

Re-emergence of natural products for drug discovery in honor of Prof. Dr. M. Iqbal Choudhary

Edited by

Hidayat Hussain, Ioannis P. Gerothanassis
and Hina Siddiqui

Published in

Frontiers in Pharmacology



FRONTIERS EBOOK COPYRIGHT STATEMENT

The copyright in the text of individual articles in this ebook is the property of their respective authors or their respective institutions or funders. The copyright in graphics and images within each article may be subject to copyright of other parties. In both cases this is subject to a license granted to Frontiers.

The compilation of articles constituting this ebook is the property of Frontiers.

Each article within this ebook, and the ebook itself, are published under the most recent version of the Creative Commons CC-BY licence. The version current at the date of publication of this ebook is CC-BY 4.0. If the CC-BY licence is updated, the licence granted by Frontiers is automatically updated to the new version.

When exercising any right under the CC-BY licence, Frontiers must be attributed as the original publisher of the article or ebook, as applicable.

Authors have the responsibility of ensuring that any graphics or other materials which are the property of others may be included in the CC-BY licence, but this should be checked before relying on the CC-BY licence to reproduce those materials. Any copyright notices relating to those materials must be complied with.

Copyright and source acknowledgement notices may not be removed and must be displayed in any copy, derivative work or partial copy which includes the elements in question.

All copyright, and all rights therein, are protected by national and international copyright laws. The above represents a summary only. For further information please read Frontiers' Conditions for Website Use and Copyright Statement, and the applicable CC-BY licence.

ISSN 1664-8714
ISBN 978-2-8325-3020-7
DOI 10.3389/978-2-8325-3020-7

About Frontiers

Frontiers is more than just an open access publisher of scholarly articles: it is a pioneering approach to the world of academia, radically improving the way scholarly research is managed. The grand vision of Frontiers is a world where all people have an equal opportunity to seek, share and generate knowledge. Frontiers provides immediate and permanent online open access to all its publications, but this alone is not enough to realize our grand goals.

Frontiers journal series

The Frontiers journal series is a multi-tier and interdisciplinary set of open-access, online journals, promising a paradigm shift from the current review, selection and dissemination processes in academic publishing. All Frontiers journals are driven by researchers for researchers; therefore, they constitute a service to the scholarly community. At the same time, the *Frontiers journal series* operates on a revolutionary invention, the tiered publishing system, initially addressing specific communities of scholars, and gradually climbing up to broader public understanding, thus serving the interests of the lay society, too.

Dedication to quality

Each Frontiers article is a landmark of the highest quality, thanks to genuinely collaborative interactions between authors and review editors, who include some of the world's best academicians. Research must be certified by peers before entering a stream of knowledge that may eventually reach the public - and shape society; therefore, Frontiers only applies the most rigorous and unbiased reviews. Frontiers revolutionizes research publishing by freely delivering the most outstanding research, evaluated with no bias from both the academic and social point of view. By applying the most advanced information technologies, Frontiers is catapulting scholarly publishing into a new generation.

What are Frontiers Research Topics?

Frontiers Research Topics are very popular trademarks of the *Frontiers journals series*: they are collections of at least ten articles, all centered on a particular subject. With their unique mix of varied contributions from Original Research to Review Articles, Frontiers Research Topics unify the most influential researchers, the latest key findings and historical advances in a hot research area.

Find out more on how to host your own Frontiers Research Topic or contribute to one as an author by contacting the Frontiers editorial office: frontiersin.org/about/contact

Re-emergence of natural products for drug discovery in honor of Prof. Dr. M. Iqbal Choudhary

Topic editors

Hidayat Hussain — Leibniz Institute of Plant Biochemistry, Germany

Ioannis P. Gerothanassis — University of Ioannina, Greece

Hina Siddiqui — University of Karachi, Pakistan

Citation

Hussain, H., Gerothanassis, I. P., Siddiqui, H., eds. (2024). *Re-emergence of natural products for drug discovery in honor of Prof. Dr. M. Iqbal Choudhary*.

Lausanne: Frontiers Media SA. doi: 10.3389/978-2-8325-3020-7

Table of contents

- 05 **Prof. Dr. M. Iqbal Choudhary-A lifetime career dedicated to remarkable services in “natural products sciences”**
Hidayat Hussain, Hina Siddiqui and Ioannis P. Gerothanassis
- 09 **Editorial: Re-emergence of natural products for drug discovery in honor of Prof. Dr. M. Iqbal Choudhary**
Hidayat Hussain, Hina Siddiqui and Ioannis P. Gerothanassis
- 12 **Potential targets and treatments affect oxidative stress in gliomas: An overview of molecular mechanisms**
Shiyu Liu, Lihua Dong, Weiyan Shi, Zhuangzhuang Zheng, Zijing Liu, Lingbin Meng, Ying Xin and Xin Jiang
- 28 **Bioactive natural products in COVID-19 therapy**
Zhonglei Wang, Ning Wang, Liyan Yang and Xian-qing Song
- 42 **Preclinical studies of NOS inhibitor T1059 vasopressor activity on the models of acute hemorrhagic shock in rats and dogs**
Marina Filimonova, Ljudmila Shevchenko, Victoria Makarchuk, Alina Saburova, Petr Shegay, Andrey Kaprin, Sergey Ivanov and Alexander Filimonov
- 54 **Antihypertensive potential of *Brassica rapa* leaves: An *in vitro* and *in silico* approach**
Rohma Abid, Muhammad Islam, Hamid Saeed, Abrar Ahmad, Fariha Imtiaz, Anam Yasmeen and Hassaan Anwer Rathore
- 69 **The bioactivities of sclareol: A mini review**
Jianbo Zhou, Xiaofang Xie, Hailin Tang, Cheng Peng and Fu Peng
- 77 **2,3,5,4'-tetrahydroxystilbene-2-O- β -D-glucoside ameliorates bleomycin-induced pulmonary fibrosis *via* regulating pro-fibrotic signaling pathways**
Tsung-Teng Huang, Chuan-Mu Chen, Lih-Geeng Chen, Ying-Wei Lan, Tse-Hung Huang, Kong Bung Choo and Kowit-Yu Chong
- 95 **Hypericin, a potential new BH3 mimetic**
Anastasia Doroshenko, Silvia Tomkova, Tibor Kozar and Katarina Stroffekova
- 109 **HAS 1: A natural product from soil-isolated *Streptomyces* species with potent activity against cutaneous leishmaniasis caused by *Leishmania tropica***
Bassel Awada, Maguy Hamie, Rana El Hajj, Ghada Derbaj, Rania Najm, Perla Makhoul, Dima Hajj Ali, Antoine G. Abou Fayad and Hiba El Hajj
- 123 **Ethanol extract of *Origanum syriacum* L. leaves exhibits potent anti-breast cancer potential and robust antioxidant properties**
Joelle Mesmar, Rola Abdallah, Kamar Hamade, Serine Baydoun, Najlaa Al-Thani, Abdullah Shaito, Marc Maresca, Adnan Badran and Elias Baydoun

- 146 **Oxysterols in catfish skin secretions (*Arius bilineatus*, Val.) exhibit anti-cancer properties**
Jassim M. Al-Hassan, Mohammad Afzal, Sosamma Oommen, Yuan Fang Liu and Cecil Pace-Asciak
- 156 **Potential effects of cannabinoids on audiovestibular function: A narrative review**
Joaquin Guerra, Vinogran Naidoo and Ramon Cacabelos
- 168 **The use of African medicinal plants in cancer management**
Goabaone Gaobotse, Srividhya Venkataraman, Pheny D. Brown, Kabo Masisi, Tebogo E. Kwape, David O. Nkwe, Gaolathe Rantong and Abdullah Makhzoum



OPEN ACCESS

EDITED BY

Apostolos Zarros,
Pharmacological Research Observatory,
United Kingdom

REVIEWED BY

Jeremy Everett,
University of Greenwich, United Kingdom
Jarkko Rautio,
University of Eastern Finland, Finland

*CORRESPONDENCE

Hidayat Hussain,
✉ Hidayat.Hussain@ipb-halle.de,
✉ hussainchem3@gmail.com
Hina Siddiqui,
✉ hinahej@gmail.com
Ioannis P. Gerothanassis,
✉ igeroth@uoi.gr

SPECIALTY SECTION

This article was submitted to Experimental Pharmacology and Drug Discovery, a section of the journal Frontiers in Pharmacology

RECEIVED 08 December 2022

ACCEPTED 12 January 2023

PUBLISHED 26 January 2023

CITATION

Hussain H, Siddiqui H and Gerothanassis IP (2023), Prof. Dr. M. Iqbal Choudhary-A lifetime career dedicated to remarkable services in "natural products sciences". *Front. Pharmacol.* 14:1119419. doi: 10.3389/fphar.2023.1119419

COPYRIGHT

© 2023 Hussain, Siddiqui and Gerothanassis. This is an open-access article distributed under the terms of the [Creative Commons Attribution License \(CC BY\)](https://creativecommons.org/licenses/by/4.0/). The use, distribution or reproduction in other forums is permitted, provided the original author(s) and the copyright owner(s) are credited and that the original publication in this journal is cited, in accordance with accepted academic practice. No use, distribution or reproduction is permitted which does not comply with these terms.

Prof. Dr. M. Iqbal Choudhary-A lifetime career dedicated to remarkable services in "natural products sciences"

Hidayat Hussain^{1*}, Hina Siddiqui^{2*} and Ioannis P. Gerothanassis^{3*}

¹Department of Bioorganic Chemistry, Leibniz Institute of Plant Biochemistry, Halle (Saale), Germany, ²H.E.J. Research Institute of Chemistry, International Center for Chemical and Biological Sciences, University of Karachi, Karachi, Pakistan, ³Section of Organic Chemistry and Biochemistry, Department of Chemistry, University of Ioannina, Ioannina, GR, Greece

KEYWORDS

M. Iqbal Choudhary, scientist, scientific achievements, drug discovery, bioorganic, medicinal chemistry

Short biography

It is a great honor and a pleasure for us to serve as the Guest Editors for this especial issue of "Frontier in Pharmacology" dedicated to Prof. Dr. Muhammad Iqbal Choudhary on his pioneering contributions in the field of Bioorganic, Synthetic, and Natural Product Chemistry. This special collection, honoring Prof. Dr. M. Iqbal Choudhary on his immense scientific contributions, and S and T (Science and Technology) capacity building services, represents an excellent opportunity to celebrate a remarkable chemist.



Prof. Dr. M. Iqbal Choudhary was born on 11 September 1959 in Karachi, Pakistan and completed his undergraduate studies at the University of Karachi. He completed his Ph. D. degree under the supervision of Prof. Dr. Atta-ur-Rahman FRS, a renowned natural product chemist, at the H. E. J. Research Institute of Chemistry, University of Karachi in 1987. He completed his doctoral research work from the Pennsylvania State University, United States

during 1985–86. Later he did his post-doctoral studies at the Department of Chemistry, Cornell University and Department of Medicinal Chemistry, Purdue University, United States. He was also a Senior Fulbright Fellow at the Scripps Institute of Oceanography, University of California at San Diego, United States.

Career and scientific achievements

Prof. Dr. M. Iqbal Choudhary now serves as a Distinguished National and Meritorious Professor, Director at the International Center for Chemical and Biological Sciences (ICCBS), H. E. J. Research Institute of Chemistry (www.iccs.edu), and Dr. Panjwani Center for Molecular Medicine and Drug Research, University of Karachi, Karachi, Pakistan. In addition, he is also serving as the Coordinator General COMSTECH [Organization of Islamic Cooperation (OIC) Ministerial Standing Committee on Scientific and Technological Cooperation] (www.comstech.org), and the Vice President of Central and South Asia of the World Academy of Sciences (TWAS). He is among the most leading scientists of Pakistan and he is also the author of over 1,266 research publications in reputed international journals, as well as 64 US patents. Notably, the cumulative impact factor of his publications is over 2,550 (calculated in Dec. 2022) and his citations exceeding 36,700 (h-Index: 80). Under his direct supervision, over 100 Ph. D. students have graduated. In addition to this, several hundred foreign students, including women students' researchers, from Nigeria, Nepal, Bangladesh, Sri Lanka, Iran, Kazakhstan, Sudan, Cameroon, Ethiopia, Mauritius, Jordan, Lebanon, Indonesia, China, Burkina Faso, and Egypt, have been trained for their doctoral and post doctoral studies at his laboratories. He has served as a visiting faculty member in many prestigious universities all over the world, including Purdue University, Cornell University, Scripps Institution of Oceanography, Pennsylvania State University, University Rhode Island, and various top Universities in the China, United Kingdom, Malaysia, Saudi Arabia, Kazakhstan, and Iran.

Prof. Choudhary has written or edited 94 books, including "Solving Problems with NMR Spectroscopy, Edition 2" (Academic Press (Elsevier), USA in the years 2006 and 2015) and "Bioassay Techniques for Drug Development" (Harwood Academic Publishers, Amsterdam) (1999). Currently, he is the editor of many other prestigious international book series and several international science journals, including "Mini Reviews in Medicinal Chemistry", and "Current Bioactive Compounds" and the rest.

Honors and awards

Prof. Choudhary has been awarded several prestigious national and international awards, including the Friendship Award by the Chinese Government (2022), Gold Medal conferred by the International Turkic Academy (ITA), Kazakhstan 2022; Mustafa (PBUH) Prize and Award (Laureate) in Bioorganic Chemistry (Mustafa PBUH Science and Technology Foundation) 2021; Appointed by UNESCO as a UNESCO Chair holder on Medicinal and Bio-Organic Natural Product Chemistry (2020); President's

International Fellowship Initiative (PIFI), "Distinguished Scientist Award" Chinese Academy of Sciences (2020); Doctor of Science (D.Sc.) from Al-Farabi Kazakh National University, Kazakhstan (2019) and University of Karachi (2005); COMSTECH Award in Chemistry (2010); Civil Award *Hilal-e-Imtiaz* by the President of Pakistan (2007); Civil Award *Sitara-e-Imtiaz* by the President of Pakistan (2001); First Khwarizmi International Award and Prize from the President of the Islamic Republic of Iran (2006); Economic Cooperation Organization (ECO) Excellence Awards in Education 2006 from the President of Azerbaijan; Distinguished National Professor by the Higher Education Commission (2004); the Academy of Sciences for the Developing World (TWAS) (2003); Civil Award *Tamgha-i-Imtiaz* by the President of Pakistan (1999); Prof. Riazuddin Siddiqui Gold Medal of Pakistan Academy of Sciences (1992); The Third World Academy of Science (Trieste, Italy) Young Scientists Award (1994); National Book Foundation Prize for the Best Science Book (1995); and Fellow, Prof. Abdussalam (Nobel Laureate) Prize in Chemistry (1989).

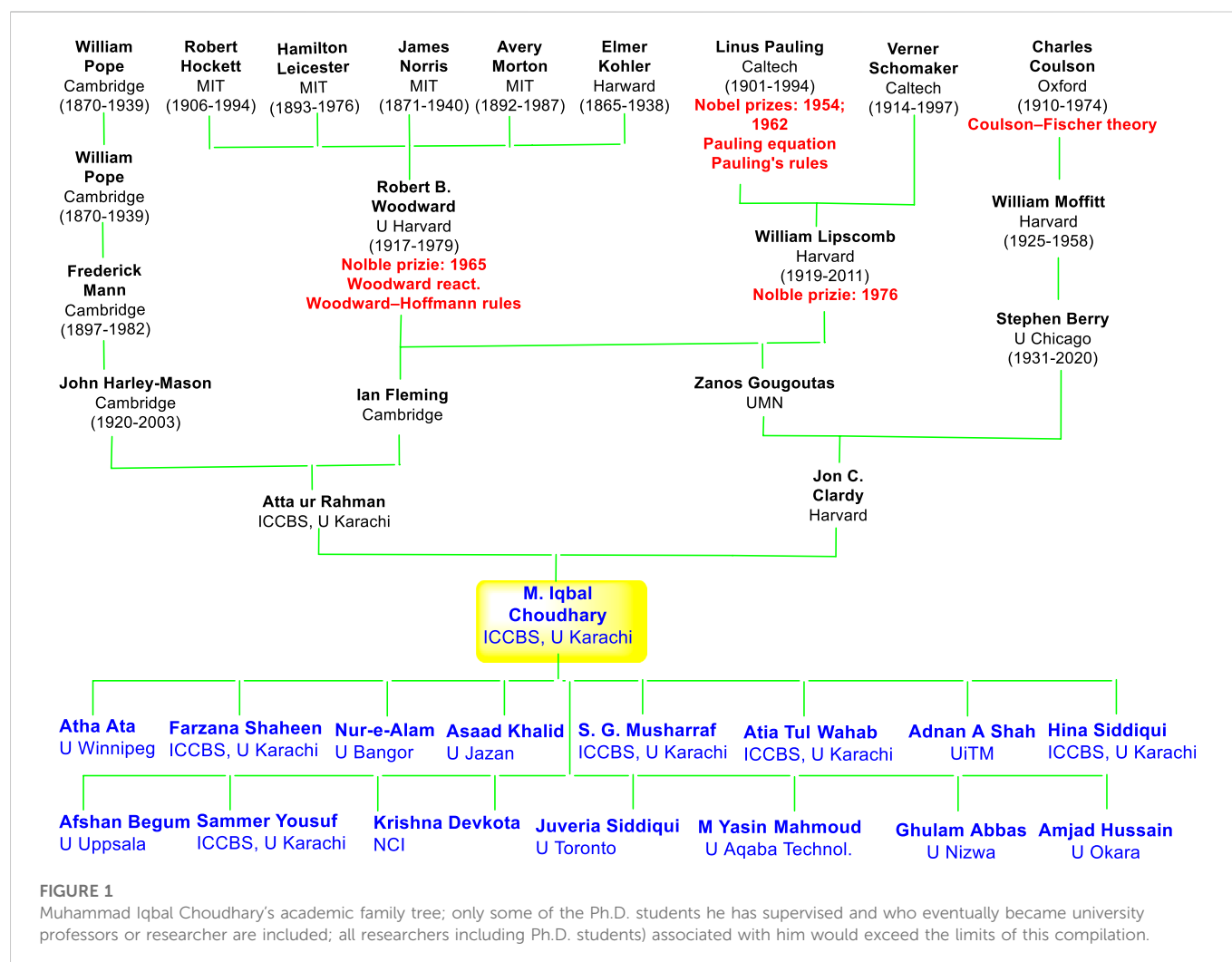
Prof. Choudhary was a Visiting Professor at several international universities, including the University of Rhode Island, USA; Manchester Metropolitan University, United Kingdom; King Saud University; King Abdulaziz University, Saudi Arabia; Al-Farabi Kazakh National University, Kazakhstan, University Malaysia Pahang, Malaysia; National Pharmaceutical Chemistry of Human University of Chinese Medicine, China; Guangxi Normal University and State Key Laboratory for Chemistry and Molecular Engineering of Medicine Resources, China; T.C.M. and Hospital of Southwest Medical University Luzhou, Sichuan, China.

Key contributions

Establishment of higher education institutions

Prof. Choudhary is currently leading two large institutions, the ICCBS (A UNESCO Cat. II center), and the COMSTECH. Under the dynamic leadership of Prof. Dr. Choudhary the ICCBS has emerged as one of the finest academic and research institutions in the developing world. He has led the major expansion of this premier research institution since 2002, both in terms of infrastructure and academic excellence. The institute received the prestigious IsDB (Islamic Development Bank) Prize twice (2004 and 2010) for the best science institution in the OIC region and selected as an UNESCO Category II Institution, and WHO Collaborating Center. As the Director of the ICCBS, Dr. Choudhary has opened the doors of state-of-the-art facilities for researchers, not only from Pakistan but also from other countries.

Prof. Choudhary has trained many young scientists from developing countries and helped them to initiate and continue their research despite the constrained environment in their countries. A large number of these young scholars have received their Ph. D. degrees based on their research work conducted under the supervision of Dr. Choudhary at the ICCBS. These scholars have developed into well-established scientists, serving their nations. Over 400 scientists (since 2004) from developing countries have been trained, which also resulted in hundreds of joint international publications. Dr. Choudhary facilitated the scientific visits of women scholars from developing countries to the ICCBS and other institutions, which have resulted in capacity building and continuity in their scientific career.



Key contributions in drug discovery

Prof. Choudhary has skillfully employed his deep knowledge of chemical principles along with biological functions in the discovery of a numerous intriguing compounds with significant therapeutic potentials (Siddiqui et al., 2020). Notably, Prof. Choudhary research group has discovered and established new clinically important enzyme inhibitors, which can be employed to stop the biological functions involved in enzyme-related disorders. His esteemed group have also discovered various new classes of lead compounds including numerous novel natural products and synthetic compounds, which possessed significant acetylcholinesterase, urease, α -glucosidase, and aromatase inhibitors. Some of these chemical entities are currently in different phases of human clinical and preclinical trials.

Dr. Choudhary and his research team have worked extensively on the plants used by the local population for the treatment of epilepsy and other neurodegenerative disorders (Shaheen et al., 2021). He along with his team has discovered isooxylitones A and B, the two most active antiepileptic secondary metabolites and patented in the United States. Interestingly these compounds were isolated from *Delphinium denudatum* and is currently in

phase 2 clinical trials. These results have been published in many international journals and patented in the United States.

Moreover, he has developed an effective nutraceutical formulation for Parkinson's disease, which has been patented and is currently in phase-II human clinical trials. Discovery of anti-leishmanial compounds is another field of his interest (Atta-ur-Rahman et al., 2012; Choudhary et al., 2005; Samdani et al., 2012). His team has successfully conducted multicenter clinical trials on the most potent compound and/or extracts from *Allium sativum* L., and *Physalis minima* L. Prof. Choudhary has identified drug candidates for the treatment of breast cancer which are several fold more active than existing clinical drugs (Choudhary et al., 2020). These drug candidates are currently in preclinical trials.

Interestingly, Prof. Choudhary has made pioneering contributions on the development of chemical entities which can reverse multidrug resistance (MDR) in *Staphylococcus aureus*, and *Pseudomonas aeruginosa*. Furthermore, Prof. Choudhary has discovered various enzyme inhibitors against various critical drug targets (enzymes involved in cancer, diabetes, peptic ulcer, and Alzheimer's disease) and antiglycating agents from natural sources, synthetic compounds, and bio-transformed metabolites.

Global S and T (science and technology) capacity building

On the platform of COMSTech (www.comstech.org), Prof. Choudhary is responsible for S&T cooperation and capacity building in member states in four continents. Since his appointment as the Coordinator General of COMSTech, OIC-COMSTech (Standing Committee of 57 Ministers of OIC member countries) has embarked on a journey of making international joint ventures, and fund raising for science and technology capacity building in largely LDCs (*Least Developed Countries*). This includes OIC's largest research mobility program, COMSTech Consortium of Excellence (CCoE), COMSTech-Africa Program in Health and STI in Niger, Uganda, Burkina Faso, Gambia, Nigeria, and Chad, Emerging Technology Initiative with IsDB and ICCI&A, Science in Exile Program (TWAS and UNESCO), Distinguished Scholars Program, OIC Technology and Innovation Portal, Research Fellowships in the fields of "Virology and Vaccine Development" with ICGEB, Women in Science Program with Women Development Organization (WDO), Technician Training Program for Capacity Building, and the Joint Research Grants Program for Young Scientists with IFS (International Foundation For Science). Besides this, under his mentorship, various technology exhibitions related to healthcare solutions, artificial intelligence, and information technology had been organized to link universities with the health industry for providing technology integrated solutions of patients.

Prof. Choudhary has helped in the establishment and strengthening of institutions, research centers, and laboratories in various countries of the developing world, including:

- Turkey: "Natural Product and Pharmacognosy Laboratory", Gazi University, Ankara.
- Nigeria: "Iqbal Choudhary Center for Natural Product Research", Benin, Nigeria
- Cameroon: "Natural Product Chemistry Center", University of Younde' I.
- Sudan: "Medicinal Plants Research Institute (MAPRI)", National Research Center, Khartoum.
- Bangladesh: "Laboratory for Research on Anti-Diabetic Plants", Dhaka.
- Kazakhstan: "Medicinal Plants Research Institute", Al-Farabi National Kazakh University.
- Sri Lanka: "Center for Advanced Research", Sir General Kotelawala Defense University, Colombo.
- Iran: "Natural Products Research Center", Shaheed Bheshti University of Medical Sciences, Tehran.

References

- Atta-ur-Rahman, Choudhary, M. I., Yousuf, S., Khan, S., Soomro, F. R., and Perveen, S. (2012). Formulations against cutaneous Leishmaniasis. US-Patent 8287921. Available at: <http://www.google.com/patents/US8287921>.
- Choudhary, M. I., Wahab, A., Siddiqui, M., Shaikh, N. N., Yousuf, S., and Atta-ur-Rahman (2020). Potent aromatase inhibitors through fungal for transformation of anti-cancer drug Testolactone: An Approach towards the treatment of breast cancer. Pakistan Patent. Available at: <https://patents.google.com/patent/US20210230214A1/en>.
- Choudhary, M. I., Yousuf, S., Ahmed, S., Yasmen, K., and Atta-ur-Rahman (2005). Antileishmanial physalins from *Physalis minima*. *Chem. Biodivers.* 2, 1164–1173. doi:10.1002/cbdv.200590086

- Saudi Arabia: "Laboratory for Bioorganic Chemistry", King Abdulaziz University, Jeddah.

Prof. Choudhary has always been a highly motivated, innovative, and hardworking researcher with gifted skills of a keen observer. As a mentor he has been a very encouraging and stimulating mentor to his students. He has this unique ability to teach students in such a way that they can visualize the concept in their mind easily, which reflects his command of the subject. He discusses science with reasoning and logic which has enabled him to supervise a large number of scholars and in this way creating a highly competitive, international and interdisciplinary working environment. Many of his former national and international students are now working in top institutions in Pakistan and the world as Professors and researchers (Figure 1). Indeed, his passion for science, work, and fascinating scientific ideas has inspired entire generations of scientists around the globe, as showed by the contributions to this Special Collection.

Ethics statement

Written informed consent was obtained from the Prof. Muhammad Iqbal. Choudhary for the publication of any potentially identifiable image.

Author contributions

HH, HS, and IPG conceptualized the study and prepared the whole manuscript.

Conflict of interest

The authors declare that the research was conducted in the absence of any commercial or financial relationships that could be construed as a potential conflict of interest.

Publisher's note

All claims expressed in this article are solely those of the authors and do not necessarily represent those of their affiliated organizations, or those of the publisher, the editors and the reviewers. Any product that may be evaluated in this article, or claim that may be made by its manufacturer, is not guaranteed or endorsed by the publisher.

- Samdani, A. J., Choudhary, M. I., Iqbal Choudhary, M., and Atta-ur-Rahman (2012). Laboratory studies and clinical trials on new Formulations from garlic extract against cutaneous Leishmaniasis. *Antimicrob. Agents* 10, 111–116. doi:10.2174/2211362611208020111
- Shaheen, F., Atta-ur-Rahman, Choudhary, M. I., Simjee, S. U., and Batool, Z. (2021). Nasally administered pharmaceutical composition for the treatment of epilepsy and related Disorders. US-Patent 322344. Available at: <https://patents.google.com/patent/US11419833B2/en>.
- Siddiqui, M., Jabeen, A., Wang, Y., Wang, W., Atta-ur-Rahman, Choudhary, M. I., et al. (2020). Whole-cell fungal-mediated structural transformation of anabolic drug metenolone acetate into potent anti-inflammatory metabolites. *J. Adv. Res.* 24, 69–78. doi:10.1016/j.jare.2020.02.009



OPEN ACCESS

EDITED AND REVIEWED BY
Filippo Drago,
University of Catania, Italy

*CORRESPONDENCE

Hidayat Hussain,
✉ hussainchem3@gmail.com
Hina Siddiqui,
✉ hinahej@gmail.com
Ioannis P. Gerothanassis,
✉ igeroth@uoi.gr

RECEIVED 23 May 2023

ACCEPTED 23 June 2023

PUBLISHED 03 July 2023

CITATION

Hussain H, Siddiqui H and
Gerothanassis IP (2023), Editorial: Re-
emergence of natural products for drug
discovery in honor of Prof. Dr. M.
Iqbal Choudhary.
Front. Pharmacol. 14:1227732.
doi: 10.3389/fphar.2023.1227732

COPYRIGHT

© 2023 Hussain, Siddiqui and
Gerothanassis. This is an open-access
article distributed under the terms of the
[Creative Commons Attribution License](#)
(CC BY). The use, distribution or
reproduction in other forums is
permitted, provided the original author(s)
and the copyright owner(s) are credited
and that the original publication in this
journal is cited, in accordance with
accepted academic practice. No use,
distribution or reproduction is permitted
which does not comply with these terms.

Editorial: Re-emergence of natural products for drug discovery in honor of Prof. Dr. M. Iqbal Choudhary

Hidayat Hussain^{1*}, Hina Siddiqui^{2*} and Ioannis P. Gerothanassis^{3*}

¹Department of Bioorganic Chemistry, Leibniz Institute of Plant Biochemistry, Halle, Germany,

²H.E.J. Research Institute of Chemistry, International Center for Chemical and Biological Sciences, University of Karachi, Karachi, Pakistan, ³Department of Chemistry, Section of Organic Chemistry and Biochemistry, University of Ioannina, Ioannina, Greece

KEYWORDS

editorial, natural product, drug discovery, plants, cancer

Editorial on the Research Topic

Re-emergence of natural products for drug discovery in honor of Prof. Dr. M. Iqbal Choudhary

Nature has always been a notable source of bioactive lead compounds and has provided unprecedented opportunities for medicinal chemists to continuously provide drug candidates as new compounds for evaluation. Natural products (NPs) and their derivatives have historically made major contributions to pharmacotherapy, in particular for cancer and infectious diseases. NPs provide intriguing chemical diversity and are considered as being irreplaceable sources of inspiration for new drug discovery and have been validated by their truly enormous contributions in the development of new lead molecules. These secondary metabolites feature diverse chemical structures, and inherently occupy biologically applicable chemical spaces. Notably, NPs and their analogs are responsible for over half of all approved drugs in current use. FDA data illustrated that NPs and their analogs represent more than one-third of all FDA-approved new lead molecules (Li and Lou, 2018).

Many renowned scientists have contributed to this topic, which includes 13 papers, original articles along with review articles that give the readers of the *Frontier in Pharmacology* an updated and new appreciation of the tremendous role played by natural products in drug discovery.

Hypericin is a penanthroperylenequinone which is a naturally occurring secondary metabolite produced by some *Hypericum* species. Hypericin was initially produced by *H. perforatum* (Brockmann et al., 1939), generally called St. John's wort, which is one of the most important members of the *Hypericum* genus. Numerous cancers including myeloid leukemia, prostate cancer, glioblastoma, and breast cancer demonstrate powerful chemo resistance which is assisted by increased expression of numerous anti-apoptotic Bcl-2 proteins. Therefore one of the more important anti-cancer strategies would be to develop inhibitors of these Bcl-2 proteins, the BH3 mimetics. Strohferkova and coworkers (Doroshenko et al.) have demonstrated that hypericin can cause critical activity in the mitochondria function and cellular ultrastructure, and also cause distribution of Bcl2 proteins. The authors proposed that the possible mechanisms of cytotoxic effects

could be due to the direct interconnection between hypericin and Bcl-2 proteins. Computational chemistry confirmed this hypothesis that hypericin interacts with BH3 and BH1 peptides.

The plant *Origanum syriacum* is employed to treat respiratory and gastrointestinal diseases in Syrian folk medicine. In addition, this plant is used to treat various respiratory diseases in Palestine, Israel and Jordan. Moreover *O. syriacum* is employed in Jordan as a pectoral, carminative, aperitif, antitussive and as an anti-stomachache. Additionally *Origanum* species were used to treat hemorrhoids, sexual diseases, internal diseases, animals bites, pains and poison in various Arab countries (Lukas et al., 2009). Mesmar et al. investigated the phytochemical content and anticancer effects of an ethanolic extract of *O. syriacum*. The authors demonstrated that this extract showed promising antioxidant effects and induced the generation of ROS in breast cancer cells (MDA-MB-231 cells). Mechanistic studies demonstrated that an *O. syriacum* extract induced G0/G1 cell cycle arrest, associated with p38 MAPK phosphorylation, protein p21enhancement and reduction of Ki67 protein. Moreover, the extract decreased the invasive and migration potentials of MDA-MB-231 cells via the deactivation of FAK (focal adhesion kinase).

Brassica rapa belongs to the family *Cru-ciferae*. The literature about this plant revealed that it demonstrated antimicrobial, antioxidant, antitumor, antiinflammatory, cardioprotective, hypolipidemic hepatoprotective, antidiabetic, nephroprotective, and analgesic effects (Paul et al., 2019). Abid et al. evaluated the antihypertensive effects of a methanolic extract the leaves of *B. rapa* and found that the highest concentration of natural products including polyphenols, flavonoids and polysaccharides to be present while an aqueous extract was rich in saponins. Moreover, the aqueous extract demonstrated promising antihypertensive potential by illustrating inhibition towards the angiotensin-converting enzyme (ACE). GC-MS analysis revealed that oleic acid was present in the *B. rapa* methanolic extract and docking analysis confirmed that this molecule is the main constituent responsible for antihypertensive effects.

Polygonum multiflorum is employed in Chinese traditional medicine to treat leptotrichia, hyperlipidaemia, inflammation and learning and memory obstructions. This plant was also reported to show hair-blackening and liver-tonic effects. Furthermore, this plant is employed in traditional medicine to treat sore scabies, pruritus, ringworm, carbuncles, scrofula, and postpartum (Lin et al., 2015). 2,3,5,4'-Tetrahydroxystilbene-2-O- β -D-glucoside (THSG) is a stilbene glycoside reported from *P. multiflorum* and literature revealed that THSG illustrated various biological effects, such as hepatoprotection, cardiovascular protection, memory enhancement, neuroprotection, anti-aging, anti-cancer, anti-oxidation, anti-osteoporosis, and anti-inflammation (Huang et al.). Chong and coworkers (Huang et al.) investigated the protective effect of THSG towards bleomycin-induced lung fibrosis. The authors found that THSG potentially attenuated lung injury via decreasing fibrosis and extracellular matrix deposition. Further studies revealed the promise that this stilbene downregulated fibronectin, TGF- β 1, CTGF, α -SMA, and TGFBR2. On the other hand, THSG upregulated SOD-1, LC3B, and catalase in the lungs of treated mice. Mechanistic studies demonstrated that THSG potentially decreased TGF- β 1-induced enhancement of

TGFBR2 expression and phosphorylation of Akt, Smad2/3, ERK1/2, and mTOR in MRC-5 cells.

The bacteria species *Streptomyces* produced numerous anti-infective potential NPs. These bacteria provided natural products with significant medical efficacy. For instance, ivermectin isolated from *S. avermitilis* is largely employed for the treatment of helminth infections. In addition, paromomycin, aminoglycoside, isolated from *S. rimosus* is used for the treatment of various parasitic infections including leishmaniasis. Awada et al. evaluated the anti-leishmanial effects of various extracts of *Streptomyces sp.* isolated and showed potent anti-leishmanial effects towards *L. tropica*. Based on bio-guided fractionation the isolation and structure elucidation of a natural product named "HAS1" which possess an acetogenins skeleton was isolated. Furthermore the isolated compound showed promising anti-leishmanial effects towards *L. tropica*.

Al-Hassan et al. phytochemically investigated the edible catfish *Arius bilineatus* and isolated twelve oxysterols including two deoxygenated steroids and cholesterol. Moreover these steroids were screened for their cytotoxic effects towards three human cancer cells including the CML cell line (K-562), breast cancer cells (MDA MB-231 and MCF-7). Cholesta-3,5,6-triol was the most active steroid towards K562 leukemic cells. Notably, steroids which featured the 5,6-epoxy group were inactive, indicating that the epoxide acquire its cytotoxic effects only after being hydrolysed to the corresponding diol precursor. Furthermore SAR showed that the importance of the C-3 hydroxyl group along with either a C-7 OH moiety and the unsaturation at C-5/C-6 or the C-5/C-6 OH groups might be replaced by a unsaturation linked with a C-7 OH group.

Filimonova and coworkers identified T1059, 1-cyclohexanoyl-2-ethylisothiourea hydrobromide and illustrated its potent eNOS and iNOS inhibitor activity along with its vasotropic effects. In an initial investigation in rats, T1059 demonstrated significant vasoconstrictive effects at relatively safe doses but was accompanied with an increase in peripheral vascular resistance in rats (Filimonova et al., 2018). In another study the same authors demonstrated that T1059 showed long-term vasoconstrictor effects (Filimonova et al., 2020) and that this molecules did not cause a potential baroreflex response in rats. Quite recently Filimonova and coworkers (Filimonova et al.) screened the T1059 vasopressor effects in rats and dogs and demonstrated significant vasoconstrictor effects. Treatment of T1059 in dogs and rats induced and enhancement in vascular tone along with significant hypertensive effects. Moreover the low dose administration of T1059, inhibited the establishment of cardiorespiratory disorders and potentially increased the survival of animals.

The COVID-19 pandemic has resulted in 639 132 486 cases being reported in addition to 6 614 082 deaths around the globe during the last 3 years. (World Health Organization, 2022). The various variants including Alpha, Beta, Gamma, Delta, and Omicron of the SARS-CoV-2 are thought to be responsible for all these cases and deaths. Natural products continuously play a tremendous role in drug discovery including for COVID-19 and are still considered as a most important strategy to defeat this ongoing pandemic. Wang et al. published a review article about the role of natural products in COVID-19 therapy. The authors included various natural products with intriguing effects towards SARS-CoV-2 and related viruses.

They discussed the effects of various natural products as anti-COVID-19 treatment from numerous natural product classes including alkaloids, peptides, steroids, triterpene glycosides, xanthenes, diterpenes, macrolides, cannabinoids, flavones, coumarins, and naphthoquinones.

Zhou et al. published an interesting review on the biological and pharmacological effects of sclareol. They described how sclareol, a diterpene reported from *S. sclarea* is applied as a traditional medicine to treat oral inflammation, arthritis, dysmenorrhea, and digestive system diseases. Moreover sclareol illustrated significant anticancer effects towards various cancer cells including leukemia (HL60), breast (MN1, MDD2, MCF-7), colon (HCT116), cervical (HeLa), lung (H1688, A549), and osteosarcoma (MG63). Additionally, sclareol illustrated anti-pathogenic and anti-inflammation effects.

Liu et al. published a comprehensive review on significant drug targets and treatments which affect oxidative stress in gliomas diseases. The authors discussed oxidative stress and its link with gliomas along with pathogenesis of gliomas and the perceived mode of action of oxidative stress in gliomas. In addition, the authors described various natural products that can be used to treat gliomas. These natural products include thymoquinone, chidamide, atovaquone, ivermectin, chloroquine, quinacrine, melatonin, chaetocin, celastrol, shikonin, chaetocin and cannabidiol. Guerra et al. described in their review article that cannabinoids have significant effects on the audiovestibular function. The authors demonstrated that the cannabinoid receptors expression in the audiovestibular pathway demonstrates their tremendous role in drug development. Notably, these drugs may be fruitful for diseases including ototoxicity, noise-induced hearing loss, and various forms of vertigo.

Gaobotse et al. provide an overview some African medicinal plants which demonstrated anticancer properties. These plants include *Dicoma anomala*, *Portulaca oleracea*, *Withania somnifera*, *Azanza garckeana*, *Cajanus cajan*, *Combretum*

caffrum, *Prunus avium*, *Prunus Africana*, *Securidaca longipedunculata*, *Annona muricata*, *Annona senegalensis*, *Aerva javanica*, *Abelmoschus esculentus*, *Flueggea virosa*, *Lagenaria siceraria*, *Xylopia aethiopica*, *Nymphaea lotus*, *Zanthoxylum chalybeum*, *Ceratonia siliqua*, *Moringa oleifera*, and *Peganum harmala*. In another article, Badivi et al. developed the formulation of bee venom-loaded liposomes coated with PEG (BV-Lipo-PEG). Cytotoxic results demonstrated that bee venom has ability to enhance the cytotoxic effects towards various cancer cells. Additionally, BV-Lipo-PEG reduce the expression levels of cyclin E genes, MMP-9, and MMP-2 while enhanced the expression level of caspases 3 and 9.

Author contributions

HH, HS, and IG wrote the manuscript. All authors contributed to the article and approved the submitted version.

Conflict of interest

The authors declare that the research was conducted in the absence of any commercial or financial relationships that could be construed as a potential conflict of interest.

Publisher's note

All claims expressed in this article are solely those of the authors and do not necessarily represent those of their affiliated organizations, or those of the publisher, the editors and the reviewers. Any product that may be evaluated in this article, or claim that may be made by its manufacturer, is not guaranteed or endorsed by the publisher.

References

- Brockmann, H., Haschad, M. N., Maier, K., and Pohl, F. (1939). Über das Hypericin, den photodynamisch wirksamen Farbstoff aus *Hypericum perforatum*. *Naturwissenschaften* 27, 550. doi:10.1007/BF01495453
- Filimonova, M. V., Shevchenko, L. I., Makarchuk, V. M., Chesnakova, E. A., Shevchuk, A. S., Filimonov, A. S., et al. (2020). Vasopressor properties of NO synthase inhibitor T1059. Part II. Hemodynamic effects on hypovolemic disorders. *Pharm. Chem. J.* 53, 1113–1117. doi:10.1007/s11094-020-02132-y
- Filimonova, M. V., Shevchenko, L. I., Makarchuk, V. M., Chesnakova, E. A., Surinova, V. I., Shevchuk, A. S., et al. (2018). Vasopressor properties of nitric oxide synthase inhibitor T1059. Part I: Synthesis, toxicity, NOS-inhibition activity, and hemodynamic effects under normotensive conditions. *Pharm. Chem. J.* 52, 294–298. doi:10.1007/s11094-018-1809-2
- Li, G., and Lou, H. X. (2018). Strategies to diversify natural products for drug discovery. *Med. Res. Rev.* 38, 1255–1294. doi:10.1002/med.21474
- Lin, L., Ni, B., Lin, H., Zhang, M., Li, X., Yin, X., et al. (2015). Traditional usages, botany, phytochemistry, pharmacology and toxicology of *Polygonum multiflorum* Thunb. *a Rev. J. Ethnopharmacol.* 159, 158–183. doi:10.1016/j.jep.2014.11.009
- Lukas, B., Schmiderer, C., Franz, C., and Novak, J. (2009). Composition of essential oil compounds from different Syrian populations of *Origanum syriacum* L. (Lamiaceae). *J. Agric. Food. Chem.* 57, 1362–1365. doi:10.1021/jf802963h
- Paul, S., Geng, C. A., Yang, T. H., Yang, Y. P., and Chen, J. J. (2019). Phytochemical and health-beneficial progress of turnip (*Brassica rapa*). *J. Food Sci.* 84, 19–30. doi:10.1111/1750-3841.14417



OPEN ACCESS

EDITED BY

Hidayat Hussain,
Leibniz Institute of Plant Biochemistry,
Germany

REVIEWED BY

Azhwar Raghunath,
University of Michigan, United States
Balaran Mohapatra,
Indian Institute of Technology Bombay,
India

*CORRESPONDENCE

Ying Xin,
xiny@jlu.edu.cn
Xin Jiang,
jiangx@jlu.edu.cn

SPECIALTY SECTION

This article was submitted to
Experimental Pharmacology and Drug
Discovery,
a section of the journal
Frontiers in Pharmacology

RECEIVED 15 April 2022

ACCEPTED 04 July 2022

PUBLISHED 22 July 2022

CITATION

Liu S, Dong L, Shi W, Zheng Z, Liu Z,
Meng L, Xin Y and Jiang X (2022),
Potential targets and treatments affect
oxidative stress in gliomas: An overview
of molecular mechanisms.
Front. Pharmacol. 13:921070.
doi: 10.3389/fphar.2022.921070

COPYRIGHT

© 2022 Liu, Dong, Shi, Zheng, Liu, Meng,
Xin and Jiang. This is an open-access
article distributed under the terms of the
[Creative Commons Attribution License](#)
(CC BY). The use, distribution or
reproduction in other forums is
permitted, provided the original
author(s) and the copyright owner(s) are
credited and that the original
publication in this journal is cited, in
accordance with accepted academic
practice. No use, distribution or
reproduction is permitted which does
not comply with these terms.

Potential targets and treatments affect oxidative stress in gliomas: An overview of molecular mechanisms

Shiyu Liu^{1,2,3}, Lihua Dong^{1,2,3}, Weiyan Shi^{1,2,3},
Zhuangzhuang Zheng^{1,2,3}, Zijing Liu^{1,2,3}, Lingbin Meng⁴,
Ying Xin^{5*} and Xin Jiang^{1,2,3*}

¹Jilin Provincial Key Laboratory of Radiation Oncology and Therapy, The First Hospital of Jilin University, Changchun, China, ²Department of Radiation Oncology, The First Hospital of Jilin University, Changchun, China, ³NHC Key Laboratory of Radiobiology, School of Public Health, Jilin University, Changchun, China, ⁴Department of Hematology and Medical Oncology, Moffitt Cancer Center, Tampa, FL, United States, ⁵Key Laboratory of Pathobiology, Ministry of Education, Jilin University, Changchun, China

Oxidative stress refers to the imbalance between oxidation and antioxidant activity in the body. Oxygen is reduced by electrons as part of normal metabolism leading to the formation of various reactive oxygen species (ROS). ROS are the main cause of oxidative stress and can be assessed through direct detection. Oxidative stress is a double-edged phenomenon in that it has protective mechanisms that help to destroy bacteria and pathogens, however, increased ROS accumulation can lead to host cell apoptosis and damage. Glioma is one of the most common malignant tumors of the central nervous system and is characterized by changes in the redox state. Therapeutic regimens still encounter multiple obstacles and challenges. Glioma occurrence is related to increased free radical levels and decreased antioxidant defense responses. Oxidative stress is particularly important in the pathogenesis of gliomas, indicating that antioxidant therapy may be a means of treating tumors. This review evaluates oxidative stress and its effects on gliomas, describes the potential targets and therapeutic drugs in detail, and clarifies the effects of radiotherapy and chemotherapy on oxidative stress. These data may provide a reference for the development of precise therapeutic regimes of gliomas based on oxidative stress.

KEYWORDS

Reactive Oxygen Species (ROS), gliomas, oxidative stress, target gene, therapeutic strategy

Introduction

Gliomas are common and arise from neuroglial progenitor cells. They are currently incurable central nervous system (CNS) tumors in adults, representing almost 80% of all malignant brain tumors (Ostrom et al., 2014). Glioma incidence and survival rate are associated with numerous factors. Brain tumor development is related to oxidative stress, therefore, it is important to understand oxidative stress mechanisms and develop novel and effective treatments.

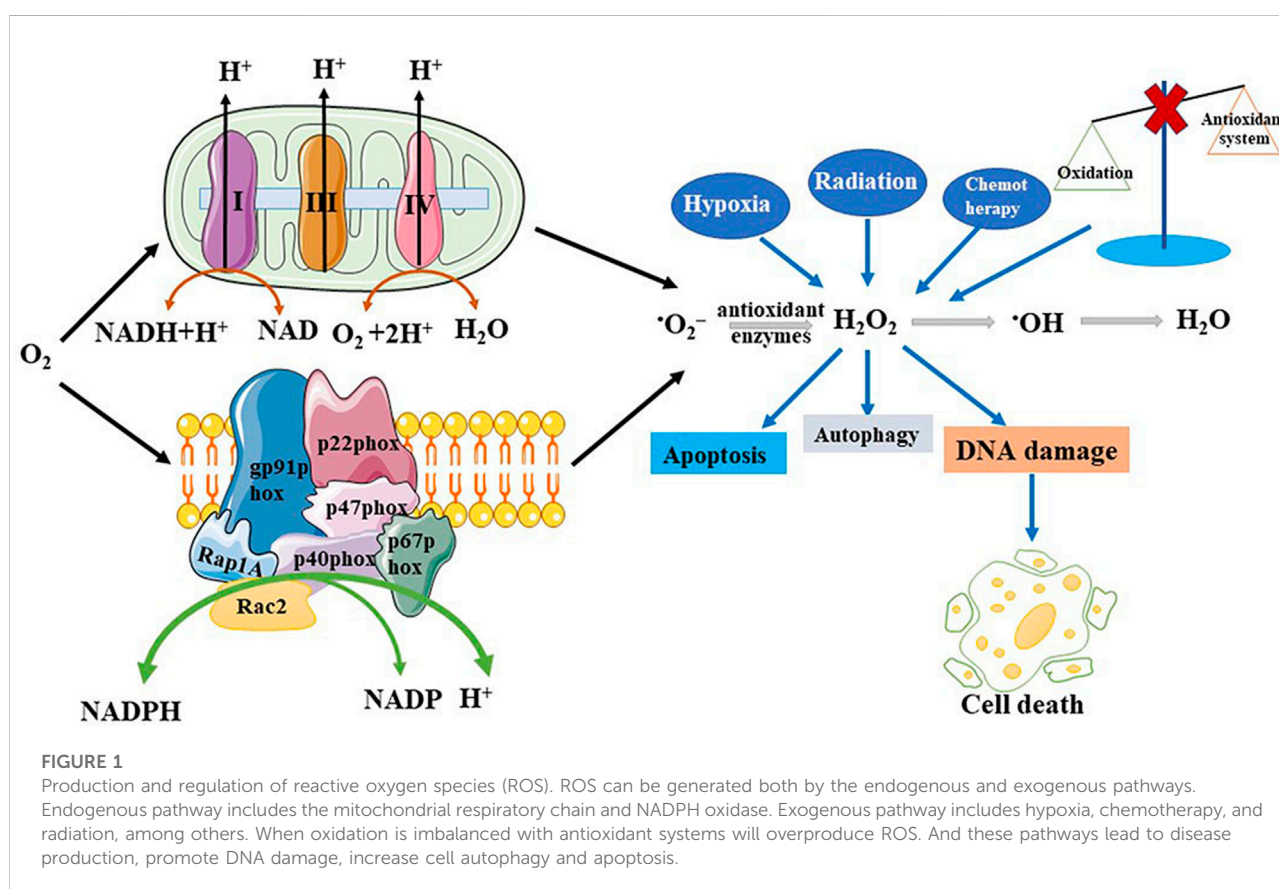
In 1990, Sohal et al. first proposed the concept of oxidative stress, either caused by an increase in free radical production or a reduction in the scavenging capacity of the body, leading to disorders in the oxidation and antioxidant systems, resulting in oxidative damage by free radical accumulation (Sohal and Allen, 1990). This process is associated with electron transfer, which affects the redox state of the organism.

The species to which oxygen converts with high reactivity are generally called reactive oxygen species (ROS), which are a type of single electron reduction product of oxygen *in vivo* (Nosaka and Nosaka, 2017). ROS are toxic but are also necessary for regulating the diverse physiological functions of living organisms.

Antioxidative therapy is an effective strategy for many diseases triggered by excess ROS. Low and well-regulated ROS levels enable the functioning of a diverse array of signaling pathways. High levels of ROS-damaged proteins, lipids, and deoxyribonucleic acid (DNA) promote clonal expansion and tumor growth by protecting initial cells from oxidative toxicity and apoptosis (Reczek and Chandel, 2017). Therefore, antioxidative therapy could be used as a research target for glioma treatment. This review describes the existing evidence for the involvement of oxidative stress in the incidence of gliomas, focuses on understanding the function of ROS, and details how to manipulate ROS in glioma treatment.

Oxidative stress overview

Any atom or molecule containing one or more unpaired electrons is defined as a free radical. ROS is a collective concept consisting of oxygen-based free radicals and some non-radical derivatives of O_2 , including hydrogen peroxide (H_2O_2), superoxide anion radicals ($\cdot O_2^-$), hydroxyl radicals ($\cdot OH$), and singlet oxygen (1O_2) (Nosaka and Nosaka, 2017). The regulation of ROS production is shown in Figure 1. ROS have beneficial biological activities and are maintained at appropriate



levels by endogenous antioxidant defenses, comprising non-enzymatic antioxidants and antioxidant enzymes. Non-enzymatic antioxidants include tocopherols, ascorbic acid, and glutathione (GSH). Generally, oxidative stress levels are measured using GSH. The antioxidant enzymes include catalase (CAT), superoxide dismutase (SOD), and glutathione peroxidase. Some endogenous pathways can generate ROS, such as the reduction of oxygen molecules during aerobic respiration, resulting in hydroxyl radicals and superoxide. Similarly, the oxidation of catecholamines and the activation of electrons in arachidonic acid co-products reduces oxygen molecules to superoxide (Betteridge, 2000). Many factors stimulate ROS production in various cell types, including cytokines, such as interleukin-1 (IL-1), tumor necrosis factor- α (TNF- α), transforming growth factor- β 1 (TGF- β 1), interferon- γ (IFN- γ), G protein-coupled receptor binding ligands angiotensin II, serotonin (5-hydroxytryptamine), bradykinin, thrombin, endothelin, and ion channel-linked receptors with neurotransmitters (e.g., acetylcholine, glutamate, glycine, and γ -aminobutyric acid) (Thannickal and Fanburg, 2000). Stimulated by growth factors, ROS act as secondary messenger molecules and initiate a signal cascade in receptor transduction, acting downstream of small guanosine triphosphate (GTP)-binding proteins and receptor tyrosine kinases (RTKs) and upstream of the mitogen-activated protein kinase (MAPK) family (Behrend et al., 2003). The MAPK family mainly consists of c-Jun N-terminal kinases (JNKs: JNK1, JNK2, and JNK3), extracellular signal-regulated kinases (ERKs: ERK1 and ERK2), and p38-MAPKs (p38-MAPK α , p38-MAPK β , p38-MAPK γ , and p38-MAPK δ) (Wada and Penninger, 2004). JNKs are activated by the phosphorylation of threonine and tyrosine residues catalyzed by MAPK kinase 4 (MKK4) and MKK7, which in turn activate ETS-like protein 1, transcription factor 2, p53, and c-Myc to promote cancer cell proliferation (Wada and Penninger, 2004). Activator protein 1 (AP-1), which is composed of c-Jun and c-Fos, is a downstream transcription factor that is activated by MAPK. It also regulates cyclin D1 and p21 to promote cell proliferation (Waris and Ahsan, 2006). ROS can also be produced through a series of exogenous processes. Exposure to exogenous substances can induce oxidative stress and damage. In the case of ionizing radiation, water decomposes to produce hydroxyl radicals. A study has suggested that the majority of the subversive effects of O₂ are due to the action of oxygen radicals and an increase in the partial pressure of oxygen or reduction in antioxidant defenses can cause cellular and tissue damage. $\bullet\text{O}_2^-$, a free radical, is produced by the monovalent reduction of O₂ (Gerschman et al., 1954). From a biological perspective, $\bullet\text{O}_2^-$ can be generated from two major sources: phagocytic nicotinamide adenine dinucleotide phosphate (NADPH) oxidase and the mitochondrial respiratory chain. Duve and Baudhuin described the process whereby peroxisomes can oxidize the substrate RH₂, reducing oxygen to hydrogen peroxide. A large

quantity of CAT can reduce hydrogen peroxide to water (O₂ + RH₂ → R₂ + H₂O₂; H₂O₂ + RH₂ → 2H₂O + O₂ + R) (De Duve and Baudhuin, 1966). Peroxisomes not only participate in ROS generation but also scavenge ROS. Previous studies have shown that NADPH oxidase (NOX) is the principal source of ROS (Brown and Griendling, 2009). NOX is mainly composed of five subunits, including gp91phox (or its homologs, NOX1 and NOX4), p22phox, p47phox, p40phox, and p67phox and two GTP-binding proteins Rap1A and Rac2 (Burtenshaw et al., 2019).

The first SOD that catalyzes the dismutation of superoxide radicals and defends against oxygen free radicals was reported in 1969 (McCord and Fridovich, 1969). Studies have shown that SOD advances the reaction between itself and superoxide anions to form H₂O₂ and O₂ ($\bullet\text{O}_2^- + \bullet\text{O}_2^- + 2\text{H}^+ \rightarrow \text{O}_2 + \text{H}_2\text{O}_2$) (Fridovich, 1997). H₂O₂ reacts with iron ions to generate $\bullet\text{OH}$ in Fenton systems, inducing the production of 5,6-dihydroxycytosine, 2,6-diamino-4-hydroxy-5-formamidopyrimidine, 8-hydroxyguanine (8-OHdG) and 4,6-diamino-5-formamidopyrimidine (Halliwell and Gutteridge, 1992). The content of these products can be measured as an index of DNA damage caused by $\bullet\text{OH}$. CAT and peroxidase are inactivated by $\bullet\text{O}_2^-$, and SOD reduces the H₂O₂ burden borne by aerobic cells by maintaining the activities of peroxidases and CAT (Flint et al., 1993). In any environment where oxygen is produced, the activities of CAT and peroxidase are compromised, and SOD minimizes this effect. However, when $\bullet\text{O}_2^-$ is used as an oxidant, it promotes the generation of H₂O₂, while SOD prevents chain reactions initiated by $\bullet\text{O}_2^-$ oxidation and reduces the generation of H₂O₂ (Liochev and Fridovich, 1994).

ROS are well established as playing dual roles as harmful and beneficial components. Overproduction of ROS can induce cell death *via* signaling pathways such as autophagy and apoptosis, resulting in oxidative stress. However, ROS at low or moderate concentrations will exert beneficial effects involving multiple cellular signaling pathways and playing various physiological roles (Valiko et al., 2007). Inflammation is a defensive immune response to stimuli, where phagocytes and endothelial cells play a central role and contain ROS generated by NADPH oxidase. Neutrophils also produce ROS that can promote inflammatory cell migration to clear foreign materials and pathogens but this also results in host tissue damage (Mittal et al., 2014). Xanthine oxidoreductase is transformed by proteases into xanthine oxidase, which is then able to transfer electrons from xanthine to oxygen to generate ROS and participate in the inflammatory pathway by inactivating MAPK phosphatase-1, leading to JNK phosphorylation in macrophages (Nomura et al., 2013). Parthanatos, also known as poly ADP-ribose polymerase-1 (PARP-1)-dependent cell death, is a newly described form of programmed brain cell death. JNK phosphorylation promotes oxidative stress-induced parthanatos by increasing intracellular ROS generation (Zheng et al., 2017).

Oxidative stress is associated with several human diseases, including diabetes, cancer, neurodegenerative diseases, cardiovascular diseases, and aging (Aruoma et al., 2006; Milkovic et al., 2014). Increased ROS production leads to disturbances in the balance between oxidation and the antioxidant defense system of the body, causing oxidative stress and this has been observed in cancer cells (Trachootham et al., 2009). Cancer cells exhibit high levels of ROS owing to aberrant signaling, which may be an obstacle to tumor generation. However, ROS can also accelerate tumor growth *via* oncogenic signaling pathways, DNA mutations, and DNA damage (Ames, 1983; Gorrini et al., 2013). DNA mutations are crucial for tumor formation. With the accumulation of ROS, the number of cellular mutations increases, and DNA is constantly damaged. The product of the direct reaction of $\bullet\text{OH}$ with guanosine is 8-oxo-7,8-dihydro-2'-deoxyguanosine (8-oxo-dG), which is moderately mutagenic and affects G→T transversion mutations (Fleming and Burrows, 2017). 8-oxo-dG can be an indicator of cellular oxidative stress, with its presence suggesting increased oxidative stress and tumor malignancy. Therefore, the modulation of ROS levels plays a significant role in potential anticancer strategies. Most cancer cells exhibit multiple genetic alterations, increased ROS generation, and altered redox status with additive oxidative stress and aerobic glycolysis, suggesting that preferential clearance of these cells by modulation of the redox modulation mechanism may be a valid strategy for cancer therapy (Trachootham et al., 2009).

Pathogenesis of gliomas

Gliomas are among the most common malignant brain tumors in adults, accounting for more than 70% of which glioblastoma (GBM) is the most malignant form. GBM accounts for 14.3% of all tumors and 49.1% of malignant tumors (Ostrom et al., 2021). The updated 2016 edition of the World Health Organization (WHO) classification of CNS tumors was the first to use molecular type and histology to define major tumor categories (Louis et al., 2016). This classification divides gliomas into four grades. Grade I mainly includes angiocentric gliomas and pilocytic astrocytomas. Grade II includes diffuse astrocytomas, oligoastrocytomas, and oligodendrogliomas. Grade III includes anaplastic astrocytomas. Finally, grade IV tumors include GBM and gliosarcomas. Traditionally, low-grade gliomas (LGGs) include grade I and grade II gliomas and high-grade gliomas (HGGs) include grade III and grade IV gliomas. However, the fifth edition of the CNS classification adopted in 2021 introduced new types and subtypes of gliomas based on molecular biomarkers (Louis et al., 2021). Currently, the standard treatment for newly diagnosed HGGs is surgical resection within a feasible range, followed by adjuvant radiotherapy (60 Gy/2 Gy/30 f) and concurrent oral

temozolomide (TMZ) from the first day of radiotherapy to the last day. Sequential chemotherapy with six cycles of adjuvant temozolomide (Tan et al., 2020). The prognosis of patients with gliomas remains poor despite standard radiotherapy and TMZ treatment. Almost all patients with GBM show disease progression after a median progression-free survival of 7–10 months. Besides radiotherapy and chemotherapy, molecular-targeted therapy is widely used, especially in recurrent gliomas, and holds the promise of providing more effective treatment options with minimal toxicity (Omuro and DeAngelis, 2013). Immunotherapy clears tumors *via* antitumor responses by the host immune system, releases antigens, regulates immune pathways, and elicits tumor-specific cytotoxic T-cells, eventually resulting in immunogenic death (Liu et al., 2021). Despite the current advent of multiple immunotherapies, they have not significantly improved the overall survival of patients with glioma, which is associated with a suppressive immune microenvironment in glioma cells. Immunosuppression of gliomas is associated with multiple biological processes, such as aerobic glycolysis, tryptophan metabolism, and arginine metabolism (Chen and Hambardzumyan, 2018). Multiple mechanisms by which glioma cells evade detection and destruction in the immune system include T-cell, NK cell, and myeloid dysfunction; M2 phenotypic conversion in tumor-associated macrophages/microglia; glioma cell cytokine and surface factor cytokine upregulation; and glioma cell microenvironment hypoxia (Grabowski et al., 2021).

Gliomas are complex microcosms that depend on growth regulatory signals sent by the tumor microenvironment and feature angiogenesis and redox state changes. Communication between non-neoplastic and neoplastic cells contributes to the formation, progression, and response to cancer treatments. Receptors on glioma cells bind to ligands secreted by normal brain parenchymal cells, which may promote glioma invasion or create a microenvironment for malignant progression (Hoelzinger et al., 2007). In addition, abnormal activation of the inflammatory response is a characteristic of GBM and inflammation can promote tumor growth and resistance to treatment (Ham et al., 2019). High ROS levels lead to the death of astrocytes through necrosis and apoptosis, affecting the degree of malignancy *via* the nuclear factor kappa enhancer-binding protein (NF- κ B) (Waris and Ahsan, 2006). Cancer development is a multi-stage process described in three stages: initiation, promotion, and progression. The initiation stage involves a non-lethal mutation in the DNA. The promotion phase is a reversible process characterized by the initiation of clonal expansion of cells through the induction of cell proliferation or inhibition of programmed cell death (i.e., apoptosis). At this stage, it is necessary to continue the existence of the tumor to promote stimulation. The final stage of carcinogenesis is irreversible and involves genetic instability and damage to chromosome integrity. The accumulation of

additional genetic damage, vascularization, invasion, and metastasis leads to the transformation of cells from benign to malignant, which means that benign preneoplastic lesions become neoplastic cancer cells (Valko et al., 2006).

Oxidative stress is particularly important in glioma pathogenesis. The nervous system is vulnerable to oxidative stress because of high oxygen metabolism in the brain (Barciszewska et al., 2019). ROS-induced oxidative stress leads to DNA damage, which affects the proliferation and apoptosis of glioma cells and increases their susceptibility to gliomas. Human MutT homolog protein 1 (hMTH1) is an enzyme that hydrolyzes 8-oxo-dGTP to the corresponding monophosphate and prevents 8-oxo-dG from accumulating in DNA. The level of oxidative stress is higher in HGGs, therefore, the accumulation of 8-oxo-dG and the expression of hMTH1 are more pronounced. Enhancing the defense against this oxidative stress could be used to treat tumors (Iida et al., 2001). A case-control study showed that the influence of antioxidant gene variations, such as SOD3 T58A, SOD2 V16A, NOS1 3'-UTR, and GPX1-46 C/T, was correlated with the risk of glioma development (Zhao et al., 2012). A study investigated the possible pathway by which H₂O₂ induced apoptosis in glioma cells and concluded that oxidative stress inhibited glioma cell growth and induced apoptosis *via* a caspase-3-dependent pathway (Liu et al., 2015). Glioma stem-like cells (GSCs) are a class of subpopulations with stem-like characteristics in glioma cells that confer self-renewal capacity and therapeutic resistance (Mittal et al., 2014). ROS is crucial for the study of therapeutic strategies for GSCs. GSCs, like normal stem cells, maintain low ROS levels, which is in contrast to the high ROS levels in cancer cells (Mittal et al., 2014).

Functional annotation analysis of differentially methylated genes in pediatric GBM and adult GBM identified ROS regulation as a vital process in pediatric GBM and ROS-related genes neutrophil cytosolic factor 1 (NCF1) and NOX4 are upregulated and play important roles in chemosensitivity and proliferation (Jha et al., 2014).

The mechanism of oxidative stress modulators in gliomas

The design of many molecular targets based on oxidative stress is essential for maximizing survival and transforming this treatment into a form of precision medicine. The following section describes several therapeutic targets that influence oxidative stress.

Oxidative stress activates multiple transcription factors, including hypoxia-inducible factor-1 α (HIF-1 α), AP-1, NF- κ B, p53, and nuclear factor erythroid 2-related factor 2 (Nrf2) (Reuter et al., 2010). Nrf2 is an important component of the cellular defense against various exogenous and endogenous stresses that can be activated in response to a series of oxidative and electrophilic stimulations (Kensler et al., 2007).

Nrf2 serves as a potential therapeutic target in gliomas since activating its expression will increase the content of target antioxidants and enzymes that protect cells from apoptosis, whereas inhibiting its expression can elevate the killing effects of antitumor therapies (Zhu et al., 2014). Kelch-like ECH-associated protein 1 (KEAP1) is an inhibitor of Nrf2, which acts by modulating Nrf2 activity. A complex consisting of Cullin 3 (Cul3), KEAP1, and ring-box 1 (RBX1) binds to E2 ubiquitin-conjugating enzyme, and Nrf2 and Nedd8 (N8) induce a conformational change that inhibits Nrf2 ubiquitination (Baird and Yamamoto, 2020). Upon recognition of oxidative stress, Nrf2 dissociates from KEAP1, translocates to the nucleus, and heterodimerizes with small musculoaponeurotic fibrosarcoma proteins (sMafs). Nrf2 and other transcription factors regulate the expression of antioxidant genes by interacting with antioxidant response elements (ARE) (Reuter et al., 2010). The KEAP1–Nrf2–ARE signaling pathway plays a significant role in protecting cells from oxidative stress. Oxidative stress-related molecules and matrix metalloproteinases (MMPs) are involved in regulating glioma migration and invasion *via* the Nrf2/ARE pathway (Deryugina et al., 1997). Downregulation of Nrf2 expression can inactivate MMP-9 and reduce the migration and invasion of gliomas (Pan et al., 2013). Heme oxygenase-1 (HO-1), a downstream molecule of Nrf2, plays a key role in regulating oxidative stress. Nuclear Nrf2 upregulates HO-1 and decreases intracellular ROS (Kanzaki et al., 2013). HO-1, which is involved in heme metabolism, catalyzes the conversion of heme to biliverdin and generates carbon monoxide during this process (Hayashi et al., 1999). HO-1 protein expression is associated with the degree of glioma malignancy and is overexpressed in HGGs. Moreover, HO-1 participates in immune cell infiltration and is associated with metastasis and angiogenesis. The mechanism of action of Nrf2 in glioma treatment is shown in Figure 2.

HIF-1 is a DNA-binding protein and is composed of two different subunits, 120 kDa HIF-1 α and 91–94 kDa HIF-1 β (Wang and Semenza, 1995). HIF-1 allows tumor cells to survive in the absence of oxygen, activating the transcription of glycolytic enzymes, glucose transporters, and vascular endothelial growth factors (Zhong et al., 1999). ROS can alter the function and activity of HIF-1 and inhibition of HIF-1 activity contributes to tumor therapy. NOX4 mRNA expression levels in GBM are markedly higher than those in other astrocytomas (Shono et al., 2008). A previous study revealed that circulating hypoxic conditions increase ROS production, activate HIF-1, and promote the growth of glioma cells by upregulating the expression of NOX4 mRNA and protein expression in GBM cells (Hsieh et al., 2011). NOX2, a downstream target gene of microRNA (miR)-34a, increases ROS levels and promotes apoptosis in glioma cells (Li et al., 2014). Therefore, knockdown of NOX2 and NOX4 during GBM progression may be a therapeutic method for counteracting the effect of hypoxia on tumor progression.

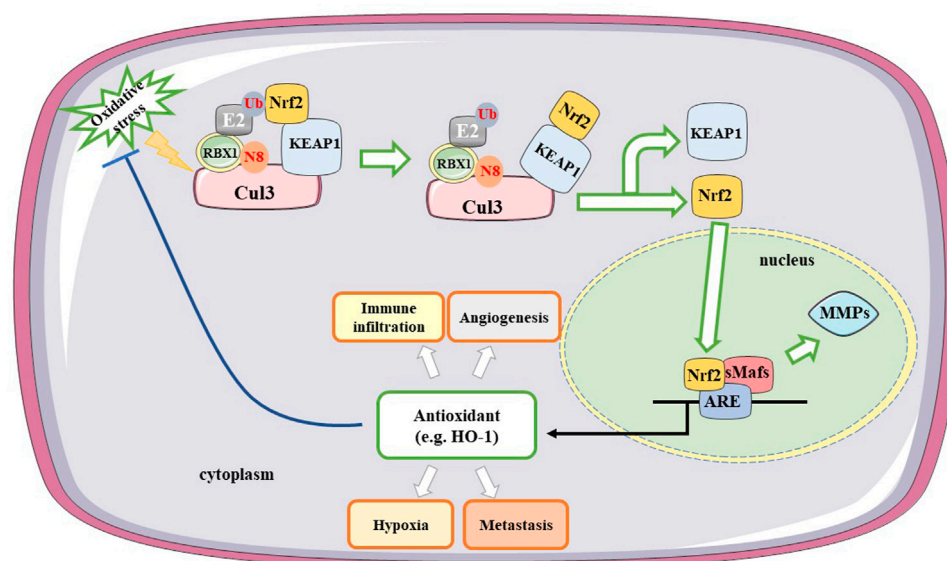


FIGURE 2

Mechanisms of Nrf2 in treating gliomas. A complex consisting of Cul3, KEAP1, and RBX1 binds to E2 ubiquitin-conjugating enzyme. Under the oxidative stress, Nrf2 induces a conformational change and dissociates from KEAP1, translocating to the nucleus. Nrf2 binds with ARE and heterodimerizes with sMafs. Downregulating Nrf2 expression inactivates MMP-9 and reduces the migration and invasion of gliomas. HO-1 as a downstream factor of Nrf2 participates in immune infiltration, hypoxia, metastasis and angiogenesis. Cul3, Cullin 3; Nrf2, nuclear factor erythroid 2-related factor 2; KEAP1, Kelch-like ECH-associated protein 1; RBX1, ring-box-1; ARE, antioxidant response elements; MMPs, matrix metalloproteinases; H₂O₂, heme oxygenase 1; sMafs, small musculoaponeurotic fibrosarcoma proteins; N8, Nedd8; Ub, Ubiquitination.

A study identified that diacylglycerol O-acyltransferase 1 (DGAT1) is highly expressed in HGGs. Inhibition of DGAT1 was shown to significantly upregulate the carnitine palmitoyltransferase 1A (CPT1A) protein, which facilitates the entry of excessive fatty acids (FAs) into the mitochondria for oxidation, resulting in mitochondrial damage, remarkable increase in GBM cell apoptosis, and ROS production (Cheng et al., 2020). Therefore, targeting DGAT1 may be a potential therapeutic approach for glioma treatment.

Epidermal growth factor receptor (EGFR) induces protein kinase C ϵ (PKC ϵ) to phosphorylate and activate I κ B kinase β (IKK β) at Ser177, increasing the expression of pyruvate kinase M2 (PKM2). NF- κ B is also involved in this process (Yang et al., 2012a). EGFR also induces ERK2 to phosphorylate PKM2 at Ser 37, which allows peptidylprolyl cis/trans isomerase NIMA-interacting 1 (PIN1) to bind to PKM2, prompting PKM2 to translocate to the nucleus, upregulating lactate dehydrogenase A (LDHA) and glucose transporter 1 (GLUT1) expression and promoting the Warburg effect (Yang et al., 2012b). A previous study indicated that the expression of PKM2 is correlated with the grade of glioma malignancy and that the level of PKM2 is lower in LGGs than in HGGs (Yang et al., 2012a). The heat shock protein (HSP) 90-PKM2-B-cell lymphoma 2 (Bcl2) axis is a potential therapeutic target in GBM treatment. In cancer cells, PKM2 affects ROS levels in two ways (Liang et al., 2017). Firstly, oxidative stress induces PKM2 translocation to the mitochondria

where it phosphorylates Bcl2 at Thr69 site with the help of the chaperone protein HSP90 α 1. This prevents the combination of Cul3-based E3 ligase and Bcl2, thereby maintaining the stability of Bcl2 and increasing the resistance of glioma cells to oxidative stress-induced apoptosis. Researchers have also found that the PKM2 389–405 peptide is an efficacious medicine that disrupts the interaction between PKM2-Bcl2 leading to an antitumor effect that hinders the development of gliomas. Secondly, Cys358 oxidation inhibits PKM2 activity, thereby activating the ROS scavenging system in response to increased ROS levels. Collectively these results indicate that PKM2 could be a potential target for developing effective treatment of GBM. The mechanism underlying PKM2 regulation is shown in Figure 3.

Protein tyrosine phosphatase non-receptor type 2 (PTPN2) was recently identified as a novel cancer target. PTPN2 is oxidized and inactivated by H₂O₂ and the expression levels of PTPN2 are increased in GBM and isocitrate dehydrogenase (IDH) wild-type gliomas. An increase in PTPN2 levels is correlated with a worse overall survival rate (Wang et al., 2018). Furthermore, another study observed this phenomenon, indicating that oxidative stress may be exploited to stimulate PTPN2 inactivation for treating gliomas (Wu et al., 2019).

Prohibitin (PHB) is a highly conserved pleiotropic protein that plays a vital role in multiple biological processes. Peroxiredoxin3 (PRDX3) is a specific peroxidase in the

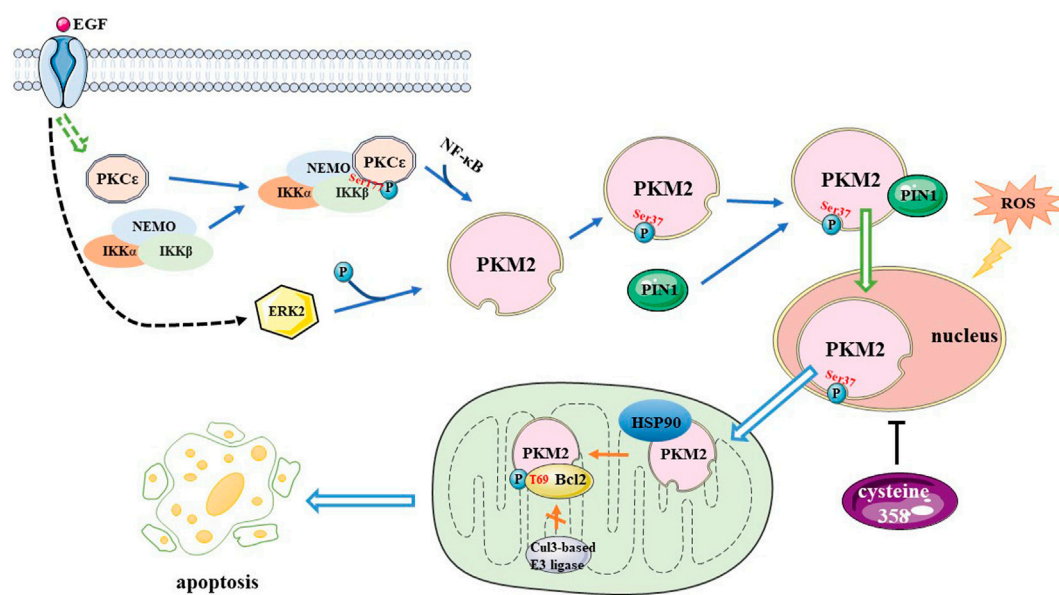


FIGURE 3

A mechanism for PKM2 regulation. EGF induces PKC ϵ generated to phosphorylate IKK β at Ser177, increasing PKM2 expression, and NF- κ B is involved in this process. EGF also activates ERK2, which phosphorylates PKM2 at the Ser37 site, allowing PIN1 to bind to it, it also promotes PKM2 translocate to nucleus. Oxidative stress induces PKM2 translocation to mitochondria and phosphorylates Bcl2 at T69 site with the help of Hsp90, preventing the Cul3-based E3 ligase from binding to Bcl2 and increasing the resistance of glioma cells to oxidative stress-induced apoptosis. Cysteine 358 oxidation inhibits PKM2 activity, activating the reactive oxygen species scavenging system. PKM2, pyruvate kinase M2; EGF, Epidermal growth factor; PKC, protein kinase C; IKK, I κ B kinase; NF- κ B, nuclear factor kappa enhancer binding protein; ERK, extracellular signal-regulated kinase; Bcl2, B-cell lymphoma 2; T, threonine; HSP90, Heat Shock Protein 90; Cul3, cullin 3

mitochondria that scavenge peroxides and protects cells from oxidative stress. PHB binds to and stabilizes PRDX3 to inhibit mitochondrial ROS accumulation and promote GSCs self-renewal. Therefore, knockout of the PHB gene significantly increases ROS levels and inhibits GSCs self-renewal (Huang et al., 2021).

The oncostatin M receptor (OSMR) is a direct signal transducer and activator of the transcription 3 (STAT3) target gene, a member of the IL-6 receptor family, and is involved in many cellular responses, such as differentiation, proliferation, and survival. The depletion of OSMR affects EGFRvIII-STAT3 signaling and significantly retards the proliferation of GBM cells, prolonging their lifespan (Jahani-Asl et al., 2016). A study examined the relationship between ROS and OSMR and found interaction with nicotinamide adenine dinucleotide (NADH) ubiquinone oxidoreductase 1/2 (NDUFS1/2). Deleting OSMR promotes the generation of ROS, sensitizes GBM cells to radiotherapy, and induces glioma cell death (Sharanek et al., 2020). It is possible to identify drugs that inhibit OSMR expression to achieve the goal of treating gliomas.

Paired box 6 (PAX6) is a DNA-binding transcription factor that downregulates the expression of the vascular endothelial growth factor A (VEGFA) gene in glioma cells to suppress tumor

cell invasion. PAX6 expression was found to be significantly reduced in GBM compared to LGGs. It has been shown that GBM cells with lower PAX6 levels survive better in a stressful environment after detachment from the culture. ROS levels increased following cell detachment and the addition of antioxidants enhanced the viability of PAX6-overexpressing cells, however, this did not recover their proliferative capacity (Chang et al., 2007).

A study that utilized proteomic analysis of cells from patients with GBM revealed that the autocrine factor midkine (MDK) promotes cell proliferation and detoxifies ROS. Inhibition of MDK expression may serve as a novel approach for GBM treatment by inducing ROS-mediated apoptosis and cell cycle arrest (Han et al., 2019).

Proteomics suggests that HOXA transcript antisense RNA myeloid-specific 1 (HOTAIRM1) is associated with mitochondrial function, and knockdown of HOTAIRM1 can increase the level of ROS and radiation sensitivity, thereby prolonging patient survival (Ahmadov et al., 2021).

Apurinic/apyrimidinic endonuclease1 (APE1), associated with checkpoint kinase 2 (Chk2), participates in the coordination of double-strand break DNA repair. Ectonucleotide pyrophosphatase/phosphodiesterase 2 (ENPP2) is a secreted protein that possesses lysophospholipase D activity

TABLE 1 Summary of studies on target genes linked to ROS in gliomas.

Target gene	Expression in gliomas	Regulatory pathway	Result	Survival	Study design	References
<i>DGAT1</i>	High	DGAT1/CPT1A/FAs	ROS↓ apoptosis↓	Low	<i>in vivo</i> , <i>in vitro</i>	Cheng et al. (2020)
<i>PKM2</i>	High	HSP90/PKM2/Bcl2	oxidative stress induced apoptosis↓	Low	<i>in vivo</i> , <i>in vitro</i>	Liang et al. (2017)
<i>PTPN2</i>	High	STAT/PTPN2	PTPN2 was inactivated and oxidated by ROS	Low	<i>in vitro</i>	Wu et al. (2019)
<i>OSMR</i>	High	OSMR/NDUFS1/2	mitochondrial respiration↑ ROS↓	Low	<i>in vivo</i> , <i>in vitro</i>	Sharanek et al. (2020)
<i>SIRT6</i>	Low	SIRT6/JAK2/STAT3	cell injury↑ ROS↓ cell growth↓	High	<i>in vitro</i>	Feng et al. (2016)
<i>SIRT6</i>	Low	miR-33a/SIRT6	apoptosis↑	High	<i>in vitro</i>	Chang et al. (2017)
<i>PHB</i>	High	miR-27a/PHB/peroxiredoxin3 (PRDX3)	ROS↓ cell growth↓ Radioresistance↓	Low	<i>in vivo</i> , <i>in vitro</i>	Huang et al. (2021)
<i>PRDM16</i>	High	miR-101/DNMT3A/PRDM16/H3K27me3 H3K4me2	ROS↑ apoptosis↑	Low	<i>in vitro</i>	Lei et al. (2016)
<i>HERPUD1</i>	High	miR-9-3p/Herpud1	H ₂ O ₂ induced apoptosis↓	Low	<i>in vitro</i>	Yang et al. (2017)
<i>ATF4</i>	High	ATF4/xCT/SCL7A11	tumor cell growth↑ xCT transporter activity↑ ferroptosis↓ ROS↓	Low	<i>in vitro</i>	Chen et al. (2017)

and hydrolyzes pyrophosphate bonds and phosphodiesterases from various substrates (Amaral et al., 2021). Oxidative stress elevates the expression levels of APE1 and PKM2 and stimulates the extracellular secretion and intracellular expression of ENPP2 in glioma cells (Cholia et al., 2018). These results revealed that glioma progression is mediated by the regulation of activity, expression levels, and the correlation of these three enzymes. Sirtuin 6 (SIRT6) is a nuclear NAD⁺-dependent histone H3 deacetylase that regulates its genomic expression and stability. An experiment revealed that mir-33a reduced ROS levels by inhibiting SIRT6 expression and decreasing cell survival following H₂O₂ treatment (Chang et al., 2017). SIRT6 suppresses the oxidative stress response while inhibiting Janus kinase 2 (JAK2)/STAT3 signaling pathway activation during glioma treatment (Feng et al., 2016). Recent studies on the target genes that influence oxidative stress in gliomas are summarized in Table 1.

The efficacy of phytocompounds in gliomas

Several studies have emphasized the relationship between oxidative stress and the emergence of drugs. However, many drugs are unable to cross the blood–brain barrier (BBB) to achieve maximum therapeutic efficacy. The BBB is composed of capillary endothelial cells, an intact basement membrane, and glial membranes surrounding astrocyte foot plates and is a barrier between the walls of brain capillaries and plasma to brain cells formed by glial cells. The BBB excludes substances

that are hazardous to the brain, protects the brain from harm, and allows particles smaller than 20 nm in diameter to cross over (Abbott et al., 2010). If a drug is converted into a small molecule, it can pass through the BBB to achieve the purpose of treatment.

Quinoxaline-1,4-dioxide derivatives are a class of synthetic heterocyclic compounds that exhibit diverse biological and pharmacological effects. They can promote cell damage by increasing ROS (Silva et al., 2019). Thymoquinone (TQ) is a drug that can penetrate the BBB and act against gliomas through its antioxidant, antimetastatic, and anti-invasive activities (Racoma et al., 2013). TQ regulates the production of superoxide in mitochondria in a dose-dependent manner and low-dose TQ inhibits superoxide production in mitochondria. ROS generation has been shown to increase with higher TQ concentrations. It has also been confirmed that TQ induces apoptosis in C6 glioma cells *via* redox-dependent MAPK proteins (Krylova et al., 2019). This provides direction for treatment options for gliomas.

Chidamide is a histone deacetylase (HDAC) inhibitor that selectively inhibits the activity of HDAC1, 2, 3, and 10 (Shi et al., 2017). The Hedgehog (Hh) signaling pathway affects glioma growth. This pathway is initiated by a combination of Patched and Hh proteins, consisting of Sonic Hh (Shh), Desert Hh, and Indian Hh (Ihh), which allows Smoothened to transmit signals to the nucleus. A basic study suggested that chidamide inactivates Hh signaling by increasing the level of miR-338-5p, increasing oxidative stress and promoting glioma cell apoptosis and necrosis (Zhou et al., 2020). Chidamide could therefore be used as a potential drug to prevent glioma development.

A review summarized that combining antiparasitic drugs, such as ivermectin, atovaquone, proguanil, quinacrine, and

mefloquine with radiotherapy could potentially enhance the radiosensitivity of HGGs by abolishing tumor hypoxia and enhancing oxidative stress (Mudassar et al., 2020). In conclusion, the combination of radiotherapy and antiparasitic drugs may be a new method for the treatment of malignant HGGs and may improve patient survival.

Quercetin (Qu), a plant-derived flavonoid, is known for its anti-tumor and anti-proliferative activities. Qu has been modified as a chemoprotective and radiosensitive agent that plays an important role in the treatment of GBM, and it has been found to inhibit oxidative stress by scavenging ROS to achieve antitumor effects (Tavana et al., 2020).

One study examined the antitumor effects of eight Cu(II) complexes with uracil-functionalized ligands in glioma cells. These compounds promoted apoptosis and autophagy in glioma cells by affecting the activities of SOD and CAT (Illán-Cabeza et al., 2020). Thus, copper (II) complexes can be used as drugs to manipulate the redox microenvironment to treat gliomas.

Melatonin, a free-radical scavenger, exerts antioxidant effects and protects the BBB under hypoxic conditions. Melatonin has been shown to significantly reduce the invasion and migration of glioma cells by inhibiting the ROS/NF- κ B/MMPs pathway (Wang et al., 2012). This indicates that melatonin has potential therapeutic applications for the treatment of gliomas.

TNF-related apoptosis-inducing ligand (TRAIL), a member of the TNF superfamily, induces apoptosis by binding to receptors that contain death domains. The fungal metabolite chaetocin is a novel TRAIL sensitizer and is an inhibitor of the histone methyltransferase SUV39H1. Chaetocin promotes apoptosis by depleting the expression of heme oxygenase 1 (HMOX1) thereby inducing ROS-dependent apoptosis (Ozy erli-Goknar et al., 2019). The increase in ROS can also affect the apoptosis and metabolism of glioma cells via the JNK-regulated metabolic pathway and ataxia telangiectasia mutated (ATM)-Yes-associated protein 1 (YAP1)-driven apoptotic pathway (Dixit et al., 2014). These results provide a basis for the combination of chaetocin and TRAIL for the treatment of gliomas.

Celastrol is one of the most important active ingredients of the traditional Chinese medicine *Tripterygium wilfordii*, which activates the JNK pathway and ROS production and inhibits the activities of mechanistic targets of rapamycin (mTOR) and Akt kinases, significantly increasing apoptosis and autophagy in glioma cells (Liu et al., 2019).

Osthole is a coumarin derived from traditional Chinese medicine. One study found that osthole is a potential drug for treating gliomas, as it increases the production of ROS and upregulates the expression of induced receptor interacting protein kinase 1 (RIP1), RIP2, and mixed lineage kinase domain-like protein (MLKL). These results confirm that osthole induces mitochondrial depolarization and necroptosis (Huangfu et al., 2021).

Shikonin, a naphthoquinone, has been studied as a preventive or therapeutic drug for the treatment of gliomas.

Shikonin dose-dependently induces ROS overproduction in glioma cells and upregulates RIP1 and RIP3 to mediate necroptosis (Lu et al., 2017).

Small molecule antioxidants containing selenium can ameliorate oxidative damage. Selenocysteine (SeC), a naturally available selenoamino acid that potentiates the production of ROS and superoxide anions, induces DNA damage, causes S-phase cell cycle arrest, and inhibits the growth of glioma cells (Wang et al., 2016).

An experiment revealed that polyphyllin VI (PPVI), a bioactive ingredient extracted from the traditional Chinese medicine *Paris polyphylla*, increases ROS accumulation, which in turn activates ROS-regulated JNK and p38 pathways and regulates the G2/M phase to inhibit glioma cell proliferation (Liu et al., 2020). Thus, PPVI might be a potential therapeutic agent for gliomas.

Deoxypodophyllotoxin (DPT), isolated from herbal plants, is used as a precursor for teniposide and etoposide phosphate. Overproduction of DPT triggers ROS-induced upregulation of PARP-1, which promotes apoptosis-inducing factor (AIF) translocation into the nucleus, causing parthanatos in glioma cells (Ma et al., 2016). This study provides novel insights for the development of an anti-glioma strategy.

Cannabidiol (CBD) is a non-psychoactive, natural ingredient extracted from cannabis. CBD has proapoptotic and antiproliferative effects and serves an anti-glioma purpose by increasing the production of ROS and the activity of GSH-associated enzymes, as well as depleting glutathione (Massi et al., 2006). Another study found a similar view that CBD induces a substantial increase in ROS, thereby inhibiting GSCs survival and self-renewal (Singer et al., 2015).

Proteomic analysis of cells following treatment with loperamide and pimozide revealed that these drugs can induce endoplasmic reticulum stress, leading to increased ROS levels and promoting cell death (Meyer et al., 2021).

Silibinin is a polyphenolic extract of *Silybum marianum*. Silibinin suppresses glycolysis in tumor cells, thereby activating autophagy. Autophagy increases H₂O₂ levels by promoting p53-mediated GSH depletion and inducing Bcl2 interacting protein 3 (BNIP3) upregulation, mitochondrial damage, and AIF translocation from the mitochondria to the nucleus, resulting in glioma cell death (Wang et al., 2020). Therapeutic agents that regulate ROS levels to provide new ideas for glioma treatment are summarized in Table 2. And the effect and pathway of these therapeutic agents pertinent to ROS are shown in Figure 4.

Effect of radiotherapy and chemotherapy on oxidative stress in gliomas

Radiotherapy and chemotherapy, as standard treatment strategies, have been rapidly developed and are widely used in

TABLE 2 Summary of studies on medicines linked to ROS in gliomas.

Medicine	Type	Study design	Cell	Pathway	Result	Reference
Thymoquinone	Chemotherapeutic agent	<i>in vitro</i>	C6	PI3K/AKT	Proliferation↓ ROS↑ Apoptosis↑	Krylova et al. (2019)
Chidamide	HDAC inhibitor	<i>in vitro</i>	U87; HS683	miR-338-5p/ Hedgehog	ROS↑ Proliferation↓ Migration↓ Invasion↓	Zhou et al. (2020)
Atovaquone	Anti-malarial drug	<i>in vivo</i> , <i>in vitro</i>	U87-MG; LN-18, SF-188; SJ-GBM2	STAT3	ROS↑ Apoptosis↑	Takabe et al. (2018)
Ivermectin	Anthelmintic drug	<i>in vitro</i>	U87; T98G	Akt/mTOR	Angiogenesis↓ Cell growth↓ ROS↑	Liu et al. (2016)
Chloroquine	Anti-malarial drug	<i>in vitro</i>	U87; LN308; U118; U251; LN229	P53	ROS↑ Autophagic vacuoles accumulation	Geng et al. (2010)
Quinacrine	Antiprotozoal agent	<i>in vivo</i> , <i>in vitro</i>	C6; GSCs	Ras/MAPK	Survival period↑ ROS↑	Wang et al. (2017)
Quercetin	Flavonoid	<i>in vitro</i>	C6	-	oxidative stress↓	Ersoz et al. (2020)
Melatonin	Indolamine	<i>in vitro</i>	T98G; U251	NF-κB/MMPs	ROS↓ migration↓ invasion↓	Wang et al. (2012)
Chaetocin	Fungal metabolite	<i>in vitro</i> , <i>in vivo</i>	U87MG; U373; T98G	HMOX1/TRAIL;P53	ROS↑ apoptosis↑	Ozy erli-Goknar et al. (2019)
Celastrol	Triterpene compound	<i>in vitro</i> , <i>in vivo</i>	U251; U87- MG; C6	ROS/JNK Akt/mTOR	G2/M phase arrest; ROS, apoptosis and autophagy↑	Liu et al. (2019)
Osthole	Coumarin derivative	<i>in vitro</i>	U87; C6	RIP1/RIP3/MLKL	ROS↑ necroptosis↑	Huangfu et al. (2021)
Shikonin	Naphthoquinone	<i>in vitro</i>	C6; SHG-44; U87; U251	RIP1/RIP3	ROS↑ necroptosis↑	Lu et al. (2017)
Selenocysteine	Selenoamino acid	<i>in vitro</i>	U251; U87	MAPK/Akt	ROS↑ DNA damage↑	Wang et al. (2016)
Polyphyllin VI	Component derived from Chinese herb Paris polyphylla	<i>in vivo</i> , <i>in vitro</i>	U251; U343; LN229; U87; HEB	JNK/P38	ROS↑ autophagy↑ apoptosis↑ cell cycle arrest	Liu et al. (2020)
Chaetocin	A histone methyltransferase inhibitor	<i>in vivo</i> , <i>in vitro</i>	A172; T98G; U87-MG	ATM/YAP1; JNK	ROS↑ apoptosis↑	Dixit et al. (2014)
Deoxypodophyllotoxin	Major lignan of plant Anthriscus sylvestris phosphate	<i>in vivo</i> , <i>in vitro</i>	C6; SHG-44; U87	PARP1	ROS↑ cell death↑	Ma et al. (2016)
Cannabidiol	A non-toxic, non-psychoactive cannabinoid	<i>in vivo</i> , <i>in vitro</i>	U251; GSC lines 387 and 3832	p-p38	ROS↑ GSC survival↓ self-renewal↓ invasion↓	Singer et al. (2015)
Silibinin	A polyphenolic extract from silybum marianum	<i>in vivo</i> , <i>in vitro</i>	U87; U251; SHG- 44; C6	Glycolysis; P53	GSH↓; H ₂ O ₂ ↑; BNIP3↑	Wang et al. (2020)
Dichloroacetate	Glycolytic inhibitor	<i>in vivo</i> , <i>in vitro</i>	GL261; U-87 MG; U-251 MG; T98G	Glucose and FAO metabolic pathways	ROS↑ autophagy↑ DNA damage↑ apoptosis↑	McKelvey et al. (2021)
Ranolazine	Partial fatty acid oxidation inhibitor	<i>in vivo</i> , <i>in vitro</i>	U87MG/ EGFRVIII; U87-MG	PTEN/ NQO1 GSTP1/ PI3K/Akt	Oxidative stress↑ apoptosis↑	Lei et al. (2020)

clinics to eliminate gliomas. However, resistance to radiation and chemotherapeutic drugs is a fundamental obstacle to improving the curative effect of gliomas. Therefore, the design and development of novel chemoradiotherapy strategies to overcome resistance have become a focus of clinical oncology research. Gliomas need to use radiotherapeutic or chemotherapeutic drugs to influence the prognosis through ROS modulation. A study demonstrated that combined treatment with radiation and salinomycin (SAL) increased

DNA damage and tumor apoptosis by increasing ROS production, which is a novel strategy to improve the efficacy of radiotherapy in cancer prevention and overcome radioresistance (Liu et al., 2018). The radioresistance of human glioma cells induced by SOD1 overexpression is related to the inhibition of late ROS accumulation and enhancement of G2/M accumulation (Gao et al., 2008). Another study revealed that adenosine triphosphate (ATP) channels can control glioma radioresistance by adjusting ROS-

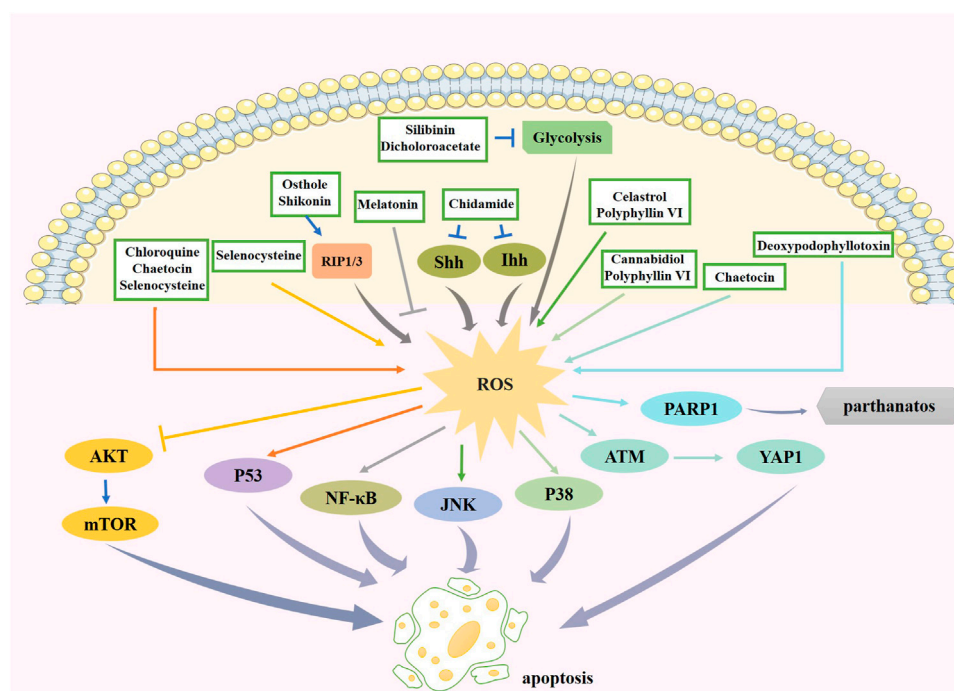


FIGURE 4

The effect and pathway of available therapeutic agents in glioma pertinent to ROS. Chidamide increases ROS production through the Hh signaling pathway. Melatonin promotes apoptosis by suppressing ROS production, leading to the reduction of its downstream factor NF- κ B. Chaetocin promotes ROS production and can promote apoptosis through the p53 pathway or the ATM/YAP1 pathway. Celastrol and polyphyllin VI promote ROS generation to induce apoptosis via JNK pathway. Osthole and shikonin increase ROS by promoting RIP1/3 expression. Increased ROS expression by selenocysteine inhibited Akt pathway on one hand and activated p53 pathway on the other hand to promote cell apoptosis. Increased ROS expression by polyphyllin VI and cannabidiol activates p38 pathway to induce apoptosis. Deoxypodophyllotoxin increases the expression of ROS and thus PARP1 expression, causing parthanatos. Silibinin and dichloroacetate can have inhibition of glycolysis and increase ROS expression. ROS, reactive oxygen species; NF- κ B, nuclear factor kappa enhancer binding protein; JNK, c-Jun N-terminal kinase; RIP1/3, receptor interacting protein kinase 1/3; ATM, ataxia telangiectasia mutated; YAP1, Yes-associated protein 1; PARP-1, poly ADP-ribose polymerase-1.

induced ERK activation; thus, inhibiting ATP channels is a potential target for glioma therapeutic development (Huang et al., 2015). One way to increase radiosensitivity is to increase intracellular ROS by 5-aminolevulinic acid treatment, which results in the radiosensitization of glioma cells (Kitagawa et al., 2015). The transcriptional activity of the HIF-1 signal induced by ROS in cyclic hypoxia was higher than that in intermittent hypoxia. Under hypoxic conditions, knockout of the HIF-1 gene inhibits uninterrupted hypoxia-induced radioresistance while increasing the overall radiosensitivity of the tumor (Hsieh et al., 2010). Outer-membrane vesicles (OMVs) from *Escherichia coli* and gold nanoparticles (AuNPs) were combined to synthesize Au-OMVs. Combining Au-OMVs with radiotherapy generated ROS to increase radiosensitization and suppress glioma cell growth (Chen et al., 2021). Proton beam radiation generates substantial amounts of ROS, which induces cell cycle redistribution and DNA damage and promotes apoptosis in GSCs (Alan Mitteer et al., 2015). The main adverse effect is a radiation-induced skin reaction, with its mechanisms including inflammation and

oxidative stress, which interact and promote each other. Direct exposure of normal cells to radiation or ROS may lead to apoptosis and necrosis, which triggers the release of anti-inflammatory cytokines (Wei et al., 2019).

During chemotherapy, when O⁶-methylguanine methyltransferase, alkylpurine-DNA-N-glycosylase, and base excision repair proteins are expressed, GBM cells are resistant to TMZ (Lee, 2016). Drug efflux transporters, the advent of GSCs, and the upregulation of autophagy are also mechanisms of TMZ resistance (Tomar et al., 2021). The curcumin analog ALZ003 increased the production of ROS and ubiquitinated the androgen receptor resulting in its degradation, which potentiated TMZ resistance. This result provides evidence to improve the efficacy in glioma patients resistant to TMZ (Chen et al., 2020). Gemcitabine combined with nanomaterials, such as AgNTs, participates in ROS-dependent mitochondrial pathway-mediated apoptosis, thereby inhibiting the activity of gliomas, indicating that AgNTs and chemotherapeutics have a synergistic effect (Yang et al., 2020). Dimethylaminomichelolide is a novel chemotherapeutic agent that induces apoptosis and autophagy by

adjusting the ROS/MAPK signaling pathway and inhibiting the Akt/mTOR signaling pathway to treat gliomas (Wang et al., 2019).

Conclusion

Gliomas are highly malignant and prone to recurrence and progression. Although a certain degree of therapeutic effect can be achieved by applying standard treatment methods, the prognosis remains unsatisfactory. Oxidative stress has an important role in the occurrence and development of glioma, as well as in treatment. Therefore, antioxidative therapy can be considered a new therapeutic strategy for the treatment of gliomas. By summarizing the components of ROS, the role of oxidative stress in gliomas pathogenesis, the effects of oxidative stress on targets such as Nrf2, NOX2, NOX4, DGAT1, PKM2, PTPN2, PHB, OSMR, and PAX6 are presented in this paper, and some phytochemicals shown to alter glioma cell growth by affecting oxidative stress are discussed. Moreover, we suggest potential targets and drugs that modify radiosensitivity and chemoresistance by affecting oxidative stress, all of which provide new directions for our enriched treatment regimens for gliomas. However, extensive basic experimental and clinical trial research are still needed to explore the selection of intervention time and dosage of drugs. In addition, the efficacy of combining antioxidant treatment with other treatments also deserves to explore.

Author contributions

Conceptualization, YX and XJ; methodology, SL; software, SL; validation, LD, YX, and XJ; formal analysis, WS and ZZ; investigation, ZL; data curation, SL; writing-original draft preparation, SL; writing-review and editing, LM, YX, and

XJ; visualization, XJ; supervision, XJ; project administration, XJ; funding acquisition, XJ. All authors have read and agreed to the published version of the manuscript.

Funding

This research was funded by the Jilin Provincial Science and Technology Foundation (Grant number: 20190201200JC).

Acknowledgments

We would like to thank Editage (www.editage.cn) for the English language editing. Figures 1, 2, 3, and 4 were modified from Servier Medical Art (<http://smart.servier.com/>), licensed under Creative Commons Attribution 3.0 Generic License (<https://creativecommons.org/licenses/by/3.0/>).

Conflict of interest

The authors declare that the research was conducted in the absence of any commercial or financial relationships that could be construed as a potential conflict of interest.

Publisher's note

All claims expressed in this article are solely those of the authors and do not necessarily represent those of their affiliated organizations, or those of the publisher, the editors and the reviewers. Any product that may be evaluated in this article, or claim that may be made by its manufacturer, is not guaranteed or endorsed by the publisher.

References

- Abbott, N. J., Patabendige, A. A., Dolman, D. E., Yusof, S. R., and Begley, D. J. (2010). Structure and function of the blood-brain barrier. *Neurobiol. Dis.* 37, 13–25. doi:10.1016/j.nbd.2009.07.030
- Ahmadov, U., Picard, D., Bartl, J., Silgner, M., Trajkovic-Arsic, M., Qin, N., et al. (2021). The long non-coding RNA HOTAIRM1 promotes tumor aggressiveness and radiotherapy resistance in glioblastoma. *Cell Death Dis.* 12, 885. doi:10.1038/s41419-021-04146-0
- Alan Mitteer, R., Wang, Y., Shah, J., Gordon, S., Fager, M., Butter, P. P., et al. (2015). Proton beam radiation induces DNA damage and cell apoptosis in glioma stem cells through reactive oxygen species. *Sci. Rep.* 5, 13961. doi:10.1038/srep13961
- Amaral, R. F., Geraldo, L. H. M., Einicker-Lamas, M., Tcls, E. S., Mendes, F., Lima, F. R. S., et al. (2021). Microglial lysophosphatidic acid promotes glioblastoma proliferation and migration via LPA(1) receptor. *J. Neurochem.* 156, 499–512. doi:10.1111/jnc.15097
- Ames, B. N. (1983). Dietary carcinogens and anticarcinogens. Oxygen radicals and degenerative diseases. *Science* 221, 1256–1264. doi:10.1126/science.6351251
- Aruoma, O. I., Grootveld, M., and Bahorun, T. (2006). Free radicals in biology and medicine: From inflammation to biotechnology. *Biofactors* 27, 1–3. doi:10.1002/biof.5520270101
- Baird, L., and Yamamoto, M. (2020). The molecular mechanisms regulating the KEAP1-NRF2 pathway. *Mol. Cell. Biol.* 40, e00099–20. doi:10.1128/MCB.00099-20
- Barciszewska, A. M., Giel-Pietraszuk, M., Perrigue, P. M., and Naskręć-Barciszewska, M. (2019). Total DNA methylation changes reflect random oxidative DNA damage in gliomas. *Cells* 8, E1065. doi:10.3390/cells8091065
- Behrend, L., Henderson, G., and Zwacka, R. M. (2003). Reactive oxygen species in oncogenic transformation. *Biochem. Soc. Trans.* 31, 1441–1444. doi:10.1042/bst0311441
- Betteridge, D. J. (2000). What is oxidative stress? *Metabolism* 49, 3–8. doi:10.1016/s0026-0495(00)80077-3
- Brown, D. I., and Griendling, K. K. (2009). Nox proteins in signal transduction. *Free Radic. Biol. Med.* 47, 1239–1253. doi:10.1016/j.freeradbiomed.2009.07.023

- Burtenshaw, D., Kitching, M., Redmond, E. M., Megson, I. L., and Cahill, P. A. (2019). Reactive oxygen species (ROS), intimal thickening, and subclinical atherosclerotic disease. *Front. Cardiovasc. Med.* 6, 89. doi:10.3389/fcvm.2019.00089
- Chang, J. Y., Hu, Y., Siegel, E., Stanley, L., and Zhou, Y. H. (2007). PAX6 increases glioma cell susceptibility to detachment and oxidative stress. *J. Neurooncol.* 84, 9–19. doi:10.1007/s11060-007-9347-x
- Chang, M., Qiao, L., Li, B., Wang, J., Zhang, G., Shi, W., et al. (2017). Suppression of SIRT6 by miR-33a facilitates tumor growth of glioma through apoptosis and oxidative stress resistance. *Oncol. Rep.* 38, 1251–1258. doi:10.3892/or.2017.5780
- Chen, D., Fan, Z., Rauh, M., Buchfelder, M., Eyupoglu, I. Y., Savaskan, N., et al. (2017). ATF4 promotes angiogenesis and neuronal cell death and confers ferroptosis in a xCT-dependent manner. *Oncogene* 36, 5593–5608. doi:10.1038/onc.2017.146
- Chen, M. H., Liu, T. Y., Chen, Y. C., and Chen, M. H. (2021). Combining augmented radiotherapy and immunotherapy through a nano-gold and bacterial outer-membrane vesicle complex for the treatment of glioblastoma. *Nanomater. (Basel)* 11, 1661. doi:10.3390/nano11071661
- Chen, T. C., Chuang, J. Y., Ko, C. Y., Kao, T. J., Yang, P. Y., Yu, C. H., et al. (2020). AR ubiquitination induced by the curcumin analog suppresses growth of temozolomide-resistant glioblastoma through disrupting GPX4-Mediated redox homeostasis. *Redox Biol.* 30, 101413. doi:10.1016/j.redox.2019.101413
- Chen, Z., and Hambardzumyan, D. (2018). Immune microenvironment in glioblastoma subtypes. *Front. Immunol.* 9, 1004. doi:10.3389/fimmu.2018.01004
- Cheng, X., Geng, F., Pan, M., Wu, X., Zhong, Y., Wang, C., et al. (2020). Targeting DGAT1 ameliorates glioblastoma by increasing fat catabolism and oxidative stress. *Cell Metab.* 32, 229–242. e8. doi:10.1016/j.cmet.2020.06.002
- Cholia, R. P., Dhiman, M., Kumar, R., and Mantha, A. K. (2018). Oxidative stress stimulates invasive potential in rat C6 and human U-87 MG glioblastoma cells via activation and cross-talk between PKM2, ENPP2 and APE1 enzymes. *Metab. Brain Dis.* 33, 1307–1326. doi:10.1007/s11011-018-0233-3
- De Duve, C., and Baudhuin, P. (1966). Peroxisomes (microbodies and related particles). *Physiol. Rev.* 46, 323–357. doi:10.1152/physrev.1966.46.2.323
- Deryugina, E. I., Bourdon, M. A., Luo, G. X., Reisfeld, R. A., and Strongin, A. (1997). Matrix metalloproteinase-2 activation modulates glioma cell migration. *J. Cell Sci.* 110 (Pt 19), 2473–2482. doi:10.1242/jcs.110.19.2473
- Dixit, D., Ghildiyal, R., Anto, N. P., and Sen, E. (2014). Chaetocin-induced ROS-mediated apoptosis involves ATM-YAP1 axis and JNK-dependent inhibition of glucose metabolism. *Cell Death Dis.* 5, e1212. doi:10.1038/cddis.2014.179
- Ersöz, M., Erdemir, A., Derman, S., Arasoglu, T., and Mansuroglu, B. (2020). Quercetin-loaded nanoparticles enhance cytotoxicity and antioxidant activity on C6 glioma cells. *Pharm. Dev. Technol.* 25, 757–766. doi:10.1080/10837450.2020.1740933
- Feng, J., Yan, P. F., Zhao, H. Y., Zhang, F. C., Zhao, W. H., Feng, M., et al. (2016). SIRT6 suppresses glioma cell growth via induction of apoptosis, inhibition of oxidative stress and suppression of JAK2/STAT3 signaling pathway activation. *Oncol. Rep.* 35, 1395–1402. doi:10.3892/or.2015.4477
- Fleming, A. M., and Burrows, C. J. (2017). 8-Oxo-7, 8-dihydroguanine, friend and foe: Epigenetic-like regulator versus initiator of mutagenesis. *DNA Repair (Amst)* 56, 75–83. doi:10.1016/j.dnarep.2017.06.009
- Flint, D. H., Emptage, M. H., Finnegan, M. G., Fu, W., and Johnson, M. K. (1993). The role and properties of the iron-sulfur cluster in *Escherichia coli* dihydroxy-acid dehydratase. *J. Biol. Chem.* 268, 14732–14742. doi:10.1016/s0021-9258(18)82394-8
- Fridovich, I. (1997). Superoxide anion radical (O₂⁻), superoxide dismutases, and related matters. *J. Biol. Chem.* 272, 18515–18517. doi:10.1074/jbc.272.30.18515
- Gao, Z., Sarsour, E. H., Kalen, A. L., Li, L., Kumar, M. G., Goswami, P. C., et al. (2008). Late ROS accumulation and radiosensitivity in SOD1-overexpressing human glioma cells. *Free Radic. Biol. Med.* 45, 1501–1509. doi:10.1016/j.freeradbiomed.2008.08.009
- Geng, Y., Kohli, L., Klocke, B. J., and Roth, K. A. (2010). Chloroquine-induced autophagic vacuole accumulation and cell death in glioma cells is p53 independent. *Neuro. Oncol.* 12, 473–481. doi:10.1093/neuonc/nop048
- Gerschman, R., Gilbert, D. L., Nye, S. W., Dwyer, P., and Fenn, W. O. (1954). Oxygen poisoning and x-irradiation: A mechanism in common. *Science* 119, 623–626. doi:10.1126/science.119.3097.623
- Gorrini, C., Harris, I. S., and Mak, T. W. (2013). Modulation of oxidative stress as an anticancer strategy. *Nat. Rev. Drug Discov.* 12, 931–947. doi:10.1038/nrd4002
- Grabowski, M. M., Sankey, E. W., Ryan, K. J., Chongsathidkiet, P., Lorrey, S. J., Wilkinson, D. S., et al. (2021). Immune suppression in gliomas. *J. Neurooncol.* 151, 3–12. doi:10.1007/s11060-020-03483-y
- Halliwell, B., and Gutteridge, J. M. (1992). Biologically relevant metal ion-dependent hydroxyl radical generation. An update. *FEBS Lett.* 307, 108–112. doi:10.1016/0014-5793(92)80911-y
- Ham, S. W., Jeon, H. Y., Jin, X., Kim, E. J., Kim, J. K., Shin, Y. J., et al. (2019). TP53 gain-of-function mutation promotes inflammation in glioblastoma. *Cell Death Differ.* 26, 409–425. doi:10.1038/s41418-018-0126-3
- Han, S., Shin, H., Lee, J. K., Liu, Z., Rabadan, R., Lee, J., et al. (2019). Secretome analysis of patient-derived GBM tumor spheres identifies midkine as a potent therapeutic target. *Exp. Mol. Med.* 51, 1–11. doi:10.1038/s12276-019-0351-y
- Hayashi, S., Takamiya, R., Yamaguchi, T., Matsumoto, K., Tojo, S. J., Tamatani, T., et al. (1999). Induction of heme oxygenase-1 suppresses venular leukocyte adhesion elicited by oxidative stress: Role of bilirubin generated by the enzyme. *Circ. Res.* 85, 663–671. doi:10.1161/01.res.85.8.663
- Hoelzinger, D. B., Demuth, T., and Berens, M. E. (2007). Autocrine factors that sustain glioma invasion and paracrine biology in the brain microenvironment. *J. Natl. Cancer Inst.* 99, 1583–1593. doi:10.1093/jnci/djm187
- Hsieh, C. H., Lee, C. H., Liang, J. A., Yu, C. Y., and Shyu, W. C. (2010). Cycling hypoxia increases U87 glioma cell radioresistance via ROS induced higher and long-term HIF-1 signal transduction activity. *Oncol. Rep.* 24, 1629–1636. doi:10.3892/or_00001027
- Hsieh, C. H., Shyu, W. C., Chiang, C. Y., Kuo, J. W., Shen, W. C., Liu, R. S., et al. (2011). NADPH oxidase subunit 4-mediated reactive oxygen species contribute to cycling hypoxia-promoted tumor progression in glioblastoma multiforme. *PLoS One* 6, e23945. doi:10.1371/journal.pone.0023945
- Huang, H., Zhang, S., Li, Y., Liu, Z., Mi, L., Cai, Y., et al. (2021). Suppression of mitochondrial ROS by prohibitin drives glioblastoma progression and therapeutic resistance. *Nat. Commun.* 12, 3720. doi:10.1038/s41467-021-24108-6
- Huang, L., Li, B., Tang, S., Guo, H., Li, W., Huang, X., et al. (2015). Mitochondrial KATP channels control glioma radioresistance by regulating ROS-induced ERK activation. *Mol. Neurobiol.* 52, 626–637. doi:10.1007/s12035-014-8888-1
- Huangfu, M., Wei, R., Wang, J., Qin, J., Yu, D., Guan, X., et al. (2021). Osthole induces necroptosis via ROS overproduction in glioma cells. *FEBS Open Bio* 11, 456–467. doi:10.1002/2211-5463.13069
- Iida, T., Furuta, A., Kawashima, M., Nishida, J., Nakabeppu, Y., and Iwaki, T. (2001). Accumulation of 8-oxo-2'-deoxyguanosine and increased expression of hMTH1 protein in brain tumors. *Neuro. Oncol.* 3, 73–81. doi:10.1093/neuonc/3.2.73
- Illán-Cabeza, N. A., Jiménez-Pulido, S. B., Hueso-Ureña, F., Ramírez-Expósito, M. J., Martínez-Martos, J. M., Moreno-Carretero, M. N., et al. (2020). Relationship between the antiproliferative properties of Cu(II) complexes with the Schiff base derived from pyridine-2-carboxaldehyde and 5, 6-diamino-1, 3-dimethyluracil and the redox status mediated by antioxidant defense systems on glioma tumoral cells. *J. Inorg. Biochem.* 207, 111053. doi:10.1016/j.jinorgbio.2020.111053
- Jahani-Asl, A., Yin, H., Soleimani, V. D., Haque, T., Luchman, H. A., Chang, N. C., et al. (2016). Control of glioblastoma tumorigenesis by feed-forward cytokine signaling. *Nat. Neurosci.* 19, 798–806. doi:10.1038/nn.4295
- Jha, P., Pia Patric, I. R., Shukla, S., Pathak, P., Pal, J., Sharma, V., et al. (2014). Genome-wide methylation profiling identifies an essential role of reactive oxygen species in pediatric glioblastoma multiforme and validates a methylome specific for H3 histone family 3A with absence of G-CIMP/isocitrate dehydrogenase 1 mutation. *Neuro. Oncol.* 16, 1607–1617. doi:10.1093/neuonc/nou113
- Kanzaki, H., Shinohara, F., Kajiya, M., and Kodama, T. (2013). The Keap1/Nrf2 protein axis plays a role in osteoclast differentiation by regulating intracellular reactive oxygen species signaling. *J. Biol. Chem.* 288, 23009–23020. doi:10.1074/jbc.M113.478545
- Kensler, T. W., Wakabayashi, N., and Biswal, S. (2007). Cell survival responses to environmental stresses via the Keap1-Nrf2-Are pathway. *Annu. Rev. Pharmacol. Toxicol.* 47, 89–116. doi:10.1146/annurev.pharmtox.46.120604.141046
- Kitagawa, T., Yamamoto, J., Tanaka, T., Nakano, Y., Akiba, D., Ueta, K., et al. (2015). 5-Aminolevulinic acid strongly enhances delayed intracellular production of reactive oxygen species (ROS) generated by ionizing irradiation: Quantitative analyses and visualization of intracellular ROS production in glioma cells *in vitro*. *Oncol. Rep.* 33, 583–590. doi:10.3892/or.2014.3618
- Krylova, N. G., Drobysh, M. S., Semenova, G. N., Kulahava, T. A., Pinchuk, S. V., Shadyro, O. I., et al. (2019). Cytotoxic and antiproliferative effects of thymoquinone on rat C6 glioma cells depend on oxidative stress. *Mol. Cell. Biochem.* 462, 195–206. doi:10.1007/s11010-019-03622-8
- Lee, S. Y. (2016). Temozolomide resistance in glioblastoma multiforme. *Genes Dis.* 3, 198–210. doi:10.1016/j.gendis.2016.04.007
- Lei, K., Gu, X., Alvarado, A. G., Du, Y., Luo, S., Ahn, E. H., et al. (2020). Discovery of a dual inhibitor of NQO1 and GSTP1 for treating glioblastoma. *J. Hematol. Oncol.* 13, 141. doi:10.1186/s13045-020-00979-y

- Lei, Q., Liu, X., Fu, H., Sun, Y., Wang, L., Xu, G., et al. (2016). miR-101 reverses hypomethylation of the PRDM16 promoter to disrupt mitochondrial function in astrocytoma cells. *Oncotarget* 7, 5007–5022. doi:10.18632/oncotarget.6652
- Li, S. Z., Hu, Y. Y., Zhao, J., Zhao, Y. B., Sun, J. D., Yang, Y. F., et al. (2014). MicroRNA-34a induces apoptosis in the human glioma cell line, A172, through enhanced ROS production and NOX2 expression. *Biochem. Biophys. Res. Commun.* 444, 6–12. doi:10.1016/j.bbrc.2013.12.136
- Liang, J., Cao, R., Wang, X., Zhang, Y., Wang, P., Gao, H., et al. (2017). Mitochondrial PKM2 regulates oxidative stress-induced apoptosis by stabilizing Bcl2. *Cell Res.* 27, 329–351. doi:10.1038/cr.2016.159
- Liochev, S. I., and Fridovich, I. (1994). The role of O₂⁻ in the production of HO₂: *In vitro* and *in vivo*. *Free Radic. Biol. Med.* 16, 29–33. doi:10.1016/0891-5849(94)90239-9
- Liu, C., Wang, L., Qiu, H., Dong, Q., Feng, Y., Li, D., et al. (2018). Combined strategy of radioactive (¹²⁵I) seeds and salinomycin for enhanced glioma chemoradiotherapy: Evidences for ROS-mediated apoptosis and signaling crosstalk. *Neurochem. Res.* 43, 1317–1327. doi:10.1007/s11064-018-2547-2
- Liu, S., Zhao, Q., Shi, W., Zheng, Z., Liu, Z., Meng, L., et al. (2021). Advances in radiotherapy and comprehensive treatment of high-grade glioma: Immunotherapy and tumor-treating fields. *J. Cancer* 12, 1094–1104. doi:10.7150/jca.51107
- Liu, W., Chai, Y., Hu, L., Wang, J., Pan, X., Yuan, H., et al. (2020). Polyphyllin VI induces apoptosis and autophagy via reactive oxygen species mediated JNK and P38 activation in glioma. *Onco. Targets. Ther.* 13, 2275–2288. doi:10.2147/OTT.S243953
- Liu, X. R., Li, Y. Q., Hua, C., Li, S. J., Zhao, G., Song, H. M., et al. (2015). Oxidative stress inhibits growth and induces apoptotic cell death in human U251 glioma cells via the caspase-3-dependent pathway. *Eur. Rev. Med. Pharmacol. Sci.* 19, 4068–4075.
- Liu, X., Zhao, P., Wang, X., Wang, L., Zhu, Y., Song, Y., et al. (2019). Celastrol mediates autophagy and apoptosis via the ROS/JNK and Akt/mTOR signaling pathways in glioma cells. *J. Exp. Clin. Cancer Res.* 38, 184. doi:10.1186/s13046-019-1173-4
- Liu, Y., Fang, S., Sun, Q., and Liu, B. (2016). Anthelmintic drug ivermectin inhibits angiogenesis, growth and survival of glioblastoma through inducing mitochondrial dysfunction and oxidative stress. *Biochem. Biophys. Res. Commun.* 480, 415–421. doi:10.1016/j.bbrc.2016.10.064
- Louis, D. N., Perry, A., Reifenberger, G., von Deimling, A., Figarella-Branger, D., Cavenee, W. K., et al. (2016). The 2016 world Health organization classification of tumors of the central nervous system: A summary. *Acta Neuropathol.* 131, 803–820. doi:10.1007/s00401-016-1545-1
- Louis, D. N., Perry, A., Wesseling, P., Brat, D. J., Cree, I. A., Figarella-Branger, D., et al. The 2021 WHO classification of tumors of the central nervous system: A summary. *Neuro. Oncol.* 23 (2021), 1231–1251. doi:10.1093/neuonc/noab106
- Lu, B., Gong, X., Wang, Z. Q., Ding, Y., Wang, C., Luo, T. F., et al. (2017). Shikonin induces glioma cell necroptosis *in vitro* by ROS overproduction and promoting RIP1/RIP3 necrosome formation. *Acta Pharmacol. Sin.* 38, 1543–1553. doi:10.1038/aps.2017.112
- Ma, D., Lu, B., Feng, C., Wang, C., Wang, Y., Luo, T., et al. (2016). Deoxy podophyllotoxin triggers parthanatos in glioma cells via induction of excessive ROS. *Cancer Lett.* 371, 194–204. doi:10.1016/j.canlet.2015.11.044
- Massi, P., Vaccani, A., Bianchessi, S., Costa, B., Macchi, P., and Parolaro, D. (2006). The non-psychoactive cannabidiol triggers caspase activation and oxidative stress in human glioma cells. *Cell. Mol. Life Sci.* 63, 2057–2066. doi:10.1007/s00018-006-6156-x
- McCord, J. M., and Fridovich, I. (1969). Superoxide dismutase. *J. Biol. Chem.* 244, 6049–6055. doi:10.1016/s0021-9258(18)63504-5
- McKelvey, K. J., Wilson, E. B., Short, S., Melcher, A. A., Biggs, M., Diakos, C. I., et al. (2021). Glycolysis and fatty acid oxidation inhibition improves survival in glioblastoma. *Front. Oncol.* 11, 633210. doi:10.3389/fonc.2021.633210
- Meyer, N., Henkel, L., Linder, B., Zielke, S., Tascher, G., Trautmann, S., et al. (2021). Autophagy activation, lipotoxicity and lysosomal membrane permeabilization synergize to promote pimozone- and loperamide-induced glioma cell death. *Autophagy* 17, 3424–3443. doi:10.1080/15548627.2021.1874208
- Milkovic, L., Siems, W., Siems, R., and Zarkovic, N. (2014). Oxidative stress and antioxidants in carcinogenesis and integrative therapy of cancer. *Curr. Pharm. Des.* 20, 6529–6542. doi:10.2174/1381612820666140826152822
- Mittal, M., Siddiqui, M. R., Tran, K., Reddy, S. P., and Malik, A. B. (2014). Reactive oxygen species in inflammation and tissue injury. *Antioxid. Redox Signal.* 20, 1126–1167. doi:10.1089/ars.2012.5149
- Mudassar, F., Shen, H., O'Neill, G., and Hau, E. (2020). Targeting tumor hypoxia and mitochondrial metabolism with anti-parasitic drugs to improve radiation response in high-grade gliomas. *J. Exp. Clin. Cancer Res.* 39, 208. doi:10.1186/s13046-020-01724-6
- Nomura, J., Busso, N., Ives, A., Tsujimoto, S., Tamura, M., So, A., et al. (2013). Febuxostat, an inhibitor of xanthine oxidase, suppresses lipopolysaccharide-induced MCP-1 production via MAPK phosphatase-1-mediated inactivation of JNK. *PLoS One* 8, e75527. doi:10.1371/journal.pone.0075527
- Nosaka, Y., and Nosaka, A. Y. (2017). Generation and detection of reactive oxygen species in photocatalysis. *Chem. Rev.* 117, 11302–11336. doi:10.1021/acs.chemrev.7b00161
- Omuro, A., and DeAngelis, L. M. (2013). Glioblastoma and other malignant gliomas: A clinical review. *Jama* 310, 1842–1850. doi:10.1001/jama.2013.280319
- Ostrom, Q. T., Bauchet, L., Davis, F. G., Deltour, I., Fisher, J. L., Langer, C. E., et al. (2014). The epidemiology of glioma in adults: A "state of the science" review. *Neuro. Oncol.* 16, 896–913. doi:10.1093/neuonc/nou087
- Ostrom, Q. T., Cioffi, G., Waite, K., Kruchko, C., and Barnholtz-Sloan, J. S. (2021). CBTRUS statistical report: Primary brain and other central nervous system tumors diagnosed in the United States in 2014–2018. *Neuro-oncology* 23, iii1–iii105. doi:10.1093/neuonc/noab200
- Ozyerli-Goknar, E., Sur-Erdem, I., Seker, F., Cingöz, A., Kayabol, A., Kahya-Yesil, Z., et al. (2019). The fungal metabolite chaetocin is a sensitizer for proapoptotic therapies in glioblastoma. *Cell Death Dis.* 10, 894. doi:10.1038/s41419-019-2107-y
- Pan, H., Wang, H., Zhu, L., Mao, L., Qiao, L., Su, X., et al. (2013). The role of Nrf2 in migration and invasion of human glioma cell U251. *World Neurosurg.* 80, 363–370. doi:10.1016/j.wneu.2011.06.063
- Racoma, I. O., Meisen, W. H., Wang, Q. E., Kaur, B., and Wani, A. A. (2013). Thymoquinone inhibits autophagy and induces cathepsin-mediated, caspase-independent cell death in glioblastoma cells. *PLoS One* 8, e72882. doi:10.1371/journal.pone.0072882
- Reczek, C. R., and Chandel, N. S. (2017). The two faces of reactive oxygen species in cancer. *Annu. Rev. Cancer Biol.* 1, 79–98. doi:10.1146/annurev-cancerbio-041916-065808
- Reuter, S., Gupta, S. C., Chaturvedi, M. M., and Aggarwal, B. B. (2010). Oxidative stress, inflammation, and cancer: How are they linked? *Free Radic. Biol. Med.* 49, 1603–1616. doi:10.1016/j.freeradbiomed.2010.09.006
- Sharaneek, A., Burban, A., Laaper, M., Heckel, E., Joyal, J. S., Soleimani, V. D., et al. (2020). OSMR controls glioma stem cell respiration and confers resistance of glioblastoma to ionizing radiation. *Nat. Commun.* 11, 4116. doi:10.1038/s41467-020-17885-z
- Shi, Y., Jia, B., Xu, W., Li, W., Liu, T., Liu, P., et al. (2017). Chidamide in relapsed or refractory peripheral T cell lymphoma: A multicenter real-world study in China. *J. Hematol. Oncol.* 10, 69. doi:10.1186/s13045-017-0439-6
- Shono, T., Yokoyama, N., Uesaka, T., Kuroda, J., Takeya, R., Yamasaki, T., et al. (2008). Enhanced expression of NADPH oxidase Nox4 in human gliomas and its roles in cell proliferation and survival. *Int. J. Cancer* 123, 787–792. doi:10.1002/ijc.23569
- Silva, L., Coelho, P., Soares, R., Prudêncio, C., and Vieira, M. (2019). Quinoxaline-1, 4-dioxide derivatives inhibitory action in melanoma and brain tumor cells. *Future Med. Chem.* 11, 645–657. doi:10.4155/fmc-2018-0251
- Singer, E., Judkins, J., Salomonis, N., Matlaf, L., Soteropoulos, P., McAllister, S., et al. (2015). Reactive oxygen species-mediated therapeutic response and resistance in glioblastoma. *Cell Death Dis.* 6, e1601. doi:10.1038/cddis.2014.566
- Sohal, R. S., and Allen, R. G. (1990). Oxidative stress as a causal factor in differentiation and aging: A unifying hypothesis. *Exp. Gerontol.* 25, 499–522. doi:10.1016/0531-5565(90)90017-v
- Takabe, H., Warnken, Z. N., Zhang, Y., Davis, D. A., Smyth, H. D. C., Kuhn, J. G., et al. (2018). A repurposed drug for brain cancer: Enhanced atovaquone amorphous solid dispersion by combining a spontaneously emulsifying component with a polymer carrier. *Pharmaceutics* 10, E60. doi:10.3390/pharmaceutics10020060
- Tan, A. C., Ashley, D. M., López, G. Y., Malinzak, M., Friedman, H. S., Khasraw, M., et al. (2020). Management of glioblastoma: State of the art and future directions. *Ca. Cancer J. Clin.* 70, 299–312. doi:10.3322/caac.21613
- Tavana, E., Mollazadeh, H., Mohtashami, E., Modaresi, S. M. S., Hosseini, A., Sabri, H., et al. (2020). Quercetin: A promising phytochemical for the treatment of glioblastoma multiforme. *Biofactors* 46, 356–366. doi:10.1002/biof.1605
- Thannickal, V. J., and Fanburg, B. L. (2000). Reactive oxygen species in cell signaling. *Am. J. Physiol. Lung Cell. Mol. Physiol.* 279, L1005–L1028. doi:10.1152/ajplung.2000.279.6.L1005
- Tomar, M. S., Kumar, A., Srivastava, C., and Shrivastava, A. (2021). Elucidating the mechanisms of Temozolomide resistance in gliomas and the strategies to overcome the resistance. *Biochim. Biophys. Acta. Rev. Cancer* 1876, 188616. doi:10.1016/j.bbcan.2021.188616

- Trachootham, D., Alexandre, J., and Huang, P. (2009). Targeting cancer cells by ROS-mediated mechanisms: A radical therapeutic approach? *Nat. Rev. Drug Discov.* 8, 579–591. doi:10.1038/nrd2803
- Valko, M., Leibfritz, D., Moncol, J., Cronin, M. T., Mazur, M., Telser, J., et al. (2007). Free radicals and antioxidants in normal physiological functions and human disease. *Int. J. Biochem. Cell Biol.* 39, 44–84. doi:10.1016/j.biocel.2006.07.001
- Valko, M., Rhodes, C. J., Moncol, J., Izakovic, M., and Mazur, M. (2006). Free radicals, metals and antioxidants in oxidative stress-induced cancer. *Chem. Biol. Interact.* 160, 1–40. doi:10.1016/j.cbi.2005.12.009
- Wada, T., and Penninger, J. M. (2004). Mitogen-activated protein kinases in apoptosis regulation. *Oncogene* 23, 2838–2849. doi:10.1038/sj.onc.1207556
- Wang, C., He, C., Lu, S., Wang, X., Wang, L., Liang, S., et al. (2020). Autophagy activated by silibinin contributes to glioma cell death via induction of oxidative stress-mediated BNIP3-dependent nuclear translocation of AIF. *Cell Death Dis.* 11, 630. doi:10.1038/s41419-020-02866-3
- Wang, G. L., and Semenza, G. L. (1995). Purification and characterization of hypoxia-inducible factor 1. *J. Biol. Chem.* 270, 1230–1237. doi:10.1074/jbc.270.3.1230
- Wang, J., Hao, H., Yao, L., Zhang, X., Zhao, S., Ling, E. A., et al. (2012). Melatonin suppresses migration and invasion via inhibition of oxidative stress pathway in glioma cells. *J. Pineal Res.* 53, 180–187. doi:10.1111/j.1600-079X.2012.00985.x
- Wang, K., Fu, X. T., Li, Y., Hou, Y. J., Yang, M. F., Sun, J. Y., et al. (2016). Induction of S-phase Arrest in human glioma cells by selenocysteine, a natural selenium-containing agent via triggering reactive oxygen species-mediated DNA damage and modulating MAPKs and AKT pathways. *Neurochem. Res.* 41, 1439–1447. doi:10.1007/s11064-016-1854-8
- Wang, P. F., Cai, H. Q., Zhang, C. B., Li, Y. M., Liu, X., Wan, J. H., et al. (2018). Molecular and clinical characterization of PTPN2 expression from RNA-seq data of 996 brain gliomas. *J. Neuroinflammation* 15, 145. doi:10.1186/s12974-018-1187-4
- Wang, Y., Ying, X., Xu, H., Yan, H., Li, X., Tang, H., et al. (2017). The functional curcumin liposomes induce apoptosis in C6 glioblastoma cells and C6 glioblastoma stem cells *in vitro* and in animals. *Int. J. Nanomedicine* 12, 1369–1384. doi:10.2147/IJN.S124276
- Wang, Y., Zhang, J., Yang, Y., Liu, Q., Xu, G., Zhang, R., et al. (2019). ROS generation and autophagosome accumulation contribute to the DMAMCL-induced inhibition of glioma cell proliferation by regulating the ROS/MAPK signaling pathway and suppressing the Akt/mTOR signaling pathway. *Onco. Targets. Ther.* 12, 1867–1880. doi:10.2147/OTT.S195329
- Waris, G., and Ahsan, H. (2006). Reactive oxygen species: Role in the development of cancer and various chronic conditions. *J. Carcinog.* 5, 14. doi:10.1186/1477-3163-5-14
- Wei, J., Meng, L., Hou, X., Qu, C., Wang, B., Xin, Y., et al. (2019). Radiation-induced skin reactions: Mechanism and treatment. *Cancer Manag. Res.* 11, 167–177. doi:10.2147/CMAR.S188655
- Wu, L., Wang, F., Xu, J., and Chen, Z. (2019). PTPN2 induced by inflammatory response and oxidative stress contributed to glioma progression. *J. Cell. Biochem.* 120, 19044–19051. doi:10.1002/jcb.29227
- Yang, H., Chen, W., Ma, J., Zhao, J., Li, D., Cao, Y., et al. (2020). Silver nanotriangles and chemotherapeutics synergistically induce apoptosis in glioma cells via a ROS-dependent mitochondrial pathway. *Int. J. Nanomedicine* 15, 7791–7803. doi:10.2147/IJN.S267120
- Yang, L., Mu, Y., Cui, H., Liang, Y., and Su, X. (2017). MiR-9-3p augments apoptosis induced by H₂O₂ through down regulation of Herpud1 in glioma. *PLoS One* 12, e0174839. doi:10.1371/journal.pone.0174839
- Yang, W., Xia, Y., Cao, Y., Zheng, Y., Bu, W., Zhang, L., et al. (2012). EGFR-induced and PKC ϵ monoubiquitylation-dependent NF- κ B activation upregulates PKM2 expression and promotes tumorigenesis. *Mol. Cell* 48, 771–784. doi:10.1016/j.molcel.2012.09.028
- Yang, W., Zheng, Y., Xia, Y., Ji, H., Chen, X., Guo, F., et al. (2012). ERK1/2-dependent phosphorylation and nuclear translocation of PKM2 promotes the Warburg effect. *Nat. Cell Biol.* 14, 1295–1304. doi:10.1038/ncb2629
- Zhao, P., Zhao, L., Zou, P., Lu, A., Liu, N., Yan, W., et al. (2012). Genetic oxidative stress variants and glioma risk in a Chinese population: A hospital-based case-control study. *BMC Cancer* 12, 617. doi:10.1186/1471-2407-12-617
- Zheng, L., Wang, C., Luo, T., Lu, B., Ma, H., Zhou, Z., et al. (2017). JNK activation contributes to oxidative stress-induced parthanatos in glioma cells via increase of intracellular ROS production. *Mol. Neurobiol.* 54, 3492–3505. doi:10.1007/s12035-016-9926-y
- Zhong, H., De Marzo, A. M., Laughner, E., Lim, M., Hilton, D. A., Zagzag, D., et al. (1999). Overexpression of hypoxia-inducible factor 1 α in common human cancers and their metastases. *Cancer Res.* 59, 5830–5835.
- Zhou, H., Han, L., Wang, H., Wei, J., Guo, Z., Li, Z., et al. (2020). Chidamide inhibits glioma cells by increasing oxidative stress via the miRNA-338-5p regulation of hedgehog signaling. *Oxid. Med. Cell. Longev.* 2020, 7126976. doi:10.1155/2020/7126976
- Zhu, J., Wang, H., Fan, Y., Lin, Y., Zhang, L., Ji, X., et al. (2014). Targeting the NF-E2-related factor 2 pathway: A novel strategy for glioblastoma (review). *Oncol. Rep.* 32, 443–450. doi:10.3892/or.2014.3259

Glossary

AgNTs silver nanotriangles	LDHA lactate dehydrogenase A
AP-1 activator protein 1	LGGs low grade gliomas
APE1 apurinic/apyrimidinic endonuclease1	MKK MAPK kinase
ARE antioxidant response elements	MMPs matrix metalloproteinases
ATP adenosine triphosphate	NADH nicotinamide adenine dinucleotide
Chk2 checkpoint kinase 2	NADPH nicotinamide adenine dinucleotide phosphate
CPT1A carnitine palmitoyltransferase 1A	Nrf2 nuclear factor erythroid 2-related factor 2
DGAT1 diacylglycerol-acyltransferase 1	OMV outer-membrane vesicles
DNA deoxyribonucleic acid	OSMR oncostatin M receptor
ENPP2 ectonucleotide pyrophosphatase/phosphodiesterase 2	PARP-1 poly ADP-ribose polymerase-1
FAs fatty acids	PKM2 pyruvate kinase M2
GBM glioblastoma	PPVI polyphyllin VI
GLUT1 glucose transporter 1	PTPN2 protein tyrosine phosphatase, non-receptor type 2
GSH glutathione	Qu quercetin
GTP guanosine triphosphate	RBX1 RING box protein 1
HDAC histone deacetylase	RIP receptor interacting protein kinase
HGGs high grade gliomas; 8-oxo-dG:8-oxo-7,8-dihydro-2'-deoxyguanosine	ROS reactive oxygen species
HIF-1 hypoxia-inducible factor-1	SAL salinomycin
HIF-1α hypoxia-inducible factor-1 α	SeC selenocysteine
HMOX1 heme oxygenase 1	SIRT6 sirtuin 6
hMTH1 homolog protein 1	SOD superoxide dismutase
HO-1 heme oxygenase 1	STAT3 signal transducer and activator of transcription 3
IDH isocitrate dehydrogenase	TGF transforming growth factor
IFN interferon	TNF tumor necrosis factor
IL-1 interleukin-1; ATF4:Activating transcription factor 4	TQ thymoquinone
JAK2 janus kinase 2	TRAIL TNF-related apoptosis-inducing ligand
KEAP1 kelch-like ECH-associated protein 1	VEGFA vascular endothelial growth factor A
	WHO World Health Organization
	YAP1 yes-associated protein 1



OPEN ACCESS

EDITED BY

Hidayat Hussain,
Leibniz Institute of Plant Biochemistry,
Germany

REVIEWED BY

Zeynab Fakhar,
University of the Witwatersrand, South
Africa
Ramendra K. Singh,
Allahabad University, India

*CORRESPONDENCE

Zhonglei Wang,
wangzl16@tsinghua.org.cn
Liyang Yang,
yangly@iccas.ac.cn
Xian-qing Song,
Song_xianqing@126.com

SPECIALTY SECTION

This article was submitted to
Experimental Pharmacology and Drug
Discovery,
a section of the journal
Frontiers in Pharmacology

RECEIVED 22 April 2022

ACCEPTED 11 July 2022

PUBLISHED 19 August 2022

CITATION

Wang Z, Wang N, Yang L and Song X-q
(2022), Bioactive natural products in
COVID-19 therapy.
Front. Pharmacol. 13:926507.
doi: 10.3389/fphar.2022.926507

COPYRIGHT

© 2022 Wang, Wang, Yang and Song.
This is an open-access article
distributed under the terms of the
[Creative Commons Attribution License](#)
(CC BY). The use, distribution or
reproduction in other forums is
permitted, provided the original
author(s) and the copyright owner(s) are
credited and that the original
publication in this journal is cited, in
accordance with accepted academic
practice. No use, distribution or
reproduction is permitted which does
not comply with these terms.

Bioactive natural products in COVID-19 therapy

Zhonglei Wang^{1,2*}, Ning Wang³, Liyan Yang^{4*} and
Xian-qing Song^{3*}

¹Key Laboratory of Green Natural Products and Pharmaceutical Intermediates in Colleges and Universities of Shandong Province, School of Chemistry and Chemical Engineering, Qufu Normal University, Qufu, China, ²School of Pharmaceutical Sciences, Tsinghua University, Beijing, China, ³General Surgery Department, Ningbo Fourth Hospital, Xiangshan, China, ⁴School of Physics and Physical Engineering, Qufu Normal University, Qufu, China

The devastating COVID-19 pandemic has caused more than six million deaths worldwide during the last 2 years. Effective therapeutic agents are greatly needed, yet promising magic bullets still do not exist. Numerous natural products (cordycepin, gallinamide A, plitidepsin, telocinobufagin, and tylophorine) have been widely studied and play a potential function in treating COVID-19. In this paper, we reviewed published studies (from May 2021 to April 2022) relating closely to bioactive natural products (isolated from medicinal plants, animals products, and marine organisms) in COVID-19 therapy *in vitro* to provide some essential guidance for anti-SARS-CoV-2 drug research and development.

KEYWORDS

natural products, COVID-19, SARS-CoV-2, cordycepin, gallinamide A, plitidepsin, telocinobufagin, tylophorine

1 Introduction

The ongoing coronavirus disease 2019 (COVID-19) pandemic, the sixth public health emergency of international concern, has resulted in 505,035,185 cases and 6,210,719 deaths worldwide during the last 2 years (at the time of writing). (World Health Organization, 2022). The Alpha, Beta, Gamma, and Delta variants of the severe acute respiratory syndrome coronavirus 2 (SARS-CoV-2) responsible for COVID-19 have created recurrent pandemic alerts. (Nasreen et al., 2022). Alarmingly, the novel Omicron (South Africa) variant was firstly confirmed on 24 November 2021. Still, it became the most predominant strain internationally within months because of its increased transmissibility and extensive immune evasion ability. (Scott et al., 2021; Del Rio et al., 2022). Up to now, the devastating Omicron variant has spread to almost all countries. Effective measures, such as vaccines, (Andrews et al., 2022; Chandrashekar et al., 2022) traditional medicine, (Liu et al., 2020; Alam et al., 2021) and small-molecule inhibitors, (Wang and Yang, 2020a; Reis et al., 2022; Sourimant et al., 2022) are greatly needed to reduce human-to-human transmission.

However, promising magic bullets still do not exist. (Kozlov, 2022). As an indispensable resource for promising compounds, natural products have attracted significant attention in countering SARS-CoV-2 infection *via* targeting its main

protease (M^{pro} , also called $3CL^{pro}$), (Jin et al., 2020; Mengist et al., 2020) RNA-dependent RNA polymerase (RdRp), (Hillen et al., 2020; Wang et al., 2021a) papain-like protease (PL^{pro}), (Yin et al., 2020; Gao et al., 2021) and spike (S) glycoprotein. (Toelzer et al., 2020; Walls et al., 2020). Building on our previously published work, (Wang and Yang, 2020b; Yang and Wang, 2021) we systematically discuss the landmark studies (published between May 2021 and April 2022) relating to bioactive natural products in COVID-19 therapy *in vitro* to support anti-SARS-CoV-2 drugs research and development.

2 Promising bioactive natural products in COVID-19 therapy

Bioactive natural products, isolated from medicinal plants, animal products, and marine organisms, are widely studied (in *in vitro*, animal models, and clinical trials) and play an important role in COVID-19 therapy. (Wei et al., 2020; Sahoo et al., 2021; Alqathama et al., 2022). Natural products are still considered one of the most positive and practical approaches to defeating the ongoing pandemic.

Tylophorine, a remarkable tylophora alkaloid, is an active pharmaceutical ingredient of the medicinal plant *Cynanchum komarovii* AL (Figure 1A) (An et al., 2001). NK007(S,R), a racemate of tylophorine malate, was prepared from S-tylophorine to improve its poor solubility. (Wang et al., 2010). NK007(S,R) displays significant inhibitory activity against SARS-CoV-2 at a half maximal effective concentration (EC_{50}) of $0.030\ \mu\text{M}$ in Vero cells, with an excellent selectivity profile (selectivity index, [SI] = 868). (Wang et al., 2021b). Hossain et al. (2022) found that tylophorine showed binding affinity ($-8.5\ \text{kcal/mol}$) against abelson murine leukemia viral oncogene homolog one protein. Additionally, NK007(S,R) exhibits excellent *in vivo* antiviral efficacy in the COVID-19 golden hamster rat model by significantly reducing viral loads in the lungs. NK007(S,R) could protect against lung injury by decreasing lung inflammation with a dose of $5\ \text{mg/kg}$. (Wang et al., 2021b). Briefly, the abovementioned evidence has highlighted the superior activity of NK007(S,R) against SARS-CoV-2 infection in *in vitro* and in the rat model. (Wang et al., 2021b). Numerous natural product-based nanomedicines have been sprung up during the past several decades in the field of medicinal chemistry, providing a valuable reference for anti-COVID-19 therapeutics. (Sharma et al., 2021). To evaluate the potential of the candidate NK007(S,R), Wang et al. (Wang et al., 2021b) prepared self-assembled poly (ethylene glycol)-poly (lactide-co-glycolide) nanoparticles, NP-NK007 and LP-NK007. The optimized NP-NK007 exhibited small particle size ($145.8\ \text{nm}$), high NK007(S,R) loading (13.10%), maximized encapsulation efficiency (87.47%), and sustained release (66.51% in 48 h). The optimal lung-targeted liposome LP-NK007 exhibited smaller particle size ($75\ \text{nm}$), higher drug

loading (36.7%), and excellent encapsulation efficiency (62.4%). Subsequent experiments implied that the nanoparticles NP-NK007 and LP-NK007 are effective SARS-CoV-2 inhibitors with higher EC_{50} values of 0.007 and $0.014\ \mu\text{M}$, respectively, because they improve the accumulation and delivered efficiency of NK007(S,R) in the lung. (Wang et al., 2021b). Collectively, NK007(S,R) NPs could provide a workable strategy for overcoming the lack of COVID-19-targeting treatment. Theoretically, more validation studies *in vivo* are needed to systematically assess the anti-SARS-CoV-2 potential of NK007(S,R)-based nanoparticles.

Venenum Bufonis (Chinese name: ChanSu), a well-known secretion of a traditional medicine animal (toad *Bufo bufo gargarizans*), is commonly used in China to treat various diseases, including heart failure, infections, toothaches, and cancers. (Tian et al., 2017; Shen et al., 2022). For example, Huachansu injection, a valuable anticancer agent, has been used in tumour treatment in China for more than 30 years. (Wu et al., 2022a). ChanSu's main active constituents are bufadienolides that have an unusual 2-pyrone ring, which contributes to their pharmacological activities *via* inhibiting Na^+/K^+ ATPase. (Prassas and Diamandis, 2008). Recently, Jin et al. (2021) demonstrated that six bufadienolides (bufalin, bufotalin, cinobufagin, cinobufotalin, resibufogenin, and telocinobufagin) have potent broad-spectrum antiviral activities *in vitro* (Figure 1B). Experiments showed that bufalin could inhibit virus replication in the nanomolar range, including MERS-CoV at a half-maximal inhibitory concentration (IC_{50}) of $0.018\ \mu\text{M}$, SARS-CoV at an IC_{50} of $0.016\ \mu\text{M}$, and SARS-CoV-2 at an IC_{50} of $0.019\ \mu\text{M}$; cinobufagin can inhibit MERS-CoV, SARS-CoV, and SARS-CoV-2 replication at IC_{50} values of 0.017 , 0.060 , and $0.072\ \mu\text{M}$; telocinobufagin can inhibit MERS-CoV, SARS-CoV and SARS-CoV-2 replication with IC_{50} values of 0.027 , 0.071 , and $0.142\ \mu\text{M}$; bufotalin, cinobufotalin and resibufogenin can inhibit the MERS-CoV, SARS-CoV and SARS-CoV-2 replication *in vitro* with high IC_{50} values (0.027 – $1.612\ \mu\text{M}$). (Jin et al., 2021). This study showed that the unusual 2-pyrone ring in bufadienolides plays an essential role in inhibiting SARS-CoV-2 replication. Subsequent dose toxicity studies ($10\ \text{mg/kg/day}$, 5 days) revealed that bufalin and cinobufagin have strong toxicity in the mouse model, while the pharmacokinetic model predicts that telocinobufagin has lower toxicity, better metabolic stability, excellent oral bioavailability, and proper anti-SARS-CoV-2 activity. (Jin et al., 2021). Taken together, telocinobufagin might be a more promising broad-spectrum inhibitor among the bufadienolides, and thus worthy of multifaceted properties investigation from *in vitro* studies to clinical practice.

Gallinamide A, possessing an α,β -unsaturated imide moiety, is a novel linear depsipeptide first isolated in 2008 from the marine cyanobacteria *Schizothrix* genus and *Symploca* sp. with critical pharmacological effects (Figure 1C) (Linington et al., 2009; Taori et al., 2009). Gallinamide A is a highly selective

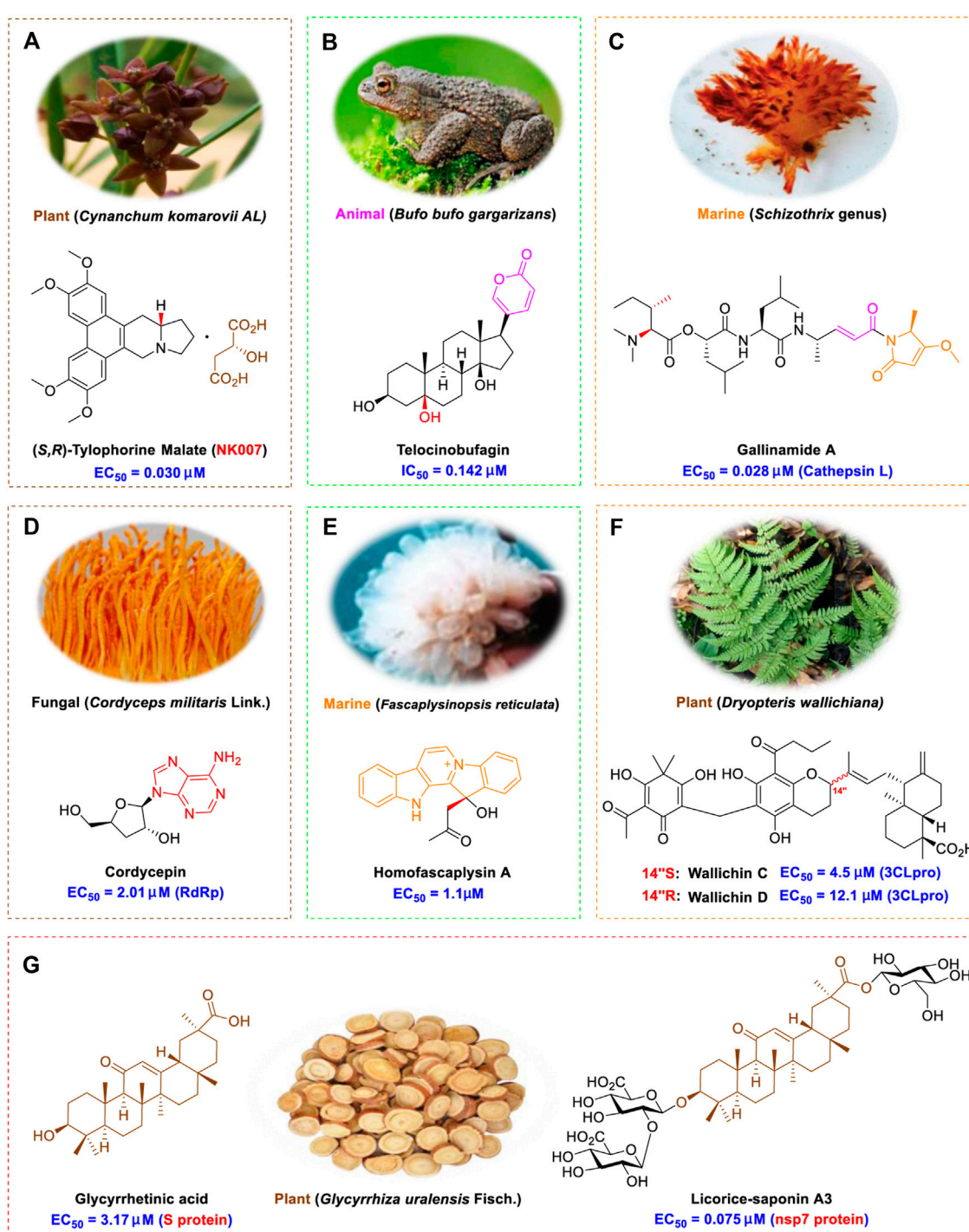


FIGURE 1

Promising natural products in COVID-19 therapy. (A) Tylophorine can be isolated from the medicinal plant *Cynanchum komarovii* AL. (B) Telocinobufagin can be isolated from the traditional medicinal animal toad *Bufo gargarizans*. (C) Gallinamide A can be isolated from the marine cyanobacteria *Schizothrix* genus. (D) Cordycepin can be isolated from the traditional medicine *Cordyceps militaris* Link. (E) Homofascaplysin A can be isolated from the marine sponge *Fascaplysinopsis reticulata*. (F) Wallichins C and D can be isolated from the medicinal fern *Dryopteris wallichiana*. (G) Licorice-saponin A3 and glycyrrhetic acid can be isolated from the medicinal plant *Glycyrrhiza uralensis* Fisch.

covalent inhibitor targeting human cathepsin L-like cysteine proteases, which is a promising drug target. (Barbosa Da Silva et al., 2022). Gerwick's group showed that gallinamide A had a 28- to 320-fold higher affinity and selectivity towards cathepsin L than cathepsin V or B. (Miller et al., 2014). *In vitro*, gallinamide A demonstrates significant bioactivity against *Trypanosoma cruzi* at an IC_{50} of 0.005 μ M by irreversible Michael addition. (Miller et al., 2014). It has been reported that gallinamide A can decrease viral load in VeroE6 cells with an IC_{90} of 0.088 μ M and inhibit SARS-CoV-2 cathepsin L-mediated endosomal entry with an EC_{50} value of 0.028 μ M in a dose-dependent manner. (Ashhurst et al., 2022). Angiotensin-converting enzyme 2 (ACE2) and transmembrane serine protease 2 (TMPRSS2) are two essential host determinants for SARS-CoV-2 infection and pathogenesis *in vivo*. (Hoffmann et al., 2020). Specifically, the S glycoprotein helps the virus enter inside the host cell *via* cellular receptor ACE2 binding; then TMPRSS2 helps SARS-CoV-2 contents fuse and release into the host cell cytosol *via* enzymatical activation of the S glycoprotein. (Liu et al., 2022). Based on combination drug therapies, Payne et al. (Ashhurst et al., 2022) recently demonstrated that the combined use of the cathepsin L inhibitor gallinamide A and the TMPRSS2 protease inhibitor nafamostat mesylate exerts a synergistic inhibitory effect in HEK-ACE2-TMPRSS2 cells *via* inhibiting multiple routes of SARS-CoV-2 entry. Taking gallinamide A as the lead, Payne et al. (Ashhurst et al., 2022) further explored and synthesized 32 analogues for the assessment of SARS-CoV-2 cathepsin L inhibitory activities; the study revealed two lead analogues of gallinamide A with EC_{50} values in the nanomolar range. Taken together, gallinamide A is a highly selective SARS-CoV-2 cathepsin L inhibitor, thus worthy of further investigation *via* combination therapies and lead optimization.

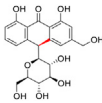
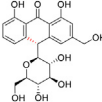
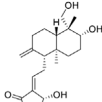
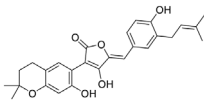
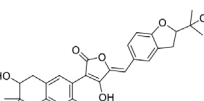
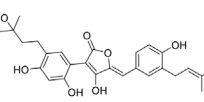
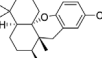
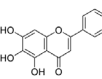
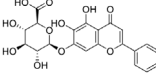
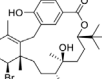
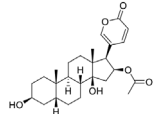
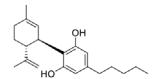
Natural products with broad-spectrum bioactivities and multi-organ protection are an essential class of anti-SARS-CoV-2 agents that play vital roles in COVID-19 therapy. (Wang and Yang, 2021). RdRp could regulate viral replication through catalyzing the RNA template-dependent development of phosphodiester bonds. (Wang et al., 2021a). The adenosine analogue cordycepin (3'-deoxyadenosine) is a unique fungal product isolated from the traditional medicine fungi *Cordyceps militaris* (Cunningham et al., 1950) and *Ophiocordyceps sinensis* (Figure 1D) (Zhou et al., 2008). Interestingly, cordycepin is known to have broad-spectrum pharmacological properties against several diseases (e.g., virulent RNA viruses) and multi-organ protective effects (e.g. acute lung injury). Specifically, cordycepin is a promising therapeutic against several viruses *in vitro*, including dengue virus, (Panya et al., 2021) Epstein-Barr virus, (Choi et al., 2019) and hepatitis C virus. (Ueda et al., 2014). Because of its close structural similarity to the cellular nucleoside adenosine (except for the absence of a hydroxyl group at the 3'-position of the five-membered ring), cordycepin is a possible potent anti-SARS-CoV-2 agent. Rabie et al. (Rabie, 2022) showed that cordycepin could inhibit SARS-CoV-2 replication in Vero E6 cells with an EC_{50} value of 2.01 μ M

and without observable cytotoxicity ($SI > 49.8$) in a time-dependent manner. It is worth noting that cordycepin is a long-acting antiviral for SARS-CoV-2 prevention with high metabolic stability, reaching maximal anti-SARS-CoV-2 potency within 1.5–2.0 days of treatment. (Rabie, 2022). With respect to the activation mechanism, cordycepin is rapidly converted *in vivo* to its mono-, di-, and triphosphate forms; then, the active form cordycepin triphosphate can serve as a substrate for the RNA-dependent RNA polymerase (RdRp) to terminate the synthesis of viral RNA sequences. (Rabie, 2022). Bibi et al. (2022) revealed that two pivotal amino acid residues (Asp760 and Asp761) play critical roles in the binding of cordycepin with RdRp. Notably, SARS-CoV-2 infection—even in mild cases—can increase the long-term risk of a broad range of cardiovascular and cerebrovascular complications in COVID-19 patients. (Wang and Yang, 2022c). In terms of organ protection, cordycepin has unique advantages. For example, cordycepin plays a key role in long-term neuroprotection for traumatic brain injury (through inhibiting neutrophil infiltration and preserving neuroinflammation), (Wei et al., 2021) protecting diabetic hearts from ischemia/reperfusion injury (*via* up-regulating AMPK/Mfn2-dependent mitochondrial fusion and expression), (Yu et al., 2021) and ameliorating cerebral ischemic damage (*via* improving the memory ability, up-regulating the level of adenosine A1 receptors, and reducing dendritic morphology scathing). (Chen et al., 2021). Thus, cordycepin has its advantages in organ protection and broad-spectrum antiviral activities. Further study is still needed, however, to evaluate its antiviral potency *in vitro*.

The marine environment is a valuable source of structurally unique natural products with diverse bioactivity targeted at life-threatening diseases, including the emerging COVID-19. (Panggabean et al., 2022; Pokharkar et al., 2022; Zhang et al., 2022). Homofascaplysin A, isolated from the marine sponge *Fascaplysinopsis reticulata* (Figure 1E), is a well-established β -carboline alkaloid reported to exhibit promising activity against many viruses, including hepatitis C virus, (Ishida et al., 2001) human coronavirus NL63, (Tsai et al., 2020) and dengue virus. (Quintana et al., 2016). Kubanek et al. (Chhetri et al., 2022) revealed that homofascaplysin A can inhibit SARS-CoV-2 replication in Calu-3 cells at an EC_{50} value of 1.1 μ M with relatively slight cytotoxicity ($SI \sim 4.55$). Additionally, Kubanek et al. (Chhetri et al., 2022) found that the viral load was substantially reduced (by >90%) for infections in harvested SARS-CoV-2 RNA after administration of 2.8 μ M of homofascaplysin A. Therefore, homofascaplysin A could be used as a unique lead compound for the rapid screening of novel analogues with promising anti-SARS-CoV-2 activity and minimal cytotoxicity.

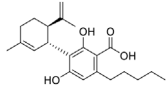
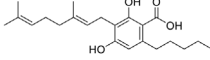
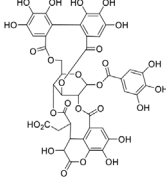
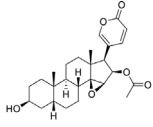
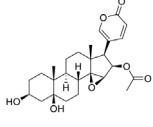
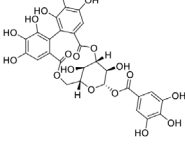
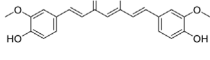
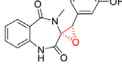
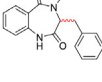
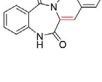
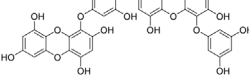
Chirality is a critical attribute of natural products. (Wang, 2019). Wallichin C and wallichin D, isolated from the medicinal fern *Dryopteris wallichiana* (Figure 1F), exhibit potent anti-SARS-CoV-2 activities in Vero-E6 cells at EC_{50} values of 4.5 and 12.1 μ M, respectively. (Socolsky et al., 2012; Hou et al., 2022). The corresponding SI values of wallichins C and D

TABLE 1 Other promising natural products for treating SARS-CoV-2 infection *in vitro*.

No.	Name	Structure	EC ₅₀ or IC ₅₀ (μM)	Strain	Refs
1	Aloin A		15.68	Vero E6 cells	Lewis et al. (2022)
2	Aloin B		17.51	Vero E6 cells	Lewis et al. (2022)
3	Andrographolide		0.034	Calu-3 cells	Sa-Ngiamsumtorn et al. (2021) , Schulte et al. (2022)
4	Aspulinone D		10.3	J774A.1 cells	Liang et al. (2022)
5	Aspulinone M		9.4	J774A.1 cells	Liang et al. (2022)
6	Aspulinone R		7.7	J774A.1 cells	Liang et al. (2022)
7	(+)-Aureol		4.00	Calu-3 cells	Chhetri et al. (2022)
8	Baicalein		1.11	<i>E. coli</i> BL21 cells	Wu et al., 2022a , Xiao et al. (2021)
9	Baicalin		8.8	Vero E6 cells	Ngwe Tun et al. (2022)
10	Bromophycolide A		6.90	Calu-3 cells	Chhetri et al. (2022)
11	Bufotalin		0.072	Vero E6 cells	Jin et al. (2021)
12	Cannabidiol		1.24	A549-ACE2 cells	Corpetti et al. (2021) , Nguyen et al. (2022)

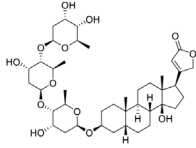
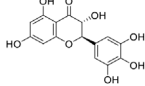
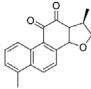
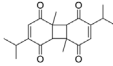
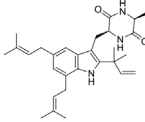
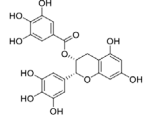
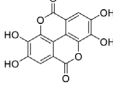
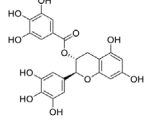
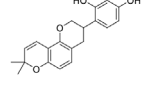
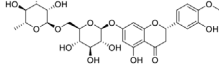
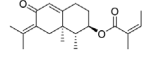
(Continued on following page)

TABLE 1 (Continued) Other promising natural products for treating SARS-CoV-2 infection *in vitro*.

No.	Name	Structure	EC ₅₀ or IC ₅₀ (μM)	Strain	Refs
13	Cannabidiolic acid		24 μg/mL	Vero E6 cells	van Breemen et al. (2022)
14	Cannabigerolic acid		37 μg/mL	Vero E6 cells	van Breemen et al. (2022)
15	Chebularic acid		9.76	Vero E6 cells	Du et al. (2021)
16	Cinobufagin		0.072	Vero E6 cells	Corpetti et al. (2021), Nguyen et al. (2022)
17	Cinobufotalin		0.399	Vero E6 cells	Jin et al. (2021)
18	Corilagin		24.9	HEK293 cells	Yang et al. (2021a)
19	Curcumin		11.9	Vero E6 cells	Bahun et al. (2022)
20	Cyclophenol		0.39	RAW264.7 cells	Thissera et al. (2021)
21	Cyclopeptin		0.40	RAW264.7 cells	Thissera et al. (2021)
22	Dehydrocyclopeptin		0.89	RAW264.7 cells	Thissera et al. (2021)
23	Dieckol		4.50	Vero E6 cells	Yan et al. (2021)

(Continued on following page)

TABLE 1 (Continued) Other promising natural products for treating SARS-CoV-2 infection *in vitro*.

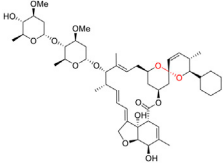
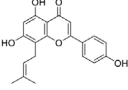
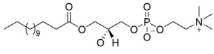
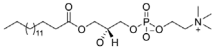
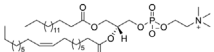
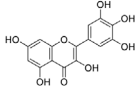
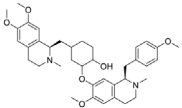
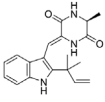
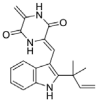
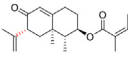
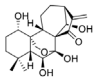
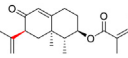
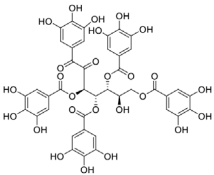
No.	Name	Structure	EC ₅₀ or IC ₅₀ (μM)	Strain	Refs
24	Digitoxin		0.059	Vero E6 cells	Caohuy et al. (2021) , Jin et al. (2021) , Caohuy et al. (2022)
25	Dihydromyricetin		1.14	Vero E6 cells	Su et al. (2021) , Xiao et al. (2021)
26	Dihydrotanshinone I		8.14	Vero E6 cells	Ma and Wang, (2022)
27	Dithymoquinone		0.275 μg/mL	Vero E6 cells	Esharkawy et al. (2022)
28	Echinulin		3.90	<u>Vero E6 cells</u>	Alhadrami et al. (2022)
29	EGCG		4.24	Vero E6 cells	Chiou et al. (2022)
30	Ellagic acid		11.8	Vero E6 cells	Bahun et al. (2022)
31	(-)-Gallocatechin gallate		5.77	Vero E6 Cells	Xiao et al. (2021)
32	Glabridin		2.5	Vero E6 cells	Ngwe Tun et al. (2022)
33	Hesperidin		51.5	Vero E6 cells	Huang et al. (2022)
34	Isopetasin		0.37	Vero E6 cells	Urda et al. (2022)

(Continued on following page)

were >35 and >11. ([Hou et al., 2022](#)). Furthermore, phloroglucinol-terpenoids wallichins C and D exhibit potent inhibitory activities in SARS-CoV-2-infected Calu-3 cells at

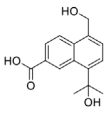
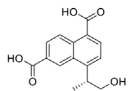
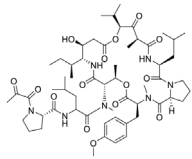
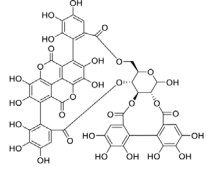
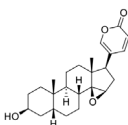
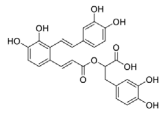
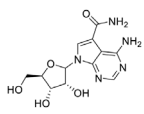
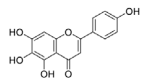
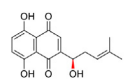
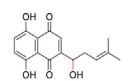
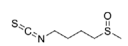
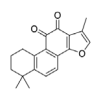
EC₅₀ values of 20.2 and 30.0 μM, with moderate cytotoxicity (SI values were 4.88 and 2.14 μM, respectively). ([Hou et al., 2022](#)). Notably, both wallichins C and D have the same core structure

TABLE 1 (Continued) Other promising natural products for treating SARS-CoV-2 infection *in vitro*.

No.	Name	Structure	EC ₅₀ or IC ₅₀ (μM)	Strain	Refs
35	Ivermectin		0.55	Vero E6 cells	Chable-Bessia et al. (2022)
36	Licoflavone C		1.34	Vero E6 cells	Corona et al. (2022)
37	LPC (14:0/0:0)		0.92	Vero E6 cells	Du et al. (2022)
38	LPC (16:0/0:0)		1.48	Vero E6 cells	Du et al. (2022)
39	LPC (16:0/18:1)		0.14	Vero E6 cells	Du et al. (2022)
40	Myricetin		0.63	Vero E6 cells	Kato et al. (2021) , Su et al. (2021)
41	Neferine		0.36	HEK293/hACE2 cells	Yang et al. (2021b)
42	(+)-Neoechinulin A		0.47	<u>Vero E6 cells</u>	Alhadrami et al. (2022)
43	Neoechinulin B		32.9	Vero E6 cells	Nishiuchi et al. (2022)
44	Neopetasin		1.26	Vero E6 cells	Urda et al. (2022)
45	Oridonin		2.16	Vero E6 cells	Zhong et al. (2022)
46	Petasin		10.79	Vero E6 cells	Urda et al. (2022)
47	PGG		3.66	Vero E6 cells	Chiou et al. (2022)

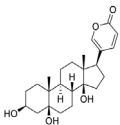
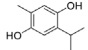
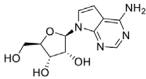
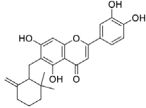
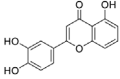
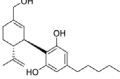
(Continued on following page)

TABLE 1 (Continued) Other promising natural products for treating SARS-CoV-2 infection *in vitro*.

No.	Name	Structure	EC ₅₀ or IC ₅₀ (μM)	Strain	Refs
48	Pinitrpenoid A		64.5	<u>Vero E6 cells</u>	Li et al. (2021b)
49	Pinitrpenoid C		76.1	<u>Vero E6 cells</u>	Li et al. (2021b)
50	Plitidepsin		0.0043	Vero E6 cells	Guisado-Vasco et al. (2022) , Sachse et al. (2022)
51	Punicalagin		6.19	Vero E6 cells	Saadh et al. (2021) Suručić et al. (2021)
52	Resibufogenin		1.606	Vero E6 cells	Jin et al. (2021)
53	Salvianolic acid A		2.49	Vero E6 cells	Zhong et al. (2022)
54	Sangivamycin		0.015	Vero E6 cells	Bennett et al. (2022)
55	Scutellarein		5.68	<i>E. coli</i> BL21 cells	Wu et al. (2022c)
56	(+)-Shikonin		4.38	Vero E6 cells	Zhao et al. (2021) , Ma et al. (2022)
57	Shikonin		4.50	Vero E6 cells	Cui and Jia (2021) , Zhao et al. (2021)
58	Sulforaphane		2.40	Caco-2 cells	Ordóñez et al. (2022)
59	Tanshinone IIA		7.82 μg/mL	Vero E6 cells	Elebeedy et al. (2022)

(Continued on following page)

TABLE 1 (Continued) Other promising natural products for treating SARS-CoV-2 infection *in vitro*.

No.	Name	Structure	EC ₅₀ or IC ₅₀ (μM)	Strain	Refs
60	Telocinobufagin		0.142	Vero E6 cells	Jin et al. (2021)
61	Thymohydroquinone		0.023 μg/mL	Vero E6 cells	Esharkawy et al. (2022)
62	Tubercidin		0.05	Calu-3 cells	Schultz et al. (2022)
63	Ugonin J		2.38	Vero E6 Cells	Chiou et al. (2021)
64	5,3',4'-trihydroxyflavone		8.22	Vero E6 cells	Zhao et al. (2021)
65	7-OH-Cannabidiol		3.60	A549-ACE2 cells	Nguyen et al. (2022)

except for the chirality at C-14 position. The study has demonstrated that the slight differences in the chirality at C-14'' S (wallichin C) or C-14'' R (wallichin D) account for differences in their antiviral activities. (Hou et al., 2022). As for the activation mechanism, Zhou et al. (Hou et al., 2022) unambiguously showed that wallichins C and D have higher selectivity and stronger interaction toward the 3CL^{pro} with K_d values of 12.0–16.6 μM, while not active against the TMPRSS2, spike glycoprotein, and ACE2 proteins. Taken together, wallichin C might be the more promising 3CL^{pro} inhibitor, thus worthy of further investigation.

Among pharmacological interventions, traditional medicine plays a positive role in the prevention and treatment of the COVID-19 pandemic. (Lyu et al., 2021; Zhan et al., 2022). For example, the Qingfei Paidu decoction has shown amazing clinical efficacy in treating COVID-19 patients. (Li Y. et al., 2021). It is crucial to support scientific foundations for the clinical use of Chinese herbal medicine by exploring the underlying molecular mechanisms. (Cui et al., 2021; De Jin et al., 2021). Ye and co-workers (Yi et al., 2022) recently indicated that licorice-saponin A3 and its aglycone glycyrrhetic acid, famous triterpenoids that could be isolated from the most frequently used medicinal plant *Glycyrrhiza uralensis* Fisch. (Figure 1G), show a remarkably different inhibitory potency against SARS-CoV-2 infection in Vero E6 cells at EC₅₀ values of 0.075 μM (targeting SARS-CoV-

2 nsp7 protein) and 3.17 μM (targeting the S protein receptor-binding domain [RBD]), respectively in a dose-dependent manner. Interestingly, licorice-saponin A3 and glycyrrhetic acid were effective in inhibiting the SARS-CoV-2 spike RBD activities, with similar IC₅₀ values of 8.3 and 10.9 μM, respectively. (Yi et al., 2022). To elucidate the remarkable difference between S-RBD inhibitory effects and their antiviral activities, the underlying molecular mechanisms were further explored by Ye and co-workers. Based on molecular docking analysis of licorice-saponin A3 with nsp7 (PDB ID:7JIT), Yi et al. (2022) propose that nsp7 is another vital target for licorice-saponin A3 *via* seven hydrogen bond interactions (binding energy −8.7 kcal/mol). Qingfei Paidu decoction extracted from 21 types of traditional Chinese medicines (including *Glycyrrhiza uralensis* Fisch.) could effectively treat COVID-19, highlighting an important contributor to the active components (such as licorice-saponin A3, glycyrrhetic acid, and so on) in herbal medicine treatment. (Wu et al., 2022b). Importantly, the results provided valuable data on the “multi-components, multiple-pathways, and multi-targets” feature of traditional herbal medicine.

Glycosylation is an important structural modification that increases water solubility, enhances pharmacological activity, and improves the bioavailability of natural products. 11) In fact, GA mainly exists in the form of functional glycosides in

licorice. At present, more than 43 saponins have been identified in licorice, many of which are glycosylated derivatives of GA. 12) These glycosylated derivatives have different sugar numbers and types and display various pharmacological activities.

3 Other promising natural products for treating SARS-CoV-2 infection

Innovative drug development is an arduous process; bioactive natural products greatly expedite the development of antiviral drugs. (Abdelmohsen et al., 2017). In addition to the abovementioned agents, numerous other natural products (Table 1) have exhibited highly efficacious anti-SARS-CoV-2 activities *in vitro* and clinical practice. For example, plitidepsin (Aplidin®), a eukaryotic translation elongation factor 1A (eEF1A) inhibitor of marine origin, was initially approved to treat multiple myeloma. (Rodon et al., 2021). Sachse et al. (2022) showed that plitidepsin is highly effective at inhibiting SARS-CoV-2 replication in a dose-dependent manner in Vero E6 cells at IC₅₀ values of 0.0052 μ M for D614G variants, 0.0039 μ M for Delta variants, and 0.0043 μ M for Omicron variants. Furthermore, White et al. (2021) showed that plitidepsin can inhibit SARS-CoV-2 replication in Vero E6 cells, hACE2-293T cells and pneumocyte-like cells at IC₅₀ values of 0.00070, 0.00073, and 0.0016 μ M, respectively, *via* targeting the host protein eEF1A. Notably, Guisado-Vasco et al. (2022) showed that plitidepsin is well-tolerated in humans and can lower viral load in SARS-CoV-2-infected chronic lymphocytic leukemia patients. Clinical trials of plitidepsin have been registered (NCT04382066 and NCT05121740) and will be reported shortly. Further study is still needed to evaluate its anti-SARS-CoV-2 potency *in vivo* and *in vitro*.

4 Conclusion and outlook

The devastating SARS-CoV-2 variants have caused over six million deaths worldwide. Natural products and small-molecule inhibitors have been widely studied (in *in vitro* studies, animal models, and clinical trials) and play an essential function in treating COVID-19. Drug research and development is a highly time-consuming process. To date, Gilead's controversial Veklury® (Remdesivir, RdRp inhibitor) was conditionally approved to combat the outbreak. (Kalil et al., 2021; Wang and Yang, 2022a). Pfizer's oral broad-spectrum candidate Paxlovid® (PF-07321332, M^{pro} inhibitor) and Merck's oral prodrug Lagevrio® (Molnupiravir, RdRp inhibitor) raise new hope for a COVID-19 cure. (Cully, 2022; Wang and Yang, 2022b). Promising clinical results have occurred, while small-molecule inhibitors still have a long way to go.

The substantial progress in treating COVID-19 patients is not sufficient. Multiple factors must be considered. The first feasible factor, optimized drug combination therapy (such as gallinamide A + remdesivir, licorice-saponin A3 + PF-07321332, telcinobufagin + molnupiravir, and cordycepin + tylophorine), targeting multiple targets, could not only enhance synergistic efficacy but also reduce drug resistance and toxicity. However, any potential combination would need to be tested *in vitro* and *in vivo* to verify the anticipated synergistic or additive effect. The second workable approach is natural product-based nanomedicines therapy. For example, the tylophorine-based lung-targeted liposome LP-NK007 could inhibit SARS-CoV-2 replication with a higher EC₅₀ value *via* improving the accumulation and efficient delivery in the lung. Third, natural product-based lead optimization offers a valuable reference for enhancing anti-SARS-CoV-2 potency and pharmacokinetic parameters. For example, taking gallinamide A as the lead, Payne et al. (Ashhurst et al., 2022) synthesized two highly selective SARS-CoV-2 cathepsin L inhibitors with nanomolar EC₅₀ values. Taken together, we hope natural products (with the help of natural product-based nanomedicines therapy, lead optimization, and drug combination) prove to be a compelling direction in COVID-19 therapy.

Author contributions

ZW conceived the review. NW, LY, and XS collected the literatures. ZW and LY wrote the manuscript. ZW and XS edited the manuscript. All authors read and approved the final version of the manuscript.

Funding

This work was supported by the project of the PhD research start-up fund of Qufu Normal University, China (Grant No. 614901 and 615201).

Conflict of interest

The authors declare that the research was conducted in the absence of any commercial or financial relationships that could be construed as a potential conflict of interest.

Publisher's note

All claims expressed in this article are solely those of the authors and do not necessarily represent those of their affiliated organizations, or those of the publisher, the editors and the reviewers. Any product that may be evaluated in this article, or claim that may be made by its manufacturer, is not guaranteed or endorsed by the publisher.

References

- Abdelmohsen, U. R., Balasubramanian, S., Oelschlaeger, T. A., Grkovic, T., Pham, N. B., Quinn, R. J., et al. (2017). Potential of marine natural products against drug-resistant fungal, viral, and parasitic infections. *Lancet. Infect. Dis.* 17 (2), e30–e41. doi:10.1016/S1473-3099(16)30323-1
- Alam, S., Sarker, M., Rahman, M., Afrin, S., Richi, F. T., Zhao, C., et al. (2021). Traditional herbal medicines, bioactive metabolites, and plant products against COVID-19: Update on clinical trials and mechanism of actions. *Front. Pharmacol.* 12, 671498. doi:10.3389/fphar.2021.671498
- Alhadrami, H. A., Burgio, G., Thissera, B., Orfali, R., Jiffri, S. E., Yaseen, M., et al. (2022). Neoechinulin A as a promising SARS-CoV-2 Mpro inhibitor: *In vitro* and *in silico* study showing the ability of simulations in discerning active from inactive enzyme inhibitors. *Mar. Drugs* 20 (3), 163. doi:10.3390/md20030163
- Alqathama, A. A., Ahmad, R., Alsaedi, R. B., Alghamdi, R. A., Abkar, E. H., Alrehaly, R. H., et al. (2022). The vital role of animal, marine, and microbial natural products against COVID-19. *Pharm. Biol.* 60 (1), 509–524. doi:10.1080/13880209.2022.2039215
- An, T. Y., Huang, R. Q., Yang, Z., Zhang, D. K., Li, G. R., Yao, Y. C., et al. (2001). Alkaloids from *Cynanchum komarovii* with inhibitory activity against the tobacco mosaic virus. *Phytochemistry* 58 (8), 1267–1269. doi:10.1016/S0031-9422(01)00382-x
- Andrews, N., Stowe, J., Kirsebom, F., Toffa, S., Rickeard, T., Gallagher, E., et al. (2022). Covid-19 vaccine effectiveness against the omicron (B.1.1.529) variant. *N. Engl. J. Med.* 386, 1532–1546. doi:10.1056/NEJMoa2119451
- Ashhurst, A. S., Tang, A. H., Fajtová, P., Yoon, M. C., Aggarwal, A., Bedding, M. J., et al. (2022). Potent anti-SARS-CoV-2 activity by the natural product gallinamide A and analogues via inhibition of cathepsin L. *J. Med. Chem.* 65 (4), 2956–2970. doi:10.1021/acs.jmedchem.1c01494
- Bahun, M., Jukić, M., Oblak, D., Kranjc, L., Bajc, G., Butala, M., et al. (2022). Inhibition of the SARS-CoV-2 3CLpro main protease by plant polyphenols. *Food Chem.* 373, 131594. doi:10.1016/j.foodchem.2021.131594
- Barbosa Da Silva, E., Sharma, V., Hernandez-Alvarez, L., Tang, A. H., Stoye, A., O'Donoghue, A. J., et al. (2022). Intramolecular interactions enhance the potency of gallinamide A analogues against *Trypanosoma cruzi*. *J. Med. Chem.* 65 (5), 4255–4269. doi:10.1021/acs.jmedchem.1c02063
- Bennett, R. P., Postnikova, E. N., Eaton, B. P., Cai, Y., Yu, S., Smith, C. O., et al. (2022). Sangivamycin is highly effective against SARS-CoV-2 *in vitro* and has favorable drug properties. *JCI insight* 7 (1), e153165. doi:10.1172/jci.insight.153165
- Bibi, S., Hasan, M. M., Wang, Y. B., Papadakis, S. P., and Yu, H. (2022). Cordycepin as a promising inhibitor of SARS-CoV-2 RNA dependent RNA polymerase (RdRp). *Curr. Med. Chem.* 29 (1), 152–162. doi:10.2174/0929867328666210820114025
- Cui, J., and Jia, J. (2021). Discovery of juglone and its derivatives as potent SARS-CoV-2 main proteinase inhibitors. *Eur. J. Med. Chem.* 225, 113789. doi:10.1016/j.ejmech.2021.113789
- Caohuy, H., Eidelman, O., Chen, T., Liu, S., Yang, Q., Bera, A., et al. (2021). Common cardiac medications potently inhibit ACE2 binding to the SARS-CoV-2 Spike, and block virus penetration and infectivity in human lung cells. *Sci. Rep.* 11, 22195. doi:10.1038/s41598-021-01690-9
- Caohuy, H., Eidelman, O., Chen, T., Yang, Q., Walton, N. I., Pollard, H. B., et al. (2022). Inflammation in the COVID-19 airway is due to inhibition of CFTR signaling by the SARS-CoV-2 Spike protein. *bioRxiv* [Preprint]. doi:10.1101/2022.01.18.476803
- Chable-Bessia, C., Boullé, C., Neyret, A., Swain, J., Hénaut, M., Merida, P., et al. (2022). Low selectivity indices of ivermectin and macrocyclic lactones on SARS-CoV-2 replication *in vitro*. *COVID* 2, 60–75. doi:10.3390/covid2010005
- Chandrasekar, A., Yu, J., McMahan, K., Jacob-Dolan, C., Liu, J., He, X., et al. (2022). Vaccine protection against the SARS-CoV-2 Omicron variant in macaques. *Cell* 185 (9), 1549–1555.e11. doi:10.1016/j.cell.2022.03.024
- Chen, Z. H., Han, Y. Y., Shang, Y. J., Zhuang, S. Y., Huang, J. N., Wu, B. Y., et al. (2021). Cordycepin ameliorates synaptic dysfunction and dendrite morphology damage of hippocampal CA1 via A1R in cerebral ischemia. *Front. Cell. Neurosci.* 15, 783478. doi:10.3389/fncel.2021.783478
- Chhetri, B. K., Tedbury, P. R., Sweeney-Jones, A. M., Mani, L., Soapi, K., Manfredi, C., et al. (2022). Marine natural products as leads against SARS-CoV-2 infection. *J. Nat. Prod.* 85, 657–665. doi:10.1021/acs.jnatprod.2c00015
- Chiou, W. C., Chen, J. C., Chen, Y. T., Yang, J. M., Hwang, L. H., Lyu, Y. S., et al. (2022). The inhibitory effects of PGG and EGCG against the SARS-CoV-2 3C-like protease. *Biochem. Biophys. Res. Commun.* 591, 130–136. doi:10.1016/j.bbrc.2020.12.106
- Chiou, W. C., Lu, H. F., Hsu, N. Y., Chang, T. Y., Chin, Y. F., Liu, P. C., et al. (2021). Ugonin J acts as a SARS-CoV-2 3C-like protease inhibitor and exhibits anti-inflammatory properties. *Front. Pharmacol.* 12, 720018. doi:10.3389/fphar.2021.720018
- Choi, S. J., Ryu, E., Lee, S., Huh, S., Shin, Y. S., Kang, B. W., et al. (2019). Adenosine induces EBV lytic reactivation through ADORA1 in EBV-associated gastric carcinoma. *Int. J. Mol. Sci.* 20 (6), 1286. doi:10.3390/ijms20061286
- Corona, A., Wycisk, K., Talarico, C., Manelfi, C., Milia, J., Cannalire, R., et al. (2022). Natural compounds inhibit SARS-CoV-2 nsp13 unwinding and ATPase enzyme activities. *ACS Pharmacol. Transl. Sci.* 5, 226–239. doi:10.1021/acspstsci.1c00253
- Corpetti, C., Del Re, A., Seguela, L., Palencia, I., Rurgo, S., De Conno, B., et al. (2021). Cannabidiol inhibits SARS-Cov-2 spike (S) protein-induced cytotoxicity and inflammation through a PPARY-dependent TLR4/NLRP3/Caspase-1 signaling suppression in Caco-2 cell line. *Phytother. Res.* 35 (12), 6893–6903. doi:10.1002/ptr.7302
- Cui, H. R., Chen, K. D., Zhang, X. Y., and Shang, H. C. (2021). Network pharmacology-based analysis on bioactive compounds and mechanisms in Yiqifumai formula in the treatment of heart failure. *TMR Mod. Herb. Med.* 4 (4), 27. doi:10.53388/mhm2021a1017001
- Cully, M. (2022). A tale of two antiviral targets—And the COVID-19 drugs that bind them. *Nat. Rev. Drug Discov.* 21 (1), 3–5. doi:10.1038/d41573-021-00202-8
- Cunningham, K. G., Manson, W. I. L. I. A. M., Spring, F. S., and Hutchinson, S. A. (1950). Cordycepin, a metabolic product isolated from cultures of *Cordyceps militaris* (Linn.) Link. *Nature* 166 (4231), 949. doi:10.1038/166949a0
- De Jin, X. A., Zhang, Y., Zhao, S., Duan, L., Duan, Y., Lian, F., et al. (2021). Potential mechanism prediction of herbal medicine for pulmonary fibrosis associated with SARS-CoV-2 infection based on network analysis and molecular docking. *Front. Pharmacol.* 12, 602218. doi:10.3389/fphar.2021.602218
- Del Rio, C., Omer, S. B., and Malani, P. N. (2022). Winter of omicron—the evolving COVID-19 pandemic. *JAMA* 327 (4), 319–320. doi:10.1001/jama.2021.24315
- Du, R., Cooper, L., Chen, Z., Lee, H., Rong, L., Cui, Q., et al. (2021). Discovery of chebulagic acid and punicalagin as novel allosteric inhibitors of SARS-CoV-2 3CLpro. *Antivir. Res.* 190, 105075. doi:10.1016/j.antiviral.2021.105075
- Du, Xinyi, Xu, Longxin, Ma, Yiming, Lu, Shuaiyao, Tang, Kegong, Qiao, Xiangyu, et al. (2022). Herbal inhibitors of SARS-CoV-2 Mpro effectively ameliorate acute lung injury in mice. *IUBMB Life* 74, 532–542. doi:10.1002/iub.2616
- Elebeedy, D., Badawy, I., Elmaaty, A. A., Saleh, M. M., Kandeil, A., Ghanem, A., et al. (2022). *In vitro* and computational insights revealing the potential inhibitory effect of Tanshinone IIA against influenza A virus. *Comput. Biol. Med.* 141, 105149. doi:10.1016/j.combiomed.2021.105149
- Esharkawy, E. R., Almalki, F., and Hadda, T. B. (2022). *In vitro* potential antiviral SARS-CoV-19-activity of natural product thymohydroquinone and dithymoquinone from *Nigella sativa*. *Bioorg. Chem.* 120, 105587. doi:10.1016/j.bioorg.2021.105587
- Gao, X., Qin, B., Chen, P., Zhu, K., Hou, P., Wojdyla, J. A., et al. (2021). Crystal structure of SARS-CoV-2 papain-like protease. *Acta Pharm. Sin. B* 11 (1), 237–245. doi:10.1016/j.apsb.2020.08.014
- Guisado-Vasco, P., Carralón-González, M. M., Aguarales-Gorines, J., Martí-Ballesteros, E. M., Sánchez-Manzano, M. D., Carnevali-Ruiz, D., et al. (2022). Plitidepsin as a successful rescue treatment for prolonged viral SARS-CoV-2 replication in a patient with previous anti-CD20 monoclonal antibody-mediated B cell depletion and chronic lymphocytic leukemia. *J. Hematol. Oncol.* 15, 4. doi:10.1186/s13045-021-01220-0
- Hillen, H. S., Kokic, G., Farnung, L., Dienemann, C., Tegunov, D., Cramer, P., et al. (2020). Structure of replicating SARS-CoV-2 polymerase. *Nature* 584 (7819), 154–156. doi:10.1038/s41586-020-2368-8
- Hoffmann, M., Kleine-Weber, H., Schroeder, S., Krüger, N., Herrler, T., Erichsen, S., et al. (2020). SARS-CoV-2 cell entry depends on ACE2 and TMPRSS2 and is blocked by a clinically proven protease inhibitor. *Cell* 181 (2), 271–280.e8. doi:10.1016/j.cell.2020.02.052
- Hossain, R., Sarkar, C., Hassan, S. M. H., Khan, R. A., Arman, M., Ray, P., et al. (2022). *In silico* screening of natural products as potential inhibitors of SARS-CoV-2 using molecular docking simulation. *Chin. J. Integr. Med.* 28 (3), 249–256. doi:10.1007/s11655-021-3504-5
- Hou, B., Zhang, Y. M., Liao, H. Y., Fu, L. F., Li, D. D., Zhao, X., et al. (2022). Target-based virtual screening and LC/MS-guided isolation procedure for identifying phloroglucinol-terpenoid inhibitors of SARS-CoV-2. *J. Nat. Prod.* 85 (2), 327–336. doi:10.1021/acs.jnatprod.1c00805

- Huang, Y., Zhou, W., Sun, J., Ou, G., Zhong, N. S., Liu, Z., et al. (2022). Exploring the potential pharmacological mechanism of hesperidin and glucosyl hesperidin against COVID-19 based on bioinformatics analyses and antiviral assays. *Am. J. Chin. Med.* 50 (2), 351–369. doi:10.1142/S0192415X22500148
- Ishida, J., Wang, H. K., Oyama, M., Cosentino, M. L., Hu, C. Q., Lee, K. H., et al. (2001). Anti-AIDS agents. 46.¹ Anti-HIV activity of harman, an anti-HIV principle from *Symplocos setchuensis*, and its derivatives. *J. Nat. Prod.* 64 (7), 958–960. doi:10.1021/np0101189
- Jin, Y. H., Jeon, S., Lee, J., Kim, S., Jang, M. S., Park, C. M., et al. (2021). Broad spectrum antiviral properties of cardiotonic steroids used as potential therapeutics for emerging coronavirus infections. *Pharmaceutics* 13 (11), 1839. doi:10.3390/pharmaceutics13111839
- Jin, Z., Du, X., Xu, Y., Deng, Y., Liu, M., Zhao, Y., et al. (2020). Structure of Mpro from SARS-CoV-2 and discovery of its inhibitors. *Nature* 582 (7811), 289–293. doi:10.1038/s41586-020-2223-y
- Kalil, A. C., Mehta, A. K., Patterson, T. F., Erdmann, N., Gomez, C. A., Jain, M. K., et al. (2021). Efficacy of interferon beta-1a plus remdesivir compared with remdesivir alone in hospitalised adults with COVID-19: A double-blind, randomised, placebo-controlled, phase 3 trial. *Lancet. Respir. Med.* 9 (12), 1365–1376. doi:10.1016/S2213-2600(21)00384-2
- Kato, Y., Higashiyama, A., Takaoka, E., Nishikawa, M., and Ikushiro, S. (2021). Food phytochemicals, epigallocatechin gallate and myricetin, covalently bind to the active site of the coronavirus main protease *in vitro*. *Adv. Redox Res.* 3, 100021. doi:10.1016/j.arres.2021.100021
- Kozlov, M. (2022). Merck's COVID pill loses its lustre: What that means for the pandemic. *Nature* [Epub ahead of print]. doi:10.1038/d41586-021-03667-0
- Lewis, D. S., Ho, J., Wills, S., Kwall, A., Sharma, A., Chavada, K., et al. (2022). Aloin isoforms (A and B) selectively inhibits proteolytic and deubiquitinating activity of papain like protease (PLpro) of SARS-CoV-2 *in vitro*. *Sci. Rep.* 12, 2145. doi:10.1038/s41598-022-06104-y
- Li, X., Gao, J., Li, M., Cui, H., Jiang, W., Tu, Z. C., et al. (2021a). Aromatic cadinane sesquiterpenoids from the fruiting bodies of *Phellinus pini* block SARS-CoV-2 Spike-ACE2 interaction. *J. Nat. Prod.* 84 (8), 2385–2389. doi:10.1021/acs.jnatprod.1c00426
- Li, Y., Li, B., Wang, P., and Wang, Q. (2021b). Traditional Chinese medicine, Qingfei Paidu decoction and xuanfei baidu decoction, inhibited cytokine production via NF- κ B signaling pathway in macrophages: Implications for coronavirus disease 2019 (COVID-19) therapy. *Front. Pharmacol.* 12, 722126. doi:10.3389/fphar.2021.722126
- Liang, X. X., Zhang, X. J., Zhao, Y. X., Feng, J., Zeng, J. C., Shi, Q. Q., et al. (2022). Aspulvins A–H, aspulvinone analogues with SARS-CoV-2 Mpro inhibitory and anti-inflammatory activities from an endophytic *Cladosporium* sp. *J. Nat. Prod.* 85 (4), 878–887. doi:10.1021/acs.jnatprod.1c01003
- Linington, R. G., Clark, B. R., Trimble, E. E., Almanza, A., Ureña, L. D., Kyle, D. E., et al. (2009). Antimalarial peptides from marine cyanobacteria: Isolation and structural elucidation of gallinamide A. *J. Nat. Prod.* 72 (1), 14–17. doi:10.1021/np8003529
- Liu, G., Du, W., Sang, X., Tong, Q., Wang, Y., Chen, G., et al. (2022). RNA G-quadruplex in TMPrSS2 reduces SARS-CoV-2 infection. *Nat. Commun.* 13, 1444. doi:10.1038/s41467-022-29135-5
- Liu, N., Li, S., Fan, K., Lu, T., and Li, T. (2020). The prevention and treatment of COVID-19 with Qingfei Paidu decoction in Shanxi China. *TMR Mod. Herb. Med.* 3 (3), 1–5.
- Lyu, M., Fan, G., Xiao, G., Wang, T., Xu, D., Gao, J., et al. (2021). Traditional Chinese medicine in COVID-19. *Acta Pharm. Sin. B* 11 (11), 3337–3363. doi:10.1016/j.apsb.2021.09.008
- Ma, C., Tan, H., Choza, J., Wang, Y., and Wang, J. (2022). Validation and invalidation of SARS-CoV-2 main protease inhibitors using the Flip-GFP and Protease-Glo luciferase assays. *Acta Pharm. Sin. B* 12 (4), 1636–1651. doi:10.1016/j.apsb.2021.10.026
- Ma, C., and Wang, J. (2022). Validation and invalidation of SARS-CoV-2 papain-like protease inhibitors. *ACS Pharmacol. Transl. Sci.* 5 (2), 102–109. doi:10.1021/acscptsci.1c00240
- Mengist, H. M., Fan, X., and Jin, T. (2020). Designing of improved drugs for COVID-19: Crystal structure of SARS-CoV-2 main protease Mpro. *Signal Transduct. Target. Ther.* 5, 67. doi:10.1038/s41392-020-0178-y
- Miller, B., Friedman, A. J., Choi, H., Hogan, J., McCammon, J. A., Hook, V., et al. (2014). The marine cyanobacterial metabolite gallinamide A is a potent and selective inhibitor of human cathepsin L. *J. Nat. Prod.* 77 (1), 92–99. doi:10.1021/np400727r
- Nasreen, S., Chung, H., He, S., Brown, K. A., Gubbay, J. B., Buchan, S. A., et al. (2022). Effectiveness of COVID-19 vaccines against symptomatic SARS-CoV-2 infection and severe outcomes with variants of concern in Ontario. *Nat. Microbiol.* 7 (3), 379–385. doi:10.1038/s41564-021-01053-0
- Nguyen, L. C., Yang, D., Nicolaescu, V., Best, T. J., Gula, H., Saxena, D., et al. (2022). Cannabidiol inhibits SARS-CoV-2 replication through induction of the host ER stress and innate immune responses. *Sci. Adv.* 8, eabi6110. doi:10.1126/sciadv.abi6110
- Ngwe Tun, M. M., Toume, K., Luvai, E., Nwe, K. M., Mizukami, S., Hirayama, K., et al. (2022). The discovery of herbal drugs and natural compounds as inhibitors of SARS-CoV-2 infection *in vitro*. *J. Nat. Med.* 76, 402–409. doi:10.1007/s11418-021-01596-w
- Nishiuchi, K., Ohashi, H., Nishioka, K., Yamasaki, M., Furuta, M., Mashiko, T., et al. (2022). Synthesis and antiviral activities of neoechinulin B and its derivatives. *J. Nat. Prod.* 85 (1), 284–291. doi:10.1021/acs.jnatprod.1c01120
- Ordóñez, A. A., Bullen, C. K., Villabona-Rueda, A. F., Thompson, E. A., Turner, M. L., Merino, V. F., et al. (2022). Sulforaphane exhibits antiviral activity against pandemic SARS-CoV-2 and seasonal HCoV-OC43 coronaviruses *in vitro* and in mice. *Commun. Biol.* 5, 242. doi:10.1038/s42003-022-03189-z
- Panggabean, J. A., Adiguna, S. B. P., Rahmawati, S. I., Ahmadi, P., Zainuddin, E. N., Bayu, A., et al. (2022). Antiviral activities of algal-based sulfated polysaccharides. *Molecules* 27 (4), 1178. doi:10.3390/molecules27041178
- Panya, A., Songprakhon, P., Panwong, S., Jantakee, K., Kaewkod, T., Tragoolpua, Y., et al. (2021). Cordycepin inhibits virus replication in dengue virus-infected Vero cells. *Molecules* 26 (11), 3118. doi:10.3390/molecules26113118
- Pokharkar, O., Lakshmanan, H., Zyryanov, G., and Tsurkan, M. (2022). *In silico* evaluation of antifungal compounds from marine sponges against COVID-19-associated mucormycosis. *Mar. Drugs* 20 (3), 215. doi:10.3390/md20030215
- Prassas, I., and Diamandis, E. P. (2008). Novel therapeutic applications of cardiac glycosides. *Nat. Rev. Drug Discov.* 7 (11), 926–935. doi:10.1038/nrd2682
- Quintana, V. M., Piccini, L. E., Zénere, J. D. P., Damonte, E. B., Ponce, M. A., Castilla, V., et al. (2016). Antiviral activity of natural and synthetic β -carbolines against dengue virus. *Antivir. Res.* 134, 26–33. doi:10.1016/j.antiviral.2016.08.018
- Rabie, A. M. (2022). Potent inhibitory activities of the adenosine analogue cordycepin on SARS-CoV-2 replication. *ACS Omega* 7, 2960–2969. doi:10.1021/acsomega.1c05998
- Reis, G., Silva, E. A., Silva, D. C., Thabane, L., Milagres, A. C., Ferreira, T. S., et al. (2022). Effect of early treatment with ivermectin among patients with Covid-19. *N. Engl. J. Med.* 386, 1721–1731. doi:10.1056/NEJMoa2115869
- Rodon, J., Muñoz-Basagoiti, J., Perez-Zsolt, D., Noguera-Julian, M., Paredes, R., Mateu, L., et al. (2021). Identification of plitidepsin as potent inhibitor of SARS-CoV-2-induced cytopathic effect after a drug repurposing screen. *Front. Pharmacol.* 12, 646676. doi:10.3389/fphar.2021.646676
- Sa-Ngiamsumtorn, K., Suksatu, A., Pewkiang, Y., Thongsri, P., Kanjanasirirat, P., Manopwisedjaroen, S., et al. (2021). Anti-SARS-CoV-2 activity of *Andrographis paniculata* extract and its major component Andrographolide in human lung epithelial cells and cytotoxicity evaluation in major organ cell representatives. *J. Nat. Prod.* 84, 1261–1270. doi:10.1021/acs.jnatprod.0c01324
- Saadth, M. J., Almaaytah, A. M., Alaraj, M., Dababneh, M. F., Sa'adeh, I., Aldalaen, S. M., et al. (2021). Punicalagin and zinc (II) ions inhibit the activity of SARS-CoV-2 3CL-protease *in vitro*. *Eur. Rev. Med. Pharmacol. Sci.* 25 (10), 3908–3913. doi:10.26355/eurrev_202105_25958
- Sachse, M., Tenorio, R., de Castro, I. F., Muñoz-Basagoiti, J., Perez-Zsolt, D., Raich-Regué, D., et al. (2022). Unraveling the antiviral activity of plitidepsin against SARS-CoV-2 by subcellular and morphological analysis. *Antivir. Res.* 200, 105270. doi:10.1016/j.antiviral.2022.105270
- Sahoo, A., Furloria, S., Swain, S. S., Panda, S. K., Sekar, M., Subramaniam, V., et al. (2021). Potential of marine terpenoids against SARS-CoV-2: An *in silico* drug development approach. *Biomedicine* 9 (11), 1505. doi:10.3390/biomedicine9111505
- Schulte, B., König, M., Escher, B. I., Wittenburg, S., Proj, M., Wolf, V., et al. (2022). Andrographolide derivatives target the KEAP1/NRF2 axis and possess potent anti-SARS-CoV-2 activity. *ChemMedChem* 17 (5), e202100732. doi:10.1002/cmdc.202100732
- Schultz, D. C., Johnson, R. M., Ayyanathan, K., Miller, J., Whig, K., Kamalia, B., et al. (2022). Pyrimidine inhibitors synergize with nucleoside analogues to block SARS-CoV-2. *Nature* 604, 134–140. doi:10.1038/s41586-022-04482-x
- Scott, L., Hsiao, N. Y., Moyo, S., Singh, L., Tegally, H., Dor, G., et al. (2021). Track Omicron's spread with molecular data. *Science* 374 (6574), 1454–1455. doi:10.1126/science.abn4543
- Sharma, V., Sharma, A., and Bharate, S. B. (2021). Natural products in mitigation of SARS-CoV infections. *Curr. Med. Chem.* 28 (22), 4454–4483. doi:10.2174/0929867327666201027153940
- Shen, Y., Cai, H., Ma, S., Zhu, W., Zhao, H., Li, J., et al. (2022). Telocinobufagin has antitumor effects in non-small-cell lung cancer by inhibiting STAT3 signaling. *J. Nat. Prod.* 85 (4), 765–775. doi:10.1021/acs.jnatprod.1c00761

- Socolsky, C., Domínguez, L., Asakawa, Y., and Bardón, A. (2012). Unusual terpenylated acylphloroglucinols from *Dryopteris wallichiana*. *Phytochemistry* 80, 115–122. doi:10.1016/j.phytochem.2012.04.017
- Sourimant, J., Lieber, C. M., Aggarwal, M., Cox, R. M., Wolf, J. D., Yoon, J. J., et al. (2022). 4'-Fluorouridine is an oral antiviral that blocks respiratory syncytial virus and SARS-CoV-2 replication. *Science* 375 (6577), 161–167. doi:10.1126/science.abj5508
- Su, H., Yao, S., Zhao, W., Zhang, Y., Liu, J., Shao, Q., et al. (2021). Identification of pyrogallol as a warhead in design of covalent inhibitors for the SARS-CoV-2 3CL protease. *Nat. Commun.* 12, 3623. doi:10.1038/s41467-021-23751-3
- Suručić, R., Travar, M., Petković, M., Tubić, B., Stojilković, M. P., Grabež, M., et al. (2021). Pomegranate peel extract polyphenols attenuate the SARS-CoV-2 S-glycoprotein binding ability to ACE2 receptor: *In silico* and *in vitro* studies. *Bioorg. Chem.* 114, 105145. doi:10.1016/j.bioorg.2021.105145
- Taori, K., Liu, Y., Paul, V. J., and Luesch, H. (2009). Combinatorial strategies by marine cyanobacteria: Symplostatin 4, an antimitotic natural dolastatin 10/15 hybrid that synergizes with the coproduced HDAC inhibitor largazole. *ChemBioChem* 10 (10), 1634–1639. doi:10.1002/cbic.200900192
- Thissera, B., Sayed, A. M., Hassan, M. H., Abdelwahab, S. F., Amaeze, N., Semler, V. T., et al. (2021). Bioguided isolation of cyclophenin analogues as potential SARS-CoV-2 Mpro inhibitors from *Penicillium citrinum* TDPEF34. *Biomolecules* 11 (9), 1366. doi:10.3390/biom11091366
- Tian, H. Y., Ruan, L. J., Yu, T., Zheng, Q. F., Chen, N. H., Wu, R. B., et al. (2017). Bufoprostenin A and Bufogargarizin C, steroids with rearranged skeletons from the toad *Bufo fargarizans*. *J. Nat. Prod.* 80 (4), 1182–1186. doi:10.1021/acs.jnatprod.6b01018
- Toelzer, C., Gupta, K., Yadav, S. K., Borucu, U., Davidson, A. D., Kavanagh Williamson, M., et al. (2020). Free fatty acid binding pocket in the locked structure of SARS-CoV-2 spike protein. *Science* 370 (6517), 725–730. doi:10.1126/science.abd3255
- Tsai, Y. C., Lee, C. L., Yen, H. R., Chang, Y. S., Lin, Y. P., Huang, S. H., et al. (2020). Antiviral action of tryptanthrin isolated from *Strobilanthes cusia* leaf against human coronavirus NL63. *Biomolecules* 10 (3), 366. doi:10.3390/biom10030366
- Ueda, Y., Mori, K., Satoh, S., Dansako, H., Ikeda, M., Kato, N., et al. (2014). Anti-HCV activity of the Chinese medicinal fungus *Cordyceps militaris*. *Biochem. Biophys. Res. Commun.* 447 (2), 341–345. doi:10.1016/j.bbrc.2014.03.150
- Urda, L., Kreuter, M. H., Drewe, J., Boonen, G., Butterweck, V., Klimkait, T., et al. (2022). The petasites hybridus CO2 extract (Ze 339) blocks SARS-CoV-2 replication *in vitro*. *Viruses* 14, 106. doi:10.3390/v14010106
- van Breemen, R. B., Muchiri, R. N., Bates, T. A., Weinstein, J. B., Leier, H. C., Farley, S., et al. (2022). Cannabinoids block cellular entry of SARS-CoV-2 and the emerging variants. *J. Nat. Prod.* 85, 176–184. doi:10.1021/acs.jnatprod.1c00946
- Walls, A. C., Park, Y. J., Tortorici, M. A., Wall, A., McGuire, A. T., Veesler, D., et al. (2020). Structure, function, and antigenicity of the SARS-CoV-2 spike glycoprotein. *Cell* 181 (2), 281–292. doi:10.1016/j.cell.2020.02.058
- Wang, K., Su, B. O., Wang, Z., Wu, M., Li, Z., Hu, Y., et al. (2010). Synthesis and antiviral activities of phenanthroindolizidine alkaloids and their derivatives. *J. Agric. Food Chem.* 58 (5), 2703–2709. doi:10.1021/jf902543r
- Wang, Z. (2019). Advances in the asymmetric total synthesis of natural products using chiral secondary amine catalyzed reactions of α , β -unsaturated aldehydes. *Molecules* 24 (18), 3412. doi:10.3390/molecules24183412
- Wang, Z., and Yang, L. (2022a). Broad-spectrum prodrugs with anti-SARS-CoV-2 activities: Strategies, benefits, and challenges. *J. Med. Virol.* 94 (4), 1373–1390. doi:10.1002/jmv.27517
- Wang, Z., and Yang, L. (2021). Chinese herbal medicine: Fighting SARS-CoV-2 infection on all fronts. *J. Ethnopharmacol.* 270, 113869. doi:10.1016/j.jep.2021.113869
- Wang, Z., and Yang, L. (2020a). GS-5734: A potentially approved drug by FDA against SARS-cov-2. *New J. Chem.* 44 (29), 12417–12429. doi:10.1039/d0nj02656e
- Wang, Z., and Yang, L. (2022b). In the age of Omicron variant: Paxlovid raises new hopes of COVID-19 recovery. *J. Med. Virol.* 94 (5), 1766–1767. doi:10.1002/jmv.27540
- Wang, Z., and Yang, L. (2022c). Post-acute sequelae of SARS-CoV-2 infection: A neglected public health issue. *Front. Public Health* 10, 908757. doi:10.3389/fpubh.2022.908757
- Wang, Z., and Yang, L. (2020b). Turning the tide: Natural products and natural-product-inspired chemicals as potential counters to SARS-CoV-2 infection. *Front. Pharmacol.* 11, 1013. doi:10.3389/fphar.2020.01013
- Wang, Z., Yang, L., and Zhao, X. E. (2021a). Co-crystallization and structure determination: An effective direction for anti-SARS-CoV-2 drug discovery. *Comput. Struct. Biotechnol. J.* 19, 4684–4701. doi:10.1016/j.csbj.2021.08.029
- Wang, Z., Ye, F., Feng, Y., Xiao, W., Song, H., Zhao, L., et al. (2021b). Discovery and nanosized preparations of (S, R)-tylophorine malate as novel anti-SARS-CoV-2 agents. *ACS Med. Chem. Lett.* 12 (11), 1840–1846. doi:10.1021/acsmchemlett.1c00481
- Wei, P., Wang, K., Luo, C., Huang, Y., Misilimu, D., Wen, H., et al. (2021). Cordycepin confers long-term neuroprotection via inhibiting neutrophil infiltration and neuroinflammation after traumatic brain injury. *J. Neuroinflammation* 18 (1), 137. doi:10.1186/s12974-021-02188-x
- Wei, X. X., Zhao, M. Z., Zhao, C., Zhang, X., Qiu, R., Lin, Y., et al. (2020). The global registry of COVID-19 clinical trials: Indicating the design of traditional Chinese medicine clinical trials. *TMR Mod. Herb. Med.* 3 (3), 140–146.
- White, K. M., Rosales, R., Yildiz, S., Kehr, T., Miorin, L., Moreno, E., et al. (2021). Plitidepsin has potent preclinical efficacy against SARS-CoV-2 by targeting the host protein eEF1A. *Science* 371 (6532), 926–931. doi:10.1126/science.abf4058
- World Health Organization WHO coronavirus (COVID-19) dashboard, 2022. Available at: <https://covid19.who.int/> (Assessed April 22, 2022).
- Wu, H., Cheng, H., Luo, S., Peng, C., Zhou, A., Chen, Z., et al. (2022a). Use of cellular metabolomics and lipidomics to decipher the mechanism of Huachansu injection-based intervention against human hepatocellular carcinoma cells. *J. Pharm. Biomed. Anal.* 212, 114654. doi:10.1016/j.jpba.2022.114654
- Wu, Q., Yan, S., Wang, Y., Li, M., Xiao, Y., Li, Y., et al. (2022b). Discovery of 4'-O-methylscutellarein as a potent SARS-CoV-2 main protease inhibitor. *Biochem. Biophys. Res. Commun.* 604, 76–82. doi:10.1016/j.bbrc.2022.03.052
- Wu, Y., Xu, L., Cao, G., Min, L., and Dong, T. (2022c). Effect and mechanism of Qingfei Paidu decoction in the management of pulmonary fibrosis and COVID-19. *Am. J. Chin. Med.* 50 (1), 33–51. doi:10.1142/S0192415X22500021
- Xiao, T., Cui, M., Zheng, C., Zhang, P., Ren, S., Bao, J., et al. (2022). Both baicalin and gallic acid effectively inhibit SARS-CoV-2 replication by targeting Mpro and Sepsis in mice. *Inflammation* 45, 1076–1088. doi:10.1007/s10753-021-01602-z
- Xiao, T., Wei, Y., Cui, M., Li, X., Ruan, H., Zhang, L., et al. (2021). Effect of dihydromyricetin on SARS-CoV-2 viral replication and pulmonary inflammation and fibrosis. *Phytomedicine* 91, 153704. doi:10.1016/j.phymed.2021.153704
- Yan, G., Li, D., Lin, Y., Fu, Z., Qi, H., Liu, X., et al. (2021). Development of a simple and miniaturized sandwich-like fluorescence polarization assay for rapid screening of SARS-CoV-2 main protease inhibitors. *Cell. Biosci.* 11, 199. doi:10.1186/s13578-021-00720-3
- Yang, L. J., Chen, R. H., Hamdoun, S., Coghi, P., Ng, J. P., Zhang, D. W., et al. (2021a). Corilagin prevents SARS-CoV-2 infection by targeting RBD-ACE2 binding. *Phytomedicine* 87, 153591. doi:10.1016/j.phymed.2021.153591
- Yang, L., and Wang, Z. (2021). Natural products, alone or in combination with FDA-approved drugs, to treat COVID-19 and lung cancer. *Biomedicines* 9 (6), 689. doi:10.3390/biomedicines9060689
- Yang, Y., Yang, P., Huang, C., Wu, Y., Zhou, Z., Wang, X., et al. (2021b). Inhibitory effect on SARS-CoV-2 infection of neferine by blocking Ca²⁺-dependent membrane fusion. *J. Med. Virol.* 93 (10), 5825–5832. doi:10.1002/jmv.27117
- Yi, Y., Li, J., Lai, X., Zhang, M., Kuang, Y., Bao, Y. O., et al. (2022). Natural triterpenoids from licorice potentially inhibit SARS-CoV-2 infection. *J. Adv. Res.* 36, 201–210. doi:10.1016/j.jare.2021.11.012
- Yin, W., Mao, C., Luan, X., Shen, D. D., Shen, Q., Su, H., et al. (2020). Structural basis for inhibition of the RNA-dependent RNA polymerase from SARS-CoV-2 by remdesivir. *Science* 368 (6498), 1499–1504. doi:10.1126/science.abc1560
- Yu, H., Hong, X., Liu, L., Wu, Y., Xie, X., Fang, G., et al. (2021). Cordycepin decreases ischemia/reperfusion injury in diabetic hearts via upregulating AMPK/Mfn2-dependent mitochondrial fusion. *Front. Pharmacol.* 12, 754005. doi:10.3389/fphar.2021.754005
- Zhan, Y. Q., Chen, R. F., Ma, Q. H., Zheng, J., Deng, X., Yang, W., et al. (2022). Efficacy and safety of phyllirin (KD-1) capsule in the treatment of moderate COVID-19: Protocol for a randomized controlled trial. *TMR Mod. Herb. Med.* 5 (1), 5. doi:10.53388/mhm2021p1204001
- Zhang, S., Pei, R., Li, M., Su, H., Sun, H., Ding, Y., et al. (2022). Cocktail polysaccharides isolated from *Ecklonia kurome* against the SARS-CoV-2 infection. *Carbohydr. Polym.* 275, 118779. doi:10.1016/j.carbpol.2021.118779
- Zhao, J., Ma, Q., Zhang, B., Guo, P., Wang, Z., Liu, Y., et al. (2021). Exploration of SARS-CoV-2 3CLpro inhibitors by virtual screening methods, FRET detection, and CPE assay. *J. Chem. Inf. Model.* 61 (12), 5763–5773. doi:10.1021/acs.jcim.1c01089
- Zhong, B., Peng, W., Du, S., Chen, B., Feng, Y., Hu, X., et al. (2022). Oridonin inhibits SARS-CoV-2 by targeting its 3C-Like protease. *Small Sci.* 2, 2100124. doi:10.1002/smcs.202100124
- Zhou, X., Luo, L., Dressel, W., Shadier, G., Krumbiegel, D., Schmidtke, P., et al. (2008). Cordycepin is an immunoregulatory active ingredient of *Cordyceps sinensis*. *Am. J. Chin. Med.* 36 (05), 967–980. doi:10.1142/S0192415X08006387



OPEN ACCESS

EDITED BY

Hidayat Hussain,
Leibniz Institute of Plant Biochemistry,
Germany

REVIEWED BY

Dario A. Vitturi,
University of Alabama at Birmingham,
United States
Abimael González-Hernández,
Universidad Nacional Autónoma de
México, Mexico

*CORRESPONDENCE

Marina Filimonova,
vladimirovna.fil@gmail.com

SPECIALTY SECTION

This article was submitted to
Experimental Pharmacology and Drug
Discovery,
a section of the journal
Frontiers in Pharmacology

RECEIVED 15 July 2022

ACCEPTED 16 September 2022

PUBLISHED 30 September 2022

CITATION

Filimonova M, Shevchenko L,
Makarchuk V, Saburova A, Shegay P,
Kaprin A, Ivanov S and Filimonov A
(2022), Preclinical studies of NOS
inhibitor T1059 vasopressor activity on
the models of acute hemorrhagic shock
in rats and dogs.
Front. Pharmacol. 13:995272.
doi: 10.3389/fphar.2022.995272

COPYRIGHT

© 2022 Filimonova, Shevchenko,
Makarchuk, Saburova, Shegay, Kaprin,
Ivanov and Filimonov. This is an open-
access article distributed under the
terms of the [Creative Commons
Attribution License \(CC BY\)](https://creativecommons.org/licenses/by/4.0/). The use,
distribution or reproduction in other
forums is permitted, provided the
original author(s) and the copyright
owner(s) are credited and that the
original publication in this journal is
cited, in accordance with accepted
academic practice. No use, distribution
or reproduction is permitted which does
not comply with these terms.

Preclinical studies of NOS inhibitor T1059 vasopressor activity on the models of acute hemorrhagic shock in rats and dogs

Marina Filimonova^{1*}, Ljudmila Shevchenko¹,
Victoria Makarchuk¹, Alina Saburova¹, Petr Shegay²,
Andrey Kaprin^{2,3}, Sergey Ivanov¹ and Alexander Filimonov¹

¹A. Tsyb Medical Radiological Research Center—Branch of the National Medical Research Radiological Center of the Ministry of Health of the Russian Federation, Obninsk, Russia, ²National Medical Research Radiological Center of the Ministry of Health of the Russian Federation, Obninsk, Russia, ³Medical Institute (RUDN University), Peoples' Friendship University of Russia, Moscow, Russia

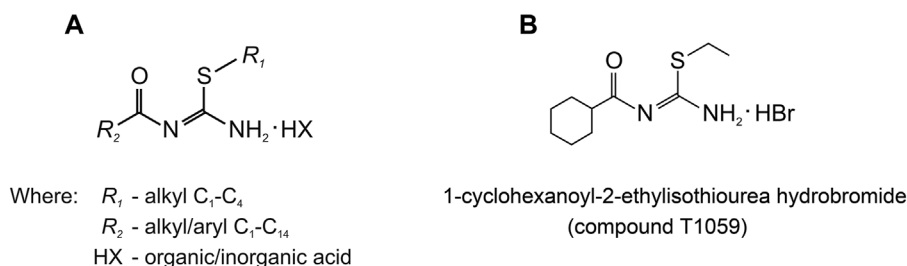
The development of new effective and safe vasopressors is one of the ways to increase the effectiveness of the treatment of hypotensive disorders, the severe forms of which remain a common cause of death in all countries of the world. Previously, we synthesized the original compound T1059, a selective inhibitor of eNOS/iNOS which has a pronounced vasoconstrictive effect. Here we show its vasopressor activity in models of the early stage of acute hemorrhagic shock in rats and dogs, as part of preclinical studies. The results indicate NOS inhibitor T1059 as a potent long-acting vasopressor. Its single parenteral administration in sufficiently safe doses (1/50–1/9 LD₅₀), caused in rats and dogs a rapid increase in vascular tone, accompanied by a prolonged hypertensive effect (within 90–120 min in rats, and within 115 min in dogs). The repeated administration of T1059 at low doses (1/3 of the first dose) made it possible to considerably (by at least 60 min) prolong a significant vasopressor effect. In all schemes, T1059 administration considerably inhibited the development of threatening cardiorespiratory disorders and significantly ($p = 0.0026–0.0098$) increased the short-term survival of experimental animals, formally extending the duration of the “golden hour” by 2 times. These data indicate that NOS inhibitors and, in particular, compound T1059, are able to create new opportunities in the treatment of hypotensive disorders, including the provision of assistance at the prehospital stage of treatment of such pathologies.

KEYWORDS

hemorrhagic shock, *in vivo* models, vasopressor activity, NOS inhibitor, rats, dogs

Abbreviations: NO, nitric oxide; NOS, nitric oxide synthase; BL, blood loss; BP, blood pressure; SBP and DBP, systolic and diastolic BP; HF, heart frequency; HR, respiratory frequency.

Molecular structure of studied compounds

**FIGURE 1**

(A) General chemical structure of N,S-substituted isothioureas, synthesized in the A. Tsyb MRRC laboratory of radiation pharmacology, exhibiting significantly NOS-inhibiting activity. (B) Molecular structure of 1-cyclohexanoyl-2-ethylisothiourea hydrobromide (compound T1059).

Introduction

The lab of radiation pharmacology of the A. Tsyb Medical Radiological Research Center (A. Tsyb MRRC) has long been interested in the chemistry and pharmacology of signaling pathway modifiers, including NO donors and NOS inhibitors. So, some time ago, while screening linear and cyclic isothioureas, we identified and synthesized a large group of isothiourea derivatives (Figure 1A) that are competitive inhibitors of NOS (Proskuryakov et al., 2002, 2005; Proskuryakov et al., 2010; Filimonova et al., 2012a). Further, we found that some compounds of this group (such as T1023, T1082, T1084) are promising for further pharmacological development—as hypoxic radioprotectors that provide effective prevention of hematopoietic and gastrointestinal acute radiation syndromes, and radiotherapy complications (Filimonova et al., 2020b, 2021, 2022b; Saburova et al., 2020), as well as antitumor, antiangiogenic agents (Filimonova et al., 2019a; 2019b; 2022a).

Along with this, one of the studied compounds, T1059, 1-cyclohexanoyl-2-ethylisothiourea hydrobromide (Figure 1B), demonstrated a high affinity for eNOS and iNOS, as well as a pronounced vasotropic activity. In preliminary studies in rats, compound T1059 had a long-term vasoconstrictive effect at a single parenteral administration (i.p, i.v. and i.m.) at relatively safe doses (5–30 mg/kg; 1/50–1/10 LD_{50}) (Filimonova et al., 2018). 2–5 min after T1059 administration and the next 70–140 min, an increase in peripheral vascular resistance (by 30%–60%) in rats was recorded. Later on, all changes in these animals normalized independently as the vascular tone weakened. In rats with various hypovolemic disorders (on models of acute hemorrhagic shock and acute endotoxemic shock), T1059 at such doses and methods of administration realized the same long-term vasoconstrictor effect (Filimonova et al., 2020a). Under these conditions, T1059-induced vasoconstriction did not cause a significant baroreflex response in rats. On these models, T1059 effect was

accompanied by a pronounced, stable hypertensive effect. It is duration significantly (7–10 times) exceeded the duration of the effects of high doses of phenylephrine with the same methods of administration.

These experimental data justified the feasibility of conducting preclinical studies of pharmacological activity and safety of T1059 as a vasopressor agent (state contract with the Ministry of Education and Science of the Russian Federation #14.N08.11.0078). The vascular and hemodynamic effects of T1059 were studied in models of hypotensive disorders of various etiology and course in small and large laboratory animals—acute hemorrhagic shock and acute endotoxemic shock in rats and dogs, gangliolytic hypotension and refractory endotoxemic vasoplegia in rats. A vast amount of data has been obtained that needs a detailed presentation. In this publication, we present the first part of the experimental data—studies on models of acute hemorrhagic hypotension in rats and dogs. We also plan to present the results obtained on models of vasodilatory disorders in a subsequent publication.

Materials and methods

Animals

Male Wistar rats (3–4 months old, 180–260 g) and male and female outbred dogs (2–4 years old, 9–19 kg) were used in these studies. Rats were purchased from the Biomedical Technology Scientific Center of Federal Biomedical Agency of Russia. Rats were housed in the vivarium of the A. Tsyb MRRC in T-3 cages under natural light conditions with forced ventilation 16 times per hour, at a room temperature 18–20°C and relative humidity 40–70%. Animals had free access to the filtered (Aquaphor, Russia) water and feed for rodents PK-120–1 (Laboratorsnab, Russia). Outbred dogs were received from the sponsor according to the Donation Agreement. Dogs were kept in single aviaries in

the A. Tsyb MRRC vivarium under similar conditions of lighting, temperature and air ventilation. The dogs were fed twice a day. The dogs' diet included Now Natural Holistic adult dog food (Petcurean, Canada), raw meat, boiled fish, meat-based soups with cereals and vegetables. Animal studies were approved by the A. Tsyb MRRC Ethical Committee, were performed in accordance with generally accepted standards for the animal treatment, based on standard operating procedures of the A. Tsyb MRRC, in accordance with the rules and requirements of the European Convention ETS/STE No 123 and international standard GLP (OECD Guide 1:1998).

T1059: Synthesis, toxicological and biochemical properties, administration

Method of T1059 synthesis was developed in the laboratory of radiation pharmacology A. Tsyb MRRC (Filimonova et al., 2015, 2018). It represents the reaction between 1-cyclohexanoylthiourea and the excess of bromethyl in an inert organic solvent at elevated temperature. Synthesis example: a mixture of 1-cyclohexanoylthiourea (3.7 g, 20 mmol), ethyl bromide (4.4 g, 40 mmol) and dry acetonitrile (10 ml) in a sealed ampoule was heated in a boiling water bath for 20 h, the residue was filtered off and recrystallized twice from 4-methyl-2-pentanone to yield a crystalline T1059 (2.8 g, 48.5%). These methods ensured a stable quality of a substance with a content of 1-cyclohexanoyl-2-ethylisothiourea hydrobromide of more than 95% and a total content of related and extraneous impurities of less than 0.5% of dry weight. Compound T1059 is a white crystalline powder substance that is easily soluble in water, acetone and chloroform, and insoluble in hexane. Its molecular weight is 295.2; spectra ^1H PMR (500 MHz, DMSO- d_6 , δ): 1.3 (m, 9H); 1.62–1.84 (m, 5H); 3.65 (m, 1H); 10.8 (b, 3H). Melting temperature is 123–125°C. In the benzene-ethanol-triethylamine system 9:1:0.1 the R_f value is 0.35. Its 1% aqueous solution is transparent and colorless with pH = 3.92 at 20°C.

Compound T1059 belong to the “moderately hazardous” class (Berezovskaya, 2003; Gad, 2007). Its acute toxicity parameters LD_{10} , LD_{16} , LD_{50} and LD_{84} estimated by the Litchfield-Wilcoxon method (Mironov, 2012) are 260, 278, 310 and 362 mg/kg i. p., respectively, for Wistar rats. With i.g. administration, the sensitivity of rats to T1059 toxic effect is reduced by 5–7 times, so in this case its LD_{10} , LD_{16} , LD_{50} , and LD_{84} values are 1,320, 1,440, 2030 and 3,480 mg/kg, respectively. With long-term administration, T1059 does not show cumulative toxic properties [cumulative toxicity Lim test (Lim et al., 1961)].

In radiological studies *in vitro* on isolated recombinant human NOS isoforms by the rate of accumulation of [^3H]-L-citrulline (van Eijk et al., 2007) T1059 effectively inhibits NOS with significant selectivity (15–30 times) to endothelial and

inducible isoforms—its IC_{50} values for nNOS, iNOS and eNOS are 60.1, 1.8 and 3.3 μM , respectively (Filimonova et al., 2018). The mechanism of inhibition of all NOS isoforms is competitive, fully reversible. Its NOS inhibitory activity *in vivo* is quite pronounced. According to EPR spectrometry with a diethyldithiocarbamate trap (Hogg, 2010), already in the first 30 min after T1059 single i.p. administration at doses 1.5–30 mg/kg, a significant decrease in spontaneous and lipopolysaccharide-induced NO production was observed in various tissues of mice. Increasing the dose of T1059 causes both the increase of the degree (from 55% to 97%) and the duration (from 1 to 4–5 h) of suppression of NO endogenous production (Filimonova et al., 2018).

In this study, T1059 was used as aqueous solutions for single and double parenteral (i.v. and i.m.) administration. T1059 solutions were prepared *ex tempore* based on water for injection (Dalchimpharm, Russia). In a rat model of acute hemorrhagic shock, T1059 was administered once, 5 or 10 mg/kg i.v. (1.0 ml/kg of 0.5% or 1% solutions; slowly, 0.1 ml/min); 30 mg/kg i.m. (2.0 ml/kg of 1.5% solution; slowly, 0.2 ml/min) or twice, 30 + 10 mg/kg i.m. (2.0 ml/kg + 0.66 ml/kg of 1.5% solution; slowly). The used doses of T1059 for rats were justified in preliminary studies in this model of hemorrhagic shock (Filimonova et al., 2020a). Control (untreated) rats received once i.v. 1.0 ml/kg of 0.9% sodium chloride for injections (Biochemist, Russia). In a model of acute hemorrhagic shock in dogs, T1059 was administered once, 3.2 mg/kg i.v. (0.25 ml/kg of 1.28% solution; slowly, 2.0 ml/min) or 9.5 mg/kg i.m. (0.5 ml/kg of 1.9% solution in two slow injections in both thighs). The doses of T1059 used in dogs were equivalent to those for rats, 10 mg/kg (i.v.) and 30 mg/kg (i.m.), taking into account the body surface area of laboratory animals (Mironov, 2012). Control (untreated) dogs received once i.v. or i.m. 0.25 ml/kg of 0.9% sodium chloride for injections.

Acute hemorrhagic hypotension models, study design

The vasopressor activity of T1059 was studied in models of acute severe hemorrhagic shock in rats and acute moderate hemorrhagic shock in dogs caused by massive blood loss (BL). In rat studies, animals were anesthetized (thiopental sodium, Sandoz, Austria; 60 mg/kg, i.p.), tracheostomy was placed, jugular vein and carotid arteries catheterizations were performed, invasive blood pressure (BP) sensors and ECG electrodes were connected, and heparin were injected (Heparin sodium, Ozon, Russia; 100 ME, i.v). After stabilization of the animal's condition, baseline ECG (standard leads) and indicators of systolic and diastolic BP (SBP and DBP), heart rate (HF) and respiratory rate (RF) were recorded using a polygraph RM-6000 (Nihon Kohden, Japan)

or the PowerLab 8/30 complex (ADInstruments, Australia). To reproduce acute severe hemorrhagic shock, blood was taken from the right carotid artery for 8–12 min in a volume of 25 ml/kg. For rats, this BL corresponds to a loss of 40% of circulating blood volume (Diehl et al., 2001). At the end of blood sampling, the registration of indicators was repeated. Then the control rats received a single i.v. injection of 0.9% sodium chloride solution (1 ml/kg), and the rats of the experimental groups were given a single injection of T1059: i.v.—at doses of 5 or 10 mg/kg (1.0 ml/kg of 0.5% or 1% solutions; slowly); i.m.—at dose of 30 mg/kg (2.0 ml/kg of 1.5% solution; slowly). Further recording of ECG and physiological parameters in these animals was continued for the next 120 min. In experiments with double i. m. administration of T1059, the first injection (30 mg/kg; 2.0 ml/kg of 1.5% solution; slowly) was given immediately after BL, and the second injection (10 mg/kg; 0.66 ml/kg of 1.5% solution; slowly)—after 70–140 min, at a time when the vasopressor effect from the first injection became weakened to a level of negligible. Further monitoring in these cases was continued until 60 min after the second injection. Euthanasia of anaesthetized rats that survived to the end of monitoring was carried out by air embolism.

For studies in dogs, animals were accustomed within 1 week to the manipulation room, short-term (10–30 min) fixations, BP measurement procedures and ECG recording. One day before the study, the hair on their limbs removed (trimmer Moser ChroMini Type 1,591, Germany) to access the necessary vessels. Baseline SBP, DBP, HF and RF were measured 30 min after sedation bromdihydrochlorophenylbenzodiazepine (elzepam, Ellara, Russia; 0.1 mg/kg, i.v.). BP и HF were measured in arteria brachialis using a veterinary tonometer petMAP graphic II (CardioCommand, United States). ECG registration was performed using a cardiograph Cardiofax GEM (Nihon Kohden, Japan). Then, controlled blood sampling in the amount of 20 ml/kg from vena cephalica or vena saphenus lateral tarsal was performed for 15–20 min using Helmflon venous catheters (20 g 1.1 × 33 mm; Helm, Germany). For dogs, such BL corresponds to a loss of 25% of circulating blood volume (Diehl et al., 2001). At the end of blood sampling, complete hemostasis was ensured and ECG and physiological parameters were recorded again. Then, the control animals received a single i.v. injection of 0.9% sodium chloride solution (0.25 ml/kg), and the dogs of the experimental groups received T1059 once: i.v.—at dose 3.2 mg/kg (0.25 ml/kg of 1.28% solution; slowly); i.m.—at dose 9.5 mg/kg (0.5 ml/kg of 1.9% solution in two injections, slowly, in both thighs). Subsequent recording of ECG and physiological parameters was continued for 120 min. Further observations and daily examination of these animals were carried out for the next 15 days.

T1059 vasopressor activity was assessed by intergroup statistical comparison of hemodynamic parameters in untreated and T1059-treated animals, as well as by the

quantitative severity and duration of the hypertensive effect. In addition, the effect of T1059 on the clinical course of the early stage of acute severe hemorrhagic shock in rats was indirectly assessed by the dynamics of ECG, external respiration parameters and Kaplan-Meier diagrams of short-term (2–3 h) survival.

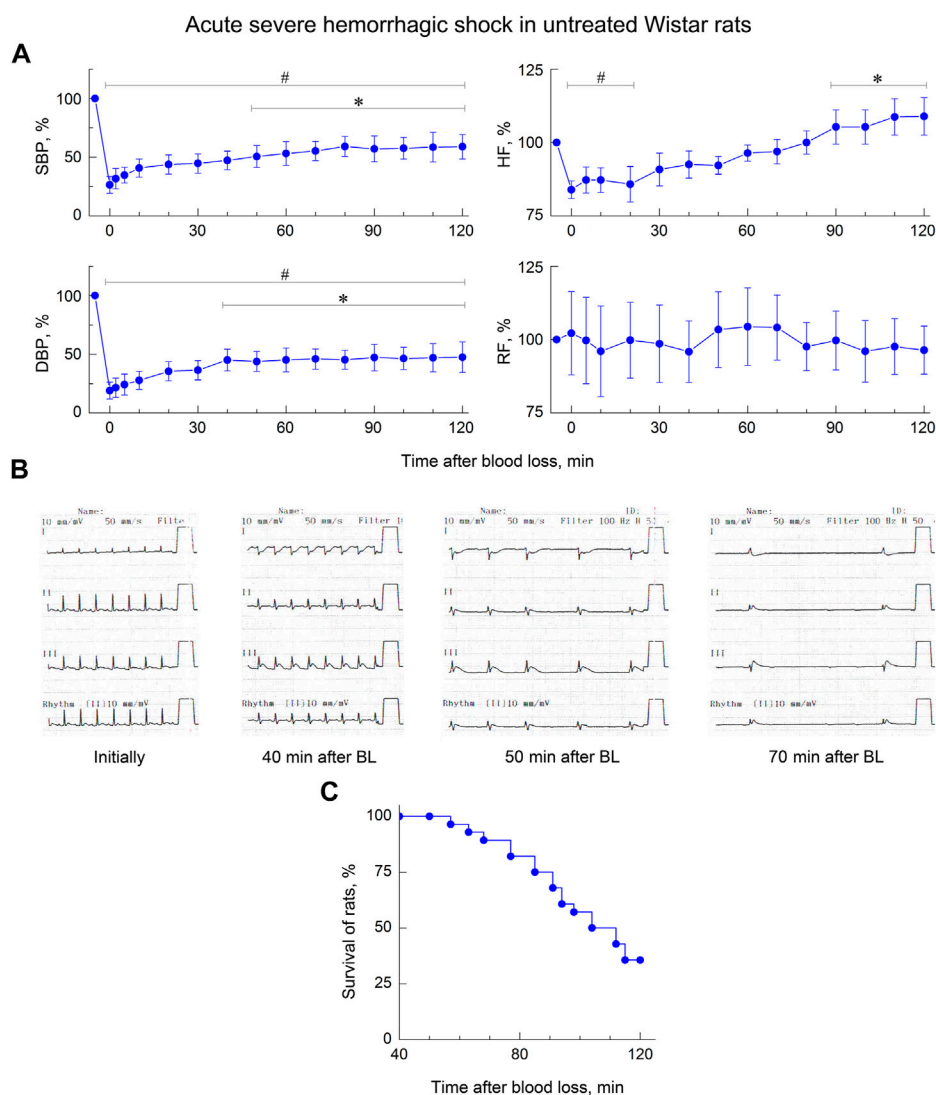
Statistical analysis

Standard parameters of variation statistics were calculated for all experimental data and their values are given (including graphically) as $M \pm SD$. For multiple intergroup and intragroup comparisons of physiological parameters, the level of significance of differences was assessed using the Kruskal-Wallis ANOVA by ranks with post hoc Mann-Whitney *U* test with Bonferroni-Holm corrections for multiple comparison (Holm, 1979); and for multiple comparisons of survival diagrams, using the χ^2 test with post hoc Cox F test with Bonferroni-Holm corrections. In all cases, effects or differences were considered statistically significant at the 5% level.

Results

Effects of T1059 on the model of acute severe hemorrhagic shock in rats

In rat studies, a simultaneous (within 8–12 min) controlled loss of 40% of circulating blood (25 ml/kg) led to the development of acute severe hemorrhagic shock in anesthetized animals. At the end of blood sampling, all experimental rats showed severe hypotension - the average values of SBP and DBP in these animals were 33 and 19 mmHg (respectively, 26% and 22% of the level before BL). The depth of hypotension in control untreated rats during the first 60–90 min after BL was partially compensated by an increase in vascular tone and acceleration of the heart rate (Figure 2A)—by this time, the mean SBP and DBP in these animals had risen to 66 and 37 mmHg (respectively, 53% and 44% of the level before BL). But such adaptation, apparently, did not significantly compensate the lack of blood flow. In most of the control rats, against the background of maintaining such a significant hypotension, manifestations of cardiorespiratory insufficiency began to increase 40–70 min after BL (Figure 2B)—total myocardial ischemia developed, atrioventricular conduction became grossly disturbed, breathing slowed down and acquired an arrhythmic, terminal character, so that cessation of respiratory movements and heart contractions was soon recorded. In this model of acute hemorrhagic shock, 18 (64%) out of 28 control rats died within 120 min of observation (Figure 2C).

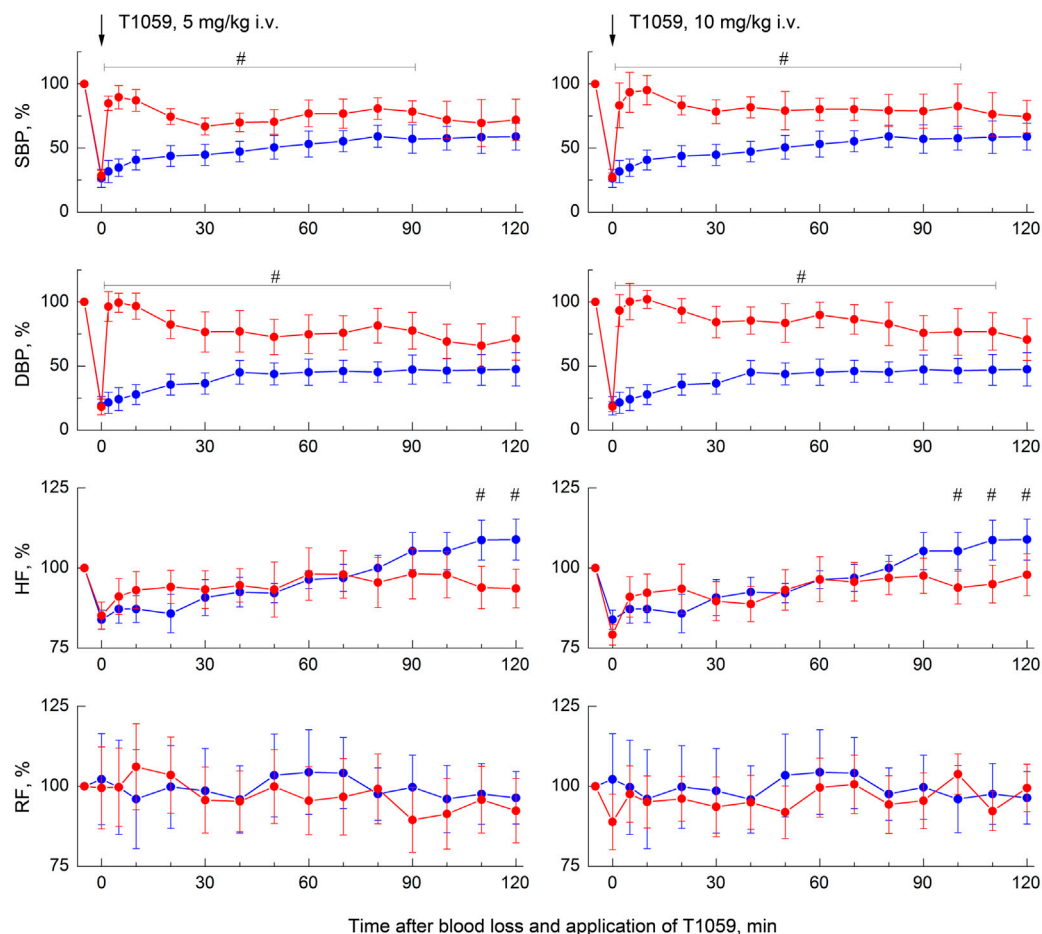
**FIGURE 2**

Early stage of acute severe hemorrhagic shock in untreated anesthetized Wistar rats. **(A)** Dynamics of indicators of systolic and diastolic blood pressure (SBP and DBP), heart frequency (HF) and respiratory frequency (RF). Data are normalized to the original values of indicators of animals and presented as percentage. Graphical deviations correspond to SD ($n = 10-28$ per point). # - significantly different vs. original value of indicator (SBP: $p < 0.00001$, $p < 0.00001$, $p < 0.00001$, $p = 0.00002$, $p = 0.00005$, $p = 0.00007$, $p = 0.00023$, $p = 0.00049$, $p = 0.00072$, $p = 0.00148$, $p = 0.00136$, $p = 0.00219$, $p = 0.00165$, $p = 0.00374$, $p = 0.00531$, respectively; DBP: $p < 0.00001$, $p < 0.00001$, $p < 0.00001$, $p < 0.00001$, $p = 0.00003$, $p = 0.00008$, $p = 0.00027$, $p = 0.00019$, $p = 0.00076$, $p = 0.00061$, $p = 0.00052$, $p = 0.00263$, $p = 0.00175$, $p = 0.00360$, $p = 0.00574$, respectively; HF: $p = 0.00311$, $p = 0.00628$, $p = 0.00543$, $p = 0.01947$, respectively). *—significantly different vs. value of indicator immediately after blood loss (SBP: $p = 0.03810$, $p = 0.02795$, $p = 0.01436$, $p = 0.00252$, $p = 0.00469$, $p = 0.00327$, $p = 0.00708$, $p = 0.00851$, respectively; DBP: $p = 0.02462$, $p = 0.03513$, $p = 0.01745$, $p = 0.00826$, $p = 0.00504$, $p = 0.00977$, $p = 0.00758$, $p = 0.01476$, $p = 0.02635$, respectively; HF: $p = 0.02914$, $p = 0.02373$, $p = 0.00668$, $p = 0.00812$, respectively). **(B)** Typical cardio-respiratory dynamics in untreated rats. Initially: BP—133/86 mmHg; HF—451 min⁻¹; sinus rhythm, no changes in the ECG; RF—62 min⁻¹. 40 min after blood loss (BL): BP—59/35; HF—417; sinus rhythm, ECG sings of myocardial ischemia; RF—38. 50 min after BL: BP—55/26; HF—146–206; sinus arrhythmia, sings of myocardial ischemia; terminal respiration, RF—7–12. 70 min after BL: BP—30/19; HF—57; complete atrioventricular block, myocardial ischemia; respiratory movements are not recorded. At 73 min a cardiac arrest was recorded. **(C)** Short-term survival of untreated rats ($n = 28$). Diagram was plotted using Kaplan-Meier method.

As in preliminary studies (Filimonova et al., 2018; 2020a) on this model of hemorrhagic shock, a single parenteral administration of T1059 after BL, caused a rapid development of a pronounced and prolonged vasoconstrictive, hypertensive effect in hypotensive rats. T1059 vasopressor activity after i.v. injections at doses of 5 or

10 mg/kg (1/50 or 1/25 LD₅₀) had a noticeable biphasic character (Figure 3). In the first 15–20 min, the effect was most pronounced and was achieved already by the 2nd minute after the injection. During this period of time, the SBP and DBP values in rats in a state of severe hemorrhagic shock were 100–120 and 75–85 mmHg

Effects of compound T1059 on the model of acute severe hemorrhagic shock in rats

**FIGURE 3**

Effect of compound T1059 with a single i.v. injection at doses of 5 mg/kg (left) and 10 mg/kg (right) on hemodynamics and external respiration of Wistar rats at an early stage of acute severe hemorrhagic shock. Red symbols and lines are indicators of T1059-treated rats ($n = 12-15$ per point), blue symbols and lines are indicators of untreated rats ($n = 10-28$). Data are normalized to the original values of indicators of animals and presented as percentage. Graphical deviations correspond to SD. # - significantly different indicators in untreated vs. T1059-treated rats (5 mg/kg, SBP: $p = 0.00002$, $p < 0.00001$, $p = 0.00004$, $p = 0.00073$, $p = 0.00462$, $p = 0.00218$, $p = 0.02964$, $p = 0.00871$, $p = 0.01053$, $p = 0.00932$, $p = 0.03817$, respectively; DBP: $p < 0.00001$, $p < 0.00001$, $p < 0.00001$, $p = 0.00006$, $p = 0.00175$, $p = 0.00322$, $p = 0.00789$, $p = 0.00648$, $p = 0.00470$, $p = 0.00091$, $p = 0.00467$, $p = 0.02306$, respectively; HF: $p = 0.03715$, $p = 0.01872$, respectively. 10 mg/kg, SBP: $p = 0.00027$, $p = 0.00008$, $p < 0.00001$, $p = 0.00036$, $p = 0.00084$, $p = 0.00053$, $p = 0.00779$, $p = 0.00092$, $p = 0.00415$, $p = 0.01930$, $p = 0.04706$, $p = 0.03021$, respectively; DBP: $p = 0.00001$, $p < 0.00001$, $p < 0.00001$, $p = 0.00005$, $p = 0.00017$, $p = 0.00063$, $p = 0.00508$, $p = 0.00024$, $p = 0.00136$, $p = 0.00790$, $p = 0.01455$, $p = 0.02643$, $p = 0.02768$, respectively; HF: $p = 0.03180$).

(respectively, 80%–95% and 90–100% of the level before BL). In the subsequent period of time, the hypertensive effect of T1059 in these animals was somewhat less pronounced—the average SBP and DBP were 85–95 и 60–70 mmHg (respectively, 70%–80% and 70%–85% of the level before BL). The duration of a significant vasopressor effect of T1059 with a single i.v. injection was high—90 min at a dose of 5 mg/kg and 100 min at a dose of 10 mg/kg. A significant increase in DBP was observed up to 100 and 110 min.

A single i. m. injection of T1059 at a dose of 30 mg/kg (1/9 LD₁₀) also caused a pronounced vasopressor effect (Figure 4, left). In this case, T1059 hypertensive effect developed less rapidly

- it increased monotonously in the first 10 min after injection, and then remained stably pronounced throughout the entire observation period. During this time period, the mean SBP and DBP in rats in severe hemorrhagic shock were 95–105 and 65–75 mmHg (respectively, 75%–85% and 80%–90% of the level before BL). The duration of a significant vasopressor effect of T1059 exceeded 120 min. Moreover, repeated i. m. administration of T1059 at a low dose (10 mg/kg) during the period when the vascular effect of the first injection (30 mg/kg) was significantly weakened allowed to prolong the vasopressor effect for at least another 60 min (Figure 4, right).

Effects of compound T1059 on the model of acute severe hemorrhagic shock in rats

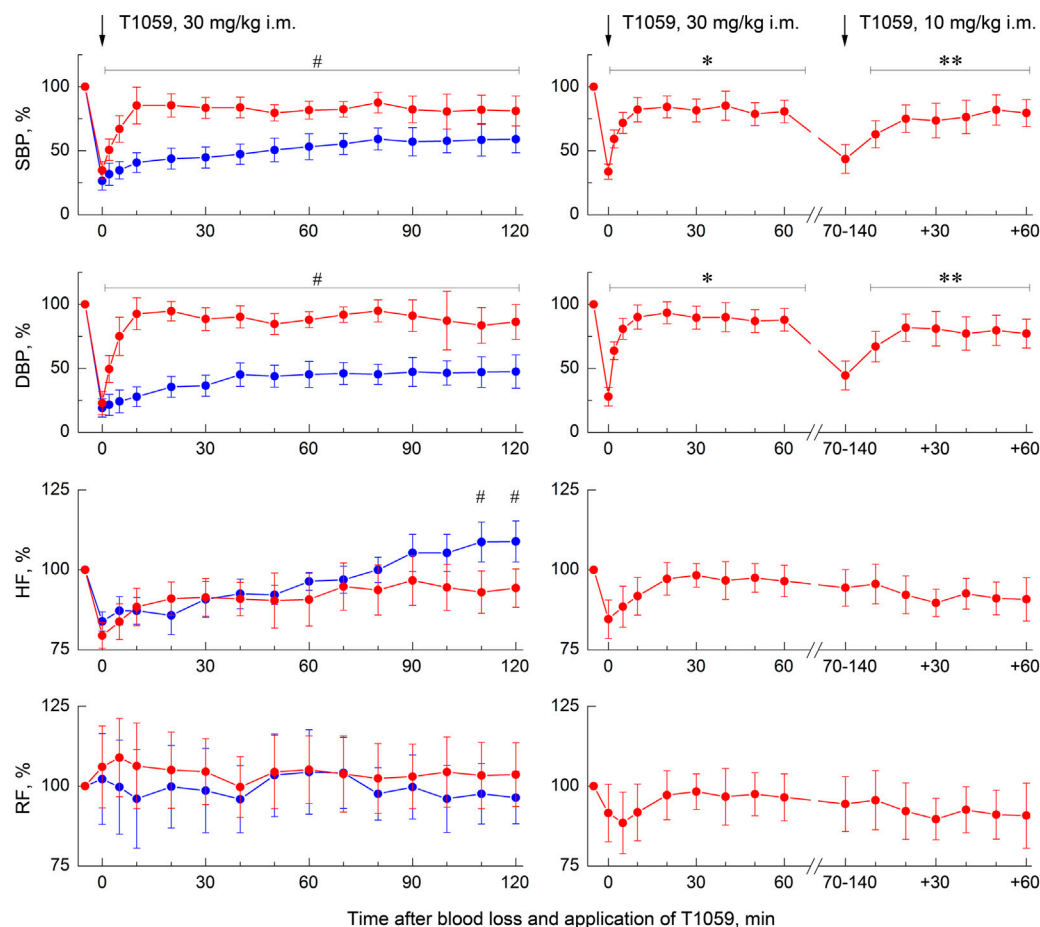


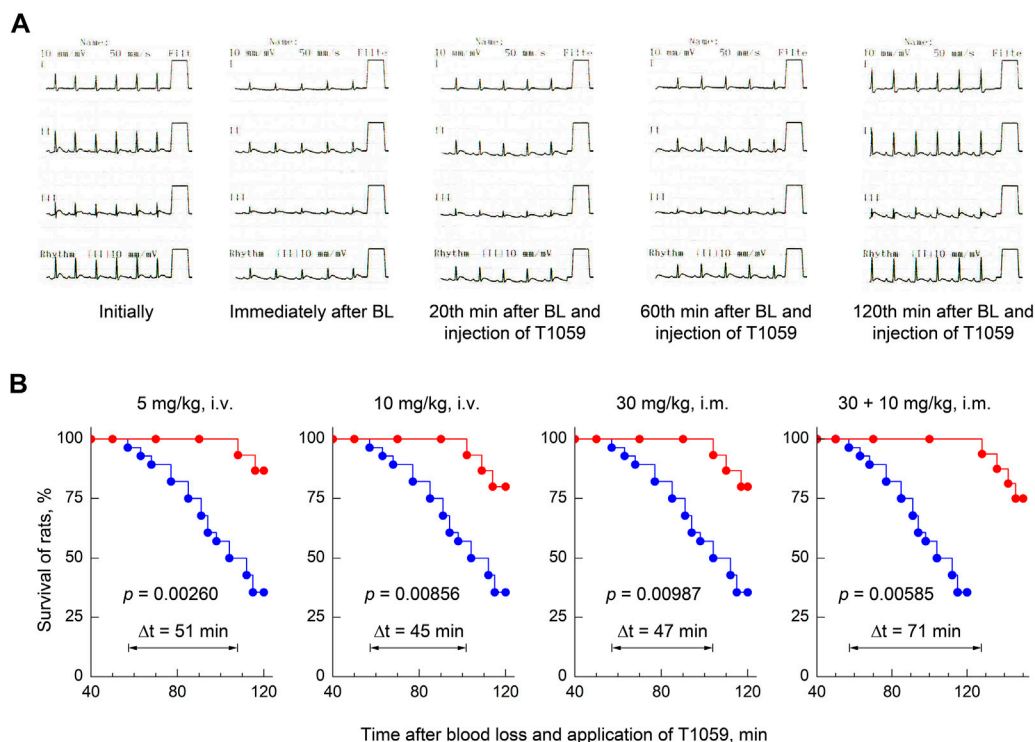
FIGURE 4

Effect of compound T1059 with a single i.m. injection at dose of 30 mg/kg (left) and two times i.m. injection at doses 30 + 10 mg/kg (right) on hemodynamics and external respiration of Wistar rats at an early stage of acute severe hemorrhagic shock. Red symbols and lines are indicators of T1059-treated rats ($n = 12-16$ per point), blue symbols and lines are indicators of untreated rats ($n = 10-28$). Data are normalized to the original values of indicators of animals and presented as percentage. Graphical deviations correspond to SD. # - significantly different indicators in untreated vs. T1059-treated rats (SBP: $p = 0.04754$, $p = 0.01182$, $p = 0.00736$, $p = 0.00598$, $p = 0.00721$, $p = 0.00907$, $p = 0.00984$, $p = 0.01070$, $p = 0.00833$, $p = 0.00645$, $p = 0.02651$, $p = 0.03076$, $p = 0.04182$, $p = 0.03287$, respectively; DBP: $p = 0.02744$, $p = 0.00056$, $p = 0.00003$, $p < 0.00001$, $p = 0.00012$, $p = 0.00290$, $p = 0.00437$, $p = 0.00305$, $p = 0.00184$, $p = 0.00076$, $p = 0.00742$, $p = 0.01539$, $p = 0.01163$, $p = 0.00906$, respectively; HF: $p = 0.02747$, $p = 0.03825$, respectively). * - significantly different with the indicator immediately after blood loss (SBP: $p = 0.00817$, $p = 0.00543$, $p = 0.00072$, $p = 0.00061$, $p = 0.00085$, $p = 0.00069$, $p = 0.00107$, $p = 0.00084$, respectively; DBP: $p = 0.00023$, $p = 0.00014$, $p = 0.00007$, $p < 0.00001$, $p = 0.00036$, $p = 0.00009$, $p = 0.00031$, $p = 0.00023$, respectively). **—significantly different with the indicator before the second injection of T1059 (SBP: $p = 0.03850$, $p = 0.02725$, $p = 0.03468$, $p = 0.02954$, $p = 0.01309$, $p = 0.02083$, respectively; DBP: $p = 0.03941$, $p = 0.00807$, $p = 0.01625$, $p = 0.02736$, $p = 0.02012$, $p = 0.02547$, respectively).

Moreover, along with the manifestations of a pronounced stable vasopressor activity of T1059, its significant influence on the clinical course of the early stage of severe acute hemorrhagic shock attracted attention. As noted above, in most control rats in this model, cardiorespiratory insufficiency increased 40–70 min after BL. The death of a significant part (64%) of these animals was recorded at the 2nd hour of observation (Figure 2). At the same time, long-term stabilization of the hemodynamics of T1059-treated animals at all doses and methods of

administration significantly “restrained” the development of threatening complications. Monitoring data indicated the increase in significant cardio-respiratory disorders only in 20%–30% of T1059-treated rats and at later periods (90–110 min after BL and T1059 administration). In most of these animals, negative symptoms were limited to mild signs of myocardial ischemia at the end of monitoring (Figure 5A). Moreover, a positive objective cardio-respiratory dynamics was accompanied by a statistically significant increase in the

Effects of compound T1059 on the model of acute severe hemorrhagic shock in rats

**FIGURE 5**

Effect of compound T1059 on the clinical course of the early stage of acute severe hemorrhagic shock in rats. **(A)** Typical cardio-respiratory dynamics in T1059-treated rats. Initially: BP—128/84 mmHg; HF—424 min⁻¹; sinus rhythm, no changes in the ECG; RF—58 min⁻¹. Immediately after blood loss (BL): BP—53/27; HF—335; sinus rhythm, R-wave depression; RF—63. 20 min after BL and injection of T1059: BP—95/66; HF—372; sinus rhythm, easing of R-wave depression, RF—60. 60 min after BL and injection of T1059: BP—120/81; HF—368; sinus rhythm, no changes in the ECG; RF—62. 120 min after BL and injection of T1059: BP—115/74; HF—404; sinus rhythm, moderate signs of myocardial ischemia; RF—59. **(B)** Effect of compound T1059 at different doses and applications on the short-term survival of rats. Red symbols and curves—survival of T1059-treated rats ($n = 15$ –16), blue symbols and curve—survival of untreated rats ($n = 28$). Diagrams were plotted using Kaplan-Meier method. p —significance level of the difference in the survival of T1059-treated vs. untreated rats; Δt —an increase in time of the non-lethal course of shock when using T1059.

short-term survival of T1059-treated rats (Figure 5B)—by 120–150 min of observation, lethality in these groups of animals was 13%–25%. Comparison of survival diagrams showed a significant (1.8–2.3 times) increase in the time of non-lethal shock in T1059-treated groups—from 57 min in control rats to 102–108 min in T1059-treated rats with a single injection (5 and 10 mg/kg, i.v. or 30 mg/kg, i.m.) and to 128 min with 2-fold injection (30 + 10 mg/kg, i.m.).

Effects of compound T1059 on the model of acute hemorrhagic shock in dogs

A less severe model of acute hemorrhagic shock was used to study the vascular and hemodynamic effects of T1059 in dogs. In this case, a less acute (within 20–25 min) controlled loss of 25% of circulating blood led to the development of moderately severe hemorrhagic shock in animals (Figure 6). 2–5 min after the end

of BL, SBP/DBP in dogs averaged 65/45 mmHg (52–55% of the level before BL). In the first 30–40 min after BL, a slight compensation of hypotension due to a moderate acceleration of the heart rate and, apparently, an increase in stroke volume was registered in control, untreated animals. And further until the end of the observation, the SBP/DBP indicators in these animals remained at the level of 75/45 mmHg (respectively, 65% and 55% of the level before BL). Further, during 120 min of the experiment (and in the next 15 days) no any death or threatening clinical symptoms and ECG changes in the control untreated group were registered.

The vasopressor activity of T1059 was studied in this model with a single parenteral administration at doses of 3.2 mg/kg (i.v.) and 9.5 mg/kg (i.m.). That is equivalent to doses of 10 and 30 mg/kg for rats, taking into account the species surface area of the animal's body (Mironov, 2012). Dogs of the experimental groups endured slow i.v. and i.m. injections of T1059 solutions easily and painlessly. No any manifestations of intoxication or

Effects of compound T1059 on the model of acute hemorrhagic shock in dogs

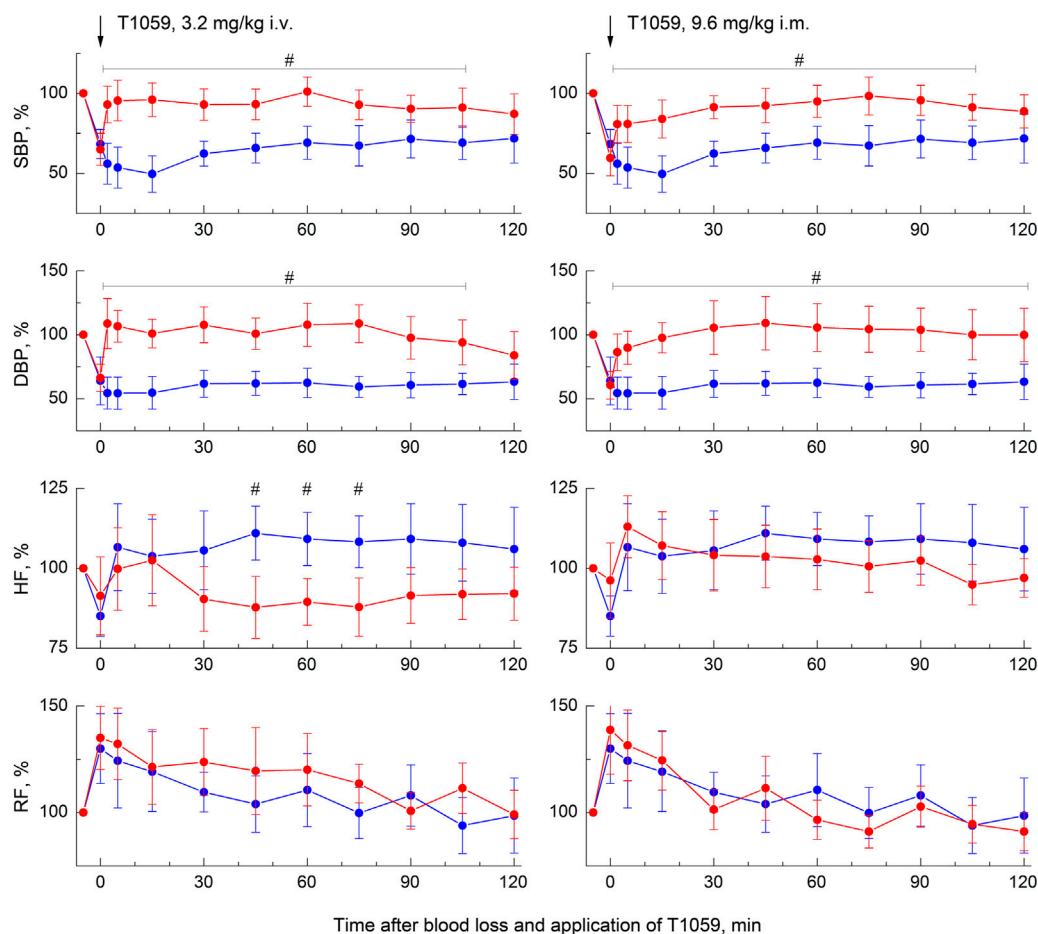


FIGURE 6

Effect of compound T1059 with a single i.v. injection at dose of 3.2 mg/kg (left) and a single i.m. injection at dose 9.6 mg/kg (right) on hemodynamics and external respiration of dogs at an early stage of acute hemorrhagic shock. Red symbols and lines are indicators of T1059-treated dogs ($n = 8$), blue symbols and lines are indicators of untreated dogs ($n = 7$). Data are normalized to the original values of indicators of animals and presented as percentage. Graphical deviations correspond to SD. #—significantly different indicators in untreated vs. T1059-treated dogs (3.2 mg/kg i.v., SBP: $p = 0.00478$, $p = 0.00253$, $p = 0.00069$, $p = 0.00625$, $p = 0.00814$, $p = 0.00167$, $p = 0.01350$, $p = 0.03902$, $p = 0.02733$, respectively. DBP: $p = 0.00017$, $p = 0.00009$, $p = 0.00034$, $p = 0.00086$, $p = 0.00295$, $p = 0.00071$, $p = 0.00053$, $p = 0.00492$, $p = 0.01768$, respectively. HF: $p = 0.00745$, $p = 0.00908$, $p = 0.01362$, respectively. 9.6 mg/kg i.m., SBP: $p = 0.02176$, $p = 0.01892$, $p = 0.00354$, $p = 0.00513$, $p = 0.00940$, $p = 0.00874$, $p = 0.00721$, $p = 0.01956$, $p = 0.02498$, respectively. DBP: $p = 0.01572$, $p = 0.00743$, $p = 0.00209$, $p = 0.00651$, $p = 0.00375$, $p = 0.00624$, $p = 0.00176$, $p = 0.00507$, $p = 0.00943$, $p = 0.02745$, respectively).

changes in the state and behavior of these animals were observed. Subsequent examinations also showed no any clinical manifestations of local damaging effects of T1059.

At the same time, T1059 in this model caused almost the same vascular and hemodynamic effects in hypotensive dogs as in hypotensive rats. After a single i.v. injection of T1059, 3.2 mg/kg, a stably pronounced hypertensive effect was observed during the first 60–75 min, it was achieved already at the 5th minute after the injection (Figure 5, left). During this time period, SBP and DBP in dogs were 110–125 and 80–90 mmHg (90%–100% and 100%–110% of pre-BL levels). In

the next 20–30 min, the effect manifestation decreased slightly - the average values of SBP and DBP were 105 and 75 mmHg (85% and 90% of pre-BL levels). The total duration of T1059 significant vasopressor effect was 115 min. After a single i.m. injection of T1059, 9.5 mg/kg, a significant effect was also observed as early as 5 min after injection (Figure 5, right). During the first 45–60 min, its manifestation increased from 100/70 mmHg (80% and 85% of pre-BL level) to 120/90 mmHg (95% and 105% of pre-BL level). The total duration of T1059 significant vasopressor effect in this case was also 115 min, and increased DBP values were observed until the end of the experiment.

Discussion

Since the discovery of the NOS/sGC/cGMP pathway of vascular relaxation in the 1980's (Furchgott and Zawadzki, 1980; Palmer et al., 1987; Rees et al., 1989), our understanding of the physiological and pathophysiological role of NO and various NOS isoforms in regulation of vascular tone and hemodynamics are constantly refined and expanded. Nevertheless, since that time, the vasoconstrictive, vasopressor ability of effective eNOS and iNOS inhibitors blocking the vascular relaxation pathway has been perceived rather as a natural property. Indeed, to date, such an activity has been shown for many NOS inhibitors containing guanidine (L-NMMA, L-NNA, L-NAME), aminoguanidine (Kilbourn et al., 1990, 1997; Wu et al., 1995; Avontuur et al., 1998), amidine (L-NIL, 7-NI, 1400 W) (Faraci and Brian, 1995; Wray et al., 1998; Kadoi and Goto, 2007) and thioamidine group (derivatives of isothiurea, L-thiocytrulline, 2-aminothiazole/thiazoline/thiazine) (Fray et al., 1994; Narayanan et al., 1995; Handy et al., 1996; Proskuryakov et al., 2002, 2004, 2010; Filimonova et al., 2012b; Nurieva et al., 2018; Alexeev et al., 2019). Apparently, the isothiurea derivative T1059 is not an exception in this series.

According to radiological studies on isolated NOS isoforms (Filimonova et al., 2018), compound T1059 is a fairly effective inhibitor of eNOS and iNOS (its IC_{50} values are 3.3 and 1.8 μ M, respectively). It not inferior in such activity to L-NMMA and L-NNA (Faraci et al., 1996; Boer et al., 2000). Apparently, the features of N-substituting radical in chemical structure of this isothiurea make it difficult to interact its thioamidine fragment with nNOS active site (its IC_{50} value is 60.1 μ M). This provides T1059 a significant (15–30 times) selectivity for eNOS and iNOS,—NOS isoforms that play a leading role in the physiological and pathophysiological regulation of vascular homeostasis and, in particular, vascular tone (Napoli and Ignarro, 2009; Forstermann and Sessa, 2012; Krol and Kapinska, 2021).

Such features of T1059 biochemical activity probably determine the presence of a pronounced vasopressor activity in this compound. In our studies on models of acute hemorrhagic shock, T1059, after a single parenteral administration in sufficiently safe doses (1/50–1/9 LD_{10}), caused in rats and dogs a rapid increase in vascular tone, accompanied by a prolonged hypertensive effect (within 90–120 min in rats, and within 115 min in dogs). The repeated administration of T1059 at low doses (1/3 of the dose of the first injection) made it possible to considerably (by at least 60 min) prolong a significant vasopressor effect.

Routine use of vasopressors is currently not recommended in the treatment of acute posthemorrhagic hypotension because of possible excessive centralization of blood flow, that can accelerate the development of multiple organ failure and aggravate « delayed » damage during

reperfusion. Options for fluid resuscitation are considered as optimal strategies. However, fluid replacement in such disorders may also be unsafe and ineffective (e.g. in uncontrolled traumatic hemorrhagic shock or in states resistant to volume therapy) or belated. So, with the loss of the “golden hour,” the chances of survival of patients with acute severe hemorrhagic shock in the preclinical setting remain low. In this regard, a significant positive effect of T1059 on the clinical course of the early stage of acute severe hemorrhagic shock in rats seems to be an important result of this study. In all schemes, T1059 administration considerably inhibited the development of threatening cardiorespiratory disorders and significantly ($p = 0.0026–0.0098$) increased the short-term survival of experimental animals, formally extending the duration of the “golden hour” by 2 times.

This “therapeutic” effect of T1059 in this case, most likely, is realized due to a fairly long stabilization of animals’ hemodynamics. It reproduces the positive effects of vasopressor support in the early stages of severe shock, that have been shown in a number of experimental works for adrenomimetics and peptide vasoconstrictors (Hakstian et al., 1961; Noura et al., 2005; Johnson et al., 2006; Sanui et al., 2006; Poloujadoff et al., 2007; Beloncle et al., 2013; Djogovic et al., 2015). At the same time, the contribution of the specific NOS inhibitory activity of T1059 to this positive effect cannot be excluded. So, a number of studies have shown the ability of some NOS inhibitors to increase short-term survival in the early stages of severe hemorrhagic shock. Such an effect can be exerted not only by NOS inhibitors with high vasopressor activity (Khazaei et al., 2012), but also by selective iNOS inhibitors (McDonald et al., 2002; Soliman, 2014). Therefore, the nature of T1059 NOS-inhibitory activity is capable of providing not only to implement vasopressor stabilization of hemodynamics in severe hemorrhagic shock, but also to limit the development of destructive processes caused by oxidative and nitrosative stresses against the background of acute hypoxia.

Conclusion

Studies on models of acute hemorrhagic hypotension in rats and dogs demonstrate that the NOS inhibitor T1059 is a potent long-acting vasopressor. It caused the rapid development of a stable and prolonged (within 90–120 min) hypertensive effect after a single parenteral administration in sufficiently safe doses (1/50–1/9 LD_{10}) in hypotensive animals. The repeated administration of T1059 at low doses made it possible to prolong the vasopressor effect. Long-term stabilization of hemodynamics in T1059-treated rats at an early stage of severe hemorrhagic shock significantly increased the short-term survival of animals. These data suggest that NOS inhibitors and, in particular, compound T1059, are able to

create new opportunities in the treatment of hypotensive disorders, including the provision of assistance at the prehospital stage of treatment of such pathologies.

Data availability statement

The raw data supporting the conclusions of this article will be made available by the authors, without undue reservation.

Ethics statement

The animal study was reviewed and approved by A. Tsyb MRRC Ethical Committee, Protocol number 1-DI-00024.

Author contributions

Conceptualization, methodology, analysis, and writing, MF and AF; chemical synthesis and analysis, LS; investigation and formal analysis, MF, VM, AF, and AS; supervision and project administration, PS, AK, and SI. All authors have read and agreed to the published version of the manuscript.

References

- Alexeev, A. A., Nurieva, E. V., Trofimova, T. P., Chesnakova, E. A., Grishin, Y. K., Lyssenko, K. A., et al. (2019). Bicyclic bridged isothioureas: Synthesis and evaluation of activity in a model of lipopolysaccharide-induced septic shock. *Mendeleev Commun.* 29, 14–16. doi:10.1016/j.mencom.2019.01.003
- Avontuur, J. A., Tutein Nolthenius, R. P., van Bodegom, J. W., and Bruining, H. A. (1998). Prolonged inhibition of nitric oxide synthesis in severe septic shock: A clinical study. *Crit. Care Med.* 26, 660–667. doi:10.1097/00003246-199804000-00012
- Beloncle, F., Meziani, F., Lerolle, N., Radermacher, P., and Asfar, P. (2013). Does vasopressor therapy have an indication in hemorrhagic shock? *Ann. Intensive Care* 3, 13. doi:10.1186/2110-5820-3-13
- Berezovskaya, I. V. (2003). Classification of substances with respect to acute toxicity for parenteral administration. *Pharm. Chem. J.* 37, 139–141. doi:10.1023/A:1024586630954
- Boer, R., Ulrich, W. R., Klein, T., Mirau, B., Haas, S., and Baur, I. (2000). The inhibitory potency and selectivity of arginine substrate site nitric-oxide synthase inhibitors is solely determined by their affinity toward the different isoenzymes. *Mol. Pharmacol.* 58, 1026–1034. doi:10.1124/mol.58.5.1026
- Diehl, K. H., Hull, R., Morton, D., Pfister, R., Rabemampianina, Y., Smith, D., et al. (2001). A good practice guide to the administration of substances and removal of blood, including routes and volumes. *J. Appl. Toxicol.* 21, 15–23. doi:10.1002/jat.727
- Djogovic, D., MacDonald, S., Wensel, A., Green, R., Loubani, O., Archambault, P., et al. (2015). Vasopressor and inotrope use in Canadian Emergency Departments: Evidence based consensus guidelines. *Can. J. Emerg. Med.* 17, 1–16. doi:10.1017/cem.2014.77
- Faraci, F. M., and Brian, J. E., Jr (1995). 7-Nitroindazole inhibits brain nitric oxide synthase and cerebral vasodilatation in response to N-methyl-D-aspartate. *Stroke* 26, 2172–2175. doi:10.1161/01.str.26.11.2172
- Faraci, W. S., Nagel, A. A., Verdries, K. A., Vincent, L. A., Xu, H., Nichols, L. E., et al. (1996). 2-amino-4-methylpyridine as a potent inhibitor of inducible NO synthase activity *in vitro* and *in vivo*. *Br. J. Pharmacol.* 119, 1101–1108. doi:10.1111/j.1476-5381.1996.tb16010.x

Funding

This research was funded by the Ministry of Education and Science of the Russian Federation (state contract #14.N08.11.0078), Ministry of Health of the Russian Federation and partially by the Russian Foundation for Basic Research and Kaluga Region, grant number 12-04-97524-p-center-a.

Conflict of interest

The authors declare that the research was conducted in the absence of any commercial or financial relationships that could be construed as a potential conflict of interest.

Publisher's note

All claims expressed in this article are solely those of the authors and do not necessarily represent those of their affiliated organizations, or those of the publisher, the editors and the reviewers. Any product that may be evaluated in this article, or claim that may be made by its manufacturer, is not guaranteed or endorsed by the publisher.

Filimonova, M., Saburova, A., Makarchuk, V., Shevchenko, L., Surinova, V., Yuzhakov, V., et al. (2021). The ability of the nitric oxide synthase inhibitor T1023 to selectively protect the non-malignant tissues. *Int. J. Mol. Sci.* 22, 9340. doi:10.3390/ijms22179340

Filimonova, M., Saburova, A., Shevchenko, L., Makarchuk, V., Shitova, A., Soldatova, O., et al. (2022b). 1-Isobutanol-2-isopropylisothiourea phosphate, T1082: A safe and effective prevention of radiotherapy complications in oncology. *Int. J. Mol. Sci.* 23, 2697. doi:10.3390/ijms23052697

Filimonova, M., Shitova, A., Soldatova, O., Shevchenko, L., Saburova, A., Podosinnikova, T., et al. (2022a). Combination of NOS-and PDK-inhibitory activity: Possible way to enhance antitumor effects. *Int. J. Mol. Sci.* 23, 730. doi:10.3390/ijms23020730

Filimonova, M. V., Makarchuk, V. M., Shevchenko, L. I., Saburova, A. S., Surinova, V. I., Izmetstieva, O. S., et al. (2020b). Radioprotective activity of the nitric oxide synthase inhibitor T1023. Toxicological and biochemical properties, cardiovascular and radioprotective effects. *Radiat. Res.* 194, 532–543. doi:10.1667/RADE-20-00046.1

Filimonova, M. V., Podosinnikova, T. S., Samsonova, A. S., Makarchuk, V. M., Shevchenko, L. I., and Filimonov, A. S. (2019b). Comparison of antitumor effects of combined and separate treatment with NO synthase inhibitor T1023 and PDK1 inhibitor dichloroacetate. *Bull. Exp. Biol. Med.* 168, 92–94. doi:10.1007/s10517-019-04655-1

Filimonova, M. V., Proskuriakov, S. I., Shevchenko, L. I., Shevchuk, A. S., Lushnikova, G. A., Makarchuk, V. M., et al. (2012a). [Radioprotective properties of isothiourea derivatives with NO-inhibitory mechanism of action]. *Radiat. Biol. Radioecol.* 52, 593–601. (In Russian).

Filimonova, M. V., Shevchenko, L. I., Makarchuk, V. M., Chesnakova, E. A., Shevchuk, A. S., Filimonov, A. S., et al. (2020a). Vasopressor properties of NO synthase inhibitor T1059. Part II. Hemodynamic effects on hypovolemic disorders. *Pharm. Chem. J.* 53, 1113–1117. doi:10.1007/s11094-020-02132-y

Filimonova, M. V., Shevchenko, L. I., Makarchuk, V. M., Chesnakova, E. A., Surinova, V. I., Shevchuk, A. S., et al. (2018). Vasopressor properties of nitric oxide synthase inhibitor T1059. Part I: Synthesis, toxicity, NOS-inhibition activity, and

hemodynamic effects under normotensive conditions. *Pharm. Chem. J.* 52, 294–298. doi:10.1007/s11094-018-1809-2

Filimonova, M. V., Shevchenko, L. I., Makarchuk, V. M., Chesnakova, E. A., and Tsyb, A. F. (2015). Inventor; medical radiological research center of the Ministry of health of the Russian federation, assignee. *Vasopressor agent. Russ. Fed. Pat. RU* 2, 552–529.

Filimonova, M. V., Trofimova, T. P., Borisova, G. S., and Mandrugina, A. A. (2012b). Antihypotensive activity of 2-acetylamin-5, 6-dihydro-4H-1, 3-thiazine for an endotoxic shock model in rats. *Pharm. Chem. J.* 46, 210–212. doi:10.1007/s11094-012-0763-7

Filimonova, M. V., Yuzhakov, V. V., Filimonov, A. S., Makarchuk, V. M., Bandurko, L. N., Korneeva, T. S., et al. (2019a). Comparative study of the effects of NOS inhibitor T1023 and bevacizumab on growth and morphology of Lewis lung carcinoma]. *Patologicheskaya Fiziologiya i Eksperimentalnaya Terapiya = Pathological Physiology Exp. Ther.* 63, 89–98. (In Russian). doi:10.25557/0031-2991.2019.02.89-98

Forstermann, U., and Sessa, W. C. (2012). Nitric oxide synthases: Regulation and function. *Eur. Heart J.* 33, 829–837. doi:10.1093/eurheartj/ehs304

Fray, C., Narayanan, K., McMillan, K., Spack, L., Gross, S. S., Masters, B. S., et al. (1994). L-thiocitrulline. A stereospecific, heme-binding inhibitor of nitric-oxide synthases. *J. Biol. Chem.* 269, 26083–26091. doi:10.1016/S0021-9258(18)47162-1

Furchgott, R. F., and Zawadzki, J. V. (1980). The obligatory role of endothelial cells in the relaxation of arterial smooth muscle by acetylcholine. *Nature* 288, 373–376. doi:10.1038/288373a0

S. G. Gad (Editor) (2007). *Animal models in toxicology*. 2nd Edition (New York: Taylor & Francis), 952.

Hakstian, R. W., Hampson, L. G., and Gurd, F. N. (1961). Pharmacological agents in experimental hemorrhagic shock. A controlled comparison of treatment with hydralazine, hydrocortisone, and levarterenol (1-norepinephrine). *Arch. Surg.* 3, 335–347. doi:10.1001/archsurg.1961.01300150009002

Handy, R. L., Wallace, P., and Moore, P. K. (1996). Inhibition of nitric oxide synthase by isothioureas: Cardiovascular and antinociceptive effects. *Pharmacol. Biochem. Behav.* 55, 179–184. doi:10.1016/S0091-3057(96)00051-2

Hogg, N. (2010). Detection of nitric oxide by electron paramagnetic resonance spectroscopy. *Free Radic. Biol. Med.* 49, 122–129. doi:10.1016/j.freeradbiomed.2010.03.009

Holm, S. (1979). A simple sequentially rejective multiple test procedure. *Scand. J. Statistics* 6, 65–70.

Johnson, K. B., Pearce, F. J., Jeffreys, N., McJames, S. W., and Cluff, M. (2006). Impact of vasopressin on hemodynamic and metabolic function in the decompensatory phase of hemorrhagic shock. *J. Cardiothorac. Vasc. Anesth.* 3, 167–172. doi:10.1053/j.jvca.2005.11.015

Kadoi, Y., and Goto, F. (2007). Effects of selective iNOS inhibition on systemic hemodynamics and mortality rate on endotoxic shock in streptozotocin-induced diabetic rats. *Shock* 28, 602–609. doi:10.1097/SHK.0b013e31804d452d

Khazaei, M., Barmaki, B., and Nasimi, A. (2012). Protective role of selective nitric oxide synthase inhibitor for treatment of decompensated hemorrhagic shock in normotensive and hypertensive rats. *Int. J. Prev. Med.* 3, 47–53. PMID: 22355477 PMID: PMC3278869.

Kilbourn, R. G., Jubran, A., Gross, S. S., Griffith, O. W., Levi, R., Adams, J., et al. (1990). Reversal of endotoxin-mediated shock by NG-methyl-L-arginine, an inhibitor of nitric oxide synthesis. *Biochem. Biophys. Res. Commun.* 172, 1132–1138. doi:10.1016/0006-291x(90)91565-a

Kilbourn, R. G., Szab, C., and Trauber, D. L. (1997). Beneficial versus detrimental effects of nitric oxide synthase inhibitors in circulatory shock: Lessons learned from experimental and clinical studies. *Shock* 7, 235–246. doi:10.1097/00024382-199704000-00001

Krol, M., and Kapinska, M. (2021). Human nitric oxide synthase-its functions, polymorphisms, and inhibitors in the context of inflammation, diabetes and cardiovascular diseases. *Int. J. Mol. Sci.* 22, 56. doi:10.3390/ijms22010056

Lim, R. K., Rink, K. G., Glass, H. G., and Soaje-Echague, E. (1961). A method for the evaluation of cumulation and tolerance by the determination of acute and subchronic median effective doses. *Arch. Int. Pharmacodyn. Ther.* 130, 336–353. PMID: 13762162.

McDonald, M. C., Izumi, M., Cuzzocrea, S., and Thiemermann, C. (2002). A novel, potent and selective inhibitor of the activity of inducible nitric oxide synthase (GW274150) reduces the organ injury in hemorrhagic shock. *J. Physiol. Pharmacol.* 53, 555–569. PMID: 12512692.

A. N. Mironov (Editor) (2012). *Guidelines for preclinical Drug research* (Moscow, Russia: Grif & Co.), 944. (In Russian). Part

Napoli, C., and Ignarro, L. J. (2009). Nitric oxide and pathogenic mechanisms involved in the development of vascular diseases. *Arch. Pharm. Res.* 32, 1103–1108. doi:10.1007/s12272-009-1801-1

Narayanan, K., Spack, L., McMillan, K., Kilbourn, R. G., Hayward, M. A., Masters, B. S., et al. (1995). S-alkyl-L-thiocitrullines. Potent stereoselective inhibitors of nitric oxide synthase with strong pressor activity *in vivo*. *J. Biol. Chem.* 270, 11103–11110. doi:10.1074/jbc.270.19.11103

Nouira, S., Elatrous, S., Dimassi, S., Besbes, L., Boukef, R., Mohamed, B., et al. (2005). Effects of norepinephrine on static and dynamic preload indicators in experimental hemorrhagic shock. *Crit. Care Med.* 3, 2339–2343. doi:10.1097/01.CCM.0000182801.48137.13

Nurieva, E. V., Trofimova, T. P., Alexeev, A. A., Proshin, A. N., Chesnakova, E. A., Grishin, Y. K., et al. (2018). Synthesis and antihypotensive properties of 2-amino-2-thiazoline analogues with enhanced lipophilicity. *Mendeleev Commun.* 28, 390–392. doi:10.1016/j.mencom.2018.07.016

Palmer, R. M. J., Ferrige, A. G., and Moncada, S. (1987). Nitric oxide release accounts for the biological activity of endothelium-derived relaxing factor. *Nature* 327, 524–526. doi:10.1038/327524a0

Poloujadoff, M. P., Borron, S. W., Amathieu, R., Favret, F., Camara, M. S., Lapostolle, F., et al. (2007). Improved survival after resuscitation with norepinephrine in a murine model of uncontrolled hemorrhagic shock. *Anesthesiology* 3, 591–596. doi:10.1097/01.anes.0000281926.54940.6a

Proskuryakov, S. Y., Filimonova, M. V., Borovaya, O. N., Kucherenko, N. G., Trishkina, A. I., Steyn, L. V., et al. (2010). Effect of NO inhibitors on hypovolemic shock-induced hypotension. *Bull. Exp. Biol. Med.* 150, 18–22. doi:10.1007/s10517-010-1057-2

Proskuryakov, S. Y., Filimonova, M. V., Verkhovskii, Y. G., Konoplyannikov, A. G., Mandrugina, A. A., Fedoseev, V. M., et al. (2004). Effect of NO synthase inhibitor 2-amino-5, 6-dihydro-4H-1, 3-thiazine on endotoxin-induced changes in hemodynamic parameters and respiration in rats. *Bull. Exp. Biol. Med.* 138, 397–400. doi:10.1007/s10517-005-0110-z

Proskuryakov, S. Y., Konoplyannikov, A. G., Skvortsov, V. G., Mandrugina, A. A., and Fedoseev, V. M. (2005). Nitric oxide synthase inhibitors containing the carboxamidine group or its isosteres. *Russ. Chem. Rev.* 74, 859–870. doi:10.1070/RC2005v07n09ABEH000923

Proskuryakov, S. Y., Kucherenko, N. G., Trishkina, A. I., Filimonova, M. V., Shevchuk, A. G., Shtein, L. V., et al. (2002). NO-inhibiting and vasotropic activity of some compounds with thioamidine group. *Bull. Exp. Biol. Med.* 134, 338–341. doi:10.1023/A:1021943811672

Rees, D. D., Palmer, R. M. J., and Moncada, S. (1989). Role of endothelium-derived nitric oxide in the regulation of blood pressure. *Proc. Natl. Acad. Sci. U. S. A.* 86, 3375–3378. doi:10.1073/pnas.86.9.3375

Saburova, A. S., Filimonova, M. V., Yuzhakov, V. V., Shevchenko, L. I., Yakovleva, N. D., Bandurko, L. N., et al. (2020). The influence of nitric oxide synthases inhibitor T1023 on the development of radiation pneumofibrosis in rats. *Radiatsionnaya Gygiena = Radiat. Hyg.* 13, 60–67. (In Russian). doi:10.21514/1998-426X-2020-13-1-60-67

Sanui, M., King, D. R., Feinstein, A. J., Varon, A. J., Cohn, S. M., and Proctor, K. G. (2006). Effects of arginine vasopressin during resuscitation from hemorrhagic hypotension after traumatic brain injury. *Crit. Care Med.* 3, 433–438. doi:10.1097/01.CCM.0000196206.83534.39

Soliman, M. M. (2014). Effects of aminoguanidine, a potent nitric oxide synthase inhibitor, on myocardial and organ structure in a rat model of hemorrhagic shock. *J. Emerg. Trauma Shock* 7, 190–195. doi:10.4103/0974-2700.136864

van Eijk, H. M., Luiking, Y. C., and Deutz, N. E. (2007). Methods using stable isotopes to measure nitric oxide (NO) synthesis in the L-arginine/NO pathway in health and disease. *J. Chromatogr. B Anal. Technol. Biomed. Life Sci.* 851, 172–185. doi:10.1016/j.jchromb.2006.08.054

Wray, G. M., Millar, C. G., Hinds, C. J., and Thiemermann, C. (1998). Selective inhibition of the activity of inducible nitric oxide synthase prevents the circulatory failure, but not the organ injury/dysfunction, caused by endotoxin. *Shock* 9, 329–335. doi:10.1097/00024382-199805000-00003

Wu, C. C., Chen, S. J., Szabo, C., Thiemermann, C., and Vane, J. R. (1995). Aminoguanidine attenuates the delayed circulatory failure and improves survival in rodent models of endotoxic shock. *Br. J. Pharmacol.* 114, 1666–1672. doi:10.1111/j.1476-5381.1995.tb14955.x



OPEN ACCESS

EDITED BY

Hina Siddiqui,
University of Karachi, Pakistan

REVIEWED BY

Kunming Qin,
Jiangsu Ocean University, China
Hanan Farouk Aly,
National Research Centre, Egypt

*CORRESPONDENCE

Hassaan Anwer Rathore,
hrathore@qu.edu.qa

†PRESENT ADDRESS

Hassaan Anwer Rathore,
Department of Pharmaceutical
Sciences, College of Pharmacy, QU
Health, Qatar University, Doha, Qatar.

†These authors have contributed equally
to this work

SPECIALTY SECTION

This article was submitted to
Experimental Pharmacology and Drug
Discovery,
a section of the journal
Frontiers in Pharmacology

RECEIVED 18 July 2022

ACCEPTED 30 August 2022

PUBLISHED 30 September 2022

CITATION

Abid R, Islam M, Saeed H, Ahmad A,
Imtiaz F, Yasmeen A and Rathore HA
(2022), Antihypertensive potential of
Brassica rapa leaves: An in vitro and in
silico approach.
Front. Pharmacol. 13:996755.
doi: 10.3389/fphar.2022.996755

COPYRIGHT

© 2022 Abid, Islam, Saeed, Ahmad,
Imtiaz, Yasmeen and Rathore. This is an
open-access article distributed under
the terms of the [Creative Commons
Attribution License \(CC BY\)](#). The use,
distribution or reproduction in other
forums is permitted, provided the
original author(s) and the copyright
owner(s) are credited and that the
original publication in this journal is
cited, in accordance with accepted
academic practice. No use, distribution
or reproduction is permitted which does
not comply with these terms.

Antihypertensive potential of *Brassica rapa* leaves: An *in vitro* and *in silico* approach

Rohma Abid^{1†}, Muhammad Islam¹, Hamid Saeed²,
Abrar Ahmad³, Fariha Imtiaz¹, Anam Yasmeen¹ and
Hassaan Anwer Rathore^{4*†}

¹Section of Pharmaceutical Chemistry, University College of Pharmacy, Allama Iqbal Campus, University of the Punjab, Lahore, Pakistan, ²Section of Pharmaceutics, University College of Pharmacy, Allama Iqbal Campus, University of the Punjab, Lahore, Pakistan, ³Section of Pharmacognosy, University College of Pharmacy, Allama Iqbal Campus, University of the Punjab, Lahore, Pakistan, ⁴Department of Pharmaceutical Sciences, College of Pharmacy, QU Health, Qatar University, Doha, Qatar

Aim: Plants contain many essential constituents and their optimization can result in the discovery of new medicines. One such plant is *Brassica rapa* that is commonly used as a vegetable to fulfill daily food requirements worldwide. This study intends to screen the phytochemicals, antihypertensive potential, GC-MS, and *in silico* analysis of the leaves of *Brassica rapa*.

Methods: Powdered leaves were subjected to proximate analysis followed by estimation of primary metabolites. Extracts were obtained by hot and cold extraction and investigated for secondary metabolites. All crude extracts were screened for their antihypertensive potential using an angiotensin-converting enzyme (ACE) inhibition assay. GC-MS analysis was carried out to standardize the extract, and an antihypertensive metabolite was confirmed using an *in silico* approach.

Results: Physicochemical evaluation resulted in moisture content ($9.10\% \pm 0.1$), total ash value ($18.10\% \pm 0.6$), and extractive values (water $9.46\% \pm 0.5$ and alcohol soluble $4.99\% \pm 0.1$), while phytochemical investigation revealed primary metabolites (total proteins $11.90 \text{ mg/g} \pm 0.9$; total fats $3.48 \text{ mg/g} \pm 0.5$; and total carbohydrates $57.45 \text{ mg/g} \pm 1.2$). Methanol extract showed the highest number of secondary metabolites including polyphenols $93.63 \text{ mg/g} \pm 0.6$; flavonoids $259.13 \text{ mg/g} \pm 0.6$; and polysaccharides $56.63 \text{ mg/g} \pm 1.4$, while water extract ($70 \text{ mg/g} \pm 2$) was rich in glycosaponins. Methanol extract showed the highest antihypertensive potential by inhibiting ACE (79.39%) amongst all extracts, compared to the standard drug captopril, which inhibited 85.81%. Standardization of methanol extract *via* GC-MS analysis revealed potent phytoconstituents, and a molecular docking study confirmed that oleic acid is the main antihypertensive metabolite.

Conclusion: We conclude that leaves of *Brassica rapa* can successfully lower hypertension by inhibiting ACE, however; *in vivo* investigations are required to confirm this antihypertensive activity.

KEYWORDS

Brassica rapa, food, antihypertensive action, ACE inhibitor and molecular docking, in silico

1 Introduction

Despite great development in the field of medicine, the disease burden is high. Plants contain many essential constituents, optimization of which can result in the discovery of new medicines. Drugs obtained from natural sources like plants are safer and economically viable. The primitive and current research evidence suggests that plants are a major source and popular medicine for maintaining health in people of the Asian subcontinent (Sheng-Ji, 2001). Drugs derived from natural origin mainly plants as food have garnered attention as potential therapeutic entities (Shoeb, 2006).

Plants included in the Brassicaceae or Cruciferae family are generally common vegetables that fulfill the daily food requirements throughout the world. The roots and green leaves of such a plant, *Brassica rapa*, are commonly called turnip and have nutritional and medicinal values (Paul et al., 2019). According to the United States Department of Agriculture's Food Data Central database, one cup of raw turnip cubes contains around 36.4 calories, 1.17 g of protein, 0.13 g of fat, 8.36 g of carbohydrates including 4.66 g of sugar, 2.34 g of fiber, 39 mg of calcium, 0.39 mg of iron, 14.3 mg of magnesium, 35.1 mg of phosphorus, 0.13 µg of vitamin K, 87.1 mg of sodium, 0.351 mg of zinc, 27.3 mg of vitamin C, and 19.5 µg of folate. *Brassica rapa* has a variety of volatile substances such as aldehydes, ketones, alcohols, and esters. It also contains flavonoids and derivatives of hydroxycinnamic acid. Turnips are also popular as fodder for animals (Taveira et al., 2009). In Perso-Arabic tradition, *Brassica rapa* was employed as a medicine for inflammation of the gall bladder, gall stones, constipation, hepatic diseases, and gastritis. The roots of turnip possess antibacterial properties and were used in the treatment of common cold (Beltagy, 2014). For a long time, the powder of seeds of *Brassica rapa* is well-known for its anticancer properties, especially in breast cancer, and the product obtained from roots has shown benefits in skin cancer. Turnip has also been a common diet and herbal remedy in Tibet, where high altitude leads to oxygen deficiency and exhaustion (Ahmadvand and Sariri, 2008).

Norlander et al. (2018) explained hypertension with reference to the current recommendation as an increase in systolic blood pressure of more than 130 mm Hg. The prevalence of primary hypertension is almost 95% and is associated with cardiac diseases, diabetes, and hyperlipidemia (Messerli et al., 2007). About 24% of the total population or 43 million individuals in the United States of America are hypertensive (Carretero and Oparil, 2000), and nearly 25% of the residents in developed countries are suffering from the problem of raised blood pressure (Lifton et al., 2001). It is

estimated that by 2025, the worldwide cases of hypertension may rise to 500 million (Norlander et al., 2018).

With a population of more than 150 million, Pakistan is dealing with the widespread issue of elevated blood pressure. In consonance with a survey study carried out in Pakistan, three-quarter of the natives is suffering from hypertension without being aware of it (Ahmad and Jafar, 2005). Recent analysis has indicated the prevalence of hypertension in Pakistan to be 20.7%, whereas high blood pressure is still manageable in underdeveloped countries with proper management of the disease (Mittal and Singh, 2010). Lifestyle choices and other major factors such as increased consumption of salt and liquor, sedentary lifestyle, being overweight, etc., are important contributors to the high prevalence of hypertension. Further causes responsible for hypertension include anxiety, traumas, and miscellaneous ecological aspects (Whelton, 1994). Diuretics, calcium channel blockers, RAAS inhibitors, and beta-blockers are mostly the drugs of choice prescribed as a single pill or in combination therapy to the population facing high blood pressure. However, their continuous use leads to many side effects, including erectile dysfunction, nervousness, muscle weakness, and frequent headaches (Williams, 2009).

Hypertension can lead to heart problems such as kidney failure, coronary heart disease, and peripheral arterial disease. Pharmacological approaches for alleviating the symptoms of hypertension tend to decline the incidence of cardiac diseases including myocardial infarction, stroke, etc. However, for the elimination and cure of hypertension, non-pharmacological therapy could be the most effective approach (Burt et al., 1995). Comini et al. (2007) stated that ACE inhibitors exert their effect by over-expression of an endothelial enzyme, nitric oxide synthase (eNOS), which is involved in the regulation of blood pressure by producing nitric oxide, a potent vasodilator.

Literature shows several studies where turnip has been investigated for many pharmacological activities, but the antihypertensive activity of the leaves of *Brassica rapa* has not been investigated. Thus, the purpose of the current study is to analyze the leaf extract of *Brassica rapa* for antihypertensive activity by applying an angiotensin-converting enzyme (ACE) inhibition assay, followed by *in silico* analysis.

2 Materials and methods

2.1 Collection of plant leaves

Approximately 15 kg leaves were collected in January 2021 from the fields of Gujranwala district of northern Punjab. The leaves were washed, and dust was removed. They

were dried in sunlight for 4–5 days. After drying, the leaves were crushed to a fine powder. The powdered form weighed almost 2,500 g and was stored in an air-tight jar. The identification and authentication of leaves were carried out by Prof. Dr. Zaheer-uddin Khan from the Botany Department of Government College University, Lahore (GCU). Voucher number GC. Herb.Bot.3721 was allocated by the GCU Lahore herbarium to the plant.

2.2 Solvent and chemicals

N-hexane (Merck, United States), chloroform (May and Baker, UK), methanol (Merck, Germany), ethanol (Merck, Germany), deionized water, hydrochloric acid (BDH, England), sulphuric acid (BDH, England), nitric acid (BDH, England), sodium carbonate, copper sulfate, potassium acetate, aluminium nitrite, acetone, sodium hydroxide, sodium chloride (E. Merck A. G Darmstadt, Germany), quercetin (Sigma, United States), bovine serum albumin (Sigma, United States), gallic acid (Sigma, United States), anhydrous glucose (Merck, Germany), Triton X (Sigma, United States), Folin–Ciocalteu's phenol reagent (Unichem Chemicals, India), anthrone reagent (Sigma, United States), monosodium phosphate (BDH, England), disodium phosphate (Riedel-de Haen, Germany), 3, 5-dinitrosalicylic acid (BDH, England), potassium sodium tartrate (BDH, England), and distilled water were used in experiments.

2.3 Preparation of plant extract

The hot and cold extraction method was used for collecting the extract from the leaves of *Brassica rapa*. Hot extraction was carried out using the Soxhlet apparatus. The extraction was carried out by using the solvents in increasing order of polarity, that is, n-hexane, chloroform, and methanol. Cold extraction was simply carried out using two polar solvents: alcohol and distilled water (Yadav and Agarwala, 2011).

2.4 Physicochemical analysis

Physicochemical analysis was performed on the leaves of *Brassica rapa* with reference to the protocols of USP (2005).

2.4.1 Moisture content

Two grams of powdered leaves were weighed and placed in the crucible. The crucible was then placed in an oven at 105 °C for 30 min. After 30 min, the crucible was taken out and weighed. The loss in weight was recorded. The method was repeated until the weight of the powder became constant. Calculation of

moisture content was carried out by using the following formula (Eq. A.1, A.2):

$$\text{Dry matter (\%)} = \frac{\text{Initial weight} - \text{final weight}}{\text{weight of dried sample}} \times 100, \quad (\text{A.1})$$

$$\text{Moisture content (\%)} = 100 - \text{Dry matter}. \quad (\text{A.2})$$

2.4.2 Ash values

2.4.2.1 Total ash

Two grams of powdered sample were taken in a pre-weighed China dish. China dish was incinerated by placing it in a muffle furnace at $675 \pm 25^\circ\text{C}$ until the sample became carbon-free. It was taken out of the furnace and allowed to cool in a desiccator at room temperature. Weight was noted, and the following formula (Eq. B.1) was used to calculate the total ash content:

$$\text{Total Ash (\%)} = \frac{\text{weight of Ash}}{\text{total weight of powder}} \times 100. \quad (\text{B.1})$$

2.4.2.2 Acid insoluble ash

Two grams of sample were measured and placed in a China dish in a muffle furnace at 675°C until it became carbon-free. It was then cooled in desiccators and weighed. The resultant ash was boiled for 5 min in 25 ml of 3N HCL and allowed to cool at room temperature. The mixture was filtered using ashless filter paper. The residue obtained was washed with hot double distilled water and again placed in the furnace. The sample was cooled and weighed when it became carbon-free. The percentage of acid insoluble ash was determined by the following formula (Eq. B.2):

$$\text{Acid Insoluble Ash (\%)} = \frac{\text{weight of acid insoluble ash}}{\text{total ash}} \times 100. \quad (\text{B.2})$$

2.4.2.3 Water insoluble ash

The ash obtained in the total ash test was boiled for 5 min with 25 ml of double distilled water and passed through ashless filter paper. The residue left on the filter paper was placed in a China dish which was allowed to incinerate in a muffle furnace at 450°C for 15 min. The weight of China dish was then measured, and an assessment of water-insoluble ash was carried out by the following formula (Eq. B.3):

$$\text{Water Insoluble Ash (\%)} = \frac{\text{weight of water insoluble ash}}{\text{total ash weight}} \times 100. \quad (\text{B.3})$$

2.4.2.4 Sulfated ash

Two grams of sample were added to a washed, dried, and pre-weighed china dish. Then, 1 ml of concentrated sulphuric acid was added. Also, it was heated on a low flame until the fumes

disappeared. This process was repeated twice, and then the China dish was placed in the muffle furnace at a temperature of $600 \pm 25^\circ\text{C}$ for 30 min. The China dish was cooled and weighed. The percentage of sulfated ash was measured using the following equation (Eq. B.4):

$$\text{Sulfated Ash (\%)} = \frac{\text{weight of sulfated ash}}{\text{weight of powder ash}} \times 100. \quad (\text{B.4})$$

2.4.3 Extractive values

2.4.3.1 Water soluble extractive value

Five grams of powder were accurately weighed and added to a conical flask containing 100 ml of double distilled water. The flask with a magnetic stirrer was placed on the hotplate to allow shaking for 24 h. The solution was filtered after 24 h. China dish was weighed and 25 ml of the filtrate was added and placed in an oven at 105°C for evaporation. After evaporation, the China dish was weighed again. Extractive value relative to dried powder was evaluated. The percentage was calculated by the following equation (Eq. C.1):

$$\begin{aligned} \text{Water soluble extractive value (\%)} \\ = \frac{\text{weight of dried extract}}{\text{weight of powder sample}} \times 100. \end{aligned} \quad (\text{C.1})$$

2.4.3.2 Alcohol soluble extractive value

Five grams of powder from the leaves of *Brassica rapa* was mixed with 100 ml of ethanol in a conical flask and was continuously shaken on a hotplate. After 24 h, it was removed from the hot plate and filtered. Twenty-five mL of filtrate in the China dish was then placed in the oven at 105°C . The weight of dried material was recorded with reference to the weight of the air-dried sample. The percentage of alcohol soluble extractive value was measured by the formula given below (Eq. C.2):

$$\begin{aligned} \text{Acid soluble extractive value (\%)} \\ = \frac{\text{weight of dried extract}}{\text{weight of powder sample}} \times 100. \end{aligned} \quad (\text{C.2})$$

2.5 Estimation of primary metabolites

2.5.1 Total protein content

Estimation of total protein content was completed by following the protocol of Lowry et al. (1951) with slight modifications. In a Falcon tube, 1 g of powdered material, 10 ml of distilled water, and five drops of Triton X were added and shaken randomly. The solution in the Falcon tube was centrifuged at 2,700 rpm for 10 min. After centrifugation, the supernatant layer was formed, from which 100 μL was taken and double distilled water was added to make the volume up to 1 ml.

To this mixture, 3 ml of reagent C and 0.2 ml of Folin–Ciocalteu reagent were added. Reagent C was prepared by combining 50 ml of reagent A and 1 ml of reagent B. Reagent A consisted of 2% sodium carbonate and 0.1 N sodium hydroxide while reagent B comprised 0.5% copper sulfate in 1% potassium sodium tartrate. The sample was incubated at room temperature for 30 min. Absorbance against a blank solution was taken at 600 nm. The blank solution was prepared in the same way as the sample solution except for the powdered sample. Bovine serum albumin (BSA) was used as a standard for protein content estimation. The absorbance of different dilutions ranging from 20–120 $\mu\text{g/ml}$ was measured and plotted against the standard curve through linear regression.

2.5.2 Total lipid content

For hot extraction with n-hexane, 50 g of powdered material was packed in a thimble, and maceration was carried out in the solvent. The temperature of $40\text{--}60^\circ\text{C}$ was maintained throughout the process of extraction. After completion of extraction, filtration was carried out, and a rotary evaporator was used to dry the filtrate. It was then transferred to a pre-weighed glass vial. The vial was then placed in an oven at 40°C for further drying. Evaluation of total lipid content was carried out after it was completely dried and weighed and expressed in mg/g of the total sample taken (Besbes et al., 2004).

2.5.3 Total carbohydrates

The formula discussed by Al-Hooti et al., 1997 for total carbohydrate determination was used by taking the difference between total lipid and total protein content from 100 (Eq. D.1).

$$\begin{aligned} \text{Total carbohydrates (\%)} = 100 - (\text{Total moisture} + \text{Total ash} \\ + \text{Total fats} + \text{Total proteins}). \end{aligned} \quad (\text{D.1})$$

2.6 Estimation of secondary metabolites

2.6.1 Determination of total polyphenols

Evaluation of phenolic content of all the five extracts of *Brassica rapa* leaves was accomplished in accordance with the experiments by Slinkard and Singleton (1977). The standard used for plotting the calibration curve in this experiment was gallic acid. Standard and stock solutions were prepared using a 1 mg/ml concentration of methanol. In individual Falcon tubes, 200 μL of sample and standard were taken. Then, 200 μL of Folin–Ciocalteu (FC) reagent was added. Two mL of 15% sodium carbonate was added after 4 min, and the final volume was achieved with 3 ml methanol. A blank solution was made which contained the same reagents except for the sample. Then, 10, 20, 40, 60, 80, 100, and 120 $\mu\text{g/ml}$ dilutions of the sample were prepared. All the samples, blank and standard were incubated at

room temperature for 2 h and absorbance was found using a UV-visible spectrophotometer at 760 nm. Total phenolic content was measured through a linear regression equation and expressed as mg/g.

2.6.2 Determination of total flavonoids

The number of flavonoids in *Brassica rapa* leaves was measured by using a method proposed by Chang et al. (2002). For the preparation of a standard solution of quercetin, methanol was used. Stock solutions of all the five extracts of samples were prepared using methanol at a concentration of 1 mg/ml. Different dilutions of the sample were made. The working solution was prepared by mixing 200 µl solution from the stock solution and standard with methanol, and the volume was made up to 1 ml. After that 100 µl of 10% (w/v) aluminum nitrate, 100 µl 1 M potassium acetate, and 4.6 ml of double distilled water were added. The blank solution had all reagents except the sample. For measuring the absorbance, all test tubes were incubated at 25°C, and absorbance was recorded using a UV spectrophotometer at a wavelength of 415 nm. Using quercetin as a reference standard, total flavonoids were then calculated.

2.6.3 Total polysaccharides

The procedure given by Hussain et al. (2008) was used for total polysaccharide content. A quantity of 200 mg taken from each of the five extracts was mixed in 80% of 7 ml of warm ethanol. The solution was run for 2 min on a vortex mixer and then centrifuged at 2,700 rpm for about 10 min. Anthrone reagent (45 mg anthrone in 100 ml chilled 85% sulphuric acid) was added drop-wise to the residue, and the same process was repeated until the solution displayed no color upon the addition of anthrone reagent. The residue was then dried, and 10 ml digestion mixture (5 ml of 25% HCl and 5 ml of double distilled water) was added. The Falcon tubes were put in an ice bath for 20 min until the temperature reached 0°C. This was followed by centrifugation for 10 min, and the supernatant was obtained. For the collection of supernatants, the whole process was repeated. The final volume was made up using distilled water; 4 ml of anthrone was added to the mixture, which was boiled in a water bath for 8 min and then chilled instantly. The blank solution did not contain the sample but contained water, ethanol, anthrone, and digestion mixture. Absorbance was taken at 630 nm by using glucose as standard. Different dilutions ranging between 10 and 120 µL were prepared for all the extracts, absorbance was recorded, and a standard curve was plotted. The linear regression equation was used to find out the values, and the results were multiplied by a factor of 0.9.

2.6.4 Total glycosaponins

Siddiqui et al. (2009) stated that 1 g of extract was taken in a 100-ml round-bottom flask, and 50 ml of methanol was added. The solution was allowed to heat on a reflux condenser for

30 min. It was repeated two times and then filtered. The filtrate was passed through the rotary evaporator until much of it evaporated, leaving behind 10 ml of filtrate in the flask; 50 ml acetone was taken in a beaker, and 10 ml of the filtrate was added drop-wise. Consequently, saponins were precipitated out. Precipitates were dried in an oven at 100°C until the weight became constant. The same method was used for the rest of the extracts. The formula used for the estimation of glycosaponins is stated below (Eq. E.1):

$$\text{Glycosaponins (mg/g)} = \frac{\text{weight of precipitate}}{\text{weight of sample}} \times 100. \quad (\text{E.1})$$

2.6.5 Fourier transform infrared (FTIR) profiling

Functional group analysis in leaves of *Brassica rapa* was completed using a Fourier transform infrared spectroscopic technique. All the extracts of leaves of *Brassica rapa* were placed on a crystal of the FTIR spectrophotometer, and spectra were recorded.

2.7 In vitro antihypertensive activity

2.7.1. Preparation of reagents

- Reagent A: 300 mM sodium chloride with pH 8.3 in 100 mM sodium borate buffer
- Reagent B: Buffer substrate solution (using 5 mM hippuryl-L-histidyl-L-leucine (HHL) and reagent A)
- Reagent C: Angiotensin-converting enzyme (ACE) solution (0.1 unit/ml).

2.7.2 Preparation of sample and standard stock solutions

Sample solutions of n-hexane, chloroform, methanol, ethanol, and water extract were made by taking 1 mg of each extract in 1 ml of sodium borate buffer pH 8.3. The reference standard solution was made using 1 mg of captopril in 1 ml of sodium borate buffer pH 8.3.

2.7.3 Angiotensin-converting enzyme (ACE) inhibition assay

The ACE inhibition assay proposed by Cushman and Cheung (1971) was performed with slight modifications. The sample for each extract was prepared by mixing 100 µl buffer substrate solution (reagent B), 40 µl extract solution, and 20 µl ACE solution (reagent C). For control, 100 µl of buffer substrate solution (reagent B), 40 µl of deionized water, and 20 µl of ACE solution (reagent C) were mixed together. Preparation of blank solution requires 100 µl of buffer substrate solution (reagent B) and 60 µl of deionized water; 100 µl of buffer substrate solution (reagent B), 40 µl of captopril solution, and 20 µl of ACE solution (reagent C) were taken to make the standard solution. All the test

tubes were incubated for 30 min, and the temperature was maintained at 37°C. To end the reaction, 250 µl of 1M HCl was added. The formation of hippuric acid occurs as a result of the reaction between angiotensin-converting enzyme (ACE) and hippuryl-L-histidyl -L-leucine (HHL). For extraction of hippuric acid, 1 ml of ethyl acetate was used and subjected to vigorous stirring in a vortex mixer for 15 s. Centrifugation of all samples was completed in 10 min. One mL of the organic layer was shifted to a test tube and heated at 100°C for 30 min until it evaporated. The residual matter was again dissolved in 1 ml of deionized water. Using a spectrophotometer, the absorbance of the sample, blank, control, and standard was measured at 228 nm. The percentage inhibition was calculated by using the following equation (Eq. F.1):

$$\begin{aligned} \text{Percentage inhibition (\%)} &= \frac{\text{test control} - \text{test solution}}{\text{test control} - \text{blank solution}} \times 100. \end{aligned} \quad (\text{F.1})$$

2.8 GC-MS analysis of methanol extract of leaves of *Brassica rapa*

GC-MS (GC system 7890A, Agilent Technologies, United States, and MS 5975C, Agilent Technologies, United States) was used for the analysis of methanolic extracts of powdered leaves of *Brassica rapa*. The capillary tube was 30 m in length and 0.25 mm in diameter with a film coating of 0.25 µm. A carrier gas, helium, with a flow rate of 0.25 ml/min was used. The extract was dissolved in methanol for preparing the sample. A sample volume of 1 µl was taken, and column pressure was set to 0.77 psi. Initially, for 5 minutes, the temperature of the oven was maintained at 100°C, which was then raised to 200°C at the rate of 10°C/min and retained for 10 min. In the end, at the rate of 25°C/min, the temperature was elevated to 325°C for 30 min and was kept constant for 10 min. Various peaks were obtained for different compounds present in the methanolic extract of *Brassica rapa* leaves. The constituents present in the extracts were interpreted by comparing the peaks to the database of the National Institute of Standards and Technology NIST20, having a minimum quality factor of 70 (Priya and Subhashini, 2016).

2.9 *In silico* molecular docking studies

Molecular modeling was performed on the selected compound using the Schrödinger Maestro Suite.

2.9.1 Preparation of protein

Three-dimensional conformation of the protein, that is, eNOS (PDB: 1D0C), was achieved with the help of the

Protein Preparation Wizard in Maestro. All the water molecules and ligands were removed from the protein structure.

2.9.2 Preparation of ligand

Oleic acid, obtained in GC-MS analysis, was selected as a ligand. For molecular modeling, a minimized structure was preferred.

2.9.3 Molecular docking analysis

Using Glide software available in Maestro, molecular docking of the selected ligand, that is, oleic acid, was carried out. Initially, for locating the binding site with the highest affinity, blind docking was conducted, and finally molecular docking was conducted using Glide 6.2 Extra Precision.

2.9.4 Molecular dynamic simulation

For an improved understanding of compounds, molecular modeling was performed for 50 ns. In the first step, using the antechamber module of Amber18, libraries, specifications for the receptor, and the ligand were generated. Charge neutralization, hydrogen atom minimization, and optimization of energy were achieved. For limitation of the hydrogen bond system, the temperature was raised to 300 K via canonical (NVT) ensemble. Keeping pressure constant through NPT equilibration was accomplished for 100 ps. Finally, the system was examined for stability using systematic simulations (Wahedi et al., 2021).

3 Results

3.1 Extraction and proximate analysis

Results of proximate analysis of *Brassica rapa* are mentioned in Table 1. Moisture content found in the leaves of *Brassica rapa* was 9.1%. Powdered roots had a percentage moisture content of 6.48 ± 0.45%, and the total ash noted in sample leaves of *Brassica rapa* was 18%. The acid insoluble ash was found to be 5.7%, water-soluble 5.20% and sulfated was 21.60%.

3.2 Determination of phytochemicals

3.2.1 Determination of primary metabolites

The primary metabolite content in all extracts of *Brassica rapa* leaves was resolute and is listed in Table 2. For determination of protein content, linear regression equation was employed $Y = 0.0101x + 0.0296$, $R^2 = 0.9452$, and calibration curve was plotted for (10, 20, 40, 60, 80, and 100 µg/ml) dilutions of bovine serum albumin (BSA).

TABLE 1 Proximate analysis of extracts of *Brassica rapa* leaf powder.

Sr no.	Physicochemical parameters	Percentage content \pm SD (% w/w)
1	Moisture content	9.1 \pm 0.1
2	Total ash	18.10 \pm 0.6
3	Acid insoluble ash	5.70 \pm 0.2
4	Water soluble ash	5.20 \pm 0.2
5	Sulfated ash	21.60 \pm 0.6
6	Alcohol soluble extractive	4.99 \pm 0.1
7	Water soluble extractive	1.1 0.5

TABLE 2 Primary metabolites (mg/g) of powdered leaves of *Brassica rapa*.

Sr no.	Primary metabolites	mg/g \pm SD
1	Total proteins	11.90 \pm 0.9
2	Total lipids	3.48 \pm 0.5
3	Total carbohydrates	57.45 \pm 1.2

3.2.2 Determination of secondary metabolites

The secondary metabolite content in all extracts of *Brassica rapa* leaves was resolute and is listed in Table 3. Analysis of all secondary metabolites through linear regression equations was performed using different standards for different metabolites. By linear regression equation, total protein content was calculated as $y = 0.0101x + 0.0296$, $R^2 = 0.9452$. Bovine serum albumin was used as standard, and a calibration curve was plotted. The highest protein content was exhibited by methanol extract of leaves, followed by water, ethanol, chloroform, and n-hexane. For evaluation of total polyphenols, regression equation used was $y = 0.0037x + 0.0178$, $R^2 = 0.9953$. Gallic acid was used as a standard for methanol extract with maximum phenolic content. Using standard curve of quercetin, the total flavonoid count was $y = 0.0024x + 0.0147$. The highest value for flavonoids was observed in methanol.

Total polysaccharide estimation was carried out using a linear regression equation $y = 0.0028 + 0.022$, $R^2 = 0.9957$, where glucose was used as a standard. The results showed

that the extract of methanol has polysaccharides in a large amount. According to our study, water extract has the highest content of saponins.

3.2.3 FTIR scanning

FTIR scans of five extracts of *Brassica rapa* are presented in Figure 1. There was a broad range of peaks at the 3,500–3,200 cm^{-1} region in n-hexane and ethanol extracts which indicated O-H stretching. Methanol and water extracts showed small but distinct peaks, whereas all three extracts of n-hexane, chloroform, and ethanol showed distinct and sharp peaks in the 3,000–2,500 cm^{-1} range for C-H stretching bonds. All extracts have shown a series of peaks in the region of 2,140–1990 cm^{-1} , which shows N=C=S stretching.

3.3.4 Estimation of ACE inhibition activity of extract of leaves of *Brassica rapa*

Angiotensin-converting enzyme (ACE) inhibition activity of a concentration (1 mg/ml) of various leaf extracts of *Brassica rapa* was analyzed. The percentage inhibition of each solution is shown in Figure 2. It is evident from the results that methanolic extract of leaf powder of *Brassica rapa* shows the highest percentage inhibition of angiotensin-converting enzyme. Hence, the methanol extract has an activity against hypertension that is comparable to the ACE inhibition activity achieved with the standard drug captopril, while n-hexane has a 35% inhibitory effect that is least comparable to the reference standard. Further *in vivo*

TABLE 3 Secondary metabolites (mg/g) of extracts of powdered leaves of *Brassica rapa*.

Extracts	Total proteins mg/g	Total polyphenols mg/g	Total flavonoids mg/g	Total polysaccharides mg/g	Total glycosaponins mg/g
n-hexane	9.78 \pm 1.2	15.82 \pm 0.7	28.54 \pm 0.5	21.53 \pm 0.4	Negative
Chloroform	13.68 \pm 1.2	74.65 \pm 0.7	151.93 \pm 1.0	26.30 \pm 0.5	Negative
Methanol	56.29 \pm 1.1	93.63 \pm 0.6	259.13 \pm 0.6	56.63 \pm 1.4	60.13 \pm 1.6
Ethanol	35.53 \pm 0.6	37.38 \pm 1.2	172.68 \pm 0.5	43.16 \pm 1.0	53.26 \pm 0.6
Water	37.18 \pm 0.9	46.66 \pm 0.5	105.08 \pm 0.4	19.02 \pm 0.4	70 \pm 2

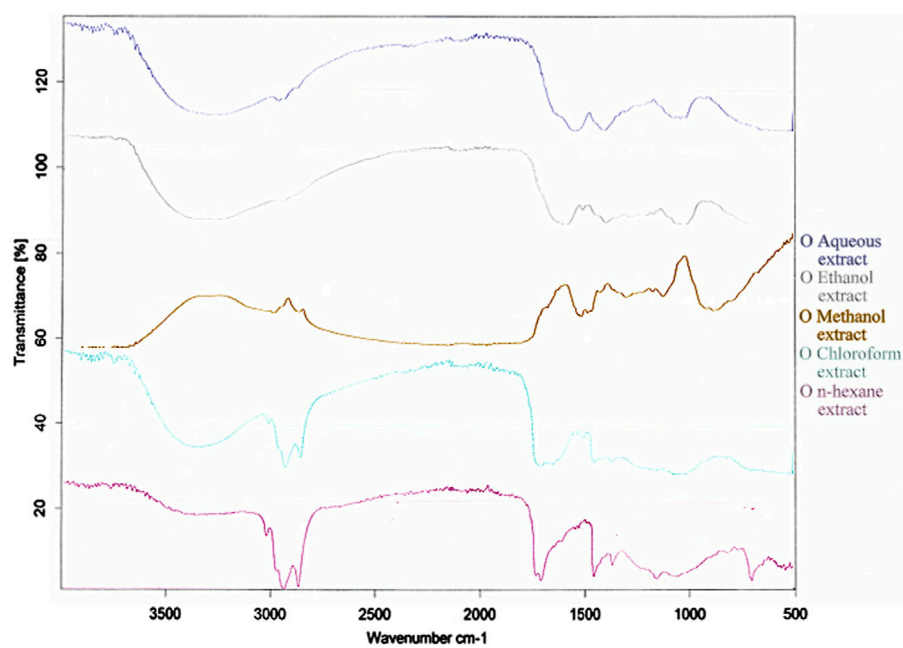


FIGURE 1
FTIR spectrum of extracts of leaves of *Brassica rapa*.

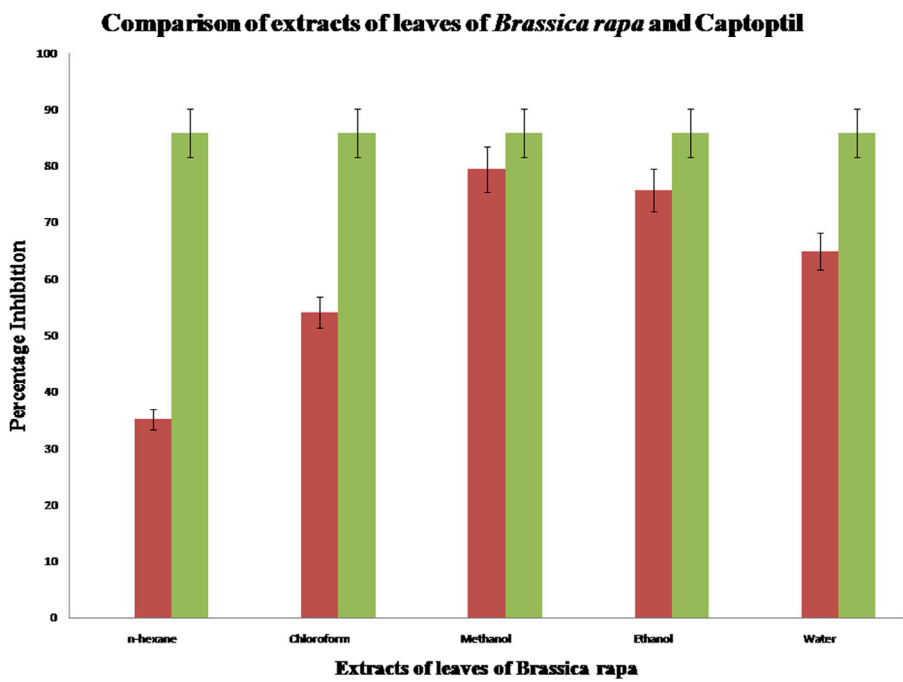


FIGURE 2
Comparison of ACE inhibition activity of extracts of leaves of *Brassica rapa* with standard captopril.

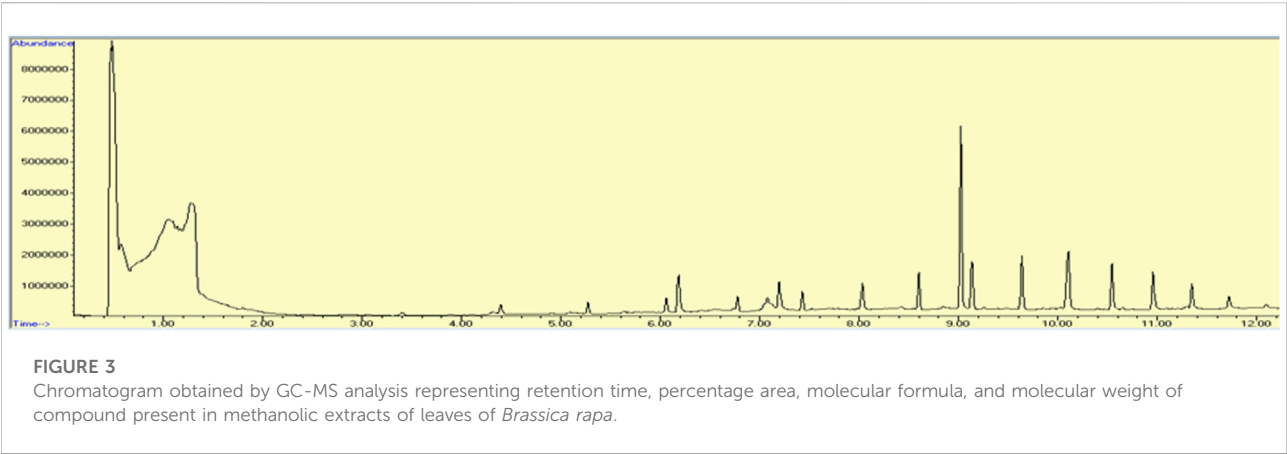


TABLE 4 GC-MS analysis of methanol extract of *Brassica rapa*.

Sr no.	Compound name	Molecular formula	Molecular weight g/mol	% area	Retention time min
1	Hexadecanoic acid, methyl ester	C17H34O2	270.45	1.10	6.184
2	Methyl stearate	C19H38O2	298.50	0.91	7.199
3	7,10,13, hexadecatrienoic acid, methyl ester	C17H28O2	264.40	1.18	7.07
4	Hexadecane, 1-chloro	C16H33Cl	260.88	0.11	8.419
5	Methyl tetradecanoate	C15H30O2	242.39	0.08	5.084
6	Hexacosane	C26H54	366.70	0.06	9.253
7	Oleic acid	C18H34O2	282.46	0.09	6.546
8	Octacosane	C28H58	394.76	0.04	10.027
9	Cholesterol	C27H46O	386.65	0.10	11.295
10	Phenol, 4-ethenyl-2,6-dimethoxy	C10H12O3	180.20	0.21	4.317
11	Octadecane	C18H38	254.49	0.03	5.483
12	Disulfide, di-tert-dodecyl	C24H50 S2	402.8	0.06	4.909
13	1,2-benzene dicarboxylic acid ethyl methyl ester	C11H12O4	208.21	0.05	6.740
14	Pentacosane	C25H52	352.68	0.12	8.848
15	Dodecane, 2,6,10-trimethyl	C15H32	212.41	0.03	7.984
16	Androst-5-ene-3,4,17,triol	C28H54O3Si3	523	0.99	10.957
17	Isopropyl myristate	C17H34O2	270.45	0.10	5.628
18	Heptasiloxane	O6Si7	292.59	0.14	13.362
19	Cyclononasiloxane, octadecamethyl	C18H54O9Si9	667.38	1.88	10.105

studies using other models can be conducted on the leaf extract of *Brassica rapa* to investigate the antihypertensive potential of the plant.

3.3.5 Estimation of GC-MS analysis of methanol extract of leaves of *Brassica rapa*

The chromatogram shown in Figure 3, names of the compounds obtained by GC-MS analysis, their retention time, % area, molecular formula, and molecular weight are listed in Table 4. The results of GC-MS evaluation showed the presence of

many compounds including straight chain alkanes, fatty acids, aromatic compounds, and siloxanes.

3.3.6 In silico molecular docking studies

The results of in silico docking studies are tabulated in Table 5. The escalated negative docking score (-4.818) depicts the high binding affinity (-51.3 kcal/mol) of the receptor–ligand complex portraying the biological activity of the compound. Figures 4A and B illustrate the 3D imaging of binding sites in the protein, while Figure 4C represents the binding site with

TABLE 5 Docking results showing G score, binding, and receptor energy.

Title	Docking score	Glide Gscore	Prime energy kcal/mol	Receptor energy kcal/mol	MMGBSA dg bind kcal/mol
Ligprep					
Oleic acid					
Glide dock					
1D0C					
Oleic acid	−4.818	−4.822			
Prime MMGBSA					
1D0C					
Oleic acid	−4.818	−4.822	−35774.8	−35687.247	−51.3
Desmond setup					
Oleic acid	−4.818	−4.822	−35774.8	−35687.247	−51.3

ligand. The docking study reveals that oleic acid can bind within the C1 pocket of endothelial nitric oxide synthase depending upon the binding affinity toward that site shown in Figure 5. In eNOS, there are two binding pockets C1 and C2, where oleic acid can possibly bind through amino acid residues such as B: ARG 608, B:GLN483, B:HIS 342, and B:ARG 486. For testing the stability of the docked compound, docking simulations were performed with the help of the Maestro-Desmond v12.3 Schrödinger software package, and the interaction of eNOS with the appropriate ligand was evaluated. The addition of water molecules was carried out by placing the docking complex in an orthorhombic box. Na⁺/Cl[−] ions were used to neutralize the charge. At normal pressure and 300 K temperature, the run time for docking simulation was 50 ns. Using the default setting, root mean square deviation (RMSD) of the protein–ligand complex and amino acids that participated in this contact were investigated. The RMSD plot of protein and ligand is shown in Figure 6. The binding of enzyme with the ligand against the interaction fraction displayed hydrogen bonding, hydrophobic and ionic interaction, and water bridges. ARG 486 and ASN 574 bind with the enzyme through strong hydrogen bonds. TRP 414, PHE 589, and PHE 709 showed hydrophobic interaction of simulation time between 50–60%. Water bridge-mediated hydrogen bonding is seen with ARG 486 residue. The binding residues in the ligand that react with the enzyme can be noted in Figure 7.

4 Discussion

The study was conducted on turnip leaves. Moisture content found in the leaves of *Brassica rapa* was 9.1% which was approximately similar to the findings of another study conducted on turnip leaves. Hammad and Abo-Zaid (2020)

conducted a study in Egypt and observed the moisture content present in powdered turnip leaves to be 9.6%. An increase in moisture content increases microbial growth and decreases the storage time and efficacy of the product (Kunle et al., 2012). Less moisture content leads to increased stability (Olujemisi et al., 2012). Turnip root powder has a percentage moisture content of $6.48 \pm 0.45\%$ as per a previous study (Mahfouz et al., 2019). Ash value is a measure of impurities present in the raw material used for drugs. The residual material that remains after the plant is incinerated gives the total ash value, while the presence of sand or silica in the plant gives the value of acid insolubility (Unit and Organization, 1992). The total percentage of ash in our sample, leaves of *Brassica rapa*, was 18% which is comparable to the results of a previous study which revealed that the ash value of powdered turnip leaves in Egypt was 12.12% (Hammad and Abo-Zaid, 2020).

Primary metabolites (carbohydrates, proteins, and lipids) are involved in plant maturation and growth. (Erb and Kliebenstein, 2020). Amongst other factors, the development and growth of an individual depends on the number of carbohydrates, proteins, and lipids present in the diet. Proteins are important in performing different body functions, for instance, nutrients transported across the cell membrane and the functioning of enzymes (Mæhre et al., 2018). According to Hammad and Abo-Zaid (2020), the percentage of fats, carbohydrates, and proteins detected in powdered leaves of *Brassica rapa* was 1.69, 41.92, and 16.44%, respectively. Our calculated values of lipid, carbohydrates, and protein are 3.48, 57.45, and 11.90%, respectively. This shows that turnip leaves have high carbohydrate content. Carbohydrates are remarkably essential in plant cell morphology as well as in metabolic processes. They mostly occur as polysaccharides and serve as anti-ulcer, laxative, hypoglycemic, immunomodulators, analgesic, expectorant, hypocholesterolemic, and anabolic.

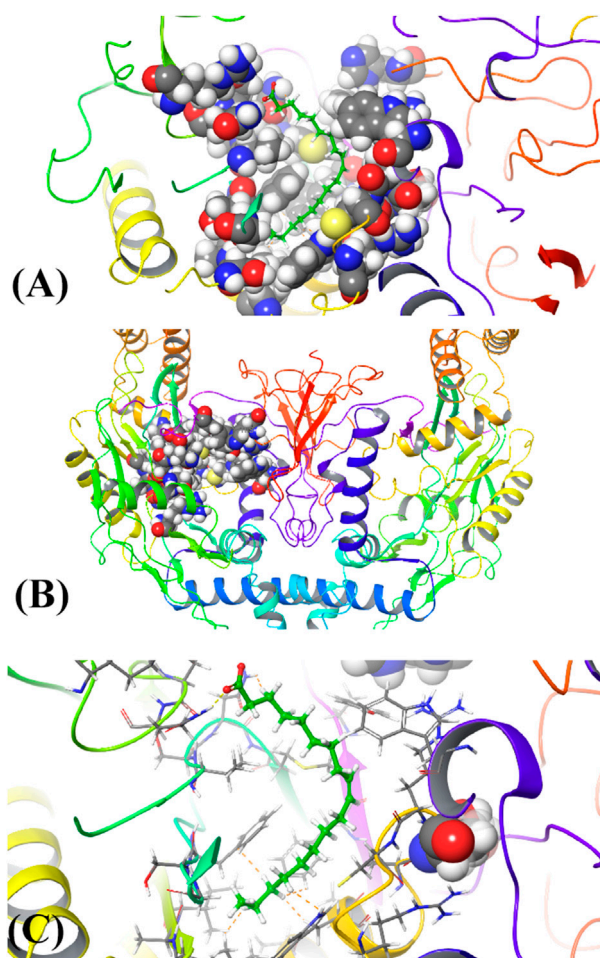


FIGURE 4

(A) 3D structure of ligand binding with c1 pocket of enzyme, (B) Horn shaped structure of enzyme with binding pocket, and (C) attachment of the ligand with the binding site of the enzyme.

They are advantageous in decreasing the toxicity of cytostatic drugs and antibiotics. The most important function is their role in the pharmacodynamics of drugs obtained from plant source (Budniak et al., 2021).

Because of their scavenging power, polyphenols are considered essential constituents of plants (Nguyen et al., 2020). Other than their role as antioxidants, flavonoids are also responsible for several therapeutic properties such as antitumor, anti-inflammatory, antiviral, antibacterial, and anti-allergy (Priecina and Karlina, 2013). Our research suggests that the methanolic extract of turnip was rich in flavonoids and polyphenols.

Glycosaponins are secondary metabolites with a large molecular weight. They are of prime importance for their cardio-protective and anti-angiogenesis inhibition of multi-drug resistance effects. Saponins play a vital role in minimizing the effects of radio and chemotherapy (Xu et al.,

2016). This study indicates that aqueous extracts of *Brassica rapa* contained glycosaponins in abundance, while glycosaponins were not detected in non-polar solvents (n-hexane and chloroform).

As stated by Chizoruo et al. (2019), the functional groups in the IR region indicate the existence of phytoconstituents in plant studies. The presence of alcohols, aldehydes, ketones, carboxylic acids, aromatic aldehydes, ethers, nitro compounds, alkanes, alkenes, and amines was shown by FTIR analysis on turnip leaves. A similar study was performed by Dhivya (2017), and our results are also in accordance with the reports of Chizoro et al.

The results of GC-MS evaluation showed the presence of many compounds, most of which are of great importance in the field of medicine. The constituents include straight chain alkanes such as pentacosane, hexacosane, octacosane, octadecane, and hexadecane. Pentacosane exhibits medicinal properties by acting

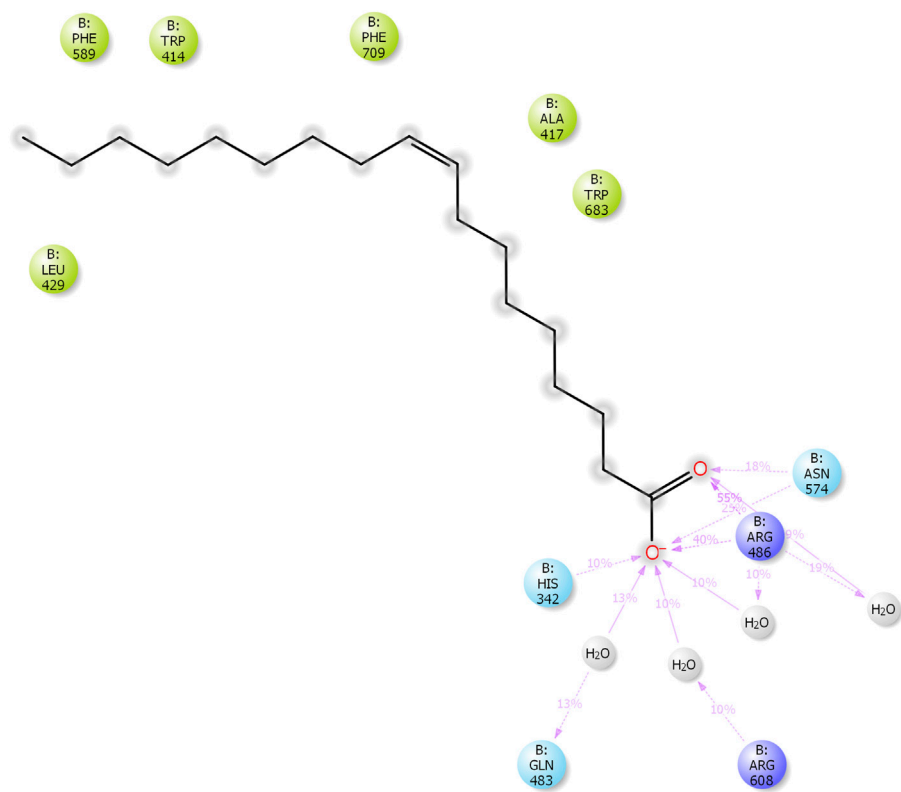


FIGURE 5
Two-dimensional ligand (oleic acid) interaction with endothelial nitric oxide synthase (eNOS). The binding of oleic acid takes place through amino acid residues; B:ARG 608, B:GLN483, B:HIS 342, and B:ARG 486.

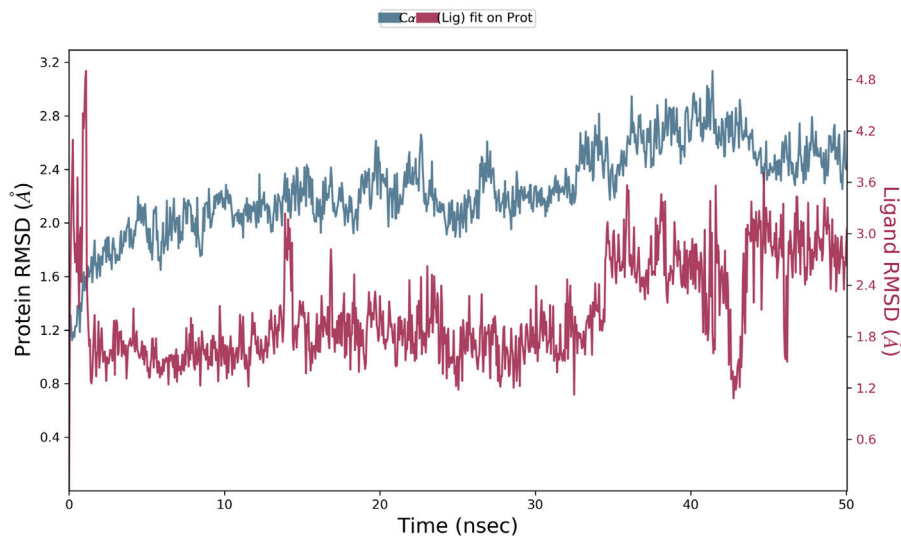


FIGURE 6
Root mean square deviation (RMSD) plot of protein and ligand.

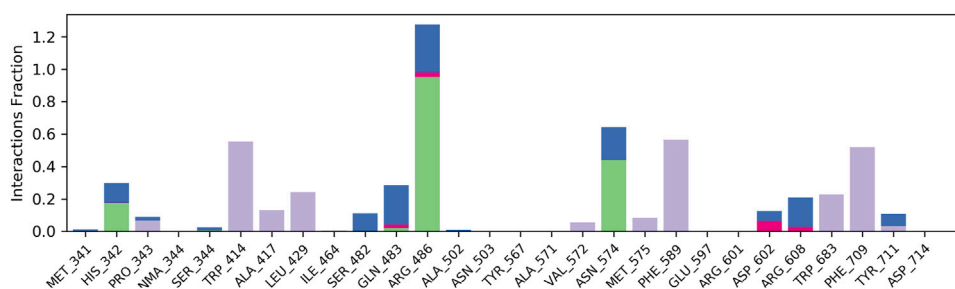


FIGURE 7

Plot of interaction fraction and amino acid residue interacting with the ligand. ARG 486 and ASN 574 bind with enzyme through strong hydrogen bonds. TRP 414, PHE 589, and PHE 709 showed hydrophobic interaction of simulation time between 50–60%. A water bridge mediated by hydrogen bonding is seen with ARG 486 residue.

as a 5- α reductase inhibitor, TNF α -inhibitor, and increasing the activity of α -mannosidase (Gomathi Priyadarshini et al., 2017), whereas hexacosane has been reported to have antifungal activity (Adeyemi et al., 2017). Studies on octacosane revealed its mosquitocidal effect (Rajkumar and Jebanesan, 2004) and is a compound with antimicrobial properties (Rai et al., 2021). Dodecane 2,6,10-trimethyl is an alkane that is antibacterial in nature (Nahid et al., 2012). The presence of cholesterol, reported in our study, is known for its antimicrobial activity (Sribalan et al., 2016). Hexadecanoic acid, methyl ester is employed as an antioxidant, 5- α reductase inhibitor, and hypocholesterolemic (Priya and Subhashini, 2016). Methyl tetradecanoate is an ester of myristic acid that possesses antioxidant, anticancer, nematocidal, and hypocholesterolemic properties (Elaiyaraja and Chandramohan, 2016). Isopropyl myristate is a long-chain fatty ester famous for its use in topical preparation and as a moisturizer (Chandrasekar et al., 2015). Methyl stearate, an ester of fatty acid, shows antifungal and antioxidant properties (Javaid et al., 2021). Siloxanes such as octadecamethyl, cyclononasiloxane, and heptasiloxane have applications in implants and skin patches (Neha et al., 2021). Research revealed that oleic acid has antimicrobial and antifungal properties (Naqvi et al., 2020). It is also used in the preparation of anticancer and antihypertensive medicines (Funari et al., 2003).

GC-MS analysis of methanol extract of *Brassica rapa* reported the presence of oleic acid as the bioactive compound. As per research conducted by Zhang et al. (2010), oleic acid is responsible for the lowering of blood pressure induced by angiotensin II via ANG II signal modulation in the blood vessels. In an *in vivo* study, a substantial reduction occurred in the number of inhibitory G-proteins when the rats were treated with oleic acid, causing an increase in vasodilation (Teres et al., 2008). Our study has also indicated that oleic acid could inhibit ACE.

In conclusion, we applied the *in silico* molecular modeling methods to verify our results whereby oleic acid was subjected to molecular docking. Excellent binding of oleic acid was observed with

the enzyme endothelial nitric oxide synthase (eNOS) which showed its antihypertensive potential. Our research is based on computational data that is in coherence with the experimental results. Some other compounds have also been detected in GC-MS, which can be further evaluated and docked for the purpose of designing a potent antihypertensive drug.

Data availability statement

The raw data supporting the conclusion of this article will be made available by the authors, without undue reservation.

Author contributions

Conceptualization: MI, HS, and HR; methodology: RA, MI, HS, AA, FI, and HR; software: AA and AY; validation: MI, AA, FI, and AY; formal analysis: RA, MI, HS, and HR; investigation: RA, MI, HS, and AA; data curation: RA, MI, HS, AA, FI, and AY; writing—original draft preparation: RA, MI, and FI; writing—review and editing: HR, MI, and HS; supervision: MI and HS. All authors have read and agreed to the published version of the manuscript.

Funding

Qatar University Startup research grant to the corresponding author. Open access funding is provided by the Qatar National Library.

Acknowledgments

Open Access funding is provided by the Qatar National Library. College of Pharmacy and QU Health cluster are

greatly acknowledged for all the support provided to the corresponding author for conducting this study.

Conflict of interest

The authors declare that the research was conducted in the absence of any commercial or financial relationships that could be construed as a potential conflict of interest.

References

- Adeyemi, M., Ekunseitan, D., Abiola, S., Dipeolu, M., Egbeyale, L., and Sogunle, O. (2017). Phytochemical analysis and GC-MS determination of *Lagenaria breviflora* R. fruit. *Int. J. Pharmacogn. Phytochem. Res.* 9, 1045–1050. doi:10.25258/phyto.v9i07.11178
- Ahmad, K., and Jafar, T. H. (2005). Prevalence and determinants of blood pressure screening in Pakistan. *J. Hypertens.* 23, 1979–1984. doi:10.1097/01.hjh.0000187258.86824.00
- Ahmadvand, S., and Sariri, R. (2008). Antimicrobial activity of crude extracts of turnip (*Brassica rapa*). *J. Pure Appl. Microbiol.* 2, 193–196.
- Al-Hooti, S., Sidhu, J., and Qabazard, H. (1997). Physicochemical characteristics of five date fruit cultivars grown in the United Arab Emirates. *Plant Foods Hum. Nutr.* 50, 101–113. doi:10.1007/BF02436030
- Beltagy, A. M. (2014). Investigation of new antimicrobial and antioxidant activities of *Brassica rapa* L. *Int. J. Pharm. Pharm. Sci.* 6, 84–88.
- Besbes, S., Blecker, C., Deroanne, C., Drira, N.-E., and Attia, H. (2004). Date seeds: Chemical composition and characteristic profiles of the lipid fraction. *Food Chem.* 84, 577–584. doi:10.1016/s0308-8146(03)00281-4
- Budniak, L., Slobodianiuk, L., Marchyshyn, S., and Ilashchuk, P. (2021). Determination of polysaccharides in *Gentiana cruciata* L. herb. *Pharmacologyonline* 2, 1473–1479.
- Burt, V. L., Whelton, P., Roccella, E. J., Brown, C., Cutler, J. A., Higgins, M., et al. (1995). Prevalence of hypertension in the US adult population: Results from the third national health and nutrition examination survey, 1988–1991. *Hypertension* 25 (3), 305–313. doi:10.1161/01.hyp.25.3.305
- Carretero, O. A., and Oparil, S. (2000). Essential hypertension: Part I: Definition and etiology. *Circulation* 101, 329–335. doi:10.1161/01.cir.101.3.329
- Chandrasekar, T., Rao, M. R. K., Kumar, R. V., Prabhu, K., Kumar, S. N., and Divya, D. (2015). GC-MS analysis, antimicrobial, antioxidant activity of an Ayurvedic medicine, *Nimbapatriadi choornam*. *J. Chem. Pharm. Res.* 7, 124–136.
- Chang, C.-C., Yang, M.-H., Wen, H.-M., and Chern, J.-C. (2002). Estimation of total flavonoid content in propolis by two complementary colorimetric methods. *J. food drug analysis* 10.
- Chizoruo, I. F., Onyekachi, I. B., and Ebere, E. C. (2019). *Trace metal, FTIR and phytochemical analysis of Viscum album leaves harvested from Pentaclethra macrophylla*. Poland: World News of Natural Sciences, 25.
- Comini, L., Bachetti, T., Cargnoni, A., Bastianon, D., Gitti, G. L., Ceconi, C., et al. (2007). Therapeutic modulation of the nitric oxide: All ace inhibitors are not equivalent. *Pharmacol. Res.* 56 (1), 42–48. doi:10.1016/j.phrs.2007.03.004
- Cushman, D. W., and Cheung, H. S. (1971). Spectrophotometric assay and properties of the angiotensin-converting enzyme of rabbit lung. *Biochem. Pharmacol.* 20, 1637–1648. doi:10.1016/0006-2952(71)90292-9
- Dhivya, K. (2017). Screening of phytoconstituents, UV-VIS spectrum and FTIR analysis of *micrococca mercurialis* (L.) benth. *Int. J. Herb. Med.* 5, 40–44.
- Elaiyaraja, A., and Chandramohan, G. (2016). Comparative phytochemical profile of *Indoneesiella echioides* (L.) Nees leaves using GC-MS. *J. Pharmacogn. Phytochemistry* 5, 158.
- Erb, M., and Kliebenstein, D. J. (2020). Plant secondary metabolites as defenses, regulators, and primary metabolites: The blurred functional trichotomy. *Plant Physiol.* 184 (1), 39–52. doi:10.1104/pp.20.00433
- Funari, S. S., Barceló, F., and Escrivá, P. V. (2003). Effects of oleic acid and its congeners, elaidic and stearic acids, on the structural properties of phosphatidylethanolamine membranes. *J. Lipid Res.* 44, 567–575. doi:10.1194/jlr.M200356-JLR200
- Gomathi Priyadarshini, A. A. E., Anthony, J., Rao, M. R. K., Prabhu, K., Ramesh, A., and Krishna, V. (2017). The GC MS analysis of one medicinal plant, *Premna tomentosa*. *J. Pharm. Sci. Res.* 9, 1595–1597.
- Hammad, E. M., and Abo-Zaid, E. M. (2020). Properties of noodles fortification with turnip leave powder. *J. Food Dairy Sci.* 11, 209–213. doi:10.21608/jfds.2020.111755
- Hussain, K., Ismail, Z., Sadikun, A., and Ibrahim, P. (2008). *Analysis of proteins, polysaccharides, glycosaponins contents of Piper sarmentosum Roxb. and anti-TB evaluation for bio-enhancing/interaction effects of leaf extracts with Isoniazid (INH)*.
- Javaid, A., Khan, I. H., and Ferdosi, M. F. (2021). Antimicrobial and other bioactive constituents of *cannabis sativus* roots from Pakistan. *Pak. J. Weed Sci. Res.* 27, 359–368. doi:10.28941/pjwsr.v27i3.984
- Kunle, O. F., Egharevba, H. O., and Ahmadu, P. O. (2012). Standardization of herbal medicines-A review. *Int. J. Biodivers. Conserv.* 4 (3), 101–112. doi:10.5897/ijbc11.163
- Lifton, R. P., Gharavi, A. G., and Geller, D. S. (2001). Molecular mechanisms of human hypertension. *Cell* 104, 545–556. doi:10.1016/s0092-8674(01)00241-0
- Lowry, O. H., Rosebrough, N. J., Farr, A. L., and Randall, R. J. (1951). Protein measurement with the Folin phenol reagent. *J. Biol. Chem.* 193, 265–275. doi:10.1016/s0021-9258(19)52451-6
- Mahfouz, M., Abd-Elnoor, A. V., EL-Razek, A., and Ragwa, I. (2019). The influence of adding turnip roots (*Brassica rapa* var. *rapa* L.) powder on the antioxidant activity and acrylamide content in some fried foods. *Alexandria Sci. Exch. J.* 40, 717–730. doi:10.21608/asejaqsae.2019.68841
- Mæhre, H. K., Dalheim, L., Edvinsen, G. K., Elvevoll, E. O., and Jensen, I.-J. (2018). Protein determination—Method matters. *Foods* 7, 5. doi:10.3390/foods7010005
- Messerli, F. H., Williams, B., and Ritz, E. (2007). Essential hypertension. *Lancet* 370, 591–603. doi:10.1016/S0140-6736(07)61299-9
- Mittal, B. V., and Singh, A. K. (2010). Hypertension in the developing world: Challenges and opportunities. *Am. J. Kidney Dis.* 55, 590–598. doi:10.1053/j.ajkd.2009.06.044
- Nahid, R., Ali, S., and Farshid, S. (2012). Antimicrobial activity and constituents of the hexane extracts from leaf and stem of *Origanum vulgare* L. ssp. *Viride* (Boiss.) Hayek. growing wild in Northwest Iran. *J. Med. Plants Res.* 6, 2681–2685.
- Naqvi, S. F., Khan, I. H., and Javaid, A. (2020). Hexane soluble bioactive components of *Chenopodium murale* stem. *Pak. J. Weed Sci. Res.* 26, 425–432. doi:10.28941/pjwsr.v26i4.875
- Neha, B., Jannavi, R., and Sukumaran, P. (2021). Phyto-pharmacological and biological aspects of *vitex negundo* medicinal plant-A review. *Cardiovasc. Dis.* 6, 7.
- Nguyen, N., Nguyen, M., Nguyen, V., LE, V., Trieu, L., LE, X., et al. (2020). “The effects of different extraction conditions on the polyphenol, flavonoids components and antioxidant activity of *Polyscias fruticosa* roots,” in *IOP conference series: Materials science and engineering* (Bristol: IOP Publishing), 022067.
- Norlander, A. E., Madhur, M. S., and Harrison, D. G. (2018). The immunology of hypertension. *J. Exp. Med.* 215, 21–33. doi:10.1084/jem.20171773
- Oluyemisi, F., Henry, O., and Peter, O. (2012). Standardization of herbal medicines-A review. *Int. J. Biodivers. Conservation* 4, 101–112.
- Paul, S., Geng, C. A., Yang, T. H., Yang, Y. P., and Chen, J. J. (2019). Phytochemical and health-beneficial progress of turnip (*Brassica rapa*). *J. Food Sci.* 84, 19–30. doi:10.1111/1750-3841.14417
- Priecina, L., and Karlina, D. (2013). “Total polyphenol, flavonoid content and antiradical activity of celery, dill, parsley, onion and garlic dried in convective and

Publisher's note

All claims expressed in this article are solely those of the authors and do not necessarily represent those of their affiliated organizations, or those of the publisher, the editors, and the reviewers. Any product that may be evaluated in this article, or claim that may be made by its manufacturer, is not guaranteed or endorsed by the publisher.

microwave-vacuum dryers," in *2nd international conference on nutrition and food Sciences*, 107–112.

Priya, S., and Subhashini, A. (2016). Phytochemical screening and GCMS analysis of methanolic extract of leaves of *Pisonia aculeata* Linn. *Int. J. Pharma Bio Sci.* 7, 317–322. doi:10.22376/ijpbs.2016.7.4.p317-322

Rai, R., Singh, R. K., and Suthar, S. (2021). Production of compost with biopesticide property from toxic weed lantana: Quantification of alkaloids in compost and bacterial pathogen suppression. *J. Hazard. Mat.* 401, 123332. doi:10.1016/j.jhazmat.2020.123332

Rajkumar, S., and Jebanesan, A. (2004). Mosquitocidal activities of octacosane from *moschosma polystachyum* linn.(lamiaceae). *J. Ethnopharmacol.* 90, 87–89. doi:10.1016/j.jep.2003.09.030

Sheng-Ji, P. (2001). Ethnobotanical approaches of traditional medicine studies: Some experiences from asia. *Pharm. Biol.* 39 (1), 74–79. doi:10.1076/phbi.39.s1.74.0005

Shoeb, M. (2006). Anti-cancer agents from medicinal plants. *Bangladesh J. Pharmacol.* 1, 35–41. doi:10.3329/bjp.v1i2.486

Siddiqui, M., Ismail, Z., Sahib, H., Helal, M., and Abdul, M. A. (2009). Analysis of total proteins, polysaccharides and glycosaponins contents of orthosiphon stamineus benth. In spray and freeze dried methanol: Water (1: 1) extract and its contribution to cytotoxic and antiangiogenic activities. *Pharmacogn. Res.* 1.

Slinkard, K., and Singleton, V. L. (1977). Total phenol analysis: Automation and comparison with manual methods. *Am. J. enology Vitic.* 28, 49–55.

Sribalan, R., Padmini, V., Lavanya, A., and Ponnuel, K. (2016). Evaluation of antimicrobial activity of glycinate and carbonate derivatives of cholesterol: Synthesis and characterization. *Saudi Pharm. J.* 24, 658–668. doi:10.1016/j.jsp.2015.05.003

Taveira, M., Fernandes, F., DE Pinho, P. G., Andrade, P. B., Pereira, J. A., and Valentão, P. (2009). Evolution of *Brassica rapa* var. *rapa* L. volatile composition by HS-SPME and GC/IT-MS. *Microchem. J.* 93, 140–146. doi:10.1016/j.microc.2009.05.011

Teres, S., Barceló-Coblijn, G., Benet, M., Alvarez, R., Bressani, R., Halver, J. E., et al. (2008). Oleic acid content is responsible for the reduction in blood pressure induced by olive oil. *Proc. Natl. Acad. Sci. U. S. A.* 105 (37), 13811–13816. doi:10.1073/pnas.0807500105

Unit, P., and Organization, W. H. (1992). *Quality control methods for medicinal plant materials*. France: World Health Organization.

USP (2005). *United States pharmacopoeia D-1*. Washington: Drug Information for the health care professional, 1. Thomas PDR. Micromedex.

Wahedi, H. M., Ahmad, S., and Abbasi, S. W. (2021). Stilbene-based natural compounds as promising drug candidates against COVID-19. *J. Biomol. Struct. Dyn.* 39, 3225–3234. doi:10.1080/07391102.2020.1762743

Whelton, P. K. (1994). Epidemiology of hypertension. *Lancet (London, Engl.* 344 (8915), 101–106. doi:10.1016/s0140-6736(94)91285-8

Williams, B. (2009). *The aorta and resistant hypertension*. Washington, DC: American College of Cardiology Foundation.

Xu, X. H., Li, T., Fong, C. M. V., Chen, X., Chen, X. J., Wang, Y. T., et al. (2016). Saponins from Chinese medicines as anticancer agents. *Molecules* 21 (10), 1326. doi:10.3390/molecules21101326

Yadav, R., and Agarwala, M. (2011). Phytochemical analysis of some medicinal plants. *J. phytology* 3, 1.

Zhang, J., Villacorta, L., Chang, L., Fan, Z., Hamblin, M., Zhu, T., et al. (2010). Nitro-oleic acid inhibits angiotensin II-induced hypertension. *Circ. Res.* 107 (4), 540–548. doi:10.1161/CIRCRESAHA.110.218404



OPEN ACCESS

EDITED BY

Hina Siddiqui,
University of Karachi, Pakistan

REVIEWED BY

Adnane Boualem,
French National Research Institute for
Agriculture, Food and Environment
(INRAE), France
Mahdi Moridi Farimani,
Shahid Beheshti University, Iran

*CORRESPONDENCE

Cheng Peng,
pengchengchengdu@126.com
Fu Peng,
pengf@scu.edu.cn

SPECIALTY SECTION

This article was submitted to
Experimental Pharmacology and
Drug Discovery,
a section of the journal
Frontiers in Pharmacology

RECEIVED 08 August 2022

ACCEPTED 14 September 2022

PUBLISHED 03 October 2022

CITATION

Zhou J, Xie X, Tang H, Peng C and
Peng F (2022), The bioactivities of
sclareol: A mini review.
Front. Pharmacol. 13:1014105.
doi: 10.3389/fphar.2022.1014105

COPYRIGHT

© 2022 Zhou, Xie, Tang, Peng and Peng.
This is an open-access article
distributed under the terms of the
[Creative Commons Attribution License](https://creativecommons.org/licenses/by/4.0/)
(CC BY). The use, distribution or
reproduction in other forums is
permitted, provided the original
author(s) and the copyright owner(s) are
credited and that the original
publication in this journal is cited, in
accordance with accepted academic
practice. No use, distribution or
reproduction is permitted which does
not comply with these terms.

The bioactivities of sclareol: A mini review

Jianbo Zhou¹, Xiaofang Xie², Hailin Tang³, Cheng Peng^{2*} and
Fu Peng^{1*}

¹Key Laboratory of Drug-Targeting and Drug Delivery System of the Education Ministry and Sichuan Province, Engineering Laboratory for Plant-Sourced Drug and Sichuan Research Center for Drug Precision Industrial Technology, West China School of Pharmacy, Sichuan University, Chengdu, China, ²State Key Laboratory of Southwestern Chinese Medicine Resources, Chengdu University of Traditional Chinese Medicine, Chengdu, China, ³Department of Breast Oncology, Sun Yat-sen University Cancer Center, Guangzhou, China

Sclareol, a diterpene alcohol isolated from the herbal and flavor plant clary sage (*Salvia sclarea* L.), is far-famed as the predominant ingredient in the refined oil of *Salvia sclarea* (L.). The empirical medicine of *Salvia sclarea* L. focused on various diseases, such as arthritis, oral inflammation, digestive system diseases, whereas the sclareol possessed more extensive and characteristic bioactivities, including anti-tumor, anti-inflammation and anti-pathogenic microbes, even anti-diabetes and hypertension. However, there is a deficiency of literature to integrate and illuminate the pharmacological attributes of sclareol based on well-documented investigations. Interestingly, sclareol has been recently considered as the potential candidate against COVID-19 and Parkinson's disease. Accordingly, the bioactive attributes of sclareol in cancer, inflammation, even pharmacology and delivery systems are reviewed for comprehensively dissecting its potential application in medicine.

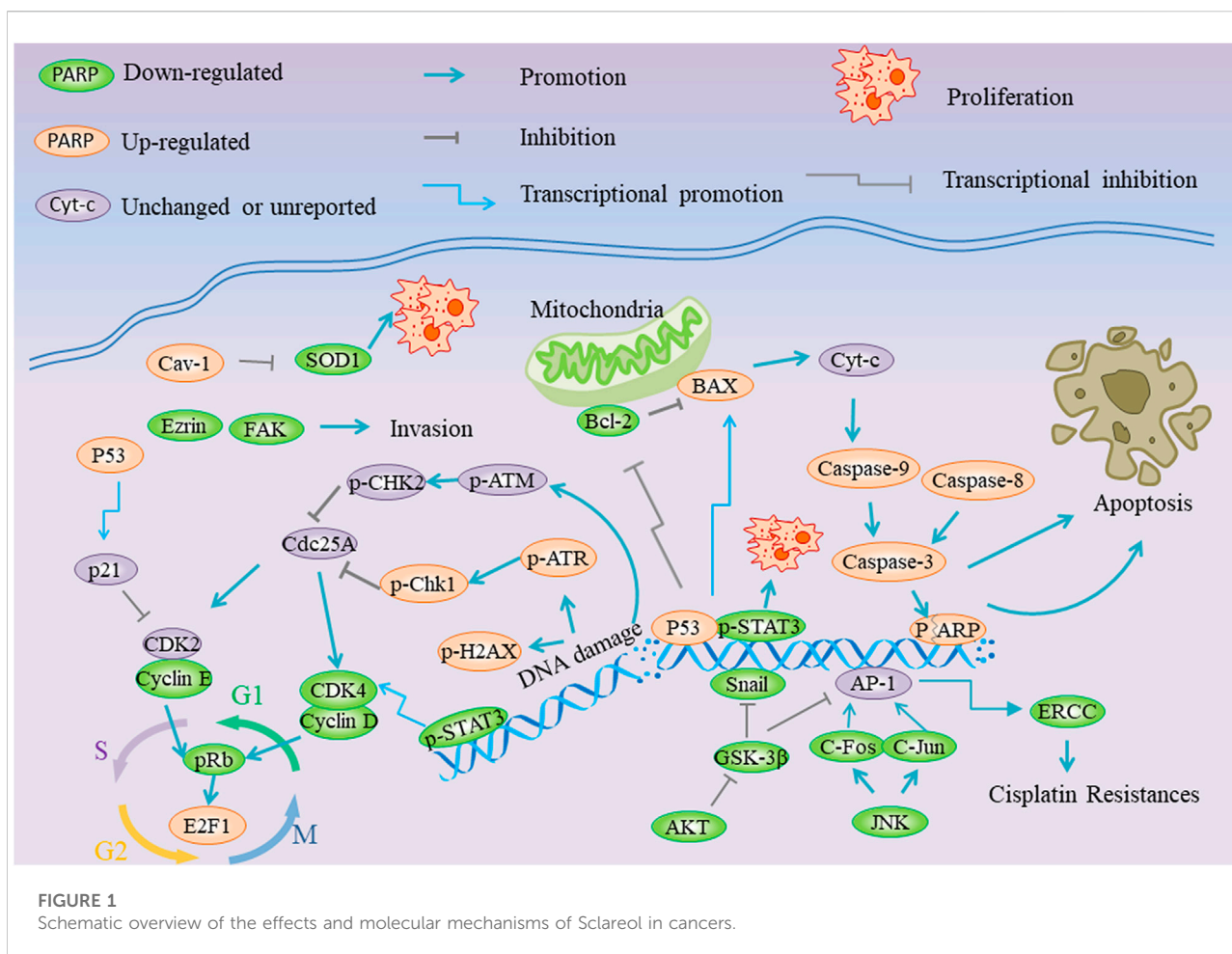
KEYWORDS

sclareol, bioactivities, cancer, inflammation, delivery

Introduction

Salvia sclarea L. (SSL, *S. sclarea*), known as clary sage, plays pivotal role in herb medicine and essential oil industry (Chalvin et al., 2021a). Notably, its essential oil has been investigated for various bioactivities including anti-oxidant, anti-bacterial, anti-fungal, anti-inflammatory, anti-diabetic, and so on (Ögütçü et al., 2008; Yuce et al., 2014; Durgha et al., 2016; Raafat and Habib, 2018). According to the early literatures, *S. sclarea* was widely applied in the empirical medicine for treatment of various diseases, such as arthritis, oral inflammation, digestive system diseases and dysmenorrhea (Peana and Moretti, 2002; Kostić et al., 2017). The remediation potential of SSL in metal polluted soils has been revealed, especially under Cadmium stress and zinc tolerance (Chand et al., 2015; Dobrikova A. et al., 2021; Dobrikova A. G. et al., 2021).

Sclareol (SCL, Labd-14-ene-8, 13-diol), a diterpene alcohol enriching in capitate oil glands of calyxes, was mainly isolated from inflorescences of *Salvia sclarea* L. (Balnova-Tsvetkova and Tsankova, 1992; Schmiderer et al., 2008; Caissard et al., 2012). It also was indispensable raw materials in the synthesis of Ambrox (ambroxide) (Günnewich et al., 2013). SCL, accounting for about 11.5–15.7% in the essential oil, was produced *via* the two steps enzymatic reaction of



Diterpene Synthase (diTPs) and a class II diTPs to substrate Geranylgeranyl Diphosphate (GGPP) and released from chloroplast (Farka et al., 2005; Caniard et al., 2012; Günnewich et al., 2013; Durgha et al., 2016). The terpenoid compositions content including SCL in *S. sclarea* were affected by geography, climate, temperature, carbon dioxide, nitrogen, plant lines, etc (Yadav et al., 2010; Kaur et al., 2015; Kumar et al., 2017; Tuttolomondo et al., 2021). SCL also existed in several other plant species, comprising *Cistus creticus* (Cistaceae), *Nicotiana glutinosa* (Solanaceae) and *Cleome spinosa* (Brassicaceae) (Caniard et al., 2012). Recently, SCL was identified one of the components of aromatic extraction products (6.9%) obtained from *Nicotiana glutinosa* L (Popova et al., 2019). As a natural flavor, SCL is widely used in cosmetics and food industry. *Salvia sclarea* L is widely planted for the extraction of SCL based on commercial purpose for its high content of SCL. SCL performed antiphotoreactive efficacy *in vitro*, and exhibited wrinkle improvement effect in clinical test (0.02% sclareol-containing cream). Furthermore, SCL inhibited ultraviolet-B inducing MMPs expression and prevented collagen degradation by down-regulating the protein expression of AP-1 transcription factors (Park et al., 2016).

There are three synthesis routes of Ambrox from sclareol, in which the classical commercial route including three reactions and two intermediates sclareolide and ambradiol (Yang et al., 2016). However, the one-pot synthesis was viewed to be convenient and environmentally friendly. Another strategy using strains, containing *Cryptococcus albidus* and *Hyphozyma roseonigra*, to transform sclareol to sclareol glycol, and then the latter was converted to Ambrox using chemical conversion (Wang et al., 2019). Here, we first summarized the pharmacological effects and molecular mechanisms underlying of the plant-derived bioactive component SCL for further investigating its role in cancer and other diseases.

Pharmacological activities of sclareol

Anti-cancer effects

As shown in Figure 1 and Table 1, SCL has performed extensive activities against cancer *via* multiple signaling pathways involving cell proliferation, apoptosis, cell cycle

TABLE 1 The effects and mechanisms of SCL against various cancers *in vivo* and *in vitro*.

Cancer Type	Model	Dose	Effects	Mechanisms	Ref
Leukemia	HL60	10 µg/ml	Proliferation ↓; G0/G1 cycle arrest and DNA cleavage ↑	No reported	Dimas et al. (1999)
Breast	MN1, MDD2	50,100 µm	DNA synthesis inhibition, cell cycle arrest in G0/G1 phase, Apoptosis ↑	No reported	Sashidhara et al. (2007)
	MCF-7	30 µm (IC ₅₀ : 31.11 µm)	Proliferation↓; Apoptosis↑	Bcl-2, p-STAT3 ↓; P53, BAX, Caspase-8, Caspase-9 ↑	Afshari et al. (2020)
Colon	HCT116	100 µm	G1 phase cycle arrest, DNA damage, Apoptosis ↑	Caspase-3, 8, 9 ↓; cleaved PARP ↑	Dimas et al. (2007)
Cervical	HeLa	5–20 µg/ml	Proliferation, chemosensitivity ↑	Cav1↑; SOD1 ↓; Cav1 downregulated SOD1 with lysosome-mediated ↑	Zhang et al. (2017)
Osteosarcoma	MG63	2, 5, 10 µm	Proliferation, Invasion ↓; Apoptosis ↑	Ezrin, FAK ↓	Mo et al. (2016)
	MG63	50,70,100 µm	mitochondrial membrane potential ↓; Apoptosis, G1 phase cycle arrest ↑	No reported	Wang et al. (2015)
Lung	H1688	25, 50,100 mm	G1 phase cycle arrest, Apoptosis, DNA damage ↑	CDK4, Cyclin D, Cyclin E, pRb, cleaved PARP, p-H2AX, p-ATR and p-Chk1↑; E2F1↓	Chen et al. (2020a)
	Cisplatin resistant A549	50, 100 µm	ERCC1↓; Drug sensitivity↑	GSK3β-AP1/Snail/JNK-AP1 ↓	Pan et al. (2020)
	H1688 mice xenograft model	300 mg/kg	tumor growth ↓	No reported	Chen et al. (2020a)
Breast	Spontaneous mouse mammary tumor	7.85 µg/mouse/day	IL-4,Treg↓; IFN-γ↑	No reported	Noori et al. (2010)
Colon	HCT116 bearing tumor mice	50 mg/kg	tumor growth ↓	Ki-67↓	Dimas et al. (2007)

Annotation: ↓, downregulated; ↑, upregulated; ref. reference.

arrest and so on. The SCL performed proliferation-suppressive effects in various cancer cells (50% of inhibitory concentration, IC₅₀ < 50 µm), including lung cancer, colon cancer, breast cancer (Paradisiss et al., 2007). In addition, cell viability assay showed that splenocytes obviously ascended after SCL treatment while cell proliferation of K562 was restricted (Noori et al., 2013).

Early studies suggested that SCL had anti-proliferation activity on leukemia cells (IC₅₀ below 20 µg/ml at 48 h), induced G0/G1 cycle arrest and DNA cleavage in HL60 cells (Dimas et al., 1999). In breast cancer cell lines MN1 and MDD2, SCL (50,100 µm) triggered the DNA synthesis inhibition, cell cycle arrest in G0/G1 phase and cell apoptosis. Docking investigations *in silicon* revealed SCL putatively targeted BRCA1 with high binding affinity in natural compounds (Hossain et al., 2022). Besides, the 13-epimer-sclareol exerted antiproliferative effect against MCF-7 cells (IC₅₀ = 11.056 µm) and induced apoptosis (10, 20 µm) (Sashidhara et al., 2007). Cellular study found that SCL induced G1 phase cycle arrest, DNA damage, and led to apoptosis by activating Caspase-3, 8, 9 and cleaved PARP in colon cancer HCT116 cells (100 µm) (Dimas et al., 2007).

The Caveolin-1(Cav1) and Superoxide Dismutase 1(SOD1) were supposed to as potential tumor suppressor and oncogene respectively. In cervical cancer cells, SCL (5–20 µg/ml) induced proliferative inhibition *via* promoting Cav1 expression and down-regulating SOD1, enhanced sensibility of MCF-7,

HepG2, SW480 and SW620 cells to bortezomib. Interestingly, Cav1 was negatively associated with SOD1 through involving the lysosome-mediated degradation of SOD1, the effect was facilitated by SCL(Zhang et al., 2017). Additionally, SCL inhibited proliferation (IC₅₀ = 14 µm), invasion and induced apoptosis (2, 5, 10 µm) in MG63 osteosarcoma cells, with the expression of Ezrin and FAK suppressed (Mo et al., 2016). Another similar study in MG63 cells implicated that SCL performed antiproliferative effect (IC₅₀ = 65.2 µm) and induced apoptosis, G1-phase cell cycle arrest and loss of mitochondrial membrane potential (Wang et al., 2015).

Moreover, the synergistic effect of SCL (50 µm) and cisplatin, doxorubicin and etoposide ameliorated drug sensitivity of breast cancer (Dimas et al., 2006). Furthermore, the up-regulation of P53, BAX, Caspase-8, Caspase-9 and down-regulation of Bcl-2 was perceived to trigger apoptosis in breast cancer MCF-7 under SCL treatment, while SCL inhibited proliferation (IC₅₀ = 27.65 µm) by suppressing the phosphorylation of STAT3, which enhanced by the combination of SCL and cyclophosphamide in the above regulative effect (Afshari et al., 2020). The cisplatin (6 mg/kg) combined with SCL (200 mg/kg) exhibited stronger tumor toxicity than cisplatin or SCL alone in A549 mice model with the down-regulation expression of cisplatin-resistant maker ERCC1. And the combination of SCL (100 µm) and cisplatin (50 µm) showed synergetic effect against survival and invasion of A549 cells. In

mechanism, SCL (50, 100 μm) inhibited ERCC1 protein expression to sensitize A549 towards cisplatin treatment through attenuating ERCC1 upstream GSK3 β -AP1/Snail and JNK-AP1 axis (Pan et al., 2020).

In vivo, SCL repressed the tumor growth by decreasing IL-4 and increasing IFN- γ level in breast cancer mice model, and notably suppressed the population of T regulatory cells (Treg) in tumor (Noori et al., 2010). SCL restricted tumor growth in xenograft model of small cell lung cancer H1688 cells, inhibited proliferation of H1688 cells and H146 cells with IC₅₀ of 42.14 and 69.96 μm at 24 h respectively. In addition, SCL induced G1 phase cycle arrest with the decreased level of CDK4, Cyclin D, Cyclin E, pRb and the increased level of E2F1. Apoptosis that SCL triggering also been reported with caspase-3 activity promoted and cleaved PARP expression elevated, and SCL elevated p-H2AX, p-ATR and p-Chk1 expression to trigger DNA damage in H1688 cells (25, 50, 100 μM) (Chen H. L. et al., 2020).

Anti-inflammatory effects

The anti-inflammatory effects of Labdane diterpenes through regulating NF- κB , nitric oxide (NO) and arachidonic acid metabolite axis had been reported, comprising andrographolide, andalusol, etc (Tran et al., 2017). As a part of labdane diterpenes family, SCL (intraperitoneal injection, 50 and 100 mg/kg) significantly attenuated inflammatory severity by inhibiting NF- κB translocation and phosphorylation of MAPK signaling in atopic dermatitis -like skin lesions model mice induced by 2,4-dinitrochlorobenzene, with local pro-inflammatory cytokine concentration reduced and T cell activation and cytokine production (IFN- γ , IL-4 and IL-17 A) inhibited (Wu et al., 2019). SCL suppressed LPS-induced lung injury in mice *via* impeding NF- κB , MAPKs and HO-1 signaling transductions (Hsieh et al., 2017).

Additionally, SCL treatment retarded arthritic severities in mice model of rheumatoid arthritis through regulating inflammatory cytokines and the population of Th17 and Th1 cells. *In vitro*, SCL weakened IL-1 β -induced expression of MMP-1, TNF- α , and IL-6 in SW982 cells *via* attenuating translocation of NF- κB and p38 MAPK/ERK/JNK pathways (Tsai et al., 2018).

Distinguishingly, the SCL induced eryptosis with the dysfunction of membrane phosphatidylserine in human erythrocytes, and partially regulated p38 kinase and casein kinase 1 α (Signoretto et al., 2016). Interestingly, SCL inhibited RANKL-induced osteoclastogenesis and osteoclast function *in vitro* (1–10 μm), which was associated with SCL-triggering the suppression of NF- κB and MAPK/ERK signaling pathways, and prevented ovariectomy -induced mouse model from bone loss *in vivo* (Jin et al., 2019). SCL has been reported to improve dysmenorrhea and inflammation

in dysmenorrhea models *in vitro* and *in vivo* *via* suppressing the Ca²⁺/MLCK/MLC20 pathway cascades (Wong et al., 2020).

The SCL performed anti-osteoarthritic activities by up-regulating TIMPs and inhibiting iNOS, COX-2 and MMPs expression in interleukin-1 β -induced rabbit chondrocytes and knee osteoarthritis model of rabbit (Zhong et al., 2015). Moreover, sclareol (10 mg/kg) was found to ameliorate LPS-induced lung injury in mice through the suppression of NF- κB and MAPK signaling and activation of heme oxygenase-1 (HO-1) expression (Hsieh et al., 2017). In addition, the mechanism research indicated that the anti-inflammatory bioactivity of SCL was contributed to inhibition of inflammatory cytokines and enhancement of antioxidant enzyme activity. Sclareol inhibited the release of NO, TNF- α and MDA in the carrageenan-induced paw edema model, and restricted the cell growth and the expression of NO, iNOS and COX-2 in LPS-stimulated RAW264.7 macrophages (Huang et al., 2012).

Anti-pathogenic microbes

The anti-microbial effect of SCL against *Candida* yeasts, including *C. albicans*, *C. glabrata*, *C. parapsilosis*, and *C. tropicalis* was almost equivalent to Fluconazole (Popova et al., 2019). The structure-activity relationship study found that the modification of branched chain and benzene ring in SCL improved its antifungal activity (Ma et al., 2018). Miaofeng et al. reported 20 derivatives of SCL, in which compound 16 performed the best fungicidal activity against *Curvularia lunata* (IC₅₀ = 12.09 $\mu\text{g}/\text{ml}$) and *Alternaria brassicae* (IC₅₀ = 14.47 $\mu\text{g}/\text{ml}$) comparing with SCL and fungicide thiabendazole (Ma et al., 2015). Moreover, the SCL was first reported to inhibit helminth growth in larval (IC₅₀ \approx 13 μm), juvenile (IC₅₀ = 5.0 μm), and adult (IC₅₀ = 19.3 μm) stages of *Schistosoma mansoni*, a pathogen of schistosomiasis. Among 14 derivatives of SCL, the most effective compound 12 enhanced cytotoxicity against larval (IC₅₀ \approx 2.2 μm), juvenile (IC₅₀ = 1.7 μm), and adult schistosomes (IC₅₀ = 9.4 μm) by interfering with arachidonic acid metabolism to regulate membrane lipid homeostasis (Crusco et al., 2019). Importantly, the wide-spectrum effect against filoviruses of SCL has been proposed, especially, SCL was considered as Ebola virus (EBOV) entry inhibitor by interfering the viral fusion process (EC₅₀ = 2.4 μm) (Chen Q. et al., 2020). In antibiotic resistance, SCL performed synergistic effect with clindamycin against Methicillin-resistant *Staphylococcus aureus* (Iobbi et al., 2021). SCL also exerted antifungal synergies with Curcumin towards various fungus, including *Candida albicans*, *C. glabrata*, *Aspergillus fumigatus* (Augustine and Avery, 2022). The derivatives of SCL were

reported more effective against plant pathogenic fungal *A. alternate* and *A. brassicae* than thiabendazole (Ma et al., 2018).

Anti-hypertensive and anti-diabetic effects

The reduction of blood pressure SCL induced was observed in normotensive and hypertensive rats, the phenomenon was probably due to ameliorated vasodilation *via* NO/cGMP signaling (Campos et al., 2017). The regulation of blood pressure mediated by SCL indicates it may be applied to cardiovascular disease as potential hypotensor. In addition, SCL was viewed as one of the bioactive components in *Salvia miltiorrhiza* and *Dalbergia odorifera* against myocardial infarction (Zhao et al., 2022). SCL improved hyperglycemia-induced renal injury (renal dysfunction, fibrosis, and inflammation) to prevent diabetic nephropathy through inducing inactivation of MAPKs and NF- κ B pathway (Han et al., 2022).

Pharmacokinetics, derivatives and pharmaceutical

Pharmacokinetic studies suggested that SCL was mainly distributed in extracellular fluid (apparent distribution volume was 21.4 L/kg), and its half-life was short (6.0 h) in rats (intravenous injection, 5.0 mg/kg) (Xiang et al., 2021). The neurotoxicity of free SCL was found in bearing tumor mice of colon cancer HCT116 cells when over 560 mg/kg, whereas 50 mg/kg SCL observed to be ineffective in toxicity (Paradissis et al., 2007). The low bioavailability attributed to its poor water solubility (0.0012 g/L) was considered as the main obstacle limiting its clinical application. The structure modification and nano-delivery systems were imported for enhancing bioactivities and pharmacokinetic properties, such water-solubility and distribution.

The aryl derivatives of SCL were synthesized by Heck coupling reaction for importing aryl in the end of SCL branch chain, in which the compound 15-(4-fluorophenyl)-sclareol (SS-12) exhibited the most effective anti-proliferation activity against PC3 cells ($IC_{50} = 0.082 \mu\text{M}$). SS-12 (0.3 μM) reshaped the balance between autophagy and apoptosis by regulating the BH3 domain protein Bcl-2 and Beclin 1. SS-12 (0.1–0.3 μM) induced autophagic cell death with the decreased level of P62 and increased expression of LC3-I, LC3-II, Beclin-1, while triggered apoptosis by blocking the Akt/mTOR pathway in PC-3 Cells (Shakeel u et al., 2015). The tumor growth of Sarcoma-180 Solid and Ascitic Tumors was dramatic suppressed on the group of SS-12 (5, 10 mg/kg i. p.) comparing with the control group treated with 5-fluorouracil (22 mg/kg i. p.) or normal saline.

Highly lipophilic sclareol was encapsulated in PLGA nanoparticles, and then the surface of nanoparticles was modified by hyaluronic acid (HA) to construct HA-NanoSCL for targeting hyaluronic acid receptor in breast cancer. The HA-NanoSCL nanosystem enhanced cytotoxicity against MCF-7 and MDA-MB-468 (0–50 μm) and uptake of SCL in MDA-MB-231 cells (Cosco et al., 2019). Interestingly, The natural and environmental-friendly nano-formulation was reported that SCLAREIN (SCL encapsulated by plant protein zein) with mean size of 120 nm, performed great stability and time-dependent release in 1 week, while the nanoparticles (loading 1 mg/ml SCL) possessed stronger cytotoxicity of MCF-7 and K562 than free SCL (Gagliardi et al., 2021).

The liposome, lipid nanoparticles (LNPs) and nanostructured lipidic carriers (NLCs) have been viewed as carriers for lipophilic SCL delivery based on SCL low water solubility and high lipophilicity. Liposomes targeting mitochondria significantly improved the apoptosis induction and cytotoxicity of SCL (Patel et al., 2010). Moreover, liposome SCL increased the distribution of SCL in the nucleus of colon cancer HCT-116 cells (Paradissis et al., 2007) and reduced the tumor growth in HCT116 xenograft mice (Dimas et al., 2007). Solid lipid nanoparticles (SLN) loading with SCL exerted excellent physicochemical features including encapsulation efficiency (EE, 89%) and drug loading (DL, 42.47 mg/g), and realized sustained drug release over 1 week and time-dependent proliferative inhibition in A549 cells comparing with plain SCL ($IC_{50} = 19 \mu\text{g/ml}$) (Hamishehkar et al., 2018). Similarly, SLN encapsulated adriamycin and SCL enhanced the antitumor effect of doxorubicin compared with free adriamycin in breast cancer 4T1 cells (Oliveira et al., 2018).

To conquer the drug resistance in cancer and facilitate chemotherapy response, combination therapy has been widely used in clinical and basic investigation. SCL was reported as an enhancer of doxorubicin (DOX) and the combination of DOX and SCL showed stronger anti-proliferative effect than free DOX and free SCL in breast cancer MDA-MB-231 and 4T1 cells. In 4T1 mice model, the nanostructured lipid carrier loading Doxorubicin and SCL (NLC-DOX-SC) exhibited better tumor inhibition than plain DOX and NCL-DOX, also performed lower cytotoxicity than the combination of free DOX and SCL in weight loss and myelosuppression (Borges et al., 2019). However, recent research indicated that NLC-SCL exerted higher encapsulation than SLN-SCL, which was contributed to the difference of lipid matrix (Borges et al., 2021). NLC-SCL performed higher anti-proliferation effect than plain SCL against MDA-MB-231 and HCT-116 cells. Moreover, NLC-SCL G2/M phase arrest in above cells (Borges et al., 2021). Various, sclareol-loaded lipid nanoparticles effectively improved metabolism and attenuated obesity process in obesity induced mice, which was attributed to the decreased expression of proinflammatory cytokines (NF- κ B and MCP-1) and adipogenesis related markers SREBP-1 (Ceri et al., 2019).

Conclusion and prospect

Although sclareol has exhibited extensive and wide-spectrum effects for attenuating cancer-related phenotypes, such as proliferation, apoptosis and cell cycle, the molecular pathways sclareol mediated remain uncharted and the present studies focusing on signaling mechanisms are not deep and comprehensive. For instance, weaver SCL is associated with ferroptosis and pyroptosis, and the relationship between SCL with m6A RNA methylation remains underlying. Investigations on structure activity relationships provide new sight to uncover the bioactivities between SCL and its analogues, while the improvement of pharmacokinetic parameters (water solubility and half-life) and targeting are entitled by delivery systems, including liposome, lipid nanoparticle, etc. Beyond anti-tumor effects, SCL also exhibited other attributes, mainly comprising anti-inflammation and anti-pathogenic microbes (fungal, schistosomiasis and Ebola virus). The classic NF- κ B and MAPK signaling pathways exerts crucial role in the anti-inflammation property of SCL. It is significant that SCL triggered immunomodulatory effects of Th17, Th1 and Treg may involve tumor microenvironment remodeling. Promisingly, SCL was identified as a novel Cav1.3 antagonist against Parkinson's disease (Wang et al., 2022). SCL was considered as candidate drug to treat or prevent SARS-CoV-2 *via* targeting Covid19 Main Protase (MPro) (Aydin et al., 2021). Sclareol as F1Fo-ATP synthase inhibitor restrained free radical production in the retinal rod, which indicated SCL could serve as a potential drug for retinal disease (Ravera et al., 2020).

Biosynthetic strategy provided new application prospect for industrial manufacture of sclareol with green and sustainable, compared to traditional extract from plants (Einhaus et al., 2022). We look forward emerging investigations to further explore the role of sclareol in combined therapy with chemotherapy or immunotherapy against cancer, even in Covid19 and Parkinson's disease.

References

- Afshari, H., Nourbakhsh, M., Salehi, N., Mahboubi_Rabbani, M., Zarghi, A., and Noori, S. (2020). STAT3-mediated apoptotic-enhancing function of sclareol against breast cancer cells and cell sensitization to cyclophosphamide. *Iran. J. Pharm. Res.* 19 (1), 398–412. doi:10.22037/ijpr.2020.112587.13843
- Augustine, C. R., and Avery, S. V. (2022). Discovery of natural products with antifungal potential through combinatorial synergy. *Front. Microbiol.* 13, 866840. doi:10.3389/fmicb.2022.866840
- Aydin, A. D., Altinel, F., Erdoğan, H., and Son Ç, D. (2021). Allergen fragrance molecules: A potential relief for COVID-19. *BMC Complement. Med. Ther.* 21 (1), 41. doi:10.1186/s12906-021-03214-4
- Balinova-Tsvetkova, A., and Tsankova, P. (1992). On the extraction of salvia sclarea L. *Flavour Fragr. J.* 7 (3), 151–154. doi:10.1002/ffj.2730070310
- Borges, G. S. M., Prazeres, P., de Souza, A. M., Yoshida, M. I., Vilela, J. M. C., Silva, A., et al. (2021). Nanostructured lipid carriers as a novel tool to deliver sclareol: Physicochemical characterisation and evaluation in human cancer cell lines. *Braz. J. Pharm. Sci.* 57. doi:10.1590/s2175-97902020000418497
- Borges, G. S. M., Silva, J. d. O., Fernandes, R. S., de Souza, A. M., Cassali, G. D., Yoshida, M. I., et al. (2019). Sclareol is a potent enhancer of doxorubicin: Evaluation of the free combination and co-loaded nanostructured lipid carriers against breast cancer. *Life Sci.* 232, 116678. doi:10.1016/j.lfs.2019.116678
- Caissard, J. C., Olivier, T., Delbecq, C., Palle, S., Garry, P. P., Audran, A., et al. (2012). Extracellular localization of the diterpene sclareol in clary sage (*Salvia sclarea* L., Lamiaceae). *PLoS One* 7 (10), e48253. doi:10.1371/journal.pone.0048253
- Campos, D. R., Celotto, A. C., Albuquerque, A. A. S., Ferreira, L. G., Monteiro, A., Coelho, E. B., et al. (2017). The diterpene sclareol vascular effect in normotensive and hypertensive rats. *Arq. Bras. Cardiol.* 109 (2), 0–122. doi:10.5935/abc.20170086
- Caniard, A., Zerbe, P., Legrand, S., Cohade, A., Valot, N., Magnard, J.-L., et al. (2012). Discovery and functional characterization of two diterpene synthases for sclareol biosynthesis in *Salvia sclarea*(L.) and their relevance for perfume manufacture. *BMC Plant Biol.* 12 (1), 119. doi:10.1186/1471-2229-12-119

Author contributions

The manuscript was written by JZ, XX, and HT revised the manuscript. CP and FP supported the study.

Funding

The study was supported by the National Natural Science Foundation of China (no.82003879 and U19A2010) the Key Project of Science and Technology Department of Sichuan Province (no. 2020YFS0053; 2021YFS0044), and Youth Talent Promotion Project of China Association for Science and Technology (CACM-2020-QNRC1-01), Project of State Administration of Traditional Chinese Medicine of China (ZYXCXTD-D-202209) and the Open Research Fund of Chengdu University of Traditional Chinese Medicine Key Laboratory of Systematic Research of Distinctive Chinese Medicine Resources in Southwest China.

Conflict of interest

The authors declare that the research was conducted in the absence of any commercial or financial relationships that could be construed as a potential conflict of interest.

Publisher's note

All claims expressed in this article are solely those of the authors and do not necessarily represent those of their affiliated organizations, or those of the publisher, the editors and the reviewers. Any product that may be evaluated in this article, or claim that may be made by its manufacturer, is not guaranteed or endorsed by the publisher.

- Cerri, G. C., Lima, L. C. F., Lelis, D. d. F., Barcelos, L. d. S., Feltenberger, J. D., Mussi, S. V., et al. (2019). Sclareol-loaded lipid nanoparticles improved metabolic profile in obese mice. *Life Sci.* 218, 292–299. doi:10.1016/j.lfs.2018.12.063
- Chalvin, C., Drevensek, S., Chollet, C., Gilard, F., Šolić, E. M., Dron, M., et al. (2021a). Study of the genetic and phenotypic variation among wild and cultivated clary sages provides interesting avenues for breeding programs of a perfume, medicinal and aromatic plant. *PLoS One* 16 (7), e0248954. doi:10.1371/journal.pone.0248954
- Chand, S., Yaseen, M., and Rajkumari Patra, D. D. (2015). Application of heavy metal rich tannery sludge on sustainable growth, yield and metal accumulation by clarysage (*Salvia sclarea* L.). *Int. J. Phytoremediation* 17 (12), 1171–1176. doi:10.1080/15226514.2015.1045128
- Chen, H. L., Gong, J. Y., Lin, S.-C., Li, S., Chiang, Y.-C., Hung, J.-H., et al. (2020a). Effects of sclareol against small cell lung carcinoma and the related mechanism: *In vitro* and *in vivo* studies. *Anticancer Res.* 40 (9), 4947–4960. doi:10.21873/anticancer.14498
- Chen, Q., Tang, K., and Guo, Y. (2020b). Discovery of sclareol and sclareolide as flavivirus entry inhibitors. *J. Asian Nat. Prod. Res.* 22 (5), 464–473. doi:10.1080/10286020.2019.1681407
- Cosco, D., Mare, R., Paolino, D., Salvatici, M. C., Cilurzo, F., and Fresta, M. (2019). Sclareol-loaded hyaluronan-coated PLGA nanoparticles: Physico-chemical properties and *in vitro* anticancer features. *Int. J. Biol. Macromol.* 132, 550–557. doi:10.1016/j.jbiomac.2019.03.241
- Crusco, A., Whiteland, H., Baptista, R., Forde-Thomas, J. E., Beckmann, M., Mur, L. A. J., et al. (2019). Antischistosomal properties of sclareol and its heck-coupled derivatives: Design, synthesis, biological evaluation, and untargeted metabolomics. *ACS Infect. Dis.* 5 (7), 1188–1199. doi:10.1021/acscinfdis.9b00034
- Dimas, K., Hatziantoniou, S., Tseleni, S., Khan, H., Georgopoulos, A., Alevizopoulos, K., et al. (2007). Sclareol induces apoptosis in human HCT116 colon cancer cells *in vitro* and suppression of HCT116 tumor growth in immunodeficient mice. *Apoptosis* 12 (4), 685–694. doi:10.1007/s10495-006-0026-8
- Dimas, K., Kokkinopoulos, D., Demetozos, C., Vaos, B., Marselos, M., Malamas, M., et al. (1999). The effect of sclareol on growth and cell cycle progression of human leukemic cell lines. *Leuk. Res.* 23 (3), 217–234. doi:10.1016/s0145-2126(98)00134-9
- Dimas, K., Papadaki, M., Tsimplouli, C., Hatziantoniou, S., Alevizopoulos, K., Pantazis, P., et al. (2006). Labd-14-ene-8, 13-diol (sclareol) induces cell cycle arrest and apoptosis in human breast cancer cells and enhances the activity of anticancer drugs. *Biomed. Pharmacother.* 60 (3), 127–133. doi:10.1016/j.biopha.2006.01.003
- Dobrikova, A., Apostolova, E., Hanč, A., Yotsova, E., Borisova, P., Sperdouli, I., et al. (2021a). Tolerance mechanisms of the aromatic and medicinal plant *Salvia sclarea* L. To excess zinc. *Plants* 10 (2), 194. doi:10.3390/plants10020194
- Dobrikova, A. G., Apostolova, E. L., Hanč, A., Yotsova, E., Borisova, P., Sperdouli, I., et al. (2021b). Cadmium toxicity in *Salvia sclarea* L.: An integrative response of element uptake, oxidative stress markers, leaf structure and photosynthesis. *Ecotoxicol. Environ. Saf.* 209, 111851. doi:10.1016/j.ecoenv.2020.111851
- Durgha, H., Thirugnanasampandan, R., Ramya, G., and Ramanth, M. G. (2016). Inhibition of inducible nitric oxide synthase gene expression (iNOS) and cytotoxic activity of *Salvia sclarea* L. essential oil. *J. King Saud Univ. - Sci.* 28 (4), 390–395. doi:10.1016/j.jksus.2015.11.001
- Einhaus, A., Steube, J., Freudenberger, R. A., Barczyk, J., Baier, T., and Kruse, O. (2022). Engineering a powerful green cell factory for robust photoautotrophic diterpenoid production. *Metab. Eng.* 73, 82–90. doi:10.1016/j.ymben.2022.06.002
- Farka, P., Hollá, M., Tekel, J., Mellen, S., and Vavrková, t. (2005). Composition of the essential oils from the flowers and leaves of *Salvia sclarea* L. (Lamiaceae) cultivated in Slovak republic. *J. Essent. Oil Res.* 17 (2), 141–144. doi:10.1080/10412905.2005.9698858
- Gagliardi, A., Voci, S., Bonacci, S., Iriti, G., Procopio, A., Fresta, M., et al. (2021). SCLAREIN (SCLAREol contained in zeIN) nanoparticles: Development and characterization of an innovative natural nanoformulation. *Int. J. Biol. Macromol.* 193, 713–720. doi:10.1016/j.jbiomac.2021.10.184
- Günnewich, N., Higashi, Y., Feng, X., Choi, K.-B., Schmidt, J., and Kutchan, T. M. (2013). A diterpene synthase from the clary sage *Salvia sclarea* catalyzes the cyclization of geranylgeranyl diphosphate to (8R)-hydroxy-copalyl diphosphate. *Phytochemistry* 91, 93–99. doi:10.1016/j.phytochem.2012.07.019
- Hamishehkar, H., Bahadori, M. B., Vandghanooni, S., Eskandani, M., Nakhilband, A., and Eskandani, M. (2018). Preparation, characterization and anti-proliferative effects of sclareol-loaded solid lipid nanoparticles on A549 human lung epithelial cancer cells. *J. Drug Deliv. Sci. Technol.* 45, 272–280. doi:10.1016/j.jddst.2018.02.017
- Han, X., Zhang, J., Zhou, L., Wei, J., Tu, Y., Shi, Q., et al. (2022). Sclareol ameliorates hyperglycemia-induced renal injury through inhibiting the MAPK/NF- κ B signaling pathway. *Phytother. Res.* 36 (6), 2511–2523. doi:10.1002/ptr.7465
- Hossain, R., Ray, P., Sarkar, C., Islam, M. S., Khan, R. A., Khalipha, A. B. R., et al. (2022). Natural compounds or their derivatives against breast cancer: A computational study. *Biomed. Res. Int.* 2022, 5886269. doi:10.1155/2022/5886269
- Hsieh, Y.-H., Deng, J.-S., Pan, H.-P., Liao, J.-C., Huang, S.-S., and Huang, G.-J. (2017). Sclareol ameliorate lipopolysaccharide-induced acute lung injury through inhibition of MAPK and induction of HO-1 signaling. *Int. Immunopharmacol.* 44, 16–25. doi:10.1016/j.intimp.2016.12.026
- Huang, G.-J., Pan, C.-H., and Wu, C.-H. (2012). Sclareol exhibits anti-inflammatory activity in both lipopolysaccharide-stimulated macrophages and the λ -carrageenan-induced paw edema model. *J. Nat. Prod.* 75 (1), 54–59. doi:10.1021/np200512a
- Iobbi, V., Brun, P., Bernabé, G., Dougué Kentsop, R. A., Donadio, G., Ruffoni, B., et al. (2021). Labdane diterpenoids from *Salvia tingitana* etl. Synergize with clindamycin against methicillin-resistant *Staphylococcus aureus*. *Molecules* 26 (21), 6681. doi:10.3390/molecules26216681
- Jin, H., Shao, Z., Wang, Q., Miao, J., Bai, X., Liu, Q., et al. (2019). Sclareol prevents ovariectomy-induced bone loss *in vivo* and inhibits osteoclastogenesis *in vitro* via suppressing NF- κ B and MAPK/ERK signaling pathways. *Food Funct.* 10 (10), 6556–6567. doi:10.1039/C9FO00206E
- Kaur, T., Bhat, H. A., Bhat, R., Kumar, A., Bindu, K., Koul, S., et al. (2015). Physico-chemical and antioxidant profiling of *Salvia sclarea* L. at different climates in north-Western Himalayas. *Acta Physiol. Plant.* 37 (7), 132. doi:10.1007/s11738-015-1879-7
- Kostić, M., Kitić, D., Petrović, M. B., Jevtović-Stoimenov, T., Jović, M., Petrović, A., et al. (2017). Anti-inflammatory effect of the *Salvia sclarea* L. ethanolic extract on lipopolysaccharide-induced periodontitis in rats. *J. Ethnopharmacol.* 199, 52–59. doi:10.1016/j.jep.2017.01.020
- Kumar, R., Kaundal, M., Sharma, S., Thakur, M., Kumar, N., Kaur, T., et al. (2017). Effect of elevated [CO₂] and temperature on growth, physiology and essential oil composition of *Salvia sclarea* L. in the Western Himalayas. *J. Appl. Res. Med. Aromatic Plants* 6, 22–30. doi:10.1016/j.jarmap.2017.01.001
- Ma, M., Feng, J., Li, R., Chen, S.-W., and Xu, H. (2015). Synthesis and antifungal activity of ethers, alcohols, and iodohydrin derivatives of sclareol against phytopathogenic fungi *in vitro*. *Bioorg. Med. Chem. Lett.* 25 (14), 2773–2777. doi:10.1016/j.bmcl.2015.05.013
- Ma, M., Feng, J., Wang, D., Chen, S. W., and Xu, H. (2018). Synthesis and antifungal activities of drimane-amide derivatives from sclareol. *Comb. Chem. High. Throughput Screen.* 21 (7), 501–509. doi:10.2174/1386207321666180925164358
- Mo, J. W., Yang, R. Z., and Zhang, D. F. (2016). Modulation of anoikis resistance in MG63 osteosarcoma cells by sclareol via inhibiting Ezrin/Fak expression. *Int. J. Clin. Exp. Pathology* 9 (7), 6795–6803.
- Noori, S., Hassan, Z. M., Mohammadi, M., Habibi, Z., Sohrabi, N., and Bayanollah, S. (2010). Sclareol modulates the Treg intra-tumoral infiltrated cell and inhibits tumor growth *in vivo*. *Cell. Immunol.* 263 (2), 148–153. doi:10.1016/j.cellimm.2010.02.009
- Noori, S., Hassan, Z. M., and Salehian, O. (2013). Sclareol reduces CD4+CD25+FoxP3+T-reg cells in a breast cancer model *in vivo*. *Iran. J. Immunol.* 10 (1), 10–21.
- Öğütçü, H., Sökmen, A., Sökmen, M., Polissiou, M., Serkedjieva, J., Daferera, D., et al. (2008). Bioactivities of the various extracts and essential oils of *Salvia limbata* C.A.Mey. and *Salvia sclarea* L.. *Turk. J. Biol.* 32 (3), 181–192.
- Oliveira, M. S., Lima, B. H. S., Goulart, G. A. C., Mussi, S. V., Borges, G. S. M., Orefice, R. L., et al. (2018). Improved cytotoxic effect of doxorubicin by its combination with sclareol in solid lipid nanoparticle suspension. *J. Nanosci. Nanotechnol.* 18 (8), 5609–5616. doi:10.1166/jnn.2018.15418
- Pan, C.-H., Chen, S.-Y., Wang, J.-Y., Tsao, S.-P., Huang, H.-Y., Wei-Chen Chiu, P., et al. (2020). Sclareol ameliorated ERCC1-mediated cisplatin resistance in A549 human lung adenocarcinoma cells and a murine xenograft tumor model by suppressing AKT-GSK3 β -AP1/Snail and JNK-AP1 pathways. *Chem. Biol. Interact.* 332, 109304. doi:10.1016/j.cbi.2020.109304
- Paradissis, A., Hatziantoniou, S., Georgopoulos, A., Psarra, A.-M. G., Dimas, K., and Demetozos, C. (2007). Liposomes modify the subcellular distribution of sclareol uptake by HCT-116 cancer cell lines. *Biomed. Pharmacother.* 61 (2-3), 120–124. doi:10.1016/j.biopha.2006.10.006
- Park, J.-E., Lee, K.-E., Jung, E., Kang, S., and Kim, Y. J. (2016). Sclareol isolated from *Salvia officinalis* improves facial wrinkles via an antiphotaging mechanism. *J. Cosmet. Dermatol.* 15 (4), 475–483. doi:10.1111/jocd.12239
- Patel, N. R., Hatziantoniou, S., Georgopoulos, A., Demetozos, C., Torchilin, V. P., Weissig, V., et al. (2010). Mitochondria-targeted liposomes improve the apoptotic and cytotoxic action of sclareol. *J. Liposome Res.* 20 (3), 244–249. doi:10.3109/08982100903347931

- Peana, A. T., and Moretti, M. D. L. (2002). "Pharmacological activities and applications of *Salvia sclarea* and *Salvia desoleana* essential oils," in *Studies in natural products chemistry*. Editor R. Atta ur (Elsevier), 391–423.
- Popova, V., Ivanova, T., Stoyanova, A., Nikolova, V., Hristeva, T., Gochev, V., et al. (2019). Terpenoids in the essential oil and concentrated aromatic products obtained from *Nicotiana glutinosa* L. Leaves. *Molecules* 25 (1), E30. doi:10.3390/molecules25010030
- Raafat, K., and Habib, J. (2018). Phytochemical compositions and antidiabetic potentials of *Salvia sclarea* L. Essential oils. *J. Oleo Sci.* 67 (8), 1015–1025. doi:10.5650/jos.ess17187
- Ravera, S., Esposito, A., Degan, P., Caicci, F., Calzia, D., Perrotta, E., et al. (2020). Sclareol modulates free radical production in the retinal rod outer segment by inhibiting the ectopic fllo-atp synthase. *Free Radic. Biol. Med.* 160, 368–375. doi:10.1016/j.freeradbiomed.2020.08.014
- Sashidhara, K. V., Rosaiah, J. N., Kumar, A., Bid, H. K., Konwar, R., and Chattopadhyay, N. (2007). Cell growth inhibitory action of an unusual labdane diterpene, 13-*epi*-Sclareol in breast and uterine cancers *in vitro*. *Phytother. Res.* 21 (11), 1105–1108. doi:10.1002/ptr.2205
- Schmiderer, C., Grassi, P., Novak, J., Weber, M., and Franz, C. (2008). Diversity of essential oil glands of clary sage (*Salvia sclarea* L., Lamiaceae). *Plant Biol.* 10 (4), 433–440. doi:10.1111/j.1438-8677.2008.00053.x
- Shakeel u, R., Rah, B., Lone, S. H., Rasool, R. U., Farooq, S., Nayak, D., et al. (2015). Design and synthesis of antitumor heck-coupled sclareol analogues: Modulation of BH3 family members by SS-12 in autophagy and apoptotic cell death. *J. Med. Chem.* 58 (8), 3432–3444. doi:10.1021/jm501942m
- Signoretto, E., Laufer, S. A., and Lang, F. (2016). Stimulating effect of sclareol on suicidal death of human erythrocytes. *Cell. Physiol. biochem.* 39 (2), 554–564. doi:10.1159/000445647
- Tran, Q. T. N., Wong, W. S. F., and Chai, C. L. L. (2017). Labdane diterpenoids as potential anti-inflammatory agents. *Pharmacol. Res.* 124, 43–63. doi:10.1016/j.phrs.2017.07.019
- Tsai, S.-W., Hsieh, M.-C., Li, S., Lin, S.-C., Wang, S.-P., Lehman, C. W., et al. (2018). Therapeutic potential of sclareol in experimental models of rheumatoid arthritis. *Int. J. Mol. Sci.* 19 (5), E1351. doi:10.3390/ijms19051351
- Tuttolomondo, T., Virga, G., Licata, M., Iacuzzi, N., Farruggia, D., and Bella, S. L. (2021). Assessment of production and qualitative characteristics of different populations of *salvia sclarea* L. Found in sicily (Italy). *Agronomy* 11 (8), 1508. doi:10.3390/agronomy11081508
- Wang, H., Xie, M., Rizzi, G., Li, X., Tan, K., and Fussenegger, M. (2022). Identification of sclareol as a natural neuroprotective Ca(v) 1.3-antagonist using synthetic Parkinson-mimetic gene circuits and computer-aided drug Discovery. *Adv. Sci.* 9 (7), e2102855. doi:10.1002/advs.202102855
- Wang, L., He, H. S., Yu, H. L., Zeng, Y., Han, H., He, N., et al. (2015). Sclareol, a plant diterpene, exhibits potent antiproliferative effects via the induction of apoptosis and mitochondrial membrane potential loss in osteosarcoma cancer cells. *Mol. Med. Rep.* 11 (6), 4273–4278. doi:10.3892/mmr.2015.3325
- Wang, X., Zhang, X., Yao, Q., Hua, D., and Qin, J. (2019). Comparative proteomic analyses of *Hyphozyma roseonigra* ATCC 20624 in response to sclareol. *Braz. J. Microbiol.* 50 (1), 79–84. doi:10.1007/s42770-019-00040-2
- Wong, J., Chiang, Y. F., Shih, Y. H., Chiu, C. H., Chen, H. Y., Shieh, T. M., et al. (2020). *Salvia sclarea* L. Essential oil extract and its antioxidative phytochemical sclareol inhibit oxytocin-induced uterine hypercontraction dysmenorrhea model by inhibiting the Ca(2+)-MLCK-MLC20 signaling cascade: An *ex vivo* and *in vivo* study. *Antioxidants (Basel)* 9 (10), E991. doi:10.3390/antiox9100991
- Wu, P.-C., Chuo, W.-H., Li, S.-C., Lehman, C. W., Lien, C. Z., Wu, C.-S., et al. (2019). Sclareol attenuates the development of atopic dermatitis induced by 2, 4-dinitrochlorobenzene in mice. *Immunopharmacol. Immunotoxicol.* 41 (1), 109–116. doi:10.1080/08923973.2018.1555846
- Xiang, Z., Chen, Y., Xiao, Q., Yu, X., Yu, X., Hu, Z., et al. (2021). GC-MS/MS method for determination and pharmacokinetics of sclareol in rat plasma after intravenous administration. *J. Chromatogr. B Anal. Technol. Biomed. Life Sci.* 1173, 122703. doi:10.1016/j.jchromb.2021.122703
- Yadav, A., Chanotiya, C. S., and Singh, A. K. (2010). Terpenoid compositions and enantio-differentiation of linalool and sclareol in *salvia sclarea* L. From three different climatic regions in India. *J. Essent. Oil Res.* 22 (6), 589–592. doi:10.1080/10412905.2010.9700406
- Yang, S., Tian, H., Sun, B., Liu, Y., Hao, Y., and Lv, Y. (2016). One-pot synthesis of (-)-Ambrox. *Sci. Rep.* 6, 32650. doi:10.1038/srep32650
- Yuce, E., Yildirim, N., Yildirim, N. C., Paksoy, M. Y., and Bagci, E. (2014). Essential oil composition, antioxidant and antifungal activities of *salvia sclarea* L. From munzur valley in tunceli, Turkey. *Cell. Mol. Biol.* 60 (2), 1–5.
- Zhang, T., Wang, T., and Cai, P. (2017). Sclareol inhibits cell proliferation and sensitizes cells to the antiproliferative effect of bortezomib via upregulating the tumor suppressor caveolin-1 in cervical cancer cells. *Mol. Med. Rep.* 15 (6), 3566–3574. doi:10.3892/mmr.2017.6480
- Zhao, S., Liu, K., Duan, J., Tao, X., Li, W., Bai, Y., et al. (2022). Identification of traditional Chinese drugs containing active ingredients for treating myocardial infarction and analysis of their therapeutic mechanisms by network pharmacology and molecular docking. *Nan Fang. Yi Ke Da Xue Xue Bao* 42 (1), 13–25. doi:10.12122/j.issn.1673-4254.2022.01.02
- Zhong, Y., Huang, Y., Santoso, M. B., and Wu, L.-D. (2015). Sclareol exerts anti-osteoarthritic activities in interleukin-1 β -induced rabbit chondrocytes and a rabbit osteoarthritis model. *Int. J. Clin. Exp. Pathol.* 8 (3), 2365–2374.



OPEN ACCESS

EDITED BY

Hina Siddiqui,
University of Karachi, Pakistan

REVIEWED BY

Xiaogang Jiang,
Soochow University, China
Ayaz Ahmed,
University of Karachi, Pakistan

*CORRESPONDENCE

Kowit-Yu Chong,
kchong@mail.cgu.edu.tw

SPECIALTY SECTION

This article was submitted to
Experimental Pharmacology and Drug
Discovery,
a section of the journal
Frontiers in Pharmacology

RECEIVED 18 July 2022

ACCEPTED 12 September 2022

PUBLISHED 04 October 2022

CITATION

Huang T-T, Chen C-M, Chen L-G,
Lan Y-W, Huang T-H, Choo KB and
Chong K-Y (2022), 2,3,5,4'-
tetrahydroxystilbene-2-O- β -D-
glucoside ameliorates bleomycin-
induced pulmonary fibrosis via
regulating pro-fibrotic
signaling pathways.
Front. Pharmacol. 13:997100.
doi: 10.3389/fphar.2022.997100

COPYRIGHT

© 2022 Huang, Chen, Chen, Lan,
Huang, Choo and Chong. This is an
open-access article distributed under
the terms of the [Creative Commons
Attribution License \(CC BY\)](https://creativecommons.org/licenses/by/4.0/). The use,
distribution or reproduction in other
forums is permitted, provided the
original author(s) and the copyright
owner(s) are credited and that the
original publication in this journal is
cited, in accordance with accepted
academic practice. No use, distribution
or reproduction is permitted which does
not comply with these terms.

2,3,5,4'-tetrahydroxystilbene -2-O- β -D-glucoside ameliorates bleomycin-induced pulmonary fibrosis *via* regulating pro-fibrotic signaling pathways

Tsung-Teng Huang^{1,2}, Chuan-Mu Chen^{3,4}, Lih-Geeng Chen⁵,
Ying-Wei Lan⁶, Tse-Hung Huang⁷, Kong Bung Choo⁸ and
Kowit-Yu Chong^{1,2,7,8,9*}

¹Department of Medical Biotechnology and Laboratory Science, College of Medicine, Chang Gung University, Taoyuan, Taiwan, ²Graduate Institute of Biomedical Sciences, Division of Biotechnology, College of Medicine, Chang Gung University, Taoyuan, Taiwan, ³Department of Life Sciences, Agricultural Biotechnology Center, National Chung Hsing University, Taichung, Taiwan, ⁴The iEGG and Animal Biotechnology Center and the Rong Hsing Research Center for Translational Medicine, National Chung Hsing University, Taichung, Taiwan, ⁵Department of Microbiology, Immunology and Biopharmaceuticals, National Chiayi University, Chiayi, Taiwan, ⁶Division of Pulmonary Biology, The Perinatal Institute of Cincinnati Children's Research Foundation, Cincinnati, OH, United States, ⁷Department of Traditional Chinese Medicine, Chang Gung Memorial Hospital at Keelung, Keelung, Taiwan, ⁸Centre for Stem Cell Research, Faculty of Medicine and Health Sciences, Universiti Tunku Abdul Rahman, Kajang, Selangor, Malaysia, ⁹Hyperbaric Oxygen Medical Research Lab, Bone and Joint Research Center, Chang Gung Memorial Hospital at Linkou, Taoyuan, Taiwan

2,3,5,4'-Tetrahydroxystilbene-2-O- β -D-Glucoside (THSG) is the main active ingredient extracted from *Polygonum multiflorum* Thunb. (PMT), which has been reported to possess extensive pharmacological properties. Nevertheless, the exact role of THSG in pulmonary fibrosis has not been demonstrated yet. The main purpose of this study was to investigate the protective effect of THSG against bleomycin (BLM)-induced lung fibrosis in a murine model, and explore the underlying mechanisms of THSG in transforming growth factor-beta 1 (TGF- β 1)-induced fibrogenesis using MRC-5 human lung fibroblast cells. We found that THSG significantly attenuated lung injury by reducing fibrosis and extracellular matrix deposition. THSG treatment significantly downregulated the expression levels of TGF- β 1, fibronectin, α -SMA, CTGF, and TGFBR2, however, upregulated the expression levels of antioxidants (SOD-1 and catalase) and LC3B in the lungs of BLM-treated mice. THSG treatment decreased the expression levels of fibronectin, α -SMA, and CTGF in TGF- β 1-stimulated MRC-5 cells. Conversely, THSG increased the expression levels of SOD-1 and catalase. Furthermore, treatment of THSG profoundly reduced the TGF- β 1-induced generation of reactive oxygen species (ROS). In addition, THSG restored TGF- β 1-induced impaired autophagy, accompany by increasing the protein levels of LC3B-II and Beclin 1. Mechanism study indicated that THSG significantly reduced TGF- β 1-induced increase of TGFBR2 expression and phosphorylation of Smad2/3, Akt, mTOR, and ERK1/2 in MRC-5 cells. These findings suggest that THSG may be considered as an anti-fibrotic drug for the treatment of pulmonary fibrosis.

KEYWORDS

THSG, bleomycin, pulmonary fibrosis, TGF- β 1, autophagy

Introduction

Idiopathic pulmonary fibrosis (IPF) is characterized by progressive and lethal symptoms of interstitial lung disease with an unclear etiology. Mortality rate of IPF is higher than many cancers, with a median survival of 3–4 years following diagnosis (Sauleda et al., 2018). Atrophic alveolar epithelial damage is associated with proliferation and activation of fibroblasts and myofibroblasts, resulting in aberrant deposition of extracellular matrix (ECM) components and extensive remodeling of lung architecture (Richeldi et al., 2017). Conventional pharmacological therapies for pulmonary fibrosis include corticosteroids alone or in combination with other immunosuppressive and immunomodulatory agents; however, the curative effects of these drugs is limited and can cause a number of side effects, such as nausea, anorexia, dyspepsia, and skin rash (Bouros and Antoniou, 2005; Richeldi et al., 2017; Gibson et al., 2020). So far, the U.S. Food and Drug Administration has approved pirfenidone and nintedanib for the use of mild-to-moderate IPF therapy, but these two drugs have only been able to retard the progression of pulmonary fibrosis (Raghu et al., 2015). Therefore, exploration of novel effective therapeutic agents for IPF is still needed.

A previous study has shown that there are many cytokines and growth factors involving in the development of fibrotic disorders (Allen and Spiteri, 2002). Among them, transforming growth factor-beta 1 (TGF- β 1) is the most studied profibrotic cytokine that is involved in the development of pulmonary fibrosis (Sime et al., 1997). This cytokine promotes fibroblasts proliferating and differentiating into active myofibroblasts, which leads to excessive collagen synthesis and ECM protein accumulation, and contribute to the recruitment of inflammatory cells (Fernandez and Eickelberg, 2012). Differentiation of fibroblasts into myofibroblasts is identified by the expression of alpha-smooth muscle actin (α -SMA), and both fibroblasts and myofibroblasts are primary sources of ECM proteins such as fibronectin and collagen (Jarman et al., 2014). Moreover, an increased expression level of TGF- β 1 in the lungs was found in lung fibrosis animal models and patients with IPF (Tanaka et al., 2010; Bao et al., 2014). Transient overexpression of TGF- β 1 by using adenoviral vectors carrying an active TGF- β 1 construct induced prolonged severe interstitial and pleural fibrosis in rat lungs (Sime et al., 1997). In addition, epithelium-specific deletion of TGF- β receptor type II protects mice from bleomycin (BLM)-induced pulmonary fibrosis, further implying that the TGF- β signaling pathway plays a central role for alveolar epithelium in fibrogenesis (Li et al., 2011). Therefore, inhibiting of the fibrogenic cytokine TGF- β 1 production and blocking the ECM

process represent a potential approach for pulmonary fibrosis therapy.

TGF- β exerts its function through binding to heteromeric receptor complexes composed of type I and type II receptors, and then triggers intracellular signaling cascades including Smad-dependent and Smad-independent pathways (Koli et al., 2008; Ahn et al., 2011). In the Smad-dependent pathway, TGF- β binds first to the type II receptor (TGFBR2), after which the type I receptor (TGFBR1) is recruited to the complex and activated by a phosphorylation event. Subsequently, the activated TGFBR1 promotes the phosphorylation of Smad2 and Smad3 that form complexes with Smad4 and allow the complex to translocate from the cytosol to the nucleus and regulate the transcription of downstream genes (Shi and Massagué, 2003). Although the Smad pathway is critical for TGF- β -mediated signaling, several studies show that TGF- β activates non-Smad signal pathways, including mitogen-activated protein kinases (MAPKs), Rho-like GTPase, and phosphatidylinositol 3-kinase (PI3K)/Akt pathways. Three well-established signaling molecules of MAPK pathways regarding TGF- β -mediated signaling consist of extracellular signal-regulated kinase 1/2 (ERK1/2), stress-activated protein kinase or c-Jun N-terminal kinase (SAPK or JNK), and p38 MAPK (Wilkes et al., 2005; Zhang, 2009; Luo et al., 2014).

Autophagy is a critical cellular homeostatic process, which plays an essential role in removing denatured proteins as well as damaged cellular components. Many cell hyperproliferative disorders, including pulmonary fibrosis, are considered to be alleviated by autophagy activation (Haspel and Choi, 2011; Cabrera et al., 2015). Autophagy defects promote the expression of α -SMA and ECM proteins (Patel et al., 2012). Studies have shown that microtubule-associated protein 1 light chain 3 beta (LC3B) expression is downregulated in lung fibrosis tissues of patients, indicating autophagy activity is decreased (Wang et al., 2018). The activation of autophagy in mice after BLM injury can reduce collagen deposition in the lungs and increase survival rate (Araya et al., 2013). Furthermore, treatment of TGF- β 1 in human lung fibroblasts inhibits autophagic processes, which may promote fibrogenesis in IPF (Patel et al., 2012). Silencing of LC3 and Beclin 1 genes or pharmacological inhibition of autophagy in human lung fibroblasts augments TGF- β 1-induced expression of fibronectin and α -SMA (Patel et al., 2012). These results indicate that TGF- β 1 is also involved in the pathogenesis of IPF via inhibiting autophagy processes and regulating fibrotic processes. In addition, the intracellular pathway PI3K/Akt suppresses autophagy through its downstream mammalian target of rapamycin (mTOR) (Jung et al., 2010). A recent study has found that activation of the mTOR pathway in lung epithelial cells promotes epithelial-mesenchymal transition (EMT) and lung injury,

leading to acceleration of pulmonary fibrosis (Saito et al., 2020). Lung fibrosis is alleviated by inhibition of the PI3K/Akt/mTOR signaling pathway in the BLM-induced pulmonary fibrosis animal model (Chitra et al., 2015). Therefore, interventions aimed at restraining the activation of Smad, MAPK, and PI3K/Akt/mTOR signaling pathways provides an attractive strategy for a potent agent against pulmonary fibrosis.

2,3,5,4'-tetrahydroxystilbene-2-O- β -D-glucoside (THSG) is one of the major bioactive constituents extracted from *Polygonum multiflorum* Thunb. (PMT; Ho Shou Wu in Chinese). Previous studies have validated that THSG exhibits various pharmacologic effects, including cardiovascular protection, hepatoprotection, neuroprotection, the promotion of hair growth, memory enhancement, anti-cancer, anti-aging, anti-osteoporosis, anti-oxidation, anti-inflammation and so on (Büchter et al., 2015; Ling and Xu, 2016; Yu et al., 2017; Wu et al., 2020; Wang et al., 2022). THSG has also been shown to exhibit anti-fibrotic effect on pressure overloaded-induced cardiac fibrosis (Peng et al., 2016). However, the protective role of THSG in pulmonary fibrosis and its potential mechanisms has not been elucidated.

The aim of the current study is to decipher the *in vitro* and *in vivo* protective efficacy of THSG against pulmonary fibrosis with molecular mechanism elucidation. Thereafter, the underlying mechanisms of THSG against TGF- β 1-induced fibrotic process of human lung fibroblasts and alveolar epithelial cells were further examined. These results provide compelling evidence for the therapeutic potential of THSG in pulmonary fibrosis.

Materials and methods

Reagents and antibodies

The recombinant human TGF- β 1 was obtained from R&D Systems (Minneapolis, MN, United States). Bovine serum albumin (BSA), Bleomycin (BLM) sulfate from *Streptomyces verticillus*, hydroxychloroquine (HCQ) sulfate, and 2,3,5,4'-tetrahydroxystilbene-2-O- β -D-glucoside (THSG) were purchased from Sigma-Aldrich (Saint Louis, MO, United States). THSG was dissolved in ddH₂O at 5 mg/ml concentration as a stock solution that was stored at -20°C. Minimum essential medium (MEM), Dulbecco's modified Eagle's medium (DMEM), sodium pyruvate (100 mM), fetal bovine serum (FBS), and antibiotic-antimycotic (100 \times) were purchased from Life Technologies (Grand Island, NY, United States). Primary antibodies against Akt, phospho (p)-Akt (Ser473), SAPK/JNK, p-SAPK/JNK (Tyr183/Tyr185), ERK1/2, p-ERK1/2 (Thr202/Tyr204), p38 MAPK, p-p38 MAPK (Thr180/Tyr182), mTOR, p-mTOR (Ser2448), Smad2/3, and p-Smad2 (Ser465/467)/Smad3 (Ser423/425) were purchased from Cell Signaling Technology (Beverly, MA, United States).

Antibodies specific to Beclin 1, catalase, connective tissue growth factor (CTGF), E-cadherin, LC3B, and TGFBR2 were purchased from Proteintech (Chicago, IL, United States). Fibronectin, SOD-1, and β -actin antibodies were supplied by Santa Cruz Biotechnology (Dallas, TX, United States). TGFBR1 antibody was obtained from Affinity Biosciences (Cincinnati, OH, United States). N-cadherin and α -SMA antibodies were purchased from ABclonal Biotechnology (Wuhan, Hubei, China). Horseradish peroxidase (HRP)-conjugated goat anti-rabbit/mouse IgG secondary antibodies were supplied by Santa Cruz Biotechnology.

Murine model of bleomycin-induced pulmonary fibrosis

Male C57BL/6 mice (8 weeks of age; body weight, 22–25 g) were obtained from the National Laboratory Animal Center (Taipei, Taiwan). The animals were housed in an air-conditioned animal facility with constant temperature and humidity, a 12/12 h light/dark cycle, and fed with a commercial diet and tap water *ad libitum*. All experimental procedures were according to the guidelines of Institutional Animal Care and Use Committee approved by Chang Gung University. The mice were randomly allocated into four groups ($n = 6$ per group) as follows: 1) control group, 2) BLM group, 3) BLM + THSG (10 mg/kg) group, and 4) BLM + THSG (30 mg/kg) group. The BLM sulfate stock was dissolved in sterile phosphate-buffered saline (PBS) at 10 mg/ml and stored in small aliquots at 4°C. Mice were anesthetized with isoflurane (Abbott Laboratories, Abbott Park, IL, United States) and BLM was administered intratracheally (1.5 mg/kg) in PBS on day 0 as previously described (Huang et al., 2015) while control animals receive an equal volume of sterile PBS. The mice of BLM + THSG groups were received THSG dissolved in 0.1 ml of sterile PBS by oral gavage five times a week, starting from the third to the 21st day after BLM instillation. On day 21, all mice were sacrificed and lung tissues were collected for the following experiments.

Culture of lung fibroblasts and alveolar epithelial cells

Human lung fibroblast cell line MRC-5 was obtained from the Bioresource Collection and Research Center (BCRC, Hsinchu, Taiwan). Human lung alveolar epithelial cell line A549 was obtained from the American Type Culture Collection (Manassas, VA, United States). MRC-5 and A549 cells were cultured in MEM and DMEM respectively, supplemented with 10% FBS, 1% sodium pyruvate, and 1% antibiotic-antimycotic solution. Cells were incubated in a humidified chamber at 37°C with 95% air and 5% CO₂.

environment. In this study, the MRC-5 cells were pretreated with various concentrations of THSG (50 and 100 $\mu\text{g/ml}$) for 24 h. Afterward, exogenous 2.5 ng/ml of TGF- β 1 was administered for 1, 6, and 24 h. Additionally, the A549 cells were pretreated with 50 and 100 $\mu\text{g/ml}$ of THSG for 2 h, and then stimulated with 5 ng/ml of TGF- β 1 for 30 min, 1, 3, and 48 h.

MTT assay

Effect of THSG on cell viability of MRC-5 cells was assessed using the *In Vitro* Toxicology Assay Kit, MTT based from Sigma-Aldrich as described previously (Huang et al., 2014). Briefly, a density of 2×10^4 cells per well was cultured in 96-well plates. After 24 h, cells were treated with various concentrations (50, 100, and 200 $\mu\text{g/ml}$) of THSG for either 24 or 48 h. According to the manufacturer's instructions, the cells were incubated with MTT solution at a concentration of 0.5 mg/ml for 4 h. Finally, formazan crystals were solubilized with the MTT solubilization solution. The absorbance of the mixture was measured at 570 nm with a SpectraMax M5 multi-mode microplate reader (Molecular Devices, Sunnyvale, CA, United States).

Measurement of reactive oxygen species production

MRC-5 cells were seeded in 96-well black wall/clear bottom plates at a density of 2×10^4 cells per well for overnight adhesion. Before experiments, cells were serum starved for 24 h, followed by treatment with THSG (50 and 100 $\mu\text{g/ml}$) for further incubation for 24 h. The cells were subsequently incubated with 2.5 ng/ml of TGF- β 1 for an additional 24 h. ROS production in cells was measured using the Total ROS/Superoxide detection kit (Enzo Life Sciences, Farmingdale, NY, United States) following the manufacturer's instructions.

Autophagy analysis

Autophagy was determined using an Autophagy Assay Kit (Sigma-Aldrich) following the manufacturer's instructions. In brief, MRC-5 cells were passaged and treated as mentioned in the ROS production assay. After the treatment, cells were incubated with an autophagosome detection reagent working solution (diluting 20 μl of the 500 \times autophagosome detection reagent with 10 ml of the stain buffer) for 45 min at 37°C. Next, cells were washed with the wash buffer for four times. The fluorescence intensity was measured at a wavelength of 520 nm using excitation wavelength at 360 nm. Relative fluorescence intensities were used to measure Intracellular autophagosome production.

Histopathological examination

The lung tissues of mice were fixed with 4% paraformaldehyde overnight and embedded in paraffin wax. The paraffin-embedded specimens were then sectioned at 5 μm and stained with hematoxylin and eosin (H&E, Sigma-Aldrich) for evaluating fibrotic lesions. The Ashcroft score was used for semi-quantitative assessment of lung fibrotic changes (Ashcroft et al., 1988). For visualization of collagen deposition, Masson's trichrome staining (Trichrome Stain (Masson) Kit, Sigma-Aldrich) was performed to examine the density and magnitude of collagen fibers in the lungs, an index of lung fibrosis.

Estimation of collagen content by sircol collagen assay

The levels of soluble collagen in the lung tissues were determined by the Sircol Collagen Assay Kit according to the manufacturer's instructions (Biocolor Ltd., Carrickfergus, United Kingdom). In brief, the lung tissue samples were incubated with acid neutralizing reagent and isolation and concentration reagent and then centrifuged. Lung extracts were incubated with Sircol dye reagent and centrifuged to precipitate the collagen-dye complex pellets. The Sircol dye was released from the pellets by using an alkali reagent (1 N NaOH, Sigma-Aldrich) and the absorbance measured at 550 nm using a SpectraMax M5 multi-mode microplate reader (Molecular Devices).

Immunohistochemical staining analysis

The lung tissue sections (5 μm thick) were deparaffinized in xylene and were treated with graded ethanol solutions for rehydration. To retrieve antigens, the sections were microwave-heated in citrate buffer (10 mM of sodium citrate, pH 6.0) and kept to boil for 10–15 min. The endogenous peroxidase were quenched by 3% hydrogen peroxide (H_2O_2) for 15 min at room temperature. After blocked with goat serum for 30 min, the sections were further incubated with primary antibodies specific to fibronectin, α -SMA, CTGF, TGF- β 1, TGFBR1, TGFBR2, SOD-1, catalase, and LC3B overnight at 4°C, prior to incubation in EnVision Detection Systems (DAKO, Glostrup, Denmark) following the manufacturer's instructions. Subsequently, the bound antibodies were visualized with 3,3'-diaminobenzidine (DAB), counterstained with hematoxylin, dehydrated by increasing the concentration of ethanol concentration gradually, cleared with xylene, and mounted in glycerol-gelatin. Images from stained slides were obtained using HistoFAXS (Tissue FAX Plus; Tissue Gnostics, Vienna, Austria).

RNA Extraction and Quantitative Real-Time Polymerase Chain Reaction

The total RNA from lung tissues were extracted using RNeasy Mini Kit (Qiagen, Valencia, CA, United States) following the protocol provided by the manufacturer. The reverse transcription of 1 µg of total RNA was performed in a solution (final volume of 20 µL) containing oligo dT primer, dNTP, and reverse transcriptase (SuperScript III, Invitrogen, Carlsbad, CA, United States). The sequences of the mouse gene-specific primers are shown as follows: forward primer 5'-TATGGGGACAATACACAAGGCT-3', reverse primer CGG GCCACCATGTTTCTTAGA-3' for SOD-1; forward primer 5'-AGCGACCAGATGAAGCAGTG-3', reverse primer 5'-TCCGCTCTCTGTCAAAGTGTG-3' for catalase; forward primer 5'-TTGCTTCAGCTCCACAGAGA-3', reverse primer 5'-TGGTTGTAGAGGGCAAGGAC-3' for TGF-β1; forward primer 5'-GCGAGAAGATGACCCAGATC-3', reverse primer 5'-CCAGTGGTACGGCCAGAGG-3' for β-actin. Quantitative RT-PCR was conducted with Roche SYBR Green Master Mix (Mannheim, Germany) according to our previously described protocol (Huang et al., 2013). Relative quantification of gene expression was calculated using a manufacturer-provided mathematical model. β-actin was used as an internal standard to normalize the expression level of each mRNA. Fold expression is based on at least three to five biological replicates for each treatment group.

Western blot analysis

After treatment with THSG and TGF-β1, the cells were harvested at the indicated times and lysed in radioimmunoprecipitation assay (RIPA) lysis buffer (Millipore Corporation, Billerica, MA, United States) containing a cocktail of protease and phosphatase inhibitor (Thermo Fisher Scientific, Waltham, MA, United States). Protein extraction and Western blot analysis were performed as described previously (Huang et al., 2014). Equal amounts of total protein from each sample were separated by 8%–12% sodium dodecyl sulfate-polyacrylamide gel electrophoresis (SDS-PAGE) and further transferred to polyvinylidene difluoride (PVDF) membranes (Millipore). Membranes were blocked with 5% non-fat skim milk or BSA in a TBST solution containing Tris-buffered saline with 0.1% Tween-20 for 1 h at room temperature, and then probed with the indicated primary antibodies overnight at 4°C. After washing steps, the membranes were probed with HRP-conjugated specific secondary antibodies for 90 min at room temperature. Finally, the immunoreactive bands were detected using the enhanced chemiluminescence (ECL) detection system (Millipore). The images of bands were quantified using the software ImageJ (National Institutes of Health, Bethesda, MD, United States) for densitometric analysis.

Statistical analysis

The data are presented as means ± standard error of the mean (SEM) from at least three different experiments. The two-tailed Student's *t*-test was used for comparing the differences between two groups, and one-way analysis of variance (ANOVA) followed by Dunnett's post hoc test was used for multiple comparisons. A value of *p* < 0.05 was considered statistically significant.

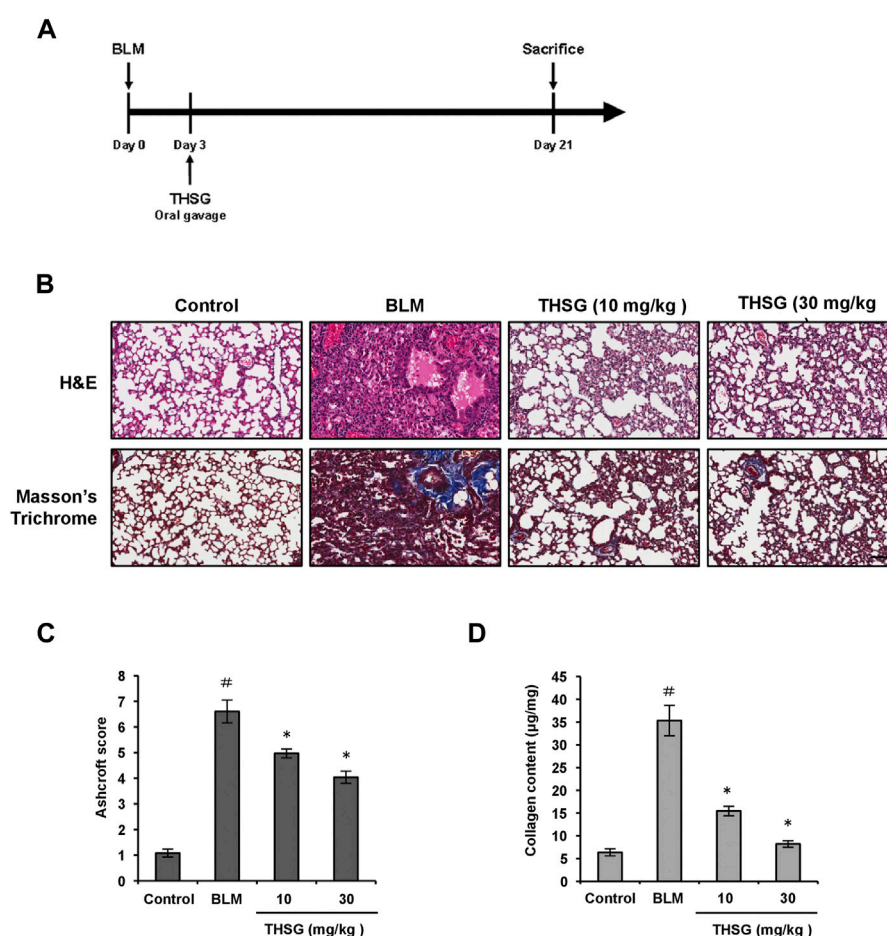
Results

2,3,5,4'-tetrahydroxystilbene-2-O-β-D-glucoside attenuates bleomycin-induced pulmonary fibrosis in mice

The mouse model of BLM-induced pulmonary fibrosis was established, and mice were treated with THSG after intratracheal installation of BLM (Figure 1A). To analyze the therapeutic effect of THSG on BLM-induced pulmonary fibrosis in mice, H&E staining, Masson's trichrome staining, and Sircol collagen assay were performed in the lung tissue sections of mice from each group. H&E staining results revealed that severely thickened alveolar walls, disturbed lung architecture, and evident fibrous hyperplasia in the lung interstitium was induced by the BLM instillation, and these pathological changes were markedly improved by the oral administration of THSG (Figure 1B). Masson's Trichrome staining showed the accumulation of ECM i.e. Collagen among the BLM-induced fibrosis model, which was significantly reduced when treated with THSG in a dose-dependent manner (Figure 1B). Consequently, Ashcroft score was used to quantify the overall grade of the fibrotic changes in the lungs (Figure 1C). The scores of the mice administered with BLM were significantly elevated compared to the control group. THSG (10 and 30 mg/kg) treatment strikingly reduced the Ashcroft score compared to the BLM model group. Similarly, analysis of collagen content in the lung tissues by Sircol collagen assay confirmed that the BLM-induced elevation of collagenous protein was clearly suppressed by THSG in a dose-dependent manner, as shown in Figure 1D.

2,3,5,4'-tetrahydroxystilbene-2-O-β-D-glucoside inhibits transforming growth factor-beta 1-induced expression of fibrotic markers in MRC-5 human lung fibroblast cells

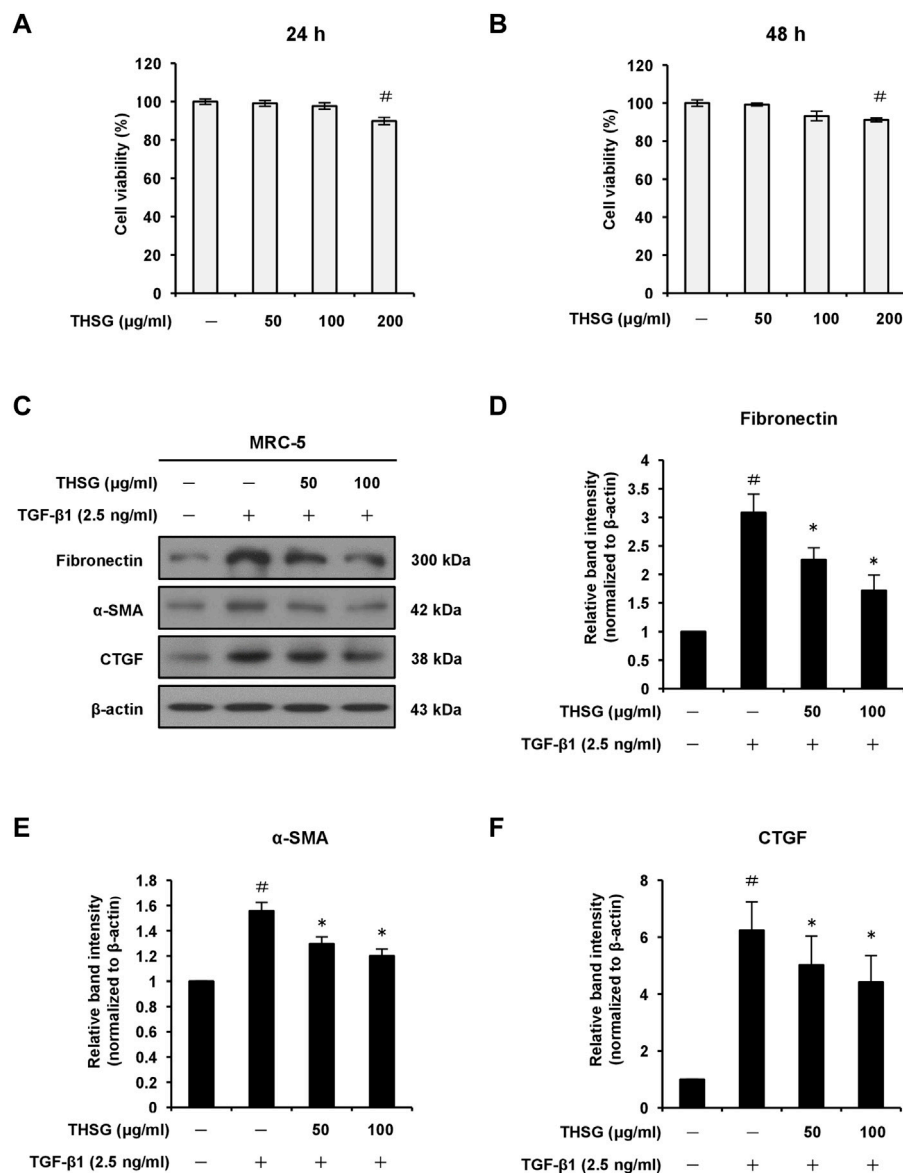
To test the impact of THSG on cell viability, MRC-5 cells were treated with 50, 100, and 200 µg/ml THSG for 24 and 48 h.

**FIGURE 1**

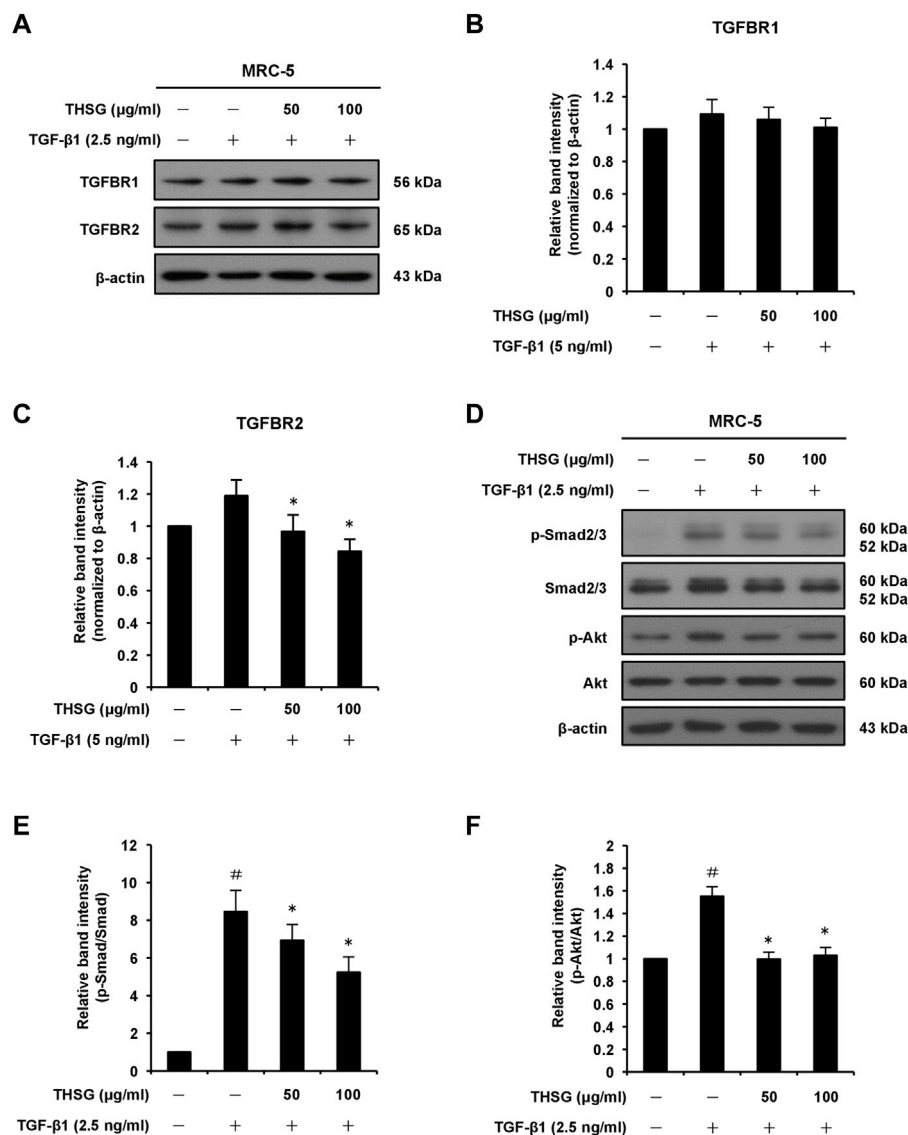
Effect of THSG on BLM-induced pulmonary fibrosis in mice. **(A)** Experimental design: Mice were intratracheally injected with BLM (1.5 mg/kg in 50 μ L of PBS) at day 0. The treatment groups received orally with THSG (10 or 30 mg/kg) once a day, five times a week from day 3 to day 20. Mice were sacrificed on day 21 and lung samples were collected for further analysis. **(B)** Representative photographs of H&E and Masson's trichrome staining of lung tissue sections in the indicated groups. Scale bar: 100 μ m. **(C)** Ashcroft fibrosis scores were used to evaluate the degree of lung fibrosis. **(D)** Detection of collagen content in the lung tissues of mice from different experimental groups by the Sircol collagen assay. Data are represented as the mean \pm SEM ($n = 6$ in each group). [#] $p < 0.05$ compared with vehicle-treated control group. ^{*} $p < 0.05$ compared with BLM group.

The results of MTT assay showed an obvious reduction in cell viability after 24 or 48 h incubation with 200 μ g/ml THSG compared with untreated control cells; however, cell viability of MRC-5 cells did not significant decrease at the concentration of 50 or 100 μ g/ml THSG (Figures 2A,B). Hence, 50 and 100 μ g/ml of THSG treatments were chosen for the following experiments. To further determine the role of THSG in pulmonary fibrosis, we examined the effect of THSG in TGF- β 1-induced myofibroblast differentiation and ECM deposition *in vitro*. As shown in Figures 2C,D, Stimulation with 2.5 ng/ml of TGF- β 1 significantly upregulated the protein level of fibronectin, while pretreatment of THSG (50 and 100 μ g/ml) for 24 h dose-dependently downregulated TGF- β 1-induced the expression of fibronectin in MRC-5 cells. We also observed that addition of TGF- β 1 significantly

increased the protein expression of the myofibroblast activation marker α -SMA, and THSG inhibited TGF- β 1-induced the expression of α -SMA in MRC-5 cells (Figures 2C,E). Additionally, CTGF is a downstream mediator of TGF- β 1 and has been suggested to play a key role in TGF- β 1-induced connective tissue cell proliferation and ECM deposition, leading to promotion and maintenance of fibrogenesis (Kothapalli et al., 1997). We assessed the protein level of CTGF by THSG after stimulation of TGF- β 1. Western blot analysis and quantitative results demonstrated that the expression of CTGF was dramatically elevated by treatment of TGF- β 1, and pretreatment of THSG for 24 h significantly attenuated TGF- β 1-induced CTGF expression in MRC-5 cells (Figures 2C,F). In short, THSG can inhibit the proliferation and activation of fibroblasts.

**FIGURE 2**

Effect of THSG on protein expression levels of fibronectin, α-SMA, and CTGF in TGF-β1-stimulated MRC-5 human lung fibroblast cells. The cells were treated with different concentrations (50, 100, and 200 μg/ml) of THSG for (A) 24 h or (B) 48 h and viability was measured by the MTT assay. (C) Following 24 h of serum starvation, cells were treated with varying concentrations (50 and 100 μg/ml) of THSG for 24 h, and then incubated with 2.5 ng/ml of TGF-β1 for an additional 24 h. The protein expression levels of fibrotic markers in whole cell lysates were determined by Western blotting and the β-actin was used as a loading control. The relative protein levels of (D) fibronectin, (E) α-SMA, and (F) CTGF were quantified by densitometry and normalized to β-actin. The results were expressed as relative units. Data are represented as the mean ± SEM of three independent experiments. [#]*p* < 0.05 compared with untreated group. ^{*}*p* < 0.05 compared with TGF-β1-treated group.

**FIGURE 3**

Effect of THSG on TGF- β receptors and TGF- β 1-induced Smad-dependent and -independent signaling pathways in MRC-5 human lung fibroblast cells. Confluent cultures of cells were serum starved for 24 h, before treatment with the indicated concentrations (50 and 100 μ g/ml) of THSG for 24 h, and then stimulated with 2.5 ng/ml of TGF- β 1 for 1 h (for TGFBR1 and TGFBR2), 6 h (for Smad2/3, Akt, ERK1/2, p38, and JNK), or 24 h (for mTOR). Whole cell lysates were prepared at the indicated times, and analyzed by Western blotting. The β -actin was used as a loading control.

(A) Representative blots of TGFBR1 and TGFBR2 are shown. The relative protein levels of (B) TGFBR1 and (C) TGFBR2 were quantified by densitometry and normalized to β -actin. (D) Representative blots of p-Smad2/3, Smad2/3, p-Akt and Akt are shown. Quantification of (E) p-Smad2/3 and (F) p-Akt proteins was achieved by densitometry with reference to the respective Smad2/3 and Akt proteins. (G) Representative blots of p-mTOR and mTOR are shown. (H) Quantification of p-mTOR protein was achieved by densitometry and normalized to mTOR protein. (I) Representative blots of p-ERK1/2, ERK1/2, p-p38, p38, p-JNK, and JNK are shown. Quantification of (J) p-ERK1/2, (K) p-p38, and (L) p-JNK proteins was achieved by densitometry with reference to the respective ERK1/2, p38, and JNK proteins. Data are represented as the mean \pm SEM of three independent experiments. # p < 0.05 compared with untreated group. * p < 0.05 compared with TGF- β 1-treated group. (a) (b)

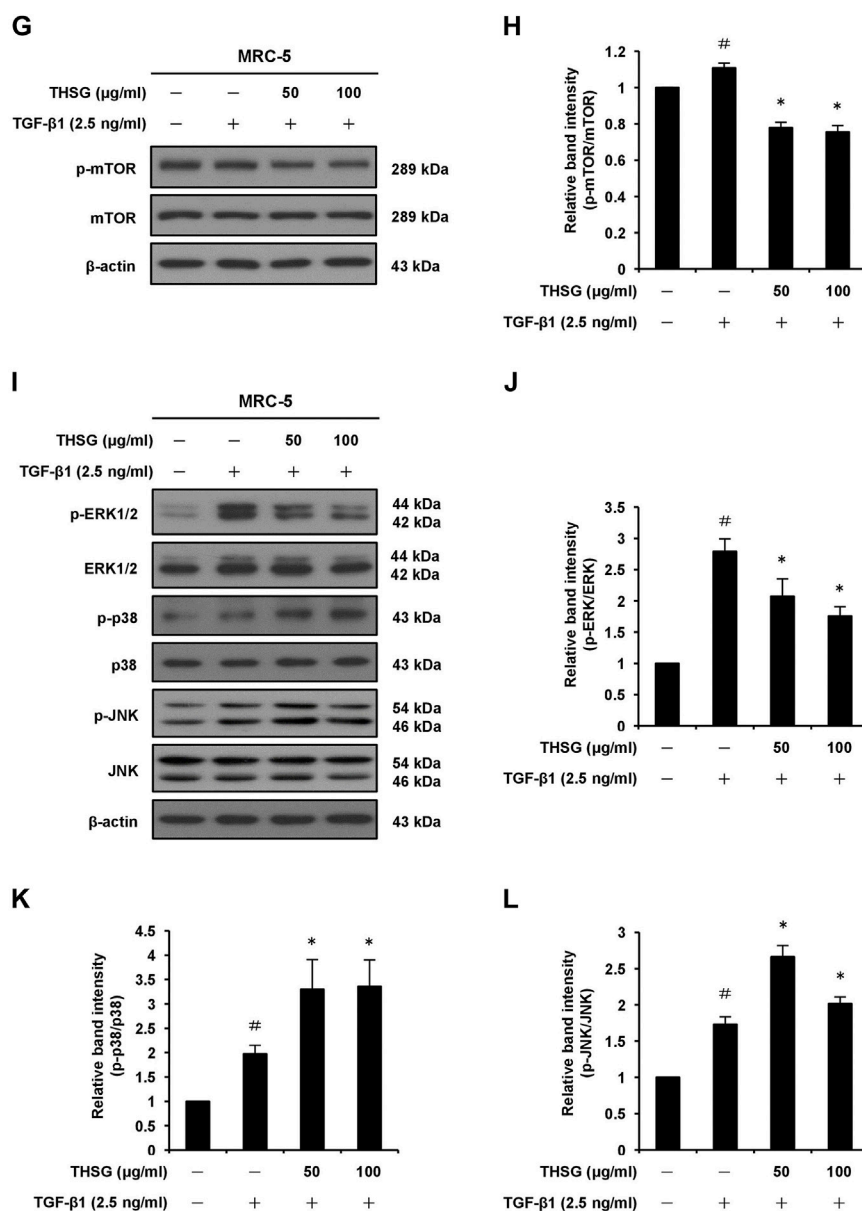


FIGURE 3
XXX

2,3,5,4'-tetrahydroxystilbene-2-O- β -D-glucoside suppresses transforming growth factor-beta 1-induced expression of epithelial–mesenchymal transition related markers in A549 human lung alveolar epithelial cells

TGF- β induces injured alveolar epithelial cells to undergo EMT, which contributes to the expansion of myofibroblasts causing the progression of fibrosis (Xu et al., 2009). Therefore, we examined whether THSG could influence TGF- β 1-induced

EMT related protein expression in A549 cells. As shown in [Supplementary Figures S1A,B](#), Western blot analysis and quantitative results showed that the protein level of the epithelial phenotype marker E-cadherin was significantly decreased after stimulation of 5 ng/ml TGF- β 1 for 48 h, while pretreatment with 100 $\mu\text{g/ml}$ of THSG for 2 h profoundly increased the expression of E-cadherin in A549 cells. In contrast, TGF- β 1 treatment upregulated the protein levels of the mesenchymal phenotype markers N-cadherin and fibronectin compared with the untreated cells. In cells pretreated with THSG, the expression levels of

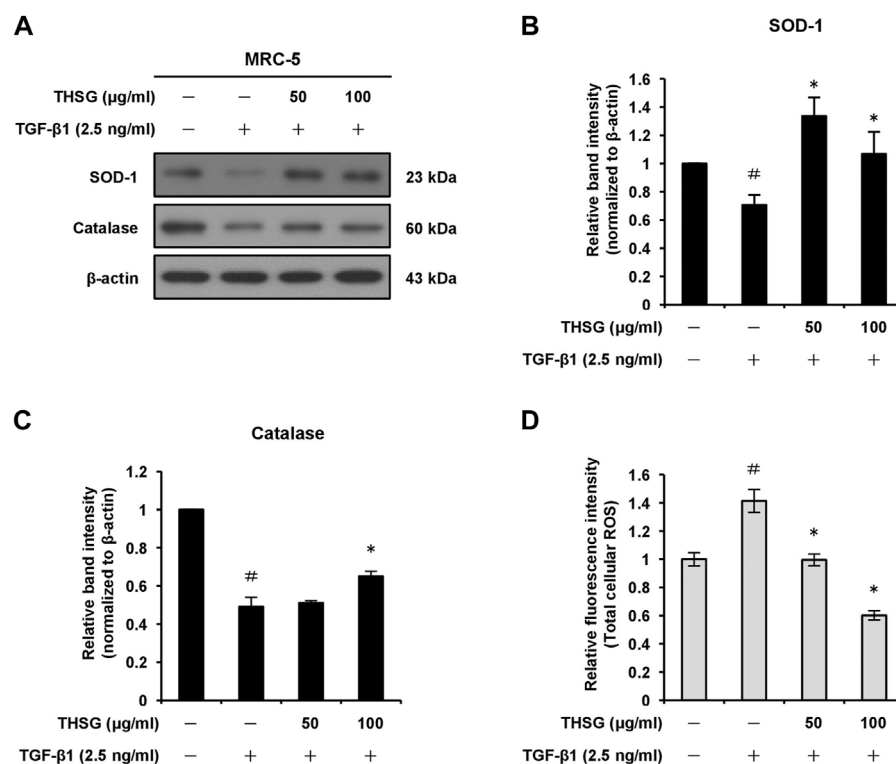


FIGURE 4

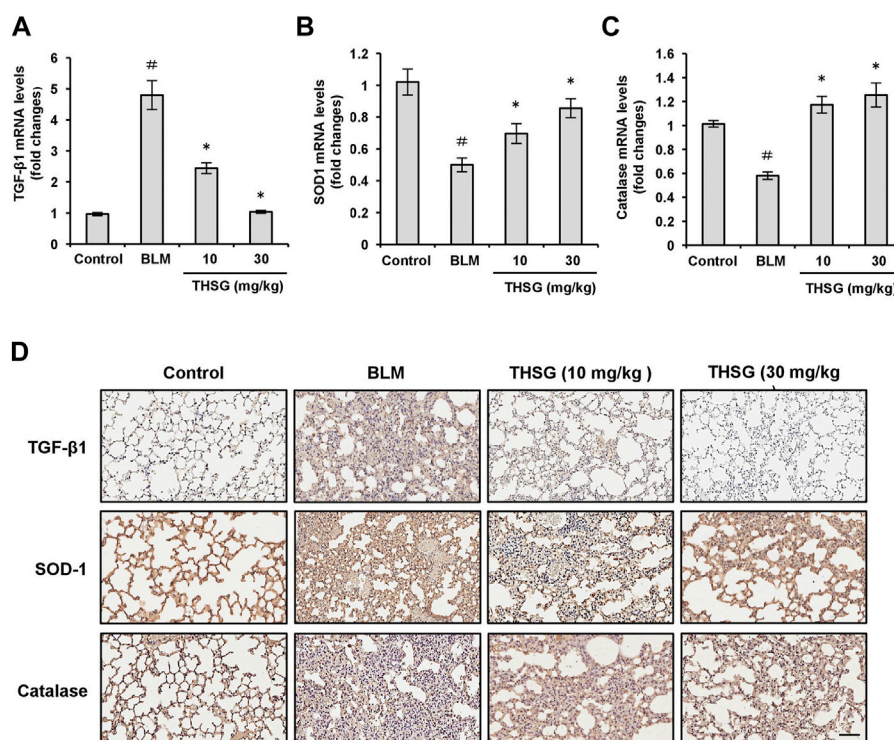
Effect of THSG on antioxidative enzymes expression and oxidative stress in TGF-β1-treated MRC-5 cells. (A) The cells were serum starved for 24 h prior to treatment with various concentrations (50 and 100 μg/ml) of THSG for 24 h, and then incubated with 2.5 ng/ml of TGF-β1 for a further 24 h. The protein expression levels of antioxidative enzymes SOD-1 and catalase in whole cell lysates by Western blotting. β-actin was used as a loading control. The relative protein levels of (B) SOD-1 and (C) catalase were quantified by densitometry and normalized to β-actin. (D) ROS production in cells subjected to different treatment was measured using a ROS detection kit. Data are represented as the mean ± SEM of three independent experiments. [#]*p* < 0.05 compared with untreated group. ^{*}*p* < 0.05 compared with TGF-β1-treated group.

N-cadherin and fibronectin proteins were obviously repressed compared to cells in the TGF-β1-treated group (Supplementary Figures S1A,C,D).

2,3,5,4'-tetrahydroxystilbene-2-O-β-D-glucoside suppresses TGFβR2 expression and transforming growth factor-beta 1-induced Smad2/3 signaling pathway

Since the TGF-β receptors (TGFβR1 and TGFβR2) represent important upstream regulators of the TGF-β/Smad signaling pathway, the effects of THSG on the expression of TGFβR1 and TGFβR2 proteins in TGF-β1-stimulated MRC-5 lung fibroblast cells were detected by Western blot analysis. The results showed that 2.5 ng/ml of TGF-β1 treatment for 1 h slightly upregulated the protein levels of TGFβR1 and TGFβR2. When cells were pretreated for 24 h with THSG (50 and 100 μg/ml) and then stimulated with TGF-β1 for 1 h, the protein level of TGFβR2 was

obviously reduced while the protein level of TGFβR1 was not affected (Figures 3A–C). Similarly, pretreatment of THSG for 2 h markedly reduced TGF-β1-induced up-regulation of the expression of TGFβR2 in A549 lung alveolar epithelial cells, but did not decrease the protein level of TGFβR1 (Supplementary Figures S2A,B,C). TGF-β1-induced fibrotic effects through activation of the canonical Smad signaling pathway in most target cells is well documented. Thus, Western blot analysis was performed to further examine the effect of THSG against TGF-β1-induced activation of Smad signaling pathway. MRC-5 cells were pretreated with THSG (50 and 100 μg/ml) for 24 h and treated with 2.5 ng/ml of TGF-β1 for 1 h. The results demonstrated that TGF-β1 induced Smad2/3 phosphorylation, however, THSG pretreatment significantly dampened TGF-β1-induced Smad2/3 phosphorylation in a dose dependent manner (Figures 3D,E). Additionally, we observed that THSG dramatically inhibited TGF-β1-induced Smad2/3 phosphorylation in A549 cells, as shown in Supplementary Figures S2A,D.

**FIGURE 5**

Effect of THSG on TGF-β1, SOD-1, and catalase expression in the lung tissues of BLM-stimulated mice. The mRNA levels of TGF-β1 (A), SOD-1 (B), and catalase (C) in the lung tissues of mice from each group on day 21 were detected by the qRT-PCR. (D) Representative photographs of immunohistochemical staining for TGF-β1, SOD-1, and catalase in the lung sections of mice from different experimental groups. Scale bar: 100 μm. Data are represented as the mean ± SEM (*n* = 6 in each group). [#]*p* < 0.05 compared with vehicle-treated control group. ^{*}*p* < 0.05 compared with BLM group.

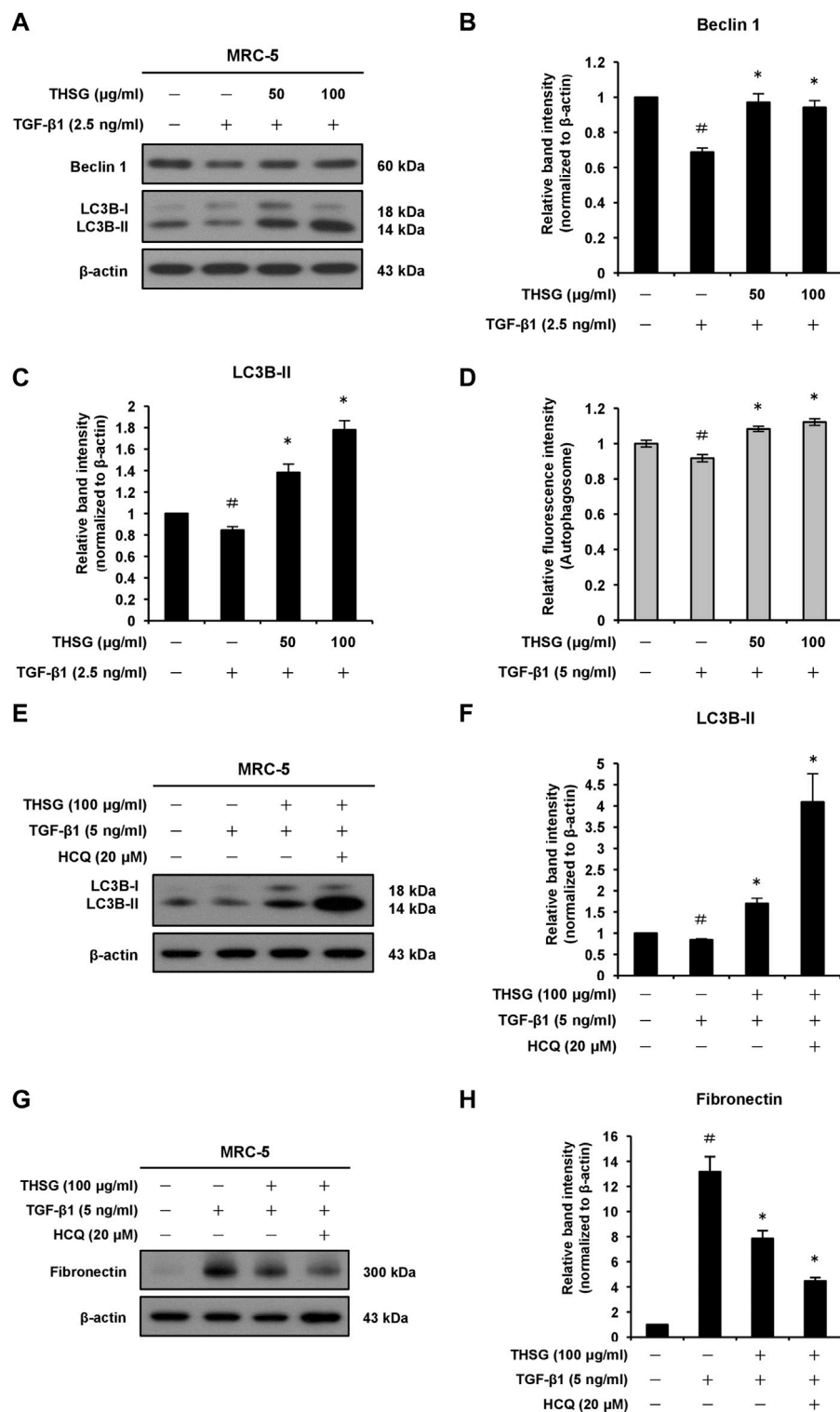
2,3,5,4'-tetrahydroxystilbene-2-O-β-D-glucoside inhibits transforming growth factor-beta 1-induced Akt, mTOR, and ERK1/2 phosphorylation

It has been reported that the non-Smad signaling pathways, including PI3K/Akt/mTOR and MAPK signaling pathways, are involved in the formation of pulmonary fibrosis (Ruan et al., 2020; Li et al., 2021). Thus, we examined whether THSG can inhibit TGF-β1-induced phosphorylation of Akt, mTOR, ERK1/2, p38, and JNK in MRC-5 human lung fibroblast cells (Figures 3D,F–L). Western blot analysis of cell lysates showed that the expression levels of p-Akt, p-mTOR, p-ERK1/2, p-p38, and p-JNK were enhanced in TGF-β1-stimulated lung fibroblasts compared to the untreated cells. Nevertheless, THSG treatment significantly reduced the expression levels of p-Akt, p-mTOR, and p-ERK1/2, but did not diminish the expression levels of p-p38 and p-JNK in TGF-β1-stimulated lung fibroblasts. Likewise, Western blot analysis also demonstrated that TGF-β1-induced phosphorylation of Akt, mTOR, and

ERK1/2 was drastically reduced by THSG treatment in A549 human lung epithelial cells, while THSG had no inhibitory effect on the expression of p-p38 and p-JNK in TGF-β1-stimulated lung epithelial cells (Supplementary Figures S2E–L).

2,3,5,4'-tetrahydroxystilbene-2-O-β-D-glucoside suppresses oxidative stress in MRC-5 human lung fibroblast cells

In order to find out whether THSG is able to induce oxidative stress in MRC-5 cells, we examined the effect of THSG on the expression levels of anti-oxidant enzymes SOD-1 and catalase in TGF-β1-stimulated MRC-5 cells using Western blot analysis. The results showed that the treatment of 2.5 ng/ml TGF-β1 decreased the protein levels of SOD-1 and catalase in MRC-5 cells as compared to the untreated cells. However, the pretreatment of THSG (50 and 100 μg/ml) for 24 h efficiently increased the expression levels of SOD-1 and catalase proteins as compared to the TGF-β1-

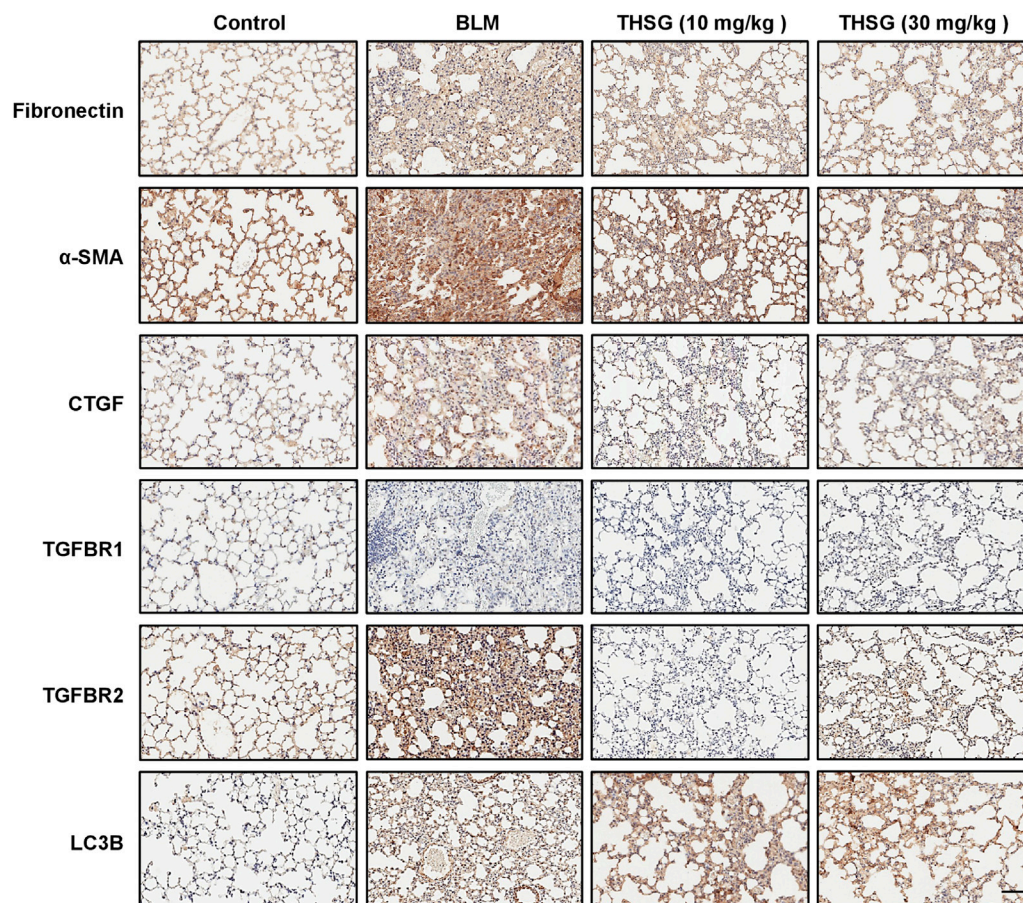
**FIGURE 6**

Effect of THSG on autophagy in MRC-5 cells treated with TGF-β1. **(A)** The cells were serum starved for 24 h, before treatment with various concentrations (50 and 100 μg/ml) of THSG for 24 h, and then incubated with 2.5 ng/ml of TGF-β1 for an additional 24 h. The protein expression levels of autophagic markers Beclin 1 and LC3B in whole cell lysates were assessed by Western blotting. The β-actin was used as a loading control. The relative protein expression levels of **(B)** Beclin 1 and **(C)** LC3B-II were quantified by densitometry and normalized to β-actin. **(D)** After treatment with the indicated concentrations of THSG for 24 h, and autophagy in cells was measured using an autophagy assay kit. **(E)** Cells were

(Continued)

FIGURE 6 (Continued)

pretreated with THSG (100 μ g/ml) for 24 h, and then subsequently stimulated with or without TGF- β 1 (5 ng/ml) or HCQ (20 μ M) for 24 h. The protein samples were collected after the treatment. Representative images of Western blotting showed the protein expression of LC3B. (F) The relative protein expression levels of LC3B-II were quantified by densitometry. (G) Representative images of Western blotting showed the protein expression of fibronectin. (H) Densitometric analysis showed the quantification of fibronectin expression. Data are represented as the mean \pm SEM of three independent experiments. # $p < 0.05$ compared with untreated group. * $p < 0.05$ compared with TGF- β 1-treated group.

**FIGURE 7**

Effect of THSG on fibronectin, α -SMA, CTGF, TGFBR1, TGFBR2, and LC3B expression in the lung tissues of BLM-stimulated mice on day 21. Representative photographs of immunohistochemical staining for fibronectin, α -SMA, CTGF, TGFBR1, TGFBR2, and LC3B in the lung sections of mice from different experimental groups. Scale bar: 100 μ m.

only treated cells (Figures 4A–C). The intracellular production of ROS in MRC-5 cells after the treatments were measured using the total ROS/Superoxide detection kit. After 24 h incubation of MRC-5 cells with 2.5 ng/ml TGF- β 1, a significant increase in ROS production was observed when compared with the untreated group. In contrast, pretreatment of the cells with THSG in doses of 50 and 100 μ g/ml markedly reduced the intracellular ROS generation in comparison to the TGF- β 1-only treated group (Figure 4D).

2,3,5,4'-tetrahydroxystilbene-2-O- β -D-glucoside decreases transforming growth factor-beta 1 expression and increases SOD-1 and catalase expression in the lung tissues of mice with bleomycin-induced pulmonary fibrosis

TGF- β 1 is a profibrotic mediator involved in myofibroblast differentiation and induction of ECM deposition. We assessed the expression level of TGF- β 1

in the lung tissues of mice from all treatment groups by quantitative real-time polymerase chain reaction (qRT-PCR) and immunohistochemistry. Quantitative RT-PCR results showed that the mRNA level of TGF- β 1 from lung tissues of mice after administration of BLM was significantly elevated compared with the untreated group, which was evidently suppressed by the treatment of THSG in a dose-dependent manner, as shown in [Figure 5A](#). These results were confirmed by immunohistochemistry ([Figure 5D](#)). BLM administration produced a significant increase in TGF- β 1 expression in lung tissues, but the increase was reduced by THSG treatment. Additionally, in order to validate the anti-oxidative effect of THSG, oxidative stress was evaluated by detecting the levels of SOD-1 and catalase in lung tissues. A significant inhibition of mRNA levels of SOD-1 and catalase was detected in the lung tissues of BLM-administrated mice as compared to the untreated group. THSG treatment restored BLM-induced reduction in the mRNA levels of SOD-1 and catalase ([Figures 5B,C](#)). Immunohistochemical staining also revealed that SOD-1 and catalase expression was reduced by BLM. In contrast, treatment with THSG increased the expression levels of SOD-1 and catalase ([Figure 5D](#)).

2,3,5,4'-tetrahydroxystilbene-2-O- β -D-glucoside induces autophagy activation in transforming growth factor-beta 1-stimulated MRC-5 human lung fibroblast cells

To define whether THSG affects autophagy in MRC-5 human lung fibroblast cells. Autophagy was monitored by the expression levels of autophagy-associated proteins Beclin 1 and LC3B using Western blot analysis. As shown in [Figures 6A–C](#), the expression levels of Beclin 1 and LC3B-II proteins were significantly decreased in the TGF- β 1-treated group in comparison with the untreated group. However, the levels of Beclin 1 and LC3B-II proteins were significantly increased in the THSG-treated groups (cells were treated with THSG in doses of 50 and 100 μ g/ml, followed by stimulation with 2.5 ng/ml of TGF- β 1) compared with that in the TGF- β 1-only treated group. In addition, the protein level of LC3B was measured after pretreated with 50 and 100 μ g/ml of THSG for 2 h and then cotreated with 5 ng/ml of TGF- β 1 for 24 h in A549 human lung alveolar epithelial cells. The protein expression level of LC3B-II was significantly increased in THSG-treated groups compared to the TGF- β 1-only treated group ([Supplementary Figures S3A,B](#)). To confirm this notion, we used an autophagy assay kit. As indicated in [Figure 6D](#), autophagosome formation decreased in TGF- β 1-treated MRC-5 cells compared to the untreated cells, while pretreatment of these cells with 50 and 100 μ g/ml of THSG

significantly increased the fluorescent intensity of autophagosomes. In addition, studies have found that treatment of chloroquine (as an inhibitor of autophagy, which inhibits lysosome fusion with the autophagosome and thereby interferes autophagic degradation process) can enhance LC3-II expression and increase the autophagosome accumulation in TGF- β 1-stimulated lung fibroblasts ([Rangarajan et al., 2016; Liu et al., 2021](#)). Therefore, we sought to demonstrate whether THSG restores TGF- β 1-induced impaired autophagy, inhibition assay by using HCQ to examine the effect of THSG is related to autophagy inhibition or an increase in autophagic flux. After adding HCQ, the expression level of LC3B-II was increased in THSG-treated cells ([Figures 6E,F](#)). Moreover, the expression of LC3B-II was significantly higher than in THSG-treated cells, indicating the enhanced autophagosome formation and an increase in autophagic flux. To further test the effect of HCQ on the expression of fibrotic marker protein induced by TGF- β 1 in THSG-treated lung fibroblasts. We found that HCQ augmented the downregulation of fibronectin by THSG ([Figures 6G,H](#)). Based on the above results, THSG-induced autophagy may partly account for the inhibitory effect of ECM proteins.

2,3,5,4'-tetrahydroxystilbene-2-O- β -D-glucoside treatment protects against pulmonary fibrosis induced by bleomycin

To assess the effect of THSG on the expression of fibronectin, α -SMA, CTGF, TGFBR1, TGFBR2, and LC3B in the lung tissue sections of mice from each group sacrificed on day 21, immunohistochemical staining was used to determine the protein expressions of these molecules. As shown in [Figure 7](#), the protein levels of fibronectin, α -SMA, CTGF, and TGFBR2 were significantly increased in the lung tissues of BLM-treated mice. In contrast, treatment with THSG (10 or 30 mg/kg) exhibited a reduced levels of fibronectin, α -SMA, CTGF, and TGFBR2 in the lung tissues of mice compared to those of BLM-treated mice. However, the expression of LC3B was markedly increased in the lung tissues of THSG-treated mice compared to the BLM-treated mice. Additionally, there were no obvious changes in the expression of TGFBR1 in the lung tissues of mice from each group.

Discussion

This study showed that THSG could alleviate lung fibrosis by suppressing ECM protein production and myofibroblast differentiation. Furthermore, THSG administration significantly ameliorates lung fibrosis in BLM-treated mice, which is similar to THSG therapeutic effects as depicted in another disease model such as fibrosis of heart and liver

(Peng et al., 2016; Long et al., 2019). In a rat model of pressure overloaded-induced cardiac fibrosis model, THSG administration significantly attenuated the upregulated protein levels of pro-fibrotic markers such as fibronectin, type I and type III collagen induced by pressure overload (Peng et al., 2016). THSG treatment also markedly decreased the protein levels of fibronectin, type I and type III collagen induced by angiotensin II in rat cardiac fibroblasts (Peng et al., 2016). Likewise, in a rodent model of carbon tetrachloride (CCl₄)-induced liver fibrosis, THSG significantly downregulated the expression of α -SMA protein in the liver tissues of rats (Long et al., 2019). In our research, treatment of THSG reduced the expression levels of α -SMA and fibronectin and collagen deposition in the lung tissues of mice exposed to BLM. THSG also decreased the protein levels of α -SMA and fibronectin in TGF- β 1-stimulated MRC-5 lung fibroblast cells. Moreover, THSG treatment significantly inhibited TGF- β expression induced by CCl₄ in rat liver tissue sections (Long et al., 2019). In a mice model of streptozotocin (STZ)-induced diabetes, THSG therapy dramatically suppressed the expression of fibronectin, CTGF, and TGF- β in kidney tissues and prevented renal injury and fibrosis (Chen et al., 2016). Similarly, our current results revealed that THSG administration effectively reduced the expression levels of TGF- β 1 and CTGF induced by BLM in lung tissues of mice.

It has been reported that the protective effect of THSG against hepatic fibrosis was exerted by strikingly decreasing CCl₄-induced phosphorylation of Smad2 and ERK1/2 in the liver tissues of rats (Long et al., 2019). Another study has shown that the phosphorylation of Smad3 was dramatically elevated in palmitic acid-stimulated cardiomyocytes, while THSG treatment significantly inhibited the up-regulation of p-Smad3 by palmitic acid (Zou and Kong, 2019). Moreover, increasing evidences have affirmed that the impediment of activation of Smad-dependent and -independent cascades including MAPK and PI3K/Akt/mTOR pathways, which effectively inhibited pulmonary fibrosis induced by BLM (Chitra et al., 2015; Liu et al., 2016; Qian et al., 2018). In harmony with these reports, the present study showed that the Smad2/3, Akt/mTOR, ERK1/2 signaling pathways were activated in TGF- β 1-mediated fibrogenic response of human MRC-5 lung fibroblast cells and A549 lung alveolar epithelial cells, whereas THSG treatment inhibited TGF- β 1-induced the phosphorylation of Smad2/3, ERK1/2, Akt, and mTOR. Accordingly, THSG efficiently suppressed TGF- β 1-induced the expression of α -SMA, fibronectin, and CTGF in MRC-5 lung fibroblast cells and the expression of fibronectin and N-cadherin in A549 lung alveolar epithelial cells by blocking Smad2/3, ERK1/2, and Akt/mTOR signaling pathways. Overall, these results indicate potential advantages of THSG in the treatment of pulmonary fibrosis diseases.

Oxidative stress plays a crucial role in pulmonary fibrosis development and acts as a mediator of fibrogenic effect of TGF- β (Liu and Gaston Pravia, 2010). Several studies have shown that

BLM administration triggers overproduction of ROS and an observed decrease in the levels of antioxidant (Huang et al., 2015; Zhao et al., 2020). Additionally, TGF- β 1 stimulation causes an appreciable increase in ROS generation in MRC-5 human lung fibroblast cells (Fang et al., 2021). Therefore, we believe that anti-fibrogenic effect of THSG may be acted by repression of oxidative stress. In this study, we demonstrated that ROS production was substantially increased while the expression levels of SOD-1 and catalase were reduced in TGF- β 1-stimulated MRC-5 human lung fibroblast cells. In contrast, THSG administration remarkably decreased the generation of ROS and efficiently enhanced the expression levels of SOD-1 and catalase. Moreover, our *in vivo* results showed that THSG increased the mRNA and protein levels of SOD-1 and catalase in lung tissues of BLM-treated mice. Similarly, in human skin fibroblasts, THSG treatment exhibited protective effects on UVB-induced premature senescence by increasing SOD level and suppressing oxidative stress (Xu and Wang, 2019). In another study, researchers reported that THSG attenuated gentamicin-induced ototoxicity in mouse cochlear UB/OC-2 cells by suppressing ROS generation and increasing the SOD activity (Wen et al., 2020). Wang et al. confirmed that THSG treatment significantly attenuated liver injury in prediabetic rats by increasing the activity of glutathione peroxidase (GPx) and SOD (Wang et al., 2020). These results indicate that THSG can depress lung fibrosis and injury induced by BLM through reducing oxidative stress.

THSG treatment has been proven to induce autophagy by upregulation of autophagy-related proteins Beclin 1, LC3-II, and ATG12 in the liver tissues of prediabetic rats (Wang et al., 2020). It was also reported that THSG significantly induced autophagy and increased the expression of LC3-II protein in human WRL-68 hepatic cells (Yang et al., 2020). Consistent with those reports above, our results revealed that THSG treatment dramatically increased the protein levels of Beclin 1 and LC3B-II in TGF- β 1-stimulated MRC-5 human lung fibroblast cells. THSG treatment also increased LC3B-II protein expression in TGF- β 1-stimulated A549 human lung alveolar epithelial cells. Besides, THSG administration increased the expression level of LC3B in the lung tissue sections of mice treated with BLM. Recent studies have shown that downregulation of p-mTOR and upregulation of LC3-II protein level, contributing to suppression of collagen deposition and EMT in primary lung fibroblasts and TGF- β 1-induced lung epithelial cells, resulting in an alleviation of lung injury and improving lung function in BLM-induced animal models (Alsayed et al., 2022; Pei et al., 2022). Accumulating evidence has also shown that the repression of TGF- β 1-induced activation of mTOR signaling in lung fibroblasts, which results in the induction of autophagy and the inhibition of myofibroblast activation and ECM production in mice model of BLM-induced pulmonary fibrosis (Li et al., 2021; Lu et al., 2022). Furthermore, THSG has been demonstrated to trigger autophagy in human hepatocytes via the inhibition of the PI3K/Akt/mTOR signaling pathway (Yang et al., 2020). Herein, these findings indicate that THSG inhibits the

TGF- β 1-induced Akt/mTOR pathway in human lung fibroblasts and alveolar epithelial cells, thereby leading to autophagy activation and subsequent alleviating lung fibrosis.

In conclusion, we demonstrate that THSG can effectively ameliorate BLM-induced pulmonary fibrosis in mice. We also provide *in vitro* evidence that THSG inhibits TGF- β 1-induced myofibroblast differentiation, ECM production, and EMT-like process in human lung fibroblasts and alveolar epithelial cells. In particular, the protective effect of THSG against BLM-induced pulmonary fibrosis is not only relevant to its anti-oxidative and anti-fibrotic properties but also autophagy activation. The potential molecular mechanisms responsible for the anti-fibrotic effect of THSG is due to repression of both Smad and non-Smad signaling pathways. Therefore, THSG may be a potential agent for the treatment of pulmonary fibrosis diseases.

Data availability statement

The original contributions presented in the study are included in the article/[Supplementary Material](#), further inquiries can be directed to the corresponding author.

Ethics statement

The animal study was reviewed and approved by the Institutional Animal Care and Use Committee of Chang Gung University (Taoyuan, Taiwan; Document CGU110-021).

Author contributions

T-TH and K-YC conceived and designed the experiments. T-TH, Y-WL, and K-YC performed the experiments. T-TH, C-MC, L-GC, Y-WL, T-HH, and K-YC analyzed the data. T-TH and K-YC wrote the original draft manuscript. T-TH, C-MC, T-HH, K-BC, and K-YC reviewed and edited the manuscript. All authors read and approved all versions of the manuscript.

Funding

The present study was supported by grants from the Ministry of Science and Technology of Taiwan (MOST-108-2314-B-182-052-MY3, MOST-108-2811-B-182-524, MOST-109-2811-B-182-512, MOST-110-2811-B-182-526, and MOST-111-2314-B-182-057) and Chang Gung Memorial Hospital, Taiwan (BMRPD-861, CORPD-1K-0021, CRRPD-1K-0013, CMRPD-1L-0131 and CMRPD-1L-0132) (K-YC). In addition, partially supported by the iEGG and Animal Biotechnology Center from the Feature Areas Research Center Program within the

framework of the Higher Education Sprout Project by the Ministry of Education in Taiwan (MOE-111-S-0023-A) (C-MC).

Conflict of interest

The authors declare that the research was conducted in the absence of any commercial or financial relationships that could be construed as a potential conflict of interest.

Publisher's note

All claims expressed in this article are solely those of the authors and do not necessarily represent those of their affiliated organizations, or those of the publisher, the editors and the reviewers. Any product that may be evaluated in this article, or claim that may be made by its manufacturer, is not guaranteed or endorsed by the publisher.

Supplementary material

The Supplementary Material for this article can be found online at: <https://www.frontiersin.org/articles/10.3389/fphar.2022.997100/full#supplementary-material>

SUPPLEMENTARY FIGURE S1

Effect of THSG on the protein expression levels of TGF- β 1-induced EMT related markers in A549 human lung alveolar epithelial cells. (A) Confluent cultures of cells were starved in medium containing 0.1% FBS for 24 h, before treatment with the indicated concentrations (50 and 100 μ g/ml) of THSG for 2 h, and then stimulated with 5 ng/ml of TGF- β 1 for a further 48 h. The expressions of epithelial phenotype marker (E-cadherin) and mesenchymal phenotype markers (fibronectin and N-cadherin) in whole cell lysates were determined by Western blotting. β -actin was used as a loading control. Representative blots of fibronectin, N-cadherin, and E-cadherin are shown. The relative protein levels of (B) fibronectin, (C) N-cadherin, and (D) E-cadherin were quantified by densitometry and normalized to β -actin. The results were expressed as relative units. Data are represented as the mean \pm SEM of three independent experiments. $\#p < 0.05$ compared with untreated group. $*p < 0.05$ compared with control (TGF- β 1-treated) group.

SUPPLEMENTARY FIGURE S2

Effect of THSG on TGF- β receptors and TGF- β 1-induced Smad-dependent and -independent signaling pathways in A549 human lung alveolar epithelial cells. The cells were starved for 24 h followed by treatment with the indicated doses (50 and 100 μ g/ml) of THSG for 2 h, and then stimulated with 5 ng/ml of TGF- β 1 for 30 min (for TGFB1, TGFB2, and Smad 2/3), 1 h (for Akt, ERK1/2, p38, and JNK), or 3 h (for mTOR). Whole cell lysates were prepared at the indicated times, and subjected to Western blotting. The β -actin was used as a loading control. (A) Representative blots of TGFB1, TGFB2, p-Smad2/3, and Smad2/3 are shown. The relative protein levels of (B) TGFB1 and (C) TGFB2 were quantified by densitometry and normalized to β -actin. (D) Quantification of p-Smad2/3 protein was achieved by densitometry and normalized to Smad2/3 protein. (E) Representative blots of p-Akt and Akt are shown. (F) Quantification of p-Akt protein was achieved by densitometry and normalized to Akt protein. (G) Representative blots of p-mTOR and mTOR are shown. (H) Quantification of p-mTOR was achieved by densitometry and normalized to mTOR. (I) Representative blots of p-ERK1/2, ERK1/2, p-p38, p38, p-JNK, and JNK are shown. Quantification of (J) p-ERK1/2, (K) p-p38, and (L) p-JNK proteins was analyzed by densitometry with reference to the respective ERK1/2, p38,

and JNK proteins. Data are represented as the mean \pm SEM of three independent experiments. $\#p < 0.05$ compared with untreated group. $*p < 0.05$ compared with TGF- β 1-treated group.

SUPPLEMENTARY FIGURE 3

Effect of THSG on autophagy in A549 cells treated with TGF- β 1. (A) The cells were starved for 24 h, before treatment with various concentrations (50 and 100 μ g/ml) of THSG for 2 h, and then incubated

with 5 ng/ml of TGF- β 1 for a further 48 h. The expression of autophagic marker LC3B in whole cell lysates were determined by Western blotting. β -actin was used as a loading control. Representative blots are shown. The relative protein expression level of (B) LC3B-II was quantified by densitometry and normalized to β -actin. Data are represented as the mean \pm SEM of three independent experiments. $\#p < 0.05$ compared with untreated group. $*p < 0.05$ compared with TGF- β 1-treated group.

References

- Ahn, J. Y., Kim, M. H., Lim, M. J., Park, S., Lee, S. L., Yun, Y. S., et al. (2011). The inhibitory effect of ginsan on TGF- β mediated fibrotic process. *J. Cell. Physiol.* 226 (5), 1241–1247. doi:10.1002/jcp.22452
- Allen, J. T., and Spiteri, M. A. (2002). Growth factors in idiopathic pulmonary fibrosis: Relative roles. *Respir. Res.* 3 (1), 13. doi:10.1186/rr162
- Alsayed, H. A., Mohammad, H. M. F., Khalil, C. M., El-Kherbetawy, M. K., and Elaidy, S. M. (2022). Autophagy modulation by irbesartan mitigates the pulmonary fibrotic alterations in bleomycin challenged rats: Comparative study with rapamycin. *Life Sci.* 303, 120662. doi:10.1016/j.lfs.2022.120662
- Araya, J., Kojima, J., Takasaka, N., Ito, S., Fujii, S., Hara, H., et al. (2013). Insufficient autophagy in idiopathic pulmonary fibrosis. *Am. J. Physiol. Lung Cell. Mol. Physiol.* 304 (1), L56–L69. doi:10.1152/ajplung.00213.2012
- Ashcroft, T., Simpson, J. M., and Timbrell, V. (1988). Simple method of estimating severity of pulmonary fibrosis on a numerical scale. *J. Clin. Pathol.* 41 (4), 467–470. doi:10.1136/jcp.41.4.467
- Bao, Z., Zhang, Q., Wan, H., He, P., Zhou, X., and Zhou, M. (2014). Expression of suppressor of cytokine signaling 1 in the peripheral blood of patients with idiopathic pulmonary fibrosis. *Chin. Med. J.* 127 (11), 2117–2120.
- Bouros, D., and Antoniou, K. M. (2005). Current and future therapeutic approaches in idiopathic pulmonary fibrosis. *Eur. Respir. J.* 26 (4), 693–702. doi:10.1183/09031936.05.00145004
- Büchter, C., Zhao, L., Havermann, S., Honnen, S., Fritz, G., Proksch, P., et al. (2015). TSG (2, 3, 5, 4'-Tetrahydroxystilbene-2-O- β -D-glucoside) from the Chinese herb *Polygonum multiflorum* increases life span and stress resistance of *Caenorhabditis elegans*. *Oxid. Med. Cell. Longev.* 124357. doi:10.1155/2015/124357
- Cabrera, S., Maciel, M., Herrera, I., Nava, T., Vergara, F., Gaxiola, M., et al. (2015). Essential role for the ATG4B protease and autophagy in bleomycin-induced pulmonary fibrosis. *Autophagy* 11 (4), 670–684. doi:10.1080/15548627.2015.1034409
- Chen, G. T., Yang, M., Chen, B. B., Song, Y., Zhang, W., and Zhang, Y. (2016). 2, 3, 5, 4'-Tetrahydroxystilbene-2-O- β -D-glucoside exerted protective effects on diabetic nephropathy in mice with hyperglycemia induced by streptozotocin. *Food Funct.* 7 (11), 4628–4636. doi:10.1039/c6fo01319h
- Chitra, P., Saiprasad, G., Manikandan, R., and Sudhandiran, G. (2015). Berberine inhibits Smad and non-Smad signaling cascades and enhances autophagy against pulmonary fibrosis. *J. Mol. Med.* 93 (9), 1015–1031. doi:10.1007/s00109-015-1283-1
- Fang, L., Wang, W., Chen, J., Zuo, A., Gao, H., Yan, T., et al. (2021). Osthole attenuates bleomycin-induced pulmonary fibrosis by modulating NADPH oxidase 4-derived oxidative stress in mice. *Oxid. Med. Cell. Longev.* 2021, 3309944. doi:10.1155/2021/3309944
- Fernandez, I. E., and Eickelberg, O. (2012). The impact of TGF- β on lung fibrosis: From targeting to biomarkers. *Proc. Am. Thorac. Soc.* 9 (3), 111–116. doi:10.1513/pats.201203-023AW
- Gibson, C. D., Kugler, M. C., Deshwal, H., Munger, J. S., and Condos, R. (2020). Advances in targeted therapy for progressive fibrosing interstitial lung disease. *Lung* 198 (4), 597–608. doi:10.1007/s00408-020-00370-1
- Haspel, J. A., and Choi, A. M. (2011). Autophagy: A core cellular process with emerging links to pulmonary disease. *Am. J. Respir. Crit. Care Med.* 184 (11), 1237–1246. doi:10.1164/rccm.201106-0966CI
- Huang, T. T., Chong, K. Y., Ojcius, D. M., Wu, Y. H., Ko, Y. F., Wu, C. Y., et al. (2013). *Hirsutella sinensis* mycelium suppresses interleukin-1 β and interleukin-18 secretion by inhibiting both canonical and non-canonical inflammasomes. *Sci. Rep.* 3, 1374. doi:10.1038/srep01374
- Huang, T. T., Lai, H. C., Ko, Y. F., Ojcius, D. M., Lan, Y. W., Martel, J., et al. (2015). *Hirsutella sinensis* mycelium attenuates bleomycin-induced pulmonary inflammation and fibrosis in vivo. *Sci. Rep.* 5, 15282. doi:10.1038/srep15282
- Huang, T. T., Wu, S. P., Chong, K. Y., Ojcius, D. M., Ko, Y. F., Wu, Y. H., et al. (2014). The medicinal fungus *Antrodia cinnamomea* suppresses inflammation by inhibiting the NLRP3 inflammasome. *J. Ethnopharmacol.* 155 (1), 154–164. doi:10.1016/j.jep.2014.04.053
- Jarman, E. R., Khambata, V. S., Cope, C., Jones, P., Roger, J., Ye, L. Y., et al. (2014). An inhibitor of NADPH oxidase-4 attenuates established pulmonary fibrosis in a rodent disease model. *Am. J. Respir. Cell. Mol. Biol.* 50 (1), 158–169. doi:10.1165/rcmb.2013-0174OC
- Jung, C. H., Ro, S. H., Cao, J., Otto, N. M., and Kim, D. H. (2010). mTOR regulation of autophagy. *FEBS Lett.* 584 (7), 1287–1295. doi:10.1016/j.febslet.2010.01.017
- Koli, K., Myllärniemi, M., Keski-Oja, J., and Kinnula, V. L. (2008). Transforming growth factor- β activation in the lung: Focus on fibrosis and reactive oxygen species. *Antioxid. Redox Signal.* 10 (2), 333–342. doi:10.1089/ars.2007.1914
- Kothapalli, D., Frazier, K. S., Welpy, A., Segarini, P. R., and Grotendorst, G. R. (1997). Transforming growth factor beta induces anchorage-independent growth of NRK fibroblasts via a connective tissue growth factor-dependent signaling pathway. *Cell. Growth Differ.* 8 (1), 61–68.
- Li, M., Krishnaveni, M. S., Li, C., Zhou, B., Xing, Y., Banfalvi, A., et al. (2011). Epithelium-specific deletion of TGF- β receptor type II protects mice from bleomycin-induced pulmonary fibrosis. *J. Clin. Invest.* 121 (1), 277–287. doi:10.1172/JCI42090
- Li, X., Ma, L., Huang, K., Wei, Y., Long, S., Liu, Q., et al. (2021). Regorafenib-attenuated, bleomycin-induced pulmonary fibrosis by inhibiting the TGF- β 1 signaling pathway. *Int. J. Mol. Sci.* 22 (4), 1985. doi:10.3390/ijms22041985
- Ling, S., and Xu, J. W. (2016). Biological activities of 2, 3, 5, 4'-tetrahydroxystilbene-2-O- β -D-glucoside in antiaging and antiaging related disease treatments. *Oxid. Med. Cell. Longev.* 4973239. doi:10.1155/2016/4973239
- Liu, Q., Chu, H., Ma, Y., Wu, T., Qian, F., Ren, X., et al. (2016). Salvianolic acid B attenuates experimental pulmonary fibrosis through inhibition of the TGF- β signaling pathway. *Sci. Rep.* 6, 27610. doi:10.1038/srep27610
- Liu, R. M., and Gaston Pravia, K. A. (2010). Oxidative stress and glutathione in TGF- β -mediated fibrogenesis. *Free Radic. Biol. Med.* 48 (1), 1–15. doi:10.1016/j.freeradbiomed.2009.09.026
- Liu, Y., Zhong, W., Zhang, J., Chen, W., Lu, Y., Qiao, Y., et al. (2021). Tetrandrine modulates rheb-mTOR signaling-mediated selective autophagy and protects pulmonary fibrosis. *Front. Pharmacol.* 12, 739220. doi:10.3389/fphar.2021.739220
- Long, T., Wang, L., Yang, Y., Yuan, L., Zhao, H., Chang, C. C., et al. (2019). Protective effects of trans-2, 3, 5, 4'-tetrahydroxystilbene 2-O- β -D-glucopyranoside on liver fibrosis and renal injury induced by CCl₄ via down-regulating p-ERK1/2 and p-Smad1/2. *Food Funct.* 10 (8), 5115–5123. doi:10.1039/c9fo01010f
- Lu, Y., Zhong, W., Liu, Y., Chen, W., Zhang, J., Zeng, Z., et al. (2022). Anti-PD-L1 antibody alleviates pulmonary fibrosis by inducing autophagy via inhibition of the PI3K/Akt/mTOR pathway. *Int. Immunopharmacol.* 104, 108504. doi:10.1016/j.intimp.2021.108504
- Luo, F., Zhuang, Y., Sides, M. D., Sanchez, C. G., Shan, B., White, E. S., et al. (2014). Arsenic trioxide inhibits transforming growth factor- β 1-induced fibroblast to myofibroblast differentiation in vitro and bleomycin induced lung fibrosis in vivo. *Respir. Res.* 15 (1), 51. doi:10.1186/1465-9921-15-51
- Patel, A. S., Lin, L., Geyer, A., Haspel, J. A., An, C. H., Cao, J., et al. (2012). Autophagy in idiopathic pulmonary fibrosis. *PLoS One* 7 (7), e41394. doi:10.1371/journal.pone.0041394
- Pei, X., Zheng, F., Li, Y., Lin, Z., Han, X., Feng, Y., et al. (2022). Niclosamide ethanolate salt alleviates idiopathic pulmonary fibrosis by modulating the PI3K-mTORC1 pathway. *Cells* 11 (3), 346. doi:10.3390/cells11030346
- Peng, Y., Zeng, Y., Xu, J., Huang, X. L., Zhang, W., and Xu, X. L. (2016). PPAR- γ is involved in the protective effect of 2, 3, 4', 5-tetrahydroxystilbene-2-O- β -D-glucoside against cardiac fibrosis in pressure-overloaded rats. *Eur. J. Pharmacol.* 791, 105–114. doi:10.1016/j.ejphar.2016.08.025

- Qian, W., Cai, X., Qian, Q., Zhang, W., and Wang, D. (2018). Astragaloside IV modulates TGF- β 1-dependent epithelial-mesenchymal transition in bleomycin-induced pulmonary fibrosis. *J. Cell. Mol. Med.* 22 (9), 4354–4365. doi:10.1111/jcmm.13725
- Raghu, G., Rochwerf, B., Zhang, Y., Garcia, C. A., Azuma, A., Behr, J., et al. (2015). An official ATS/ERS/JRS/ALAT clinical practice guideline: Treatment of idiopathic pulmonary fibrosis. An update of the 2011 clinical practice guideline. *Am. J. Respir. Crit. Care Med.* 192 (2), e3–e19. doi:10.1164/rccm.201506-1063ST
- Rangarajan, S., Kurundkar, A., Kurundkar, D., Bernard, K., Sanders, Y. Y., Ding, Q., et al. (2016). Novel mechanisms for the antifibrotic action of nintedanib. *Am. J. Respir. Cell. Mol. Biol.* 54 (1), 51–59. doi:10.1165/rcmb.2014-0445OC
- Richeldi, L., Collard, H. R., and Jones, M. G. (2017). Idiopathic pulmonary fibrosis. *Lancet* 389 (10082), 1941–1952. doi:10.1016/S0140-6736(17)30866-8
- Ruan, H., Lv, Z., Liu, S., Zhang, L., Huang, K., Gao, S., et al. (2020). Anlotinib attenuated bleomycin-induced pulmonary fibrosis via the TGF- β 1 signalling pathway. *J. Pharm. Pharmacol.* 72 (1), 44–55. doi:10.1111/jphp.13183
- Saito, M., Mitani, A., Ishimori, T., Miyashita, N., Isago, H., Mikami, Y., et al. (2020). Active mTOR in lung epithelium promotes epithelial-mesenchymal transition and enhances lung fibrosis. *Am. J. Respir. Cell. Mol. Biol.* 62 (6), 699–708. doi:10.1165/rcmb.2019-0255OC
- Sauleda, J., Núñez, B., Sala, E., and Soriano, J. B. (2018). Idiopathic pulmonary fibrosis: Epidemiology, natural history, phenotypes. *Med. Sci.* 6 (4), 110. doi:10.3390/medsci6040110
- Shi, Y., and Massagué, J. (2003). Mechanisms of TGF- β signaling from cell membrane to the nucleus. *Cell* 113 (6), 685–700. doi:10.1016/s0092-8674(03)00432-x
- Sime, P. J., Xing, Z., Graham, F. L., Csaky, K. G., and Gaudie, J. (1997). Adenovector-mediated gene transfer of active transforming growth factor- β 1 induces prolonged severe fibrosis in rat lung. *J. Clin. Invest.* 100 (4), 768–776. doi:10.1172/JCI119590
- Tanaka, K., Ishihara, T., Azuma, A., Kudoh, S., Ebina, M., Nukiwa, T., et al. (2010). Therapeutic effect of lecithinized superoxide dismutase on bleomycin-induced pulmonary fibrosis. *Am. J. Physiol. Lung Cell. Mol. Physiol.* 298 (3), L348–L360. doi:10.1152/ajplung.00289.2009
- Wang, C., Dai, S., Gong, L., Fu, K., Ma, C., Liu, Y., et al. (2022). A review of pharmacology, toxicity and pharmacokinetics of 2, 3, 5, 4'-tetrahydroxystilbene-2-O- β -D-glucoside. *Front. Pharmacol.* 12, 791214. doi:10.3389/fphar.2021.791214
- Wang, K., Zhang, T., Lei, Y., Li, X., Jiang, J., Lan, J., et al. (2018). Identification of ANXA2 (annexin A2) as a specific bleomycin target to induce pulmonary fibrosis by impeding TFEB-mediated autophagic flux. *Autophagy* 14 (2), 269–282. doi:10.1080/15548627.2017.1409405
- Wang, X., Zeng, J., Wang, X., Li, J., Chen, J., Wang, N., et al. (2020). 2, 3, 5, 4'-tetrahydroxystilbene-2-O- β -D-glucoside induces autophagy of liver by activating PI3K/Akt and Erk pathway in prediabetic rats. *BMC Complement. Med. Ther.* 20 (1), 177. doi:10.1186/s12906-020-02949-w
- Wen, Y. H., Lin, J. N., Wu, R. S., Yu, S. H., Hsu, C. J., Tseng, G. F., et al. (2020). Otoprotective effect of 2, 3, 4', 5-Tetrahydroxystilbene-2-O- β -D-glucoside on gentamicin-induced apoptosis in mouse cochlear UB/OC-2 cells. *Molecules* 25 (13), 3070. doi:10.3390/molecules25133070
- Wilkes, M. C., Mitchell, H., Penheiter, S. G., Doré, J. J., Suzuki, K., Edens, M., et al. (2005). Transforming growth factor- β activation of phosphatidylinositol 3-kinase is independent of Smad2 and Smad3 and regulates fibroblast responses via p21-activated kinase-2. *Cancer Res.* 65 (22), 10431–10440. doi:10.1158/0008-5472.CAN-05-1522
- Wu, T. Y., Lin, J. N., Luo, Z. Y., Hsu, C. J., Wang, J. S., and Wu, H. P. (2020). 2, 3, 4', 5-Tetrahydroxystilbene-2-O- β -D-glucoside (THSG) Activates the Nrf2 antioxidant pathway and attenuates oxidative stress-induced cell death in mouse cochlear UB/OC-2 cells. *Biomolecules* 10 (3), 465. doi:10.3390/biom10030465
- Xu, J., Lamouille, S., and Derynck, R. (2009). TGF- β -induced epithelial to mesenchymal transition. *Cell. Res.* 19 (2), 156–172. doi:10.1038/cr.2009.5
- Xu, M., and Wang, Y. (2019). Stilbene glucoside inhibits ultraviolet radiation B-induced photoaging in human skin fibroblasts. *J. Zhejiang Univ. Med. Sci.* 48 (6), 625–630. doi:10.3785/j.issn.1008-9292.2019.12.06
- Yang, L., Xing, W., Xiao, W. Z., Tang, L., Wang, L., Liu, M. J., et al. (2020). 2, 3, 5, 4'-Tetrahydroxy-stilbene-2-O-beta-D-glucoside induces autophagy-mediated apoptosis in hepatocytes by upregulating miR-122 and inhibiting the PI3K/Akt/mTOR pathway: Implications for its hepatotoxicity. *Pharm. Biol.* 58 (1), 806–814. doi:10.1080/13880209.2020.1803367
- Yu, W., Zhang, X., Wu, H., Zhou, Q., Wang, Z., Liu, R., et al. (2017). HO-1 is essential for tetrahydroxystilbene glucoside mediated mitochondrial biogenesis and anti-inflammation process in LPS-treated RAW264.7 macrophages. *Oxid. Med. Cell. Longev.* 1818575. doi:10.1155/2017/1818575
- Zhang, Y. E. (2009). Non-smad pathways in TGF- β signaling. *Cell. Res.* 19 (1), 128–139. doi:10.1038/cr.2008.328
- Zhao, H., Li, C., Li, L., Liu, J., Gao, Y., Mu, K., et al. (2020). Baicalin alleviates bleomycin-induced pulmonary fibrosis and fibroblast proliferation in rats via the PI3K/AKT signaling pathway. *Mol. Med. Rep.* 21 (6), 2321–2334. doi:10.3892/mmr.2020.11046
- Zou, Y., and Kong, M. (2019). Tetrahydroxy stilbene glucoside alleviates palmitic acid-induced inflammation and apoptosis in cardiomyocytes by regulating miR-129-3p/Smad3 signaling. *Cell. Mol. Biol. Lett.* 24, 5. doi:10.1186/s11658-018-0125-x



OPEN ACCESS

EDITED BY

Hina Siddiqui,
University of Karachi, Pakistan

REVIEWED BY

Anthony Faber,
Virginia Commonwealth University,
United States
Erika Cione,
University of Calabria, Italy

*CORRESPONDENCE

Katarina Stroffekova,
katarina.stroffekova@upjs.sk

SPECIALTY SECTION

This article was submitted to
Experimental Pharmacology and Drug
Discovery,
a section of the journal
Frontiers in Pharmacology

RECEIVED 11 July 2022

ACCEPTED 30 August 2022

PUBLISHED 04 October 2022

CITATION

Doroshenko A, Tomkova S, Kozar T and
Stroffekova K (2022), Hypericin, a
potential new BH3 mimetic.
Front. Pharmacol. 13:991554.
doi: 10.3389/fphar.2022.991554

COPYRIGHT

© 2022 Doroshenko, Tomkova, Kozar
and Stroffekova. This is an open-access
article distributed under the terms of the
[Creative Commons Attribution License](#)
(CC BY). The use, distribution or
reproduction in other forums is
permitted, provided the original
author(s) and the copyright owner(s) are
credited and that the original
publication in this journal is cited, in
accordance with accepted academic
practice. No use, distribution or
reproduction is permitted which does
not comply with these terms.

Hypericin, a potential new BH3 mimetic

Anastasia Doroshenko¹, Silvia Tomkova¹, Tibor Kozar² and
Katarina Stroffekova^{1*}

¹Department of Biophysics, Faculty of Natural Sciences, PJ Safarik University, Kosice, Slovakia, ²Center
of Interdisciplinary Biosciences, TIP-Safarik University, Kosice, Slovakia

Many types of cancer such as prostate cancer, myeloid leukemia, breast cancer, glioblastoma display strong chemo resistance, which is supported by enhanced expression of multiple anti-apoptotic Bcl-2, Bcl-XL and Mcl-1 proteins. The viable anti-cancer strategies are based on developing anti-apoptotic Bcl-2 proteins inhibitors, BH3 mimetics. Our focus in past years has been on the investigating a new potential BH3 mimetic, Hypericin (Hyp). Hyp is a naturally occurring photosensitive compound used in photodynamic therapy and diagnosis. We have demonstrated that Hyp can cause substantial effects in cellular ultrastructure, mitochondria function and metabolism, and distribution of Bcl2 proteins in malignant and non-malignant cells. One of the possible mechanisms of Hyp action could be the direct interactions between Bcl-2 proteins and Hyp. We investigated this assumption by *in silico* computer modelling and *in vitro* fluorescent spectroscopy experiments with the small Bcl2 peptide segments designed to correspond to Bcl2 BH3 and BH1 domains. We show here that Hyp interacts with BH3 and BH1 peptides in concentration dependent manner, and shows the stronger interactions than known BH3 mimetics, Gossypol (Goss) and ABT-263. In addition, interactions of Hyp, Goss and ABT263, with whole purified proteins Bcl-2 and Mcl-1 by fluorescence spectroscopy show that Hyp interacts stronger with the Bcl-2 and less with Mcl-1 protein than Goss or ABT-263. This suggest that Hyp is comparable to other BH3 mimetics and could be explore as such. Hyp cytotoxicity was low in human U87 MG glioma, similar to that of ABT263, where Goss exerted sufficient cytotoxicity, suggesting that Hyp acts primarily on Bcl-2, but not on Mcl-1 protein. In combination therapy, low doses of Hyp with Goss effectively decreased U87 MG viability, suggesting a possible synergy effect. Overall, we can conclude that Hyp as BH3 mimetic acts primarily on Bcl-2 protein and can be explored to target cells with Bcl-2 over-expression, or in combination with other BH3 mimetics, that target Mcl-1 or Bcl-XL proteins, in dual therapy.

KEYWORDS

Bcl-2 proteins, BH3 mimetics, hypericin, gossypol, cancer

Introduction

Programmed cell death (apoptosis) is a particularly conserved process that maintains healthy cell populations within tissues. Apoptosis is tightly regulated and disrupting its control mechanisms is the underlying cause of cancer initiation and expansion. B-cell lymphoma-2 (Bcl-2) family of proteins are the main regulators of apoptosis (Vaux and Korsmeyer, 1999; Danial and Korsmeyer, 2004). The Bcl-2 family consists of multi BH domain anti- (Bcl-2, Bcl-XL, Mcl-1, Bfl-1, Bcl-W, and Bcl-B) and pro-apoptotic members (Bax, Bak and Bok). The Bcl-2 family also contains a group of BH3-only proteins (Bad, Bim, Bmf, Bik, Hrk, Bid, Puma, Noxa), which can serve as sensitizers or direct activators of apoptosis (Cory et al., 2003; Llambi et al., 2011). The balanced system of protein-protein interactions between multi BH domain anti- and pro-apoptotic Bcl-2 proteins, and/or BH3-only proteins manages either cell survival or death (Llambi et al., 2011). A cell's ability to undergo apoptosis strongly depends on the presence of BH3-only proteins and their interaction with anti-apoptotic members.

Cancer cells escape apoptosis by the upregulating of anti-apoptotic Bcl2 proteins (Bcl2, Bcl-XL and Mcl1), and this upregulation significantly adds to tumor progression, poor prognosis, and chemo resistance (Vogler, 2014; Correia et al., 2015; Gong et al., 2016). Thus, these proteins and their interactions represent attractive targets for new anticancer treatments (Davids and Letai, 2012; Vela and Marzo, 2015). The Bcl-2 proteins structural studies (X-ray crystallography and NMR) revealed a hydrophobic groove comprised of BH3, BH2 and BH1 domain on the surface of anti-apoptotic Bcl-2 family proteins that binds the BH3 domain of their pro-apoptotic partners (Petros et al., 2004). Based on this interaction, different strategies have been employed. There were studies of peptides that mimic BH3 motifs of pro-apoptotic Bak, Bax or BH3-only proteins (Wang et al., 2000a; DeBartolo et al., 2012; Raghav et al., 2012), or use of small molecules that inhibit pro-survival Bcl2 proteins (Wang et al., 2000b; O'Neill et al., 2004; Wang et al., 2006; Azmi and Mohammad, 2009; Davids and Letai, 2012). More than 25 small molecules, termed BH3 mimetics, with diverse chemical structures were designed as inhibitors of anti-apoptotic Bcl2 proteins (Bcl2, BclXL and Mcl1), and are currently used in preclinical and clinical studies (Wang et al., 2000a; Wang et al., 2000b; O'Neill et al., 2004; Wang et al., 2006; Azmi and Mohammad, 2009; Davids and Letai, 2012; Raghav et al., 2012; Vela and Marzo, 2015). The available BH3 mimetics are either naturally occurring (Gossypol, Chelerythrine, Antimycin A) or artificially synthesized (HA14-1, ABT 263, BI-21C6), and it is very likely that a number of new BH3 mimetics will appear (Tzung et al., 2001; Chmura et al., 2000; Oltersdorf et al., 2005; Rega et al., 2007; Trudel et al., 2007; Tse et al., 2008; Azmi and Mohammad, 2009; Voss et al., 2010; Lian et al., 2011).

Recently, we have demonstrated that Hypericin (Hyp) has the potential to be used as a BH3 mimetic. Hyp is a naturally

occurring compound in plants of the genus *Hypericum* and some endophytic fungi, such as the *Dermocybe* (Agostinis et al., 2002; Dewick, 2002; Miskovsky, 2002). It is a photosensitive phenanthroperylenequinone with the high quantum yield of singlet oxygen (Agostinis et al., 2002; Miskovsky, 2002). Hyp and its derivatives were the subjects of investigations for a long time due to their antitumor, antiviral and antidepressant properties (Miskovsky, 2002; Theodossiou et al., 2009; Berlanda et al., 2010; Karioti and Bilia, 2010; Kepp et al., 2014). The Hyp phototoxic effects have been extensively explored in normal and malignant mammalian cell lines, bacteria, and viruses (Theodossiou et al., 2009; Karioti and Bilia, 2010; de Andrade et al., 2021). There are extensive reviews published regarding Hyp subcellular localization and its potential cellular targets based on the cell death mechanisms triggered by the Hyp photodynamic action (Agostinis et al., 2002; Kiesslich et al., 2006; de Andrade et al., 2021). Currently, Hyp is used as a photosensitizer in photodynamic therapy (PDT) of tumors, inflammatory diseases, and infections (Miskovsky, 2002; Karioti and Bilia, 2010; de Andrade et al., 2021). Due to its hydrophobic properties, Hyp freely crosses the cell membrane and accumulates mainly in membranous organelles such as ER, mitochondria, Golgi apparatus and lysosomes (Rizzuto et al., 1998; Annis et al., 2001; Gajkowska et al., 2001; de Brito and Scorrano, 2010; Balogova et al., 2013). It has been claimed that Hyp and its derivatives are compounds with a minimal cytotoxicity prior to illumination (Miskovsky, 2002; Theodossiou et al., 2009). However, there is growing evidence to contrary, including our recent work (Martinez-Poveda et al., 2005; Gyenge et al., 2013; Larisch et al., 2013; Larisch et al., 2014; Huntosova et al., 2017; Stroffekova et al., 2019). It has been shown that Hyp can accumulate in normal and tumor mammalian cells at a similar level and can display light-independent cytotoxicity in a wide range of concentrations (Blank et al., 2004; Mandel et al., 2007). Hyp also exhibited significant antiproliferative and anti-metastatic light-independent effects (Uzdensky et al., 2003; Noell et al., 2011). In the neuronal tissue, Hyp preferentially accumulated in glial and connective tissues including glioma tumors, whereas it entered into neurons at much lower level (Uzdensky et al., 2003; Noell et al., 2011).

In our recent work, we have shown, that Hyp presence in human endothelial and glioma cells resulted in significant light-independent effects on ultrastructure, mitochondria function and metabolism, and Bcl2 proteins' distribution and synthesis (Huntosova et al., 2017). There are multiple molecular mechanisms that can explain Hyp light independent effects, for example, the reduction of intracellular pH, enzymes' inhibition in cytoplasm, mitochondria or endoplasmic reticulum (ER) (Sureau et al., 1996; Gyenge et al., 2013; Dzurova et al., 2014), or interaction between Hyp and intracellular proteins (Agostinis et al., 1995; Agostinis et al., 1996; Halder et al., 2005; Lakowicz, 2006). However, these mechanisms are not well understood in detail and require more investigation. Based on Hyp accumulation in

BH domain peptides sequence

wtBH3 **scBH3**
 VVHLTLRQAGD**DF**SRRYRRDFAE MSS VVHLTLRQAGD**AA**SRAYRRFAE MSS

wtBH1 **scBH1**
 RGRFATVVE**EL**FRDGVN**WR**IVAF RGRFATVVE**AA**FRAGV**AA**IVAF

Bcl-2 sequence

10	20	30	40	50
MAHAGRTG YD	NREIVM KY IH	Y KLSQR G YEW	DAGDVGAAPP	GAAPAPGIFS
60	70	80	90	100
SQPGHTPHPA	ASRDVPARTS	PLQTPAAPGA	AAGPALSPVP	PVVHLTLRQA
110	120	130	140	150
GDDFSRR YRR	DFAE SSQLH	LTFPTARG RF	ATVVEELFRD	GVN WR IVAF
160	170	180	190	200
FEFGGVMCVE	SVNREMSPLV	DNIAL WMTEY	LNRHLHT W IQ	DNGGW

Mcl-1 sequence

10	20	30	40	50
MFGLKRNAVI	GLNI Y CGGAG	LGAGSGGATR	PGGRLLATEK	EASARREIGG
60	70	80	90	100
GEAGAVIGGS	AGASPPSTLT	PDSRRVARPP	PIGAEPDVT	ATPARLLFFA
110	120	130	140	150
PTTRAAPLEE	MEAPAADAIM	SPEEELD G YE	PEPLGKRPV	LPILLELVGES
160	170	180	190	200
GNNTSTDGSL	PSTPPPAEEE	EDEL Y RQSL	IIS Y RLREQA	TGAKDTKPMG
210	220	230	240	250
RSRATSRKAL	ETLRRVGDGV	QRNHETAFQG	MLRKLDIKNE	DDVKSLSRV
260	270	280	290	300
IHFVSDGVTN	W GRIVTLISF	GAFVAKHLKT	INQESCIPL	AESITDVLVR
310	320	330	340	350
TKRD W LVKQR	G WDGFVEFFH	VEDLEGGIRN	VLLAFAGVAG	VGAGL Y VLIR

FIGURE 1

Amino acid sequences of Bcl2 BH1 and BH3 peptides, and Bcl2 and Mcl1 proteins.

membranous organelles such as ER and mitochondria that are also primary activity sites for members of Bcl2 family (Rizzuto et al., 1998; Annis et al., 2001; Gajkowska et al., 2001; de Brito and Scorrano, 2010; Balogova et al., 2013) and our previous findings regarding Hyp effects on Bcl-2 protein distribution (Huntosova et al., 2017; Stroffekova et al., 2019), we explored the Bcl-2-Hyp interactions as one possible mechanism to explain Hyp light independent effects.

To summarize the above mentioned facts and findings, Hyp displayed effects at several sub-cellular levels. Hyp, like other known BH3 mimetics, played a key role in triggering apoptosis, caused changes in cellular ultrastructure, mitochondria function and metabolism, and in changed the distribution of Bcl-2 proteins in malignant and non-malignant cells (Huntosova et al., 2017). In addition, we have demonstrated that one of the mechanisms underlying these light independent effects can be a direct interaction between Hyp and Bcl-2 protein (Stroffekova et al., 2019).

In the present study, we tried to explore this interaction further. We have compare interaction of two BH3 mimetics, Gossypol (Goss) and ABT263, with the Bcl-2 protein BH1 and BH3 peptides and the whole purified Bcl-2 and Mcl-1 proteins to the Hyp interaction with

these peptides and proteins. In addition, we explored the effects of these compounds on the viability of human glioma U87 MG cells and on the expression levels of Bcl-2 and Mcl-1 proteins. We have found that Hyp interacts more strongly with Bcl-2 and less with Mcl-1 protein than ABT263 or Goss. Incubation of U87 MG cells with Hyp and Goss downregulated Bcl-2 and upregulated Mcl-1 proteins. Hyp and ABT263 affected U87 MG viability insufficiently, where Goss decreased viability up to 20% in time and concentration manner. This suggests, that Hyp is interacting preferably with Bcl-2 protein similarly to ABT263, and Mcl-1 upregulation rescues viability of U87 MG cells. Further, we explored the use of Hyp and Goss combination treatment. In this treatment, we were able to reduce Goss concentration to reach a significant decrease in U87 MG viability. This finding indicates that Hyp can be explored in the drug combination therapy, however, more detailed study regarding this fact is required.

Materials and methods

Chemicals and reagents

An immortal cell line culture of malignant U87 MG human glioma cells was purchased from Cell Lines Services (CLS, Germany). Dulbecco's modified Eagle medium (D-MEM) with high glucose (4,500 mgL⁻¹) was obtained from ThermoFisher (Slovakia) and FBS was purchased from Sigma Aldrich (Slovakia). Hyp was purchased from Gibco-Invitrogen (France). 3-(4,5-Dimethyl-2-thiazolyl)-2,5-diphenyl-2H-tetrazolium bromide (MTT reagent), phosphate-buffered saline solution (PBS) and Dimethyl sulfoxide (DMSO) were obtained from Sigma Aldrich (Slovakia). ABT263, Gossypol, and purified whole Bcl2 and Mcl1 proteins were purchased from Abcam (Slovakia). Bcl2 BH1 and BH3 peptides were custom made by GeneCust (France) in HPLC purity (≥80%). Sodium chloride NaCl, Triton X-100, sodium deoxycholate, sodium dodecyl sulfate SDS, Tris, and Laemmli buffer were purchased from Sigma-Aldrich (Slovakia). Halt™ Protease and Phosphatase Inhibitor Cocktail was obtained from ThermoFisher Scientific (Slovakia).

Cell culture protocol - U87 MG cells were plated and maintained according to propagation protocols onto 35 mm Petri culture dishes (SPL, Switzerland). The cells grew in the dark as monolayer up to 80% confluence, at 37°C in a humidified 5% CO₂ atmosphere. After reaching confluence, cells were incubated with either Hyp or Goss or their combination, and then processed in the MTT assay, or used for whole cell lysates in Western blot analysis.

Hypericin and gossypol protocol

Hyp and Goss stock solutions were in dimethyl sulfoxide (DMSO) at concentration of 5 and 20 x10⁻³ M, respectively. Hyp and Goss were further diluted to final concentrations of 1, 5, 10,

15 and 30 μM in the cell culture medium. For all experiments, the final content of DMSO was less than 0.1%. Cells were incubated with either Hyp or Goss or their combination for 24 or 48 h in the dark in the presence of 5% CO_2 humidified atmosphere at 37°C.

MTT cell viability assay

U87 MG cells (2×10^3 cells per well) were plated in 96-well plates. Appropriate culture medium was added to the each well, and cells were incubated at 37°C for the indicated times. MTT stock solution was at concentration 5 mg/ml in PBS. MTT was first diluted in fresh serum free medium (1:10) and then added into each well to a final volume of 100 μL . Yellowish MTT solution is converted to dark blue water-insoluble crystals of MTT formazan by mitochondrial dehydrogenases in live cells. Cells were then incubated for 2 h in the dark (5% CO_2 , 37°C). Medium was then aspirated and formazan crystals were dissolved in 100 μL DMSO per well. The absorbance of soluble formazan was measured with a microplate reader (GloMax, Promega) at 590 nm. Cell viability was displayed as the percentage of treated cells relative to the control ones. The EC50 values have been calculated by online tool Quest Graph™ EC50 Calculator (AAT Bioquest. <https://www.aatbio.com/tools/ec50-calculator>).

Fluorescence spectra measurements

Fluorescence spectra measurements were performed by a spectrofluorometer with 150W Xenon lamp (RF-5301 PC, Shimadzu, Japan). Samples were placed in a fluorimeter in the cuvette with volume 0.7 ml (Hellma 104.002-QS, Germany) and path length 10 mm. All spectra were recorded at room temperature, and in the range of wavelengths from 290 to 400 nm. Measurements were carried out in either DMSO or phosphate buffered saline solution (PBS) (pH 7.4) (Sigma Aldrich, Slovakia). Excitation wavelengths were 275 and 280 nm, respectively, which corresponded to the presence of tyrosine (Y) and tryptophan (W) residues in BH domain peptides and Bcl2 and Mcl1 proteins (Figure 1). Bcl2 protein BH1 (26 AA) and BH3 (24 AA) domain peptides were designed and described in detail previously (Stroffekova et al., 2019). In peptides with scrambled sequence, AAs important for ligand interaction were substituted with alanines (A). Peptide stocks were prepared at 2 mM concentration in DMSO. Hyp, Goss and ABT263 stock solutions were also prepared in DMSO at 100 μM and 1 mM concentration. Final concentration of BH1 and BH3 peptides used in experiments was 1 μM in each sample.

The fluorimeter setting includes excitation wavelengths, interval, speed of measurements, excitation and emission bandwidths. The excitation wavelength for BH1-sc and BH1-wt was 280nm, for BH3-sc and BH3-wt was 275 nm. For the BH1 peptides measurements, excitation and emission

bandwidths were 3 nm. In measurements with the BH3 peptides, excitation and emission bandwidths were 5 and 10 nm. In all measurements we have used 1 nm intervals and medium speed setting.

The final concentration of Bcl-2 and Mcl-1 protein used in measurements was 1 μM . Measurements were carried out in phosphate-buffered saline solution (PBS), pH7.4. The Bcl2 and Mcl1 proteins were tested in both excitation wavelengths at 280 and 275 nm that are inherent for tryptophan (W) and tyrosine (Y) fluorescence, respectively. The Bcl-2 protein displayed a stronger signal due to higher number of W in comparison with Mcl-1. Due to this fact, we have used 3 and 5 nm excitation and emission bandwidth for Bcl-2, and higher values of 5 and 5 nm for Mcl1. The Hyp, Goss, and ABT263 were added directly to a cuvette in increasing concentration ratio with proteins 1:1, 1:5, 1:10, 1:20, 1:30 μM . Fluorescence signals were analyzed by Origin software (OriginLab, United States).

From the measured peptide/protein fluorescence spectra, we have derived the Stern-Volmer plots of F_0/F versus $[Q]$, where $[Q]$ is the ligand concentration (Berlanda et al., 2010). The Stern-Volmer quenching constants K_d and the correlation coefficient of each curve were calculated from the slope of the regression curves using Eq (1).

$$\frac{F_0}{F} = 1 + K_{sv} [Q] = 1 + K_d [Q] = 1 + k_q \tau_0 [Q] \quad (1)$$

In this equation, K_{sv} is the Stern-Volmer quenching constant, k_q is the bimolecular quenching constant, τ_0 is the lifetime of the fluorophore in the absence of quencher, and $[Q]$ is the quencher concentration.

Western blot (WB)

Confluent adherent U87 MG cells were washed 2X with ice-cold PBS. Subsequently, cells were lysed and homogenized in radioimmunoprecipitation (RIPA) buffer (150 mM sodium chloride, 1% Triton X-100, 0.5% sodium deoxycholate, 0.1% sodium dodecyl sulfate, 50 mM Tris, pH 8) with the inhibitor cocktail (1:100 dilutions, Halt™ Protease and Phosphatase Inhibitor Cocktail, respectively). The total protein content in the whole cell lysates was determined by the BCA protein assay (Pierce Chemical Co., Rockford, IL). For WB analysis, 20 μg of total protein per well was loaded onto 10% or 15% polyacrylamide gels and subjected to electrophoresis. The separated proteins were transferred to a nitrocellulose membrane (0.45 μm ; Amersham Protran, Germany). Membranes were rinsed 3X with Tris-buffered saline with 0.1% Tween 20 (TBST) and then incubated with a blocking buffer. Mcl1, GAPDH and Bcl2 proteins in the membranes were blocked with 1% BSA and 1% dry nonfat milk in PBS, respectively, for 1 h at room temperature. After 3X wash with TBST, membranes were incubated overnight at 4°C with primary antibodies: anti-Bcl2

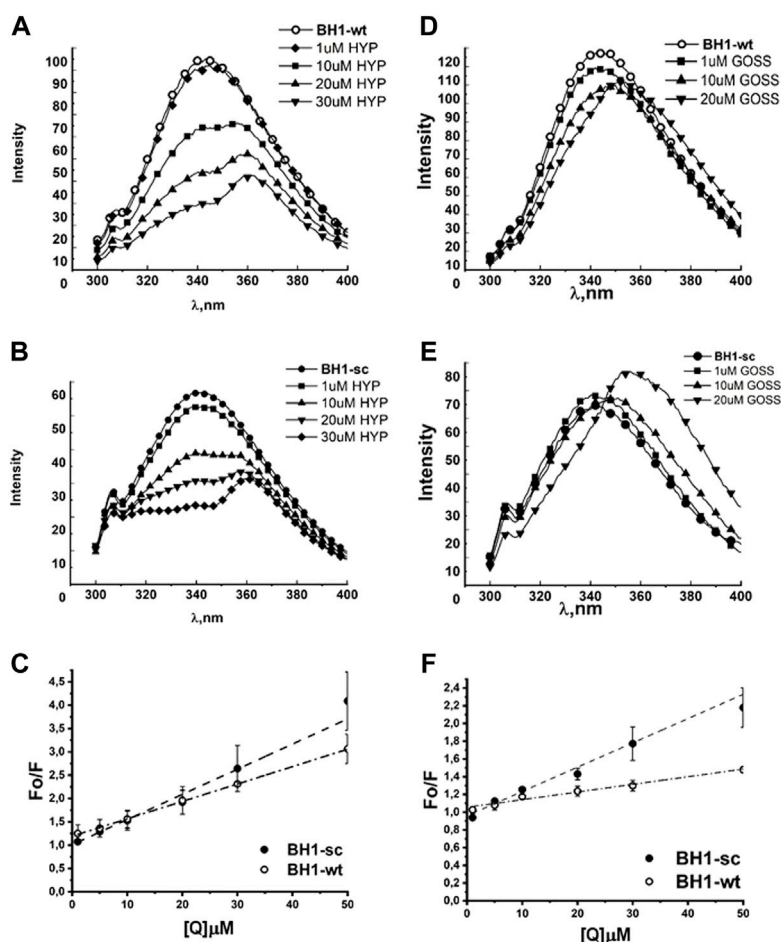


FIGURE 2

Hyp displays stronger quenching of BH1 peptides fluorescence spectra than Goss. The BH1-sc and BH1-wt fluorescence quenching spectra with different concentration of Hyp (A,B) and Goss (D,E). (C) The linear fit of Stern-Volmer curves for BH1-sc and BH1-wt corresponding to quenching spectra in (A,B). (F) The linear fit of Stern-Volmer curves for BH1-sc and BH1-wt corresponding to quenching spectra in (D,E). All of the measurements were done in three independent measurements according to protocols described in Methods section.

(1:100 dilution, ab196495, Abcam, Cambridge, UK), anti-Mcl1 (1:200, ab32087, Abcam, Cambridge, UK), and anti-GAPDH (1:2,500, ab9485, Abcam, Cambridge, UK) was used as loading control. Membranes were rinsed 3X with TBST and antibody bound proteins were detected and visualized using the Western Breeze Chromogenic Kit (ThermoFisher Scientific, Waltham, MA, United States). The protein band optical densities (O.D.) were analyzed by ImageJ software. After normalization to GAPDH, the O.D. are presented in the histograms that represent the means of 3 measurements. The error bars represent the standard deviations.

Statistical analysis

Experiments were repeated in at least three independent repetitions for all conditions. Statistical analysis was carried

out by either Student's *t*-test or ANOVA using SigmaPlot (Ver. 12.0; SystatSoftw. Inc.). A *p* < 0.05 was considered significant.

Results

Bcl2 BH peptides' fluorescence spectra measurements

Previous research from our laboratory has shown that our designed and custom made peptides (Figure 1), corresponding to BH1 and BH3 domains of Bcl2 protein, interact with Hyp and known BH3 mimetic ABT263 (Stroffekova et al., 2019). Both, BH1 and BH3 peptides contain one endogenous fluorescent amino acid, tryptophan (W18) and tyrosine (Y17), respectively.

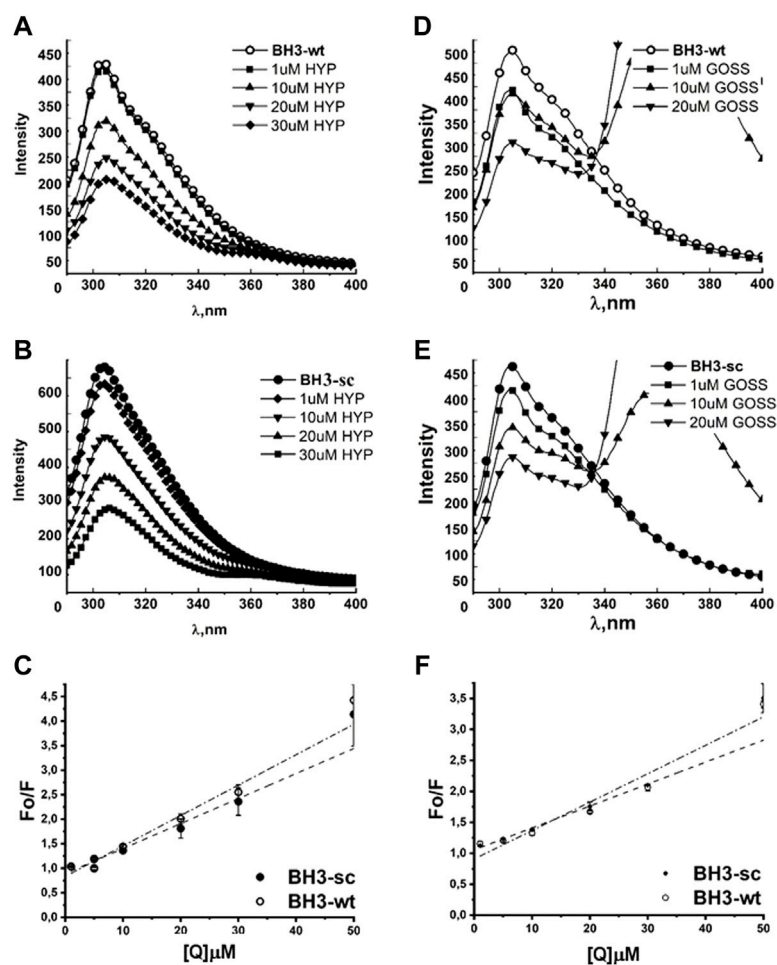


FIGURE 3

Hyp displays stronger quenching of BH3 peptides fluorescence spectra than Goss. The Fluorescence quenching spectra of BH3-sc and BH3-wt with different concentration of Hyp (A,B) and Goss (D,E). (C) The linear fit of Stern-Volmer curves for BH3-sc and BH3-wt corresponding to quenching spectra in (A,B). (F) The linear fit of Stern-Volmer curves for BH3-sc and BH3-wt corresponding to quenching spectra in (D,E). All of the measurements were done in three independent measurements according to protocols described in Methods section.

Here, we show and compare the BH1 and BH3 peptides interactions with Hyp and another plant based BH3 mimetic, gossypol (Goss). We have studied changes in the fluorescence spectra of Figure 2) and BH3 peptides (Figure 3) with respect to the different concentrations of Hyp and Goss in DMSO. The BH1-wt and BH1-sc spectra in the absence of ligands display maximum intensity at 342 and 343 nm, respectively. These values correspond to a typical W maximum intensity in nonpolar environment.

Figure 2 shows the fluorescence emission spectra of BH1-wt and BH1-sc peptides in nonpolar solvent DMSO. Peptides were dissolved in DMSO at the final concentration of 1 μ M. The BH1-wt and BH1-sc spectra were recorded within 300–400 nm range with 280 nm excitation wavelength. We observed increased W fluorescence quenching with increasing Hyp concentrations in both fluorescence spectra of BH1-wt and BH1-sc peptides

(Figure 2A–C). At the high Hyp concentrations of 20 and 30 μ M, we observed red shift of the fluorescence maximum from 342 to 362 nm. In the presence of Goss, we observed W fluorescence quenching with increasing Goss concentrations in both fluorescence spectra of BH1-wt and BH1-sc peptides (Figure 2D, E). However, the level of quenching by Goss was clearly less pronounced than quenching by Hyp.

From the measured peptide fluorescence spectra, we have derived the Stern–Volmer curves of F_0/F versus $[Q]$, as shown in peptides (Figure 2C, F), where $[Q]$ is the Hyp and Goss concentration, respectively. The Stern–Volmer quenching constants K_d (Table 1) and the correlation coefficient of each curve were calculated from the slope of the regression curves using Eq (1) in Methods.

The correlation coefficients in the presence of Hyp and Goss were $R = 0.99$ and 0.98 for BH1-wt and BH1-sc, respectively. A

TABLE 1 Stern-Volmer constants for BH1 and BH3 peptides interactions with Hyp or Goss.

 $K_d \times 10^{12} \text{ LM}^{-1}\text{s}^{-1}$

Peptide	Hyp	Goss
BH1-wt	0.5447 ± 0.0000342	2.738 ± 0.00298
BH1-sc	0.405 ± 0.0000974	0.86 ± 0.000889
BH3-wt	0.493 ± 0.000409	3.546 ± 0.00258
BH3-sc	0.417 ± 0.000339	4.588 ± 0.00513

typical fluorescence life time (τ_0) of small biopolymers without the quencher is usually around 10^{-8} s (Theodossiou et al., 2009; Karioti and Bilia, 2010). Using this value, we calculated Hyp quenching constants for our peptides at values 5.4 and $4.05 \times 10^{11} \text{ LM}^{-1}\text{s}^{-1}$ for BH1-wt and BH1-sc, respectively. Further, we calculated Goss quenching constants for BH1 peptides at values 2.738 and $0.86 \times 10^{12} \text{ LM}^{-1}\text{s}^{-1}$ for BH1-wt and BH1-sc, respectively.

Next, we tested BH3-sc and BH3-wt peptides interactions with either Hyp or Goss (Figure 3). In the absence of ligands, the BH3-wt and BH3-sc spectra display maximum intensity at 304 and 308 nm, respectively. These values correspond well with a typical tyrosine (Y) maximum intensity in nonpolar environment (Berlanda et al., 2010). In both BH3 peptides spectra, we observed a decrease in fluorescence intensity with increasing concentration of either Hyp (Figure 3A–C) or Gossypol (Figure 3D–F), which indicates interactions between peptides and used ligands. In the presence of Goss high concentration of $10\text{--}20 \mu\text{M}$, we observed decreased tyrosine fluorescence and another fluorescence peak at maximum of 370nm, which is due to Goss itself (Supplementary Figure S1).

We have fitted the Stern-Volmer curves of measured spectra (Figure 3C, F). The Stern-Volmer quenching constants K_d derived from linear fits of BH3-wt and BH3-sc peptides with either Hyp or Goss are in Table 1. The correlation coefficients for Hyp interaction with peptides were $R = 0.966$ and 0.968 for BH3-wt and BH3-sc, respectively. The correlation coefficients for Goss interaction with peptides were $R = 0.97$ and 0.98 for BH3-wt and BH3-sc, respectively. Further we calculated quenching constants for Hyp and Goss. Hyp quenching constants were determined at values 4.93 and $4.17 \times 10^{11} \text{ LM}^{-1}\text{s}^{-1}$ for BH3-wt and BH3-sc, respectively. Goss quenching constants were determined at values 3.54 and $4.59 \times 10^{12} \text{ LM}^{-1}\text{s}^{-1}$ for BH3-wt and BH3-sc, respectively.

Next, we have compared our results from fluorescence emission spectra of BH1 and BH3 peptides with the predicted strength of interaction from our *in silico* experiments (Stroffekova et al., 2019). The predicted strength of interactions based on QPLD docking (Stroffekova et al., 2019) and results from fluorescence emission spectra of BH1 and

TABLE 2 Comparison of predicted and measured strength of interaction between BH peptides and selected BH3 mimetics.

Peptid	Predicted strength of interaction	Measured strength of interaction by fluorescence quenching
wBH1	Goss > Hyp > ABT-263	Hyp > ABT-263 > Goss
scBH1	Goss ~ ABT-263 > Hyp	ABT-263 > Hyp > Goss
wBH3	Goss > Hyp ~ ABT-263	ABT-263 > Hyp > Goss
scBH3	Goss > ABT-263 > Hyp	ABT-263 > Hyp > Goss

BH3 peptides obtained here and in (Stroffekova et al., 2019) are in Table 2.

Bcl2 and Mcl1 proteins' fluorescence spectra measurements

In the next step, we have investigated interaction of known BH3 mimetics, Goss and ABT263, and Hyp in more physiologically relevant situation. We studied the interaction of these compounds with whole purified Bcl2 and Mcl1 proteins in the phosphate buffered saline (PBS) solution at pH 7.4. Figure 1 shows amino acid sequences of used BH peptides as well as Bcl2 and Mcl1 proteins, which we used in our experiments. Both, BH1 and BH3 peptides contain only one fluorescent amino acid, tryptophan (W) and tyrosine (Y), respectively. In contrast, whole proteins contain several fluorescent amino acid residues. Bcl2 protein contains six Y and five W residues, where Mcl1 protein has five Y and only three W residues. Therefore, we had measured fluorescence spectra of both proteins with excitation wavelength 275 and 280 nm. This gave us opportunity to see whether the changes in the spectra depends more on the emission from W or Y.

Figure 4 shows the fluorescence quenching spectra of Bcl2 and Mcl1 proteins at $1 \mu\text{M}$ concentration with different concentration of selected BH3 mimetics Hyp, Goss and ABT-263. Bcl2 protein spectra measured with excitation wavelength either 275 or 280 nm displayed spectra with maximum at $318 \pm 2 \text{ nm}$ corresponding to combination of signals originated in Y and W residues, respectively. Here, we show data measured with 280 nm excitation (Figure 4A–C). In Bcl2 protein spectra, we have observed fluorescence signal quenching with increasing compound concentrations, with the strongest quenching by Hyp.

The Mcl1 protein spectra measured with excitation wavelength either 275 or 280 nm displayed spectra with two distinctive peaks at 308 ± 2 and $323 \pm 2 \text{ nm}$ corresponding to signals originated in Y and W residues, respectively. Here, we show data measured with 275 nm excitation (Figure 4D–F), where the distinction of two peaks was more pronounced. In

Mcl1 protein spectra, we have observed fluorescence signal quenching with increasing compound concentrations, with the strongest quenching by Goss. Further, we have also fitted the Stern-Volmer curves of measured spectra (Figure 5). The Stern-Volmer quenching constants K_d derived from linear fits of Bcl2 and Mcl1 with ligands are in Table 3. The correlation coefficient for compound interaction with Bcl2 protein was 0.98 for all ligands. The correlation coefficient for compound interaction with Mcl-1 protein was 0.98 for Hyp and ABT-263, and 0.97 for Goss.

Next, we have compared the predicted strength of interaction between Bcl2 or Mcl1 and selected BH3 mimetics based on the QPLD docking (Stroffekova et al., 2019) with the results from the fluorescence quenching measurements. The measured strength of interaction differs from the predicted order.

The Hyp and Goss cytotoxicity in U87 MG cells

To analyze whether inhibition of anti-apoptotic Bcl-2 proteins is sufficient to induce glioma cell death, we used two different BH3 mimetics, Hyp and Goss, in this study. Based on our fluorescent quenching measurements with the BH peptides and whole Bcl2 and Mcl1 proteins, we concluded that Hyp and Goss interact with these proteins.

To test these interactions further, we have tested cell viability in the presence of Hyp and Goss in human U87 MG glioma cell line by MTT assay. We have used Hyp and Goss in concentration 1, 5, 10, 15, 30 μ M. U87 MG cell viability after 24 and 48h incubation of cells with either Hyp or Goss is shown in Figure 6. In all used concentrations, Hyp after 24h slightly decreased cell viability by 5–7% at 1–10 μ M Hyp (Figure 6A). However, this decrease is not sufficient to render the compound cytotoxic. After 48h treatment, there was no significant effect on cell viability except for 10 μ M concentration of Hyp, where we detected decrease in viable cells to 78% (Figure 6A, $p < 0.021$). Incubation of U87 MG cells with Goss for 24h resulted in the similar effect on viability as with Hyp (Figure 6B). Goss after 24h slightly decreased cell viability by 6–10% at 1–10 μ M Goss. In contrast, after 48h Goss caused significant decrease ($p < 0.0001$) in cell viability below 20% at concentration above 10 μ M (Figure 6B). The EC50 for Goss (48h) has been determined at 8.45 μ M. Consequently, Goss exhibited stronger effect on U87 MG cell viability than Hyp.

To explore this further, we have also investigated Mcl1 and Bcl2 protein level of expression in U87 MG cells after 24 and 48h incubation with either Hyp or Goss (Figure 6C, D). Hyp and Goss caused downregulation of Bcl2 and upregulation of Mcl1 protein in time and concentration dependent manner, where 10 μ M Hyp (48h) caused the 1.7fold increase of Mcl1.

In the next step, we did pilot experiments regarding the possibility of Goss and Hyp combined effect. We used the subthreshold Goss concentration of 5 μ M and used two Hyp concentrations 0.5 and 10 μ M (Figure 7). In comparison with the 10 μ M Hyp alone, presence of 5 μ M Goss significantly decreased cell viability to 55%. In addition, even low 0.5 μ M concentration of Hyp in combination 5 μ M Goss resulted in the significant decrease in cell viability to 53%, where 5 μ M Goss alone did not. These results indicate a possible synergy between two compounds.

Discussion

In various examples of human cancer lines such as prostate cancer, myeloid leukemia, breast cancer, glioblastoma etc., it has been demonstrated that they have heightened expression of multiple anti-apoptotic Bcl-2 proteins (Bcl-2, Bcl-XL and Mcl-1) and have displayed strong chemo resistance (Wei et al., 2011; Sadahira et al., 2014; Vogler, 2014; Correia et al., 2015; Gong et al., 2016; Frame et al., 2020). It has been also demonstrated that inhibition of only one anti-apoptotic member in these cells is not sufficient to trigger apoptosis. The various Bcl-2/Bcl-XL inhibitors, including ABT263, upregulated Mcl1 in malignant cells and rendered them resistant to these compounds (Wei et al., 2011; Zhao et al., 2013; Wang et al., 2014; Lee et al., 2018). The upregulated Mcl1 can also inhibit autophagy, which could augment apoptosis in cancer cells (Maiuri et al., 2007; Voss et al., 2010). Therefore, it is of interest to explore new possible BH3 mimetics and to test them in the combination with known Bcl-2 proteins inhibitors or other cancer treatments to achieve possible synergy.

In this work, we have investigated further the interaction of Hyp, a naturally occurring compound, with anti-apoptotic Bcl-2 family members Bcl-2 and Mcl-1. As shown earlier, Hyp interacted with BH1 and BH3 peptides of Bcl-2 protein similar to known Bcl-2 inhibitor ABT263, and our QPLD docking data indicated that Hyp could interact with Bcl-2 and Mcl-1 similar to pan-Bcl-2 BH3 mimetic, Goss (Stroffekova et al., 2019).

First, we investigated interactions of BH domain peptides from Bcl-2 protein, BH1 and BH3, with Hyp and Goss. BH1 and BH3 domain are part of a hydrophobic pocket in Bcl-2 proteins, which play an important role in the interaction between anti- and pro-apoptotic Bcl-2 proteins. These domains are also part of the interacting site for BH3 mimetics (Wang et al., 2000b; Wang et al., 2006). We have studied changes in the fluorescence spectra of BH1 (Figure 2) and BH3 peptides (Figure 3) with respect to the different concentrations of Hyp and Goss in DMSO. We observed increased W fluorescence quenching with increasing Hyp and Goss concentrations in both fluorescence spectra of BH1-wt and BH1-sc peptides (Figure 2). These findings are in good agreement with our previous results (Stroffekova et al.,

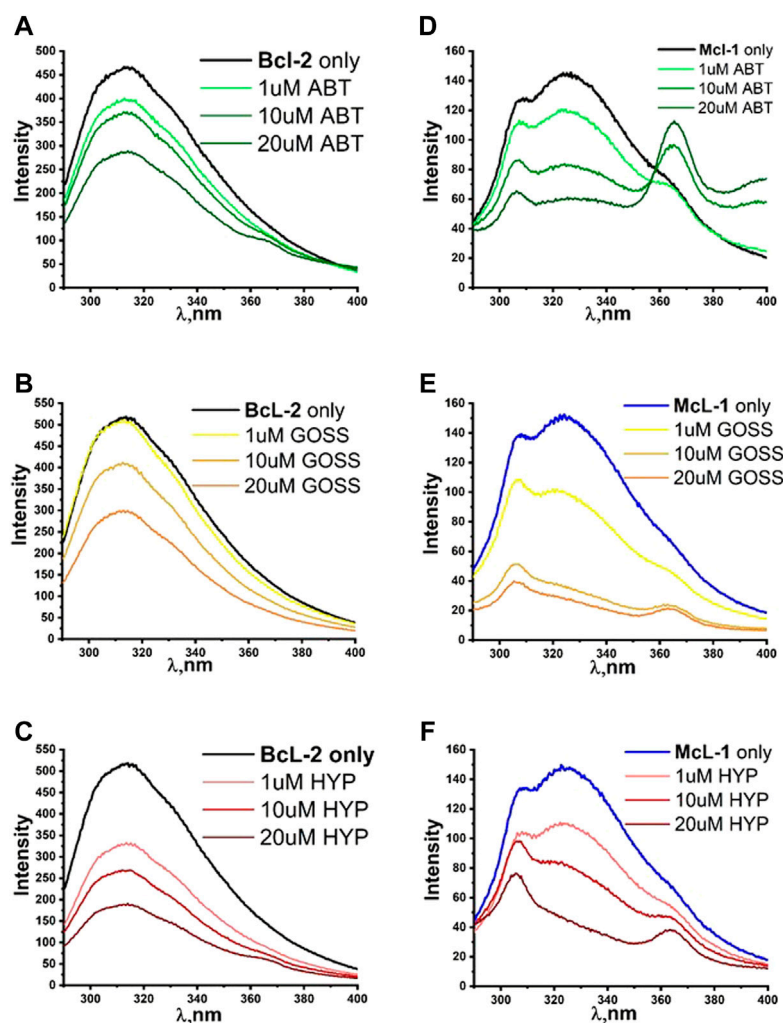


FIGURE 4

The fluorescence quenching spectra of Bcl2 and Mcl1. The fluorescence quenching spectra of Bcl2 (A–C) and Mcl1 (D–F) proteins (1 μ M) with different concentration of ABT263, Goss and Hyp in PBS. Bcl2 spectra were measured with excitation wavelength of 280 nm and Mcl1 spectra with excitation wavelength of 275 nm.

2019), and further confirm Hyp interaction with the BH1 peptides. We have observed that the level of quenching by Goss was clearly less pronounced than quenching by Hyp, indicating that Hyp interaction with BH1 peptides is stronger. At the high Hyp concentrations of 20 and 30 μ M, we have noticed a red shift of the maximum fluorescence peak to 362 nm. The red shift in spectra may be observed due to several reasons such as change in hydrogen bonds, dipole moment or change of solvent (Kepp et al., 2014). In our case, where we increased Hyp concentration, the reason for the red shift may be caused by increased hydrogen bonds between Hyp and peptide.

The BH3-wt and BH3-sc peptide fluorescent spectra (Figure 3) display maximum intensity at 304 and 308 nm, respectively, which correspond well with a typical Y maximum intensity in nonpolar environment. Similar to

observation with BH1 peptides, we have noticed a fluorescence quenching with increasing concentration of either Hyp or Goss, which indicates interactions between peptides and used ligands. In the presence of Goss high concentration of 10–20 μ M, we observed decreased tyrosine fluorescence and another fluorescence peak at maximum of 370 nm, which is due to Goss itself (Supplementary Figure S1). The Stern-Volmer quenching constants K_d (Table 1) derived from the BH1 and BH3 peptides fluorescent spectra for Hyp and Goss are at values larger than the limiting diffusion rate constant of the biomolecule ($\sim 10^{10}$ $\text{LM}^{-1}\text{s}^{-1}$), and therefore they indicate the static quenching and some type of binding interaction (Shea et al., 1997; Lakowicz, 2006; Muino and Callis, 2009).

The findings from the BH1 and BH3 peptides helped us to determine the best concentration range of Hyp, ABT263 and Goss

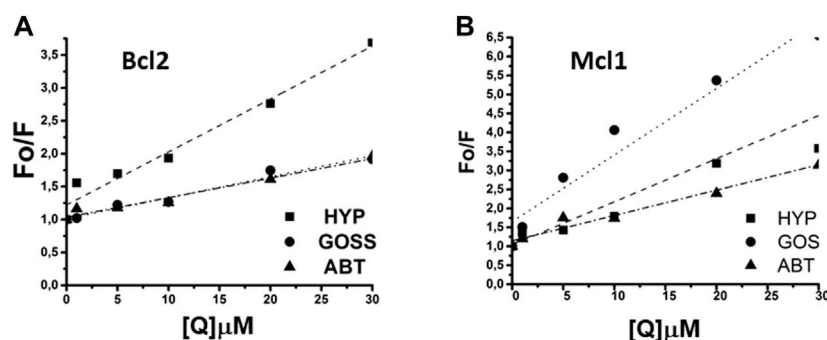


FIGURE 5

The linear fit of Stern-Volmer curves for Bcl2 and Mcl1 proteins. (A) The linear fit for Bcl2 and (B) for Mcl1 protein interaction with Hyp, Gossypol, and ABT263.

TABLE 3 The Stern-Volmer constants for Bcl2 and Mcl1 proteins with Hyp, Gossypol, and ABT263.

$K_d \times 10^{14} \text{ LM}^{-1}\text{s}^{-1}$

Protein	Hyp	Goss	ABT263
Bcl2 (280nm)	0.08048±0.007	0.03191±0.00264	0.02971±0.00258
Mcl1 (275nm)	0.08825±0.00888	0.17994±0.00206	0.06566±0.00622

for investigating their interaction with Bcl-2 and Mcl-1 proteins. Figure 4 shows the fluorescence quenching spectra of Bcl-2 and Mcl-1 protein (1 μM) with different concentration of selected BH3 mimetics, Hyp, Goss and ABT-263. In Bcl-2 spectra, we have observed fluorescence signal quenching with increasing compound concentrations of all compounds, with the strongest quenching by Hyp. The decrease in fluorescence intensity with increasing concentration of compounds strongly indicates interactions between Bcl-2 protein and used ligands. In the case of Bcl-2 protein, Hyp seemed to have the strongest effect, followed by Goss and ABT-263, which seem to have similar strength of interactions. In Mcl-1 spectra, we have observed fluorescence signal quenching with increasing compound concentrations, with the strongest quenching by Goss. In spectra measured with ABT-263, we have observed additional peak of $364 \pm 2 \text{ nm}$ at high ABT263 concentrations, which corresponds to ABT-263 fluorescence (Supplementary Figure S1). The decrease in fluorescence intensity with increasing concentration of compounds strongly indicates interactions between Mcl-1 protein and used ligands. In case of Mcl-1 protein, Goss seemed to have the strongest effect, followed by Hyp and then ABT263.

We have compared obtained results from the fluorescence quenching measurements with the predicted strength of interaction between Bcl-2 or Mcl-1 and selected BH3 mimetics based on the QPLD docking (Stroffekova et al.,

2019). It is clear that predicted values differ from the measurements. The differences may be rooted in the polarity of the environment and differences in the protein structure used in the QPLD docking and actual protein structure in PBS.

In the next step, we tested the response of human U87 MG glioma cells to the treatment by Hyp and Goss alone, and their combination. Hyp did not substantially affected cell viability either at 24 or 48h incubation (Figure 6). This finding is in good agreement with our previously published results (Huntosova et al., 2017), and it suggests that Hyp did not inhibit all of the anti-apoptotic Bcl-2 proteins in U87 MG cells. This is similar to our findings that U87 MG cells show a significant resistance to ABT263 (Stroffekova et al., 2019). In contrast, Goss, known panBcl-2 inhibitor (Kiesslich et al., 2006), caused significant effect ($p < 0.0001$) after 48h on cell viability at concentration of 10 μM and higher. The cell viability decreased below 10% (Figure 6). These findings are in good agreement with published information regarding the Goss cytotoxicity (Shea et al., 1997; Sadahira et al., 2014). The difference between U87 MG sensitivity towards Hyp, ABT263 and Goss may reside in upregulation of anti-apoptotic Mcl-1 (Zhao et al., 2013; Wang et al., 2014; Lee et al., 2018) and/or Bcl-XL proteins (Zhao et al., 2013; Wang et al., 2014; Kotschy et al., 2016; Caenepeel et al., 2018; Lee et al., 2018; Seiller et al., 2020). To elucidate the effects of Hyp and Goss further, we have looked at the Mcl-1 and Bcl-2 protein level of expression in U87 MG cell (Figure 6), and have found that Hyp and Goss downregulated Bcl-2 and upregulated Mcl-1 proteins. The upregulated Mcl-1 and different affinities of Hyp and Goss towards Mcl-1 may underlie different U87 MG sensitivity towards Hyp and Goss. In addition, differences may also be caused by off-target effects such as ER stress, increased oxidative stress and induction of autophagy, which were shown for many BH3 mimetics, including ABT737, gossypol, and obatoclax (Voss et al., 2010; Opydo-Chanek et al., 2017). The cytotoxicity of BH3 mimetics and their effects depend on the framework of expressed anti- and pro-apoptotic Bcl-2 proteins, and on off-target mechanisms involving activation of alternative cell

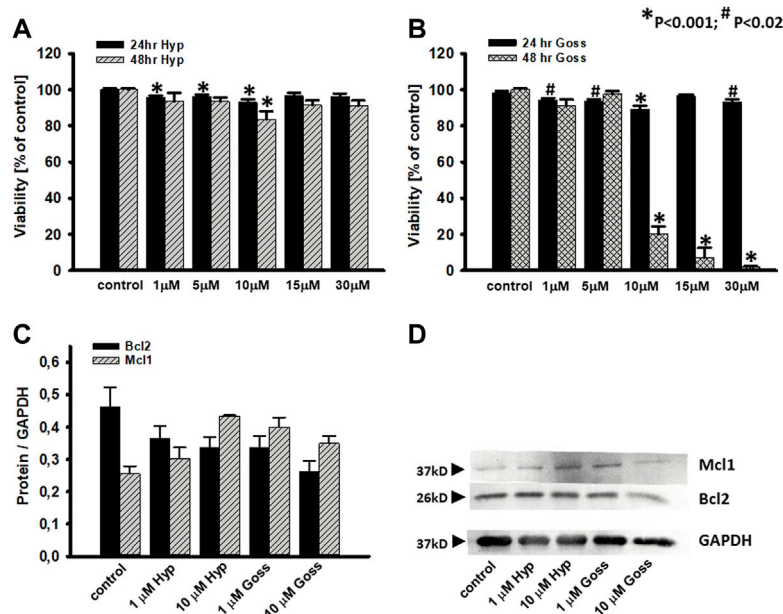


FIGURE 6

Effects of Hyp or Goss on U87 MG cells viability and Bcl2 and Mcl1 protein levels. (A) Cell viability in the presence of Hyp and (B) Goss for 24 and 48 h. (C) The optical density band histograms of Bcl2 and Mcl1 normalized against GAPDH after 48 h incubation with Hyp or Goss. The histograms represent average of three independent experiments and the error bars represent the standard deviations from the average values. All experiments were repeated in triplicates. (D) Expression of Mcl1 and Bcl2 proteins in U87 MG whole cell lysates after 48 h incubation with Hyp or Goss was examined by western blot analysis. GAPDH was used as a housing protein.

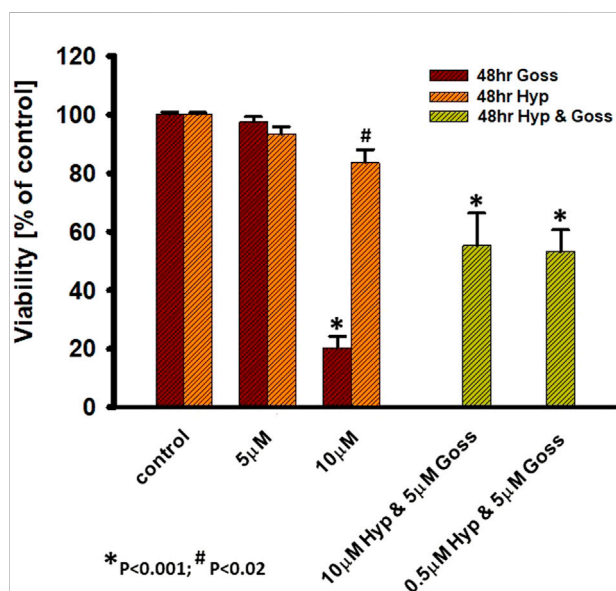


FIGURE 7

Hyp and Goss have synergetic effect on U87 MG cells viability. Cell viability in the presence of Hyp and Goss for 48 h.

death modes and modulation of multiple signaling pathways. There are still numerous questions regarding the pharmacological effects of BH3 mimetics that contribute to their cytotoxic activity (Vela and Marzo, 2015).

One of the possible strategies to overcome the cancer cell resistance towards Bcl-2 or Mcl-1 inhibitors is to use combination of both inhibitors (Seiller et al., 2020). We have tested combination treatment of Hyp and Goss on U87 MG cells. We have found that low 0.5 μ M concentration of Hyp in combination 5 μ M Goss resulted in a significant decrease in cell viability to 53% (Figure 7), suggesting that combination treatment is effective and enables to use low doses of compounds. Further, this pilot results suggest indicate a possible synergy between two compounds, however there have to be more detailed study of this phenomena and underlying mechanisms.

Conclusion

In this work, we have investigated interactions of BH domain peptides from Bcl-2 protein, BH1 and BH3, with Hyp and Goss. By fluorescence quenching method, we have shown that Hyp and

Goss interact with BH1 and BH3 peptides in concentration dependent manner. Hyp displayed stronger fluorescent quenching in both peptides than Goss indicating stronger Hyp interaction. Further, we have compared the interactions of known BH3 mimetics, Goss and ABT-263, with whole purified proteins, Bcl-2 and Mcl-1 to those of Hyp. Hyp also displayed the stronger fluorescent quenching in the interaction with the Bcl-2 protein than ABT263 and Goss. In the interactions with the Mcl-1 protein, Goss displayed the strongest effect, followed by Hyp and ABT-263. These findings suggested that Hyp interacts with Bcl-2 proteins in similar manner as the other BH3 mimetics. In human glioma U87 MG cell line, Hyp cytotoxicity was low, similar to that of ABT263, where Goss exerted sufficient cytotoxicity. This suggests that Hyp acts primarily on Bcl-2, but not on Mcl-1 protein. In addition, Hyp and Goss downregulated Bcl-2 and upregulated Mcl-1 proteins in U87 MG cells. In combination therapy, low doses of Hyp with Goss effectively decreased U87 MG viability, suggesting a possible synergy effect. Overall, we can conclude that Hyp as BH3 mimetic acts primarily on Bcl-2 protein. Thus, it can be used to treat malignancies depending on Bcl-2 over-expression, or in combination with other BH3 mimetics, that target Mcl-1 or Bcl-XL proteins, in dual targeting therapy.

Data availability statement

The original contributions presented in the study are included in the article/Supplementary Materials, further inquiries can be directed to the corresponding author.

Author contributions

Conception and design: KS and TK. Acquisition of data: AD, ST, KS, and TK. Analysis and interpretation of data: AD, ST, KS, and TK. Writing, review, and/or revision of manuscript: KS.

References

- Agostinis, P., Donella-Deana, A., Cuveele, J., Vandenbogaerde, A., Sarno, S., Merlevede, W., et al. (1996). A comparative analysis of the photosensitized inhibition of growth-factor regulated protein kinases by hypericin-derivatives. *Biochem. Biophys. Res. Commun.* 220, 613–617. doi:10.1006/bbrc.1996.0451
- Agostinis, P., Vandenbogaerde, A., Donella-Deana, A., Pinna, L.A., Lee, K.T., Goris, J., et al. (1995). Photosensitized inhibition of growth factor-regulated protein kinases by hypericin. *Biochem. Pharmacol.* 49, 1615–1622. doi:10.1016/0006-2952(95)00097-j
- Agostinis, P., Vantighem, A., Merlevede, W., and de Witte, P.A.M. (2002). Hypericin in cancer treatment: More light on the way. *Int. J. Biochem. Cell Biol.* 34 (3), 221–241. doi:10.1016/s1357-2725(01)00126-1
- Annis, M.G., Zamzami, N., Zhu, W., Penn, L.Z., Kroemer, G., Leber, B., et al. (2001). Endoplasmic reticulum localized Bcl-2 prevents apoptosis when redistribution of cytochrome c is a late event. *Oncogene* 20, 1939–1952. doi:10.1038/sj.onc.1204288
- Azmi, A.S., and Mohammad, R.M. (2009). Non-peptidic small molecule inhibitors against Bcl-2 for cancer therapy. *J. Cell. Physiol.* 218, 13–21. doi:10.1002/jcp.21567
- Balogova, L., Maslanakova, M., Dzurova, L., Miskovsky, P., and Stroffekova, K. (2013). Bcl-2 proapoptotic proteins distribution in U-87 MG glioma cells before and after hypericin photodynamic action. *Gen. Physiol. Biophys.* 32, 179–187. doi:10.4149/gpb_2013021
- Berlanda, J., Kiesslich, T., Engelhardt, V., Krammer, B., and Plaetzer, K. (2010). Comparative *in vitro* study on the characteristics of different photosensitizers employed in PDT. *J. Photochem. Photobiol. B* 100, 173–180. doi:10.1016/j.jphotobiol.2010.06.004
- Blank, M., Lavie, G., Mandel, M., Hazan, S., Orenstein, A., Meruelo, D., et al. (2004). Antimetastatic activity of the photodynamic agent hypericin in the dark. *Int. J. Cancer* 111, 596–603. doi:10.1002/ijc.20285

Funding

Present work was supported by the EU ERDF grant OPENMED (ITMS2014+: 313011V455), by the Slovak Grant Agency VEGA 1/0425/15, 1-0421-18 and 1/0557/20; and by the Slovak Research and Development Agency APVV-16-0158.

Acknowledgments

We would like to thank Matus Galis for technical assistance with the U87 MG viability studies and Mgr. Kurt Magsamen, PJ Safarik University in Kosice, Slovakia for editing the manuscript.

Conflict of interest

The authors declare that the research was conducted in the absence of any commercial or financial relationships that could be construed as a potential conflict of interest.

Publisher's note

All claims expressed in this article are solely those of the authors and do not necessarily represent those of their affiliated organizations, or those of the publisher, the editors and the reviewers. Any product that may be evaluated in this article, or claim that may be made by its manufacturer, is not guaranteed or endorsed by the publisher.

Supplementary material

The Supplementary Material for this article can be found online at: <https://www.frontiersin.org/articles/10.3389/fphar.2022.991554/full#supplementary-material>

- Caenepeel, S., Brown, S.P., Belmontes, B., Moody, G., Keegan, K.S., Chui, D., et al. (2018). AMG 176, a selective MCL1 inhibitor, is effective in hematologic cancer models alone and in combination with established therapies. *Cancer Discov.* 8, 1582–1597. doi:10.1158/2159-8290.CD-18-0387
- Chmura, S.J., Dolan, M.E., Cha, A., Mauceri, H.J., Kufe, D.W., and Weichselbaum, R.R. (2000). *In vitro* and *in vivo* activity of protein kinase C inhibitor chelerythrine chloride induces tumor cell toxicity and growth delay *in vivo*. *Clin. Cancer Res.* 6, 737–742.
- Correia, C., Lee, S.H., Meng, X.W., Vincelette, N.D., Knorr, K.L., Ding, H., et al. (2015). Emerging understanding of bcl-2 biology: Implications for neoplastic progression and treatment. *Biochim. Biophys. Acta* 1853 (7), 1658–1671. doi:10.1016/j.bbamer.2015.03.012
- Cory, S., Huang, D. C., and Adams, J. M. (2003). The bcl-2 family: Roles in cell survival and oncogenesis. *Oncogene* 22, 8590–8607. doi:10.1038/sj.onc.1207102
- Danial, N. N., and Korsmeyer, S. J. (2004). Cell death: Critical control points. *Cell* 116, 205–219. doi:10.1016/s0092-8674(04)00046-7
- Davids, M.S., and Letai, A. (2012). Targeting the B-cell lymphoma/leukemia 2 family in cancer. *J. Clin. Oncol.* 30, 3127–3135. doi:10.1200/JCO.2011.37.0981
- de Andrade, G.P., Menegassi de Souza, T.F., Cerchiaro, G., da Silva Pinhal, M.A., Orzari Ribeiro, A., and Girao, M.J.B.C. (2021). Hypericin in photobiological assays: An overview. *Photodiagnosis Photodyn. Ther.* 35, 102343. doi:10.1016/j.pdpdt.2021.102343
- de Brito, O.M., and Scorrano, L. (2010). An intimate liaison: Spatial organization of the endoplasmic reticulum-mitochondria relationship. *EMBO J.* 29, 2715–2723. doi:10.1038/emboj.2010.177
- DeBartolo, J., Dutta, S., Reich, L., and Keating, A.E. (2012). Predictive Bcl-2 family binding models rooted in experiment or structure. *J. Mol. Biol.* 422, 124–144. doi:10.1016/j.jmb.2012.05.022
- Dewick, P.M. (2002). *Medicinal natural products: A biosynthetic approach*. 2 ed. New Jersey: Wiley.
- Dzurova, L., Petrovajova, D., Nadova, Z., Huntosova, V., Miskovsky, P., and Stroffekova, K. (2014). The role of anti-apoptotic protein kinase Ca in response to hypericin photodynamic therapy in U-87 MG cells. *Photodiagnosis Photodyn. Ther.* 11, 213–226. doi:10.1016/j.pdpdt.2014.02.010
- Frame, S., Saladino, C., MacKay, C., Atrash, B., Shelldrake, P., McDonald, E., et al. (2020). Fadracilid (CYC065), a novel CDK inhibitor, targets key prosurvival and oncogenic pathways in cancer. *PLoS ONE* 15 (7), e0234103. doi:10.1371/journal.pone.0234103
- Gajkowska, B., Motyl, T., Olszewska-Badarczuk, H., and Godlewski, M.M. (2001). Expression of BAX in cell nucleus after experimentally induced apoptosis revealed by immunogold and embedment-free electron microscopy. *Cell Biol. Int.* 25, 725–733. doi:10.1006/cbir.2001.0768
- Gong, J.N., Khong, T., Segal, D., Yao, Y., Riffkin, C.D., Garnier, J.M., et al. (2016). Hierarchy for targeting prosurvival BCL2 family proteins in multiple myeloma: Pivotal role of MCL1. *Blood* 128, 1834–1844. doi:10.1182/blood-2016-03-704908
- Gyenge, E.B., Luscher, D., Forny, P., Antoniol, M., Geisberger, G., Walt, H., et al. (2013). Photodynamic mechanisms induced by a combination of hypericin and a chlorin based-photosensitizer in head and neck squamous cell carcinoma cells. *Photochem. Photobiol.* 89, 150–162. doi:10.1111/j.1751-1097.2012.01217.x
- Halder, M., Chowdhury, P.K., Das, R., Mukherjee, P.W., Atkins, M., and Petrich, J.W. (2005). Interaction of glutathione S-transferase with hypericin: A photophysical study. *J. Phys. Chem. B* 109, 19484–19489. doi:10.1021/jp051645u
- Huntosova, V., Novotova, M., Nichtova, Z., Balogova, L., Maslanakova, M., Petrovajova, D., et al. (2017). Assessing light-independent effects of hypericin on cell viability, ultrastructure and metabolism in human glioma and endothelial cells. *Toxicol. In Vitro* 40, 184–195. doi:10.1016/j.tiv.2017.01.005
- Karioti, A., and Bilia, A.R. (2010). Hypericins as potential leads for new therapeutics. *Int. J. Mol. Sci.* 11, 562–594. doi:10.3390/ijms11020562
- Kepp, O., Senovilla, L., Vitale, I., Vacchelli, E., Adjemian, S., Agostinis, P., et al. (2014). Consensus guidelines for the detection of immunogenic cell death. *Oncoimmunology* 3, e955691. doi:10.4161/21624011.2014.955691
- Kiesslich, T., Krammer, B., and Plaetzer, K. (2006). Cellular mechanisms and prospective applications of hypericin in photodynamic therapy. *Curr. Med. Chem.* 13 (18), 2189–2204. doi:10.2174/092986706777935267
- Kotschy, A., Szlavik, Z., Murray, J., Davidson, J., Maragno, A.L., Le Toumelin-Brazat, G., et al. (2016). The MCL1 inhibitor S63845 is tolerable and effective in diverse cancer models. *Nature* 538, 477–482. doi:10.1038/nature19830
- Lakowicz, J.R. (2006). *Principles of fluorescence spectroscopy*. 3rd edition. Springer. ISBN 9780387312781 Germany.
- Larisch, P., Verwanger, T., Linecker, M., and Krammer, B. (2014). The interrelation between a pro-inflammatory milieu and fluorescence diagnosis or photodynamic therapy of human skin cell lines. *Photodiagnosis Photodyn. Ther.* 11, 91–103. doi:10.1016/j.pdpdt.2014.01.002
- Larisch, P., Verwanger, T., Onder, K., and Krammer, B. (2013). *In vitro* analysis of photosensitizer accumulation for assessment of applicability of fluorescence diagnosis of squamous cell carcinoma of epidermolysis bullosa patients. *Biomed. Res. Int.* 2013, 521281. doi:10.1155/2013/521281
- Lee, Y.C., Wang, L.J., Huang, C.H., Shi, Y.J., and Chang, L.S. (2018). ABT-263-induced MCL1 upregulation depends on autophagy-mediated 4EBP1 downregulation in human leukemia cells. *Cancer Lett.* 432, 191–204. doi:10.1016/j.canlet.2018.06.019
- Lian, J., Wu, X., He, F., Karnak, D., Tang, W., Meng, Y., et al. (2011). A natural BH3 mimetic induces autophagy in apoptosis-resistant prostate cancer via modulating Bcl-2–Beclin1 interaction at endoplasmic reticulum. *Cell Death Differ.* 18, 60–71. doi:10.1038/cdd.2010.74
- Llambi, F., Moldoveanu, T., Tait, S.W.G., Bouchier-Hayes, L., Temirov, J., McCormi, L.L., et al. (2011). A unified model of mammalian BCL-2 protein family interactions at the mitochondria. *Mol. Cell* 44, 517–531. doi:10.1016/j.molcel.2011.10.001
- Maiuri, M.C., Criollo, A., Tasdemir, E., Vicenc, J.M., Tajeddine, N., Hickman, J.A., et al. (2007). BH3-only proteins and BH3 mimetics induce autophagy by competitively disrupting the interaction between Beclin 1 and Bcl-2/Bcl-XL. *Autophagy* 3 (4), 374–376. doi:10.4161/auto.4237
- Mandel, M., Blank, M., Hazan, S., Keisari, Y., and Lavie, G. (2007). ANTI-cancer activities of hypericin in the dark. *Photochem. Photobiol.* 74, 120–125. doi:10.1562/0031-8655(2001)074<0120:acaohi>2.0.co;2
- Martinez-Poveda, B., Quesada, A.R., and Medina, M.A. (2005). Hypericin in the dark inhibits key steps of angiogenesis *in vitro*. *Eur. J. Pharmacol.* 516, 97–103. doi:10.1016/j.ejphar.2005.03.047
- Miskovsky, P. (2002). Hypericin—a new antiviral and antitumor photosensitizer: Mechanism of action and interaction with biological macromolecules. *Curr. Drug Targets* 3, 55–84. doi:10.2174/1389450023348091
- Muino, P.L., and Callis, P.R. (2009). Solvent effects on the fluorescence quenching of tryptophan by amides via electron transfer. Experimental and computational studies. *J. Phys. Chem. B* 113, 2572–2577. doi:10.1021/jp711513b
- Noell, S., Mayer, D., Strau, W.S., Tatagi, M.S., and Ritz, R. (2011). Selective enrichment of hypericin in malignant glioma: Pioneering *in vivo* results. *Int. J. Oncol.* 38, 1343–1348. doi:10.3892/ijo.2011.968
- Oltersdorf, T., Elmore, S.W., Shoemaker, A.R., Armstrong, R.C., Augeri, D.J., Bel, B.A., et al. (2005). An inhibitor of Bcl-2 family proteins induces regression of solid tumours. *Nature* 435, 677–681. doi:10.1038/nature03579
- O'Neill, J., Manion, M., Schwartz, P., and Hockenbery, D.M. (2004). Promises and challenges of targeting Bcl-2 anti-apoptotic proteins for cancer therapy. *Biochim. Biophys. Acta* 1705, 43–51. doi:10.1016/j.bbcan.2004.09.004
- Opydo-Chanek, M., Gonzalo, O., and Marzo, I. (2017). Multifaceted anticancer activity of BH3 mimetics: Current evidence and future prospects. *Biochem. Pharmacol.* 136, 12–23. doi:10.1016/j.bcp.2017.03.006
- Petros, A.M., Olejniczak, E.T., and Fesik, S.W. (2004). Structural biology of the Bcl-2 family of proteins. *Biochim. Biophys. Acta* 1644, 83–94. doi:10.1016/j.bbamer.2003.08.012
- Raghav, P.K., Verma, Y.K., and Gangenahalli, G.U. (2012). Peptide screening to knockdown bcl-2's anti-apoptotic activity: Implications in cancer treatment. *Int. J. Biol. Macromol.* 50, 796–814. doi:10.1016/j.ijbiomac.2011.11.021
- Rega, M.F., Leone, M., Jung, D., Cotton, N.J., Stebbins, J.L., and Pellecchia, M. (2007). Structure based discovery of a new class of Bcl-xL antagonists. *Bioorg. Chem.* 35, 344–353. doi:10.1016/j.bioorg.2007.03.001
- Rizzuto, R., Pinton, P., Carrington, W., Fay, F.S., Fogarty, K.E., Lifshitz, L.M., et al. (1998). Close contacts with the endoplasmic reticulum as determinants of mitochondrial Ca²⁺ responses. *Science* 280, 1763–1766. doi:10.1126/science.280.5370.1763
- Sadahira, K., Sagawa, M., Nakazato, T., Uchida, H., Ikeda, Y., Okamoto, S., et al. (2014). Gossypol induces apoptosis in multiple myeloma cells by inhibition of interleukin-6 signaling and Bcl-2/Mcl-1 pathway. *Int. J. Oncol.* 45, 2278–2286. doi:10.3892/ijo.2014.2652
- Seiller, C., Maiga, S., Touzeau, C., Bellanger, C., Kervoele, C., Descamps, G., et al. (2020). Dual targeting of BCL2 and MCL1 rescues myeloma cells resistant to BCL2 and MCL1 inhibitors associated with the formation of BAX/BAK hetero-complexes. *Cell Death Dis.* 11, 316. doi:10.1038/s41419-020-2505-1
- Shea, L.D., Omann, G.M., and Linderman, J.J. (1997). Calculation of diffusion-limited kinetics for the reactions in collision coupling and receptor cross-linking. *Biophys. J.* 73, 2949–2959. doi:10.1016/S0006-3495(97)78323-1

- Stroffekova, K., Tomkova, S., Huntosova, V., and Kozar, T. (2019). Importance of Hypericin-Bcl2 interactions for biological effects at subcellular levels. *Photodiagnosis Photodyn. Ther.* 28, 38–52. doi:10.1016/j.pdpdt.2019.08.016
- Sureau, F., Miskovsky, P., Chinsky, L., and Turpin, P.Y. (1996). Hypericin-induced cell photosensitization involves an intracellular pH decrease. *J. Am. Chem. Soc.* 118, 9484–9487. doi:10.1021/ja961783k
- Theodossiou, T.A., Hothersall, J.S., DeWitte, P.A., Pantos, A., and Agostinis, P. (2009). The multifaceted photocytotoxic profile of hypericin. *Mol. Pharm.* 6, 1775–1789. doi:10.1021/mp900166q
- Trudel, S., Li, Z.H., Rauw, J., Tiedemann, R.E., Wen, X.Y., and Stewart, A.K. (2007). Preclinical studies of the pan-Bcl inhibitor obatoclax (GX015-070) in multiple myeloma. *Blood* 109, 5430–5438. doi:10.1182/blood-2006-10-047951
- Tse, C., Shoemaker, A.R., Adickes, J., Anderson, M.G., Chen, J., Jin, S., et al. (2008). ABT-263: A potent and orally bioavailable bcl-2 family inhibitor. *Cancer Res.* 68, 3421–3428. doi:10.1158/0008-5472.CAN-07-5836
- Tzung, S.P., Kim, K.M., Basanez, G., Giedt, C.D., Simon, J., Zimmerberg, J., et al. (2001). Antimycin A mimics a cell-death-inducing Bcl-2 homology domain 3. *Nat. Cell Biol.* 3, 183–191. doi:10.1038/35055095
- Uzdensky, A.B., Bragin, D.E., Kolosov, M.S., Kubin, A., Loew, H.G., and Moan, J. (2003). Photodynamic effect of hypericin and a water-soluble derivative on isolated crayfish neuron and surrounding glial cells. *J. Photochem. Photobiol. B* 72, 27–33. doi:10.1016/j.jphotobiol.2003.08.008
- Vaux, D.L., and Korsmeyer, S.J. (1999). Cell death in development. *Cell* 96, 245–254. doi:10.1016/s0092-8674(00)80564-4
- Vela, L., and Marzo, I. (2015). Bcl-2 family of proteins as drug targets for cancer chemotherapy: The long way of BH3 mimetics from bench to bedside. *Curr. Opin. Pharmacol.* 23, 74–81. doi:10.1016/j.coph.2015.05.014
- Vogler, M. (2014). Targeting BCL2-Proteins for the treatment of solid tumours. *Adv. Med.* 2014, 943648. doi:10.1155/2014/943648
- Voss, V., Senft, C., Lang, V., Ronellenfitsch, M.W., Steinbach, J.P., Seifert, V., et al. (2010). The pan-Bcl-2 inhibitor (-)-gossypol triggers autophagic cell death in malignant glioma. *Mol. Cancer Res.* 8, 1002–1016. doi:10.1158/1541-7786.MCR-09-0562
- Wang, B., Ni, Z., Dai, X., Qin, L., Li, X., Xu, L., et al. (2014). The Bcl-2/xL inhibitor ABT-263 increases the stability of Mcl-1 mRNA and protein in hepatocellular carcinoma cells. *Mol. Cancer* 13, 98. doi:10.1186/1476-4598-13-98
- Wang, G., Nikolovska-Coleska, Z., Yang, C.Y., Wang, R., Tang, G., Guo, J., et al. (2006). Structure-based design of potent small-molecule inhibitors of anti-apoptotic Bcl-2 proteins. *J. Med. Chem.* 49, 6139–6142. doi:10.1021/jm060460o
- Wang, J.L., Liu, D.X., Zhang, Z.J., Shan, S.M., Han, X.B., Srinivasula, S.M., et al. (2000). Structure-based discovery of an organic compound that binds Bcl-2 protein and induces apoptosis of tumor cells. *Proc. Natl. Acad. Sci. U. S. A.* 97, 7124–7129. doi:10.1073/pnas.97.13.7124
- Wang, J.L., Zhang, Z.J., Choksi, S., Shan, S., Lu, Z., Croce, C.M., et al. (2000). Cell permeable bcl-2 binding peptides: A chemical approach to apoptosis induction in tumor cells. *Cancer Res.* 60, 1498–1502.
- Wei, J., Stebins, J.L., Kitada, S., Dash, R., Zhai, D., Placzek, W.J., et al. (2011). An optically pure apogossypolone derivative as potent pan-active inhibitor of anti-apoptotic Bcl-2 family proteins. *Front. Oncol.* 1, 28. doi:10.3389/fonc.2011.00028
- Yang, J., Jing, Z.H., Jie, J. J., and Guo, P. (2009). Fluorescence spectroscopy study on the interaction between Gossypol and bovine serum albumin. *J. Mol. Struct.* 920, 227–230. doi:10.1016/j.molstruc.2008.10.053
- Zhao, C., Yin, S., Dong, Y., Guo, X., Fan, L., Ye, M., et al. (2013). Autophagy-dependent EIF2AK3 activation compromises ursolic acid-induced apoptosis through upregulation of MCL1 in MCF-7 human breast cancer cells. *Autophagy* 9, 196–207. doi:10.4161/auto.22805



OPEN ACCESS

EDITED BY

Hidayat Hussain,
Leibniz Institute of Plant Biochemistry,
Germany

REVIEWED BY

Muzamil Yaqub Want,
Roswell Park Comprehensive Cancer
Center, United States
Chaitanya Verma,
The Ohio State University, United States

*CORRESPONDENCE

Antoine G. Abou Fayad,
aa328@aub.edu.lb
Hiba El Hajj,
he21@aub.edu.lb

*These authors share first authorship

*These authors have contributed equally
to this work and share senior authorship

SPECIALTY SECTION

This article was submitted to
Experimental Pharmacology and Drug
Discovery,
a section of the journal
Frontiers in Pharmacology

RECEIVED 19 August 2022

ACCEPTED 26 September 2022

PUBLISHED 10 October 2022

CITATION

Awada B, Hamie M, El Hajj R, Derbaj G,
Najm R, Makhoul P, Ali DH,
Abou Fayad AG and El Hajj H (2022), HAS
1: A natural product from soil-isolated
Streptomyces species with potent
activity against cutaneous leishmaniasis
caused by *Leishmania tropica*.
Front. Pharmacol. 13:1023114.
doi: 10.3389/fphar.2022.1023114

COPYRIGHT

© 2022 Awada, Hamie, El Hajj, Derbaj,
Najm, Makhoul, Ali, Abou Fayad and El
Hajj. This is an open-access article
distributed under the terms of the
[Creative Commons Attribution License](https://creativecommons.org/licenses/by/4.0/)
(CC BY). The use, distribution or
reproduction in other forums is
permitted, provided the original
author(s) and the copyright owner(s) are
credited and that the original
publication in this journal is cited, in
accordance with accepted academic
practice. No use, distribution or
reproduction is permitted which does
not comply with these terms.

HAS 1: A natural product from soil-isolated *Streptomyces* species with potent activity against cutaneous leishmaniasis caused by *Leishmania tropica*

Bassel Awada^{1,2†}, Maguy Hamie^{1,2†}, Rana El Hajj^{3†},
Ghada Derbaj^{1,2}, Rania Najm⁴, Perla Makhoul^{1,2}, Dima Hajj Ali¹,
Antoine G. Abou Fayad^{1,2*†} and Hiba El Hajj^{1,2*†}

¹Department of Experimental Pathology, Immunology and Microbiology, Faculty of Medicine, American University of Beirut, Beirut, Lebanon, ²Center for Drug Discovery, American University of Beirut, Beirut, Lebanon, ³Department of Biological Sciences, Beirut Arab University, Beirut, Lebanon, ⁴College of Medicine, Mohammed Bin Rashid University of Medicine and Health Sciences, Dubai, United Arab Emirates

Cutaneous Leishmaniasis (CL) is a neglected tropical disease, classified by the World Health Organization (WHO) as one of the most unrestrained diseases. The Syrian war and the significant displacement of refugees aggravated the spread of this ailment into several neighboring countries in the Eastern Mediterranean Region (EMR). In Syria, *Leishmania tropica* is identified as one of the most aggressive and endemic identified species, causing localized or generalized lesions, often chronic or relapsing. Pentavalent antimonial drugs are currently used as first line treatment against CL. Nonetheless, these drugs exhibit several limitations, including the repetitive painful injections, high cost, poor availability, and mainly systemic toxicity. Besides, the emergence of acquired parasitic resistance hinders their potency, stressing the need for new therapies to combat CL. Natural products (NPs) epitomize a valuable source in drug discovery. NPs are secondary metabolites (SMs) produced by plants, sponges, or a wide variety of organisms, including environmental microorganisms. The EMR is characterized by its immense biodiversity, yet it remains a relatively untapped area in drug discovery. NPs of the region were explored over the last 2 decades, but their discoveries lack biogeographical diversity and are limited to the Red Sea. Here, we isolated previously uncultured environmental soil-dwelling *Streptomyces* sp. HAS1, from Hasbaya region in southeast Lebanon. When fermented in one of our production media named INA, HAS1 produced a crude extract with significant potency against a clinical *Leishmania tropica* isolate. Using bio-guided fractionation, the bioactive compound was purified and the structure was elucidated by NMR and LC-HRMS. Our findings establish NPs as strong candidates for treating *Leishmania tropica* and further dwells on the importance of these natural sources to combat microbial infections.

KEYWORDS

soil extract, streptomyces, *Leishmania tropica*, cutaneous leishmaniasis, natural products, bio-guided fractionation

Introduction

Cutaneous Leishmaniasis (CL) is a parasitic disease caused by the protozoan *Leishmania* species. CL is classified by the World Health Organization (WHO) as one of the most significant neglected tropical diseases (Cavalli and Bolognesi, 2009), affecting around 12 to 15 million people worldwide, and 600,000 to one million new cases occurring annually (Reithinger, 2016; Torres-Guerrero et al., 2017). Particularly, the last decade witnessed an alarming increase in CL incidence (Bailey et al., 2017). CL is endemic in various areas including the Americas, the Mediterranean basin, the Middle East and Central Asia. In the Eastern Mediterranean (EMR) region, Syria partakes the highest prevalence of CL (Mcdowell et al., 2011). Moreover, the Syrian crisis led to increased frightening numbers of CL (Al-Salem et al., 2016), across Syria itself, and its neighboring countries following the displacement of refugees who fled the war (Saroufim et al., 2014; Sharara and Kanj, 2014; Hayani et al., 2015; Burza et al., 2018; Rehman et al., 2018; Bizri et al., 2021). Clinically, CL is characterized by localized or generalized lesions, often chronic or relapsing, on exposed parts of the body (Sharma et al., 2005; Steverding, 2017; Burza et al., 2018). The severity of these clinical manifestations is variable and depends on the causative species among other factors (Torres-Guerrero et al., 2017). The most prominent etiologic agents of CL in the Middle East region are *Leishmania tropica* (*L. tropica*) and *Leishmania major* (Roberts, 2005; Masmoudi et al., 2013; Fakhra et al., 2016), with a predominance of *L. tropica* among Syrian refugees (Saroufim et al., 2014; Bizri et al., 2021). Various therapeutic approaches exist for CL, with multiple variables affecting the type of applied treatment (Heras-Mosteiro et al., 2017). In addition to physical approaches, remedies can be administered topically, orally, or systemically (Palumbo, 2009; Eiras et al., 2015; Heras-Mosteiro et al., 2017; Briones Nieva et al., 2021). Pentavalent antimonials are the first line of defense against CL, with an extensive use of Meglumine antimoniate (Glucantime) (Esfandiarpour and Alavi, 2002; Palumbo, 2009; Eiras et al., 2015; Briones Nieva et al., 2021). These drugs can be injected intra-lesionally, intramuscularly, or intravenously (Palumbo, 2009; Eiras et al., 2015; Briones Nieva et al., 2021). Nonetheless, they exhibit numerous adverse effects such as their painful repetitive injections and systemic toxicity (Torres-Guerrero et al., 2017; Garza-Tovar et al., 2020). Moreover, several reports documented the emergence of resistant parasites to these therapies (Kazemi-Rad et al., 2013a; Kazemi-Rad et al., 2013b; Mohebbi et al., 2019; Ozbilgin et al., 2020). Among the emerging treatments of CL, the potency of an immunomodulatory drug, Imiquimod (Arevalo et al., 2001; Firooz et al., 2006; Arevalo et al., 2007; Miranda-Verastegui et al., 2009) and its analog 1-(3-methoxyphenyl)-N-methylimidazo [1,2-a]quinoxalin-4-amine (EAPB0503) (El Hajj et al., 2018) was reported. Yet, the use of Imiquimod as

first-line therapy and the clinical use of its derivative against CL are still out of reach. Thus, the discovery of new alternative drugs capable of efficiently eliminating CL while inducing minimal side effects is fundamental.

Natural products (NPs), also known as secondary metabolites (SMs), originate from a plethora of organisms including environmental microorganisms and remain an important source in the field of anti-infective drug discovery (Pink et al., 2005; Chin et al., 2006). Indeed, approximately 50% of all antimicrobials discovered over the last 4 decades were NPs, their derivatives, or their mimics (Newman and Cragg, 2020). Among NPs, different examples are reported with anti-leishmanial potency (Gervazoni et al., 2020; Carter et al., 2021). Yet, these NPs were produced from a small pool of bacteria, limiting the opportunity to find novel molecules with specific targets and selective toxicity against *Leishmania* species, particularly *L. tropica* (Zhu et al., 2011; Zhu et al., 2012). Thus, the quest for these molecules against this endemic parasite in the EMR, requires the search for uncultured bacteria. Such microbes can typically be found in untapped geographical locations whose full potential was not yet unraveled (Cordell, 2000; Tulp and Bohlin, 2002; Lefevre et al., 2008). The EMR is a great example of unexploited biodiverse area, where the antimicrobial drug discovery was almost exclusively made at the level of the Red Sea. In this study, we purified NPs synthesized by uncultured environmental bacteria inhabiting the soil of Lebanon, and explored their anti-leishmanial activity against a clinical *L. tropica* isolate from a CL patient.

Materials and methods

Soil sample collection and bacterial isolation

Soil samples were collected from Hasbaya (HAS), Koura (KR) and Bchamoun (BCH) specific regions in Lebanon. Each of the isolates was named after the region it originated from and the order of its isolation. For example, HAS1 is the first bacterium isolated from the soil of the Hasbaya region, while BCH 8 and KR 24 correspond to 8th and 24th bacterial isolates from the Bchamoun and Koura regions respectively. Soil samples were collected in a sterile container and transported to the laboratory for further processing. The soil was first dried for 7 days at 37°C. Afterward, 3 g of the dried sample were dissolved in 100 ml of autoclaved distilled water and incubated at 55°C for 30 min. Subsequently, serial dilutions (1/5, 1/10, 1/100, and 1/1,000) of the soil suspension were performed in a final volume of 1 ml. These dilutions, along with the original soil solution, were inoculated on soil agar (30 g dried soil, 18 g bacteriological agar, and 10 g corn starch in 1 L distilled water) or on International *Streptomyces* Project-3 (ISP3) agar (20 g oats, 18 g bacteriological agar, and 2.5 ml ISP3 trace elements in

TABLE 1 Composition of the 14 different production media.

Media

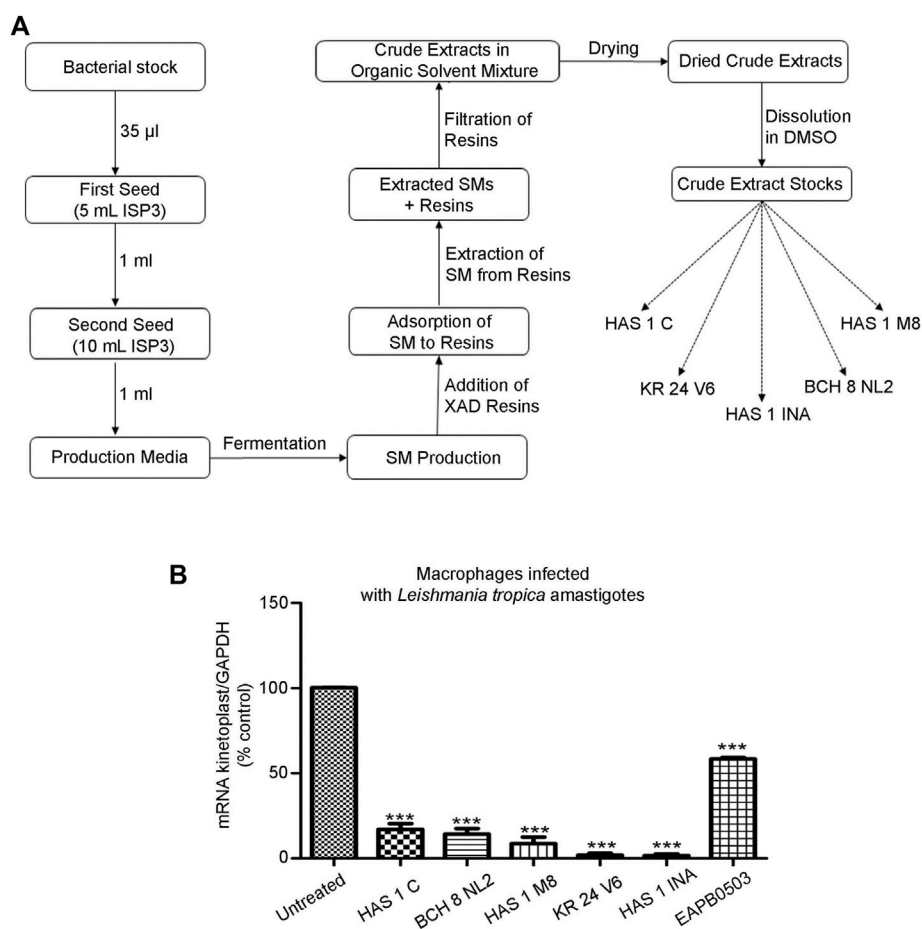
Components (g/L)	V	Veg	A	B	C	INA	Ra3	GPMY	V6	AF/MS	GYM	M8	NL2	COM
Potato starch								20						
Peptone		5	4				2		5					
Soluble starch	24	20									20	30		
Dextrose	1									20				
Meat extract	3	2	4						5			2		
Yeast extract	5	3	2				4	5	5	2	4	2	2.5	
Malt extract							10	5				10		
Soybean meal		2	2							6				
Glucose						10			20		4	10		25
Tryptose	5													
Maltose			20											
Dextrin			10											
CaCO ₃		1		0.1	0.1	5				4		3	10	2
Glycerol				20		30	5	20						
Glycine				2.5	2.5							4		
Hydrolyzed casein									3					
NaCl				1	1	2			1.5	1				2
KH ₂ PO ₄				1	1									0.15
FeSO ₄				0.1	0.1									
MgSO ₄ ·7H ₂ O				0.1	0.1									
MgCl ₂ ·6H ₂ O							2							
Tween 60					20									
Molasses													20	
Soy flour													15	25
Dried beer yeast														3
Ammonium Sulfate														2
Soybean Oil														3
pH	7.2	7	7	7	7	7.3	7.4	7.02	7.05	7.3	7	7	7.8	8.4

1 L distilled water, pH = 7.8). The plates were then incubated at 28°C for 14 days. Once colonies started to appear, they were purified *via* continuous subculturing on ISP3 agar. When pure cultures were obtained, bacteria were stored at -80°C in a 50% aqueous glycerol solution.

Secondary metabolite production and extraction

A starter culture, known as the first seed, was initiated by inoculating 35 µl of the bacterial stock in 5 ml of liquid ISP3 (20 g oats and 2.5 ml ISP3 trace elements in 1 L distilled water). This suspension was then incubated at 28°C at 130 rpm for 48 h, before 1 ml was transferred into 10 ml of sterile ISP3 media. This second seed was subjected to identical incubation conditions, after which, 1 ml was used to inoculate 50 ml of each of our

14 different media to induce SM production (Table 1). The cultures were then incubated under the same conditions for 7 days. Then, 1 ml of Amberlite XAD 16N resins was added to each culture and left for 3–4 h to adsorb the SMs. The resin and cell pellets were centrifuged and consequently extracted with methanol. The methanol solution was then defatted with hexane and the layer was evaporated to dryness. The crude was resuspended with ethyl acetate and extracted with 1M HCl. The organic layer was then evaporated to dryness and resuspended in DMSO for further purification by HPLC (Figure 1A). A Phenomenex Luna® 5 µm C18 column 100 Å 250 × 10 mm was used and a gradient from 5 to 95% B in 40 min with (A) H₂O + 0.1% FA and (B) ACN + 0.1% FA at a flow rate of 5 ml/min at room temperature. Elution was monitored at 220 and 280 nm. Accordingly, the crude extracts stocks were named HAS1 INA, C and M8 (corresponding to the crude produced by the bacterium HAS1 in medium INA, C and

**FIGURE 1**

Crude extracts produced by environmental bacteria derived from Lebanese soil inhibit *L. tropica* amastigotes replication. **(A)**. Pipeline of secondary metabolite production by environmental bacteria isolated from soils collected from selected region across Lebanon. Bacteria from Hasbaya (HAS), Koura (KR) and Bchamoun (BCH) were fermented in a collection of 14 different production media. XAD resins were added 14 days post bacterial inoculation to adsorb the SMs, which were then extracted *via* organic solvents. The overall SMs collected from an isolate in a specific medium were named after the isolate followed by the medium name, for example HAS1 INA. **(B)**. Real-time quantitative PCR detection of THP-1 derived macrophages infected with patient-derived *L. tropica* amastigotes treated with 0.01 µg/ml of crude extracts HAS1 C, BCH8 NL2, HAS1 M8, KR24 V6, and HAS1 INA for 24 h. Briefly, THP-1 monocytes were differentiated into macrophages, activated with LPS, and infected with *L. tropica* with a ratio of one parasite/three cells. Treatment with 0.01 µg/ml of the crude extracts or 1 µM of EAPB0503 was then performed for 24 h. The results are shown as percentage of untreated infected macrophages. Amastigote transcripts were evaluated by Syber green RT-PCR using kinetoplast specific primers and their percentage of expression was normalized to GAPDH. Results are expressed as percentage of the untreated control (±) SEM and are representative of at least three independent experiments. To validate statistical significance, t-tests were used with *** representing *p*-values < 0.001.

M8 respectively), BCH 8 NL2 (corresponding to the crude produced by the bacterium BCH8 in medium NL2), and KR24 V6 (corresponding to the crude produced by the bacterium KR24 in medium V6).

HAS1 isolate characterization

Since extracts of HAS1 isolate exhibited the highest potency against *L. tropica*, HAS1 INA was chosen for further purification. HAS1 was subjected to genomic DNA extraction using the

QIAamp DNA Mini Kit (Qiagen). The resulting genomic DNA was used as a template for the preparation of whole-genome sequencing libraries through the Nextera XT library prep kit (Illumina GmbH). The libraries were then sequenced on the Illumina MiniSeq sequencer, 2 × 150 bp. Trimmomatic (Bolger et al., 2014) was used for quality control and trimming of the reads, while assembly was achieved through Unicycler (Wick et al., 2017) on Galaxy. The resulting FASTA file was fed into KmerFinder 3.2 to determine the bacterial species (Larsen et al., 2014). Based on the sequencing results, HAS1 was characterized according to the taxonomic description of the

Actinobacteria as follows: first, to visualize the morphology and color of the mycelium, HAS1 was streaked on the ISP3 agar. Second, the isolate was tested for its resistance to sodium chloride (NaCl) through its culture on agar 5,339 (10 g of casein peptone, 5 g of yeast extract, and 20 g of agar in 1 L of distilled water, pH = 7) containing various percentages of NaCl. Third, the isolate's pH tolerance was investigated by culturing it on ISP2 agar (10 g of malt extract, 4 g of yeast extract, 4 g of glucose, and 15 g of agar in 1 L of distilled water) with different pH levels. For all three tests, the plates were then incubated at 28°C for 10 days before the observation of the growth which was recorded and documented. The biochemical fingerprints of HAS1 were evaluated using the API 20E kit (BioMérieux), according to the manufacturer's recommendations.

High performance liquid chromatography mass spectrometry (HPLC-MS)

Measurements were performed using an AB Sciex X500R QTOF ESI mass spectrometer. LC flow was split to 500 nL/min before entering the ion source. Mass spectra were acquired in centroid mode ranging from 150 to 1,000 m/z, resolution $R = 30,000$. A Luna Omega C18, 150 × 2.1 mm, 1.6 μ m column was used, injection volume = 1 μ L. A gradient of A) H₂O + 0.1% FA and B) MeCN + 0.1% FA at a flow rate of 0.55 ml/min was used to achieve separation. Gradient conditions start at 5% B, increase to 10% B in 1 min, then to 35% B from minute 1→15, then to 50% B from minute 15→22, and finally to 80% B from minute 22→25. After a 1-min hold at 80% B, the system was re-equilibrated for 5 min with the initial conditions. UV data was acquired using a PDA (wavelength 200–800 nm \pm 8 nm), MS detection was performed simultaneously.

Leishmania tropica promastigotes culture

L. tropica promastigotes were isolated from biopsies of CL patients as described (El Hajj et al., 2018). Sample collection was approved by the Institutional Review Board of the American University of Beirut (PALK.IK.01) (El Hajj et al., 2018). Parasites were maintained in RPMI-1640 (Lonza) supplemented with 10% Fetal Bovine Serum (FBS), 100IU/ml streptomycin/penicillin (Sigma).

Macrophage culture, infection, and treatment

Human monocytic THP-1 cells (American Type Culture Collection ATCC TIB-202) were seeded at a density of one million cells/well in six well-plates, and grown in RPMI medium supplemented with 10% Fetal Bovine Serum, 1%

penicillin-streptomycin, and 1% glutamine. The differentiation of monocytes into macrophages was performed as described (El Hajj et al., 2018). Briefly, the differentiation was induced using 50 ng/ml of phorbol 12-myristate 13-acetate (PMA, Sigma) overnight. The adherent differentiated macrophages were then activated using 1 μ g/ml of lipopolysaccharide (LPS) for 4 h. The activated macrophages were subsequently infected with the patient-derived *L. tropica* promastigotes at the ratio of one parasite/3 macrophages. After a 24 h incubation at 37°C, non-internalized parasites were washed out with phosphate buffer saline (PBS). Subsequently, the media was replenished, and a final concentration of 0.01 μ g/ml of the crude extracts or the fractions (HAS1 INA Hexane, HAS1 INA chloroform, HAS1 INA Ethyl Acetate, and HAS1 INA Water) or 1 μ g/ml of the purified compounds (HAS1 F1, HAS1 F2, HAS1 F3, and HAS1 F4) were added and incubated for 24 h at 37°C. EAPB0503 was used as positive control (El Hajj et al., 2018). The drug was prepared as a 0.1M stock in DMSO and stored at -80°C. Working solutions of 1 μ M were freshly prepared in culture media.

Anti-amastigote activity

After 24 h of incubation with the respective treatments, infected macrophages with amastigotes were washed with PBS, scraped, and collected in microcentrifuge tubes. Tubes were centrifuged at 1,200 rpm for 5 min at 4°C. The supernatant was discarded. The anti-amastigote activity was assessed by quantitative real time PCR and by Immunofluorescence assay.

Hematoxylin and eosin (H&E) stain

Activated macrophages seeded onto coverslips in six well-plates were subjected to H&E staining. Following infection with *L. tropica* promastigotes at the ratio of one parasite/3 macrophages, and treatment for 24 h with either HAS1-F1 or HAS1-F2, cells were fixed with methanol for 1 min. The coverslips were then covered in Hematoxylin (Fisher Scientific, Canada) and a counterstaining was performed for 30 s before rinsing for 5 min with water. Subsequently, the coverslips were dipped in an alcoholic eosin Y solution (Leica Microsystems, Canada), and rinsed with deionized water before mounting on slides.

Anti-promastigote activity

To investigate the anti-promastigote activity of the crude extract HAS1 INA and its bioactive fractions (HAS1-F1 and HAS1-F2), a blind counting assay was performed. First, 100 μ L per well of *L. tropica* promastigote culture (10^6 cells/mL) were

TABLE 2 Sequence of primers used in the q-RT-PCR for detection of kinetoplast and the housekeeping gene GAPDH.

Primer	Sequence
Kinetoplast Forward Primer	5'- CCT ATT TTA CAC CAA CCC CCA gT-3'
Kinetoplast Reverse Primer	5'- ggg TAg ggg CgT TCT gCg AAA-3'
GAPDH Forward Primer	5'- CAT ggC CTT CCg TgT TCC TA-3'
GAPDH Reverse Primer	5'- CCT gCT TCA CCA CCT TCT TgA T-3'

added in round-bottom 96-well plates. Then, 100 μ L of various dilutions of the treatments were added to each well, to obtain final concentrations between 0.01 and 1 μ g/ml for HAS1 INA and between 0.5 and 10 μ g/ml for HAS1-F1 and HAS1-F2. The plates were then incubated at 25°C for 24 h, then transferred to 37°C for 20 min to reduce parasite motility. The motile promastigotes were then counted using a hemocytometer.

Quantitative real-time PCR

Total RNA was extracted using the RNeasy Plus Mini Kit (Qiagen). cDNA synthesis was performed using 1 μ g of the RNA of each sample as a template, using the iScript cDNA Synthesis Kit (BIO-RAD). Syber green qRT PCR was then completed using the BIORAD-CFX96 machine as described (El Hajj et al., 2018). Primers for amastigote detection target the minicircle kinetoplast DNA (kDNA) (Table 2). Primers for the housekeeping Glyceraldehyde-3-Phosphate dehydrogenase GAPDH, are also listed in Table 2. The PCR cycles included a denaturation step for 3 min at 95°C, followed by 39 cycles of (denaturation for 15 s at 95°C, annealing for 1 min at 57°C, elongation for 30 s at 72°C), and a final elongation for 5 min at 72°C. Percentage of expression was calculated according to the Livak method (Schmittgen and Livak, 2008).

Immunofluorescence microscopy

P6 well plates were seeded with activated macrophages infected with *L. tropica* (1 parasite per three cells) for 24 h and treated with HAS1 F1 or HAS1 F2 for 24 h. After 24 h, coverslips were fixed in 4% paraformaldehyde for 20 min. Permeabilization was performed in Triton (0.2%) for 10 min. Following one PBS wash, a blocking step for 30 min with PBS-10% FBS was performed. A conjugated FITC anti-Leishmania Major Surface Protease (Gp63) monoclonal antibody (CEDARLANE CLP005F) was used at the dilution of 1:1000. Staining of nuclei was performed using 1 μ g/ml of Hoechst 33,342 in trihydrochloride trihydrate solution (Invitrogen, H33342) for 5 min. Finally, coverslips were mounted onto slides using a Prolong Anti-fade kit (Invitrogen, P36930).

Images were acquired by the Zeiss Axio microscope (Zeiss, Germany) and analyzed using ZEN software.

Cytotoxicity on PBMCs

To assess the cytotoxicity of HAS1 INA, Has1-F1, and HAS1-F2, trypan blue exclusion assay was performed on human Peripheral Blood Mononuclear Cells (PBMCs). PBMCs were isolated using a Ficoll gradient from left-over peripheral blood specimens collected from the American University of Beirut Medical Center. PBMCs were seeded in 96-cell plates at the density of 200,000 cells/mL in RPMI media supplemented with 20% FBS and 1% penicillin-streptomycin. The cells were then incubated with different concentrations of HAS-F1 or HAS1-F2 (1, 5, or 10 μ g/ml) or with 0.01 μ g/ml of HAS1 INA for 24 h, and the number of living cells was counted using a hemocytometer.

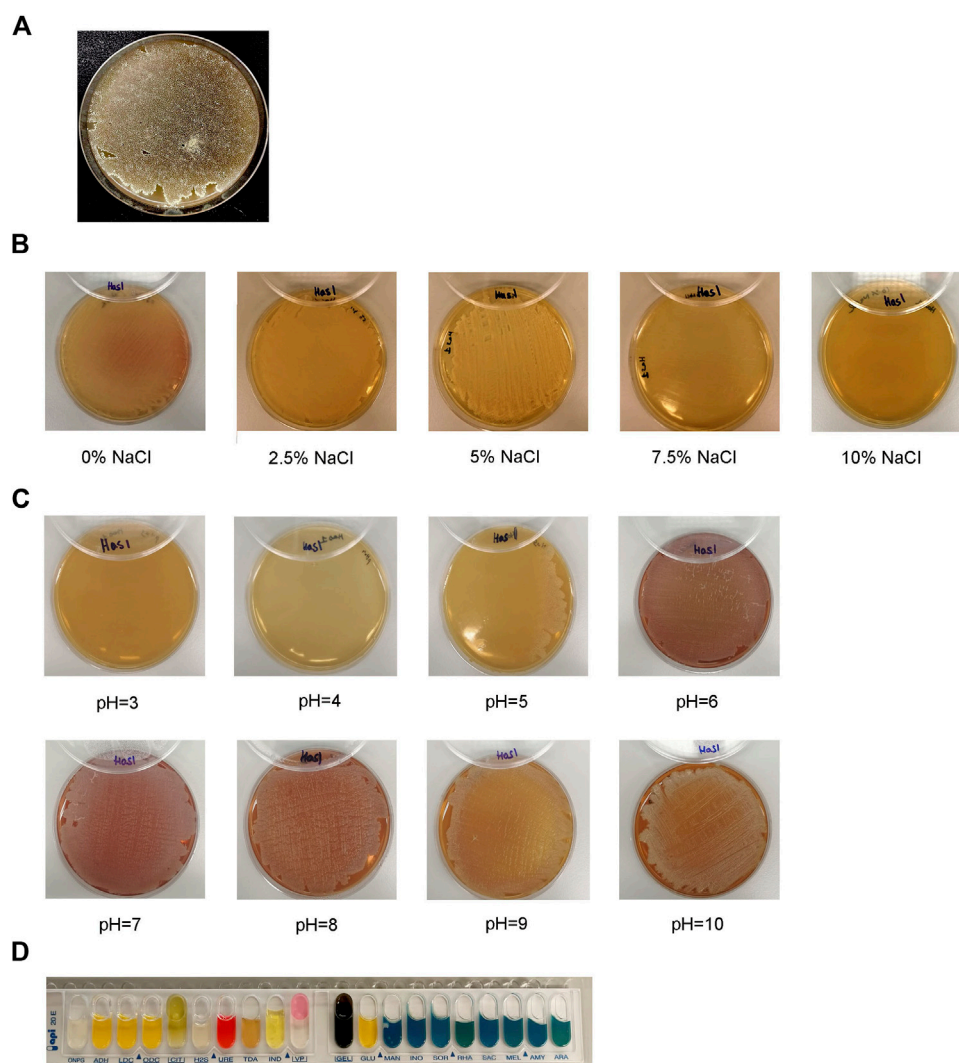
Statistical analysis

Graphs were plotted and analyzed using GraphPad Prism. The statistical significance was validated for each treatment using an unpaired *t*-test with the non-treated control. *p*-values < 0.05 were considered as significant. *, **, *** were used for *p*-value < 0.05, <0.01 and <0.001 respectively.

Results

Crude extracts from soil isolated bacteria of different Lebanese areas exhibit a potency against a clinical *Leishmania tropica* isolate

The EMR is an unexploited biodiverse area when pertaining to antimicrobial drug discovery. We first collected soil samples from specific regions in Lebanon: Hasbaya (HAS), Koura (KR), and Bchamoun (BCH). The isolation of crude extracts from different soils is described in Figure 1A. The production of secondary metabolites does not only depend on the growth of bacteria, but also on the conditions imposed by the medium and the surroundings. For instance, the carbon source plays an important role for the precursors and energy required for the synthesis of biomass building blocks and secondary metabolites production (Torres-Bacete et al., 2005). Thus, designing an appropriate production medium is an important step in the production of secondary metabolites. The crude extract of isolates from our collection of environmental bacteria from different soil samples were cultured in 14 different production media (Table 1), and tested for their antileishmanial activity, against a *Leishmania tropica* clinical isolate. The antileishmanial effect was assessed by quantifying the expression of *Leishmania*-

**FIGURE 2**

Morphological, physiological, and biochemical characterization of the bacterial isolate HAS1. **(A)** Growth, shape, color of the mycelium of the isolate HAS1 and spore formation on ISP3 agar 10 days after bacterial inoculation with an incubation at 28°C. **(B)** Physiological characterization of HAS1 isolate using bacterial growth on the 5,339 agar with different NaCl concentrations (0, 2.5, 5, 7.5 and 10%) after incubation for 10 days at 28°C. **(C)** Growth of HAS1 on ISP2 agar with different pH (3, 4, 5, 6, 7, 8, 9, and 10) after a 10 days at 28°C. **(D)** Biochemical testing of HAS1 using the API 20E kit.

kinetoplast reflecting the multiplication of amastigotes within macrophages infected with *L. tropica* (El Hajj et al., 2018). Among all tested crude extracts in different production media, five extracts from three soil sources and different production media were able to significantly reduce the kinetoplast transcript levels at a concentration as low as 0.01 µg/ml (Figure 1B), and exhibited a significantly higher potency than EAPB0503, used as positive control (El Hajj et al., 2018) (Figure 1B). While HAS1 C and BCH8 NL2 and HAS1 M8 significantly reduced the multiplication of *L. tropica* amastigotes to less than 20%, KR24 V6 and HAS1 INA almost cleared the parasites (Figure 1B). Notably, HAS1 INA showed the most prominent

inhibition of amastigote multiplication with a decline in kinetoplast expression surpassing 98%, when compared to the untreated control (p -value < 0.0001) (Figure 1B). Hence the remainder of the present study was based on the bio-guided fractionation of this crude extract to identify novel antileishmanial compounds.

HAS1 producing strain characterization

Using KmerFinder 3.2, HAS1 was most significantly identified as *Streptomyces* sp. CB00271 (q -value = 67,548.74;

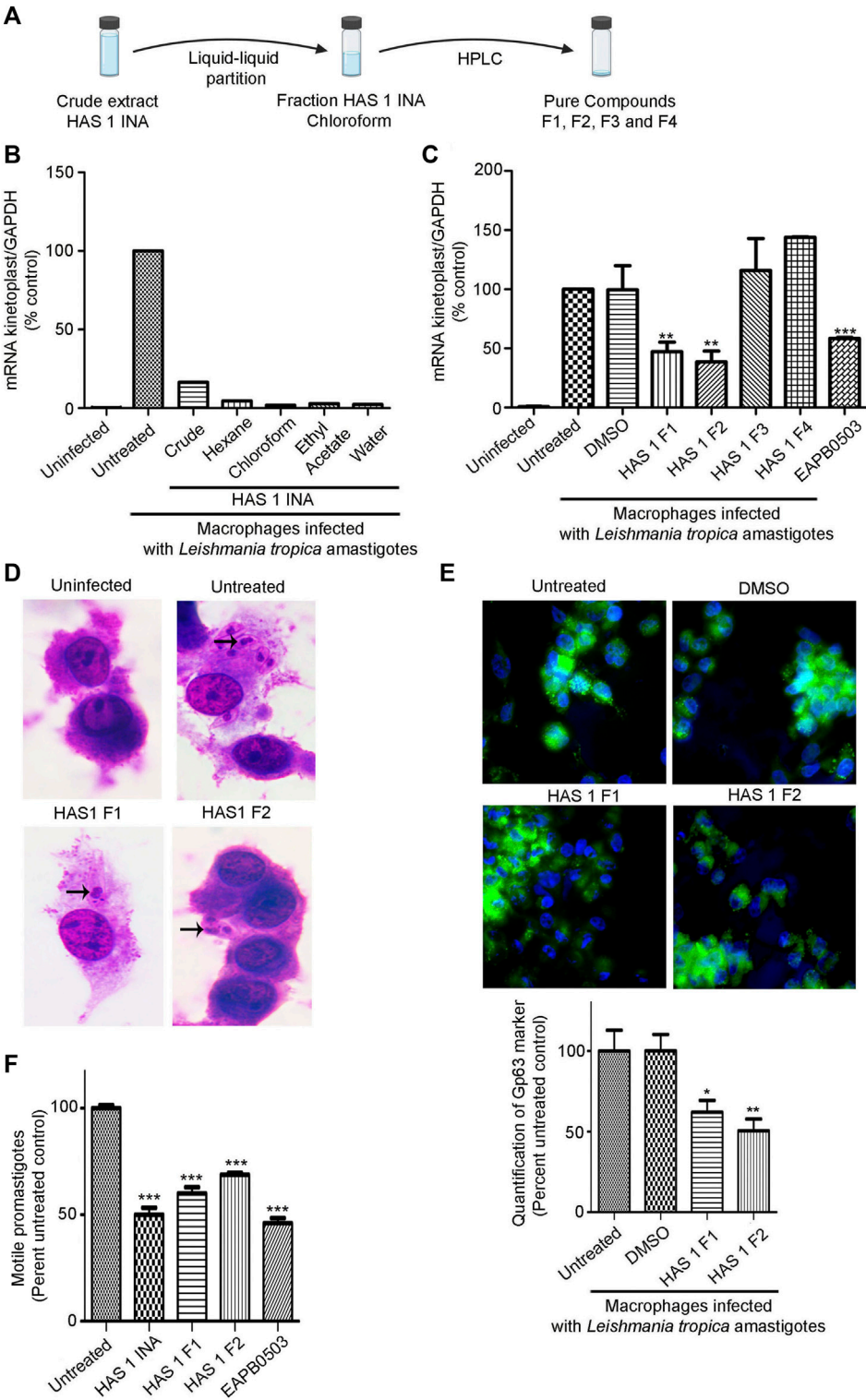


FIGURE 3
Bio-guided fractionation of the antileishmanial compounds of HAS1 INA. (A). An upscaled fermentation of the HAS1 INA crude was first subjected to liquid-liquid partition generating four fractions: HAS1 INA Hexane, HAS1 INA chloroform, HAS1 INA Ethyl Acetate, and HAS1 INA Water. HAS1 INA chloroform was further fractionated into four pure compounds using HPLC: HAS1-F1, HAS1-F2, HAS-F3, and HAS1-F4. (B,C). Real-time quantitative PCR detection of THP-1 derived macrophages infected with patient-derived *L. tropica* amastigotes treated with 0.01 µg/ml of HAS1 INA fractions and the crude extract (B) or with 1 µg/ml of the pure compounds for 24 h or with 1 µM of EAPB0503 for 24 h (C). Amastigote (Continued)

FIGURE 3 (Continued)

transcripts were evaluated by Syber green RT-PCR using kinetoplast specific primers and their percentage of expression was normalized to GAPDH. Results are expressed as percentage of the untreated control (\pm) SEM and are representative of at least three independent experiments (C) and one representative experiment for (B). To validate statistical significance, t-tests were used with ** representing p -values < 0.01 , and *** representing p -values < 0.001 . (D). H&E staining of THP-1 derived macrophages infected with patient-derived *L. tropica* amastigotes treated with 1 μ g/ml of HAS1-F1 or HAS1-F2 for 24 h. (E). Immunofluorescence microscopy of THP-1 derived macrophages infected with patient-derived *L. tropica* amastigotes treated with 1 μ g/ml of HAS1-F1 or HAS1-F2. The Gp63 surface parasite was stained with an anti-Gp63 antibody (green), and nuclei were stained with Hoechst 33,342 (blue). The graph shows the quantification of GP63 as averages from 50 different cells which were then expressed as percentage of the untreated control (\pm) SEM. To validate statistical significance, t-tests were used with * representing p -values < 0.05 , and ** representing p -values < 0.01 . (F). Blind count of motile promastigotes of *L. tropica* treated with 0.01 μ g/ml of HAS1 INA, 1 μ g/ml of HAS1-F1 or HAS1-F2, or 1 μ M of EABP0503 for 24 h. Results are expressed as percentage of the untreated control (\pm) SEM and are representative of at least three independent experiments. To validate statistical significance, t-tests were used with *** representing p -values < 0.001 .

p -value = 1.0e-26). Thus, HAS1 was characterized by standard tests for *Streptomyces*. On ISP3 agar (Figure 2A), HAS1 presented a substrate mycelium with a sand yellow color (RAL 1002) and an aerial mycelium with an oyster white color (RAL 1013). This bacterium formed spores as well. HAS1 was also able to grow normally on the agar 5,339 when the NaCl content was lower or equal to 5%. Whereas minimal growth was observed on the same agar when it contained 7.5% NaCl and no growth was observed at a NaCl percentage of 10 (Figure 2B).

On ISP2 agar, HAS1 showed no growth at pH three or 4, while it grew on the same type of agar when the pH was superior or equal to 5 (Figure 2C). Finally, using the API 20E kit, HAS1 was able to ferment glucose (GLU-positive) and produce acetoin (VP-positive), and proved to possess both the urease (URE-positive) and gelatinase (GEL-positive) enzymes (Figure 2D).

HAS1-F1 and HAS1-F2 fractions of HAS1 INA are the bioactive compounds exhibiting the antileishmanial activity against *L. tropica* isolate

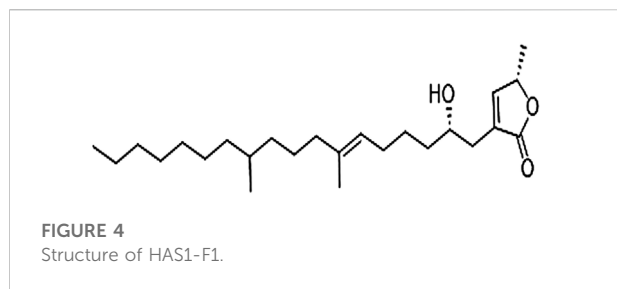
The prominent activity of HAS1 INA crude extract prompted us to isolate the bioactive compounds from this mixture. An upscaled fermentation was produced and the SMs were first segregated *via* liquid-liquid partition (Figure 3A). Among the four obtained fractions in Hexane, chloroform, Ethyl Acetate and water, the HAS1 chloroform fraction revealed the most prominent decrease in amastigote multiplication ($>98\%$), at a concentration of 0.01 μ g/mL as compared to the untreated control (Figure 3B). Therefore, this fraction was considered for further purification. After HPLC, HAS1 INA chloroform generated four distinct fractions named HAS1-F1, HAS1-F2, HAS1-F3, and HAS1-F4 (Figure 3C). Upon testing their biological activity against *L. tropica* amastigotes, all HAS1 fractions did not result in significant anti-leishmanial activity at the concentration of 0.01 μ g/ml. Importantly, at the concentration of 1 μ g/ml, HAS1-F1 and HAS1-F2 showed a significant decrease in kinetoplast transcript expression to 47% (p -value = 0.0170) and 38% (p -value = 0.0029) respectively, as

compared to the untreated control (Figure 3C). Importantly, the potency of both fractions was higher than that of EABP0503, used as positive control (El Hajj et al., 2018) (Figure 3C). The infection of macrophages and the effect HAS1-F1 and HAS1-F2 fractions were then verified by H&E stain (Figure 3D), and quantified using the *Leishmania* Glycoprotein Gp63. Indeed, treatment with 1 μ g/ml of HAS1-F1 or HAS1-F2 significantly decreased the percentage of amastigotes, as compared to untreated or DMSO treated controls (Figure 3E). In more details, HAS1-F1 lessened the percentage of intracellular parasites to 62% (p -value = 0.0122), while HAS1-F2 reduced the percentage of internalized amastigotes to 50% (p -value = 0.0012). As for vehicle control, DMSO did not affect the replication of the intramacrophage amastigotes (Figures 3C,E). Importantly, no cytotoxic effect of either fractions on human peripheral blood mononuclear cells was observed, even at concentrations reaching 5 and 10 μ g/ml (Supplementary Figure S1).

We then assessed the potency of HAS1 INA and its bioactive fractions on the promastigote stages of the used *L. tropica* isolate. Interestingly, treatment of promastigotes with HAS1 INA, HAS1-F1, or HAS1-F2 decreased the motile promastigotes count (Figure 3F). Indeed, HAS one INA at the concentration of 0.01 μ g/ml exhibited the same potency as EABP0503 (positive control) and decreased the motile promastigote count to around 50% (p -value < 0.0001). HAS1-F1 or HAS1-F2, used at the concentration of 1 μ g/ml, also exhibited a significant effect on *L. tropica* motile promastigote count, but were less potent than the crude extract or the positive control, and led to decrease of 40% (p -value < 0.0001) and 32% (p -value < 0.0001) respectively (Figure 3F). Altogether, our results demonstrate the anti-leishmanial activity of HAS1-F1 and HAS1-F2 bioactive fractions on both the promastigote and amastigotes stages of the tested clinical *Leishmania tropica* isolate.

Structure elucidation of HAS-1 bioactive fraction F1

To elucidate the structure of the two active fractions, HAS1-F1 and HAS1-F2 were run on HPLC-MS (high resolution) in ESI



positive mode. HAS1-F1 gave a peak with m/z of 449.3585 for $[M + Na]$ and 427.3779 for $[M + H]$. The molecular formula generated from these peaks was $C_{26}H_{50}O_4$ with two double bonds. As for HAS1-F2, the peak had an m/z of 393.3443 for $[M + H]$ and a molecular formula of $C_{25}H_{45}O_3$ with four double bonds. While investigating the HPLC-MS of the crude extracts and the various fractions, HAS1-F2 was revealed as a shunt product from biosynthesis, that disappeared overtime when the fermentation was left longer. Hence the possible structure of HAS1-F1 was solely investigated using a Bruker 500 MHz Ascend HD NMR. The elucidation revealed an α -angelica lactone ring and an alcohol on the beta position of the ring (Figure 4). The remaining portion is a fatty acid (Figure 4). This is characteristic to acetogenins that have previously been reported from *Streptomyces* sp. (Taechowisan et al., 2016).

Discussion

Cutaneous Leishmaniasis remains one of the most important neglected tropical diseases worldwide (Cavalli and Bolognesi, 2009) with an alarming increase in CL incidence reported over the past decade (Bailey et al., 2017). In the EMR, Syria is characterized by the highest prevalence of CL (Mcdowell et al., 2011). The economic deterioration and the war in this country led to a huge displacement of refugees from endemic areas, leading to alarming increases of CL in the neighboring countries including Lebanon (Saroufim et al., 2014; Sharara and Kanj, 2014; Hayani et al., 2015; Al-Salem et al., 2016; Burza et al., 2018; Rehman et al., 2018; Bizri et al., 2021). *L. tropica* is among the most prevalent etiologic agents of CL among Syrian refugees (Saroufim et al., 2014; Bizri et al., 2021).

The treatment of CL still heavily relies on drugs exhibiting a plethora of adverse effects. In that sense, a staple among first-line CL therapies is the pentavalent antimonial Glucantime, which requires excessive repeated parenteral injections inducing localized painful sensation and systemic toxicity (Frezard et al., 2009). Moreover, resistance to Glucantime is emerging, reducing its efficiency in combating CL (Guerin et al., 2002). Second-line drugs against CL such as the antifungal Amphotericin B and the antiprotozoal Pentamidine still pose issues when utilized clinically as they also generate systemic toxicity (Oliveira et al., 2011). Although Miltefosine

was recognized as a good candidate for the bedside treatment of CL, evidence from preclinical and clinical studies pointed to the limitations of its use (Monge-Maillo and Lopez-Velez, 2015).

Natural Products were historically, and remain an invaluable source for drug discovery (Newman and Cragg, 2020). This interest in exploiting NPs to create new drug scaffolds has extended to include neglected tropical diseases. Accordingly, leishmaniasis was the target of many studies investigating the inhibitory effects of NPs on its causative species. The majority of NPs with antileishmanial activity originate from plants, namely those which are a part of traditional or folk medicine. Numerous plant-derived crude extracts and fractions revealed their ability to inhibit the replication of *Leishmania* sp. Promastigotes and amastigotes. Using bio-guided fractionation, a variety of structurally diverse antileishmanial pure compounds from NPs were isolated (Rocha et al., 2005; Gervazoni et al., 2020; Carter et al., 2021). In particular, the flavonol Quercetin and the flavonoid Rutin (Mehwish et al., 2019), the sesquiterpene (-)- α -Bisabolol (Corpas-Lopez et al., 2016), Epigallo-catechin 3-O-Gallate (Saduqi et al., 2019) inhibited the proliferation of both promastigotes and amastigotes of *L. tropica*. Furthermore, all these NPs demonstrated lower cytotoxicity levels when compared to the pentavalent antimonial control drug both *in vitro* and *in vivo*. Therefore, NPs offer a vital pool of structurally variable molecules that can compete in both effectiveness and safety with the clinically utilized antileishmanials.

The anti-infective efficacy of NPs depended historically on a genus of environmental bacteria known as *Streptomyces* (Antoraz et al., 2015; Quinn et al., 2020). The exploitation of *Streptomyces* sp. in the discovery of novel anti-parasitic agents is typically less common. Nevertheless, these bacteria yielded compounds with important medical efficacy. Ivermectin, a macrocyclic lactone from *Streptomyces avermitilis* is widely used to treat helminth infections (Chabala et al., 1980). The aminoglycoside Paromomycin from *Streptomyces rimosus* var. *Paromomycinus*, is prescribed for several parasitic infections including leishmaniasis (Wiwanitkit, 2012). We evaluated the anti-leishmanial potential of crude extracts produced by environmental *Streptomyces*, isolated from the understudied niche of the Lebanese soil. The crude extracts produced by *Streptomyces* species from Hasbaya region were the most potent in inhibiting intra-macrophagic *L. tropica* amastigotes *in vitro*. At a concentration as low as 0.01 μ g/ml, the crude HAS1 INA caused an almost complete inhibition of the replication of the intracellular amastigotes of an *L. tropica* clinical isolate. This immense activity has not been previously recorded for plants derived extracts tested as antileishmanial compounds against patient-derived internalized *L. tropica* amastigotes. In that sense, the methanolic extract of the leaves of *Myrtus communis* inhibited amastigote replication with an IC_{50} of 40.8 μ g/ml (Mahmoudvand et al., 2015), while the alcoholic extract of *Pistacia khinjuk* fruits decreased the

growth rate of intramacrophage amastigotes with an IC_{50} of 37.3 $\mu\text{g/ml}$ (Ezatpour et al., 2015).

Following bio-assayed fractionation, two novel compounds HAS1-F1 and HAS1-F2 inhibited the replication of these parasites. Our results follow a recent trend that revolves around screening NPs from *Streptomyces* for activity against *Leishmania* species. Indeed, an extract produced by *Streptomyces* sp. VITBVK2, isolated from a soil sample of a salt pan effectively killed intramacrophage *L. donovani* amastigotes at a dose of 100 $\mu\text{g/ml}$, and yielded same activity than Miltefosine (Sreedharan and Bhaskara Rao, 2017). Our crude extracts and their bioactive fractions exhibited anti-leishmanial potency 100 to 1,000 folds lower than the extract of VITBVK2. Under the same line, *Streptomyces* sp. isolated from Mediterranean sponges produced the cyclodepsipeptide Valinomycin and the indolocarbazole alkaloid Staurosporine, whose antileishmanial activities were unraveled for the first time. Both compounds inhibited the proliferation of *L. major* promastigotes with IC_{50} values less than 0.11 and 5.3 μM respectively (Pimentel-Elardo et al., 2010). HAS1-F1 and HAS1-F2 inhibited the replication of *L. tropica* amastigotes at doses of 2.3 and 2.5 μM , which are of similar order to that of Staurosporine. Beyond CL, compounds secreted by ants-associated *Streptomyces* sp. inhibited *L. donovani*, the causative agent of another spectrum of leishmaniasis, the fatal visceral leishmaniasis. Indeed, Ortega et al. isolated four known molecules (Mer-A2026B, piericidin-A1, Dinactin, and Nigericin) from three different *Streptomyces* sp. originating from attine ants and reported their antileishmanial activity against *L. donovani* promastigotes (Ortega et al., 2021). Importantly, Dinactin and Nigericin showed superior action than Miltefosine, and were extremely effective in the eradication of the intramacrophage *L. donovani* amastigotes with IC_{50} values of 0.018 and 0.129 μM respectively. Although these compounds are of higher order of activity than HAS1-F1 and HAS1-F2, their cytotoxicity against THP-1 macrophages was extremely elevated (Ortega et al., 2019). The same research group further isolated from the ant-associated *Streptomyces* sp. ISID311, three structurally related macrolides, Cyphomycin, Caniferolide C, and GT-35 which all displayed activity against *L. donovani* promastigotes and intracellular amastigotes (Ortega et al., 2021). Cyphomycin inhibited the replication of intracellular amastigotes with a concentration similar to the HAS1 derived compounds (2.32 μM) while demonstrating low cytotoxicity. Caniferolide C and GT-35 were more potent (IC_{50} of 0.091 and 0.073 μM respectively) yet showcased intense cytotoxic effects on macrophages.

HAS1-F1 and HAS1-F2 belong to a family of compounds named acetogenins. These polyketide natural products were extensively investigated for their antileishmanial activities. Squamocin and Senegalene were efficient in reducing the proliferation of *L. major* and *L. donovani* promastigotes *in vitro*. The compounds had minimal effective concentrations (MECs), where negative growth was observed, ranging between 25 and 50 $\mu\text{g/ml}$ after 24 h (Sahpaz et al., 1994). Moreover, Squamocin alongside with Rolliniastatine one lysed the promastigotes of several

Leishmania strains at a dose of 5 $\mu\text{g/ml}$, similar to the control drug pentamidine (Fevrier et al., 1999). Our results showed around five folds higher efficacy of HAS1-F1 and HAS1-F2, against *L. tropica* amastigotes. Nonetheless, the expression levels of the *Leishmania*-specific kinetoplast markers and its Gp63 decreased significantly upon treatment with either drug as compared to the Untreated infected controls, likely suggestive of an anti-parasitic mode of action. This finding is in line with previously isolated acetogenins such as Rolliniastatin one which limited the replication of both intracellular amastigotes as well as the extracellular promastigotes of *L. donovani* (Raynaud-Le Grandic et al., 2004). Furthermore, four acetogenins isolated from the seeds of *Porcelia macrocarpa* showed anti-leishmanial activity on the amastigotes of *L. infantum*. Among these, the compound (2S,3R,4R)-3-hydroxy-4-methyl-2-(eicos-11'-yn-19'-enyl) butanolide had an IC_{50} of 29.9 μM with no cytotoxic effects on the NCTC cell line (Brito et al., 2022). Although most of the compounds in this family originate from plants, recent evidence shows that *Streptomyces* species can generate acetogenins. In that regard, *Streptomyces* sp. VE2, was able to secrete acetogenins with antibacterial and antioxidant activities (Taechowisan et al., 2016). Therefore, our study is the first to report the isolation of novel acetogenins from a previously uncultured *Streptomyces* sp. HAS1, that were able to inhibit the replication of *L. tropica* amastigotes *in vitro*. Our work marks the first recorded case about establishing a pipeline that screens SMs produced by bacteria against *L. tropica*, the major causative agent of CL in the EMR region, and foreshadows the invaluable opportunities to screen SMs produced by *Streptomyces* for CL treatment.

Data availability statement

The datasets presented in this study can be found in online repositories. The names of the repository/repositories and accession number(s) can be found below: <https://www.ncbi.nlm.nih.gov/bioproject/PRJNA873891>.

Ethics statement

The studies involving human participants were reviewed and approved by Sample collection was approved by the Institutional Review Board of the American University of Beirut (PALK.IK.01). The patients/participants provided their written informed consent to participate in this study.

Author contributions

BA, MH, RH, GD, RN, PM and DA, performed experiments; BA, MH, and RH analyzed results; BA, AF and HH made the Figures; AF and HH designed the research; BA, AF and HH wrote the paper.

Funding

This work was made possible through the support from the Medical Practice Plan (Faculty of Medicine, American University of Beirut).

Acknowledgments

We thank the American University of Beirut Core Facilities for providing access to their imaging, Animal Care, and core culture facilities. We also thank the Office of Grants and Contracts at the American University of Beirut. The authors would also like to acknowledge the National Council for Scientific Research of Lebanon (CNRS-L) for granting a doctoral fellowship to BA. This fellowship was offered in collaboration with the American University of Beirut (AUB).

Conflict of interest

The authors declare that the research was conducted in the absence of any commercial or financial relationships that could be construed as a potential conflict of interest.

References

- Al-Salem, W. S., Pigott, D. M., Subramaniam, K., Haines, L. R., Kelly-Hope, L., Molyneux, D. H., et al. (2016). Cutaneous leishmaniasis and conflict in Syria. *Emerg. Infect. Dis.* 22, 931–933. doi:10.3201/eid2205.160042
- Antoraz, S., Santamaria, R. I., Diaz, M., Sanz, D., and Rodriguez, H. (2015). Toward a new focus in antibiotic and drug discovery from the *Streptomyces* arsenal. *Front. Microbiol.* 6, 461. doi:10.3389/fmicb.2015.00461
- Arevalo, I., Tulliano, G., Quispe, A., Spaeth, G., Matlashewski, G., Llanos-Cuentas, A., et al. (2007). Role of imiquimod and parenteral meglumine antimoniate in the initial treatment of cutaneous leishmaniasis. *Clin. Infect. Dis.* 44, 1549–1554. doi:10.1086/518172
- Arevalo, I., Ward, B., Miller, R., Meng, T. C., Najjar, E., Alvarez, E., et al. (2001). Successful treatment of drug-resistant cutaneous leishmaniasis in humans by use of imiquimod, an immunomodulator. *Clin. Infect. Dis.* 33, 1847–1851. doi:10.1086/324161
- Bailey, F., Mondragon-Shem, K., Hotez, P., Ruiz-Postigo, J. A., Al-Salem, W., Acosta-Serrano, A., et al. (2017). A new perspective on cutaneous leishmaniasis: Implications for global prevalence and burden of disease estimates. *PLoS Negl. Trop. Dis.* 11, e0005739. doi:10.1371/journal.pntd.0005739
- Bizri, N. A., Alam, W., Khoury, M., Musharrafieh, U., Ghosn, N., Berri, A., et al. (2021). The association between the Syrian crisis and cutaneous leishmaniasis in Lebanon. *Acta Parasitol.* 66, 1240–1245. doi:10.1007/s11686-021-00395-3
- Bolger, A. M., Lohse, M., and Usadel, B. (2014). Trimmomatic: A flexible trimmer for Illumina sequence data. *Bioinformatics* 30, 2114–2120. doi:10.1093/bioinformatics/btu170
- Briones Nieva, C. A., Cid, A. G., Romero, A. I., Garcia-Bustos, M. F., Villegas, M., and Bermudez, J. M. (2021). An appraisal of the scientific current situation and new perspectives in the treatment of cutaneous leishmaniasis. *Acta Trop.* 221, 105988. doi:10.1016/j.actatropica.2021.105988
- Brito, I. A., Thevenard, F., Costa-Silva, T. A., Oliveira, S. S., Cunha, R., De Oliveira, E. A., et al. (2022). Antileishmanial effects of acetylene acetogenins from seeds of *Porcelia macrocarpa* (warm.) R.E. Fries (annonaceae) and semisynthetic derivatives. *Molecules* 27, 893. doi:10.3390/molecules27030893
- Burza, S., Croft, S. L., and Boelaert, M. (2018). Leishmaniasis. *Lancet* 392, 951–970. doi:10.1016/S0140-6736(18)31204-2
- Carter, N. S., Stamper, B. D., Elbarbry, F., Nguyen, V., Lopez, S., Kawasaki, Y., et al. (2021). Natural products that target the arginase in *Leishmania* parasites hold therapeutic promise. *Microorganisms* 9, 267. doi:10.3390/microorganisms9020267
- Cavalli, A., and Bolognesi, M. L. (2009). Neglected tropical diseases: Multi-target-directed ligands in the search for novel lead candidates against trypanosoma and *Leishmania*. *J. Med. Chem.* 52, 7339–7359. doi:10.1021/jm9004835
- Chabala, J. C., Mrozik, H., Tolman, R. L., Eskola, P., Lusi, A., Peterson, L. H., et al. (1980). Ivermectin, a new broad-spectrum antiparasitic agent. *J. Med. Chem.* 23, 1134–1136. doi:10.1021/jm00184a014
- Chin, Y. W., Balunas, M. J., Chai, H. B., and Kinghorn, A. D. (2006). Drug discovery from natural sources. *AAPS J.* 8, E239–E253. doi:10.1007/BF02854894
- Cordell, G. A. (2000). Biodiversity and drug discovery—a symbiotic relationship. *Phytochemistry* 55, 463–480. doi:10.1016/s0031-9422(00)00230-2
- Corpas-Lopez, V., Merino-Espinosa, G., Diaz-Saez, V., Morillas-Marquez, F., Navarro-Moll, M. C., and Martin-Sanchez, J. (2016). The sesquiterpene (-)-alpha-bisabolol is active against the causative agents of Old World cutaneous leishmaniasis through the induction of mitochondrial-dependent apoptosis. *Apoptosis* 21, 1071–1081. doi:10.1007/s10495-016-1282-x
- Eiras, D. P., Kirkman, L. A., and Murray, H. W. (2015). Cutaneous leishmaniasis: Current treatment practices in the USA for returning travelers. *Curr. Treat. Options Infect. Dis.* 7, 52–62. doi:10.1007/s40506-015-0038-4
- El Hajj, R., Bou Youness, H., Lachaud, L., Bastien, P., Masquefa, C., Bonnet, P. A., et al. (2018). EAPB0503: An Imiquimod analog with potent *in vitro* activity against cutaneous leishmaniasis caused by *Leishmania* major and *Leishmania tropica*. *PLoS Negl. Trop. Dis.* 12, e0006854. doi:10.1371/journal.pntd.0006854
- Esfandiarpour, I., and Alavi, A. (2002). Evaluating the efficacy of allopurinol and meglumine antimoniate (Glucantime) in the treatment of cutaneous leishmaniasis. *Int. J. Dermatol.* 41, 521–524. doi:10.1046/j.1365-4362.2002.01526.x
- Ezatpour, B., Saedi Dezaki, E., Mahmoudvand, H., Azadpour, M., and Ezzatkah, F. (2015). *In vitro* and *in vivo* antileishmanial effects of *Pistacia khinjuk* against *Leishmania tropica* and *Leishmania major*. *Evid. Based. Complement. Altern. Med.* 2015, 149707. doi:10.1155/2015/149707
- Fakhar, M., Pazoki Ghohe, H., Rasooli, S. A., Karamian, M., Mohib, A. S., Ziari Hezarjaribi, H., et al. (2016). Genetic diversity of *Leishmania tropica* strains isolated

Publisher's note

All claims expressed in this article are solely those of the authors and do not necessarily represent those of their affiliated organizations, or those of the publisher, the editors and the reviewers. Any product that may be evaluated in this article, or claim that may be made by its manufacturer, is not guaranteed or endorsed by the publisher.

Supplementary material

The Supplementary Material for this article can be found online at: <https://www.frontiersin.org/articles/10.3389/fphar.2022.1023114/full#supplementary-material>

SUPPLEMENTARY FIGURE S1

Cytotoxicity testing of HAS1-F1 and HAS1-F2. Peripheral blood mononuclear cells were incubated with different concentrations of HAS1-F1 or HAS1-F2 (1, 5, or 10 µg/ml) for 24 h. Living cells were counted using the Trypan Blue exclusion dye assay. Results are expressed as percentage of the untreated control (±) SEM are representative of three independent experiments. To validate statistical significance, t-tests were used, and no significance was recorded when comparing any of the treatment groups to the control group.

from clinical forms of cutaneous leishmaniasis in rural districts of Herat province, Western Afghanistan, based on ITS1-rDNA. *Infect. Genet. Evol.* 41, 120–127. doi:10.1016/j.meegid.2016.03.031

Fevrier, A., Ferreira, M. E., Fournet, A., Yaluff, G., Inchausti, A., Rojas De Arias, A., et al. (1999). Acetogenins and other compounds from *Rollinia emarginata* and their antiprotozoal activities. *Planta Med.* 65, 47–49. doi:10.1055/s-1999-13961

Firooz, A., Khamesipour, A., Ghoorchi, M. H., Nassiri-Kashani, M., Eskandari, S. E., Khatami, A., et al. (2006). Imiquimod in combination with meglumine antimoniate for cutaneous leishmaniasis: A randomized assessor-blind controlled trial. *Arch. Dermatol.* 142, 1575–1579. doi:10.1001/archderm.142.12.1575

Frezard, F., Demicheli, C., and Ribeiro, R. R. (2009). Pentavalent antimonials: New perspectives for old drugs. *Molecules* 14, 2317–2336. doi:10.3390/molecules14072317

Garza-Tovar, T. F., Sacriste-Hernandez, M. I., Juarez-Duran, E. R., and Arenas, R. (2020). An overview of the treatment of cutaneous leishmaniasis. *Fac. Rev.* 9, 28. doi:10.12703/r/9-28

Gervazoni, L. F. O., Barcellos, G. B., Ferreira-Paes, T., and Almeida-Amaral, E. E. (2020). Use of natural products in leishmaniasis chemotherapy: An overview. *Front. Chem.* 7, 579891. doi:10.3389/fchem.2020.579891

Guerin, P. J., Oliaro, P., Sundar, S., Boelaert, M., Croft, S. L., Desjeux, P., et al. (2002). Visceral leishmaniasis: Current status of control, diagnosis, and treatment, and a proposed research and development agenda. *Lancet. Infect. Dis.* 2, 494–501. doi:10.1016/s1473-3099(02)00347-x

Hayani, K., Dandashli, A., and Weisshaar, E. (2015). Cutaneous leishmaniasis in Syria: Clinical features, current status and the effects of war. *Acta Derm. Venereol.* 95, 62–66. doi:10.2340/00015555-1988

Heras-Mosteiro, J., Monge-Maillo, B., Pinart, M., Lopez Pereira, P., Reveiz, L., Garcia-Carrasco, E., et al. (2017). Interventions for old World cutaneous leishmaniasis. *Cochrane Database Syst. Rev.* 12, CD005067. doi:10.1002/14651858.CD005067.pub5

Kazemi-Rad, E., Mohebbi, M., Khadem-Erfan, M. B., Hajjaran, H., Hadighi, R., Khamesipour, A., et al. (2013a). Overexpression of ubiquitin and amino acid permease genes in association with antimony resistance in *Leishmania tropica* field isolates. *Korean J. Parasitol.* 51, 413–419. doi:10.3347/kjp.2013.51.4.413

Kazemi-Rad, E., Mohebbi, M., Khadem-Erfan, M. B., Saffari, M., Raoofian, R., Hajjaran, H., et al. (2013b). Identification of antimony resistance markers in *Leishmania tropica* field isolates through a cDNA-AFLP approach. *Exp. Parasitol.* 135, 344–349. doi:10.1016/j.exppara.2013.07.018

Larsen, M. V., Cosentino, S., Lukjancenko, O., Saputra, D., Rasmussen, S., Hasman, H., et al. (2014). Benchmarking of methods for genomic taxonomy. *J. Clin. Microbiol.* 52, 1529–1539. doi:10.1128/JCM.02981-13

Lefevre, F., Robe, P., Jarrin, C., Ginolhac, A., Zago, C., Auriol, D., et al. (2008). Drugs from hidden bugs: Their discovery via untapped resources. *Res. Microbiol.* 159, 153–161. doi:10.1016/j.resmic.2007.12.011

Mahmoudvand, H., Ezzatkah, F., Sharififar, F., Sharifi, I., and Dezaki, E. S. (2015). Antileishmanial and cytotoxic effects of essential oil and methanolic extract of *Myrtus communis* L. *Korean J. Parasitol.* 53, 21–27. doi:10.3347/kjp.2015.53.1.21

Masmoudi, A., Hariz, W., Marrekchi, S., Amouri, M., and Turki, H. (2013). Old World cutaneous leishmaniasis: Diagnosis and treatment. *J. Dermatol. Case Rep.* 7, 31–41. doi:10.3315/jdcr.2013.1135

Mcdowell, M. A., Rafati, S., Ramalho-Ortigao, M., and Ben Salah, A. (2011). Leishmaniasis: Middle East and north africa research and development priorities. *PLoS Negl. Trop. Dis.* 5, e1219. doi:10.1371/journal.pntd.0001219

Mehwish, S., Khan, H., Rehman, A. U., Khan, A. U., Khan, M. A., Hayat, O., et al. (2019). Natural compounds from plants controlling leishmanial growth via DNA damage and inhibiting trypanothione reductase and trypanothione synthetase: An *in vitro* and *in silico* approach. *3 Biotech.* 9, 303. doi:10.1007/s13205-019-1826-1

Miranda-Verastegui, C., Tulliano, G., Gyorkos, T. W., Calderon, W., Rahme, E., Ward, B., et al. (2009). First-line therapy for human cutaneous leishmaniasis in Peru using the TLR7 agonist imiquimod in combination with pentavalent antimony. *PLoS Negl. Trop. Dis.* 3, e491. doi:10.1371/journal.pntd.0000491

Mohebbi, M., Kazemirad, E., Hajjaran, H., Kazemirad, E., Oshaghi, M. A., Raoofian, R., et al. (2019). Gene expression analysis of antimony resistance in *Leishmania tropica* using quantitative real-time PCR focused on genes involved in trypanothione metabolism and drug transport. *Arch. Dermatol. Res.* 311, 9–17. doi:10.1007/s00403-018-1872-2

Monge-Maillo, B., and Lopez-Velez, R. (2015). Miltefosine for visceral and cutaneous leishmaniasis: Drug characteristics and evidence-based treatment recommendations. *Clin. Infect. Dis.* 60, 1398–1404. doi:10.1093/cid/civ004

Newman, D. J., and Cragg, G. M. (2020). Natural products as sources of new drugs over the nearly four decades from 01/1981 to 09/2019. *J. Nat. Prod.* 83, 770–803. doi:10.1021/acs.jnatprod.9b01285

Oliveira, L. F., Schubach, A. O., Martins, M. M., Passos, S. L., Oliveira, R. V., Marzochi, M. C., et al. (2011). Systematic review of the adverse effects of cutaneous leishmaniasis treatment in the New World. *Acta Trop.* 118, 87–96. doi:10.1016/j.actatropica.2011.02.007

Ortega, H. E., Ferreira, L. L. G., Melo, W. G. P., Oliveira, A. L. L., Ramos Alvarenga, R. F., Lopes, N. P., et al. (2019). Antifungal compounds from *Streptomyces* associated with attine ants also inhibit *Leishmania donovani*. *PLoS Negl. Trop. Dis.* 13, e0007643. doi:10.1371/journal.pntd.0007643

Ortega, H. E., Lourenzon, V. B., Chevrette, M. G., Ferreira, L. L. G., Alvarenga, R. F. R., Melo, W. G. P., et al. (2021). Antileishmanial macrolides from ant-associated *Streptomyces* sp. ISID311. *Bioorg. Med. Chem.* 32, 116016. doi:10.1016/j.bmc.2021.116016

Ozbilgin, A., Zeyrek, F. Y., Guray, M. Z., Culha, G., Akyar, I., Harman, M., et al. (2020). Determination of antimony resistance mechanism of *Leishmania tropica* causing cutaneous leishmaniasis in Turkey. *Mikrobiyol. Bul.* 54, 444–462. doi:10.5578/mb.69702

Palumbo, E. (2009). Current treatment for cutaneous leishmaniasis: A review. *Am. J. Ther.* 16, 178–182. doi:10.1097/MJT.0b013e3181822e90

Pimentel-Elardo, S. M., Kozyska, S., Bugni, T. S., Ireland, C. M., Moll, H., and Hentschel, U. (2010). Anti-parasitic compounds from *Streptomyces* sp. strains isolated from Mediterranean sponges. *Mar. Drugs* 8, 373–380. doi:10.3390/md8020373

Pink, R., Hudson, A., Mouries, M. A., and Bendig, M. (2005). Opportunities and challenges in antiparasitic drug discovery. *Nat. Rev. Drug Discov.* 4, 727–740. doi:10.1038/nrd1824

Quinn, G. A., Banat, A. M., Abdelhameed, A. M., and Banat, I. M. (2020). *Streptomyces* from traditional medicine: Sources of new innovations in antibiotic discovery. *J. Med. Microbiol.* 69, 1040–1048. doi:10.1099/jmm.0.001232

Raynaud-Le Grandic, S., Fourneau, C., Laurens, A., Bories, C., Hocquemiller, R., and Loiseau, P. M. (2004). *In vitro* antileishmanial activity of acetogenins from Annonaceae. *Biomed. Pharmacother.* 58, 388–392. doi:10.1016/j.biopha.2004.02.007

Rehman, K., Walochnik, J., Mischlinger, J., Alaliss, B., Allan, R., and Ramharter, M. (2018). Leishmaniasis in northern Syria during civil war. *Emerg. Infect. Dis.* 24, 1973–1981. doi:10.3201/eid2411.172146

Reithinger, R. (2016). Global burden of cutaneous leishmaniasis. *Lancet. Infect. Dis.* 16, 1004–1005. doi:10.1016/S1473-3099(16)30195-5

Roberts, M. T. (2005). Current understandings on the immunology of leishmaniasis and recent developments in prevention and treatment. *Br. Med. Bull.* 75-76, 115–130. doi:10.1093/bmb/ldl003

Rocha, L. G., Almeida, J. R., Macedo, R. O., and Barbosa-Filho, J. M. (2005). A review of natural products with antileishmanial activity. *Phytomedicine* 12, 514–535. doi:10.1016/j.phymed.2003.10.006

Sadui, M., Sharifi, I., Babaei, Z., Keyhani, A., Mostafavi, M., Hakimi Parizi, M., et al. (2019). Anti-leishmanial and immunomodulatory effects of epigallocatechin 3-O-gallate on *Leishmania tropica*: Apoptosis and gene expression profiling. *Iran. J. Parasitol.* 14, 521–533.

Sahpaz, S., Bories, C., Loiseau, P. M., Cortes, D., Hocquemiller, R., Laurens, A., et al. (1994). Cytotoxic and antiparasitic activity from *Annona senegalensis* seeds. *Planta Med.* 60, 538–540. doi:10.1055/s-2006-959566

Saroufim, M., Charafeddine, K., Issa, G., Khalifeh, H., Habib, R. H., Berry, A., et al. (2014). Ongoing epidemic of cutaneous leishmaniasis among Syrian refugees, Lebanon. *Emerg. Infect. Dis.* 20, 1712–1715. doi:10.3201/eid2010.140288

Schmittgen, T. D., and Livak, K. J. (2008). Analyzing real-time PCR data by the comparative C(T) method. *Nat. Protoc.* 3, 1101–1108. doi:10.1038/nprot.2008.73

Sharara, S. L., and Kanj, S. S. (2014). War and infectious diseases: Challenges of the Syrian civil war. *PLoS Pathog.* 10, e1004438. doi:10.1371/journal.ppat.1004438

Sharma, N. L., Mahajan, V. K., Kanga, A., Sood, A., Katoch, V. M., Mauricio, I., et al. (2005). Localized cutaneous leishmaniasis due to *Leishmania donovani* and *Leishmania tropica*: Preliminary findings of the study of 161 new cases from a new endemic focus in Himachal Pradesh, India. *Am. J. Trop. Med. Hyg.* 72, 819–824. doi:10.4269/ajtmh.2005.72.819

Sreedharan, V., and Bhaskara Rao, K. V. (2017). Efficacy of protease inhibitor from marine *Streptomyces* sp. VITBVK2 against *Leishmania donovani* - an *in vitro* study. *Exp. Parasitol.* 174, 45–51. doi:10.1016/j.exppara.2017.02.007

Steverding, D. (2017). The history of leishmaniasis. *Parasit. Vectors* 10, 82. doi:10.1186/s13071-017-2028-5

- Taechowisan, T., Singtotong, C., and Phutdhawong, W. S. (2016). Antibacterial and antioxidant activities of acetogenins from *Streptomyces* sp. VE2; an endophyte in *vernonia cinerea* (L.) less. *J. Appl. Pharm. Sci.* 6, 067–072. doi:10.7324/japs.2016.60810
- Torres-Bacete, J., Arroyo, M., Torres-Guzman, R., De La Mata, I., Acebal, C., and Castillon, M. P. (2005). Optimization of culture medium and conditions for penicillin acylase production by *Streptomyces lavendulae* ATCC 13664. *Appl. Biochem. Biotechnol.* 126, 119–132. doi:10.1385/abab:126:2:119
- Torres-Guerrero, E., Quintanilla-Cedillo, M. R., Ruiz-Esmenjaud, J., and Arenas, R. (2017F1000). *Leishmaniasis a Rev.* 6, 750.
- Tulp, M., and Bohlin, L. (2002). Functional versus chemical diversity: Is biodiversity important for drug discovery? *Trends Pharmacol. Sci.* 23, 225–231. doi:10.1016/s0165-6147(02)02007-2
- Wick, R. R., Judd, L. M., Gorrie, C. L., and Holt, K. E. (2017). Completing bacterial genome assemblies with multiplex MinION sequencing. *Microb. Genom.* 3, e000132. doi:10.1099/mgen.0.000132
- Wiwanitkit, V. (2012). Interest in paromomycin for the treatment of visceral leishmaniasis (kala-azar). *Ther. Clin. Risk Manag.* 8, 323–328. doi:10.2147/TCRM.S30139
- Zhu, F., Ma, X. H., Qin, C., Tao, L., Liu, X., Shi, Z., et al. (2012). Drug discovery prospect from untapped species: Indications from approved natural product drugs. *PLoS One* 7, e39782. doi:10.1371/journal.pone.0039782
- Zhu, F., Qin, C., Tao, L., Liu, X., Shi, Z., Ma, X., et al. (2011). Clustered patterns of species origins of nature-derived drugs and clues for future bioprospecting. *Proc. Natl. Acad. Sci. U. S. A.* 108, 12943–12948. doi:10.1073/pnas.1107336108



OPEN ACCESS

EDITED BY
Hina Siddiqui,
University of Karachi, Pakistan

REVIEWED BY
Angela Bisio,
University of Genoa, Italy
Saima Rasheed,
University of Karachi, Pakistan

*CORRESPONDENCE
Abdullah Shaito,
abdshaito@qu.edu.qa
Marc Maresca,
m.maresca@univ-amu.fr
Elias Baydoun,
eliasbay@aub.edu.lb

SPECIALTY SECTION
This article was submitted to
Experimental Pharmacology and Drug
Discovery,
a section of the journal
Frontiers in Pharmacology

RECEIVED 14 July 2022
ACCEPTED 12 September 2022
PUBLISHED 10 October 2022

CITATION
Mesmar J, Abdallah R, Hamade K,
Baydoun S, Al-Thani N, Shaito A,
Maresca M, Badran A and Baydoun E
(2022), Ethanolic extract of *Origanum
syriacum* L. leaves exhibits potent anti-
breast cancer potential and robust
antioxidant properties.
Front. Pharmacol. 13:994025.
doi: 10.3389/fphar.2022.994025

COPYRIGHT
© 2022 Mesmar, Abdallah, Hamade,
Baydoun, Al-Thani, Shaito, Maresca,
Badran and Baydoun. This is an open-
access article distributed under the
terms of the [Creative Commons
Attribution License \(CC BY\)](#). The use,
distribution or reproduction in other
forums is permitted, provided the
original author(s) and the copyright
owner(s) are credited and that the
original publication in this journal is
cited, in accordance with accepted
academic practice. No use, distribution
or reproduction is permitted which does
not comply with these terms.

Ethanolic extract of *Origanum syriacum* L. leaves exhibits potent anti-breast cancer potential and robust antioxidant properties

Joelle Mesmar¹, Rola Abdallah¹, Kamar Hamade²,
Serine Baydoun³, Najlaa Al-Thani⁴, Abdullah Shaito^{5*},
Marc Maresca^{6*}, Adnan Badran⁷ and Elias Baydoun^{1*}

¹Department of Biology, American University of Beirut, Beirut, Lebanon, ²UMRT INRE 1158 BioEcoAgro, Laboratoire BIOPI, University of Picardie Jules Verne, Amiens, France, ³Breast Imaging Section, Imaging Institute, Cleveland Clinic Foundation, Cleveland, OH, United States, ⁴Research and Development Department, Barzan Holdings, Doha, Qatar, ⁵Biomedical Research Center, College of Medicine, and Department of Biomedical Sciences at College of Health Sciences, Qatar University, Doha, Qatar, ⁶Aix-Marseille University, CNRS, Centrale Marseille, iSm2, Marseille, France, ⁷Department of Nutrition, University of Petra, Amman, Jordan

Background: Breast cancer (BC) is the second most common cancer overall. In women, BC is the most prevalent cancer and the leading cause of cancer-related mortality. Triple-negative BC (TNBC) is the most aggressive BC, being resistant to hormonal and targeted therapies. Hypothesis/Purpose: The medicinal plant *Origanum syriacum* L. is a shrubby plant rich in bioactive compounds and widely used in traditional medicine to treat various diseases. However, its therapeutic potential against BC remains poorly investigated. In the present study, we screened the phytochemical content of an ethanolic extract of *O. syriacum* (OSEE) and investigated its anticancer effects and possible underlying mechanisms of action against the aggressive and highly metastatic human TNBC cell line MDA-MB-231. Methods: MTT, trans-well migration, and scratch assays were used to assess cell viability, invasion, or migration, respectively. Antioxidant potential was evaluated *in vitro* using the DPPH radical-scavenging assay and levels of reactive oxygen species (ROS) were assessed in cells in culture using DHE staining. Aggregation assays were used to determine cell-cell adhesion. Flow cytometry was used to analyze cell cycle progression. Protein levels of markers of apoptosis (BCL-2, pro-Caspase3, p53), proliferation (p21, Ki67), cell migration, invasion, or adhesion (FAK, E-cadherin), angiogenesis (iNOS), and cell signaling (STAT3, p38) were determined by immunoblotting. A chorioallantoic Membrane (CAM) assay evaluated *in ovo* angiogenesis. Results: We demonstrated that OSEE had potent radical scavenging activity *in vitro* and induced the generation of ROS in MDA-MB-231 cells, especially at higher OSEE concentrations. Non-cytotoxic concentrations of OSEE attenuated cell proliferation and induced G₀/G₁ cell cycle arrest, which was associated with phosphorylation of p38 MAPK, an increase in the levels of tumor suppressor protein p21, and a decrease of proliferation marker protein Ki67. Additionally, only higher concentrations of OSEE were able to attenuate inhibition of proliferation induced by the ROS scavenger N-acetyl cysteine (NAC), indicating that the anti-proliferative effects

of OSEE could be ROS-dependent. OSEE stimulated apoptosis and its effector Caspase-3 in MDA-MB-231 cells, in correlation with activation of the STAT3/p53 pathway. Furthermore, the extract reduced the migration and invasive properties of MDA-MB-231 cells through the deactivation of focal adhesion kinase (FAK). OSEE also reduced the production of inducible nitric oxide synthase (iNOS) and inhibited *in ovo* angiogenesis. Conclusion: Our findings reveal that OSEE is a rich source of phytochemicals and has robust anti-breast cancer properties that significantly attenuate the malignant phenotype of MDA-MB-231 cells, suggesting that *O. syriacum* may not only act as a rich source of potential TNBC therapeutics but may also provide new avenues for the design of novel TNBC drugs.

KEYWORDS

herbal medicine, phytochemical content, breast cancer, metastasis, oxidative stress, reactive oxygen species, ROS, *Origanum syriacum* L

1 Introduction

Cancer is a leading cause of death worldwide, having claimed an estimated 10 million deaths in 2020. Breast cancer (BC) is the most common cause of new cancer cases and the fifth leading-cause of cancer-related deaths (Who, 2021). Moreover, the incidence of BC has increased significantly in recent years to become the world's most prevalent cancer (Breast Cancer, 2021). Despite significant advancements in treatment regimens and modalities, treatment of most types of breast cancer is still limited to surgery, chemotherapy, and irradiation. Hormone replacement therapy can be used for breast cancer subtypes that are positive for the estrogen receptor (ER) or progesterone receptor (PR), while targeted therapies using antibodies, like trastuzumab, is effective against breast cancers that over-express human epidermal growth factor receptor (HER2). Triple-negative breast cancer (TNBC) accounts for 10–20% of BC cases. Lacking the overexpression of HER2 and being negative for ER and PR, TNBC does not respond to targeted or hormone replacement therapies. As such, TNBC is an aggressive BC subtype that is associated with poor prognosis (Breastcancer.org), mandating that alternative treatment approaches be sought. In this regard, therapeutic approaches using plant sources have been gaining interest and popularity (Howes, 2018). Contextually, women have an inclination for the use of natural products and herbal remedies as these are claimed to be safer alternatives without significant side effects compared with conventional medicines (Cassidy, 2003). Furthermore, plants have a long history in the treatment of cancer and have been a source of several anticancer drugs (Cragg and Newman, 2005; Buyel, 2018).

Origanum syriacum L. is an aromatic perennial shrub native to the Mediterranean region and widely used in culinary practices. It has also been traditionally used in folk medicine to relieve stomach pain and in the treatment of colds and toothaches (Alwafa et al., 2021). In recent years, it has been reported to be rich in bioactive compounds such as flavonoids,

glycosides, terpenes, and phenols (Mesmar et al., 2022). These bioactive compounds bestow the plant with various pharmacological properties including antioxidant, anti-inflammatory, anticancer, antimicrobial, and neuroprotective effects, among others (Alwafa et al., 2021). Importantly, its extracts have been documented to inhibit the proliferation of human BC MCF-7 cells (Al-Kalaldeh et al., 2010; Husein et al., 2014) and leukemic TH-1 cells (Ayesh et al., 2014). This prompted the investigation of the effects of the plant in the context of the aggressive TNBC subtype, using MDA-MB-231 BC cells as an *in vitro* model of TNBC.

In this study, we screened the phytochemical constituents of an ethanolic extract of *O. syriacum* (OSEE) and tested its effect on the malignant phenotype of MDA-MB-231 cells, aiming to uncover the possible molecular mechanisms behind its anticancer activity. We report that OSEE has a potent antioxidant activity. Importantly, OSEE inhibited the proliferation of TNBC cells by causing a G₀/G₁ phase arrest, concomitant with a decrease of Ki67 levels and an increase of p21 levels. OSEE significantly inhibited MDA-MB-231 cell growth and metastatic properties by inhibiting proliferative signaling, activating suppressors of cell growth, enhancing apoptotic cell-death machinery, reducing migration and invasion of MDA-MB-231 cells, in addition to inhibiting angiogenesis in a process that correlated with inhibition of iNOS. Mechanistically, OSEE inhibited STAT3 signaling and activated the p38 MAPK pathway, implicating a crosstalk between p21, p53, iNOS, and reactive oxygen species (ROS).

2 Materials and methods

2.1 *O. syriacum* ethanolic extract

Leaves of *O. syriacum* were collected from South of Lebanon in the spring season (April–June) of 2020 and 2021. The plant was identified as *Origanum syriacum* L. by Mohammad Al Zein, a

plant taxonomist at the Biology Department, American University of Beirut (AUB), and a voucher specimen has been deposited at the Post Herbarium (AUB), under number MSA 2020–1. The leaves were rinsed and air-dried in the dark at room temperature, then ground into a fine powder and suspended in 80% ethanol [20 ml of distilled water and 80 ml of absolute ethanol (Fisher Scientific; U.K)] for 72 h in the dark. The suspension was then filtered, dried using a rotary vacuum evaporator and lyophilized. The obtained powder was dissolved in 80% ethanol at a concentration of 200 mg/ml and stored at 4°C.

2.2 Phytochemical analysis

Test for tannins: 5 ml of distilled water was added to 0.5 g of the plant extract and ultrasonicated for 15 min at 80°C. The mixture was filtered, cooled down to room temperature, and five drops of 0.1%-FeCl₃ added to the filtrate. Brownish green or blue-black coloration indicated the presence of tannins (Keo et al., 2017).

Test for resins: 5 ml of distilled water was added to 0.5 g of the plant extract and ultrasonicated for 15 min at 30°C. Then, the mixture was filtered. The presence of resins was indicated by turbidity of the filtrate (Keo et al., 2017).

Test for saponins: 5 ml of distilled water was added to 0.5 g of the plant extract and ultrasonicated for 15 min at 80°C. The mixture was filtered, cooled down to room temperature, and then shaken until the formation of a stable persistent froth, which indicated the presence of saponins (Keo et al., 2017).

Test for phenolic compounds: 0.5 g of the plant extract was mixed with 5 ml of ethanol and ultrasonicated for 15 min at 30°C. The mixture was filtered and 2 ml of distilled water added to the filtrate followed by a few drops of 5%-FeCl₃. The presence of phenolic compounds was determined by the appearance of a dark green color (Keo et al., 2017).

Test for flavonoids: 1 ml of 2% NaOH solution was mixed with 0.2 g of the plant extract. This produced a concentrated, yellow-colored solution. Then, few drops of diluted acid were added to the mixture, which made the solution colorless, indicating the presence of flavonoids (Mir et al., 2013).

Test for quinones: 0.5 g of the plant extract was added to 5 ml of ethanol and ultrasonicated for 15 min at 30°C. The mixture was filtered and 1 ml of concentrated H₂SO₄ was added to 1 ml of filtrate. The appearance of a red color indicated the presence of quinones (Keo et al., 2017).

Test for steroids: 5 ml of ethanol was added to 0.5 g of the plant extract and ultrasonicated for 15 min at 30°C. The mixture was filtered and the filtrate was evaporated to dryness. A few milligrams of the dried extract were dissolved in 1 ml of chloroform and 1 ml of glacial acetic acid, and then 1 ml of concentrated H₂SO₄ was added to the side of the test tube and mixed with the solution. The presence of steroids was indicated by appearance of a green color (Keo et al., 2017).

Test for cardiac glycosides: 5 ml of ethanol was added to 0.5 g of the plant extract and ultrasonicated for 15 min at 30°C. The mixture was filtered and the filtrate was evaporated to dryness. A few milligrams of the dried extract were dissolved in 1 ml of glacial acetic acid and few drops of 2%-FeCl₃, and then 1 ml of concentrated H₂SO₄ was added to the side of the test tube. The presence of a brown ring indicated the presence of cardiac glycosides (Keo et al., 2017).

Test for terpenoids: 0.5 g of the plant extract was added to 5 ml of chloroform and ultrasonicated for 15 min at 30°C. The mixture was filtered and 2 ml of concentrated H₂SO₄ added to the side of the test tube. The presence of a reddish-brown color indicated the presence of terpenoids (Keo et al., 2017).

Test for anthraquinones: 0.5 g of the plant extract was added to 4 ml of benzene. The mixture was filtered, and 10% ammonia solution was added. After shaking, the presence of a red or violet color indicated the presence of anthraquinones (Basiru et al., 2013).

Test for anthocyanins: 5 ml of ethanol was added to 0.5 g of the plant extract and ultrasonicated for 15 min at 30°C. Then, 1 ml of NaOH was added to 1 ml of the extract and heated for 5 min at 100°C. The presence of a bluish-green color indicated the presence of anthocyanin (Bassal et al., 2021).

Test for essential oils: 5 ml of ethanol was added to 0.5 g of the plant extract and ultrasonicated for 15 min at 30°C. Then, 100 µl of 1 M NaOH was added to the filtrate followed by a few drops of 1 M HCl. The formation of a white precipitate indicated the presence of essential oils (Keo et al., 2017).

2.3 LC-MS

2.3.1 Sample preparation

Sample was filtered through 0.22 µm PTFE membrane filters and placed in glass vials for further LC-MS analysis.

2.3.2 LC-MS data acquisition

The LC-MS analysis was performed using a single quadrupole LC-MS-2020 mass spectrometer (Shimadzu Corporation, Kyoto, Japan), which was equipped with an electrospray ion source (ESI).

UPLC separation was performed using a Kinetex C18 (1.7 µm, 100 mm × 2.1 mm, Phenomenex, Torrance, CA, United States) column. The column temperature was maintained at 40°C. The injected volume was 10 µL. Water and methanol, both supplemented with 0.1% formic acid, were used as mobile phases.

A stepwise gradient method, presented in Table 1, was used for elution, at a flow rate of 0.4 ml/min.

MS data were collected in the negative ion mode, over a m/z range of 50–1,500. The parameters of electrospray ionization (ESI) source were set as follows: ESI probe temperature 350°C, DL temperature 250°C, heat block temperature 200°C, ESI probe voltage 4.5 kV, detector voltage 1.6 kV, DL voltage 100 V, Q-array RF voltage 60 V, and nebulizing gas flow 1.5 L/min.

TABLE 1 Chromatographic gradient conditions for the analysis of *O. Syriacum* ethanolic crude extract.

Time (min)	Methanol (%)	Water (%)
0	10.0	90.0
5	20.0	80.0
8	40.0	60.0
11	50.0	50.0
13	60.0	40.0
16	80.0	20.0
17	90.0	10.0
19	10.0	90.0
21	10.0	90.0

2.4 Cell culture

Human breast cancer cells MDA-MB-231 (American Type Culture Collection, Manassas, VA) were maintained in DMEM high-glucose medium supplemented with 10% fetal bovine serum (FBS) (both from Sigma-Aldrich, St. Louis, MO, United States) and 1% penicillin/streptomycin (Lonza, Switzerland) and kept in a humidified chamber (37°C and 5% CO₂).

2.5 Cell viability assay

MDA-MB-231 cells (5×10^3) were seeded in 96-well plates and allowed to grow until they reached 30–40% confluence. The cells were then treated with increasing concentrations of OSEE and incubated for a total period of 72 h. Cell viability was measured by the reduction of 3-(4,5-dimethylthiazol-2-yl)-2,5-diphenyltetrazolium bromide (MTT; Sigma-Aldrich, St. Louis, MO, United States). Cell growth was determined as the proportional viability of the treated cells compared with the ethanol vehicle-treated cells, the viability of which is set to be 100%. In cell viability assays with N-acetyl cysteine (NAC; Sigma-Aldrich, St. Louis, MO, United States), 5 mM NAC was added to the cells for 30 min before OSEE treatment. Assays were performed in triplicate and repeated three times. Data are presented as mean values \pm standard error of the mean (SEM).

2.6 DPPH (α , α -diphenyl- β -picrylhydrazyl) antioxidant activity assay

The antioxidant activity of the ethanolic extract of *O. syriacum* leaves was measured using the DPPH-radical-scavenging assay as previously described but with some modifications (Moraes-De-Souza et al., 2008). DPPH (cat#

D9312, Sigma-Aldrich Co.) is a free radical used as a colorimetric probe to evaluate the antioxidant properties of plant extracts and constituents: the color of the solution changes from purple to pale yellow. 0.5 ml of different concentrations of OSEE (50, 100, 200, 400, and 600 μ g/ml) was mixed with 0.5 ml of DPPH solution (0.5 mM in methanol) and 3 ml of methanol. The blank consisted of 0.5 ml of 80% ethanol, 0.5 ml of DPPH solution and 3 ml of methanol. Mixed samples were then kept in the dark for 30 min and the OD was measured at a wavelength of 517 nm using a spectrophotometer. The DPPH-scavenging activity of each concentration of the extract was calculated using the formula: % radical-scavenging activity = [(OD blank—OD plant extract at each concentration)]/(OD blank)] \times 100. Ascorbic acid was used as a standard.

2.7 Dihydroethidium staining

MDA-MB-231 cells were seeded in 12-well plates and incubated until they reached 50% confluence. The cells were then treated for 24 h with the indicated concentrations of OSEE; media containing less than 1% ethanol was used as the vehicle control. After incubation, the medium was removed and the cells were washed twice with ice-cold phosphate-buffered saline (PBS). DHE stain (6 μ M) was added and the cells were incubated in the dark for 45 min. Then the stain was removed, the cells were washed once with cold PBS, and visualized using a ZEISS Axio Observer.

2.8 Microscopic analysis of apoptotic morphological changes

Cells were grown in 6-well tissue-culture plates in the absence or presence of the indicated concentrations of OSEE. Morphological changes characteristic of apoptotic cells were determined after 24 and 48 h using an inverted phase-contrast microscope (objectives 10 \times , 20 \times , and 40 \times).

2.9 Flow cytometry analysis of cell cycle

Cells were grown in 10-mm tissue-culture plates for 24 h before the addition of OSEE or ethanol at a concentration equivalent to that present in OSEE as a vehicle control. After incubation, cells were harvested, washed twice, resuspended in 500 μ l PBS, fixed with an equal volume of 100% ethanol, and incubated at -20° C for at least 12 h. Cells were then pelleted, washed twice with PBS and permeabilized in 0.1% Triton X-100/PBS and incubated for 15 min on ice. Afterwards cells were pelleted, resuspended in PBS containing 40 μ g/ml propidium iodide and 25 μ g/ml RNase A, and incubated at 37°C for 5 min.

Cell samples were then analyzed with the BD FACSCanto II Flow Cytometry System (Becton Dickinson) and data acquired using the FACSDiva 6.1 software.

2.10 Wound-healing assay

MDA-MB-231 cells were grown in 12-well tissue-culture plates until confluent. A scrape was made through the confluent monolayer using a sterile 200- μ L plastic pipette tip. The culture medium was then removed, the cells were washed twice with PBS (Sigma-Aldrich, St. Louis, MO, United States) to remove cellular debris, and incubated at 37°C in fresh medium in the presence or absence of the indicated concentrations of OSEE. Photomicrographs of the wound were taken at baseline (0 h) and for the 4–10 h period considered, using an inverted phase-contrast microscope (objective 10 \times). The width of the wound was expressed as the average \pm SEM between the measurements taken at time zero and the corresponding time points.

2.11 Trans-well migration chamber assay

The migratory ability of MDA-MB-231 cells was also assessed with trans-well inserts (8 μ m pore size; BD Biosciences, Bedford, MA, United States). Cells were seeded at a density of 1.0×10^5 cells per well, into the upper chamber of the insert, and treated with less than 1% ethanol, as a vehicle control, or the indicated concentrations of OSEE. DMEM supplemented with 10% fetal bovine serum was placed into the bottom wells in the system as a chemo-attractant and then the plates were incubated at 37°C for 24 h. Cells were then washed, and non-penetrating cells were removed from the upper surface of the filter with a sterile cotton swab. Cells that had migrated through to the lower surface of the insert were fixed with 4% formaldehyde, stained with DAPI, and counted under a fluorescence microscope. Assay was repeated three times and data were presented as mean values \pm SEM.

2.12 Matrigel invasion assay

The invasiveness of the MDA-MB-231 cells was evaluated using a BD Matrigel Invasion Chamber (8- μ m pore size; BD Biosciences, Bedford, MA, United States). Briefly, cells were seeded at a density of 1.0×10^5 cells per well, into the upper chamber of the insert, and treated with less than 1% ethanol, as a vehicle control, or the indicated concentrations of OSEE. DMEM supplemented with 10% fetal bovine serum was placed into the bottom wells of the chamber as a chemo-attractant and then incubated at 37°C for 24 h. Cells were then washed, and non-penetrating cells were removed from the upper

surface of the filter with a sterile cotton swab. Cells that had penetrated through the Matrigel to the lower surface of the insert were fixed with 4% formaldehyde, stained with DAPI, and counted under a fluorescence microscope. Assay was repeated three times and data were presented as mean values \pm SEM.

2.13 Adhesion assay

MDA-MB-231 cells were grown in the presence or absence of OSEE for 24 h and then seeded onto collagen-coated 24-well tissue-culture dishes in duplicate. Cells were incubated at 37°C for 1 h and unattached cells were removed by gently washing the wells twice with PBS. The number of adherent cells was determined by the MTT reduction assay, as described above.

2.14 Chorioallantoic membrane assay

Fertilized chicken eggs were incubated at 38°C and 60% relative humidity for 10 days. Afterwards, the highly vascularized CAM was dropped by drilling a 1-cm² hole through the eggshell into the air sac. OSEE was then applied onto the CAM to test its effect on blood vessel growth. After 24 h, pictures of the CAM were taken and the angiogenic response was analyzed using the AngioTool software, which quantifies the length of the vessels and number of junctions.

2.15 Whole-cell extracts and western blotting analysis

For whole-cell lysates, cells were washed twice with PBS and lysed in 2% SDS, 60 mM Tris lysis buffer (pH 6.8) and centrifuged at 5,000 *g* for 10 min. The protein concentration of the supernatant was determined using the Bradford protein assay kit (Biorad, Hercules, CA, United States) and 25–30- μ g aliquots were resolved by 10% sodium dodecyl sulfate-polyacrylamide gel electrophoresis before being transferred to a polyvinylidene difluoride membrane (Immobilon PVDF; Biorad) and blocked for 1 h at room temperature with 5% non-fat dry milk in TBST (TBS and 0.05% Tween 20). Immunodetection was performed by incubating the membrane with specific primary antibodies at 4°C overnight. Horseradish peroxidase-conjugated anti-IgG was used as secondary antibody and immunoreactive bands were detected using the ECL substrate kit (Thermo Scientific, Rockford, IL, United States), according to the manufacturer's instructions. All primary and secondary antibodies were purchased from Cell Signaling (Cell Signaling Technology, Inc., Danvers, MA, United States).

2.16 Statistical analysis

Results were evaluated using Student's *t*-test. For the comparison of more than two means, ANOVA was used using one-way ANOVA (with Dunnett's post hoc test) or two-way ANOVA (with Tukey–Kramer's post hoc test). Data were presented as mean \pm SEM and a *p*-value of <0.05 was considered as statistically significant.

3 Results

3.1 Phytochemical screening

O. syriacum has many primary and secondary bioactive metabolites (Mesmar et al., 2022). Extensive HPLC analyses and the phytochemical bioactives of *O. syriacum* have been reported in several studies (Alma et al., 2003; Dorman et al., 2004; Mesmar et al., 2022). Apigenin, naringenin, rosmarinic acid, carvacrol, carveol, thymoquinone, thymol, and caffeic acid are some of the reported molecules (Alma et al., 2003; Dorman et al., 2004; Mesmar et al., 2022). Here we confirmed the presence of several classes of phytochemical compounds in OSEE. Table 2 shows that OSEE contains tannins, phenols, flavonoids, quinones, steroids, terpenoids as well as cardiac glycosides and essential oils.

3.2 LC-MS of *O. Syriacum* crude extract

Metabolites were principally identified by matching masses and retention times of pure standards. Six compounds were identified as shown in Table 3 and Figure 1.

TABLE 2 Phytochemical screening of *O. syriacum* ethanolic crude extract.

Metabolite	OSEE
Tannins	+
Resins	+
Saponins	-
Phenols	+
Flavonoids	+
Quinones	+
Sterols and steroids	+
Cardiac glycosides	+
Terpenoids	+
Anthraquinones	-
Anthocyanins	-
Essential oils	+

(-): absent; (+): present.

3.3 OSEE inhibits the proliferation of MDA-MB-231 breast cancer cells

Several of the bioactives reported to be present in *O. syriacum* have been shown to have potent anti-BC effects. Naringenin, apigenin, carvacrol, thymoquinone, thymol, and rosmarinic acid were shown to reduce the malignant phenotype of BC cell lines (Kanno et al., 2005; Demain and Vaishnav, 2011; Lee et al., 2019; Messeha et al., 2020; Sampaio et al., 2021). Knowing that the unfractionated plant extract may often have more potent activities than a single or a few of its phytochemicals, it was thought prudent to investigate the anti-cancerous effects of *O. syriacum* leaves in a triple-negative human BC cell line (TNBC), MDA-MB-231. To this end, we examined the anti-proliferative activity of OSEE against MDA-MB-231 cells. The effect of various concentrations (0, 50, 100, 200, 400 and 600 μ g/ml) of the extract on the proliferation of human TNBC MDA-MB-231 cells was assessed at 24, 48, and 72 h of treatment. Results showed that OSEE treatment decreased cell viability in a concentration- and time-dependent manner (Figure 2A). For example, at 48 h of treatment, cell viability using 50, 100, 200, 400 and 600 μ g/ml of OSEE to treat MDA-MB-231 cells was 77.4 ± 5.1 , 68.4 ± 9.5 , 45.5 ± 7.9 , 28.2 ± 2.9 , and $20.2 \pm 6.9\%$ that of control cells, respectively (Figure 2A). The half-maximal inhibitory concentration (IC_{50}) was 875, 179.4, and 125.4 μ g/ml at 24, 48, and 72 h, respectively. Based on these IC_{50} values, 100 and 200 μ g/ml OSEE were used in further experiments.

To confirm the anti-proliferative effects of OSEE, protein lysates from OSEE-treated MDA-MB-231 cells were immunoblotted with an antibody against Ki67, a widely used biomarker for the evaluation of cell proliferation and the prognosis of many cancers. Particularly, Ki67 is highly expressed in TNBC, which is associated with its aggressive pathologic features and poor clinical outcomes (Yang C et al., 2018). Figure 2B, shows that treatment of MDA-MB-231 cells with 100 and 200 μ g/ml OSEE caused a remarkable decrease in Ki-67 protein levels by 0.83- and 0.67-fold, compared with vehicle-treated control cells, respectively (Figure 2B). The decrease in Ki67 protein levels seems to be concentration-dependent (Figure 2B). These data confirm data from Figure 2A, suggesting that OSEE does indeed interfere with the cell proliferation process in MDA-MB-231 cells.

3.4 OSEE has potent antioxidant activity and can increase the generation of ROS in MDA-MB-231 cells

ROS are implicated in many aspects of health and disease, including signaling processes. There is a delicate balance between oxidative stress and antioxidant mechanisms inside the cell, ensuring that physiological functions are maintained, and proper defense mechanisms are in place. Any disturbance of

TABLE 3 Compounds identified from *O. Syriacum* ethanolic crude extract.

Compound name	Elemental composition	[M-H] ⁻ precursor ion (<i>m/z</i>)	RT (min)
Vicenin-1	C ₂₆ H ₂₈ O ₁₄	563.14	5.23
Vicenin-2	C ₂₇ H ₃₀ O ₁₅	593.15	4.82
Orientin	C ₂₁ H ₂₀ O ₁₁	447.09	5.60
Isoorientin	C ₂₁ H ₂₀ O ₁₁	447.09	5.82
Vitexin	C ₂₁ H ₂₀ O ₁₀	431.09	6.11
Isovitexin	C ₂₁ H ₂₀ O ₁₀	431.09	6.71

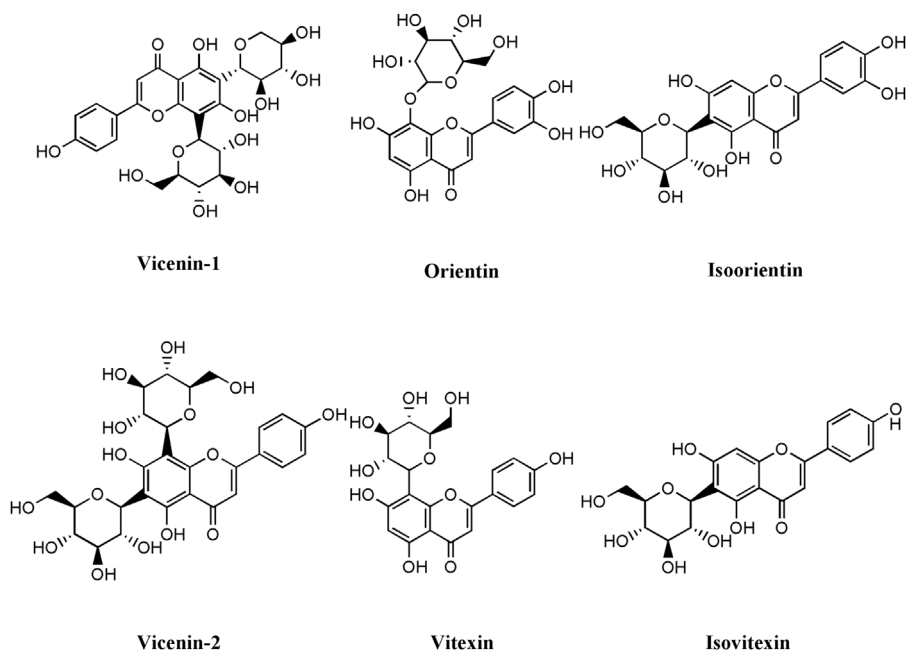


FIGURE 1

Structures of the compounds identified from *O. Syriacum* ethanolic crude extract using LC-MS.

this balance may lead to pathological outcomes. Notably, both ROS and antioxidants have been shown to play either anti- or pro-cancerous roles. Indeed, phytochemicals and other natural products have been reported to act as anti- or pro-oxidant agents, depending on the context, in a biphasic and concentration-dependent manner. For example, dietary supplementation with the antioxidant N-acetyl cysteine (NAC) can promote cancer progression and metastasis (Liou and Storz, 2010; Chio and Tuveson, 2017; Shaito et al., 2020). *O. syriacum* has been reported to contain many bioactive molecules with high antioxidant potential, such as polyphenols. In this study, OSEE antioxidant potential was evaluated *in vitro* using the DPPH-radical-scavenging assay. OSEE exhibited significant free-radical-scavenging activity which was concentration-dependent

(Figure 3A). Despite this significant antioxidant-radical-scavenging activity of OSEE in the test tube *in vitro* (Figure 3A), we tested the effect of OSEE on ROS generation in MDA-MB-231 cells in culture. Indeed, MDA-MB-231 cells treated with increasing concentrations of OSEE, showed increased DHE fluorescence as the concentration of OSEE increased (Figure 3B), indicating that OSEE increases the levels of ROS generation in MDA-MB-231 cells.

Reactive oxygen species function like a double-edged sword in cancer progression, depending on their concentration in the cell and the stage of cancer. ROS have been reported to either enhance tumorigenesis and promote tumor progression by causing DNA damage and inducing pro-oncogenic pathways, or to induce cell death and apoptosis of cancer cells (Shaito et al., 2020; Oyenih et al.,

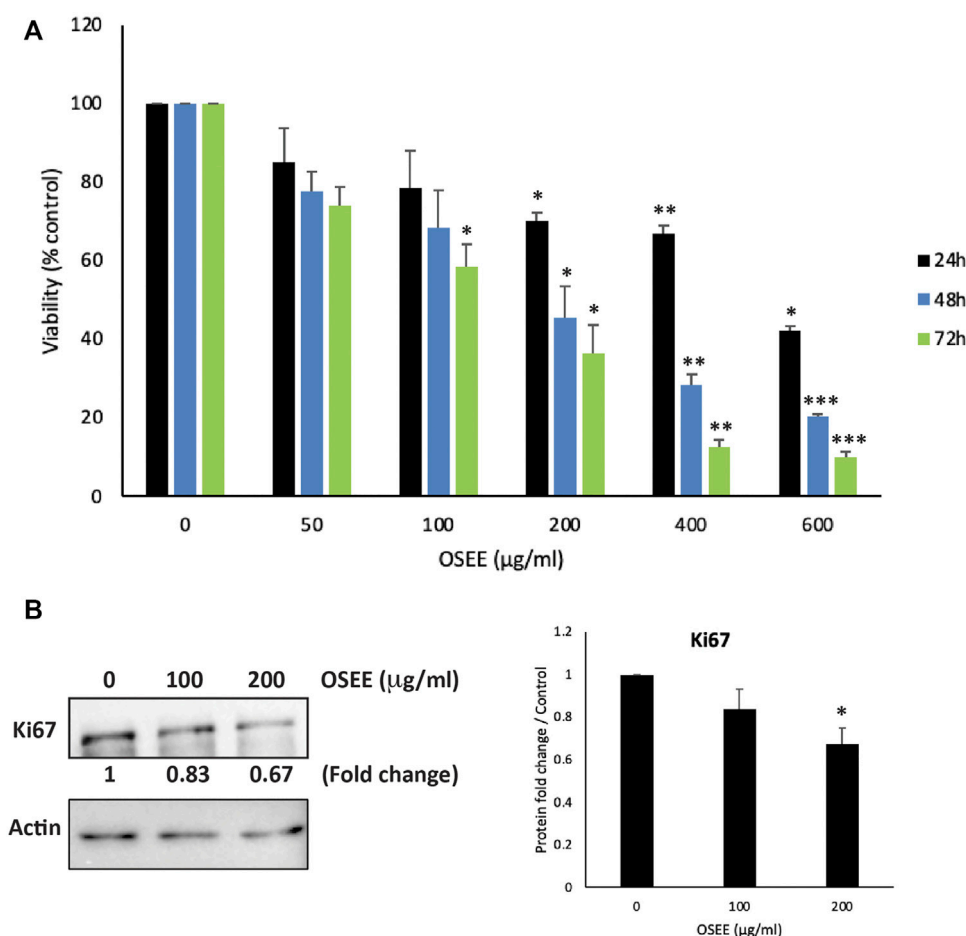


FIGURE 2

O. syriacum inhibits cellular proliferation of MDA-MB-231 breast cancer cells. (A) MDA-MB-231 cells were treated or not with the indicated concentrations of *O. syriacum* ethanolic extract (OSEE) for 24, 48, and 72 h. For vehicle control, a concentration of ethanol equivalent to that present in OSEE was used. Cell viability was monitored using the metabolism-based MTT assay, as described in Materials and Methods. (B) MDA-MB-231 cells were incubated for 24 h with and without the indicated concentrations of OSEE. Cells were then lysed, and protein lysates were subject to Western blotting with a Ki67 antibody. Data represent the mean \pm SEM of three independent experiments ($n = 3$) carried out in triplicate and expressed as a percentage of the corresponding control cells. Statistical analysis was performed using one-way ANOVA followed by LSD post-hoc test (* $p < 0.05$, ** $p < 0.005$, *** $p < 0.001$).

2022; Oyenih et al., 2022). To investigate whether OSEE exerts anti-proliferative effects on MDA-MB-231 cells through ROS generation, MDA-MB-231 cells were first pre-treated with NAC to dampen ROS generation, followed by treatment with OSEE at various concentrations. Cell proliferation and viability were then assessed for a period of 3 days. NAC, acting as a ROS scavenger, can by itself inhibit proliferation of MDA-MB-231 cells at 24 h (data not shown), 48 h, and 72 h of treatment (Figure 3C). Figure 3C also shows that treatment with NAC augmented the inhibition of proliferation of MDA-MB-231 cells treated with lower concentrations of OSEE (50 and 100 µg/ml). However, NAC treatment was not able to blunt the inhibition of proliferation of MDA-MB-231 cells induced by higher concentrations of OSEE (200, 400 and 600 µg/ml); on the

contrary, OSEE attenuated NAC-induced inhibition of proliferation (Figure 3C). These data indicate that the anti-proliferative effects of OSEE may depend on the levels of ROS generation inside the cell, confirming the biphasic concentration-dependent effects reported for other natural antioxidants.

3.5 OSEE induces cell-cycle arrest of MDA-MB-231 cells at G₀/G₁ phase

To investigate the mode of the anti-proliferative effect induced by OSEE in MDA-MB-231 cells, the cell-cycle distribution of these cells was assessed, using PI staining

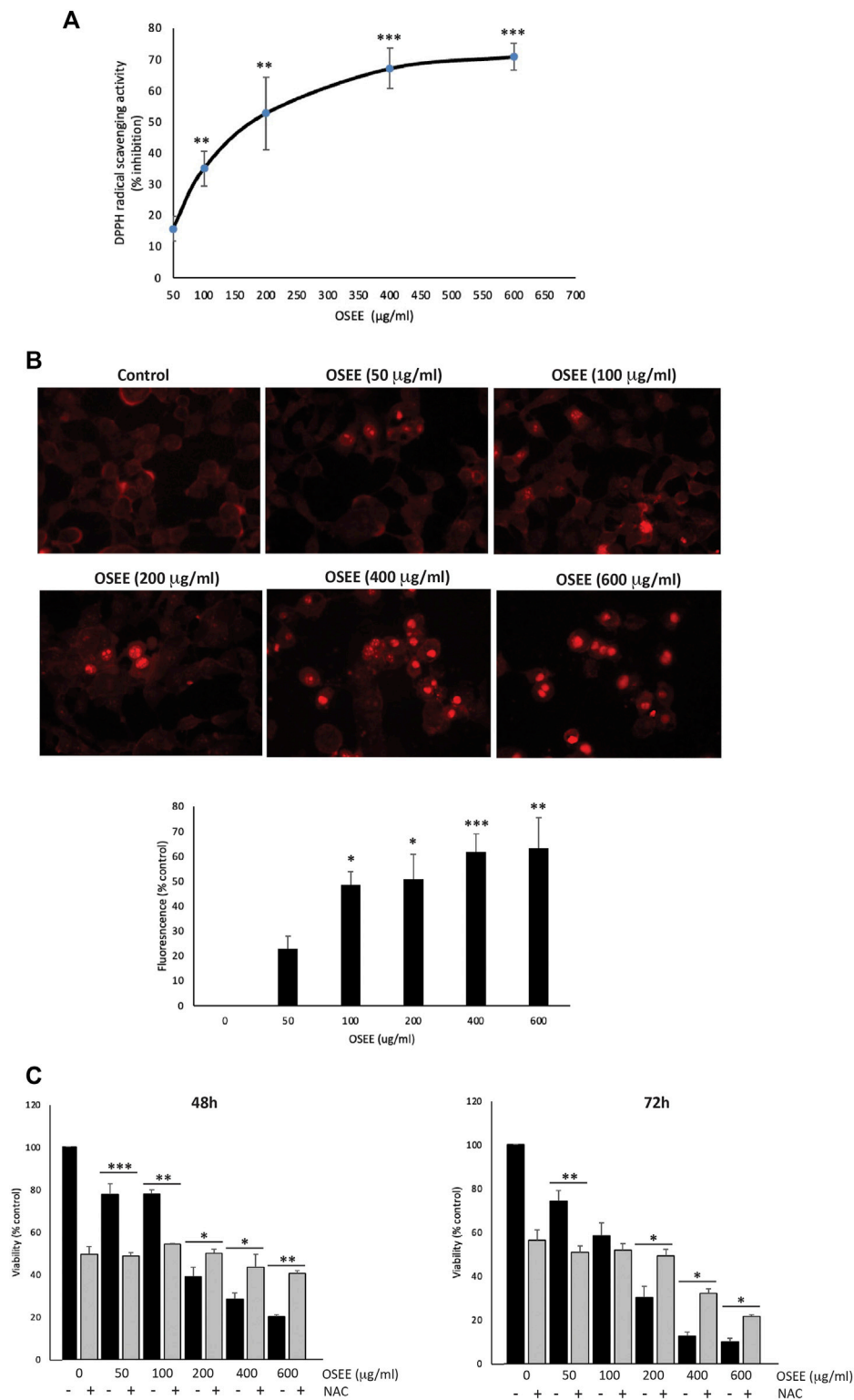
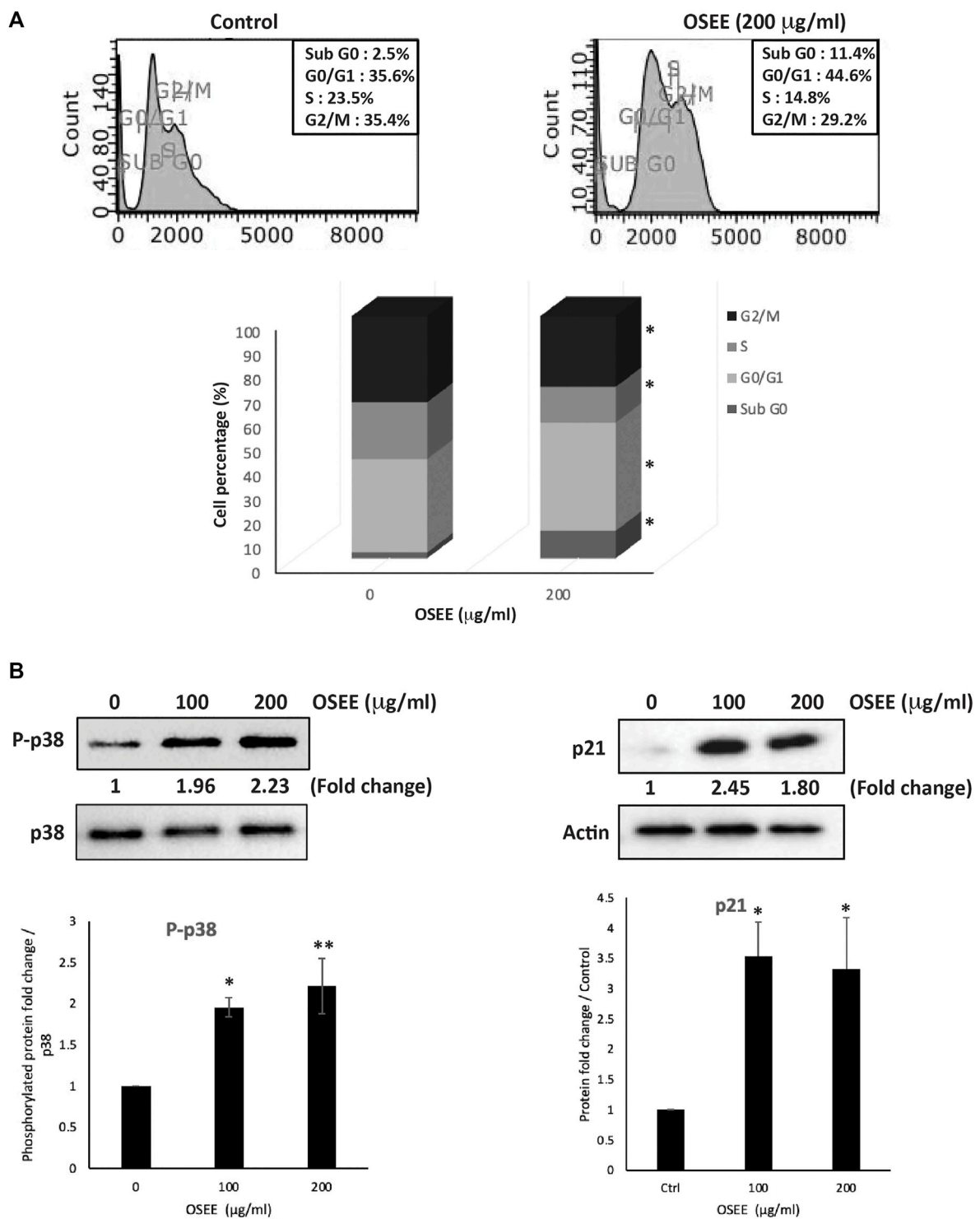


FIGURE 3
O. syriacum has remarkable antioxidant potential and can increase the generation of ROS in MDA-MB-231 cells. **(A)** The antioxidant activity of the indicated concentrations of OSEE was measured by 2,2-di-phenyl-1-picrylhydrazyl (DPPH) radical scavenging capacity assay as described in Materials and Methods. Data represent the means \pm SEM of three independent experiments. **(B)** Fluorescent images of dihydroethidium (DHE)-stained MDA-MB-231 cells. Cells were treated with and without the indicated concentrations of OSEE for 24 h and stained with DHE, as indicated in Materials and Methods, to measure intracellular ROS production. **(C)** MDA-MB-231 cells were pre-treated with NAC (10 mM) for 30 min and then with OSEE at the indicated concentrations. Cell viability was measured using the MTT assay at the indicated time points. OSEE-treated cells without NAC pre-treatment were used for comparison. Values represent the means \pm SEM of three independent experiments performed in triplicates and expressed as percentage of vehicle-treated control cells (* p < 0.05, ** p < 0.005, *** p < 0.001).

**FIGURE 4**

O. syriacum induces G₀/G₁ cell cycle arrest in MDA-MB-231 cells. (A) MDA-MB-231 cells were incubated with OSEE (200 µg/ml) or ethanol as a vehicle control for 24 h. Cells were then harvested, fixed, stained with propidium iodide, and analyzed by flow cytometry as described in Materials and Methods. Data represent the mean ± SEM of three independent experiments. Statistical analysis was performed using one-way ANOVA (**p* < 0.05, ***p* < 0.005) (B) MDA-MB-231 cells were treated with or without increasing concentrations of OSEE for 24 h. Proteins were then extracted and the levels of phosphor-p38 and p21 were analyzed by Western blotting, with total-p38 and β-actin as loading controls, respectively. Data represent the mean ± SEM of three independent experiments (* denotes a *p* < 0.05 and ** denotes a *p* < 0.005).

followed by flow cytometry, at 24 h of treatment with 200 $\mu\text{g/ml}$ OSEE. Figure 4A, shows that OSEE induced an arrest at the G_0/G_1 phase of the cell cycle. The percentage of cells in G_0/G_1 phase increased in OSEE-treated cells (44.6 ± 0.8 vs 36.5 ± 2.1 in control cells), accompanied by a concomitant decrease in the percentage of cells in the S phase (14.8 ± 1.0 vs 23.5 ± 1.3 in control cells), suggesting that OSEE triggers a G_1 phase arrest and inhibits entry into the S phase (Figure 4A). The cell cycle data also revealed that untreated control cells hardly exhibit any sub- G_0 DNA (Figure 4A). Treatment of cells with OSEE caused a significant increase in the sub- G_0 cell population, indicative of apoptosis (Figure 4A).

The p38 MAPK (mitogen-activated protein kinase) pathway has been widely associated with anti-proliferative functions by regulating cell cycle progression and inducing apoptosis to maintain cellular homeostasis (Lafarga et al., 2009; Martínez-Limón et al., 2020). Western blotting analysis of the levels of the active phosphorylated form of p38 indicated significant activation of p38 following treatment of MDA-MB-231 cells with 100 or 200 $\mu\text{g/ml}$ OSEE (1.96 ± 0.11 - and 2.23 ± 0.33 -fold increases, respectively) (Figure 4B). Our results also show that the levels of a downstream effector of p38, the cell cycle regulator protein p21 (Lafarga et al., 2009), which inhibits progression of the cell cycle, increased remarkably upon treating the cells with OSEE (Figure 4B), further confirming the cell cycle data.

3.6 OSEE induces intrinsic apoptosis in MDA-MB-231 cells

To follow up on sub- G_0 cell cycle data and to confirm the apoptosis status in OSEE-treated MDA-MB-231 cells, the cells were examined 24 h after treatment with OSEE. Analysis of OSEE-treated cells using an inverted phase-contrast microscope showed an OSEE concentration-dependent decrease in the total number of cells per microscopic field, and the appearance of apoptotic cells characterized by cell shrinkage, membrane blebbing, and nuclear abnormalities (Figure 5A). Further analysis of OSEE-treated and DAPI-stained cells showed condensation of nuclear material, chromatin lysis, and the presence of apoptotic bodies, all indicative of possible induction of apoptosis by OSEE treatment (Figure 5B).

Central to the execution of apoptosis is the processing of procaspase-3 to the active form, caspase-3. To gain further insight into the mechanism of apoptosis induced by OSEE, we examined the levels of procaspase-3 protein. The results showed a significant decrease in procaspase-3 levels in cells treated with 100 and 200 $\mu\text{g/ml}$ OSEE (0.58 ± 0.18 - and 0.52 ± 0.11 -fold reductions, respectively), suggesting that OSEE enhanced the proteolytic processing of procaspase-3, and

consequently augmented caspase activation and induced the intrinsic apoptotic cascade (Figure 5C).

The B-cell lymphoma 2 antiapoptotic protein, BCL-2, also plays an important role in the intrinsic apoptosis pathway and has been shown to contribute to chemoresistance in many cancers (Yip and Reed, 2008), implying that targeting BCL-2 could have a potential role in the treatment of TNBC. In our study, OSEE-treated cells showed a decrease in BCL-2 protein levels in a concentration-dependent manner, achieving a significant difference from the control at 200 $\mu\text{g/ml}$ of OSEE (Figure 5C). These data further confirm that OSEE induces cell death by targeting apoptotic mechanisms.

3.7 OSEE inhibits the STAT3 signaling pathway

To analyze the molecular signaling behind OSEE-induced apoptosis, we assessed the expression levels of p53 and STAT3 (signal transducer and activator of transcription 3 protein), in MDA-MB-231 cells treated with OSEE at 100 $\mu\text{g/ml}$ and 200 $\mu\text{g/ml}$ for 24 h. STAT3 is a transcription factor with established oncogenic properties. It is activated by phosphorylation, inducing its dimerization and subsequent translocation to the nucleus, where it reportedly has been shown to inhibit endogenous expression of p53 protein. Our results showed a significant decrease in the phosphorylation of STAT3 by 0.49 ± 0.05 - and 0.44 ± 0.02 -fold in cells treated with 100 $\mu\text{g/ml}$ and 200 $\mu\text{g/ml}$ OSEE, compared to vehicle control-treated cells (Figure 6). Moreover, a significant increase was observed in the phosphorylation of p53 upon treatment of MDA-MB-231 cells with 200 $\mu\text{g/ml}$ of OSEE (Figure 6). These data suggest that OSEE inhibits STAT3 signaling, resulting in the activation of p53, and therefore induction of intrinsic apoptosis mediated by caspase-3.

3.8 OSEE increases the aggregation of MDA-MB-231 cells

Epithelial-mesenchymal transition (EMT) is a complex cellular program and a hallmark of the progression of tumor cells towards metastasis. During EMT, epithelial cells acquire a mesenchymal phenotype, characterized by the loss of cell-cell adhesion and an increase in their migratory and invasive properties. MDA-MB-231 cells have undergone a high degree of EMT, and a drug that is designed for the treatment of TNBC is expected to reverse EMT by allowing the cells to regain their epithelial properties such as cell-cell adhesion. To this end, we evaluated the effect of the OSEE extract on the cell-cell adhesion properties of MDA-MB-231 cells in suspension in a cell-aggregation assay. Figure 7A shows that OSEE caused a concentration-dependent increase in cell-cell aggregates

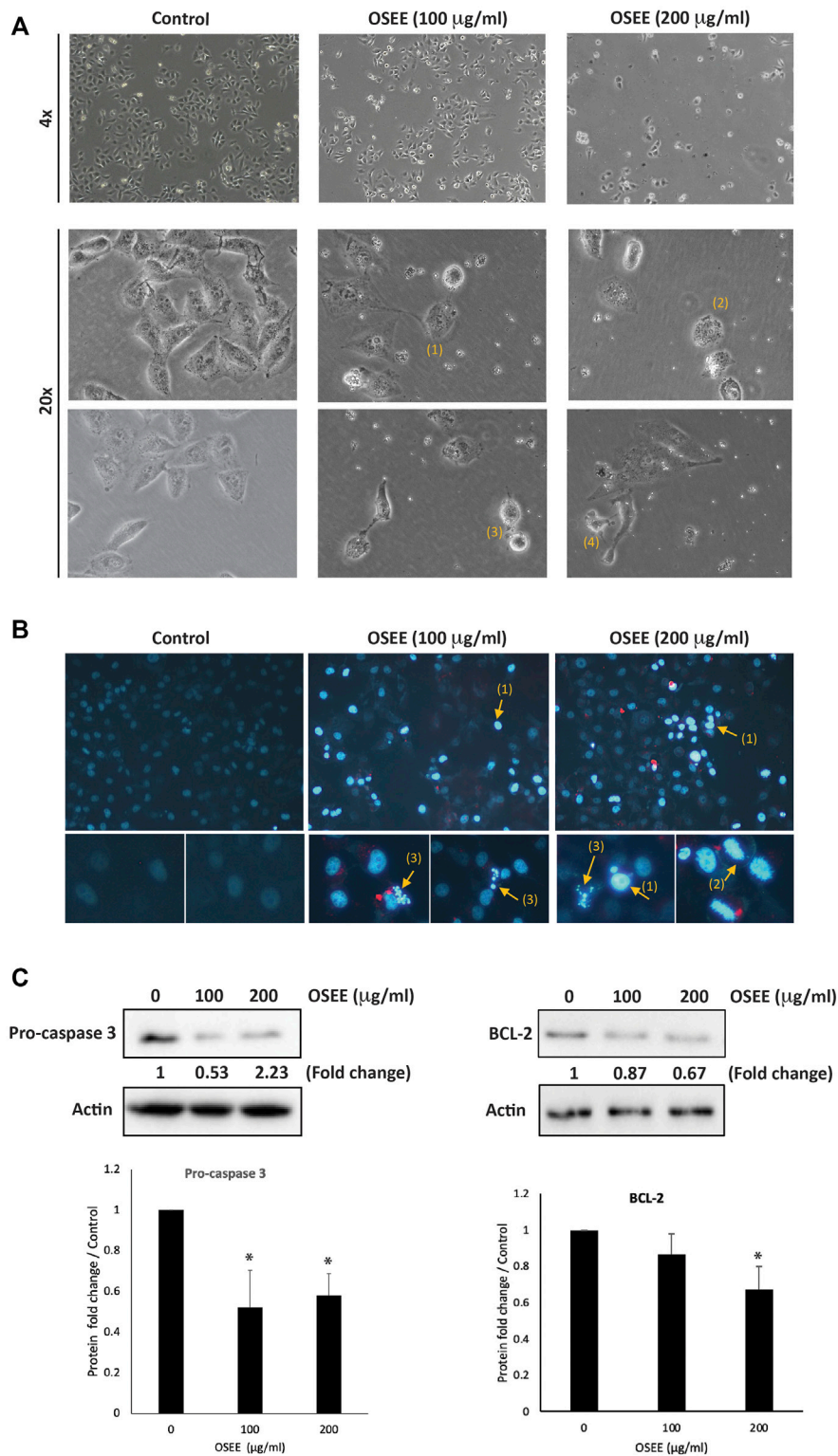
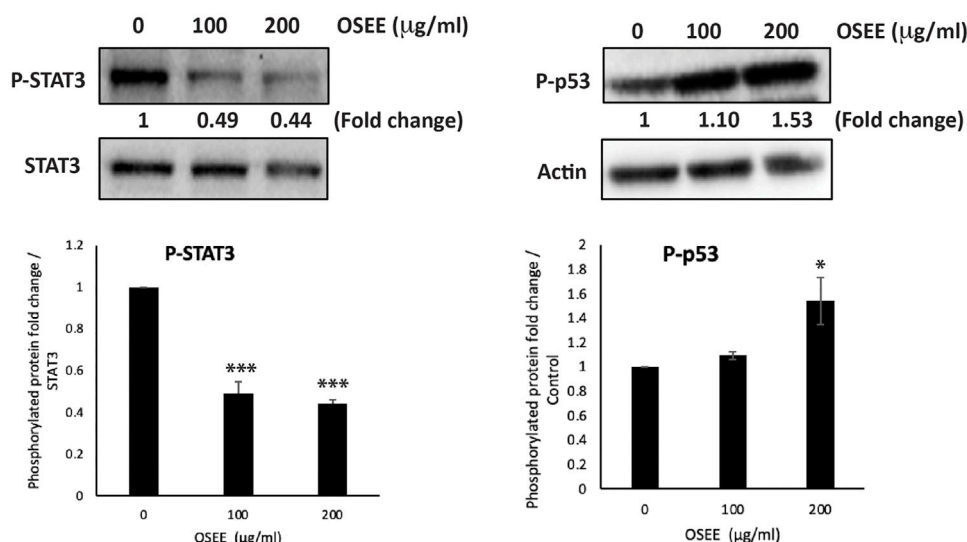


FIGURE 5
O. syriacum induces apoptosis in MDA-MB-231 cells. **(A)** MDA-MB-231 cells were treated with and without the indicated concentrations of OSEE for 24 h. Morphological changes were observed by light microscopy. Arrows show (1) cell shrinkage, (2) membrane blebbing, (3) apoptotic bodies, and (4) echinoid spikes. **(B)** Cells were incubated with OSEE at the indicated concentrations for 24 h and stained with 4',6-diamidino-2-
(Continued)

FIGURE 5 (Continued)

phenylindole (DAPI) to visualize nuclei. Nuclear morphological changes and apoptosis were then assessed using a fluorescence microscope. Arrows indicate (1) condensation of nuclear material, (2) cell swelling and chromatin lysis, and (3) apoptotic bodies. **(C)** Cells were treated with and without the indicated concentrations of OSEE for 24 h. Protein levels of pro-caspase 3 and BCL-2 were determined by Western blotting. Immunoblotting for β -actin was used as a loading control. Data represent the mean of three \pm SEM independent experiments ($n = 3$). (* denotes a $p < 0.05$).

**FIGURE 6**

O. syriacum inhibits the STAT3 signaling pathway in MDA-MB-231 cells. MDA-MB-231 cells were treated with and without the indicated concentrations of OSEE for 24 h and protein lysates were examined for the phosphorylation of STAT3 and levels of phospho-p53 by Western blotting. Values represent the mean \pm SEM of three independent experiments ($n = 3$). * $p < 0.05$ and *** $p < 0.001$.

compared to the control cells, with significant 43 ± 6.4 and $63.5 \pm 3\%$ increases, 1 h after OSEE treatment at 100 $\mu\text{g/ml}$ and 200 $\mu\text{g/ml}$, respectively.

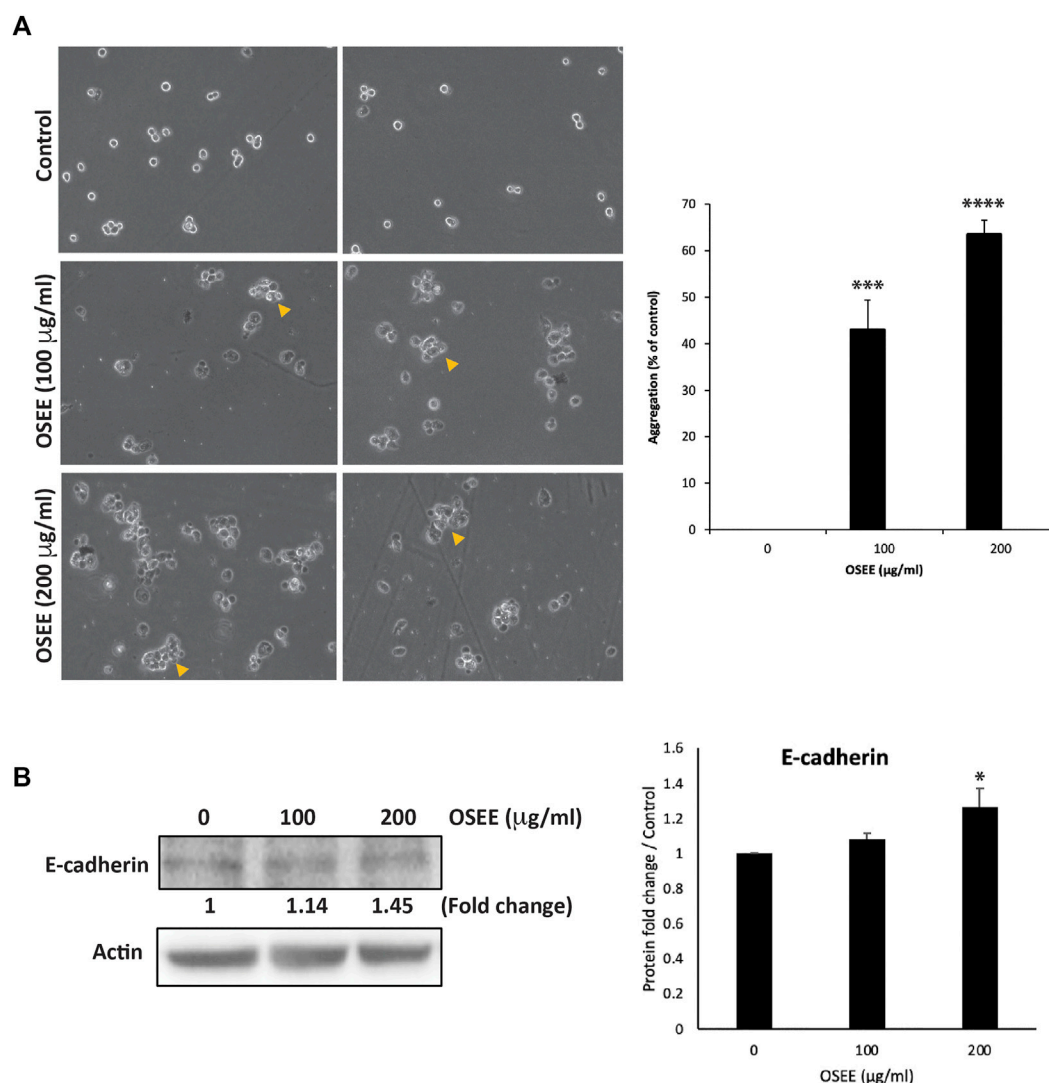
Cadherins are adhesion receptors that mediate homotypic cell-cell adhesion, and the loss of E-cadherin-mediated cell-cell contact is associated with malignant transformation by inducing EMT, leading to tumor metastasis. Here, MDA-MB-231 cells treated with 100 $\mu\text{g/ml}$ and 200 $\mu\text{g/ml}$ of OSEE showed an increase in E-cadherin protein levels in a concentration-dependent manner, by 1.14 ± 0.03 - and 1.45 ± 0.11 -fold that of untreated control cells, respectively (Figure 7B).

3.9 OSEE reduces the migration and the invasive properties of MDA-MB-231 cells

Having established that OSEE affects cell-cell interactions, we assessed the effect of the extract on cell migration, a main characteristic of the malignant phenotype. Although cell

migration is essential in many physiological processes such as wound repair, tissue formation, and proper immune response, its deregulation contributes to the initial steps of cancer metastasis as cells spread away from the primary tumor site. The effect of OSEE on the migration of MDA-MB-231 cells was examined using assays for wound healing and trans-well migration. Figure 8A shows that OSEE decreased the migration of MDA-MB-231 cells, as demonstrated by a decrease in the ability of those cells to migrate and fill the scratched area. For example, 10 h after the scratch was applied to a confluent monolayer, the migration of MDA-MB-231 cells treated with OSEE at 200 $\mu\text{g/ml}$ was 0.67 ± 0.4 -fold that of the control cells (Figure 8A). This inhibition of migration was further confirmed using the trans-well migration assay: OSEE caused a marked decrease in the cell migration ability of MDA-MB-231 cells since only $7.8 \pm 0.2\%$ of cells were able to cross from the upper to the lower chamber (Figure 8B).

Cell invasion is an integral component of the early stages of cancer metastasis, highlighting the ability of cancer cells that have

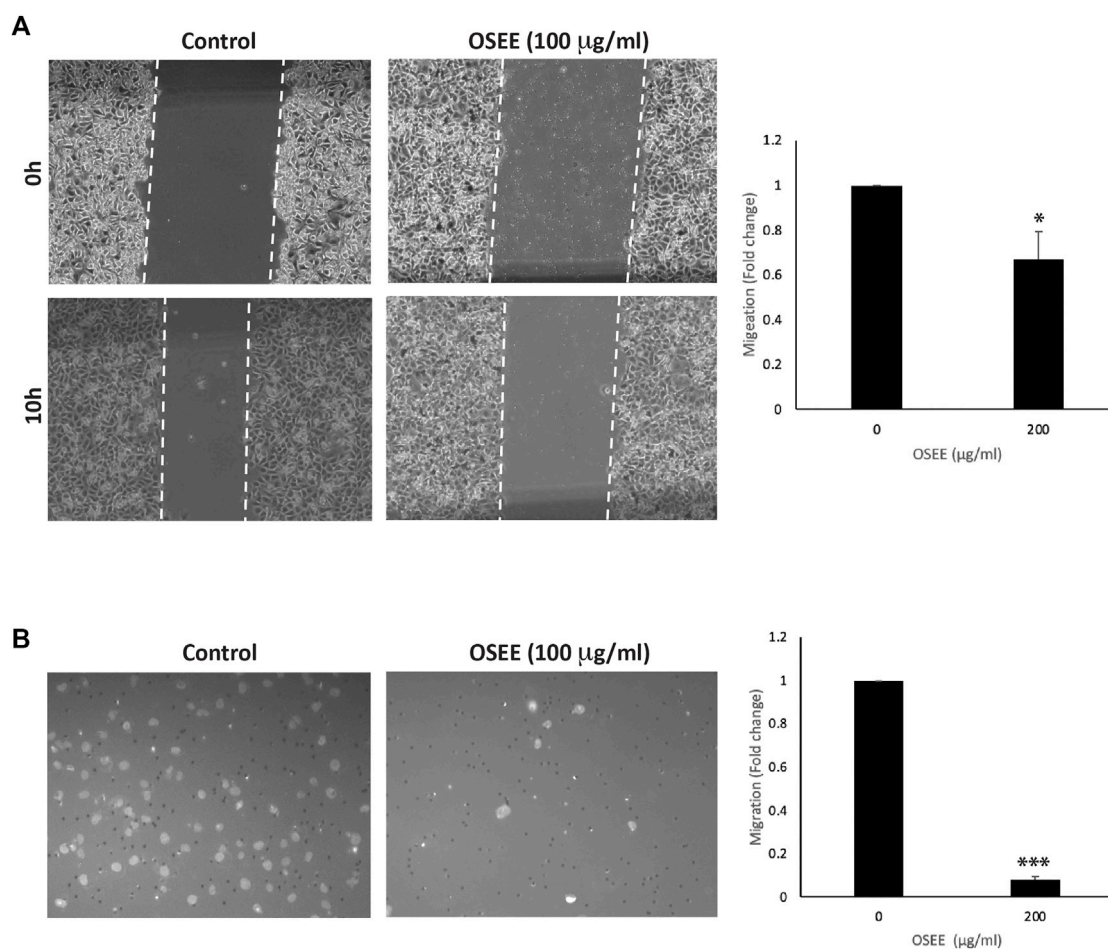
**FIGURE 7**

O. syriacum increases the cell-cell aggregation of MDA-MB-231 cells. **(A)** MDA-MB-231 cells were incubated with and without the indicated concentrations of OSEE and subjected to a cell-aggregation assay as described in Materials and Methods. Micrographs of cells were taken after 1 h and the percentage of cell-cell aggregates was measured using the following equation: % aggregation = $(1 - N_t/N_c) \times 100$, where N_t is the number of single cells in the control and N_c is the number of single cells in the treated sample. **(B)** MDA-MB-231 cells were incubated with and without the indicated concentrations of OSEE for 24 h, and whole-cell protein lysates were analyzed for E-cadherin protein levels by Western blotting. β -actin was used as a loading control. Data represent the mean \pm SEM of three independent experiments ($n = 3$). * $p < 0.05$, *** $p < 0.001$, **** $p < 0.0001$.

spread away from the primary tumor site to invade secondary sites of metastasis. To this end, we examined the effect of OSEE on the invasive potential of MDA-MB-231 cells using matrigel-coated trans-well chambers in the presence or absence of OSEE (100 $\mu\text{g/ml}$ and 200 $\mu\text{g/ml}$). The results showed that the number of cells that invaded the matrigel matrix to reach the bottom chamber was significantly reduced by OSEE treatment, by as much as $65 \pm 3.1\%$ and $89 \pm 1.7\%$, for 100 $\mu\text{g/ml}$ and 200 $\mu\text{g/ml}$, respectively, compared with the control (Figure 9A). This

reduction seems to be concentration-dependent and suggests that OSEE effectively reduces the invasive potential of MDA-MB-231 cells.

Focal adhesion kinase (FAK) has a major role in facilitating and promoting the migration and invasiveness of tumor cells (Luo and Guan, 2010; Tai et al., 2015; Lai et al., 2018; Shen et al., 2018). Here we report that 200 $\mu\text{g/ml}$ OSEE caused a 0.74 ± 0.17 -fold decrease in the phosphorylation of FAK within 5 min of treatment (Figure 9B). The decrease was

**FIGURE 8**

O. syriacum inhibits the migration of MDA-MB-231 cells. **(A)** A confluent culture of MDA-MB-231 cells was wounded by scratching with a pipette tip. The cells were then incubated with and without the indicated concentrations of OSEE. After 10 h, the wound was photographed using an inverted phase-contrast microscope and then measured and analyzed. Values represent the fold change in migration compared to vehicle control cells. **(B)** MDA-MB-231 cells were incubated overnight with and without the indicated concentrations of OSEE in Boyden chamber trans-well inserts as described in Materials and Methods. Migrating cells at the bottom of the chamber were stained with DAPI, imaged, and then counted and analyzed. Values represent the average of three independent experiments and are represented as mean \pm SEM (* p < 0.05, *** p < 0.001).

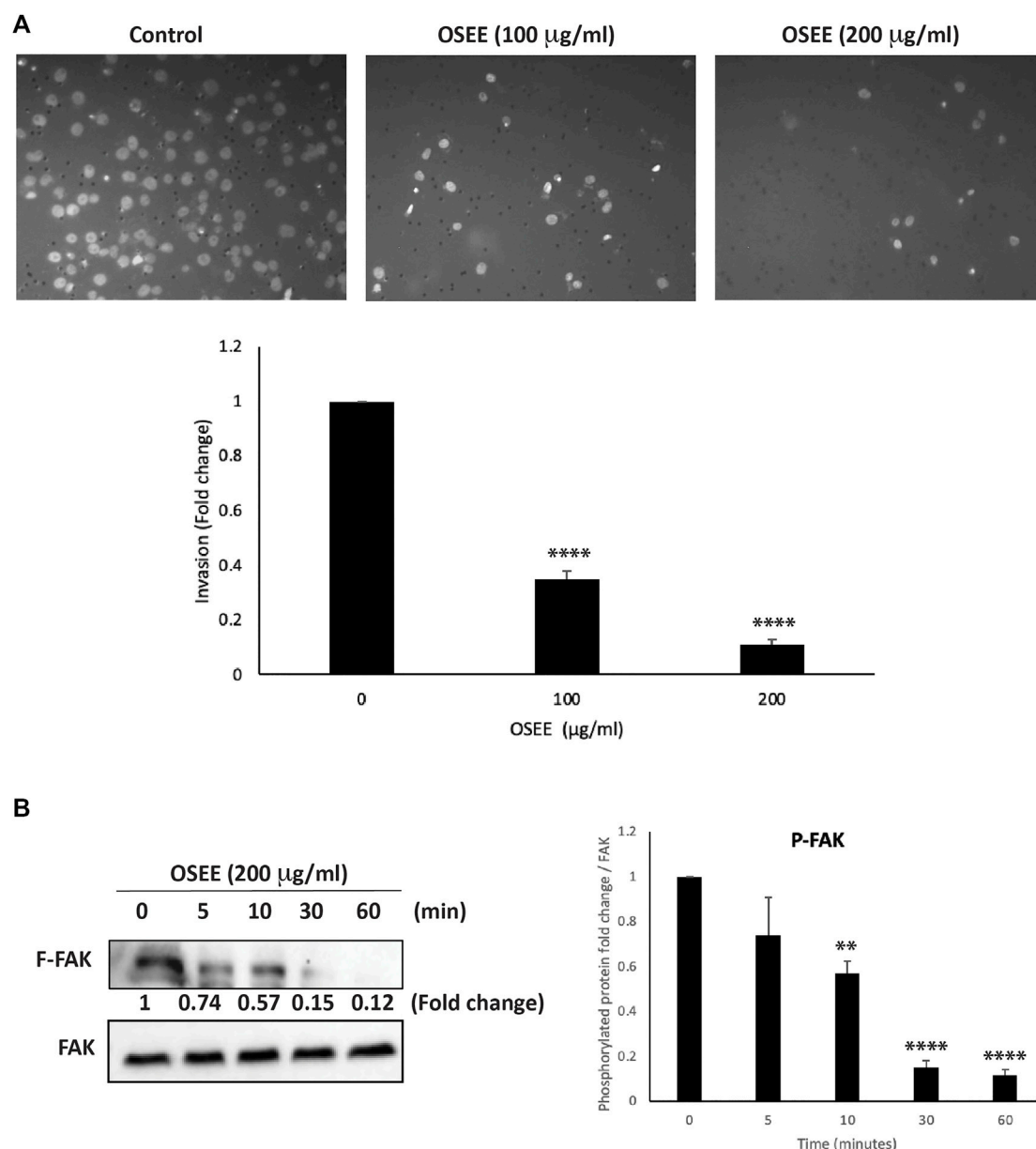
significant as early as 10 min and was 0.12 ± 0.02 -fold that of control levels after 1 h of treating MDA-MB-231 cells with OSEE. By impacting the migratory and invasive properties of MDA-MB-231 cells, OSEE can potentially reduce metastasis, the main cause of poor prognosis of TNBC tumors.

3.10 OSEE reduces the levels of iNOS and inhibits angiogenesis *in ovo*

Angiogenesis plays a crucial role in tumor growth and metastasis by providing oxygen and nutrients to proliferating cells through the formation of new blood vessels. To test the effect of OSEE on angiogenesis, the chick-embryo chorioallantoic-membrane (CAM) assay was performed. The findings demonstrated that 200 µg/ml of

OSEE applied to the surface of the highly vascularized CAM membrane for 24 h caused a significant inhibition of new blood vessel formation (a reduction of $44 \pm 5.3\%$, compared to the control) and a decrease in the number of junctions (a decrease of $56 \pm 12.8\%$ compared to the control) (Figure 10A).

Nitric oxide is a main mediator of angiogenesis. Hence, the anti-angiogenic potential of OSEE was further investigated by testing its effect on cytokine-induced expression of inducible nitric oxide synthase (iNOS), a main producer of nitric oxide. Our results showed that OSEE treatment at 100 µg/ml and 200 µg/ml caused a significant decrease in iNOS levels by 0.78 ± 0.06 - and 0.75 ± 0.02 -fold, respectively, compared to the control (Figure 10B). This indicates that OSEE interferes with the production of nitric oxide, leading to a reduction of angiogenesis.

**FIGURE 9**

O. syriacum reduces the invasive potential of MDA-MB-231 cells. **(A)** MDA-MB-231 cells were incubated overnight with and without the indicated concentrations of OSEE in Boyden chamber trans-well inserts pre-coated with Matrigel as described in Materials and Methods. Cells that invaded the Matrigel were stained with DAPI, imaged, and then counted and analyzed. Values represent the fold change in migration of the ethanol-treated control. The experiment was repeated three times ($n = 3$) and data represent the mean \pm SEM (** $p < 0.005$, **** $p < 0.0001$). **(B)** Cells were treated with and without 200 $\mu\text{g/ml}$ OSEE at different time points and the phosphorylation of FAK was assessed at those points by Western blotting, using total-FAK as loading control. The Western blot is representative of three independent experiments ($n = 3$). ** $p < 0.005$, **** $p < 0.0001$.

4 Discussion

Breast cancer (BC) cells sustain proliferative signaling, evade growth suppressors, and resist cell death, providing them with a growth advantage over normal cells. In addition, cancer cells are highly migratory, can activate invasion, and induce angiogenesis.

Therefore, new cancer therapeutic strategies have focused on compounds with multiple targets or on combination approaches that mix or design hybrid compounds, particularly to treat aggressive hard-to-treat cancers such as TNBC (Kucuksayan and Ozben, 2017). Plants are rich in secondary metabolites with strong antitumor functions, including terpenoids,

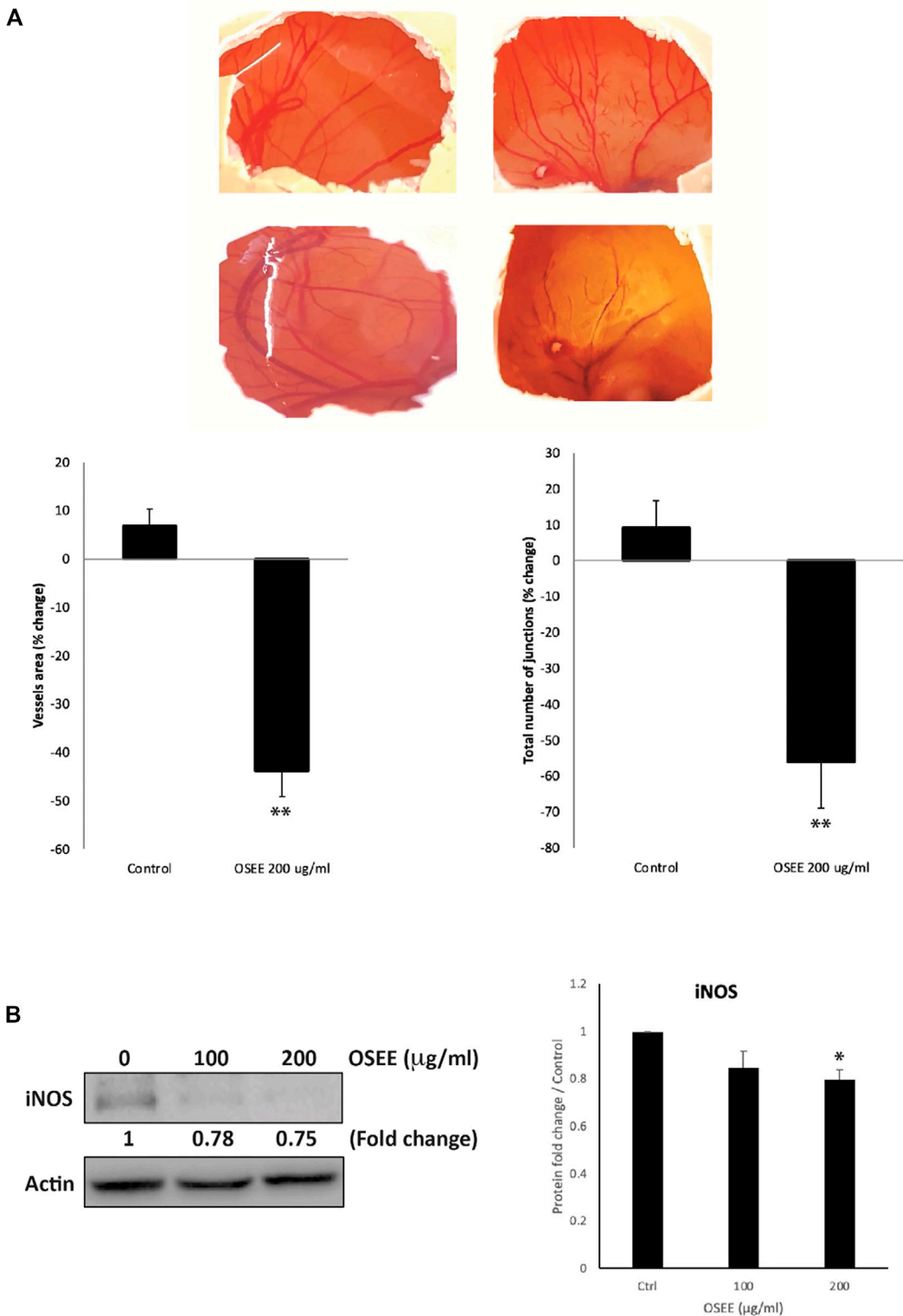


FIGURE 10
O. syriacum inhibits angiogenesis in ovo and reduces iNOS levels in MDA-MB-231 cells. **(A)** OSEE was applied to the chorioallantoic membrane (CAM) of fertilized chicken eggs as described in Materials and Methods. Upper panel of **(A)** shows images of CAM acquired 24 h later to score the angiogenic response. Lower panel of **(A)** shows analysis of the acquired images. Total vessel length and total number of junctions were quantified in both the OSEE-treated and control CAMs using the AngioTool software and represented as percentage change with respect to the control (* denotes $p < 0.05$ and ** $p < 0.01$). **(B)** The protein levels of iNOS were determined by Western blotting in MDA-MB-231 cells treated with or without the indicated concentrations of OSEE for 24 h. The Western blot is representative of three independent experiments. The bar graph represents the quantification of three independent Western blots and the data represent the mean \pm SEM of three independent experiments ($n = 3$). * $p < 0.05$.

phenolics, and alkaloids. Our study confirmed that *O. syriacum* contains several classes of these phytochemical compounds, e.g., phenols, flavonoids, quinones, steroids, terpenoids, tannins, cardiac glycosides and essential oils. This is in agreement with other studies showing that *O. syriacum* ethanolic extract contains terpenoids (Kamel et al., 2001), flavonoids, carotenoids, and phenols such as thymol and carvacrol (El-Moneim et al., 2014; Alonazi et al., 2021). These plant-derived natural compounds have been gaining more attention as therapeutic options because of their ability to evade resistance by the cancer cells while producing minimal side effects. In fact, natural compounds can solely target cancer cells, or can complement the effects of other chemotherapeutic drugs by sensitizing cancer cells and modulating drug-drug interactions (Scaria et al., 2020). Many natural compounds have been developed into staple anticancer drugs such as the antimetabolic paclitaxel from *Taxus brevifolia* and vinblastine from *Catharanthus roseus*, pro-apoptotic pomiferin from *Maclura pomifera* and *Dereis Malaccensis*, and anti-angiogenic flavopiridol from *Dysoxylum binectariferum* Hook. f and combretastatin A-4 phosphate from *Combretum caffrum*, among others (Greenwell and Rahman, 2015; Hassan, 2019). Plants from the *Origanum* genus in particular, have been shown to have strong anti-tumorigenic properties. For example, *O. vulgare* inhibits cell proliferation and induces apoptosis in human colon, stomach, hepatocarcinoma, and BC cell lines (Lombrea et al., 2020); *O. compactum* attenuates the proliferation of breast, lung and hepatoma cancer cell lines (Bouyahya et al., 2020); and *O. majorana* inhibits tumor growth and metastasis of numerous cancers including breast, colon, lung, pancreatic, lymphoblastic leukemia, and hepatocarcinoma (Bouyahya et al., 2021). Of particular interest, *O. syriacum* has been shown to exhibit an anti-proliferative effect on MCF-7 BC cells (Al-Kalaldeh et al., 2010; Husein et al., 2014) as well as human leukemia THP-1 cells (Ayesh et al., 2014). Furthermore, several phytochemicals present in *O. syriacum* have been reported to have anti-breast cancer potential. Some examples include naringenin, apigenin, carvacrol, thymoquinone, thymol, and rosmarinic which have been reported to impact the cancerous phenotype of BC cell lines (Kanno et al., 2005; Demain and Vaishnav, 2011; Lee et al., 2019; Messeha et al., 2020; Sampaio et al., 2021). In this study, LC-MS analysis of OSEE revealed the presence of vicenin-1, vicenin-2, orientin, isoorientin, vitexin, and isovitexin, all of which are flavonoid C-glycosides. Interestingly, vitexin, isovitexin, vicenin-1, and vicenin-2 are glycosides of apigenin (Engelhardt et al., 1993), which has anti-breast cancer activities and is reported to be present in *O. syriacum*, as discussed. In addition, these compounds were reported to have anti-cancerous activities, for example: vitexin against human leukaemia U937 cells, oesophageal cancer cells EC109; orientin against human cervical adenocarcinoma HeLa cells, oesophageal cancer EC109 cells, prostate cancer PC-3, DU-145 and LNCaP cells; isoorientin against liver hepatocellular carcinoma HepG2 cells;

vicenin-2 against colorectal cancer HT29 cells, hepatocellular carcinoma HepG2, CA3, SNU-387, and HCCLM3 cells, prostate cancer cells PC-3, DU-145 and LNCaP (Nagaprashantha et al., 2011; Lee et al., 2012; Yuan et al., 2013; Guo et al., 2014; Yuan et al., 2014; Yang D et al., 2018; Huang et al., 2020). In the case of breast cancer, vitexin (Kim et al., 2018), orientin, and isoorientin (Czemplik et al., 2016) were reported to have anti-cancerous effects against MCF-7 breast cancer cells, which are not TNBC cells. Collectively, there are limited studies on the effect of these compounds in BC in general, and TNBC in particular, demanding investigation in future studies. Here, it is critical to mention that oftentimes, the whole herb or its crude extract may have more potent activity than a single or a combination of its bioactive constituents. This may partly be due to inherent synergistic effects between the various bioactive constituents, which could be lost when one or several bioactives are separately used (Rasoanaivo et al., 2011; Caesar and Cech, 2019; Zhao et al., 2020). The mechanism of this synergy has not been elucidated, yet several mechanisms may be operating in parallel (Caesar and Cech, 2019). For example, synergy could be due to the low bioavailability and poor pharmacokinetics of the individual bioactives, while the combination of bioactives may impart enhanced bioavailability (Caesar and Cech, 2019; Zhao et al., 2020). Future studies should test the anti-cancerous activities of single or combined bioactives of OSEE versus the activity of the whole extract. Overall, our results show that OSEE as a crude extract has potent *in vitro* anti-breast cancer activities and highlight OSEE as a potential source of natural compound(s) with anti-cancerous activities. Notwithstanding, further *in vivo* studies are needed to validate OSEE efficacy and safety in the treatment of TNBC.

We demonstrated that OSEE dose-dependently inhibited MDA-MB-231 proliferation. OSEE reduced the levels of the proliferation marker Ki67, which is highly expressed in TNBC and is associated with its aggressive pathologic features and poor clinical outcomes (Yang C et al., 2018). Reducing the levels of Ki67 further confirmed the potential of OSEE as a source of future TNBC therapeutics. We also showed that OSEE arrested MDA-MB-231 at the G₀/G₁ phase of the cell cycle. We investigated the potential correlation of the p38 MAPK (mitogen-activated protein kinase) pathway in OSEE-induced inhibition of MDA-MB-231 cell proliferation with cell cycle arrest. p38 signaling has been widely associated with anti-proliferative functions by regulating cell cycle progression and inducing apoptosis to maintain cellular homeostasis (Lafarga et al., 2009; Martínez-Limón et al., 2020). In addition, we showed that the levels of a downstream effector of p38, the cell cycle inhibitor protein p21 (Lafarga et al., 2009), increased remarkably with OSEE treatment. Overall, we showed that OSEE can inhibit proliferation of MDA-MB-231 cells and induce cell cycle arrest of TNBC cells at G₀/G₁ in a pathway that may involve p38/p21 signaling and downregulation of Ki67.

Reactive oxygen species are free radicals that occur in the body as by-products of mitochondrial and peroxisomal metabolism or the activity of certain enzymes like NADPH-oxidases (NOXs). ROS, at low concentrations, mediate important physiological processes, but an uncontrolled increase in their levels may precipitate pathological states. Therefore, it is critical to keep their levels under homeostatic control to avoid cellular oxidative stress resulting from an imbalance between the production of ROS and other reactive species and their elimination by cellular antioxidant systems (Posadino et al., 2019). Importantly, chronic slight elevations of ROS levels can cause cellular damage that may lead to carcinogenesis (Moloney and Cotter, 2018; Slika et al., 2022). However, this is not always the case as ROS was reported to have both pro- and anti-cancerous effects (Chio and Tuveson, 2017; Moloney and Cotter, 2018), dependent on ROS concentrations in the cell (Kong et al., 2000; De Sá Junior et al., 2017). Indeed, when ROS levels rise beyond a certain cytotoxic threshold, for example through exogenous application, they can cause the selective death of cancer cells mainly by apoptosis (Kong et al., 2000; De Sá Junior et al., 2017; Raza et al., 2017). Building on these results, targeting ROS signaling and inducing oxidative stress and/or inhibiting antioxidant processes has been envisaged as a mechanism for anticancer therapy (Chio and Tuveson, 2017; Kim et al., 2019). Nevertheless, the role of ROS in cancer therapy is full of intricacies and there are disputes over whether pro-oxidative or anti-oxidative therapies will be the effective course for the management of cancer (De Sá Junior et al., 2017). To complicate the situation even more, natural antioxidants themselves have been reported to either elevate or suppress ROS levels in cancer cells, and as a result, natural antioxidants have been reported to have either pro- or anti-cancerous effects depending on their concentration (Wang et al., 2021). Our results confirm this notion since OSEE exhibited high antioxidant potential *in vitro* by scavenging the DPPH radicals, but elevated ROS generation in MDA-MB-231 cells in culture. This was further manifested as a biphasic anti-proliferative effect mediated by OSEE in the presence of NAC as a ROS scavenger. Indeed, our results showed that only higher concentrations of OSEE were able to mitigate the inhibition of proliferation induced by the ROS, while lower concentrations of OSEE augmented this effect, indicating that the anti-proliferative effects of OSEE can be ROS-dependent in a biphasic manner. Biphasic concentration-dependent effects have been reported for many natural antioxidants (Shaito et al., 2020).

Cancer is a complex multifactorial disease mediated by multiple signaling pathways that regulate the expression of a wide array of genes implicated in tumor initiation, progression and metastasis, including the STAT3 signaling pathway. This pathway plays an important role in signaling associated with cellular proliferation, migration, invasion, and angiogenesis (Yuan et al., 2015). High levels of activated STAT3 have been observed in several types of cancer, including human BC (Levy

and Inghirami, 2006). Activated STAT3 induces cancer transformation by affecting cellular pathways related to cell growth, apoptosis, and tumorigenesis. Interestingly, several studies have shown that STAT3 is constitutively activated in invasive BCs, but not benign tumors, indicating that STAT3 is mainly involved in tumor progression and metastasis, rather than tumor initiation (Watson and Miller, 1995; Ranger et al., 2009; Resemann et al., 2014). STAT3 has been attributed to have a key role in cell cycle regulation by mediating the progression of cells from G₁ to S phase through the upregulation of D-cyclins and cell division cycle 25 A phosphatase (Cdc25A) and associated downregulation of cell cycle regulator proteins p21 and p27 (Leslie et al., 2006). In agreement with the roles of STAT3, our results showed that OSEE inhibited STAT3, activated p21, and induced G₀/G₁ cell cycle arrest. Moreover, ROS-mediated activation of p38 is reportedly implicated in cell cycle arrest at G₀/G₁ and induction of apoptosis in several cancers (Martínez-Limón et al., 2020). In this instance, p38 has been reported to activate p21, p27, or p57 (Martínez-Limón et al., 2020). Collectively, our findings suggest that OSEE exerts its anti-proliferative effects against BC by regulating several pathways, including those for STAT3, ROS, p38 MAP kinase, p21, and Ki67, satisfying the multi-target requirement of an effective anticancer therapeutic strategy, as already discussed.

STAT3 inhibits apoptosis by modulating key apoptosis regulators such as the pro-survival survivin (Gritsko et al., 2006), BCL-2 (Real et al., 2002), and p53 (Sp et al., 2021). As the “guardian of the genome,” p53 is critical in cell fate decisions in response to stress signals by inducing an arrest of the cell cycle, promoting DNA repair, and eliciting apoptosis. The activity of p53 is dependent on its quantity, integrity, and post-translational modification (Lacroix et al., 2006). For example, p53 phosphorylation at the N-terminal sites has been associated with increased protein stabilization and activity (Lacroix et al., 2006). Particularly, phosphorylation at the Ser15 site has been shown to be induced by almost all kinds of stress, disrupting the interaction of p53 with its major negative regulator MDM2 and increasing its binding to acetyltransferase P300 (Ito et al., 2001). Phosphorylation of mutant p53 at Ser15 restored its conformation to the wild-type form. Prospective therapies co-targeting STAT3 and p53 are sought to overcome cancer drug resistance (Pham et al., 2020). In this regard, several plant-derived compounds have been shown to exert their anticancer properties through inhibition of STAT3-signalling pathways. For example, the naturally occurring phytoalexin resveratrol inhibits the growth, progression and metastasis of BC cells by directly affecting STAT3 and its upstream regulators (Kohandel et al., 2021). Curcumin was also shown to suppress STAT3-signaling pathways and inhibit the growth of several cancers including breast, prostate, and pancreatic cancers (Hutzen et al., 2009; Lin et al., 2009; Liu et al., 2018). Here we reported similar results where OSEE induced apoptosis and downregulated the expression of STAT3. OSEE

also induced the phosphorylation of p53, further supporting its multi-target properties. Phosphorylation of p53 can be associated with OSEE anticancer properties by stabilizing p53 to restore/increase its transcriptional activities. Moreover, OSEE treatment induced an accumulation of cells in the sub-G₀ phase, activation of caspase-3, and downregulation of BCL-2, indicating that OSEE potentially induces p53-dependent intrinsic apoptosis in TNBC. In total, our data indicate that OSEE-induced apoptosis of MDA-MB-231 may be executed through a pathway involving STAT3, p53, p21, caspase-3, and BCL-2.

Epithelial-mesenchymal transition (EMT) is a hallmark of cancer progression to metastasis and involves loss of cell-cell adhesion and cell-extracellular matrix (ECM) linkages, crucial steps of metastasis (Singh and Settleman, 2010), and the association of TNBC with EMT is well documented (Jang et al., 2015; Jalaieddine et al., 2019). In our study, OSEE increased the formation of cell-cell aggregates, indicating enhanced cell-cell adhesion of MDA-MB-231 cells. This was concomitant with an increase in E-cadherin levels, suggesting that OSEE interferes with tumor growth and dissemination by acting on single migratory tumor cells rather than on migration of cell-clusters. Furthermore, MDA-MB-231 cells have reduced cellular adhesion and low levels of E-cadherin, having undergone extensive EMT (Jalaieddine et al., 2019). Increased levels of E-cadherin and cellular adhesion by OSEE treatment of MDA-MB-231 cells may indicate that OSEE has reversed EMT in these cells. Given that drug resistance is correlated with the extent of EMT (Du and Shim, 2016), it may be speculated that OSEE can reverse chemoresistance.

Patients with metastatic TNBC have a poor prognosis (Kassam et al., 2009). This is related to the robust invasive and migratory abilities of TNBC cells (Chang et al., 2013). The enhancement of cell migration and invasion is an essential part of the multistep process of cancer metastasis. It involves the dysregulation of cell-cell junctions and cell adhesion, and the degradation of ECM by proteases such as metalloproteinases (MMPs) (Mcgowan and Duffy, 2008; Dufour et al., 2011). In our study, wound-healing assays and trans-well migration and invasion assays were conducted to confirm the anti-migratory and anti-invasive properties of OSEE. Indeed, OSEE inhibited TNBC cell migration and invasion. Similarly, it has been demonstrated that *O. majorana*, a close relative of *O. syriacum*, also inhibited migration and invasion of TNBC cells through a mechanism involving the inhibition of MMP-2 and MMP-9 (Al Dhaheri et al., 2013). The expression of MMPs has been shown to be regulated by STAT3-mediated signaling processes (Alsamri et al., 2019), inviting a future investigation of the ability of OSEE to inhibit the invasive potential of MDA-MB231 through its action on STAT3/MMPs. Moreover, we showed that OSEE inhibited activation of FAK, which is normally overexpressed in cancer cells, and its high level correlates with the invasiveness and metastasis of human cancer (Weiner et al., 1993; Taliaferro-Smith et al., 2015; Choi et al., 2016). Whether OSEE-induced inhibition of migration and invasiveness of TNBC cells takes place solely through

FAK-signaling or whether other routes are also involved remains to be tested in future studies. Overall, by enhancing cell adhesion and attenuating cell migration and invasion, OSEE may potentially inhibit TNBC metastasis.

Tumors upregulate vascularization through angiogenesis in order to acquire nutrients and grow, and for later metastasis. Angiogenesis is associated with cancer invasion and metastasis (Brem et al., 1977; Brem et al., 1978). Particularly, TNBC has been associated with high microvascular density and consequently poor prognosis. Therefore, innovative cancer therapies have been directed to anti-angiogenic therapies to block tumor growth and metastasis (Braicu et al., 2016). This involves targeting pro-angiogenic factors such as inducible nitric oxide synthase (iNOS), which regulates the production of nitric oxide in response to external stimuli. Indeed, the expression of iNOS has been shown to be associated with microvascular density and to serve as a marker for the clinical staging of metastasis in gastric carcinoma (Song et al., 2002) and TNBC (Firger, 2015). Inhibition of iNOS was successful in decreasing TNBC aggressiveness, metastasis to the lungs in particular (Firger, 2015; Granados-Principal et al., 2015). Here, we showed that OSEE exhibits significant anti-angiogenic potential by reducing the formation of capillaries (decreased vessel length and junction number) on the chicken-egg CAM. This effect was correlated with a decrease in the levels of iNOS, suggesting that OSEE blocks angiogenesis through iNOS-mediated signaling pathways. Vascular endothelial growth factor (VEGF) is the predominant angiogenic factor of invasive human BC cells (Relf et al., 1997). VEGF expression is elevated in TNBC patients and is associated with poor prognosis (Linderholm et al., 2009). Extracts from *O. majorana* inhibit angiogenesis by downregulation of VEGF secretion (Al Dhaheri et al., 2013). It is possible that OSEE-induced inhibition of angiogenesis takes place through a similar mechanism, in addition to downregulation of iNOS. The anti-angiogenic potential of *O. syriacum* further cements its potential use to develop anti-TNBC therapeutics.

5 Conclusion

In summary, our findings demonstrate that the ethanolic extract of *O. syriacum* (OSEE) exhibits potent anti-tumor growth and anti-metastatic effects on the aggressive phenotype of TNBC by modulating the processes of cell adhesion, migration, invasion, and angiogenesis through the inhibition of STAT3 signaling and activation of p38 MAPK signaling pathways. Moreover, OSEE caused cell cycle arrest, activated apoptosis, and inhibited angiogenesis in MDA-MB-231 cells. Therefore, due to its ability to modulate multiple pathways, OSEE is a potential source of candidate therapeutic anti-cancer agents. This warrants future investigation of OSEE as a source of novel compounds that can be used for multi-targeting of TNBC.

Data availability statement

The original contributions presented in the study are included in the article/Supplementary Material, further inquiries can be directed to the corresponding authors.

Author contributions

Conceptualization: EB, AS, RA, and JM designed the project; formal analysis: EB, AS, SB, NA, AB, RA, KH, MM, and JM analyzed and interpreted the data; resources: EB, AS, and AB; data curation: EB, AS, SB, NA, AB, RA, MM, KH, MM, and JM; writing: original draft preparation: EB, JM, and AS; writing: review and editing: EB, AS, SB, NA, AB, RA, KH, MM, and JM; supervision: EB and AS; funding acquisition, EB, AS, and AB. All authors read and approved the final manuscript.

Funding

This work was funded by the University Research Board of the American University of Beirut, Lebanon by a grant to EB and the University of Petra, Jordan by a grant to AB. Publication fees APC were covered by Barzan Holdings, Doha, Qatar by a grant to AS.

References

- Al Dhaheri, Y., Attoub, S., Arafat, K., Abuqamar, S., Viallet, J., Saleh, A., et al. (2013). Anti-metastatic and anti-tumor growth effects of *Origanum majorana* on highly metastatic human breast cancer cells: inhibition of NF κ B signaling and reduction of nitric oxide production. *PLoS One* 8, e68808. doi:10.1371/journal.pone.0068808
- Al-Kalaldeh, J. Z., Abu-Dahab, R., and Afifi, F. U. (2010). Volatile oil composition and antiproliferative activity of *Laurus nobilis*, *Origanum syriacum*, *Origanum vulgare*, and *Salvia triloba* against human breast adenocarcinoma cells. *Nutr. Res.* 30, 271–278. doi:10.1016/j.nutres.2010.04.001
- Alma, M. H., Mavi, A., Yildirim, A., Digrak, M., and Hirata, T. (2003). Screening chemical composition and *in vitro* antioxidant and antimicrobial activities of the essential oils from *Origanum syriacum* L. growing in Turkey. *Biol. Pharm. Bull.* 26, 1725–1729. doi:10.1248/bpb.26.1725
- Alonazi, M. A., Jemel, I., Moubayed, N., Alwhibi, M., El-Sayed, N. N. E., and Ben Bacha, A. (2021). Evaluation of the *in vitro* anti-inflammatory and cytotoxic potential of ethanolic and aqueous extracts of *Origanum syriacum* and *Salvia lanigera* leaves. *Environ. Sci. Pollut. Res. Int.* 28, 19890–19900. doi:10.1007/s11356-020-11961-z
- Alsamri, H., El Hasasna, H., Al Dhaheri, Y., Eid, A. H., Attoub, S., and Itratni, R. (2019). Carnosol, a natural polyphenol, inhibits migration, metastasis, and tumor growth of breast cancer via a ROS-dependent proteasome degradation of STAT3. *Front. Oncol.* 9, 743. doi:10.3389/fonc.2019.00743
- Alwafa, R. A., Mudalal, S., and Mauriello, G. (2021). *Origanum syriacum* L. (za'atar), from raw to go: a review. *Plants (Basel)* 10, 1001. doi:10.3390/plants10051001
- Ayesh, B. M., Abed, A. A., and Faris, D. M. (2014). *In vitro* inhibition of human leukemia THP-1 cells by *Origanum syriacum* L. and *Thymus vulgaris* L. extracts. *BMC Res. Notes* 7, 612–616. doi:10.1186/1756-0500-7-612
- Basiru, A., Ibukun, E., Edobor, G., Ojo, O., and Onikanni, S. (2013). Qualitative and quantitative analysis of phytochemicals in *Senecio bialfrae* leaf. *Int. J. Invent Pharm. Sci.* 1, 428–432.
- Bassal, H., Hijazi, A., Farhan, H., Trabolsi, C., Ahmad, B. S., Khalil, A., et al. (2021). Study of the antioxidant and anti-inflammatory properties of the biological extracts of *Psophocarpus tetragonolobus* using two extraction methods. *Molecules* 26, 4435. doi:10.3390/molecules26154435
- Bouyahya, A., Chamkhi, I., Benali, T., Guaouguaou, F. E., Balahbib, A., El Omari, N., et al. (2021). Traditional use, phytochemistry, toxicology, and pharmacology of *Origanum majorana* L. *J. Ethnopharmacol.* 265, 113318. doi:10.1016/j.jep.2020.113318
- Bouyahya, A., Zengin, G., Belmehdi, O., Bourais, I., Chamkhi, I., Taha, D., et al. (2020). *Origanum compactum* Benth., from traditional use to biotechnological applications. *J. Food Biochem.* 44, e13251. doi:10.1111/jfbc.13251
- Braicu, C., Chiorean, R., Irimie, A., Chira, S., Tomuleasa, C., Neagoe, E., et al. (2016). Novel insight into triple-negative breast cancers, the emerging role of angiogenesis, and antiangiogenic therapy. *Expert Rev. Mol. Med.* 18, e18. doi:10.1017/erm.2016.17
- Breastcancer (2021). Org triple negative breast cancer [Online]. Available: <https://www.breastcancer.org/symptoms/types/triple-negative> (accessed on 28 December 2021).
- Brem, S. S., Gullino, P. M., and Medina, D. (1977). Angiogenesis: a marker for neoplastic transformation of mammary papillary hyperplasia. *Science* 195, 880–882. doi:10.1126/science.402692
- Brem, S. S., Jensen, H. M., and Gullino, P. M. (1978). Angiogenesis as a marker of preneoplastic lesions of the human breast. *Cancer* 41, 239–244. doi:10.1002/1097-0142(197801)41:1<239::aid-cnrcr2820410133>3.0.co;2-x
- Buyel, J. F. (2018). Plants as sources of natural and recombinant anti-cancer agents. *Biotechnol. Adv.* 36, 506–520. doi:10.1016/j.biotechadv.2018.02.002
- Caesar, L. K., and Cech, N. B. (2019). Synergy and antagonism in natural product extracts: when 1 + 1 does not equal 2. *Nat. Prod. Rep.* 36, 869–888. doi:10.1039/c9np00011a

Acknowledgments

The authors would like to thank the URB of the American University of Beirut, University of Petra, and Barzan Holdings for their funding. The authors also thank Sandra Hillman for editing the manuscript and Mohammad Al Zein for taxonomic identification of *Origanum Syriacum* L.

Conflict of interest

NA was employed by the company Barzan Holdings.

The remaining authors declare that the research was conducted in the absence of any commercial or financial relationships that could be construed as a potential conflict of interest.

Publisher's note

All claims expressed in this article are solely those of the authors and do not necessarily represent those of their affiliated organizations, or those of the publisher, the editors and the reviewers. Any product that may be evaluated in this article, or claim that may be made by its manufacturer, is not guaranteed or endorsed by the publisher.

- Cassidy, A. (2003). Are herbal remedies and dietary supplements safe and effective for breast cancer patients? *Breast Cancer Res.* 5, 300–302. doi:10.1186/bcr724
- Chang, Q., Bournazou, E., Sansone, P., Berishaj, M., Gao, S. P., Daly, L., et al. (2013). The IL-6/JAK/Stat3 feed-forward loop drives tumorigenesis and metastasis. *Neoplasia* 15, 848–862. doi:10.1593/neo.13706
- Chio, I. I. C., and Tuveson, D. A. (2017). ROS in cancer: the burning question. *Trends Mol. Med.* 23, 411–429. doi:10.1016/j.molmed.2017.03.004
- Choi, S. K., Kim, H. S., Jin, T., Hwang, E. H., Jung, M., and Moon, W. K. (2016). Overexpression of the miR-141/200c cluster promotes the migratory and invasive ability of triple-negative breast cancer cells through the activation of the FAK and PI3K/AKT signaling pathways by secreting VEGF-A. *BMC Cancer* 16, 570. doi:10.1186/s12885-016-2620-7
- Cragg, G. M., and Newman, D. J. (2005). Plants as a source of anti-cancer agents. *J. Ethnopharmacol.* 100, 72–79. doi:10.1016/j.jep.2005.05.011
- Czemplik, M., Mierziak, J., Szopa, J., and Kulma, A. (2016). Flavonoid C-glucosides derived from flax straw extracts reduce human breast cancer cell growth *in vitro* and induce apoptosis. *Front. Pharmacol.* 7, 282. doi:10.3389/fphar.2016.00282
- De Sá Junior, P. L., Câmara, D. a. D., Porcacchia, A. S., Fonseca, P. M. M., Jorge, S. D., Araldi, R. P., et al. (2017). The roles of ROS in cancer heterogeneity and therapy. *Oxid. Med. Cell. Longev.* 2017, 2467940. doi:10.1155/2017/2467940
- Demain, A. L., and Vaishnav, P. (2011). Natural products for cancer chemotherapy. *Microb. Biotechnol.* 4, 687–699. doi:10.1111/j.1751-7915.2010.00221.x
- Dorman, H. J., Bachmayer, O., Kosar, M., and Hiltunen, R. (2004). Antioxidant properties of aqueous extracts from selected Lamiaceae species grown in Turkey. *J. Agric. Food Chem.* 52, 762–770. doi:10.1021/jf034908v
- Du, B., and Shim, J. S. (2016). Targeting epithelial-mesenchymal transition (EMT) to overcome drug resistance in cancer. *Molecules* 21, 965. doi:10.3390/molecules21070965
- Dufour, A., Sampson, N. S., Li, J., Kuscus, C., Rizzo, R. C., Deleon, J. L., et al. (2011). Small-molecule anticancer compounds selectively target the hemopexin domain of matrix metalloproteinase-9. *Cancer Res.* 71, 4977–4988. doi:10.1158/0008-5472.CAN-10-4552
- El-Moneim, A., Afify, M., Esawy, S., El-Hadidy, E., and Abdel-Salam, M. (2014). Antioxidant content and cytotoxicity of *Origanum syriacum* L. *Adv. Food Sci.* 36, 58–64.
- Engelhardt, U. H., Finger, A., and Kuhr, S. (1993). Determination of flavone C-glycosides in tea. *Z. Leb. Unters. Forsch.* 197, 239–244. doi:10.1007/BF01185278
- Firger, J. (2015). Nitric oxide inhibitors hit target for triple-negative breast cancer. *J. Nat. Cancer Inst.* 107, djv235. doi:10.1093/jnci/djv235
- Granados-Principal, S., Liu, Y., Guevara, M. L., Blanco, E., Choi, D. S., Qian, W., et al. (2015). Inhibition of iNOS as a novel effective targeted therapy against triple-negative breast cancer. *Breast Cancer Res.* 17, 25. doi:10.1186/s13058-015-0527-x
- Greenwell, M., and Rahman, P. K. S. M. (2015). Medicinal plants: their use in anticancer treatment. *Int. J. Pharm. Sci. Res.* 6, 4103–4112. doi:10.13040/IJPSR.0975-8232.6(10).4103-12
- Gritsko, T., Williams, A., Turkson, J., Kaneko, S., Bowman, T., Huang, M., et al. (2006). Persistent activation of stat3 signaling induces survivin gene expression and confers resistance to apoptosis in human breast cancer cells. *Clin. Cancer Res.* 12, 11–19. doi:10.1158/1078-0432.CCR-04-1752
- Guo, Q., Tian, X., Yang, A., Zhou, Y., Wu, D., and Wang, Z. (2014). Orientin in *Trollius chinensis* Bunge inhibits proliferation of HeLa human cervical carcinoma cells by induction of apoptosis. *Monatsh. Chem.* 145, 229–233. doi:10.1007/s00706-013-1011-x
- Hassan, B. (2019). “Plants and cancer treatment,” in *Medicinal Plants—Use in Prevention and Treatment of Diseases [Internet]*. Editors B. A. R. Hassan (London: IntechOpen) Available at: <https://www.intechopen.com/chapters/70522> (Accessed September 15, 2022).
- Howes, M. R. (2018). The evolution of anticancer drug discovery from plants. *Lancet. Oncol.* 19, 293–294. doi:10.1016/S1470-2045(18)30136-0
- Huang, G., Li, S., Zhang, Y., Zhou, X., and Chen, W. (2020). Vicenin-2 is a novel inhibitor of STAT3 signaling pathway in human hepatocellular carcinoma. *J. Funct. Foods* 69, 103921. doi:10.1016/j.jff.2020.103921
- Husein, A. I., Ali-Shtayeh, M. S., Jondi, W. J., Zatar, N. a.-A., Abu-Reidah, I. M., and Jamous, R. M. (2014). *In vitro* antioxidant and antitumor activities of six selected plants used in the traditional Arabic Palestinian herbal medicine. *Pharm. Biol.* 52, 1249–1255. doi:10.3109/13880209.2014.886274
- Hutzen, B., Friedman, L., Sobo, M., Lin, L., Cen, L., De Angelis, S., et al. (2009). Curcumin analogue GO-Y030 inhibits STAT3 activity and cell growth in breast and pancreatic carcinomas. *Int. J. Oncol.* 35, 867–872. doi:10.3892/ijo.00000401
- Ito, A., Lai, C. H., Zhao, X., Saito, S., Hamilton, M. H., Appella, E., et al. (2001). p300/CBP-mediated p53 acetylation is commonly induced by p53-activating agents and inhibited by MDM2. *EMBO J.* 20, 1331–1340. doi:10.1093/emboj/20.6.1331
- Jalaliddine, N., El-Hajjar, L., Dakik, H., Shaito, A., Saliba, J., Safi, R., et al. (2019). Pannexin1 is associated with enhanced epithelial-to-mesenchymal transition in human patient breast cancer tissues and in breast cancer cell lines. *Cancers (Basel)* 11, 1967. doi:10.3390/cancers11121967
- Jang, M. H., Kim, H. J., Kim, E. J., Chung, Y. R., and Park, S. Y. (2015). Expression of epithelial-mesenchymal transition-related markers in triple-negative breast cancer: ZEB1 as a potential biomarker for poor clinical outcome. *Hum. Pathol.* 46, 1267–1274. doi:10.1016/j.humpath.2015.05.010
- Kamel, M. S., Assaf, M. H., Hasanean, H. A., Ohtani, K., Kasai, R., and Yamasaki, K. (2001). Monoterpene glucosides from *Origanum syriacum*. *Phytochemistry* 58, 1149–1152. doi:10.1016/S0031-9422(01)00386-7
- Kanno, S., Tomizawa, A., Hiura, T., Osanai, Y., Shouji, A., Ujibe, M., et al. (2005). Inhibitory effects of naringenin on tumor growth in human cancer cell lines and sarcoma S-180-implanted mice. *Biol. Pharm. Bull.* 28, 527–530. doi:10.1248/bpb.28.527
- Kassam, F., Enright, K., Dent, R., Dranitsaris, G., Myers, J., Flynn, C., et al. (2009). Survival outcomes for patients with metastatic triple-negative breast cancer: implications for clinical practice and trial design. *Clin. Breast Cancer* 9, 29–33. doi:10.3816/CBC.2009.n.005
- Keo, S., Meng, C., Oeung, S., Nov, V., Lon, S., Vichet, T., et al. (2017). Preliminary phytochemical screening of selected medicinal plants of Cambodia. *Asian JPharmacog* 1, 16–23.
- Kim, S. J., Kim, H. S., and Seo, Y. R. (2019). Understanding of ROS-inducing strategy in anticancer therapy. *Oxid. Med. Cell. Longev.* 2019, 5381692. doi:10.1155/2019/5381692
- Kim, S. J., Pham, T. H., Bak, Y., Ryu, H. W., Oh, S. R., and Yoon, D. Y. (2018). Orientin inhibits invasion by suppressing MMP-9 and IL-8 expression via the PKCα/ERK/AP-1/STAT3-mediated signaling pathways in TPA-treated MCF-7 breast cancer cells. *Phytomedicine* 50, 35–42. doi:10.1016/j.phymed.2018.09.172
- Kohandel, Z., Farkhondeh, T., Aschner, M., Pourbagher-Shahri, A. M., and Samarghandian, S. (2021). STAT3 pathway as a molecular target for resveratrol in breast cancer treatment. *Cancer Cell Int.* 21, 468. doi:10.1186/s12935-021-02179-1
- Kong, Q., Beel, J. A., and Lillehei, K. O. (2000). A threshold concept for cancer therapy. *Med. Hypotheses* 55, 29–35. doi:10.1054/mehy.1999.0982
- Kucuksayan, E., and Ozben, T. (2017). Hybrid compounds as multitarget directed anticancer agents. *Curr. Top. Med. Chem.* 17, 907–918. doi:10.2174/1568026616666160927155515
- Lacroix, M., Toillon, R. A., and Leclercq, G. (2006). p53 and breast cancer, an update. *Endocr. Relat. Cancer* 13, 293–325. doi:10.1677/erc.1.01172
- Lafarga, V., Cuadrado, A., Lopez De Silanes, I., Bengoechea, R., Fernandez-Capitillo, O., and Nebreda, A. R. (2009). p38 Mitogen-activated protein kinase- and HuR-dependent stabilization of p21(Cip1) mRNA mediates the G(1)/S checkpoint. *Mol. Cell. Biol.* 29, 4341–4351. doi:10.1128/MCB.00210-09
- Lai, H., Zhao, X., Qin, Y., Ding, Y., Chen, R., Li, G., et al. (2018). FAK-ERK activation in cell/matrix adhesion induced by the loss of apolipoprotein E stimulates the malignant progression of ovarian cancer. *J. Exp. Clin. Cancer Res.* 37, 32. doi:10.1186/s13046-018-0696-4
- Lee, C. Y., Chien, Y. S., Chiu, T. H., Huang, W. W., Lu, C. C., Chiang, J. H., et al. (2012). Apoptosis triggered by vitexin in U937 human leukemia cells via a mitochondrial signaling pathway. *Urecol. Rep.* 28, 1883–1888. doi:10.3892/or.2012.2000
- Lee, H. H., Jung, J., Moon, A., Kang, H., and Cho, H. (2019). Antitumor and anti-invasive effect of apigenin on human breast carcinoma through suppression of IL-6 expression. *Int. J. Mol. Sci.* 20, 3143. doi:10.3390/ijms2013143
- Leslie, K., Lang, C., Devgan, G., Azare, J., Berishaj, M., Gerald, W., et al. (2006). Cyclin D1 is transcriptionally regulated by and required for transformation by activated signal transducer and activator of transcription 3. *Cancer Res.* 66, 2544–2552. doi:10.1158/0008-5472.CAN-05-2203
- Levy, D. E., and Inghirami, G. (2006). STAT3: a multifaceted oncogene. *Proc. Natl. Acad. Sci. U. S. A.* 103, 10151–10152. doi:10.1073/pnas.0604042103
- Lin, L., Hutzen, B., Ball, S., Foust, E., Sobo, M., Deangelis, S., et al. (2009). New curcumin analogues exhibit enhanced growth-suppressive activity and inhibit AKT and signal transducer and activator of transcription 3 phosphorylation in breast and prostate cancer cells. *Cancer Sci.* 100, 1719–1727. doi:10.1111/j.1349-7006.2009.01220.x

- Linderholm, B., Hellborg, H., Johansson, U., Elmberger, G., Skoog, L., Lehtiö, J., et al. (2009). Significantly higher levels of vascular endothelial growth factor (VEGF) and shorter survival times for patients with primary operable triple-negative breast cancer. *Ann. Oncol.* 20, 1639–1646. doi:10.1093/annonc/mdp062
- Liou, G. Y., and Storz, P. (2010). Reactive oxygen species in cancer. *Free Radic. Res.* 44, 479–496. doi:10.3109/10715761003667554
- Liu, Y., Wang, X., Zeng, S., Zhang, X., Zhao, J., Zhang, X., et al. (2018). The natural polyphenol curcumin induces apoptosis by suppressing STAT3 signaling in esophageal squamous cell carcinoma. *J. Exp. Clin. Cancer Res.* 37, 303. doi:10.1186/s13046-018-0959-0
- Lombrea, A., Antal, D., Ardelean, F., Avram, S., Pavel, I. Z., Vlaia, L., et al. (2020). A recent insight regarding the phytochemistry and bioactivity of *Origanum vulgare* L. essential oil. *Int. J. Mol. Sci.* 21, 9653. doi:10.3390/ijms21249653
- Luo, M., and Guan, J. L. (2010). Focal adhesion kinase: a prominent determinant in breast cancer initiation, progression and metastasis. *Cancer Lett.* 289, 127–139. doi:10.1016/j.canlet.2009.07.005
- Martínez-Limón, A., Joaquín, M., Caballero, M., Posas, F., and De Nadal, E. (2020). The p38 pathway: from biology to cancer therapy. *Int. J. Mol. Sci.* 21, 1913. doi:10.3390/ijms21061913
- Mcgowan, P. M., and Duffy, M. J. (2008). Matrix metalloproteinase expression and outcome in patients with breast cancer: analysis of a published database. *Ann. Oncol.* 19, 1566–1572. doi:10.1093/annonc/mdn180
- Mesmar, J., Abdallah, R., Badran, A., Maresca, M., and Baydoun, E. (2022). *Origanum syriacum* phytochemistry and pharmacological properties: A comprehensive review. *Molecules* 27, 4272. doi:10.3390/molecules27134272
- Messeha, S. S., Zarmouh, N. O., Asiri, A., and Soliman, K. F. A. (2020). Rosmarinic acid-induced apoptosis and cell cycle arrest in triple-negative breast cancer cells. *Eur. J. Pharmacol.* 885, 173419. doi:10.1016/j.ejphar.2020.173419
- Mir, M., Sawhney, S. S., and Jassal, M. M. S. (2013). Qualitative and quantitative analysis of phytochemicals of *Taraxacum officinale*. *J. Pharm. Pharmacol.* 2, 001–005.
- Moloney, J. N., and Cotter, T. G. (2018). ROS signalling in the biology of cancer. *Semin. Cell Dev. Biol.* 80, 50–64. doi:10.1016/j.semcdb.2017.05.023
- Moraes-De-Souza, R., Oldoni, T., Regitano-D'Arce, M., and Alencar, S. (2008). Antioxidant activity and phenolic composition of herbal infusions consumed in Brazil: antioxidant activity of compounds in infusions of herbs consumed in Brazil. *Cienc. Tecnol. Aliment.* 6, 41–47. doi:10.1080/11358120809487626
- Nagaprasanth, L. D., Vatsyayan, R., Singhal, J., Fast, S., Roby, R., Awasthi, S., et al. (2011). Anti-cancer effects of novel flavonoid vicenin-2 as a single agent and in synergistic combination with docetaxel in prostate cancer. *Biochem. Pharmacol.* 82, 1100–1109. doi:10.1016/j.bcp.2011.07.078
- Oyenihi, O. R., Oyenihi, A. B., Alabi, T. D., Tade, O. G., Adeyanju, A. A., and Oguntibeju, O. O. (2022). Reactive oxygen species: key players in the anticancer effects of apigenin? *J. Food Biochem.* 46, e14060. doi:10.1111/jfbc.14060
- Pham, T.-H., Park, H.-M., Kim, J., Hong, J. T., and Yoon, D.-Y. (2020). STAT3 and p53: dual target for cancer therapy. *Biomedicines* 8, 637. doi:10.3390/biomedicines8120637
- Posadino, A. M., Giordo, R., Cossu, A., Nasrallah, G. K., Shaito, A., Abou-Saleh, H., et al. (2019). Flavonoid-induced ROS generation modulates PKC biphasic effect of resveratrol on endothelial cell survival. *Biomolecules* 9, 209. doi:10.3390/biom9060209
- Ranger, J. J., Levy, D. E., Shahalizadeh, S., Hallett, M., and Muller, W. J. (2009). Identification of a Stat3-dependent transcription regulatory network involved in metastatic progression. *Cancer Res.* 69, 6823–6830. doi:10.1158/0008-5472.CAN-09-1684
- Rasoanaivo, P., Wright, C. W., Willcox, M. L., and Gilbert, B. (2011). Whole plant extracts versus single compounds for the treatment of malaria: synergy and positive interactions. *Malar. J.* 1, S4. doi:10.1186/1475-2875-10-S1-S4
- Raza, M. H., Siraj, S., Arshad, A., Waheed, U., Aldakheel, F., Alduraywish, S., et al. (2017). ROS-modulated therapeutic approaches in cancer treatment. *J. Cancer Res. Clin. Oncol.* 143, 1789–1809. doi:10.1007/s00432-017-2464-9
- Real, P. J., Sierra, A., De Juan, A., Segovia, J. C., Lopez-Vega, J. M., and Fernandez-Luna, J. L. (2002). Resistance to chemotherapy via Stat3-dependent overexpression of Bcl-2 in metastatic breast cancer cells. *Oncogene* 21, 7611–7618. doi:10.1038/sj.onc.1206004
- Relf, M., Lejeune, S., Scott, P. A., Fox, S., Smith, K., Leek, R., et al. (1997). Expression of the angiogenic factors vascular endothelial cell growth factor, acidic and basic fibroblast growth factor, tumor growth factor β -1, platelet-derived endothelial cell growth factor, placenta growth factor, and pleiotrophin in human primary breast cancer and its relation to angiogenesis. *Cancer Res.* 57, 963–969.
- Resemann, H. K., Watson, C. J., and Lloyd-Lewis, B. (2014). The Stat3 paradox: a killer and an oncogene. *Mol. Cell. Endocrinol.* 382, 603–611. doi:10.1016/j.mce.2013.06.029
- Sampaio, L. A., Pina, L. T. S., Serafini, M. R., Tavares, D. D. S., and Guimarães, A. G. (2021). Antitumor effects of carvacrol and thymol: a systematic review. *Front. Pharmacol.* 12, 702487. doi:10.3389/fphar.2021.702487
- Scaria, B., Sood, S., Raad, C., Khanafer, J., Jayachandiran, R., Pupulin, A., et al. (2020). Natural health products (NHPs) and natural compounds as therapeutic agents for the treatment of cancer; mechanisms of anti-cancer activity of natural compounds and overall trends. *Int. J. Mol. Sci.* 21, 8480. doi:10.3390/ijms21228480
- Shaito, A., Posadino, A. M., Younes, N., Hasan, H., Halabi, S., Alhababi, D., et al. (2020). Potential adverse effects of resveratrol: a literature review. *Int. J. Mol. Sci.* 21, 2084. doi:10.3390/ijms21062084
- Shen, J., Cao, B., Wang, Y., Ma, C., Zeng, Z., Liu, L., et al. (2018). Hippo component YAP promotes focal adhesion and tumour aggressiveness via transcriptionally activating THBS1/FAK signalling in breast cancer. *J. Exp. Clin. Cancer Res.* 37, 175. doi:10.1186/s13046-018-0850-z
- Singh, A., and Settleman, J. (2010). EMT, cancer stem cells and drug resistance: an emerging axis of evil in the war on cancer. *Oncogene* 29, 4741–4751. doi:10.1038/onc.2010.215
- Slika, H., Mansour, H., Wehbe, N., Nasser, S. A., Iratni, R., Nasrallah, G., et al. (2022). Therapeutic potential of flavonoids in cancer: ROS-mediated mechanisms. *Biomed. Pharmacother.* 146, 112442. doi:10.1016/j.biopha.2021.112442
- Song, Z. J., Gong, P., and Wu, Y. E. (2002). Relationship between the expression of iNOS, VEGF, tumor angiogenesis and gastric cancer. *World J. Gastroenterol.* 8, 591–595. doi:10.3748/wjg.v8.i4.591
- Sp, N., Kang, D. Y., Lee, J. M., Bae, S. W., and Jang, K. J. (2021). Potential antitumor effects of 6-gingerol in p53-dependent mitochondrial apoptosis and inhibition of tumor sphere formation in breast cancer cells. *Int. J. Mol. Sci.* 22, 4660. doi:10.3390/ijms22094660
- Tai, Y. L., Chen, L. C., and Shen, T. L. (2015). Emerging roles of focal adhesion kinase in cancer. *Biomed. Res. Int.* 2015, 690690. doi:10.1155/2015/690690
- Taliaferro-Smith, L., Oberlick, E., Liu, T., McGlothlen, T., Alcaide, T., Tobin, R., et al. (2015). FAK activation is required for IGF1R-mediated regulation of EMT, migration, and invasion in mesenchymal triple negative breast cancer cells. *Oncotarget* 6, 4757–4772. doi:10.18632/oncotarget.3023
- Wang, Y., Qi, H., Liu, Y., Duan, C., Liu, X., Xia, T., et al. (2021). The double-edged roles of ROS in cancer prevention and therapy. *Theranostics* 11, 4839–4857. doi:10.7150/thno.56747
- Watson, C., and Miller, W. (1995). Elevated levels of members of the STAT family of transcription factors in breast carcinoma nuclear extracts. *Br. J. Cancer* 71, 840–844. doi:10.1038/bjc.1995.162
- Weiner, T. M., Liu, E. T., Craven, R. J., and Cance, W. G. (1993). Expression of focal adhesion kinase gene and invasive cancer. *Lancet* 342, 1024–1025. doi:10.1016/0140-6736(93)92881-s
- Who Breast cancer. 2021 Available: <https://www.who.int/news-room/fact-sheets/detail/cancer> (accessed on 28 December 2021).
- Yang, C., Zhang, J., Ding, M., Xu, K., Li, L., Mao, L., et al. (2018). Ki67 targeted strategies for cancer therapy. *Clin. Transl. Oncol.* 20, 570–575. doi:10.1007/s12094-017-1774-3
- Yang, D., Zhang, X., Zhang, W., and Rengarajan, T. (2018). Vicenin-2 inhibits Wnt/ β -catenin signaling and induces apoptosis in HT-29 human colon cancer cell line. *Drug Des. devel. Ther.* 12, 1303–1310. doi:10.2147/DDDT.S149307
- Yip, K. W., and Reed, J. C. (2008). Bcl-2 family proteins and cancer. *Oncogene* 27, 6398–6406. doi:10.1038/onc.2008.307
- Yuan, J., Zhang, F., and Niu, R. (2015). Multiple regulation pathways and pivotal biological functions of STAT3 in cancer. *Sci. Rep.* 5, 17663. doi:10.1038/srep17663
- Yuan, L., Wang, J., Xiao, H., Wu, W., Wang, Y., and Liu, X. (2013). MAPK signaling pathways regulate mitochondrial-mediated apoptosis induced by isorientin in human hepatoblastoma cancer cells. *Food Chem. Toxicol.* 53, 62–68. doi:10.1016/j.fct.2012.11.048
- Yuan, L., Wei, S., Wang, J., and Liu, X. (2014). Isoorientin induces apoptosis and autophagy simultaneously by reactive oxygen species (ROS)-related p53, PI3K/Akt, JNK, and p38 signaling pathways in HepG2 cancer cells. *J. Agric. Food Chem.* 62, 5390–5400. doi:10.1021/jf500903g
- Zhao, Q., Luan, X., Zheng, M., Tian, X. H., Zhao, J., Zhang, W. D., et al. (2020). Synergistic mechanisms of constituents in herbal extracts during intestinal absorption: Focus on natural occurring nanoparticles. *Pharmaceutics* 12, 128. doi:10.3390/pharmaceutics12020128



OPEN ACCESS

EDITED BY

Hina Siddiqui,
University of Karachi, Pakistan

REVIEWED BY

Begum Rokeya,
Bangladesh University of Health
Sciences (BUHS), Bangladesh
Malgorzata Bialek,
Kielanowski Institute of Animal
Physiology and Nutrition (PAN), Poland

*CORRESPONDENCE

Jassim M. Al-Hassan,
jassim5577@hotmail.com

SPECIALTY SECTION

This article was submitted to
Experimental Pharmacology and Drug
Discovery,
a section of the journal
Frontiers in Pharmacology

RECEIVED 22 July 2022

ACCEPTED 03 October 2022

PUBLISHED 14 October 2022

CITATION

Al-Hassan JM, Afzal M, Oommen S,
Liu YF and Pace-Asciak C (2022),
Oxysterols in catfish skin secretions
(*Arius bilineatus*, Val.) exhibit anti-
cancer properties.
Front. Pharmacol. 13:1001067.
doi: 10.3389/fphar.2022.1001067

COPYRIGHT

© 2022 Al-Hassan, Afzal, Oommen, Liu
and Pace-Asciak. This is an open-access
article distributed under the terms of the
[Creative Commons Attribution License](#)
(CC BY). The use, distribution or
reproduction in other forums is
permitted, provided the original
author(s) and the copyright owner(s) are
credited and that the original
publication in this journal is cited, in
accordance with accepted academic
practice. No use, distribution or
reproduction is permitted which does
not comply with these terms.

Oxysterols in catfish skin secretions (*Arius bilineatus*, Val.) exhibit anti-cancer properties

Jassim M. Al-Hassan^{1*}, Mohammad Afzal¹,
Sosamma Oommen¹, Yuan Fang Liu² and Cecil Pace-Asciak^{2,3}

¹Department of Biological Sciences, Faculty of Science, Kuwait University, Kuwait, Kuwait, ²Program in Translational Medicine, Peter Gilgan Centre for Research and Learning (PGCRL), The Hospital for Sick Children, Toronto, ON, Canada, ³Department of Pharmacology, University of Toronto, Toronto, ON, Canada

The edible catfish *Arius bilineatus*, (Valenciennes) elaborates a proteinaceous gel-like material through its epidermis when threatened or injured. Our on-going studies on this gel have shown it to be a complex mixture of several biologically active molecules. Anti-cancer studies on lipid fractions isolated from the gel-like materials showed them to be active against several cancer cell lines. This prompted us to investigate further the lipid composition of the catfish epidermal gel secretions (EGS). Analysis of the lipid fraction of EGS resulted in identification of 12 oxysterols including cholesterol and 2 deoxygenated steroids i.e., 7 α -hydroxy cholesterol, 7 β -hydroxycholesterol, 5,6 epoxcholesterol, 3 β -hydroxycholest-5-ene-7-one and cholesta-3,5-dien-7-one. Progesterone, cholest-3,5-diene, cholesta-2,4-diene, cholest-3,5,6-triol and 4-cholesten-3-one were found as minor components, and were identified through their MS, ¹HNMR and FTIR spectral data and were compared with those of the standards. Cholest-3,6-dione, cholesta-4,6-diene-3-one, cholesta-2,4-diene, and cholesta-5,20(22)-dien-3-ol were found only in trace amounts and were identified by GC/MS/MS spectral data. Since cholesterol is the major component of EGS, the identified oxysterols (OS) are presumably cholesterol oxidation products. Many of the identified OS are known important biological molecules that play vital physiological role in the producer and recipient organisms. We report herein the effects of these sterols on three human cancer cell lines *in vitro*, i.e., K-562 (CML cell line), MDA MB-231 (estrogen positive breast cancer cell line) and MCF-7 (estrogen negative breast cancer cell line). Interestingly significant ($p < 0.05$) dose differences were observed between tested OS on cell types used. The presence of these sterols in EGS may help explain some aspects of the physiological activities of fraction B (FB) prepared from EGS, such as enhanced wound and diabetic ulcer healing, anti-inflammatory action and cytotoxic activities reported in our previous studies. The anti-proliferative actions of some of these oxysterols especially the cholesterol 3,5,6-triol (#5) as established on selected cancer cell lines in this study support our previous studies and make them candidates for research for human application.

KEYWORDS

epidermal secretions, inflammation, lipids, oxysterols, wound healing, cancer

1 Introduction

The catfish (*Arius bilineatus*, Valenciennes) was misidentified by fish taxonomists as *Arius thalassinus*, Ruppell. All our publications citing a single catfish species prior to 1988 used their identification (Al-Hassan, et al., 1988). *A. bilineatus*, Valenciennes is an edible catfish consumed by some inhabitants of the Gulf. It elaborates copious amounts of proteinaceous EGS when threatened or injured. This gelatinous material adheres to the fish skin, even though the fish is a fast swimmer and darts in different directions while being towed to the surface on-line.

Fishes with scales on their skin were observed to secrete mucus through their epidermis when they are caught. It was reported that this mucus contains fatty acids, immunoglobulins, lectins, and lysozymes besides glycoproteins (Tiralongo et al., 2020). The mucus was thought to provide skin protection against infection and to help the fish swim fast. However, the catfish *A. bilineatus*, Val. secretes proteinaceous gel-like secretions when stressed or injured. This epidermal gel secretion (EGS) was found to contain biologically active lipids and proteins (Al-Hassan, et al., 1986; Al-Hassan et al., 1987a; Al-Hassan et al., 1987b). EGS lipid fraction of *A. bilineatus*, Val. contains neutral lipids, glycolipids, and phospholipids. Previous analysis of the lipid fraction indicated the presence of several steroidal compounds (Al-Hassan et al., 1986).

Previously, we postulated that EGS has a protective role for *A. bilineatus* against injury (Al-Hassan et al., 1987b). Results from our laboratory have indicated that protein and lipid content of the EGS display pharmacological activities on blood vessels, blood components, inflamed lesions, cellularity in wound healing in animal model and accelerates diabetic foot ulcer healing in human (Al-Hassan et al., 1983; Al-Hassan, 1990; Al-Hassan et al., 1991), chronic back and joint pain and reduction of inflammation in human (Al-Hassan, 1990; Al-Hassan et al., 2006). Fraction B (FB) containing the catfish lipids was found to kill pancreatic cancer cells, to inhibit CD44 expression and stemness and to alter cancer cell metabolism (Al-Hassan et al., 2021).

Oxysterols can be endogenously produced from cholesterol by enzymatic and/or non-enzymatic oxidative processes or can be absorbed from dietary sources (Ballantine et al., 1980; Vatassery et al., 1997; Carvalho et al., 2010; Luliano, 2011; Chung et al., 2013). It is commonly known that OS show diverse biological activities including cytotoxic (Zmijewski et al., 2009; Carvalho et al., 2011), pro-apoptotic, and pro-inflammatory events (Hwang, 1991; Olkkonen and Hynynen, 2009). In addition, OS, have been implicated in numerous biochemical (Schroepfer, 2000; Bielska et al., 2012; Brown 2012) and pharmacological actions with special emphasis on cellularity (Larsson, et al., 2006; Vejux et al., 2009; Vejux and Lizard, 2009). Recently, it was established that furan fatty acids and Cholesta-3,5-diene (S5, compound #9 in this study), a component of catfish lipids was found to recruit neutrophils and fibroblasts to promote wound healing (Al-Hassan et al., 2020). The

anti-inflammatory activity has been attributed to furan fatty acids in the lipid fraction of *Perna Canaliculus* (Murphy et al., 2002; Wakimoto et al., 2011). Cholesta-3,5-diene was found at high level in dog cornea (Cenedella et al., 1992). Fraction B which contains furan fatty acids and oxysterols reduces all pro-inflammatory cytokines and elevates all anti-inflammatory cytokines when injected IP into diabetic animals, as measured in serum after 8 weeks of daily FB treatment (Jassim M. Al-Hassan, unpublished).

An important observation made by one of us (JMH) influenced the direction of this research study. On several occasions, during fishing for catfish for research during the past 46 years, another catfish species (*Arius tenuispenis*, Day) was found to suffer from skin tumors, while *A. bilineatus*, Val. (the subject of this research study) never had such tumors. This raised the question why was this so? This was followed by a determination to investigate EGS for the presence of oxysterols.

Encouraged by our exciting results when FB was applied for treatment of the several health problems cited above, we made it the aim of the present study to focus on the oxysterol content of the lipid fraction of EGS (hence that of FB), as a step towards further understanding the role of each individual OS (tested individually) in the control of inflammation, cancer, diabetes, pain, wound and diabetic ulcer healing, as well as other observed pharmacological activities of FB and its lipid components.

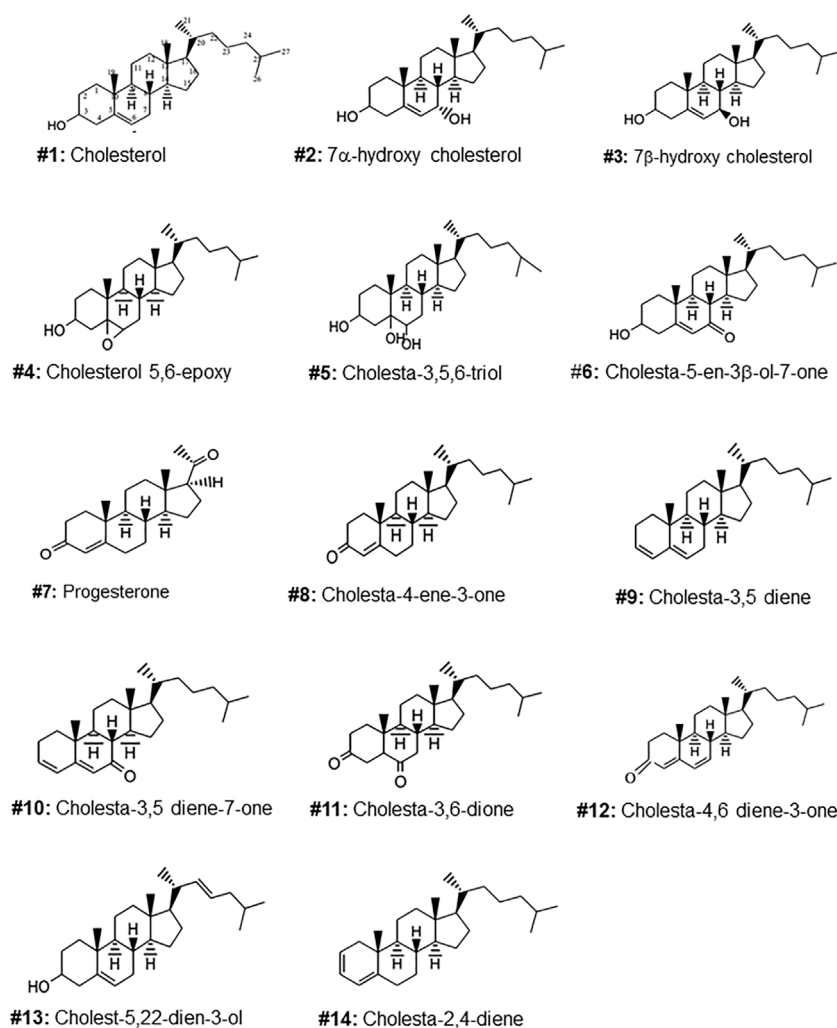
Investigation for oxysterols (OS) and steroids in EGS resulted in identification of twelve oxysterols including cholesterol and two deoxygenated steroids. As EGS was elaborated after shock or injury, the role of each oxysterol and that of the deoxygenated steroids to the fish has yet to be established. The absence of tumors on the skin of *A. bilineatus*, Val. and the discovery of the oxysterols in its EGS encouraged us further to investigate their anti-proliferative activities on selected cancer cell lines.

Since cholesterol is the major steroid component of EGS, the identified oxysterols (OS) are cholesterol oxidation products. Many of the identified OS are known important biological molecules that play vital physiological roles in the producer and recipient organisms (Selley et al., 1996; Staprans et al., 1998; Bjorkhem, 2013). In our study we investigated the effects of these OS on three human cancer cell lines *in vitro*, i.e. K-562 (CML line), MDA MB-231 (estrogen positive breast cancer line) and MCF-7 (breast cancer line estrogen negative). We expect our findings may help to advance new therapies for the active described compounds especially #5 in Figure 1, as supplements to already existing therapies for the specific cancers investigated herein and potentially other cancers.

2 Materials and methods

2.1 Definition of oxysterols

In the subsequent text, OS refers to oxygen (epoxide or keto or hydroxyl)-containing functional groups attached to ring A or

**FIGURE 1**

Molecular structures of the steroids isolated from the gel of *Arius bilineatus*. Each structure is assigned with a number to annotate further in the manuscript text.

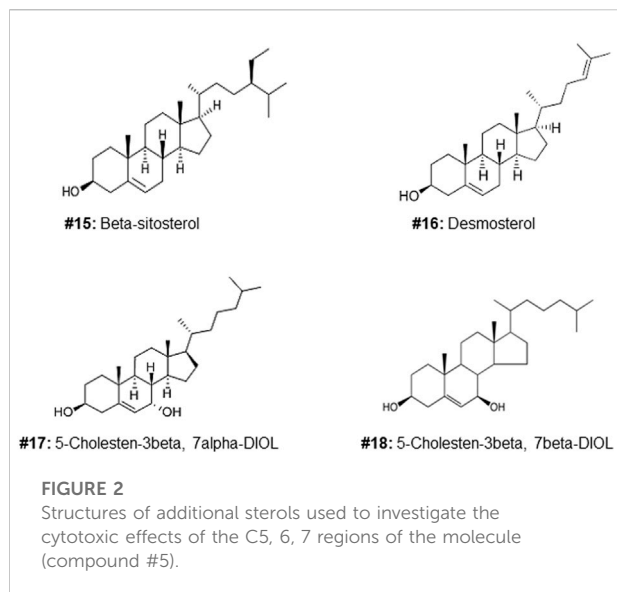
B or the side chain of the cholesterol molecule. Several non-oxygenated derivatives of cholesterol (deoxygenated/dehydrated) are referred to as deoxygenated steroids in this nomenclature for convenience of presentation. Cholesterol is a steroid. Structures are shown in Figures 1, 2.

2.1.1 Materials and instrumentation

All analytical grade solvents were freshly redistilled before lipid extraction. Solvents and aluminum coated thin layer chromatography (TLC) plates, coated with fluorescent Kieselgel-60 F₂₅₄, preparative layer chromatography (PLC) and Kieselgel-60 silica gel (0.063–0.100 mm) were obtained from Merck (Darmstadt, Germany). BSTFA + TMCS (99:1, v/v) (Kit # 33154-U) for derivatization of steroids was purchased

from Supelco (Bellefonte, PA, United States). Standard steroids, phosphomolybdic acid, and vanillin were obtained from Sigma-Aldrich, United States. Quantification of OS was done using GC/MS/MS spectrometry.

All OS used in the cancer studies *in vitro* were purchased from Sigma-Aldrich, Oakville, ON, Canada) and Steraloids (Newport, RI, United States). RPMI 1640, fetal bovine serum (FBS), antibiotics (penicillin and streptomycin), phosphate buffered saline (PBS) trypan blue and trypsin-ethylenediamine tetra acetic acid (trypsin-EDTA) were purchased from Wisent Inc. (St. Bruno, Quebec). Cell lines were purchased from ATCC (Manassas, VA, United States), WST-1 reagent from Sigma-Aldrich, Oakville, ON, Canada, SFM PMI medium from Thermo Fisher Scientific, Waltham, MA, United States.



2.1.2 Analytical instruments and conditions

All spectral measurements including FTIR, ^1H NMR, ^{13}C NMR, GC/MS, and GC-MS/MS were made in Science Analytical Facilities (SAF), Faculty of Science, KU. The GC/MS spectral data were obtained using Agilent-6890 instrument and Trace GC Ultra GC/MS DFS Bremen, Germany. ^1H NMR, ^{13}C NMR data were collected using a 400 MHz NMR (Bruker AC 400, Bruker Co., Switzerland) instrument using deuterated chloroform as a solvent. The analytical conditions for the GC/MS system, used for the analyses of oxysterols were given in [Supplementary Table S1](#).

2.2 Skin and muscle tissue sample preparation for lipid extraction

Analysis of the catfish skin and muscle for oxysterols after removal of EGS from the skin was important, considering the popular myth that consuming cooked catfish with its skin intact provides nutritional and pharmacological benefits. To detect oxysterols in skin or muscle of catfish, after removal of EGS, the catfish was repeatedly washed with distilled water accompanied with gentle massaging to ensure removal of any residual EGS. The skin was then carefully removed with a scalpel, homogenized, and freeze-dried. Samples of the flesh immediately under the skin, as well as deep lying flesh, were collected, homogenized, and freeze-dried. Both skin and muscle freeze-dried materials were stored under nitrogen in the dark at -80°C until use. Lipids in the freeze-dried samples were separately extracted using the same lipid extraction procedure as for the EGS material described below.

2.2.1 Preparation of fraction B from catfish epidermal gel secretions

Catfish epidermal gel secretions were collected as described previously ([Al-Hassan et al., 1986](#); [Al-Hassan et al., 1987b](#)). The gel-like material was fractionated to yield Fraction B (FB), containing lipids (13.4%) and proteins (85%) utilizing procedures described in the two published US patents ([Al-Hassan, 2013](#); [Ali 2020](#)). Protein content in FB was assayed with Bradford's method ([Bradford, 1976](#)) employing Coomassie Blue, and the protein concentration was calculated from the standard curve at λ 595 nm generated with bovine albumin. The linear curve obtained was used to calculate total proteins in FB. The lipid percent content of FB was calculated using methods described in ([Al-Hassan, 2013](#); [Ali 2020](#)).

2.2.2 Lipid extraction from epidermal gel secretions

Total lipid content of the freeze-dried gel material (5 g) was obtained by extraction with 20–30 ml of chloroform-methanol-isopropanol solvent mixture (2:1:0.25, v/v/v) for 72 h at room temperature under nitrogen environment. The extracted lipids were collected by filtration under vacuum. The remaining solid was re-extracted twice with fresh solvent mixture. The extraction solvent mixture was then pooled and evaporated using a rotary evaporator. The total lipid extract (1.36 g) was re-dissolved in chloroform-methanol (2:1 v/v) solvent mixture for lipid fractionation by silica gel column chromatography.

2.2.3 Fractionation of lipids using column chromatography

The extracted lipid material (1.36 g) was applied to a 30×2 cm column packed with silica gel (70–100 mesh, 100–200 μm particle size; Woelm Pharma) in petroleum spirit ($40-60^\circ\text{C}$). The column was first eluted with distilled petroleum spirit ($40/60^\circ$) to give neutral lipids (NL) (glycerides), followed by a mixture of petroleum spirit:chloroform (1:1 v/v), with a gradual increase of chloroform to 100%, or with petroleum spirit-diethyl ether (8:2, v/v) and 50 ml fractions were collected (we call these fractions also neutral lipid). After TLC analyses of the collected fractions, portions of the same composition were pooled and concentrated on a rotary evaporator. Each concentrated fraction was redissolved in chloroform, passed through a normal phase silica Sep-Pak and analyzed by Agilent GC/MS system.

2.2.4 Purification of oxysterols from the lipid fraction

Analysis for oxysterols in the lipid fractions was carried out using preparative thick layer chromatographic plates (PLC) and thin layer chromatographic plates (TLC). For initial separation of the lipids PLC plates were used. The neutral lipid (petroleum spirit:chloroform column fraction) fraction separated from chromatography column was applied on a PLC plate with the help of an autoliner TLC applicator (Desaga, Sarstedt TLC

applicator AS 30, Numbrecht, Germany) and the plate was chromatogrammed in a chromatography solvent chamber containing a mixture of heptane-ethyl acetate (1:1, v/v). After the solvent front reached half the plate, the plate was removed from the chamber and dried under nitrogen environment. The plate was then re-chromatogrammed in a mixture of hexane-diethyl ether-acetic acid (30:19:1, v/v/v). The plate, after drying, was covered with a glass sheet and one side edge of the plate was stained with 1% vanillin solution in 100 ml sulphuric acid-ethanol solution (1:4, v/v) followed by heating the side edge of the plate at 110°C, while keeping the rest of the plate cold. Steroids and oxysterols on the stained part of the PLC plate appeared as a spectrum of different colors. The corresponding unstained bands were scratched off from the PLC plate and the adsorbent was eluted with chloroform:methanol (2:1, v/v). After filtration, the solvent was evaporated under a stream of nitrogen gas and the residue was applied to a TLC plate and chromatogrammed as for the PLC separation above. The side edge of the separated bands was stained with 1% vanillin solution in 100 ml sulphuric acid-ethanol solution (1:4, v/v) followed by heating the side edge of the plate at 110°C. Oxysterols on the stained part of the TLC plate appeared as a spectrum of different colors. The corresponding unstained band of each oxysterol was scratched off from the TLC plate and the adsorbent was eluted with chloroform:methanol (2:1, v/v). After filtration, the solvent was evaporated under a stream of nitrogen gas and the residue was analyzed by GC/MS, FTIR, ¹HNMR, ¹³CNMR and GC/MS/MS. Spectral data were compared with those of reference spectra. Purity and authenticity of individual compounds were confirmed by TLC and by GC/MS against standards.

2.2.5 Lipid saponification

For confirmation of the type and number of oxysterols in EGS and to make sure that no oxysterols were missed during extraction and purification procedures, saponification was carried out on the total extracted lipids using 3 different methods for comparison purposes. These methods were: 1) Saponification by refluxing in 5 M methanolic NaOH, for 2 h; 2) Reaction with 0.35 N ethanolic KOH for 12 h at 25°C; 3) Incubation in 2 N NaOH mixed with dioxane for 12 h at 25°C. Water (25 ml) was added to the saponification reaction mixture of each procedure, followed by the addition of chloroform (75 ml) and mixed. Dioxane was evaporated after the addition of water under nitrogen. The saponified lipids obtained from each of the saponification procedures were acidified with 2 N HCl and extracted with chloroform. The organic layer was separated, dried over anhydrous sodium sulphate and vacuum evaporated. The residue was then dissolved in chloroform:methanol (2:1; v/v) and one spot from each of the three reactions along with one spot from the neutral lipids were applied to a TLC plate and chromatogrammed in heptane:ethyl acetate (1:1, v/v) mixture till the solvent front reached half the plate. The plate was dried under nitrogen, followed by a

second development in hexane:diethylether:acetic acid (30:19:1, v/v/v). The chromatogram was stained with vanillin reagent to detect oxysterols. Samples from the saponified products were analyzed for OS by GC/MS.

2.3 Cytotoxic effects of oxysterols on three human cancer cell lines

K562, MCF-7, MDA MB-231 cells were expanded as per instructions from the Company (ATCC). The cell medium was replaced with fresh RPMI/1% FBS/PS medium. For the studies, the cells were starved for 2 h in a tissue culture flask in SFM RPMI medium. 1e4 cells/well were then added to 96-well plastic plates and conditioned overnight, then centrifuged, replaced with fresh medium with RPMI/1% FBS/PS. The desired amount of each test oxysterol was dissolved in ethanol to make up the concentration needed and was then dried down in a siliconized glass tube then 5 µl ethanol was added, followed by addition of cell medium to make up a concentration of 0.02 µg/µl. The required aliquots were added to each well to which 50 µl conditioned cell medium had been added to make up 100 µl total well volume. The wells were then incubated overnight (<20 h) in 96-well plates. Then 10 µl WST-1 reagent (Roche) was added to each well and incubated for 4 h, then each well was read on a plate reader at 450 nm with 650 nm as reference. Cells were tested for cell viability using trypan blue exclusion method as a routine practice after passaging and counting the cells.

2.4 Statistical analysis

GraphPad Prism statistical analysis software (Version 5.0a) was used to perform all statistical analysis. Data are expressed as mean ± standard error. Comparison between multiple groups was performed by ANOVA followed by Bonferroni's posttest or Dunnett's test. Pairwise comparisons were performed by *t*-test. A *p*-value of ≤0.05 was considered to represent statistically significant differences between samples.

3 Results

3.1 Identification of the purified oxysterols from epidermal gel secretion

The TLC purified oxysterols were analyzed by GC/MS, GC/MS/MS, ¹HNMR, ¹³CNMR and FTIR and their spectral data were compared with those of reference standards (Supplementary Tables S2–S5). The following 13 cholesterol derivatives and cholesterol were identified, and their molecular structures are shown in Figure 1. Cholesterol, 7α-hydroxy cholesterol, 7β-hydroxycholesterol, 5,6 epoxycholesterol, 3β-hydroxycholest-5-

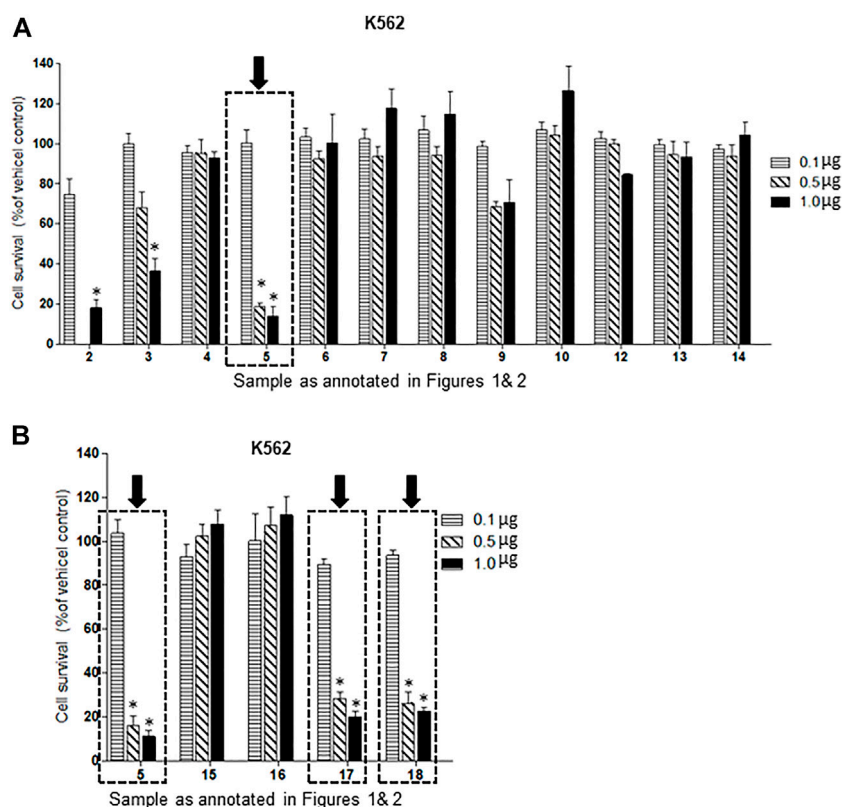


FIGURE 3

(A,B): Dose-response comparison of the cytotoxic effects of various sterols (as % of ethanol vehicle control) shown to be present in EGS in this study on K562 CML, a human cancer cell line *in vitro*. The cell survival data presented as percentage of vehicle control determine the significant potency of triols #5, #17 and #18 in the tested cell line ($n = 3$, $p < 0.05$, One-way ANOVA with Dunnett's post-test to compare response of different dosages).

ene-7-one, cholest-3,5-diene and cholesta-3,5-dien-7-one were identified by comparing GC/MS/MS, ^1H NMR, ^{13}C NMR and FTIR spectral data with those of reference standards. Progesterone, cholest-3,5,6-triol and 4-cholesten-3-one were found as minor components, and were identified by comparing their MS, ^1H NMR and FTIR spectral data with those of standards and library data base. Cholest-3,6-dione, cholesta-4,6-diene-3-one, cholesta-2,4-diene, and cholesta-5,20(22)-dien-3-ol were found only in trace amounts and were identified by comparing their GC/MS data with library data base (Supplementary Table S5).

3.2 Search for oxysterol in the skin and flesh of the catfish

Analysis of lipids from skin of the catfish, showed the presence of cholesterol and alpha tocopherol with small amounts of free fatty acids and acylglycerols, with no trace of oxysterols. Analysis of the flesh whether located immediately

under the skin or deep in muscle layers also showed the presence of only acylglycerols and free fatty acids with a trace amount of tocopherol and cholesterol.

3.3 Cytotoxic effects of oxysterols

Of the oxysterol detected in EGS, the most active on all three cell lines was cholesta-3,5,6-triol (#5 in Figure 1) with the K562 leukemic cell line being the most responsive within 0.5–1 µg/100 µl assay volume (Figures 3A,B). Of the two breast cancer cell lines, the MDA MB-231 cell line (Figures 4A,B) was more responsive within this dose range than the MCF-7 cell line (Figures 5A,B). Interestingly the 5,6-epoxide precursor (#4 in Figure 1) of cholesta-3,5,6-triol was not appreciably active, suggesting that the epoxide derives its activity after hydrolysis to the more stable and probably more water soluble triol. Four additional hydroxy cholesterol (#15, 16, 17, 18 in Figure 2) were available commercially which served to investigate the importance of the hydroxyl groups of the

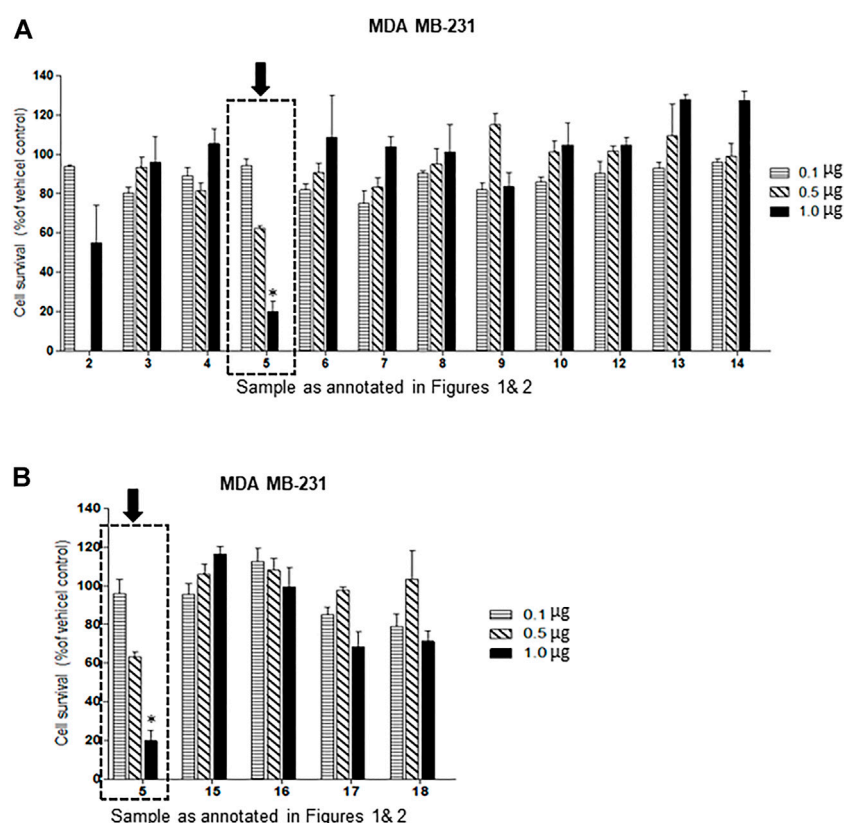


FIGURE 4

(A,B): Dose-response comparison of the cytotoxic effects of various sterols (as % of ethanol vehicle control) shown to be present in EGS in this study on MDA MB-231 an estrogen receptor negative breast cell line *in vitro*. The cell survival data presented as percentage of vehicle control determine the significant potency of only triol #5 in the tested cell line ($n = 3$, $p < 0.05$, One-way ANOVA with Dunnett's post-test to compare response of different dosages).

3,5,6 triol in #5 for apoptotic activity, i.e. we compared oxysterols #15–18 with oxysterol #5 (Figures 3B, 4B, 5B). Interestingly, while all 4 oxysterols possessed the 3-hydroxyl group, oxysterols #17 and #18 lacked the 5,6 diol of oxysterol #5, but instead possessed a double bond at C5, 6 as in cholesterol, and a hydroxyl group at C7. Yet #17 and #18 but not #15 and #16 were active as #5 on K562 cells suggesting the importance of C3 hydroxyl group combined with either a C7 hydroxyl group and the double bond at C5,6 or the C5,6 hydroxyl groups could be replaced by a double bond linked with C7 hydroxyl group (Figures 2, 3). The two breast cancer lines were less responsive but still selective for #5 in Figure 1, the cholesta- 3,5,6 triol.

4 Discussion

Our studies related to *A. bilineatus*, Val. proved that EGS was composed of biologically active proteins and lipids. This is contrary to the reported composition of fish mucus (Tiralongo et al., 2020). The lipid fraction of EGS was found to be essential

for several activities of Fraction B prepared from EGS. Analysis of the lipid fraction indicated the presence of several steroidal compounds. Further search for oxysterols in EGS resulted in twelve oxysterols including cholesterol and two deoxygenated steroids. As it was found that EGS was elaborated after shock or injury, the role of each oxysterol and that of the deoxygenated steroids in the fish during injury or disease has yet to be established.

The presence of oxysterols in the skin of an edible fish has been demonstrated in this study. This will open new venues in fishmeal research with emphasis on pharmacological implications of its oxysteroidal contents. Our results demonstrate that catfish with its skin intact may provide more than nourishing fish proteins and the commonly known fish lipids, such as triglycerides, cholesterol and fatty acids. It can also provide other lipids of biological and pharmacological importance in the neutral lipid fraction as well as glycolipids, and phospholipids.

Healing of wounds and badly infected, highly inflamed non-healing diabetic foot ulcers (some with osteomyelitis) with potent

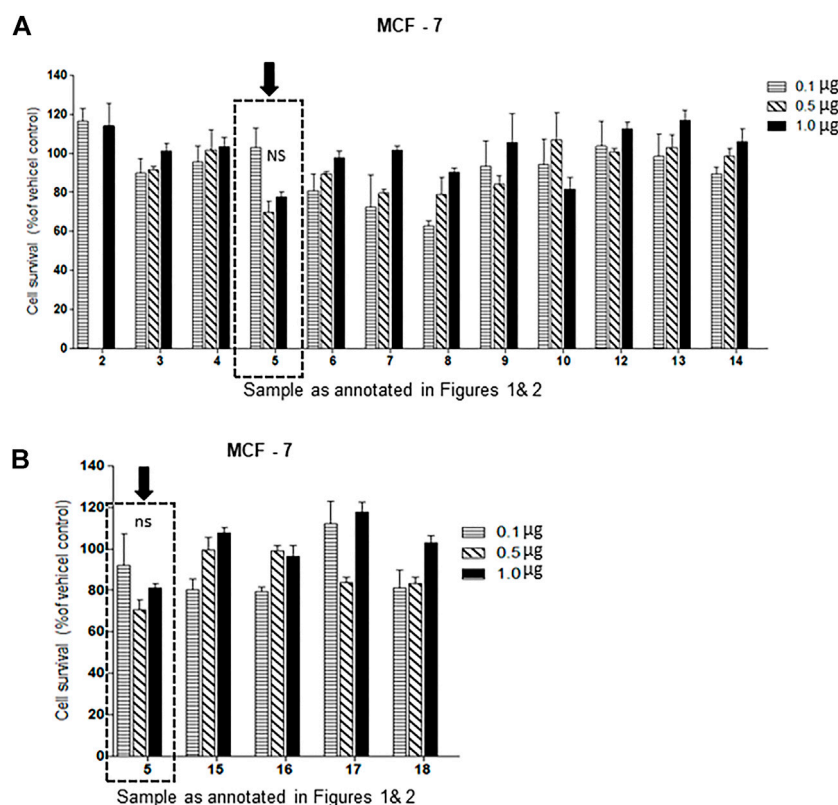


FIGURE 5

(A,B): Dose-response comparison of the cytotoxic effects of various sterols (as % of ethanol vehicle control) shown to be present in EGS in this study on MCF-7 an estrogen receptor positive breast cell line *in vitro*. Interestingly the cell survival data presented as percentage of vehicle control shows that trials #5 and others are weakly (non-significant) active in MCF-7 cell line ($n = 3$, $p < 0.05$, One-way ANOVA with Dunnett's post-test to compare response of different dosages).

preparations from EGS has been previously reported by us and may be supported by the presence of oxysterols (Al-Hassan et al., 1983; Al-Hassan, 2013; Al-Hassan et al., 2020; Ali 2020). All these activities have been experienced and demonstrated in the EGS and we predict that some of these activities may be correlated with the presence of oxysterols in the epidermal gel material. The available evidence suggests that the androgenic potential of EGS may also be explained based on oxysterols present in the EGS (Wang, et al., 2010).

It was interesting that Cholesta-3,5-diene (cholesterylene; S5, herein labeled #9) which was found in EGS and its FB fraction promotes wound healing (Al-Hassan et al., 2020). The role of each oxysterol found in EGS in the wound and diabetic ulcer healing when FB was applied to these lesions has yet to be established. Analysis of the skin and the flesh of the catfish showed no oxysterols in either of them. The claimed benefits of catfish consumers may be due to incomplete washing of the catfish, leaving some EGS on its skin before cooking, or it could be due to components other than oxysterols in the cooked catfish (anecdotal evidence).

Reports indicate that the OS mixture may result from the free radical oxidation of cholesterol (Bascoul et al., 1986). This is the main lipid component of the fish secreted gel with epoxidation of the C5,6 double bond and its hydrolysis to form cholesterol 3,5,6 triol (#5) a very stable and probably very soluble compound.

We unexpectedly identified interesting dose differences between each OS tested between the three cell types used and between the series of compounds identified. Of these, one in particular (3,5,6-trihydroxy cholesterol metabolite, #5 in Figure 1) was the most potent anti-cancer compound, while its precursor compound, the 3-hydroxy-5,6-epoxide derivative (#4 in Figure 1) was inactive within the doses tested.

The presence of these sterols in EGS may help explain some aspects of the physiological activities of preparations from EGS such as enhanced wound healing and anti-inflammatory and cytotoxic activities reported in our previous studies. These results support our postulate that the skin secretion of catfish may play an important protective role for the fish against injury and disease. The OS which showed anti-cancer activities against selected human cancer cell lines (Figure 3), particularly the

potent cholesta-3,5,6 triol, #5 in Figure 1, can be candidates for translational application for curing certain human cancer diseases.

5 Conclusion

The presence of twelve OS and two deoxygenated sterols in EGS and its FB fraction helps to unravel some of the physiological and therapeutic roles OS provide to the catfish *A. bilineatus*, Val. Our results show that the different OS discovered in EGS may possess different pharmacological activities and that their role could be beneficial to the catfish and may help explain how the catfish heals its wounds and how its skin has not been seen with skin tumors.

The presence of OS together with the other pharmacologically active components found in EGS provides further evidence that EGS is elaborated for the protection of the catfish against possible injuries or skin diseases. The application of FB, which is prepared from EGS for treatment of different human and animal health problems can be considered as an extension to the benefits provided by EGS to the catfish. The action of some OS on selected cancer cell lines reported in this study is exciting. It could inspire other valuable studies based on other active components from the marine environment. Understanding the individual physiological role of each of these OS in EGS may help appreciate their role in our observed wound and diabetic ulcer healing and other physiological activities analogous to those reported here on cancer cells. Thus, results of the present study may lead to correlate various biological activities with the presence of specific OS as shown herein together with the biological activities of the other active molecules found in EGS.

Data availability statement

The raw data supporting the conclusions of this article will be made available by the authors, without undue reservation.

Author contributions

JMA-H and CP-A managed the chemistry and the cancer studies respectively and wrote the respective parts of the manuscript. MA supervised the chemistry Lab work and SO carried out the separation and the identification of the OS.

References

Al-Hassan, J. M., Afzal, M., Ali, M., Thomson, M., Fatima, T., Fayad, S., et al. (1986). Lipid composition of the epidermal gel secretion from the Arabian Gulf

Funding

This work was supported by Kuwait University research grant #SL04/09 for which the authors are thankful. DigiBiomics Inc, Canada (Meraj Khan) carried out the statistics and Figure presentation and submitted the revised manuscript to the Journal.

Acknowledgments

We are grateful to Mohammad Al-Naki for his generous donation of the research boat and to Abdulredha H. Ghadanfar for providing his boat for our research. Special thanks are due to The Family of Yousef Khalid Al-Adsani for their generous financial donation. Sincere thanks are due to Hussein Ali Nasser Al-Qattan and his sons Bashar and Ali for their financial and administrative contribution to our research. Jassim M. Al-Hassan (the PI) contributed financially to this project. The authors thankfully acknowledge assistance of Science Analytical Facilities (SAF) at KU using their General Facility Project instruments (# GS01/01, GS03/01, GS01/03) for spectroscopic analysis.

Conflict of interest

The authors declare that the research was conducted in the absence of any commercial or financial relationships that could be construed as a potential conflict of interest.

Publisher's note

All claims expressed in this article are solely those of the authors and do not necessarily represent those of their affiliated organizations, or those of the publisher, the editors and the reviewers. Any product that may be evaluated in this article, or claim that may be made by its manufacturer, is not guaranteed or endorsed by the publisher.

Supplementary material

The Supplementary Material for this article can be found online at: <https://www.frontiersin.org/articles/10.3389/fphar.2022.1001067/full#supplementary-material>

catfish, *Arius thalassinus*, Ruppell. *Comp. Biochem. Physiol. B* 85, 41–47. doi:10.1016/0305-0491(86)90218-x

- Al-Hassan, J. M., Clayton, D., Thomson, M., and Criddle, R. S. (1988). Taxonomy and distribution of arid catfishes from the Arabian Gulf. *J. Nat. Hist.* 22, 473–487. doi:10.1080/00222938800770331
- Al-Hassan, J. M. (1990). Diabetic ulcer healing preparations from the skin of the Arabian Gulf catfish (f32 *Arius bilineatus*, Val.), A Novel and effective treatment. *Int. J. Tissue React.* XII, 121–135.
- Al-Hassan, J. M., Dyson, M., Young, S. R., Thomson, M., and Criddle, R. S. (1991). Acceleration of wound healing responses induced by preparations from the epidermal secretions of the Arabian Gulf catfish, *Arius bilineatus*, Valenciennes. *J. Wilderness Med.* 2, 153–163. doi:10.1580/0953-9859-2.3.153
- Al-Hassan, J. M., Hinek, A., Renno, W. M., Wang, Y., Liu, Y. F., Guan, R., et al. (2020). Potential mechanism of dermal wound treatment with preparations from the skin gel of arabian Gulf catfish: A unique furan fatty acid (F6) and cholesta-3, 5-diene (S5) recruit neutrophils and fibroblasts to promote wound healing. *Front. Pharmacol.* 11, 899. doi:10.3389/fphar.2020.00899
- Al-Hassan, J. M., Ramadan, A., Thomson, M., Ali, M., Afzal, M., Abdel- Razek, M., et al. (2006). Healing of back pain and some other neurological problems using preparations from the skin of the arabian Gulf catfish (*Arius bilineatus*, val.). *Exp. Biol. Annu. Meet. Am. Soc. Biochem. Mol. Biol.* 8, PA487. Abstract No. 330.
- Al-Hassan, J. M., Thomson, M., Ali, M., and Criddle, R. S. (1987b). Toxic and pharmacologically active secretions from the Arabian Gulf catfish. *Arius Thalass. Ruppell. J. Toxicol. Toxin Rev.* 6, 1–43.
- Al-Hassan, J. M., Thomson, M., and Criddle, R. S. (1983). Accelerated wound healing by a preparation from skin of the Arabian Gulf catfish. *Lancet* 1, 1043–1044. doi:10.1016/s0140-6736(83)92665-x
- Al-Hassan, J. M., Thomson, M., Summers, B., and Criddle, R. S. (1987a). Protein composition of the threat induced epidermal secretion from the Arabian Gulf catfish, *Arius thalassinus*, Ruppell. *Comp. Biochem. Physiol. B* 88, 813–822. doi:10.1016/0305-0491(87)90249-5
- Al-Hassan, J. M. (2013). United States patent for method of making an anti-Inflammatory Composition. *Pat. No* 8, 551532-B2.
- Al-Hassan, J. M., Wei, D., Chakraborty, S., Conway, T., Rhea, P., Wei, B., et al. (2021). Fraction B from catfish epidermal secretions kills pancreatic cancer cells, inhibits CD44 expression and stemness, and alters cancer cell metabolism. *Front. Pharmacol.* 12, 659590. doi:10.3389/fphar.2021.659590
- Ali, J. M. H. (2020). Method of preparing a therapeutic composition using a preparation from epidermal gel secretions of catfish. United States patent. *U. S. Pat. No* 10568, 915.
- Ballantine, J. A., Roberts, J. C., and Morris, R. J. (1980). The sterols of crustaceans: *Decapods* (sub-order *macrura*). *Comp. Biochem. Physiology Part B Biochem.* 67, 75–79. doi:10.1016/0305-0491(80)90271-0
- Bascul, J., Domergue, N., Olle, M. A., and CrAstes de Paulet, A. (1986). Autoxidation of cholesterol in tallows heated under deep frying conditions: Evaluation of oxysterols by GLC and TLC-FID. *Lipids* 2, 383–387. doi:10.1007/BF02534932
- Bielska, A. A., Scholesinger, P., Covey, D. F., and Ory, D. S. (2012). Oxysterols as non-genomic regulators of cholesterol homeostatis. *Trends endocrinol. Metab.* 3, 99–106.
- Bjorkhem, I. (2013). Five decades with oxysterols. *Biochimie* 95, 448–454. doi:10.1016/j.biochi.2012.02.029
- Bradford, M. A. (1976). Rapid and sensitive method for the quantitation of microgram quantities of protein utilizing the principle of protein-dye binding. *Anal. Biochem.* 72, 248–254. doi:10.1016/0003-2697(76)90527-3
- Brown, A. J. (2012). Cholesterol versus other sterols: How do they compare as physiological regulators of cholesterol homeostasis? *Eur. J. Lipid Sci. Technol.* 114, 617–623. doi:10.1002/ejlt.201100295
- Carvalho, J. F., Silva, M. M., Moreira, J. N., Simoes, S., and Melo, M. L. (2010). Sterols as anticancer agents: Synthesis of ring-B oxygenated sterols, cytotoxic profile, and comprehensive SAR analysis. *J. Med. Chem.* 53, 7632–7638. doi:10.1021/jm1007769
- Carvalho, J. F. S., Silva, C. M. M., Moreira, J. N., Simoes, S., and Sa e Melo, M. L. (2011). Selective cytotoxicity of oxysterols through structural modulation on rings A and B. Synthesis, *in vitro* evaluation, and sar. *J. Med. Chem.* 54 (18), 6375–6393. doi:10.1021/jm200803d
- Cenedella, R. J., Linton, L. L., and Moore, C. P. (1992). Cholesterylene, a newly recognized tissue lipid, found at high levels in the cornea. *Biochem. Biophys. Res. Commun.* 186, 1647–1655. doi:10.1016/s0006-291x(05)81597-9
- Chung, M. L., Lee, K., and Lee, C. Y. (2013). Profiling of oxidized lipid products of marine fish under acute oxidative stress. *Food Chem. Toxicol.* 53, 205–213. doi:10.1016/j.fct.2012.11.047
- Hwang, P. L. (1991). Biological activities of oxygenated sterols: Physiological and pathological implications. *Bioessays* 13, 583–589. doi:10.1002/bies.950131108
- Larsson, D. A., Baird, S., Nyhalah, J. D., Yuan, X. M., and Li, W. (2006). Oxysterol mixtures in atheroma-relevant proportions, display synergistic and proapoptotic effects. *Free Radic. Biol. Med.* 41, 902–910. doi:10.1016/j.freeradbiomed.2006.05.032
- Luliano, L. (2011). Pathways of cholesterol oxidation via non-enzymatic mechanisms. *Chem. Phys. Lipids* 164, 457–468. doi:10.1016/j.chemphyslip.2011.06.006
- Murphy, K. J., Mooney, B. D., Mann, N. J., Nichols, P. G., and Sinclair, A. J. (2002). Lipid, FA, and sterol composition of New Zealand green lipped mussel (*Perna canaliculus*) and Tasmanian blue mussel (*Mytilus edulis*). *Lipids* 37, 587–595. doi:10.1007/s11745-002-0937-8
- Olkkonen, V. M., and Hynynen, R. (2009). Interactions of oxysterols with membranes and proteins. *Mol. Asp. Med.* 30, 123–133. doi:10.1016/j.mam.2009.02.004
- Schroepfer, G. J., Jr. (2000). Oxysterols:modulators of cholesterol metabolism and other processes. *Physiol. Rev.* 80, 361–554. doi:10.1152/physrev.2000.80.1.361
- Selley, M. L., McGuinness, J. A., and Ardlie, N. G. (1996). The effect of cholesterol oxidation products on human platelet aggregation. *Thromb. Res.* 83, 449–461. doi:10.1016/0049-3848(96)00154-5
- Staprans, I., Pan, X. M., Rapp, J. H., and Feingold, K. R. (1998). Oxidized cholesterol in the diet accelerates the development of aortic atherosclerosis in cholesterol-fed rabbits. *Arterioscler. Thromb. Vasc. Biol.* 18, 977–983. doi:10.1161/01.atv.18.6.977
- Tiralongo, F., Messina, G., Lombardo, B. M., Longhitano, L., Li Voti, G., and Tibullo, D. (2020). Skin mucus of marine fish as a source for the development if antimicrobial agents. *Font. Mar. Sci.* doi:10.3389/fmars.2020.541853
- Vatassery, G. T., Quach, H. T., Smith, W. E., and Ungar, F. (1997). Oxidation of cholesterol in synaptosomes and mitochondria isolated from rat brains. *Lipids* 32, 879–886. doi:10.1007/s11745-997-0113-1
- Vejud, A., and Lizard, G. (2009). Cytotoxic effects of oxysterols associated with human diseases: Induction of cell death (apoptosis and/or oncosis), oxidative and inflammatory activities, and phospholipidosis. *Mol. Asp. Med.* 30, 153–170. doi:10.1016/j.mam.2009.02.006
- Vejud, A., Malvitte, L., and Lizard, G. (2009). Side effects of oxysterols: Cytotoxicity, oxidation, inflammation, and phospholipidosis. *Braz. J. Med. Biol. Res.* 4, 545–556. doi:10.1590/s0100-879x2008000700001
- Wakimoto, T., Kondo, H., Nil, H., Kimura, K., Egami, Y., Oka, Y., et al. (2011). Furan fatty acids as anti-inflammatory components from the green-lipped mussel *Perna canaliculus*. *PNAS* 108, 17533–17535.
- Wang, S., Rijk, J. C., Riethoff-Poortman, J. H., Van Kuijk, S., Peijnenburg, A. A., and Bovee, T. F. (2010). Bovine liver slices combined with an androgen transcriptional activation assay: An *in-vitro* model to study the metabolism and bioactivity of steroids. *Anal. Bioanal. Chem.* 397, 631–641. doi:10.1007/s00216-010-3605-z
- Zmijewski, M. A., Li, W., Zjawiony, J. K., Sweatman, T. W., Chen, J., Miller, D. D., et al. (2009). Photo-conversion of two epimers (20R and 20S) of pregna-5, 7-diene-3beta, 17alpha, 20-triol and their bioactivity in melanoma cells. *Steroids* 74, 218–228. doi:10.1016/j.steroids.2008.10.017



OPEN ACCESS

EDITED BY

Hidayat Hussain,
Leibniz Institute of Plant Biochemistry,
Germany

REVIEWED BY

Abir El-Alfy,
Medical College of Wisconsin,
United States
Luana Lionetto,
Sapienza University of Rome, Italy

*CORRESPONDENCE

Joaquin Guerra,
✉ neuroorl@euroespes.com

SPECIALTY SECTION

This article was submitted to
Experimental Pharmacology
and Drug Discovery,
a section of the journal
Frontiers in Pharmacology

RECEIVED 02 August 2022

ACCEPTED 23 November 2022

PUBLISHED 20 December 2022

CITATION

Guerra J, Naidoo V and Cacabelos R
(2022), Potential effects of cannabinoids
on audiovestibular function: A
narrative review.
Front. Pharmacol. 13:1010296.
doi: 10.3389/fphar.2022.1010296

COPYRIGHT

© 2022 Guerra, Naidoo and Cacabelos.
This is an open-access article
distributed under the terms of the
[Creative Commons Attribution License](#)
(CC BY). The use, distribution or
reproduction in other forums is
permitted, provided the original
author(s) and the copyright owner(s) are
credited and that the original
publication in this journal is cited, in
accordance with accepted academic
practice. No use, distribution or
reproduction is permitted which does
not comply with these terms.

Potential effects of cannabinoids on audiovestibular function: A narrative review

Joaquin Guerra^{1*}, Vinogran Naidoo² and Ramon Cacabelos³

¹Neuro-Otology Unit, EuroEspes Biomedical Research Center, Institute of Medical Science and Genomic Medicine, Bergondo, Corunna, Spain, ²Department of Neuroscience, International Center of Neuroscience and Genomic Medicine, EuroEspes Biomedical Research Center, Bergondo, Corunna, Spain, ³Genomic Medicine, EuroEspes Biomedical Research Center, Institute of Medical Science and Genomic Medicine, Bergondo, Corunna, Spain

The growing interest in the development of drugs that target the endocannabinoid system has extended to conditions that affect the audiovestibular pathway. The expression of cannabinoid (CB) receptors in that pathway has been widely demonstrated, indicating a therapeutic potential for drug development at this level. These medications may be beneficial for conditions such as noise-induced hearing loss, ototoxicity, or various forms of vertigo of central or peripheral origin. The therapeutic targets of interest include natural or synthetic compounds that act as CB1/CB2 receptor agonists/antagonists, and inhibitors of the endocannabinoid-degrading enzymes FAAH and MAGL. Furthermore, genetic variations implicated in the response to treatment and the development of related disorders such as epilepsy or migraine have been identified. Direct methods of administering these medications should be examined beyond the systemic strategy.

KEYWORDS

hearing, vertigo, cannabinoids, cannabis, THC-tetrahydrocannabinol, CBD-cannabidiol

1 Introduction

Auditory and vestibular disorders comprise a heterogeneous group of conditions that have different pathophysiological mechanisms. Depending on the disease, they may affect different structures of the inner ear, cochleovestibular nerve, central signaling or processing nuclei. At the same time, these disorders can either increase or decrease sensory and neural excitability. For example, increased sensory and neural excitability occurs during an acute vestibular crisis (e.g., vestibular neuritis, migraine, and labyrinthitis) or during tinnitus. By contrast, in other disorders such as chronic vestibular hypofunction or age-related hearing loss, there is a deterioration of sensory and neural activity (Peelle and Wingfield, 2016). The neurochemistry of these audiovestibular disorders includes diverse neurotransmitters with excitatory (glutamate, acetylcholine), inhibitory (GABA, glycine), modulatory (histamine, noradrenaline) and other actions (enkephalin, motilin, somatostatin, dopamine and

serotonin) (Guerra and Cacabelos, 2019). As a result, and depending on the case, therapeutic approaches differ, with depressive drugs administered in cases of increased neuronal excitability, and stimulants prescribed in cases of decreased neuronal activity.

Regardless of their etiology, acute vestibular disorders are treated with vestibular sedatives. Most of the medications used to treat audiovestibular syndromes are also used to treat central nervous system (CNS) disorders. Anticholinergics, antihistamines, benzodiazepines, calcium-channel blockers and dopamine receptor antagonists minimize nystagmus and vegetative symptoms that include tachycardia, sweating, nausea, and vomiting. To avoid delaying vestibular compensation, prescribing those drugs that have sedative effects should be used in the short term (Hain and Uddin, 2003). Drugs that decrease oxidative stress and inflammation and increase cochlear vascularization can be used to slow hearing loss. Antioxidants, neurotrophic factors, calcium-channel blockers, vasodilators, antihistaminergic, steroid, and other anti-inflammatory and antiapoptotic agents are also commonly used to treat auditory disorders. However, the majority of these drugs are only protective and there is weak evidence of their efficacy (Sha and Schacht, 2016).

Knowledge of the patient's pharmacogenetic profile is essential for reducing the risk of adverse effects and for optimizing treatment response; this prescription of pharmacogenetic profile-based strategies improves the therapeutic response. Single nucleotide polymorphisms (SNPs) in genes encoding drug-metabolizing enzymes, drug transporters and drug targets are primarily responsible for the variations in individual drug response. One of the potential consequences of using pharmacogenomics in clinical trials and molecular therapeutics is that a given disease may be treated based on genomic and biological markers, selecting drugs optimized for individual patients or for groups of patients with similar genomic profiles. This aspect has been little explored in the scientific literature (Guerra and Cacabelos, 2019).

The endocannabinoid (EC) system is distributed widely in the brain and is also expressed in the audiovestibular pathway (Gong et al., 2006; Chi and Kandler, 2012; Trattner, Berner, Grothe and Kunz, 2013). There has been increased interest in the development of drugs that act either as an agonist or antagonist on the EC system. This review summarizes current understanding on the role of the EC system for the future use and development of natural- or synthetically-derived compounds that act on the audiovestibular pathway. To pursue those objectives, it is necessary to fully understand the properties of the EC system and the pharmacogenetic profiles of drugs that act on the EC system.

2 The endocannabinoid system

CB1 (encoded by CNR1 gene, locus 6q15) and CB2 (encoded by CNR2 gene, locus 1p36.11) are the 2 G protein-coupled

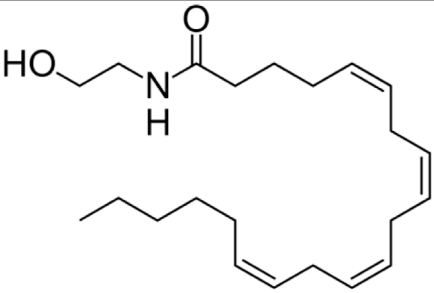
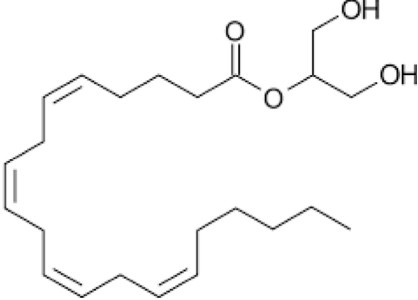
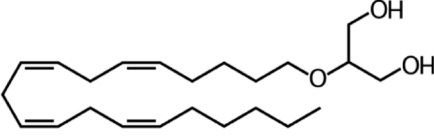
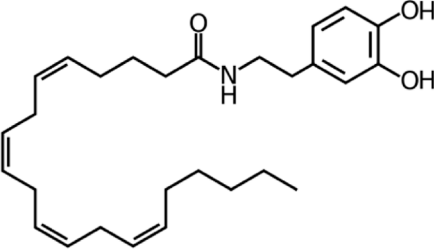
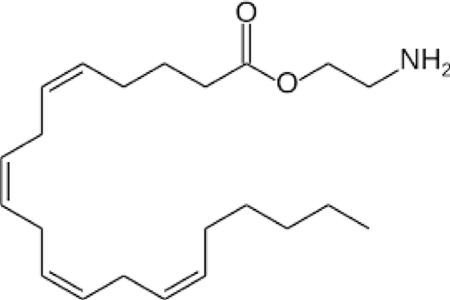
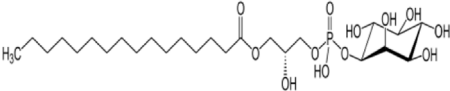
cannabinoid (CB) receptors. Activation of the Gi/G_o subunits reduces intracellular cAMP and increases MAPK levels. CB1 can occasionally activate the G-protein G_s thereby enhancing cAMP levels and the CB2 G_{12/13} subunits thus activating the MAPK-ERK signaling pathway. Most of the CB receptors in the CNS are CB1 receptors whose function is primarily neuromodulatory through inhibiting GABAergic and glutamatergic neurotransmission. However, CB2 receptors are functionally anti-inflammatory. Other clinically cannabinoid orphan receptors of interest in this review are GPR18 (13q32.3), GPR55 (2q37.1 locus) and GPR119 (Xq26.1 locus), that also encode G protein-coupled receptors (Lu and Mackie, 2016; Zou and Kumar, 2018; Kilaru and Chapman, 2020). Regarding endogenous cannabinoids (CBs), six ligands that act as neurotransmitters have been identified: arachidonylethanolamine (anandamide/AEA), 2-arachidonoylglycerol (2-AG), 2-arachidonoylglycerol ether (noladin ether) N-arachidonoyl-dopamine (NADA), Virodhamine, and lysophosphatidylinositol (LPI) (Gallelli et al., 2018). Some of these molecules have anti-inflammatory, sedative, or analgesic properties that are of interest in several audiovestibular disorders, with AEA and 2-AG being the most clinically relevant (Zogopoulos, Vasileiou, Patsouris and Theocharis, 2013). Fatty acid amide hydrolase (FAAH, encoded by FAAH gene, locus 1p33) and monoacylglycerol lipase (MAGL, encoded by MGLL gene, locus 3q21.3) are the enzymes responsible for the degradation of the endocannabinoids (Lu and Mackie, 2016; Zou and Kumar, 2018; Kilaru and Chapman, 2020).

3 Cannabinoids: Targets, effects and pharmacogenomics

More than one hundred CBs derived from the *Cannabis sativa* plant have been identified. Of these, tetrahydrocannabinol (THC), cannabidiol (CBD) and cannabinol (CBN) are the most studied and for which the most clinical data are available (Chandra et al., 2020).

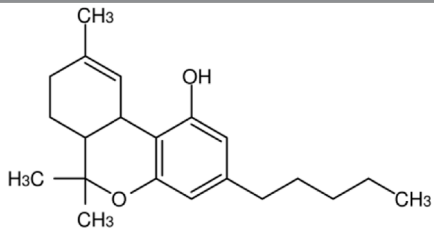
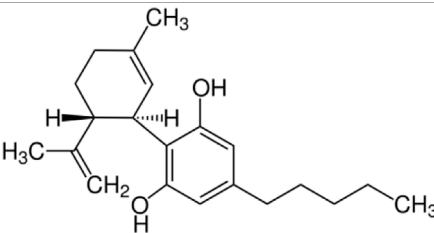
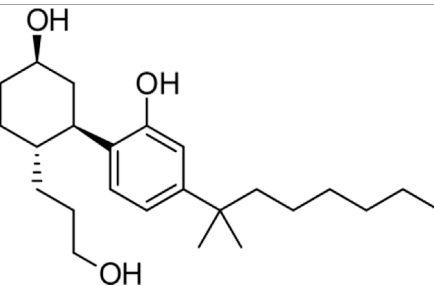
In addition to the commercialization of cannabinoid-containing medications and supplements, several clinical studies are currently investigating the effects of 1) synthetic cannabinoid-derived drugs (CB1/CB2 receptor agonists/antagonists), and 2) non-cannabinoid-derived compounds (MAGL/FAAH inhibitors) that belong to a part of a different class of biologically active molecules, that regulate the EC system. These compounds have been used in clinical trials and observational studies to manage treatment-resistant epilepsy (Devinsky et al., 2016), ALS (amyotrophic lateral sclerosis) (Weber et al., 2010), MS (multiple sclerosis) (Collin, Davies, Mutiboko and Ratcliffe, 2007; Zajicek et al., 2012), Alzheimer's disease (Herrmann et al., 2019), schizophrenia (Leweke et al., 2012; McGuire et al., 2018), acute and chronic pain (van de Donk

TABLE 1 Profile of the different cannabinoids and drugs that act on the cannabinoid system that may be effective in the treatment of audiovestibular disorders.

Drug and properties		Targets	
	Name: Anandamide IUPAC name: (5Z,8Z,11Z,14Z)-N-(2-hydroxyethyl)icosa-5,8,11,14-tetraenamide Molecular mass: 347.53 g·mol ⁻¹ Molecular formula: C ₂₂ H ₃₇ NO ₂ Category: Endocannabinoids	Agonists CB1; TRPV1	
	Name: 2-Arachidonoylglycerol (2-AG) IUPAC name: 1,3-dihydroxypropan-2-yl (5Z,8Z,11Z,14Z)-icosa-5,8,11,14-tetraenoate Molecular mass: 378.3 g·mol ⁻¹ Molecular formula: C ₂₃ H ₃₈ O ₄ Category: Endocannabinoids	Agonists CB1; CB2	
	Name: 2-Arachidonyl glyceryl ether (2-AGE; Noladin ether) IUPAC name: 2-[(5Z,8Z,11Z,14Z)-icosa-5,8,11,14-tetraenoxy]propane-1,3-diol Category: Endocannabinoids Molecular mass: 364.56 g·mol ⁻¹ Molecular formula: C ₂₃ H ₄₀ O ₃	Agonists CB1; CB2 (<i>weak</i>)	
	Name: N-Arachidonoyl dopamine (NADA) IUPAC name: (5Z,8Z,11Z,14Z)-N-[2-(3,4-dihydroxyphenyl)ethyl]icosa-5,8,11,14-tetraenamide Molecular mass: 439.63 g·mol ⁻¹ Molecular formula: C ₂₈ H ₄₁ NO ₃ Category: Endocannabinoids	Agonists CB1; TRPV1	
	Name: Virodhamine (O-arachidonoyl ethanolamine; O-AEA) IUPAC name: 2-aminoethyl (5Z,8Z,11Z,14Z)-icosa-5,8,11,14-tetraenoate Molecular mass: 347.53 g·mol ⁻¹ Molecular formula: C ₂₂ H ₃₇ NO ₂ Category: Endocannabinoids	Agonists CB2	Antagonists CB1
	Name: Lysophosphatidylinositol (LPI, lysoPI) IUPAC name: [(2S)-2-hydroxy-3-[hydroxy-[(2R,3S,5R,6R)-2,3,4,5,6-pentahydroxycyclohexyl]oxyphosphoryl]oxypropyl] acetate Molar mass: 572.629 g·mol ⁻¹ Molecular formula: C ₂₅ H ₄₉ O ₁₂ P Category: Endocannabinoids	Agonists GPR55	

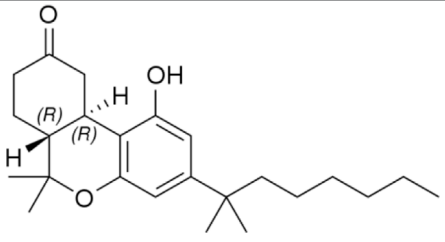
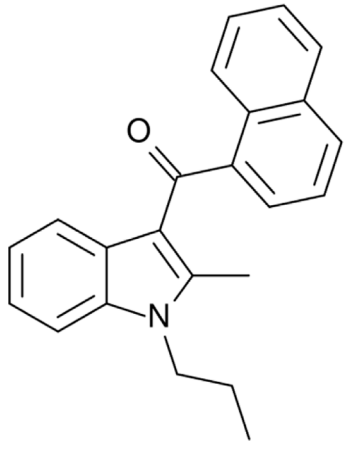
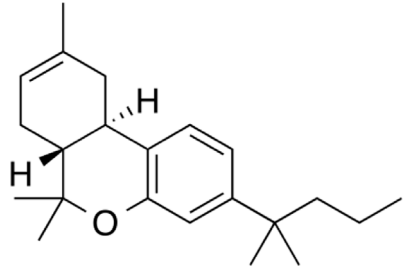
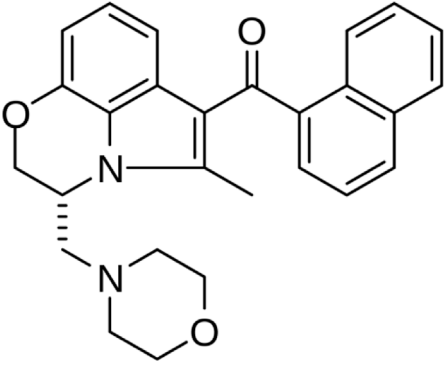
(Continued on following page)

TABLE 1 (Continued) Profile of the different cannabinoids and drugs that act on the cannabinoid system that may be effective in the treatment of audiovestibular disorders.

Drug and properties		Targets	
	<p>Name: THC/Dronabinol IUPAC name: (6aR,10aR)-6,6,9-trimethyl-3-pentyl-6a,7,8,10a-tetrahydrobenzo [c]chromen-1-ol Molar mass: 314.469 g·mol−1 Molecular formula: C₂₁H₃₀O₂ Category: Phytocannabinoids/Synthetic cannabinoids</p>	<p>Agonists CB1; CB2</p>	
	<p>Name: Cannabidiol IUPAC name: 2-[(1R,6R)-3-methyl-6-prop-1-en-2-ylcyclohex-2-en-1-yl]-5-pentylbenzene-1,3-diol Molar mass: 314.469 g·mol−1 Molecular formula: C₂₁H₃₀O₂ Category: Phytocannabinoids</p>	<p>Agonists HTR1A; HTR2A; TRPA1</p>	<p>Activators PPARG; TRPV1; TRPV2; TRPV3; TRPV4; ADORA1</p>
		<p>Inverse agonists GPR12</p>	
		<p>Antagonists CB1; CB2; GPR55; HTR3A</p>	<p>Inhibitors PTGS1; PTGS2; ACAT1; IDO1; NQO1; CAT; SOD; AANAT; NAAA</p>
		<p>Modulators CB1</p>	<p>Stimulators HMGCR; GSR; GSR; GPX</p>
		<p>Potentiators GLRA3</p>	<p>Other targets GLRA1; GPR18; CHRNA7; OPRD1; OPRM1; CACNA1G CACNA1H; CACNA1I; TRPM8; VDAC1</p>
	<p>Name: CP 55,940 IUPAC name: 2-[(1R,2R,5R)-5-hydroxy-2-(3-hydroxypropyl)cyclohexyl]-5-(2-methyloctan-2-yl)phenol Molar mass: 376.581 g·mol−1 Molecular formula: C₂₄H₄₀O₃ Category: Synthetic cannabinoids</p>	<p>Agonists CB1; CB2; HTR5A</p>	<p>Antagonists GPR55</p>

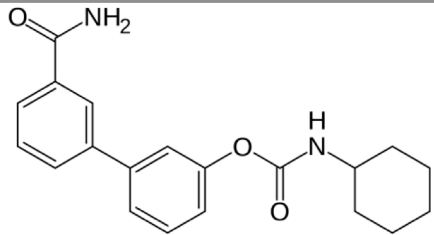
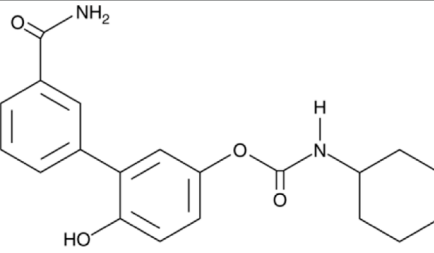
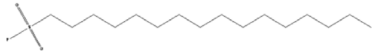
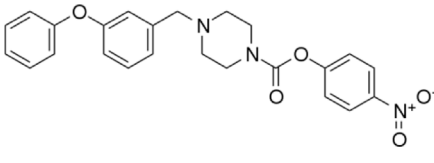
(Continued on following page)

TABLE 1 (Continued) Profile of the different cannabinoids and drugs that act on the cannabinoid system that may be effective in the treatment of audiovestibular disorders.

Drug and properties	Targets
 <p>Name: Nabilone IUPAC name: (6aR,10aR)-1-hydroxy-6,6-dimethyl-3-(2-methyloctan-2-yl)-7,8,10,10a-tetrahydro-6aH-benzo [c]chromen-9-one Molar mass: 372.549 g·mol⁻¹ Molecular formula: C₂₄H₃₆O₃ Category: Synthetic cannabinoids</p>	<p>Agonists CB1 (<i>partial</i>); CB2 (<i>partial</i>)</p>
 <p>Name: JWH-015 IUPAC name: (2-methyl-1-propylindol-3-yl)-naphthalen-1-ylmethanone Molar mass: 327.427 g·mol⁻¹ Molecular formula: C₂₃H₂₁NO Category: Synthetic cannabinoids</p>	<p>Agonists CB2; CB1 (<i>weak</i>)</p>
 <p>Name: Dimethylbutyl-deoxy-Delta-8-THC (JWH-133) IUPAC name: (6aR,10aR)-6,6,9-trimethyl-3-(2-methylpentan-2-yl)-6a,7,10,10a-tetrahydrobenzo [c]chromene Molar mass: 312.497 g·mol⁻¹ Molecular formula: C₂₂H₃₂O Category: Synthetic cannabinoids</p>	<p>Agonists CB2</p>
 <p>Name: WIN55,212-2 IUPAC name: [(11R)-2-methyl-11-(morpholin-4-ylmethyl)-9-oxa-1-azatricyclo [6.3.1.0^{4,12}]dodeca-2,4 (12),5,7-tetraen-3-yl]-naphthalen-1-ylmethanone Molar mass: 338.407 g·mol⁻¹ Molecular formula: C₂₀H₂₂N₂O₃ Category: Synthetic cannabinoids</p>	<p>Agonists CB1; CB2; PPARα; PARγ</p>

(Continued on following page)

TABLE 1 (Continued) Profile of the different cannabinoids and drugs that act on the cannabinoid system that may be effective in the treatment of audiovestibular disorders.

Drug and properties		Targets
	<p>Name: URB597 (KDS-4103)</p> <p>IUPAC name: [3-(3-carbamoylphenyl)phenyl] N-cyclohexylcarbamate</p> <p>Molar mass: 338.407 g•mol⁻¹</p> <p>Molecular formula: C₂₀H₂₂N₂O₃</p> <p>Category: Endocannabinoid reuptake inhibitor</p>	<p>Inhibitor</p> <p>FAAH</p>
	<p>Name: URB937</p> <p>IUPAC name: N-cyclohexyl-carbamic acid, 3'-(aminocarbonyl)-6-hydroxy [1,1'-biphenyl]-3-yl ester</p> <p>Molar mass: 338.407 g•mol⁻¹</p> <p>Molecular formula: C₂₀H₂₂N₂O₄</p> <p>Category: Endocannabinoid reuptake inhibitor</p>	<p>Inhibitor</p> <p>FAAH</p>
	<p>Name: AM374</p> <p>IUPAC name: Hexadecanesulfonyl fluoride</p> <p>Molar mass: 308.219 g•mol⁻¹</p> <p>Molecular formula: C₁₆H₃₃FO₂S</p> <p>Category: Endocannabinoid reuptake inhibitor</p>	<p>Inhibitor</p> <p>FAAH</p> <p>Other targets</p> <p>PPT1</p>
	<p>Name: JZL195</p> <p>IUPAC name: 4-nitrophenyl 4-(3-phenoxybenzyl)piperazine-1-carboxylate</p> <p>Molar mass: 433.464 g•mol⁻¹</p> <p>Molecular formula: C₂₄H₂₃N₃O₅</p> <p>Category: Endocannabinoid reuptake inhibitor</p>	<p>Inhibitor</p> <p>FAAH; MAGL</p>
<p>Name: Dietressa[®]</p> <p>Category: Synthetic cannabinoid antibodies</p>		<p>Antagonists</p> <p>CB1</p>
<p>Name: Brizantin[®]</p> <p>Category: Synthetic cannabinoid antibodies</p>		<p>Antagonists</p> <p>CB1</p>

et al., 2018; Weizman et al., 2018), and several other conditions (Kogan and Mechoulam, 2007; Perin et al., 2020; Khalsa et al., 2022). Since many of the above-mentioned and other nervous system disorders also affect the auditory and vestibular pathway, and are associated with dizziness, nystagmus and auditory symptoms, these molecules may help address several types of audiovestibular disorders. Moreover, symptoms that show these neurological diseases appear in peripheral audiovestibular pathology, such as nystagmus, tinnitus or hearing loss (Baguley et al., 2013; Zwergal and Dieterich, 2020).

THC and its synthetic derivative dronabinol are CB1/CB2 receptor agonists. They mimic the effects of ECs in the CNS and modulate the excitatory effect of other neurotransmitters including glutamate. These agents may adversely enhance the tachycardic response of anticholinergics and sympathomimetics and can cause tinnitus, ataxia, and seizures as side effects. Dronabinol's

half-life is 25–36 h, while its metabolites can last up to 59 h. Nabilone, another synthetic cannabinoid that mimics THC, has a more variable half-life, ranging from 2 to 35 h (Cacabelos, 2012). The analogous use of THC and its synthetic derived drugs with opioid derived drugs, antidepressants and anticonvulsants requires a dose reduction due to greater analgesic efficacy and/or higher drug toxicity caused by down-regulation of transporter efflux or enzymatic inhibition (Vázquez et al., 2020). The pharmacogenetic profile of cannabinoid derivatives is still under development, especially with regard to new synthetic derivatives. Dronabinol's mechanistic genes are *CNR1* and *CNR2*, and it acts as an agonist. Its metabolic genes are *CYP3A4*, *CYP2C9*, *CYP2C19*, *CYP1A2*, *CYP2B6*, *CYP2D6*, *CYP1A1*, *CYP2J2*, *CYP3A5*, *CYP3A7*, *CYP1B1*, *CYP2A6*, *CES1* and *PTGS1*, and the transporter genes include *ABCG2*, *ABCB1* and *ABCC1*. Nabilone displays the same

mechanistic genes as Dronabinol, but it binds partially to its receptors; *CYP2C9*, *CYP3A4*, *CYP2C8*, *CYP2E1* and *CYP2J2* are its metabolic genes.

Cannabidiol, however, is a non-competitive CB1/CB2 receptor antagonist. It reduces neuronal hyperexcitability by modulating Ca^{2+} entry *via* GPR55 and TRPV1 receptors, and by inhibiting ENT-1-receptor-mediated adenosine reuptake (Ibeas Bih et al., 2015). It has a half-life of 18–32 h and causes somnolence, sedation, diarrhea, and changes in appetite as its side effects. It may reduce the adverse effects caused by THC and its derivatives. Drug-drug interactions include regular medications such as anticonvulsants, statins or common analgesics (Vázquez et al., 2020; Davis et al., 2021). The mechanistic genes of cannabidiol are much broader, with diverse targets, as seen in Table 1. *CYP3A4*, *CYP2C19*, *CYP1A2*, *CYP2B6*, *CYP2C9*, *UGT1A7*, *UGT1A9*, *UGT2B7*, *UGT2B17*, *CYP1A1*, *CYP1B1*, *CYP2C8*, *CYP2D6*, *CYP2E1*, *CYP3A5*, *CYP2A6*, *CYP3A7*, *CYP2J2*, *CES1*, *AANAT*, *FAAH*, *ALOX5*, *ALOX15*, and *CRYZ* are its metabolic genes. Transporter genes associated with cannabidiol include *ABCC1*, *ABCG2*, *SLC29A1*, and *ABCB1* (Cacabelos, 2012; Wishart et al., 2017).

CNR1 and *CNR2* variants show mixed results in terms of cannabis dependency. *CNR1*, -64 + 1046T>G and c.-63-9c.1359G>A variants show an association with drug dependency, while 597T>C -64 + 1046T>G c.*3475A>G are also linked to drug dependency in single studies, although with no replication of results. The *CNR2* 188A>G and 946C>T variants alter its CB2 receptor function in human embryonic kidney-293 cells. Because the *COMT* rs4680 472A>G Val158Met variant is linked to memory impairment, alterations in executive function, and psychosis, the use of cannabis derivatives should be approached with caution with corresponding adjustments in prescribed doses. The *FAAH* 385C>APro129Thr variant may be involved in excessive consumption of cannabis, although other authors did not find any association between *FAAH* variants. The *ABCB1* rs10456423455C>T Ile1145Ile variant is associated with cannabis dependency (Hryhorowicz et al., 2018).

CB1 antagonists such as rimonabant, surinabant and other diarylpyrazole derivatives have been experimentally and clinically evaluated for treating conditions unrelated to audiovestibular symptoms such as obesity or addiction disorders. However, their use has raised safety concerns due to CNS or cardiac side effects (Christopoulou and Kiortsis, 2011; Klumpers et al., 2013). Therefore, its role in treating the conditions described in this review is not defined.

Unfortunately, little is known regarding the half-life, adverse effects and pharmacogenetic profiles of other drugs of interest described in this review. One of the primary reasons is that those drugs have been used solely for research purposes. These include CB1/CB2 agonists (CP 55,940, JWH-015 and WIN55,212-2) CB1 agonists (JWH-133), CB1 antagonists (Dietressa® and Brizantin®), *FAAH* inhibitors (URB597, URB937, and

AM374) and *FAAH*/*MAGL* inhibitors (JZL195). The targets of these compounds are listed in Table 1 (Cacabelos, 2012; Wishart et al., 2017).

4 The cannabinoid system and the vestibular pathway

The association of the EC system in the vestibular pathway has been previously demonstrated by early reports that indicated that the audiovestibular pathway expresses CB1 receptors. The density of these receptors in this pathway was initially reported as modest, but functionally significant (Newsham-West et al., 1998). Furthermore, CB2 receptors are expressed in the vestibular and cochlear nuclei (Gong et al., 2006; Baek et al., 2008), with lower distribution and relevance than CB1 receptors. The EC system interacts with the different vestibular pathways such as the vestibulocerebellar tract (Suárez et al., 2008). Optogenetically-induced plasticity and motor adaptation in the cerebellum are dependent on EC signaling. When vestibular stimuli are paired with relatively small amplitude Purkinje cell calcium responses, this Purkinje cell activation induces decreased vestibulo-ocular reflex gain. By contrast, pairing with large magnitude calcium responses promotes vestibulo-ocular reflex gain. This indicates that EC signaling acts downstream of Purkinje cell calcium elevation (Bonnan et al., 2021). CB1 receptors modulate the vestibular reflex, as indicated by their activation following unilateral vestibular deafferentation in rats. However, their expression does not change during vestibular compensation (Ashton et al., 2004). In rats, bilateral vestibular deafferentation causes lifelong spatial memory impairments and hippocampal dysfunction (Baek et al., 2010), that is associated with CB1 receptor down-regulation in the CA3 area of the rat hippocampus (Baek et al., 2011).

4.1 Cannabinoids and vestibular disorders

Despite the abundance of data indicating the presence and participation of the EC system in the vestibular pathway, there are currently only a few publications (Schon et al., 1999; Pradeep et al., 2008) and just one clinical trial (Barchukov et al., 2015), which limits their clinical impact.

In animal models, the administration of the potent non-selective CB receptor agonist CP-55,940 affects the vestibular pathway, comparable to the action of certain metabotropic glutamate receptor agonists, generating dizziness. These effects are sustained and involve neurons in the medial vestibular nucleus (Newsham-West et al., 1998). TRPV1 pathways, which are targets of CBD, are associated with motion sickness processes as observed in *Trpv1*-null mice (Inpravit et al., 2018). Anecdotal case-reports indicate a reduction or suppression of congenital, and pendular nystagmus associated with multiple

sclerosis in cannabis users (Schon et al., 1999; Pradeep et al., 2008). However, the use of nabilone has no effect on nystagmus, indicating that the use of THC agonists alone may not be sufficient to suppress it (Schon et al., 1999). The inhibitory action of CB agonists, and other compounds found in *Cannabis Sativa*, may suppress nystagmus; however, the lack of evidence pointing to the dosages used in the case reports limits these conclusions (Schon et al., 1999; Pradeep et al., 2008). A clinical trial evaluated the role of active-release preparations containing CB receptor antagonists (marketed in Russia under the Dietressa® and Brizantin® brands); these preparations incorporated antibodies against the CB1 receptor. In that study, patients were evaluated over 1 h after the test dose (1 tablet) of the preparation/placebo. In the follow-up period, the preparation/placebo (1 tablet) was given four times at 30-min intervals. The tolerance to accelerations in a model of vertigo with healthy subjects was increased, with no change in nystagmus duration or recovery time (Barchukov et al., 2015). In theory, cannabinoid antagonists may be advantageous during vestibular compensation. However, there are concerns about these products, related to the utilization of ultra-low doses of the active substance and limited information regarding their molecular properties.

Potential uses of CBs for other symptoms associated with vestibular disorders are described below.

4.1.1 Seizures

Vestibular epilepsy is a rare condition that affects areas in the temporal cortex responsible for motor coordination. Its key characteristics are the presence of rapidly-discharging EEG activity and a favorable response to antiepileptic therapy (Hewett and Bartolomei, 2013). On the other hand, several anticonvulsants including diazepam, gabapentin and carbamazepine are used to treat several vestibular disorder subtypes, even those unrelated to seizures (Casani et al., 2021). CBD is a proposed drug indicated for treating epilepsy. Its brand-labelled product (Epidyolex®) is currently used to treat severe resistant epilepsies such as severe myoclonic epilepsy of infancy (Dravet syndrome; SCN1A gene, locus 2q24.3) (Scheffer et al., 2021). The anti-epileptic action of CBD can be explained by: 1) generating anti-glutamatergic activity and lowering neuronal excitability via GPR55 receptor antagonism and adenosine tone control; 2) activating 5HT1A receptors; and 3) modifying intracellular calcium levels. Other CB1 receptor agonists (WIN55,212-2) also have an anticonvulsant effect, similar to the anti-epileptic action of CBD (Colangeli et al., 2017). Inhibiting EC degradation has also been considered as a potential therapy for epilepsy. FAAH inhibitors (URB597, AM374) suppress hippocampal discharges and improve short- and long-term cognitive performance in rats by increasing blood-brain levels of anandamide (Karanian et al., 2007; Colangeli et al., 2017). Long-term usage of compounds (e.g., palmitoylethanolamide) that target the atypical CB receptors GPR55 and GPR11 has neuroprotective

and neuromodulatory advantages in preventing epileptic convulsions in mice when combined with FAAH inhibitors (Post et al., 2018). Several antiepileptic drugs, however, are used to treat vestibular problems such as vestibular paroxysmia or central nystagmus (Strupp et al., 2011). Nonetheless, administering CBD or other CBs in these cases remains to be evaluated (Morano et al., 2020). Variants in the genes that encode aldehyde oxygenase (AOX1 rs6729738 CC) and diamine oxidase (ABP1 rs12539) increase the likelihood of an antiepileptic response. Since CBD produces an antioxidant effect, this could explain that finding. By contrast, SLC15A1 rs1339067 TT carriers exhibit a decreased antiepileptic response, indicating that this transporter limits CBD activity. EC receptor GPR18 expression in white matter is reduced by rs1339067, and hippocampal HTR3E serotonergic receptor expression is decreased by rs3749442, thus modulating the drug response in treatment-resistant epilepsy (Davis et al., 2021).

4.1.2 Headache

Many patients with migraine describe neuro-otological symptoms such as phonophobia and vertigo. Vestibular migraine is a distinct entity whose diagnostic criteria include at least five episodes of migraine with/without aura and vestibular symptoms of moderate or severe intensity, lasting between 5 min and 72 h. In addition, at least half of the episodes must be associated with at least one of the following three migrainous features: 1) headache with at least two of the following four characteristics: 1) unilateral location; 2) pulsating quality; 3) moderate or severe intensity; 4) aggravation by routine physical activity; 2) photophobia and phonophobia; 3) visual aura; and 3) not better accounted for by another vestibular disorder (Lempert et al., 2012). Cannabis and its derivatives are efficacious for controlling pain and are viable agents for treating migraine and other headaches. The EC system acts via CB1 and CB2 receptors to alleviate pain, whereas pain stimulation occurs through TRPV1 receptors. MAGL and FAAH regulates EC levels; this analgesia affects the meninges and brainstem (Leimuranta et al., 2018). Central EC deficiency (as observed in the cerebrospinal fluid), specifically AEA and 2-AG, is a potential cause of migraine (Russo, 2016). Cannabis consumption reduces the intensity of migraine attacks but its long-term use produces tolerance (Cuttler, Spradlin, Cleveland and Craft, 2020). Moreover, a better prophylactic control was shown after treatment with medical cannabis, although with sparse evidence (Poudel et al., 2021). Both THC and CBD are responsible for this anti-migraine effect, but with the ideal ratio of these compounds yet to be determined (Mechtler et al., 2021). In preclinical studies, FAAH inhibitors used for the preventive control of migraine increased anandamide and palmitoylethanolamide levels, but has no effect in response to an acute migraine attack (Greco et al., 2020). The use of the FAAH inhibitor URB937 reduces hyperalgesia and c-Fos expression in the trigeminal caudal nucleus (TNC) and locus coeruleus in rodents. This response was accompanied by decreased neuronal gene expression of nitric oxide synthase, calcitonin gene-related peptide and cytokines (Greco et al., 2020; Greco et al., 2021a); using dual inhibitors of FAAH and MAGL produce similar effects

(Greco et al., 2021b). Several rare, non-sense mutations in CNR1 increase the predisposition to developing migraine (Smith et al., 2017). CNR1 carriers with the HT6 haplotypic variant, for example, are most susceptible with an increased likelihood of headache together with nausea and photophobia (Juhász et al., 2009). CNR2 and FAAH variants do not appear to be involved in migraine (Smith et al., 2017).

4.1.3 Vomiting

Vomiting is one of the symptoms associated with a vestibular crisis; despite the limited data, THC and other agonists appear to be effective in decreasing chemotherapy-induced vomiting (Whiting et al., 2015). This central antiemetic action occurs *via* the activation of CB1 receptors, and possibly TRPV1 in the dorsal vagal complex (Darmani, 2010). But contrary to popular belief, one side effect of frequent cannabis use is vomiting (Castaneto et al., 2014). Moreover, the suggested best treatment for this hyperemesis, which is associated with THC and its plasma high levels (Chu and Cascella, 2022), is discontinuing THC consumption (Sorensen et al., 2016). THC may cause desensitizing, pharmacogenetic, or tolerance effects following its binding to CB1 receptors, as well as antagonizing the peripheral emetic effect *versus* the central antiemetic effect. However, its pathophysiology remains unclear (Sorensen et al., 2016). Although AEA alone does not diminish reduce vomiting in animal models, URB597 attenuates and even suppresses vomiting caused by chemotherapy and nicotine (Parker et al., 2009).

5 The cannabinoid system and the auditory pathway

EC signaling modulates neurotransmission within auditory circuits and contributes to their development (Chi and Kandler, 2012; Trattner et al., 2013). CB1-receptor knockout mice have lower auditory thresholds at hearing frequencies greater than 8 kHz in their audiograms, than wild type mice. In terms of central auditory processing, these knockout mice outperform wild-type mice in identifying gaps in low-pass noise bursts (Toal et al., 2016). CB2 receptors are found in several areas of the inner ear, including the Organ of Corti, stria vascularis, spiral ligament, and spiral ganglion cells (Ghosh et al., 2018). CB2 receptor activation is involved in protecting against drug-induced hearing loss (Martín-Saldaña et al., 2016; Dhukhwa et al., 2021).

5.1 Cannabinoids and hearing disorders

There are few publications on auditory pathology than on the effect of cannabis on hearing disorders. Considering the use of CB agonists, in animal models, JWH-015, a CB2 agonist that is also a weak CB1 agonist, is otoprotective against cisplatin exposure. CB2 antagonists reverse this effect (Ghosh et al., 2018). Furthermore, another pharmacological agonist (JWH-133)

activates CB2 receptors, produces an anti-inflammatory effect in the inner ear, and increases microcirculation following exposure to bacterial endotoxins (Weiss et al., 2021). Although these results appear promising, they were performed in animal models, and therefore the translational implications for humans are quite limited given the absence of studies in this regard.

As mentioned previously, CBD modulates the TRPV1 receptor. TRPV1 and other TRPs are up-regulated when exposed to an ototoxic agent (Kitahara et al., 2005) and can exert dual effects on hearing function, depending on which drug acts on TRP channels. For example, capsaicin would be protective while an aminoglycoside would exacerbate the inflammatory response (Ramkumar et al., 2022). TRPV1 activity begins after the activation of NOX3 NADPH oxidase and STAT1 and STAT3 transcription factors that mediate oxidative stress, which cause inflammation and cochlear apoptosis (Ramkumar et al., 2022). CBD may theoretically be an otoprotective drug, but no reports to date have demonstrated its efficacy in this regard.

Concerning tinnitus, several reviews have demonstrated a detrimental effect of cannabis and its derivatives on the development of tinnitus. Based on data obtained from animal models, null or even negative effects of CB1 receptor agonists on tinnitus have been reported in response to noise exposure and the use of ototoxic drugs (Zheng et al., 2010; Zheng et al., 2015; Berger et al., 2017). In humans, these findings have also been observed according to the results of surveys and clinical trials; paradoxically, a patient with intracranial hypertension showed tinnitus relief following dronabinol consumption (Narwani et al., 2020). Auditory excitability extends to the auditory cortex and may account for the auditory hallucinations reported in some subjects (Nestoros et al., 2017). It is unknown whether the use of cannabinoid antagonists may be effective for controlling tinnitus.

6 Conclusion

The present review shows that the EC system regulates audiovestibular function. The few but significant references to the use of CB agonists/antagonists, and MAGL/FAAH inhibitors that act on the EC system indicate that they may be effective for treating audiovestibular disorders. The neuromodulatory effects of those compounds would act on symptoms as diverse as dizziness, nystagmus, nausea, vomiting, tinnitus or headache across different vestibular syndromes of central and peripheral origin (linked or not to neurological pathology), in some cases with inhibitory effects, particularly CB agonists, with sedative action and excitatory effects in others, and with compensatory or protective functions, as is typical in the case of CB antagonists. A critical aspect concerning the use of drugs that act on the EC system is the absence and/or variability of doses used in all studies, even in those studies performed in animal models. This severely limits the application of EC system-targeting drugs and standardization in

humans. A further issue that requires discussion is the lack of pharmacogenetic profiles for most cannabinoid derivatives, which affects all conditions that may benefit from their use. However, an understanding of the pharmacogenetics of the cannabinoid derivatives dronabinol, nabilone and cannabidiol is undoubtedly invaluable. Genes related to the metabolism and/or to the mechanisms of action of these drugs contribute to problems with therapeutic efficacy and safety of those agents. A pharmacogenomic strategy to optimize the use of drugs that interact with the EC system is required for successful, personalized therapy. Finally, whereas systemic drug administration allows for wider drug distribution to exert central and peripheral effects, the effects of local delivery of these agents to the inner ear *via* more invasive direct approaches are unknown. This application would be particularly appealing for those drugs with peripheral action or those with minimal CNS effects.

Author contributions

Made substantial contributions to conception and design of the review and interpretation, JG, read, adjusted and approved the final manuscript, VN and RC.

References

- Ashton, J., Zheng, Y., Liu, P., Darlington, C., and Smith, P. (2004). Immunohistochemical characterisation and localisation of cannabinoid CB1 receptor protein in the rat vestibular nucleus complex and the effects of unilateral vestibular deafferentation. *Brain Res.* 1021 (2), 264–271. doi:10.1016/j.brainres.2004.06.065
- Back, J., Zheng, Y., Darlington, C., and Smith, P. (2011). Cannabinoid CB1 receptor expression and affinity in the rat hippocampus following bilateral vestibular deafferentation. *Neurosci. Lett.* 487 (3), 330–334. doi:10.1016/j.neulet.2010.10.050
- Back, J., Zheng, Y., Darlington, C., and Smith, P. (2008). Cannabinoid CB2 receptor expression in the rat brainstem cochlear and vestibular nuclei. *Acta Otolaryngol.* 128 (9), 961–967. doi:10.1080/00016480701796944
- Back, J., Zheng, Y., Darlington, C., and Smith, P. (2010). Evidence that spatial memory deficits following bilateral vestibular deafferentation in rats are probably permanent. *Neurobiol. Learn. Mem.* 94 (3), 402–413. doi:10.1016/j.nlm.2010.08.007
- Baguley, D., McFerran, D., and Hall, D. (2013). Tinnitus. *Lancet* 382 (9904), 1600–1607. doi:10.1016/S0140-6736(13)60142-7
- Barchukov, V., Zhavbert, E., Dugina, Y., and Epstein, O. (2015). The use of release-active antibody-based preparations for vertigo prevention in adults. *Bull. Exp. Biol. Med.* 160 (1), 61–63. doi:10.1007/s10517-015-3098-z
- Berger, J., Coomber, B., Hill, S., Alexander, S., Owen, W., Palmer, A., et al. (2017). Effects of the cannabinoid CB1 agonist ACEA on salicylate ototoxicity, hyperacusis and tinnitus in Guinea pigs. *Hear. Res.* 356, 51–62. doi:10.1016/j.heares.2017.10.012
- Bonnan, A., Rowan, M., Baker, C., Bolton, M., and Christie, J. (2021). Autonomous Purkinje cell activation instructs bidirectional motor learning through evoked dendritic calcium signaling. *Nat. Commun.* 12 (1), 2153. doi:10.1038/s41467-021-22405-8
- R. Cacabelos (Editor) (2012). *World guide for drug use and pharmacogenomics* (Spain: EuroEspes Publishing; A Coruña).
- Casani, A., Gufoni, M., and Capobianco, S. (2021). Current insights into treating vertigo in older adults. *Drugs Aging* 38 (8), 655–670. doi:10.1007/s40266-021-00877-z
- Castaneto, M., Gorelick, D., Desrosiers, N., Hartman, R., Pirard, S., and Huestis, M. (2014). Synthetic cannabinoids: Epidemiology, pharmacodynamics, and clinical implications. *Drug Alcohol Depend.* 144, 12–41. doi:10.1016/j.drugalcdep.2014.08.005
- Chandra, S., Lata, H., and ElSohly, M. (2020). Propagation of cannabis for clinical research: An approach towards a modern herbal medicinal products development. *Front. Plant Sci.* 11, 958. doi:10.3389/fpls.2020.00958
- Chi, D., and Kandler, K. (2012). Cannabinoid receptor expression at the MNTB-LSO synapse in developing rats. *Neurosci. Lett.* 509 (2), 96–100. doi:10.1016/j.neulet.2011.12.047
- Christopoulou, F., and Kiortsis, D. (2011). An overview of the metabolic effects of rimonabant in randomized controlled trials: Potential for other cannabinoid 1 receptor blockers in obesity. *J. Clin. Pharm. Ther.* 36 (1), 10–18. doi:10.1111/j.1365-2710.2010.01164.x
- Chu, F., and Cascella, M. (2022). *Treasure Island: StatPearls. Cannabinoid Hyperemesis Syndrome.*
- Colangeli, R., Pierucci, M., Benigno, A., Campiani, G., Butini, S., and Di Giovanni, G. (2017). The FAAH inhibitor URB597 suppresses hippocampal maximal dentate afterdischarges and restores seizure-induced impairment of short and long-term synaptic plasticity. *Sci. Rep.* 7 (1), 11152. doi:10.1038/s41598-017-11606-1
- Collin, C., Davies, P., Mutiboko, I., and Ratcliffe, S. (2007). Randomized controlled trial of cannabis-based medicine in spasticity caused by multiple sclerosis. *Eur. J. Neurol.* 14 (3), 290–296. doi:10.1111/j.1468-1331.2006.01639.x
- Cuttler, C., Spradlin, A., Cleveland, M., and Craft, R. (2020). Short- and long-term effects of cannabis on headache and migraine. *J. Pain* 21 (5-6), 722–730. doi:10.1016/j.jpain.2019.11.001
- Darmani, N. (2010). Mechanisms of broad-spectrum antiemetic efficacy of cannabinoids against chemotherapy-induced acute and delayed vomiting. *Pharmaceuticals* 3 (9), 2930–2955. doi:10.3390/ph3092930
- Davis, B., Beasley, T., Amaral, M., Szaflarski, J., Gaston, T., Perry Grayson, L., et al. (2021). Pharmacogenetic predictors of cannabidiol response and tolerability in treatment-resistant epilepsy. *Clin. Pharmacol. Ther.* 110 (5), 1368–1380. doi:10.1002/cpt.2408
- Devinsky, O., Marsh, E., Friedman, D., Thiele, E., Laux, L., Sullivan, J., et al. (2016). Cannabidiol in patients with treatment-resistant epilepsy: An open-label interventional trial. *Lancet. Neurol.* 15 (3), 270–278. doi:10.1016/S1474-4422(15)00379-8
- Dhukhwa, A., Al Aameri, R., Sheth, S., Mukherjee, D., Rybak, L., and Ramkumar, V. (2021). Regulator of G protein signaling 17 represents a novel target for treating cisplatin induced hearing loss. *Sci. Rep.* 11 (1), 8116. doi:10.1038/s41598-021-87387-5

Acknowledgments

JG wants to acknowledge Adria Pijuan Monroy and Iria Rodriguez Lopez for being the inspiration to prepare this article.

Conflict of interest

The authors declare that the research was conducted in the absence of any commercial or financial relationships that could be construed as a potential conflict of interest.

Publisher's note

All claims expressed in this article are solely those of the authors and do not necessarily represent those of their affiliated organizations, or those of the publisher, the editors and the reviewers. Any product that may be evaluated in this article, or claim that may be made by its manufacturer, is not guaranteed or endorsed by the publisher.

- Gallelli, C., Calcagnini, S., Romano, A., Koczwara, J., de Ceglia, M., Dante, D., et al. (2018). Modulation of the oxidative stress and lipid peroxidation by endocannabinoids and their lipid analogues. *Antioxidants* 7 (7), 93. doi:10.3390/antiox7070093
- Ghosh, S., Sheth, S., Sheehan, K., Mukherjee, D., Dhukhwa, A., Borse, V., et al. (2018). The endocannabinoid/cannabinoid receptor 2 system protects against cisplatin-induced hearing loss. *Front. Cell. Neurosci.* 12, 271. doi:10.3389/fncel.2018.00271
- Gong, J., Onaivi, E., Ishiguro, H., Liu, Q., Tagliaferro, P., Brusco, A., et al. (2006). Cannabinoid CB2 receptors: Immunohistochemical localization in rat brain. *Brain Res.* 1071 (1), 10–23. doi:10.1016/j.brainres.2005.11.035
- Greco, R., Demartini, C., Francavilla, M., Zanolini, A., and Tassorelli, C. (2021b). Dual inhibition of FAAH and MAGL counteracts migraine-like pain and behavior in an animal model of migraine. *Cells* 10 (10), 2543. doi:10.3390/cells10102543
- Greco, R., Demartini, C., Zanolini, A., Casini, I., De Icco, R., Reggiani, A., et al. (2021a). Characterization of the peripheral FAAH inhibitor, URB937, in animal models of acute and chronic migraine. *Neurobiol. Dis.* 147, 105157. doi:10.1016/j.nbd.2020.105157
- Greco, R., Demartini, C., Zanolini, A., Tumelero, E., Reggiani, A., Misto, A., et al. (2020). FAAH inhibition as a preventive treatment for migraine: A pre-clinical study. *Neurobiol. Dis.* 134, 104624. doi:10.1016/j.nbd.2019.104624
- Guerra, J., and Cacabelos, R. (2019). Pharmacoeigenetics of vertigo and related vestibular syndromes. *Pharmacoeigenetics* 10, 755–779. doi:10.1016/B978-0-12-813939-4.00028-0
- Hain, T., and Uddin, M. (2003). Pharmacological treatment of vertigo. *CNS Drugs* 17 (2), 85–100. doi:10.2165/00023210-200317020-00002
- Herrmann, N., Ruthirakuhan, M., Gallagher, D., Verhoeff, N., Kiss, A., Black, S., et al. (2019). Randomized placebo-controlled trial of nabilone for agitation in Alzheimer's disease. *Am. J. Geriatr. Psychiatry* 27 (11), 1161–1173. doi:10.1016/j.jagp.2019.05.002
- Hewett, R., and Bartolomei, F. (2013). Epilepsy and the cortical vestibular system: Tales of dizziness and recent concepts. *Front. Integr. Neurosci.* 7, 73. doi:10.3389/fnint.2013.00073
- Hryhorowicz, S., Walczak, M., Zakerska-Banaszak, O., Slomski, R., and Skrzypczak-Zielinska, M. (2018). Pharmacogenetics of cannabinoids. *Eur. J. Drug Metab. Pharmacokinet.* 43, 1–12. doi:10.1007/s13318-017-0416-z
- Ibeas Bih, C., Chen, T., Nunn, A., Bazelot, M., Dallas, M., and Whalley, B. (2015). Molecular targets of cannabidiol in neurological disorders. *Neurotherapeutics* 12 (4), 699–730. doi:10.1007/s13311-015-0377-3
- Inprasit, C., Lin, Y., Huang, C., Wu, S., and Hsieh, C. (2018). Targeting TRPV1 to relieve motion sickness symptoms in mice by electroacupuncture and gene deletion. *Sci. Rep.* 8 (1), 10365. doi:10.1038/s41598-018-23793-6
- Juhasz, G., Lazary, J., Chase, D., Pegg, E., Downey, D., Toth, Z., et al. (2009). Variations in the cannabinoid receptor 1 gene predispose to migraine. *Neurosci. Lett.* 461 (2), 116–120. doi:10.1016/j.neulet.2009.06.021
- Karanian, D., Karim, S., Wood, J., Williams, J., Lin, S., Makriyannis, A., et al. (2007). Endocannabinoid enhancement protects against kainic acid-induced seizures and associated brain damage. *J. Pharmacol. Exp. Ther.* 322 (3), 1059–1066. doi:10.1124/jpet.107.120147
- Khalsa, J., Bunt, G., Blum, K., Maggirwar, S., Galanter, M., and Potenza, M. (2022). Review: Cannabinoids as medicinals. *Curr. Addict. Rep.* 7, 1–17. doi:10.1007/s40429-022-00438-3
- Kilaru, A., and Chapman, K. (2020). The endocannabinoid system. *Essays Biochem.* 64 (3), 485–499. doi:10.1042/EBC20190086
- Kitahara, T., Li, H., and Balaban, C. (2005). Changes in transient receptor potential cation channel superfamily V (TRPV) mRNA expression in the mouse inner ear ganglia after kanamycin challenge. *Hear. Res.* 201 (1–2), 132–144. doi:10.1016/j.heares.2004.09.007
- Klumpers, L., Roy, C., Ferron, G., Turpault, S., Poitiers, F., Pinquier, J., et al. (2013). Surinabant, a selective cannabinoid receptor type 1 antagonist, inhibits Δ^9 -tetrahydrocannabinol-induced central nervous system and heart rate effects in humans. *Br. J. Clin. Pharmacol.* 76 (1), 65–77. doi:10.1111/bcp.12071
- Kogan, N., and Mechoulam, R. (2007). Cannabinoids in health and disease. *Dialogues Clin. Neurosci.* 9 (4), 413–430. doi:10.31887/DCNS.2007.9.4/nkogan
- Leimuranta, P., Khiroug, L., and Giniatullin, R. (2018). Emerging role of (Endo) Cannabinoids in migraine. *Front. Pharmacol.* 9, 420. doi:10.3389/fphar.2018.00420
- Lempert, T., Olesen, J., Furman, J., Waterston, J., Seemungal, B., Carey, J., et al. (2012). Vestibular migraine: Diagnostic criteria. *J. Vestib. Res.* 22 (4), 167–172. doi:10.3233/VES-2012-0453
- Leweke, F., Piomelli, D., Pahlisch, F., Muhl, D., Gerth, C., Hoyer, C., et al. (2012). Cannabidiol enhances anandamide signaling and alleviates psychotic symptoms of schizophrenia. *Transl. Psychiatry* 2 (3), e94. doi:10.1038/tp.2012.15
- Lu, H., and Mackie, K. (2016). An introduction to the endogenous cannabinoid system. *Biol. Psychiatry* 79 (7), 516–525. doi:10.1016/j.biopsych.2015.07.028
- Martín-Saldaña, S., Trinidad, A., Ramil, E., Sánchez-López, A., Coronado, M., Martínez-Martínez, E., et al. (2016). Spontaneous cannabinoid receptor 2 (CB2) expression in the cochlea of adult albino rat and its up-regulation after cisplatin treatment. *PLOS ONE* 11 (8), e0161954. doi:10.1371/journal.pone.0161954
- McGuire, P., Robson, P., Cubala, W., Vasile, D., Morrison, P., Barron, R., et al. (2018). Cannabidiol (CBD) as an adjunctive therapy in schizophrenia: A multicenter randomized controlled trial. *Am. J. Psychiatry* 175 (3), 225–231. doi:10.1176/appi.ajp.2017.17030325
- Mechtler, L., Gengo, F., and Bargnes, V. (2021). Cannabis and migraine: It's complicated. *Curr. Pain Headache Rep.* 25 (3), 16. doi:10.1007/s11916-020-00931-2
- Morano, A., Fanella, M., Albin, M., Cifelli, P., Palma, E., Giallonardo, A., et al. (2020). Cannabinoids in the treatment of epilepsy: Current status and future prospects. *Neuropsychiatr. Dis. Treat.* 16, 381–396. doi:10.2147/NDT.S203782
- Narwani, V., Bourdillon, A., Nalamada, K., Manes, R., and Hildrew, D. (2020). Does cannabis alleviate tinnitus? A review of the current literature. *Laryngoscope* 130 (6), 1147–1155. doi:10.1002/lary.2479
- Nestoros, J., Vakonaki, E., Tzatzarakis, M., Alegakis, A., Skondras, M., and Tsatsakis, A. (2017). Long lasting effects of chronic heavy cannabis abuse. *Am. J. Addict.* 26 (4), 335–342. doi:10.1111/ajad.12529
- Newsham-West, D., Darlington, L. C., and Smith, P. (1998). Potent effects of a selective cannabinoid receptor agonist on some Guinea pig medial vestibular nucleus neurons. *Eur. J. Pharmacol.* 348 (1), R1–R2. doi:10.1016/S0014-2999(98)00237-4
- Parker, L., Limebeer, C., Rock, E., Litt, D., Kwiatkowska, M., and Piomelli, D. (2009). The FAAH inhibitor URB-597 interferes with cisplatin- and nicotine-induced vomiting in the *Suncus murinus* (house musk shrew). *Physiol. Behav.* 97, 121–124. doi:10.1016/j.physbeh.2009.02.014
- Peelle, J., and Wingfield, A. (2016). The neural consequences of age-related hearing loss. *Trends Neurosci.* 39 (7), 486–497. doi:10.1016/j.tins.2016.05.001
- Perin, P., Mabou Tagne, A., Enrico, P., Marino, F., Cosentino, M., Pizzala, R., et al. (2020). Cannabinoids, inner ear, hearing, and tinnitus: A neuroimmunological perspective. *Front. Neurol.* 11, 505995. doi:10.3389/fneur.2020.505995
- Post, J., Loch, S., Lerner, R., Remmers, F., Lomazzo, E., Lutz, B., et al. (2018). Antiepileptogenic effect of Subchronic Palmitoylethanolamide treatment in a mouse model of acute epilepsy. *Front. Mol. Neurosci.* 11, 67. doi:10.3389/fnmol.2018.00067
- Poudel, S., Quinonez, J., Choudhary, J., Au, Z., Paesani, S., Thiess, A., et al. (2021). Medical cannabis, headaches, and migraines: A review of the current literature. *Cureus* 13, e17407. doi:10.7759/cureus.17407
- Pradeep, A., Thomas, S., Roberts, E., Proudlock, F., and Gottlob, I. (2008). Reduction of congenital nystagmus in a patient after smoking cannabis. *Strabismus* 16 (1), 29–32. doi:10.1080/09273790701821063
- Ramkumar, V., Sheth, S., Dhukhwa, A., Al Ameri, R., Rybak, L., and Mukherjee, D. (2022). Transient receptor potential channels and auditory functions. *Antioxid. Redox Signal.* 36 (16–18), 1158–1170. doi:10.1089/ars.2021.0191
- Russo, E. (2016). Clinical endocannabinoid deficiency reconsidered: Current research supports the theory in migraine, fibromyalgia, irritable bowel, and other treatment-resistant syndromes. *Syndromes. Cannabis Cannabinoid Res.* 1 (1), 154–165. doi:10.1089/can.2016.0009
- Scheffer, I., Halford, J., Miller, I., Nabbout, R., Sanchez-Carpintero, R., Shiloh-Malawsky, Y., et al. (2021). Add-on cannabidiol in patients with Dravet syndrome: Results of a long-term open-label extension trial. *Epilepsia* 62 (10), 2505–2517. doi:10.1111/epi.17036
- Schon, F., Hart, P., Hodgson, T., Pambakian, A., Ruprah, M., Williamson, E., et al. (1999). Suppression of pendular nystagmus by smoking cannabis in a patient with multiple sclerosis. *Neurology* 53 (9), 2209–2210. doi:10.1212/wnl.53.9.2209-a
- Sha, S., and Schacht, J. (2016). Emerging therapeutic interventions against noise-induced hearing loss. *Expert Opin. Invest. Drugs* 26 (1), 85–96. doi:10.1080/13543784.2017.1269171
- Smith, D., Stanley, C., Foss, T., Boles, R., and McKernan, C. (2017). Rare genetic variants in the endocannabinoid system genes CNR1 and DAGLA are associated with neurological phenotypes in humans. *PLOS ONE* 12 (11), e0187926. doi:10.1371/journal.pone.0187926
- Sorensen, C., DeSanto, K., Borgelt, L., Phillips, K., and Monte, A. (2016). Cannabinoid hyperemesis syndrome: Diagnosis, pathophysiology, and treatment—A systematic review. *J. Med. Toxicol.* 13 (1), 71–87. doi:10.1007/s13181-016-0595-z
- Strupp, M., Thurtell, M., Shaikh, A., Brandt, T., Zee, D., and Leigh, R. (2011). Pharmacotherapy of vestibular and ocular motor disorders, including nystagmus. *J. Neurol.* 258 (7), 1207–1222. doi:10.1007/s00415-011-5999-8
- Suárez, J., Bermúdez-Silva, F., Mackie, K., Ledent, C., Zimmer, A., Cravatt, B., et al. (2008). Immunohistochemical description of the endogenous cannabinoid system in the rat cerebellum and functionally related nuclei. *J. Comp. Neurol.* 509 (4), 400–421. doi:10.1002/cne.21774
- Toal, K., Radziwon, K., Holford, D., Xu-Friedman, M., and Dent, M. (2016). Audiograms, gap detection thresholds, and frequency difference limens in cannabinoid receptor 1 knockout mice. *Hear. Res.* 332, 217–222. doi:10.1016/j.heares.2015.09.013

- Trattner, B., Berner, S., Grothe, B., and Kunz, L. (2013). Depolarization-induced suppression of a glycinergic synapse in the superior olivary complex by endocannabinoids. *J. Neurochem.* 127 (1), 78–90. doi:10.1111/jnc.12369
- Van de Donk, T., Niesters, M., Kowal, M., Olofsen, E., Dahan, A., and van Velzen, M. (2018). An experimental randomized study on the analgesic effects of pharmaceutical-grade cannabis in chronic pain patients with fibromyalgia. *Pain* 160 (4), 860–869. doi:10.1097/j.pain.0000000000001464
- Vázquez, M., Guevara, N., Maldonado, C., Guido, P., and Schaiquevich, P. (2020). Potential pharmacokinetic drug-drug interactions between cannabinoids and drugs used for chronic pain. *Biomed. Res. Int.* 2020, 3902740–3902749. doi:10.1155/2020/3902740
- Weber, M., Goldman, B., and Truniger, S. (2010). Tetrahydrocannabinol (THC) for cramps in amyotrophic lateral sclerosis: A randomised, double-blind crossover trial. *J. Neurol. Neurosurg. Psychiatry* 81 (10), 1135–1140. doi:10.1136/jnnp.2009.200642
- Weiss, B., Freytag, S., Kloos, B., Haubner, F., Sharaf, K., Spiegel, J., et al. (2021). Cannabinoid receptor 2 agonism is capable of preventing lipopolysaccharide induced decreases of cochlear microcirculation – a potential approach for inner ear pathologies. *Otol. Neurotol.* 42 (9), e1396–e1401. doi:10.1097/MAO.0000000000003280
- Weizman, L., Dayan, L., Brill, S., Nahman-Averbuch, H., Hendler, T., Jacob, G., et al. (2018). Cannabis analgesia in chronic neuropathic pain is associated with altered brain connectivity. *Neurology* 91 (14), e1285–e1294. doi:10.1212/WNL.0000000000006293
- Whiting, P., Wolff, R., Deshpande, S., Di Nisio, M., Duffy, S., Hernandez, A., et al. (2015). Cannabinoids for medical use: A systematic review and meta-analysis. *JAMA* 313 (24), 2456–2473. doi:10.1001/jama.2015.6358
- Wishart, D., Feunang, Y., Guo, A., Lo, E., Marcu, A., Grant, J., et al. (2017). DrugBank 5.0: A major update to the DrugBank database for 2018. *Nucleic Acids Res.* 46 (D1), D1074–D1082. doi:10.1093/nar/gkx1037
- Zajicek, J., Hobart, J., Slade, A., Barnes, D., and Mattison, P. (2012). Multiple sclerosis and extract of cannabis: Results of the MUSEC trial. *J. Neurol. Neurosurg. Psychiatry* 83 (11), 1125–1132. doi:10.1136/jnnp-2012-302468
- Zheng, Y., Reid, P., and Smith, P. (2015). Cannabinoid CB1 receptor agonists do not decrease, but may increase acoustic trauma-induced tinnitus in rats. *Front. Neurol.* 6, 60. doi:10.3389/fneur.2015.00060
- Zheng, Y., Stiles, L., Hamilton, E., Smith, P., and Darlington, C. (2010). The effects of the synthetic cannabinoid receptor agonists, WIN55, 212-2 and CP55, 940, on salicylate-induced tinnitus in rats. *Hear. Res.* 268 (1-2), 145–150. doi:10.1016/j.heares.2010.05.015
- Zogopoulos, P., Vasileiou, I., Patsouris, E., and Theocharis, S. (2013). The role of endocannabinoids in pain modulation. *Fundam. Clin. Pharmacol.* 27 (1), 64–80. doi:10.1111/fcp.12008
- Zou, S., and Kumar, U. (2018). Cannabinoid receptors and the endocannabinoid system: Signaling and function in the central nervous system. *Int. J. Mol. Sci.* 19 (3), 833. doi:10.3390/ijms19030833
- Zwergal, A., and Dieterich, M. (2020). Vertigo and dizziness in the emergency room. *Curr. Opin. Neurol.* 33 (1), 117–125. doi:10.1097/WCO.0000000000000769



OPEN ACCESS

EDITED BY

Hidayat Hussain,
Leibniz Institute of Plant Biochemistry,
Germany

REVIEWED BY

Mohamed S. Nafie,
Suez Canal University, Egypt
Laiba Arshad,
Forman Christian College, Pakistan
Ibrahim Malami,
Usmanu Danfodiyo University, Nigeria
Sreelatha Sarangapani,
TLL, Singapore

*CORRESPONDENCE

Goabaone Gaobotse,
✉ gaobotseg@biust.ac.bw
Kabo Masisi,
✉ masisik@biust.ac.bw
Abdullah Makhzoum,
✉ makhzoum@biust.ac.bw

SPECIALTY SECTION

This article was submitted to
Experimental Pharmacology and Drug
Discovery,
a section of the journal
Frontiers in Pharmacology

RECEIVED 12 December 2022

ACCEPTED 03 February 2023

PUBLISHED 14 February 2023

CITATION

Gaobotse G, Venkataraman S, Brown PD,
Masisi K, Kwape TE, Nkwe DO, Rantong G
and Makhzoum A (2023), The use of
African medicinal plants in
cancer management.
Front. Pharmacol. 14:1122388.
doi: 10.3389/fphar.2023.1122388

COPYRIGHT

© 2023 Gaobotse, Venkataraman, Brown,
Masisi, Kwape, Nkwe, Rantong and
Makhzoum. This is an open-access article
distributed under the terms of the
[Creative Commons Attribution License](https://creativecommons.org/licenses/by/4.0/)
(CC BY). The use, distribution or
reproduction in other forums is
permitted, provided the original author(s)
and the copyright owner(s) are credited
and that the original publication in this
journal is cited, in accordance with
accepted academic practice. No use,
distribution or reproduction is permitted
which does not comply with these terms.

The use of African medicinal plants in cancer management

Goabaone Gaobotse^{1*}, Srividhya Venkataraman²,
Phenyo D. Brown¹, Kabo Masisi^{1*}, Tebogo E. Kwape¹,
David O. Nkwe¹, Gaolathe Rantong¹ and Abdullah Makhzoum^{1*}

¹Department of Biological Sciences and Biotechnology, Faculty of Sciences, Botswana International University of Science and Technology, Palapye, Botswana, ²Virology Laboratory, Department of Cell and Systems Biology, University of Toronto, Toronto, ON, Canada

Cancer is the third leading cause of premature death in sub-Saharan Africa. Cervical cancer has the highest number of incidences in sub-Saharan Africa due to high HIV prevalence (70% of global cases) in African countries which is linked to increasing the risk of developing cervical cancer, and the continuous high risk of being infected with Human papillomavirus. In 2020, the risk of dying from cancer amongst women was higher in Eastern Africa (11%) than it was in Northern America (7.4%). Plants continue to provide unlimited pharmacological bioactive compounds that are used to manage various illnesses, including cancer. By reviewing the literature, we provide an inventory of African plants with reported anticancer activity and evidence supporting their use in cancer management. In this review, we report 23 plants that have been used for cancer management in Africa, where the anticancer extracts are usually prepared from barks, fruits, leaves, roots, and stems of these plants. Extensive information is reported about the bioactive compounds present in these plants as well as their potential activities against various forms of cancer. However, information on the anticancer properties of other African medicinal plants is insufficient. Therefore, there is a need to isolate and evaluate the anticancer potential of bioactive compounds from other African medicinal plants. Further studies on these plants will allow the elucidation of their anticancer mechanisms of action and allow the identification of phytochemicals that are responsible for their anticancer properties. Overall, this review provides consolidated and extensive information not only on diverse medicinal plants of Africa but on the different types of cancer that these plants are used to manage and the diverse mechanisms and pathways that are involved during cancer alleviation.

KEYWORDS

sub-Saharan Africa, medicinal plants, cancer, bioactive compounds, cancer management, anticancer mechanism

1 Introduction

Over the past years, plants have gained momentum in research for the alleviation of major human diseases such as cancer and HIV/AIDS (Nkwe et al., 2021; Makhzoum and Hefferon, 2022). Plants have been used in the production of anti-HIV recombinant proteins to circumvent issues associated with the use of antiretroviral drugs (Tremouillaux-Guiller et al., 2020; Gaobotse et al., 2022a). Cancer, like HIV/AIDS, is a major cause of global morbidity and mortality. The World Health Organization (WHO) reported that cancer is the second leading cause of death globally and was responsible for an estimated 9.6 million deaths in 2018 (WHO, 2020). Approximately 70% of deaths from cancer occur in low and

middle-income countries which are mostly in Africa. It is estimated that 13% of global annual deaths are due to lung, colorectal, stomach, liver, and breast cancers (WHO, 2020). It is also estimated that by the year 2030, cancer related deaths will increase to 17 million (Adeloye et al., 2016). According to (WHO, 2020), in Africa, the prevalence of cancer is higher in men than women. More than 19.3 million new cases of cancer were registered worldwide in the year 2020 and these numbers are expected to rise to 28.4 million by the year 2040 (Sung et al., 2021). In the same year of 2020, there were 10 million reported deaths due to different types of cancers across the world. In addition, female breast cancer has now surpassed lung cancer as the most diagnosed cancer in the world (Sung et al., 2021). However, lung cancer remains the leading cause of mortality amongst all the different types of cancer, causing an estimated 1.8 million deaths in the year 2020. This is equivalent to 18% of all cancer related deaths globally. On the other hand, female breast cancer contributed to only 6.9% of all global cancer related deaths in 2022 (Sung et al., 2021). Throughout history, human beings have acquired knowledge on the medicinal uses of plants and have applied this knowledge in folk medicine to treat different diseases (El-Seedi et al., 2013; Ouelbani et al., 2016). It is estimated that 80% of the world population still rely on plant-based material for primary healthcare while traditional medicine usage accounts for 60% of the world population (El-Seedi et al., 2013). Due to low income or long distances from urban treatment centers, many people in Africa commonly use medicinal plants for cancer treatment (Kabbaj et al., 2012; El-Seedi et al., 2013). Moreover, some Africans believe that medicinal plants are more effective than synthetic drugs in managing diseases such as cancer. However, comprehensive compilation of information on these medicinal plants of Africa is insufficient. The documented use of medicinal plants in Africa dates back a couple of centuries, although it might have been there earlier than that (Sawadogo et al., 2012; Ntie-Kang et al., 2013). Cancer remains one of the leading causes of death globally despite advancements in cancer management strategies. Although there have been recent efforts in the production of cancer vaccines in different host plants for different types of cancer (Gaobotse et al., 2022b), there is a need to explore medicinal plants further for cancer management strategies. This review is a compilation of information on diverse medicinal plants of Africa, found in different countries of the continent, that have been used in the management of different types of cancer.

Cancer is the third leading cause of premature death in sub-Saharan Africa, responsible for one in 7 deaths. In 2020, there were 801, 392 new cases of cancer with an estimated 520, 158 deaths in sub-Saharan Africa. In women, the most common types of cancer are breast (129, 400) and cervical cancer (110, 300) which together are responsible for three out of 10 cancer diagnoses. In men, the most common types of cancer are prostate (77, 300), liver (24, 700) and colorectal cancer (23, 000) (Bray et al., 2021; Bray et al., 2022).

The rich flora of Africa results from a vast difference in environmental and climatic conditions such as deserts, savannah, and tropical rain forests. Some of these plants have been used in traditional medicine to treat symptoms of cancer with reports that of all pharmaceutical drugs used, a quarter of them have been derived from plants originally used in traditional medicine (Sawadogo et al., 2012). Treatment of patients across Africa varies from one region to

another and this is mostly influenced by the plants, protocols and recipes used. In West Africa, more than half of plants with anticancer metabolites are shrubs and the explants commonly used are the roots and stem barks, with methanol extracts contributing approximately 60% of the used extracts (Sawadogo et al., 2012). (Sawadogo et al., 2012) have shown that phytochemicals with high cytotoxicity towards many cancer cell lines are diterpenes, triterpenes and steroids. Leukaemia, breast, colon, and lung cancer cell lines have shown great sensitivity toward phytochemicals isolated from plants with anticancer activity in West Africa (Usman et al., 2022). *Brassica rapa*, which is found across almost all regions of Africa, has phytochemicals such as phenanthrene, diarylheptanoids and others with cytotoxic activity towards various human cancer cell lines (Wu et al., 2013). The African cabbage has been used by traditional healers to treat tumors and its extracts have been shown to be cytotoxic to carcinoma cell lines in mice (Bala et al., 2010). *Colocasia esculenta*, a tropical plant found in most regions of Africa, is said to produce fibers which antagonize the growth of colon cancer cells in rats (Brown et al., 2005) and its aqueous extracts inhibit breast and lung tumors (Kundu et al., 2012).

Twenty-three (23) anticancer plants that are native to Africa will be discussed in this review. These plants are *Dicoma anomala*, a perennial herb; *Fagaropsis* which are shrubs or deciduous trees with buttress roots; *Tribulus terrestris*, which is a small, silky, and hairy herb; *Portulaca oleracea*, which is an annual succulent plant and *Withania somnifera*, a small, bushy, evergreen shrub. Other plants that will be discussed are the semi-deciduous tree called *Azanza garckeana*; *Cajanus cajan*, which is a perennial legume; *Combretum cafrum*, which is an African bush willow tree; and the flowering cherry plants called *Prunus avium* and *Prunus africana*. The review will also look at the tree species *Securidaca longipedunculata*; the shrub *Annona senegalensis*; the tropical fruit tree *Annona muricata*; the shrub plant *Aerva javanica* and the flowering plant *Abelmoschus esculentus*. The review will also discuss the dioecies *Flueggea virosa*; the climbing vine called *Lagenaria siceraria*; the aromatic evergreen called *Xylopia aethiopica*; the flowering perennial aquatic *Nymphaea lotus* as well as the deciduous shrub called *Zanthoxylum chalybeum*. The Mediterranean evergreen *Ceratonia siliqua*; the perennial softwood vegetable *Moringa oleifera* and the perennial herbaceous *Peganum harmala* will also be discussed in the review.

Amongst these 23 plants, *T. terrestris* can be consumed in diet. The leaves, fruits, and shoots of this plant can be cooked and consumed. *Portulaca oleracea* is an edible weed with high nutrition. It also has nutraceutical value that helps in the prevention, treatment, and management of some human diseases (Gunaratne et al., 2022). In India, *Withania coagulans* is used to ferment milk during cheese production (Ahmad et al., 2017). *Azanza garckeana* is a valuable source of fruits which are consumed while green or a bit ripe (Ochokwu et al., 2015). *Cajanus cajan* is a good source of protein and its seeds are cooked and consumed as peas (Talari and Shakappa, 2018). *Prunus avium* fruits comprise of a fleshy edible mesocarp as well as an edible protective exocarp (Usenik et al., 2015). However, the endocarp of the fruit is inedible. The leaves of *S. longipedunculata* are cooked and consumed while they are young while the roots of this plant are poisonous. The ripe fruits of *A. senegalensis* are edible while the flowers of the plant are used for food seasoning (Donhouedé et al., 2022). The fruits of *A. muricata* are also

consumed raw or cooked. *Abelmoschus esculentus* is an important vegetable crop whose immature fruits can be consumed as vegetables (Gemedie et al., 2015). The fruits of *F. virosa* are only edible when mature. The fruits, seeds, leaves, and oil of *L. siceraria* are edible (Zahoor et al., 2021). The tubers of *N. lotus* are consumed raw or roasted (Lim, 2014). The leaves of *Z. chalybeum* are dried and used as powdered vegetable (Balama et al., 2015).

2 Traditional African medicinal plants used in the management of different cancers

2.1 *Dicoma anomala*

Dicoma anomala is a perennial herb that is typically called stomach or fever bush. It is a member of the family Asteraceae. It has an erect stem covered with thin hairs as well as an underground tuber (Balogun and Ashafa, 2017). It is native to sub-Saharan Africa, and, in South Africa, it is widely distributed in the Free State, Gauteng, KwaZulu-Natal, Limpopo, Mpumalanga, Northern Cape, and North West provinces. This plant has been used traditionally in Africa to treat diseases such as colds, coughs, fever, ulcers, and diabetes (Balogun and Ashafa, 2017). It has wide ethnomedical uses and its roots are universally used to treat diseases that affect animals and humans. Among the different species of *Dicoma*, *D. anomala*, *D. zeyheri*, *D. capensis* and *D. schinzii* have been utilized for their medicinal properties and were duly classified based on their phytochemical composition. Some of these phytochemicals are acetylenic compounds, flavonoids, phenolic acids, phytosterols, sesquiterpenes and triterpenes. They are non-toxic to normal non-cancerous cells. These compounds occur primarily in the leaves and roots and have been used to treat various cancers such as prostate, kidney, ovarian and breast cancers (Greenwell and Rahman, 2015; Maroyi, 2018). *D. anomala* Sond roots have shown antiproliferative effects against MCF-7 breast cancer cells wherein sesquiterpene conjugated to silver nanoparticles demonstrated anticancer properties by causing oxidative damage in the cancerous cells (Shafiq et al., 2020). *Dicoma capensis* aqueous extracts have also shown anticancer properties against breast cancer cell lines such as MCF-12A, MDA-MB-231 and MCF-7 (Asita et al., 2015).

2.2 *Fagaropsis*

The genus *Fagaropsis* belongs to the family Rutaceae and is widely distributed in Africa. *Fagaropsis* are mostly shrubs or deciduous trees with buttress roots. The plant species *Fagaropsis angolensis* is found in Angola, Ethiopia, Kenya, Namibia, Tanzania, Uganda, and Zimbabwe; *F. hildebrandtii* is primarily found in Ethiopia, Kenya, Somalia, and Tanzania while *F. velutina* and *F. glabra* occur endemically in Madagascar (Sun et al., 2021). *F. angolensis* whole root methanol extracts have been shown to exhibit antitumor activity against throat cancer cells (Hep2) at an IC_{50} value of $10.05 \pm 2.15 \mu\text{g/mL}$. Whole root and root-stem methanol extracts showed high degrees of anticancer effects against CT26 colon cancer cells with IC_{50} values of $8.33 \pm$

$1.42 \mu\text{g/mL}$ and $5.25 \pm 0.35 \mu\text{g/mL}$ respectively (Yiaile, 2017). *F. angolensis* stem bark methanolic extracts demonstrated significant activity against DU-145 prostate cancer cells and HCC 1395 breast cancer cells at IC_{50} values of $12.8 \pm 1.1 \mu\text{g/mL}$ and $53.9 \pm 5.6 \mu\text{g/mL}$ respectively (Misonge et al., 2019). Anticancer effects of methanol extracts of the bark of *F. angolensis* against HCC 1395 cells were also reported by (Onyancha et al., 2018). Despite its anticancer activities, *F. angolensis* has shown high levels of toxicity on Vero cells. Therefore, more research is needed to evaluate the precise dosages of the active anticancer ingredients in this plant to mitigate toxicity issues and validate them for their use in folklore medicine.

2.3 *Tribulus terrestris*

Tribulus terrestris is a small, silky and hairy herb which is indigenous to tropical regions, including Africa, and is a member of the Zygophyllaceae family (Hashim et al., 2014). Methanol extracts of *T. terrestris* showed strong inhibition against SK-OV-3 ovarian carcinoma cells and MCF-7 breast cancer cells with IC_{50} values of $89.4 \mu\text{g/mL}$ and $74.1 \mu\text{g/mL}$ respectively (Abbas et al., 2022). *Tribulus terrestris* occurs as a perennial herb and is known for its antineoplastic effects against a wide range of human cancers. The high anticancer potential of *T. terrestris* has been attributed to its high content of steroidal saponins which have been shown to induce programmed cell death in MCF-7s by eliciting both extrinsic and intrinsic apoptotic pathways (Osbourne, 2003; Sun et al., 2003; Sparg et al., 2004; Kim et al., 2011; Angelova et al., 2013; Faizal and Geelen, 2013). (Patel et al., 2021) reported *in silico* studies implicating the anticancer properties to active saponin compounds such as nautigenin saponin that could be essential in the treatment of breast cancer. *T. terrestris* fruit extracts are capable of inhibiting autophagy in TW2.6 and SAS oral cancer cells and can impact cell proliferation, growth, cell migration and invasion of neoplastic/metastatic cancer cells (Shu et al., 2021).

2.4 *Portulaca oleracea*

Portulaca oleracea is a common succulent plant that is often referred to as Purslane. It belongs to the genus *Portulaca* in the family Portulacaceae and is abundant in most regions of Africa such as Botswana (Uddin et al., 2014). The polysaccharides of *P. oleracea* L., POL-P3b, have shown inhibition of tumors by means of cell cycle arrest, elicitation of DNA damage and induction of apoptosis (Zhao et al., 2013). (Jia et al., 2021) demonstrated that there was a high-level induction of TNF- α , IFN- γ and IL-12 when POL-P3b was co-administered with a dendritic cell vaccine in mouse models, implicating Th1 immune response modulation by POL-P3b. Therefore, POL-P3b serves as an adjuvant that stimulates maturation and augment the antigen presentation capability of the Dendritic Cell (DC) vaccine. Additionally, POL-P3b upregulated the expression levels of MyD88, NF- κ B and TLR4 in the DC vaccine and promoted Th1 cytokine secretion. The Ki 67 index is closely associated with the degree of tumor malignancy (Bleckmann et al., 2016; Christensen et al., 2016) and a combination of the DC vaccine and POL-P3b was found to be

capable of reducing Ki 67 expression. Also, this combination triggered more significant apoptotic characteristics such as nuclear fragmentation, massive shrinkage of cells and high numbers of TUNEL-positive cells when compared to either the DC vaccine alone or POL-P3b alone. Additionally, higher immunomodulatory properties were observed in immune mice when administered with POL-P3b (Jia et al., 2021). Lymphocyte proliferation elicited by LPS and Con A was augmented, the CD4+/CD8+ ratio increased and the expression of cytokines, including that of TNF- α , IFN- γ , IL-4 and IL-12p70, was also significantly enhanced, suggesting that the POL-P3b adjuvant administered along with the vaccine can upregulate immune response reactions in mice. CD31, CD34 and VEGF expressions were more pronouncedly diminished when a combination of POL-P3b and the DC vaccine was administered and there was a synergistic suppression of angiogenesis. POL-P3b as an adjuvant for the DC vaccine also demonstrated diminished mortality and prolonged survival of tumor-bearing mice, showing the anti-tumor effect of POL-P3b. Therefore, POL-P3b functions as a highly propitious dietary adjuvant for the DC vaccine, inducing DC maturation. POL-P3b, in addition to inhibiting tumor growth by increasing tumor apoptosis, also inhibited lung metastasis, and induced non-toxic side effects in mouse models (Jia et al., 2021). Therefore, POL-P3b holds great promise as an efficient and safe immunomodulatory agent capable of regulating DC maturation and enhancing immune responses of the DC vaccine against breast cancer (Liu et al., 2021). isolated two novel amide glycosides, oleraciamide E and oleraciamide F, containing similar molecular structures from *P. oleracea* L. wherein oleraciamide E demonstrated anticholinesterase activity with an IC₅₀ value of 52.43 ± 0.33 M and exhibited scavenging activity in 1,1-diphenyl-2-picrylhydrazyl (DPPH) radical quenching assays with an IC₅₀ value of 24.64 ± 0.33 M which indicate antioxidant effects.

2.5 *Withania somnifera*

Withania somnifera is a small, bushy, evergreen shrub widely distributed across the world and abundant in South Africa and Botswana. It is a member of the Solanaceae family (Gaurav et al., 2015). It has been shown that *W. somnifera* root extracts can inhibit vimentin, a protein normally found in regions of metastasis, thus suggesting its counteracting effects on tumour formation in breast cancer (Yang et al., 2013). The anticancer potential of *W. somnifera* has been mainly attributed to Withanolide and Withaferin A, which are two principal phytochemicals from this plant. *In vivo*, in mice, it was reported that *W. somnifera*, through the activities of Withanolide and Withaferin-A, modulate different signalling pathways such as apoptosis, autophagy and reactive oxygen species (ROS) pathways (Shikder et al., 2020). In male Swiss albino mice, extracts from *W. somnifera* were shown to inhibit lung adenoma (Senthilnathan et al., 2006a) while the root extracts of this plant were shown to prevent ROS-induced injury in model mice (Senthilnathan et al., 2006b). Ethanol extracts of the roots of *W. somnifera* were shown to inhibit the proliferation of A549 lung cancer cells through the downregulation of PI3K, which reduced metastasis (Vamsi et al., 2020). *In vitro*, Withaferin-A has been shown to reduce the proliferation of the human breast cancer cell

line MDA-MB-231 by inhibiting the two-pore domain potassium (K2P9) channel TASK-3 (Zúñiga et al., 2020). Withaferin-A has also been shown to inhibit the proliferation of other cancer cell lines such as the cervical cancer cell lines (HeLa, SKGII, ME180) and ovarian cancer cell lines (OKV-18 and SKOV3) (Sari et al., 2020). The activity of Withaferin-A against these cells is said to be brought about by the upregulation of the tumour suppressor p53 coupled with cell growth arrest and DNA damage signalling (Sari et al., 2020). Withanolides have been shown to inhibit the proliferation of MCF-7s by inducing apoptosis, inducing the overexpression of Hsp70 and reducing the expression of ER in MCF-7s (Chen et al., 2008). Withanolides were also found to suppress TGF- β 1 and TNF- α induced Epithelial-Mesenchymal Transition (EMT) in the lung cancer cell lines H129 and A549 (Yang et al., 2013). Table 1 shows bioactive compounds of *Withania*, the plant parts they are derived from, the different types of cancer that they target, and their mechanisms of action during cancer alleviation.

2.6 *Azanza garckeana*

Azanza garckeana is a semi-deciduous tree and a member of the Malvaceae family that is commonly found in East and Southern Africa. According to (Michael et al., 2015), on evaluating phytochemicals of the seeds of this plant, it was discovered that they have tannins, saponins, flavonoids, alkaloids, phenols, glycosides and carotenoids. The benzopyrone ring structure, known for its antioxidant properties, is integral to flavonoids, making flavonoids to have antioxidant behaviour. This antioxidant activity is able to fight and remove free radicals in biological systems and inhibit the development of tumors (Michael et al., 2015). The seeds of *A. garckeana* are said to be able to reduce cancer development due to their possession flavonoids, which are able to interfere with oestrogen synthase, an enzyme that produces oestrogen (Okwu, 2005). A complex formed between Mansone G and β -Cyclodextrin, which are some of the phytochemicals extracted from *A. garckeana*, was found to exhibit high levels of cytotoxicity towards A549 lung cancer cells (Bioltif et al., 2020). Figure 1 shows the leaves of *Portulaca oleracea*, *Tribulus terrestris*, *A. garckeana* and *Withania somnifera*.

2.7 *Cajanus cajan*

Ovarian cancer is the second most prevalent gynecological malignancy and one of the most lethal cancers. The major challenge in the treatment of ovarian cancer is the emergence of multi-drug resistance during chemotherapy. Cajanol is derived from *Cajanol cajan* roots and has a multitude of pharmacological activities such as anti-tumor properties. Cajanol inhibits NF- κ B phosphorylation and nuclear ectopia by interfering with PI3K expression and the phosphorylation of Akt. This diminishes the transcription and translation of the permeability glycoprotein and eventually decreases cancer related multi-drug resistance that is induced by the efflux of paclitaxel (Sui et al., 2021). *Cajanus cajan* is a medicinal plant that is native to the Southwest of Nigeria. It is grown for food in Nigeria (Ashidi et al., 2010). *C. cajan* synthesizes cajanin stilbene acid (CSA) which shares structural analogies with

TABLE 1 *Withania* bioactive compounds, plant parts they are derived from, their target cancers, and their mechanisms of action.

Bioactive molecules	Parts used	Cancer cell line/Experiment	Mechanism of action
Withaferin A (WA)	Leaves	Breast cancer cell lines; MCF-7 and MDA-MB-231	Inhibited the expression of ER, HSF1 and RET; increased the expression of p21, phospho-p38 MAPK, and p53 in MCF-7s Zhang et al. (2011)
		Mouse models and breast cancer cells	Blocked cell proliferation, diminished tumor growth and promoted FOXO3a and Bim-dependent apoptosis Stan et al. (2008)
		Ovarian cancer cells	Blocked cell growth, induced cell cycle arrest and apoptosis, targeted Notch1 and Notch3 downregulation Zhang et al. (2012)
		Breast cancer cell lines; 4T1 (mouse breast), SCID mice, Balb/c mice, Nu/nu mice	Decreased tumor growth and enabled chemoprevention Thaiparambil et al. (2011)
	Roots	Prostate PC-3 xenografts in nude mice	Inhibited proteasomal chymotrypsin-like activity and tumor growth Yang et al. (2007)
		Breast cancer cell lines; SUM159 and MCF-7	Induced apoptosis and showed antiproliferative activity Hahm et al. (2014)
	Fruits	Liver cancer cells HepG2	Notably changed chromatin structure (uniform condensation, fragmentation) Abutaha (2015)
L-asparaginase	Fruits	Human leukemia cells	Inhibited lymphoblastic leukemia Oza et al. (2010)
Withaferin A and Withanolide D	Roots	B16F-10 melanoma cells in C57BL/6 mice	Showed significant antitumor activity Leyon and Kuttan (2004)
<i>Withania somnifera</i>	Leaves	Human glioma cell lines (A172, YKG1 and U118MG)	Inhibited cell proliferation and increased the expression of NCAM and mortalin Kataria et al. (2011)
<i>Withania somnifera</i> and Withaferin	Leaves	Breast carcinoma (MCF-7), human normal fibroblasts (TIG-3) and colon carcinoma (HCT116)	Enhanced DNA damage and oxidative stress; downregulated ING1, LHX3, TPX2 and TFAP2A Widodo et al. (2010)
<i>Withania somnifera</i>	Roots	Prostate cancer cells (PC-3)	Inhibited cell proliferation and arrested cell cycle in G2/M phase; downregulated the expression of COX-2 and IL-8 Balakrishnan et al. (2017)
<i>Withania somnifera</i> and cisplatin	Roots	Colon (HT-29) cancer cells and breast (MDA-MB-231) cancer cells	Inhibited cell proliferation, promoted mitochondrial dysfunction, and generated ROS Henley et al. (2017)

estrogen. CSA exerts antiestrogenic and anticancer activities towards estrogen receptor (ER α)-positive breast cancer cells. Particularly, it shows cytotoxicity towards MCF-7 cells resistant to tamoxifen while exhibiting low cytotoxicity towards ER α -negative breast tumor cells ([Fu et al., 2015](#)). This cytotoxicity is independent of the cellular p53 status. CSA binds to the same site as tamoxifen and 17 β -estradiol on ER α . Thus, CSA displays its anticancer properties against ER α -positive breast cancer cells by interacting with and inhibiting ER α . The cytotoxicity of CSA towards MCF-7s resistant to tamoxifen indicates its promise as a tamoxifen alternative for treatment of breast cancer. When combined with tamoxifen, CSA enables synergistic cytotoxicity and promotes p53 protein expression. Cajanol, scientifically known as 5-hydroxy-3-(4-hydroxy-2-methoxyphenyl)-7-methoxychroman-4-one, is an isoflavone isolated from the roots of *C. cajan*. In MCF-7s, cajanol causes cell cycle arrest at the G2/M phase while inducing apoptosis through a mitochondrial pathway mediated by ROS ([Luo et al., 2010](#)). This leads to the disintegration of the outer membrane of the mitochondria and the release of cytochrome C followed by the elicitation of the caspase-3 and caspase-9 cascade which causes apoptosis. In COR-L23 lung cancer cells, *C. cajan* was shown to have anticancer activity with an IC₅₀ value of 5–10 μ g/mL. It was reported

that stilbenes longistylins A and C present in the leaf extracts of the plant were responsible for this anticancer property ([Ashidi et al., 2010](#)).

2.8 *Combretum caffrum*

The bark of *Combretum caffrum*, the African bush willow tree, is a source of natural phenolic stilbene compounds called combrestatins ([Pettit et al., 1987](#)). Among these combrestatins, combrestatin A-4 (CA4) is the most efficient as an antitumor agent. CA4 inhibits tubulin polymerization, augments vascular permeability, and abrogates blood flow into tumors ([Simoni et al., 2006](#)). A drug candidate, Ecust004, has been developed as an optimized agent derived from the structure-activity investigations of the sulfamate derivatives of CA4 and Erianin. This is a strong inhibitor of steroid sulfatase and tubulin in addition to exhibiting antiproliferative activity against tumor cells at low concentrations. This sulfate modification augments the pharmacokinetic profiles and bioavailability of the parental CA4 and Erianin natural compounds ([Raobaikady et al., 2005](#); [Foster et al., 2008](#); [Visagie et al., 2015](#)). Ecust004 inhibits tumor

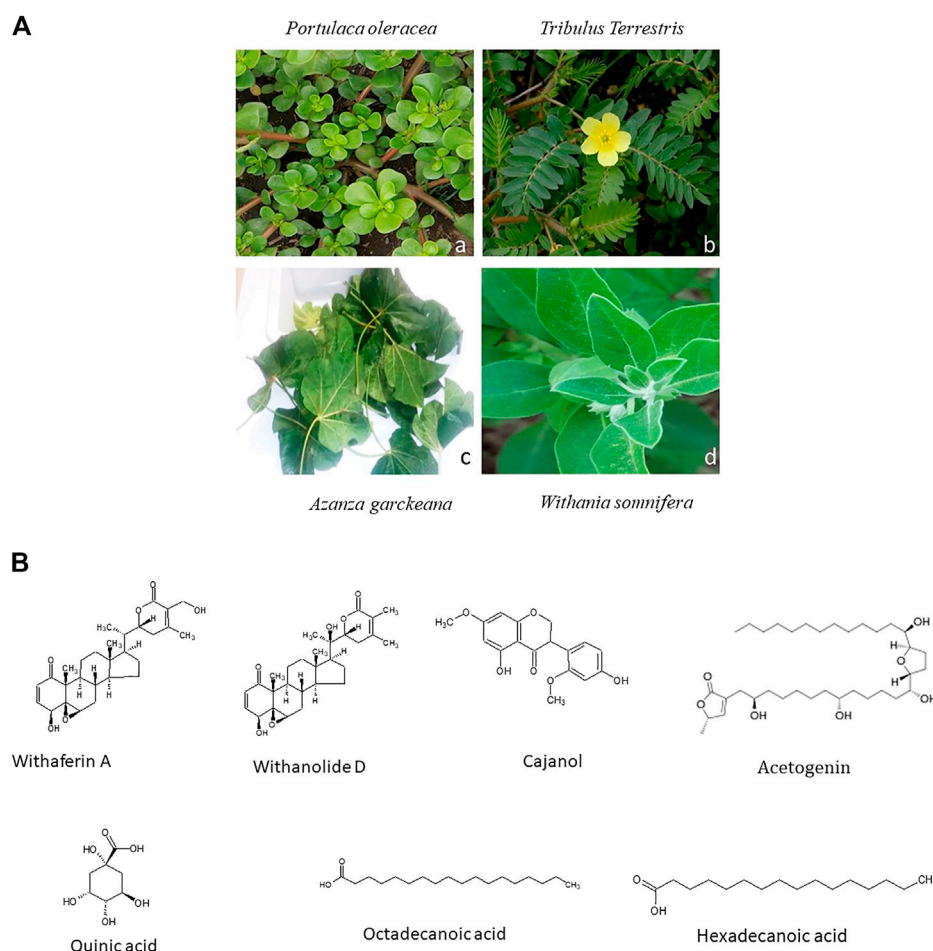


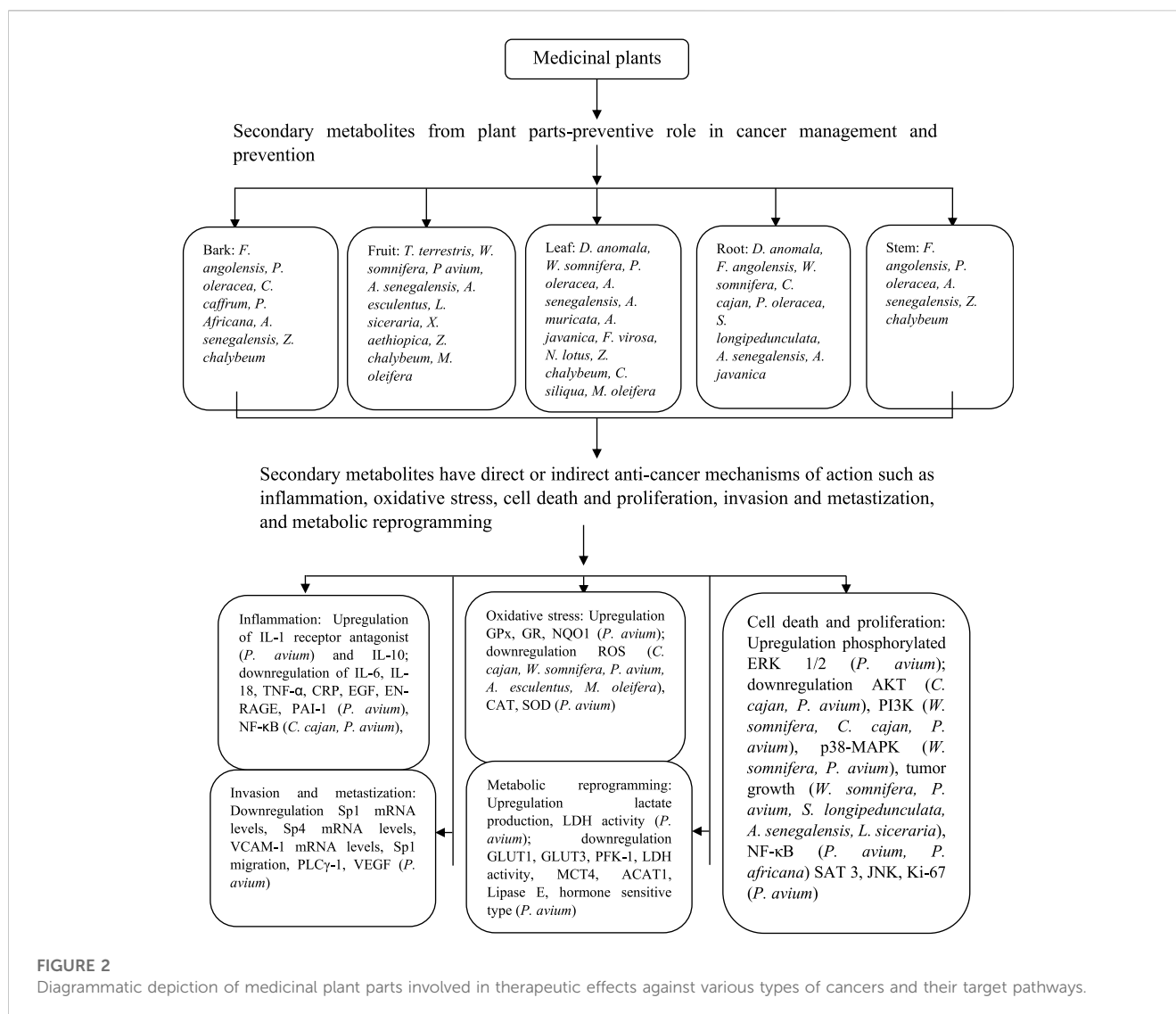
FIGURE 1

(A) Images of a selected African Medicinal Plants species used for Cancer management. Leaves of *Portulaca oleracea* are fleshy and oval (a) (Source: <https://www.terrepromise.ca/en/products/lettuce/greens/> [accessed 12 Oct 2022]), *Tribulus Terrestris* leaves are opposite each other and unequal in size (b) (Source: https://www.zimbabweflora.co.zw/speciesdata/image-display.php?species_id=132940&image_id=4 [accessed 3 Nov 2022]), Harvested leaves of *Azanza garckeana* showing a linear midrib fissure (c), *Withania somnifera* leaves are broadly ovate with curvy margins (d) (Source: [https://www.magicgardenseeds.co.uk/The-Good-To-Know/Winter-Cherry-\(Withania-somnifera\)-A.WIT01-](https://www.magicgardenseeds.co.uk/The-Good-To-Know/Winter-Cherry-(Withania-somnifera)-A.WIT01-) [accessed 27 October 2022]). (B) Structures of some Phytochemicals derived from African Medicinal Plants.

proliferation *in vivo* and *in vitro* in addition to diminishing cell viability, migration, and invasion of MCF-7 and MDA-MB-231 cells at low dosages. Combrestatins comprise a category of closely analogous stilbenes including combretastatins A, dihydrostilbenes or combretastatins B, phenanthrenes or combretastatins C and macrocyclic lactones or combretastatins D which are all derived from the bark of *C. caffrum*. Some of these compounds are the strongest antitubulin agents ever known. Owing to the structural simplicity of these substances, several analogs have been synthesized. Amongst these, Combrestatin A4 phosphate is the most tested substance in preclinical and clinical trials (Karatoprak et al., 2020). This water-soluble prodrug is rapidly metabolized in the body to combrestatin A4 that displays antitumor, antiproliferative, anti-inflammatory and antioxidant activities. Nano-formulations of CA4 phosphate have important advantages such as increased water solubility, drug targeting capabilities, improved efficiency, protracted half-lives in circulation and lesser side effects.

Therefore, combrestatins are favorable candidates for novel tumor therapeutics.

Combrestatins have been shown to be active against many human cancer cell lines and combrestatin A-4 is the strongest in terms of potency. Their principal action is their interaction with the colchicine binding site of the tubulin β subunit and the disruption of tubulin polymerization into microtubules (Izuegbuna, 2022). CA4 has been shown to be cytotoxic towards some cancer cell lines such as the leukemia cell line, P-388, which is resistant to daunorubicin (McGown and Fox, 1990). It acts by disrupting cell signaling pathways involved in the maintenance and regulation of the cytoskeleton of the endothelial cells occurring in the tumor vasculature, thus causing the selective disruption of blood flow through the tumors. Thereupon, these tumor cells undergo necrosis. Intriguingly, while enabling disruption of blood supply into the tumor cells, CA4 maintains normal blood flow into adjacent normal tissues (Nihei et al., 1999). CA4 activity is not dependent on temperature. This contrasts with colchicine, which interacts with a



similar binding site on the tubulin molecule. The complexation of CA4 tubulin occurs easily even on ice (Nam, 2003). Another CA4 sodium phosphate (CA4P) pro-drug has also been synthesized. The action of CA4P is like that of CA4. It leads to microtubule depolymerization and represses tumor cell angiogenesis (Tozer et al., 2002). CA4P eventually induces apoptosis in tumor cells (Iyer et al., 1998), although it has been reported that it results in cell death through molecular pathways, rather than apoptosis, such as the mitotic catastrophe pathways (Nabha et al., 2001). These pathways, which lead to cell death, make combrestatin a powerful anticancer compound of high efficacy (Jaroch et al., 2016).

2.9 *Prunus avium*

Prunus avium (Sweet cherry) is a plant that is widely distributed in the north of Africa (Osafu et al., 2017). Dark sweet cherry is a rich source of phenolics and is characterized by its anti-invasive and anticancer activities. *Prunus avium* phenolics inhibit MDA-MB-

453 breast cancer cells by triggering cell signaling pathways that elicit apoptosis and disrupt cell invasion. Amongst these phenolics, anthocyanins have shown augmented chemopreventative properties (Layosa et al., 2021). Polyphenols, especially anthocyanins, are well known for their anti-inflammatory, cytoprotective and antioxidant properties (Tsuda et al., 2000; Li et al., 2014; Huang et al., 2018; Silva et al., 2020). Table 2 shows examples of anticancer bioactive compounds found in *P. avium* and outcomes of their experimental uses.

2.10 *Prunus africana*

Prunus africana is a widely distributed tree of African origin which is primarily found in Southern and Central Africa (Komakech et al., 2022). In previous ethnomedical studies, the bark decoction of *P. africana* was used to treat prostate cancers (Grace et al., 2003; Ochwang'i et al., 2014; Tugume et al., 2016). In *vivo* studies, mice with transgenic adenocarcinoma in their prostate were fed with *P. africana* and demonstrated a significant decrease in the incidence of

TABLE 2 Biological properties of *Prunus avium* extracts and their bioactive compounds that target hallmarks of cancer.

Cancer hallmark	Biological model/ Type of study	Experiment	Outcome
Oxidative stress	<i>In vitro</i> : Hep2G cells	Incubation with extract of sweet cherries	↓ Intracellular ROS Acero et al. (2019)
	<i>In vitro</i> : Caco-2 cells	Co-incubation with sweet cherry extract and H ₂ O ₂	↓ Carbonyl proteins ↓ Intracellular ROS restored GSH/GSSG ratio Matias et al. (2016)
	<i>In vitro</i> : SH-SY5Y cells	Pre-incubation with sweet cherry extract prior to H ₂ O ₂ administration	↓ Intracellular ROS ↑ GSH ↑ GR ↑ NQO1 Antognoni et al. (2020)
	<i>In vivo</i> : Wistar rats	High fructose-diet with freeze-dried sweet cherry	↑ GPx ↑ GR ↓ Catalase ↓ SOD Inhibition of lipid peroxidation Dziadek et al. (2019)
	<i>In vivo</i> : Human subjects	Consumption of sweet cherries	↑ Plasma lipophilic antioxidant capacity ↑ Plasma hydrophilic antioxidant capacity ↑ Urinary antioxidant capacity ↑ Lipophilic oxygen radical absorbance capacity ↓ Ferric reducing ability of plasma Kelley et al. (2006) ; Prior et al. (2007) ; Garrido et al. (2010)
Inflammation	<i>In vivo</i> : Wistar rats	High fructose-diet along with freeze-dried sweet cherry	↓ CRP ↑ IL-10 Dziadek et al. (2019)
	<i>In vivo</i> : Diet-induced obese mice	Diet supplemented with cyanidin-3-glucoside, cyanidin-3-rutinoside and pelargonidin-3-glucoside extracted from sweet cherries	↓ IL-6 ↓ Inducible NO synthase ↓ TNF-α ↓ NF-κB (Wu et al., 2016)
	<i>In vivo</i> : Human subjects	Daily consumption of sweet cherries	↓ CRP ↓ EGF ↓ Endothelin 1 ↓ EN-RAGE ↓ Ferritin ↓ IL-18 ↓ PAI-1 ↑ IL-1 receptor antagonist ↓ Ferritin Kelley et al. (2013)
	<i>In vitro</i> : HeLa cells	Incubation with sweet cherry crude extract	↓ Cell viability Pacífico et al. (2014)
Cell death and proliferation	<i>In vitro</i> : MKN45 cells	Incubation with sweet cherry extract	↓ Cell viability Serra et al. (2011)
	<i>In vivo</i> : MDA-MB453 cells xenograft mice model	Oral administration of sweet cherry whole extract	↓ Tumor growth ↑ Phosphorylated ERK 1/2 ↓ AKT ↓ STAT3 ↓ p38-MAPK ↓ JNK ↓ NF-κB ↓ Ki-67 Noratto et al. (2020)
Invasion and metastization	<i>In vitro</i> : MDA-MB453 cells	Incubation with sweet cherry extract enriched in anthocyanins	↓ Sp1 mRNA levels ↓ Sp4 mRNA levels ↓ VCAM-1 mRNA levels ↓ Sp1 ↓ Migration ↓ PLCγ-1 ↓ VEGF ↓ Cell motility Layosa et al. (2021)
Metabolic reprogramming	<i>In vitro</i> : PNT1A cells	Incubation with sweet cherry extract	↑ Lactate production ↓ GLUT1 ↓ GLUT3 ↓ PFK-1 ↑ LDH activity ↓ MCT4 Silva et al. (2020)
	<i>In vivo</i> : MDA-MB453 cells; xenograft mice mode	Oral administration of sweet cherry extract enriched with anthocyanins	↓ ACAT1 ↓ lipase E, hormone sensitive type Noratto et al. (2020)

4↑ = increase/upregulation; ↓ decrease/downregulation.

prostate cancer when compared to control mice fed with casein ([Shenouda et al., 2007](#)). Likewise, in human *in vivo* studies, *P. africana* bark extracts induced 50% inhibition of the growth of human prostate cancer (PC-3). It also elicited notable apoptosis

in vitro in the PC-3 cell line ([Shenouda et al., 2007](#)). The anticancer property of the *P. africana* stem bark is attributed to several novel bioactive compounds such as β-amyrin, N-butylbenzene-sulfonamide, β-sitosterol, β-sitosterol-3-O-glucoside, ferulic acid,

tartaric acid, oleanolic acid, lauric acid and ursolic acid (Komakech and Kang, 2019). However, *P. africana* is an endangered species and the supply of the *P. africana* stem bark does not meet global demand (Cunningham et al., 2016). A micropropagation protocol has been developed for *P. africana* towards enabling drug development in the future for the treatment of prostate cancer (Komakech et al., 2022). The presence of β -Sitosterol in *P. Africana* has been attributed to its anti-prostate cancer properties wherein it induces apoptosis in human prostate cancer cells during the development of carcinoma in prostate lymph-nodes (von Holtz et al., 1998; Awad et al., 2000). Also, the 2,3-dihydro-3,5-dihydroxy-6-methyl-4H-pyran-one in extracts of *P. africana* is capable of inactivating NF-kB which could account for its proapoptotic and antiproliferative activities on PC-3 cancer cells. Additionally, the occurrence of benzoic acid in these extracts could be responsible for its activity against cancer as earlier studies showed that derivatives of benzoic acid hinder growth of prostate cancer cells thus precluding oncogene expression by the inhibition of histone deacetylases (Anantharaju et al., 2017).

2.11 *Securidaca longipedunculata*

Securidaca longipedunculata Fresen (violet tree) belongs to the family Polygalaceae, which is called the mother of all medicines in Northern Nigeria. Traditional medical practitioners use extracts of *Securidaca longipedunculata* to manage cancer in Africa (Saidu et al., 2015). The antiproliferative effects of *S. longipedunculata* on Ehrlich ascites carcinoma *in vivo* and *in vitro* are due to the downregulation of angiogenesis and the elicitation DNA fragmentation (Lawal et al., 2012). Root bark extracts of *S. longipedunculata* have been reported to repress proliferation and stimulate apoptosis in U87 brain tumor cells through the cleavage of Poly-ADP-Ribose Polymerase (Ngulde et al., 2019). Ethanolic extracts of the plant hindered the proliferation of the U87 cells. The most polar fraction of these extracts accounted for this activity with an IC_{50} value of 20.535 μ g/mL. When administered at 10 mg/kg, the extracts augmented the lifespan of tumor-harboring mice by decreasing tumor cell viability (Ngulde et al., 2019). Several active compounds have been identified in *Securidaca longipedunculata* including xanthenes (muchimangins), methyl-salicylate, benzyl benzoates, bisdesmosidic saponins and triterpene saponins, of which xanthenes have been implicated in antitumor and cytotoxic activities (Mitaine-Offier et al., 2010; Dibwe et al., 2014; Zuo et al., 2016; Obasi et al., 2018; Klein-Júnior et al., 2020). Saponins in *Securidaca longipedunculata* induced apoptosis and inhibited the migration and invasion of cervical cancer cells (Obasi et al., 2018). Xanthenes of in *S. longipedunculata* impeded the proliferation of lung cancer cells and functioned as an elicitor of apoptosis (Zuo et al., 2016).

2.12 *Annona senegalensis*

Annona senegalensis, which is often called wild soursop, is a 2 to 5-m-tall shrub with alternate, oblong, simple, blue to greenish leaves. It is an important plant in Northern Nigeria and all its parts have been found to be useful in medicine. It contains a plethora of

phytochemicals including alkaloids, glycosides, flavonoids, saponins, anthocyanins, tannins, and steroids (Potchoo et al., 2008; Johnson et al., 2017; Musa et al., 2017). Extracts from this plant have been shown to have antitumor activity in hepatocellular carcinoma induced by N-diethylnitrosamine in male Wistar rats. *A. senegalensis* n-hexane extracts have shown anticancer effects by augmenting liver architecture, enhancing antioxidant defense systems, downregulating anti-apoptotic, pro-inflammatory, angiogenic, farnesyl transferase and alpha-fetoprotein mRNA expression and upregulating P21 and P53 tumor suppressor mRNAs (Yakubu et al., 2020).

2.13 *Annona muricata*

Annona muricata is a tropical fruit tree that belongs to the family Annonaceae. This plant is widely cultivated in African countries such as Angola and some West African countries where its products such as fruits are consumed as food. *Annona muricata* is a plant of great applicability in traditional medicine. Ethanol extracts from the leaves of this plant contain several phytochemicals such as alkaloids, tannins, flavonoids, cardiac glycosides, reducing sugars, triterpenoids and saponins (Gavamukulya et al., 2014). Aqueous extracts of the leaves contain terpenoids, alkaloids, coumarin, flavonoids, fatty acids, steroids, phenols, saponins and tannins while ethyl acetate fractions contain saponins, phenols, flavonoids, polyphenols, and tannins (Agu and Okolie, 2017). *Annona muricata* expresses over 45 acetogenins in its leaves and seeds (Gleye et al., 1998). The ethyl acetate fraction of *A. muricata* leaves induced cytotoxic and antiproliferative activity against breast cancer cells by significantly decreasing mitochondrial membrane integrity, leading to the elicitation of apoptosis in the cells (Hadisaputri et al., 2021). This apoptotic mechanism was identified by alterations in cell morphology and the expression levels of caspase-3, caspase-9 and Bcl-2 mRNAs that were involved in the cytotoxic activity induced by the ethyl acetate fractions on MCF-7 cells (Jabir et al., 2021). prepared silver nanoparticles (AgNPs) by using *A. muricata* as a reducing agent and studying its potential as a novel therapeutic strategy against cancer. Specifically, the ability of these nanoparticles to decrease NLRP3 inflammasome activity by inducing autophagy was examined. The AgNPs showed antiproliferative effects against AMJ-13 and THP-1 cells through the stimulation of apoptosis by damaging the mitochondria and inducing the p53 protein pathway (Jabir et al., 2021). This AgNP-elicited autophagy decreased the levels of IL-1 β and NLRP3 inflammasome activation. This study showed that *A. muricata* AgNPs could serve as a robust anticancer agent by inducing apoptosis and autophagy and causing inhibition of tumorigenesis (Eritja et al., 2017; Galluzzi et al., 2017). *Annona muricata* contains two important phytochemicals; acetogenins and flavonoids which have both been implicated in several pharmacological activities (Fang et al., 1993; Yang et al., 2015; Al-Dabbagh et al., 2018). Annonacin, the main acetogenin in *A. muricata*, has anticancer activities against skin, breast and endometrial cancers mediated by cell cycle arrest and the inhibition of other cellular signaling pathways (Yap et al., 2017; Yiallouris et al., 2018; Roduan et al., 2019). There is growing evidence that this antitumor activity is enabled by the induction

of apoptosis in several breast and colon cancer cell lines (Rady et al., 2018). Additionally, the G1 phase cell cycle arrest has been reported to be involved in the antitumor activity of *A. muricata* leaf extracts. Both annonacin and ethyl acetate *A. muricata* bark extracts showed selective and robust cytotoxicity against DU-145 prostate carcinoma cells with respective IC₅₀ values of $0.1 \pm 0.07 \mu\text{M}$ and $55.501 \pm 0.55 \mu\text{g/mL}$. Normal RWPE-1 prostate cells were not affected. The chemotherapeutic agent, docetaxel, was, however, devoid of such selectivity. Moreover, when docetaxel was administered in combination with *A. muricata* ethyl acetate bark extracts, its impact against DU-145 cells was enhanced by 50% (Foster et al., 2020). This was attributed to a non-apoptotic mechanism mediating cell death. Annonacin and bark extracts of *A. muricata* acted as selective cytotoxic compounds with antiangiogenic and antimetastatic potential. Leaf methanolic extracts of *A. muricata* (LMAM) showed inhibitory effects on the growth of MCF-7s (Naik and Sellappan, 2020) in a dose-dependent fashion and without causing cytotoxic effects against normal breast cancer cells. This was achieved through an apoptotic pathway (Pieme et al., 2014). Caspase-3 was found to be upregulated, serving as a determinant of apoptosis. LMAM arrested cell cycle at the G1 phase and blocked the G1/S transition attributed to the activation of apoptosis and sub-G0/G1 cell cycle arrest. LMAM displayed major inhibitory activity against MCF-7 cancer cells with an IC₅₀ value of 85.55 mg/mL.

2.14 *Aerva javanica*

Aerva javanica is a shrub that belongs to the Amaranthaceae family of plants. This plant is native to tropical African countries and has been reported to have anticancer properties in Ethiopia (Ayele, 2018). During its use in the treatment of breast cancer, the roots of *A. javanica* are ground into powder and mixed with blood from bats. This mixture is then consumed by the cancer patient early in the morning before breakfast (Teklehaymanot, 2009). The callus and leaf methanol extracts of *A. javanica* were tested against MCF-7s (Teklehaymanot, 2009; Abate et al., 2022) and were found to induce DNA fragmentation and cytotoxicity, which are indicators of apoptosis.

2.15 *Abelmoschus esculentus*

Abelmoschus esculentus, also known as Okra, is a native African plant of the family Malvaceae. It has been historically been used to treat different ailments such as constipation, hypoglycaemia, inflammation and microbial infections (de Sousa Ferreira Soares et al., 2012). The seeds of *A. esculentus* contain flavonoids such as isoquercitrin which have shown cytotoxicity towards carcinoma cell lines; MCF-7 (breast cancer), HepG2 (liver cancer) and HeLa (cervical cancer) (Agregán et al., 2022). Okra flower extracts, which are rich in flavonoids, are capable of inhibiting cell proliferation in colorectal tumors and this inhibitory activity has been found to be due to the dysfunction of the mitochondria which is caused by the activation of p53 and the elicitation of apoptosis and senescence. In mice models, flavonoids in *A. esculentus* have shown cancer preventative activities which precluded tumor appearance. Okra flower phytochemicals positively impacted liver cancer

prognosis while Okra ethyl acetate extracts showed inhibitory activity against HepG2 cells at concentration ranges between 62.5 and 1,000 $\mu\text{g/mL}$ (Solomon et al., 2016). Therefore, Okra flowers were shown to be a valuable source of anticancer molecules which could augment the health of cancer patients. A novel lectin has been found in Okra seeds and it promotes antitumor effects in MCF-7s wherein it inhibits cell growth. It also enhances p21, caspase-3 and caspase-9 expression in the carcinogenic cells (Monte et al., 2014). Cerium oxide (CeO₂) nanoparticles were generated using *A. esculentus* as a stabilizing and reducing agent. Exposure of HeLa cells to these CeO₂ nanoparticles at 10–125 $\mu\text{g/mL}$ resulted in the loss of cell viability in the cervical cancer cells in a dose-dependent fashion (Ahmed et al., 2021). *Abelmoschus esculentus* has been shown to exhibit anticancer effects due to its high antioxidant activity against free radicals (Arapitsas, 2008; Ahmed and Kumar, 2016). It is a source of polysaccharides, flavonoids, terpenoids, tannins, alkaloids, enzymes, proteins, and vitamins (Musthafa et al., 2021) demonstrated the apoptotic potential of *A. esculentus* lectins against human glioblastoma cells by the modulation of the caspase-3 and caspase-7 gene expression and the downregulation of CLOCK and Bmal1 circadian genes, implicating a correlation between these circadian genes and apoptotic cell death. Increased cytotoxicity, morphological changes, increased intracellular ROS generation and anti-migratory activity were also observed. Due to these effects, *A. esculentus* extracts can be considered as adjunct therapy in alleviating human glioblastoma. Furthermore, pulp extracts of *A. esculentus* were used to synthesize gold nanoparticles which showed enhanced anticancer effects (Devanesan and AlSalhi, 2021). Silver nanoparticles made using *A. esculentus* flower extracts showed antiproliferative, apoptotic and cytotoxic effects against A-549 and TERT-4 cancer cell lines. Quercetin diglucoside and isoquercitrin identified in *A. esculentus* were shown to be potentially anti-ROS and thus could be used in cancer treatment (Taiwo et al., 2021).

2.16 *Flueggea virosa*

Flueggea virosa is widely distributed in Southern Africa. *Flueggea virosa* leaves and twigs were used to isolate flueggeines A 1) and B 2) indolizidine alkaloids, the latter of which showed notable inhibitory activities against the growth of breast cancer cells MDA-MB-231s (estrogen-independent) and MCF-7s (estrogen-dependent) with IC₅₀ values of 147 ± 3 and $135 \pm 5 \text{ nM}$ respectively. This suggested that cell proliferation was inhibited irrespective of estrogen receptor status (Zhao et al., 2011).

2.17 *Lagenaria siceraria*

Lagenaria siceraria is a native African climbing plant that belongs to the Cucurbitaceae family (Abebe, 2016). (Mondal and Swamy, 2020) identified BGL24, a novel PP2-type lectin in the phloem exudate of this plant, which is also called Bottle gourd. This lectin displayed high specificity for chito-oligosaccharides. BGL24 showed moderate cytotoxicity towards MDA-MB-231 breast cancer cells but did not impact normal splenocytes.

The latex sap of *L. siceraria* (LSL) markedly elicited lymphocyte proliferation and demonstrated potent cytotoxicity against cancer both *in vivo* and *in vitro* (Vigneshwaran et al., 2016). LSL caused tumor regression and drastically impacted tumoral neovasculature. Additionally, LSL stimulated the apoptotic signaling cascade in tumor cells through the activation of caspase-3 and the induction of apoptotic cellular events. Therefore, LSL possesses immunopotentiating properties which negatively impact tumor progression by attacking angiogenesis and inducing programmed cell death, which are major hallmarks of cancer. Bottle gourd juice (BGJ) was examined for its chemopreventive properties against croton oil and 7,12-dimethylbenz(a)anthracene (DMBA) and was found to elicit skin papillomagenesis in murine models (Kumar et al., 2013). BGJ caused drastic reductions in the incidence, latency, number, multiplicity, size, and volume of the papillomas. This chemopreventive effect was mediated by reducing loss of stratification, decreasing the number of epithelial layers, diminishing dermal infiltration and protection from several cytoplasmic changes. Therefore, BGJ consumption could help in the inhibition of skin cancer.

2.18 *Xylopia aethiopica*

Cytotoxic metabolites have been identified in methanol extracts of *X. aethiopica* and were found to inhibit the growth of multidrug resistant and drug-sensitive cancer cell lines (Kuede et al., 2015). Among these metabolites, flavone elicited apoptosis in CCRF-CEM leukemia cells through the disruption of the mitochondrial membrane potential and isoquinoline triggered apoptosis *via* the production of ROS, implicating these compounds as antiproliferative agents against drug-resistant cancers. Essential oils obtained from *Xylopia aethiopica* sourced from Cameroon and Chad were found to be abundant in monoterpene hydrocarbons such as β -phellandrene, β -pinene, γ -terpinene and sabinene. Oxygenated monoterpenes were highly prevalent, amongst which terpinen-4-ol was most significant (Bakarnga-Via et al., 2014). Hydroethanolic extracts of *X. aethiopica* showed antiproliferative activity against HCT116 colon cancer cells as well as KG1a and U937 leukemia cell lines. *Xylopia ethiopica* extracts also demonstrated antiproliferative effects on human cervical cancer cells. Furthermore, α -cadinol and terpinen-4-ol in essential oils isolated from *X. ethiopica* were found to be active against laryngeal, lung, ovarian, breast, gastric and colon cancer cell lines (Bakarnga-Via et al., 2014). Additionally, β -pinene, a monoterpene found in this oil, showed notable cytotoxic activity against epidermal skin and breast cancer cell lines. Fruit extracts of *X. aethiopica* caused the activation of caspase-3 and led to the cleavage of cytoskeletal proteins and the elicitation of DNA fragmentation factors, condensation of chromatin, formation of apoptotic bodies and eventually apoptosis as observed through morphological analysis (Fulda and Debatin, 2006; Ribeiro et al., 2021). (Adaramoye et al., 2011) showed that fruit extracts of *X. aethiopica* caused antiproliferative activity against human cervical carcinoma cells causing cell cycle arrest and elevated levels of p53 and p21 gene transcripts. Caspase-3 activation and apoptotic cell death have been demonstrated in MBA-MD-231 breast cancer cells upon exposure to hydroethanol extracts sourced from the

Cameroonian varieties of *X. aethiopica* fruits (Choumessi et al., 2012).

2.19 *Nymphaea lotus*

Nymphaea lotus belongs to the family Nymphaeaceae and is a perennial aquatic flowering plant that is native to Egypt and grown in several regions in Madagascar, West Africa, and Central Africa (Slocum, 2005). Hydroethanolic leaf extracts of *N. lotus* contain saponins, tannins, flavonoids, phenolics and triterpenoids but are lacking in alkaloids. These extracts have been shown to have anti-inflammatory and cytotoxic activities along with high antioxidant potential against Jurkat and MCF-7s, properties that are attributed to the occurrence of abundant flavonoids and phenolics as well as micro/macro-elements such as sulfur, phosphorus, manganese, magnesium, zinc and copper (Saleem et al., 2001; Elegami et al., 2003; Laszczyk, 2009; Afolayan et al., 2013; Oyeyemi et al., 2015; N'guessan et al., 2021). These properties may account for the use of the leaves of *Nymphaea lotus* in traditional anticancer treatments.

2.20 *Zanthoxylum chalybeum*

Zanthoxylum chalybeum is a deciduous shrub with a rounded but open crown. It can grow between 1.5 and 40 cm in diameter, with large woody spines that can grow up to 2 cm long. It is a widely used traditional medicine in East Africa and can be harvested from the wild for local use as tea, medicine, toothbrush, and timber. *Zanthoxylum chalybeum* is reported to exhibit anti-cervical cancer properties, where part of the plant used is pound before adding water to drink (Tugume et al., 2016; Omara et al., 2020). Significant antiproliferative effects of crude extracts of alkaloids from *Zanthoxylum* species were observed against human cervical cancer cells (HeLa), human gastric cancer cells (SGC-7901), human hepatocyte carcinoma cells (Hep G2) and human colorectal adenocarcinoma cells (HT29), ranging from 60.71% to 93.63% at 200 μ g/mL concentration (Tian et al., 2017). *Zanthoxylum* contains quaternary alkaloids which have been shown to be potential anti-cancer candidates that can penetrate through the cell membranes of carcinomas (Yung et al., 2016) and can attract the negative charges on DNA (Bai et al., 2006). Based on their structural skeleton, these quaternary alkaloids have been shown to belong to the berberine type, tetrahydroberberine type, benzophenanthridine type, benzyltetrahydroisoquinoline type and aporphine type (Tian et al., 2017). In *Z. chalybeum*, the amount of quaternary alkaloids account for 83.4%. Bioactivity tests on *Zanthoxylum* showed both high inhibitory rates against cancer cells and high quaternary alkaloid content, therefore justifying its use in traditional anticancer medications. The active ingredients responsible for the anticancer activity of this plant include skimmianine, furoquinoline, benzophenanthridine, alkaloids, chelerythrine and nitidine, aporphine alkaloids, tembetarine, N-methylisocorydine, N-methylisocorydine (menisperine) and berberine, phenylethylamine, candicine, alkamide, fagaramide, dihydrochelerythrine, lupeol and sesamin (Omara et al., 2020).

2.21 *Ceratonia siliqua*

Ceratonia siliqua is a Mediterranean evergreen plant that is abundantly distributed in North African countries such as Algeria, Morocco, Tunisia, and Egypt (Kaderi et al., 2015). Common ethnomedicinal uses of *Ceratonia siliqua* include treatment of gastrointestinal diseases, diarrhea, constipation and colon cancer (Benarba and Pandiella, 2018). These medicinal properties may chiefly be due to the presence of fibers and phenolic compounds (Rtibi et al., 2017). (Ghanemi et al., 2017) demonstrated that *C. siliqua* leaf phenolic extracts inhibited the growth of HTC-116 and CT-26 cell lines, in a dose dependent manner, confirming earlier similar findings by (Custódio et al., 2013).

2.22 *Moringa oleifera*

Moringa oleifera, a member of the Moringaceae family, is a drumstick tree which was first used medically by the ancient Egyptians before its cultivation around the globe which spread its medicinal benefits (Abd-Rabou et al., 2017). *Moringa oleifera* was found to be effective in treating colon cancer (Al-Asmari et al., 2015). The plant owes its anticancer properties to the presence of quercetin, kaempferol, β -D-glucopyranoside, tetracanoate, β -sitosterol glucoside, isothiocyanate (Kaur, 2015), hexadecenoic acid and eugenol (Al-Asmari et al., 2015). (Suphachai, 2014) reported the growth inhibition of hepatocarcinoma (HepG2), colorectal adenocarcinoma (Caco-2), and breast adenocarcinoma (MCF-7) cell lines by dichloromethane leaf extracts of *Moringa oleifera* with IC₅₀ values between 112 and 113 μ g/mL. Recently, *in vitro* and *in vivo* anticancer activities of *M. oleifera* have been reported. In their study (Barhoi et al., 2021), identified quinic acid, octadecanoic acid and hexadecanoic acid (palmitic acid) as the active compounds during the activity of aqueous extracts of *M. oleifera* on Ehrlich ascites carcinoma (EAC) and Hep2 (Human laryngeal carcinoma) cells. They reported that, *in vivo*, aqueous extracts of *M. oleifera* led to a reduction in tumor weight and tumor volume in tumor bearing mice, consequently elongating the life span of the mice. Additionally, *in vitro*, the extracts of *M. oleifera* were toxic to both Hep2 and EAC cancer cell lines. Apoptosis was also induced through the alteration of the mitochondrial membrane potential in the EAC cells (Barhoi et al., 2021).

It has also been recently shown that methanolic extracts of *M. oleifera* leaves led to a reduction in cell growth in cervical cancer cells (Pandey and Khan, 2021). The cervical cancer cells were reported to have undergone apoptosis. The anticancer potential of the *M. oleifera* leaf extracts was due to the inhibitory activity of the extracts on Jab-1, which is an important biomarker associated with the development of different cancers (Pandey and Khan, 2021). The inhibition of *M. oleifera* on Jab-1 led to its downregulation. There was also an increase in the expression of the tumor suppressor p27, which led to cell growth arrest at the G0/G1 phase.

Methanol extracts of *M. oleifera* leaves have also been reported to have apoptotic effects on PC-3 prostate cancer cells (Khan et al., 2020). The anticancer activity of *M. oleifera* leaf methanolic extracts was due to the induction of ROS-mediated apoptosis and the activation of caspase-3 activity in the prostate cancer cells. Cell

cycle arrest at the G0/G1 phase and changes in the expression of genes of the Hedgehog signalling pathway were also observed (Khan et al., 2020).

Moringa oleifera leaf extracts have been shown to have anticancer activity on the human squamous cell carcinoma 15 cell line (SCC15). In their study (Luetragoon et al., 2020), reported that the proliferation of SCC15 cells treated with *M. oleifera* leaf extracts was inhibited. The extracts were shown to induce cell cycle arrest at the G2/M phase and apoptosis in the cells. Cell migration and colony formation were also inhibited in the cells. Furthermore, there was a downregulation of the anti-apoptotic marker Bcl-2 and an upregulation of both Bax and caspase-3 (Luetragoon et al., 2020).

Through the activity of its bioactive compound 4-[(α -L-Rhamnosyloxy) benzyl] isothiocyanate (MIC-1), which is found in the seeds, *M. oleifera* has been reported to inhibit the migration and proliferation of renal cancer cells (Xie et al., 2022). This regulatory activity is said to be brought about by the regulation of the PTP1B-dependent Src/Ras/Raf/ERK signalling pathway in 786-O hypertriploid renal cell carcinoma (RCC) cancer cells. MCI-1 from *M. oleifera* seeds also induced cell cycle arrest and caused the downregulation of the expression of cell cycle-related proteins in the 786-O cells (Xie et al., 2022).

2.23 *Peganum harmala*

Peganum harmala is a perennial herbaceous plant with a woody underground root stalk. It is a member of the Nitriaceae family and mostly grows in temperate deserts and Mediterranean regions (Alves-Silva et al., 2017). reported the ethnomedicinal uses of *P. harmala* as a remedy for the treatment of breast, liver, and bone cancer. It is also considered as a treatment for other different types of cancer (Kabbaj et al., 2012). *Peganum harmala* seeds from Morocco are ground with honey during cancer treatment. Despite the ethnomedicinal uses of *P. harmala*, the plant is also toxic and may cause hallucinogenic effects because of the presence of β -carboline such as harmaline, harmine, harmalol, harmol, tetrahydroharmine, and the quinazoline derivatives vasicinone and deoxyvasicinone (Passos and Mironidou-Tzouveleki, 2016). Table 3 gives a summary of some of the *in vivo* and *in vitro* studies that has been carried out on plants that have been discussed in the manuscript as well as the identified bioactive compounds in these plants and the effects of these compounds on cancer progression.

3 Semi-synthetic studies for new drugs derived from natural compounds for optimizing anticancer activity

Over 25% of drugs used for combating human diseases are directly sourced from plants and another 25% are chemically modified natural products (Amin et al., 2009). Polyphenols constitute a plethora of naturally occurring compounds found in vegetables and fruits. Their health-enhancing characteristics and their application in the prophylaxis and therapy of many human cancers are well known. Several anti-cancer drugs are altered forms

TABLE 3 A summary of pharmacological information of all the medicinal plants that have been discussed in the manuscript.

Plant species	Bioactive compounds	Cell line/Experiment	Effects	References
<i>Dicoma anomala</i>	Acetylenic compounds, flavonoids, phenolic acids, phytosterols, sesquiterpenes and triterpenes	MCF-7 breast cancer cells	Reduction of proliferation, oxidative damage of the cells	Shafiq et al. (2020)
<i>Fagaropsis angolensis</i>	Alkaloids, glycosides, phenols, tannins, steroids, and flavonoids	Hep2 throat cancer cells, CT 26-CL 25 colon cancer cells	Antiproliferation of cell lines, induction of programmed cell death by apoptotic pathways	Yiaile (2017)
<i>Tribulus terrestris</i>	Saponin compounds such as nautigenin saponin	TW2.6 and SAS oral cancer cells	Inhibition of autophagy, inhibition of cell growth and proliferation, invasion of neoplastic cancer cells	Shu et al. (2021)
<i>Portulaca oleracea</i>	POL-P3b, Glycosides such as oleraciamide E and oleraciamide F	Mice models	High level induction of TNF- α , IFN- γ and IL-12, tumor growth inhibition, induction of apoptosis	Jia et al. (2021)
<i>Withania somnifera</i>	Withaferin A and Withanolide D	B16F-10 melanoma cells in C57BL/6 mice	Significant inhibition of tumor activity	Leyon and Kuttan (2004)
<i>Azanza garckeana</i>	Mansone G, β -Cyclodextrin	A549 lung cancer cells	High toxicity towards the cells	Bioltif et al. (2020)
<i>Cajanus cajan</i>	Stilbenes longistylin A and C, β -sitosterol, pinostrobin	COR-L23 lung cancer cells	Cytotoxicity towards the cells, cell growth arrest	Ashidi et al. (2010)
<i>Combretum caffrum</i>	Combrestatins such as combrestatin A-4 (CA-4)	Leukemia cell line, P-388	Disruption cell signaling pathways, selective disruption of blood flow through tumors	McGown and Fox (1990)
<i>Prunus avium</i>	Phenolics, anthocyanins	Wistar rats	Inhibition of lipid peroxidation, decrease in catalase	Dziadek et al. (2019)
<i>Prunus africana</i>	Alkaloids, glycosides, phenols, tannins, steroids, and flavonoids	Hep2 throat cancer cells, CT 26-CL-25 colon cancer cells	Antiproliferative effect against the cells	Yiaile (2017)
<i>Securidaca longipedunculata</i>	Benzyl benzoates, bisdesmosidic saponins and triterpene saponins	U87 brain tumor cells	Inhibition of proliferation, induction of apoptosis	Ngulde et al. (2019)
<i>Annona senegalensis</i>	Alkaloids, glycosides, flavonoids, saponins, anthocyanins, tannins, and steroids	Male Wistar rats	Augmentation of liver architecture, upregulation of p21 and p53	Yakubu et al. (2020)
<i>Annona muricata</i>	Terpenoids, alkaloids, coumarin, flavonoids, fatty acids, steroids	MCF-7 breast cancer cells	Morphology alterations, induction of apoptosis	Jabir et al. (2021)
<i>Aerva javanica</i>	Phenolics, flavonoids, lignins, terpenes, glycosides, and alkaloids	MCF-7 breast cancer cells	Antiproliferation, apoptosis induction through DNA fragmentation and cytotoxicity towards the cells	Abate et al. (2022)
<i>Abelmoschus esculentus</i>	Flavonoids such as isoquercitrin	HepG2 liver cancer cells	Cytotoxicity towards the cells	Agregán et al. (2022)
<i>Flueggea virosa</i>	Flueggines A 1) and B 2) indolizidine alkaloids	MDA-MB-231 breast cancer cells	Growth inhibition of the cells, inhibition of proliferation	Zhao et al. (2011)
<i>Lagenaria siceraria</i>	PP2-type lectin BGL24	MDA-MB-231 breast cancer cells	Moderate toxicity towards the cells	Mondal and Swamy (2020)
<i>Xylopi aethiopica</i>	Flavonoids, alkaloids	CCRF-CEM leukemia cells	Induction of apoptosis, disruption of the mitochondrial membrane potential, production of ROS	Kuete et al. (2015)
<i>Nymphaea lotus</i>	Saponins, tannins, flavonoids, phenolics and triterpenoids	MCF-7 breast cancer cells	Anti-inflammation, cytotoxicity, high oxidant activity	N'guessan et al. (2021)
<i>Zanthoxylum chalybeum</i>	Alkaloids, furoquinoline, benzophenanthridine, alkaloids, chelerythrine and nitidine, aporphine alkaloids, tembetarine, N-methylisocorydine	HeLa cervical cancer cells	Antiproliferative effects on the cells	Omara et al. (2020)
<i>Ceratonia siliqua</i>	Phenolic compounds	HTC-116 and CT-26 colon cancer cell lines	Growth inhibition	Ghanemi et al. (2017)
<i>Moringa oleifera</i>	Quercetin, kaempferol, β -D-glucopyranoside, tetracanoate, β -sitosterol glucoside, isothiocyanate	MDA-MB-231 breast cancer cells and HCT-8 ileocecal cancer cells	Reduction in cell survival, reduction in colony formation, increase in apoptosis	Al-Asmari et al. (2015)
<i>Peganum harmala</i>	Phenols, tannins, flavonoids and anthocyanins	RT112 human bladder carcinoma cells	Antioxidant activity	Al-Asmari et al. (2015)

of these natural compounds. Etoposide (VP-16, epipodophyllotoxin) is an anticancer drug derived semi-synthetically from a non-alkaloid lignan, podophyllotoxin sourced from the rhizomes and dried roots of *Podophyllum emodi* or *Podophyllum peltatum* (Kluska and Woźniak, 2021). Etoposide has been widely employed in cancer chemotherapy to combat various types of cancer such as adrenocortical carcinoma (Paragliola et al., 2020), brain tumors (Ruggiero et al., 2020), breast cancer (Atienza et al., 1995), leukemia (Economides et al., 2019), testicular carcinoma (Alsdorf et al., 2019) and small cell lung carcinoma (Noronha et al., 2020).

Polyphenols enhance the therapeutic action of etoposide by augmenting its cytotoxicity in various cancer cell lines like the retinoblastoma (Sreenivasan and Krishnakumar, 2015), glioblastoma (Ramachandran et al., 2012), breast cancer (Ermakova et al., 2006), cervical cancer (Ruíz et al., 2018), liver cancer (Jia et al., 2016), gastric cancer (Yu et al., 2011; Jia et al., 2016), osteosarcoma (Ferreira de Oliveira et al., 2018), lymphoma (Noda et al., 2007; Li et al., 2008), colon cancer (HWANG et al., 2007; Amiri et al., 2013), head and neck cancer (Heiduschka et al., 2014) and leukemia (Mahbub et al., 2015; Papież et al., 2016). This effect of polyphenols is caused by an increase in DNA damage and apoptosis, production of ROS and arrest of the cell cycle. Investigations on the human breast cancer cell line, MDAMB-231 revealed that flavonoids such as cyanidin, fisetin, (–)-catechin, kaempferol, naringenin, genistein and quercetin, blocked the DNA damage checkpoints and the respective repair pathways. These polyphenols inhibited Chk1 Ser345 phosphorylation induced by etoposide, and this led to the abrogation of the ATR-Chk1 pathway (Kuo et al., 2016). Hence, polyphenols can enhance the therapeutic action of etoposide chemotherapy by rendering the cancer cells more drug sensitive (Fiorito et al., 2014). synthesized a select group of natural and semi-synthetic 1,4-Naphthoquinones whose activity in inhibiting cell growth was studied *in vitro* on six human cancer cell lines. Among these compounds, only lapachol and its acetate as well as 3-geranyllawsone showed the highest activity with 15–22 μ M IC₅₀ values. Several novel anticancer drugs currently under commercial production are derived from natural plant sources and these include etoposide, irinotecan, topotecan, taxotere, taxol, teniposide, vinorelbine, vincristine and vinblastine (Wang, 1998). Thus, natural products serve as the most important source of novel anticancer agents.

Therefore, 1,4-Naphthoquinones constitute a major category of natural products found in plants. Plumbagin (obtained from *Plumbago*, *Nepenthes Drosera* spp.), juglone (sourced from the black walnut, *Juglans nigra* L. (Juglandaceae), and the K vitamins are significant examples of these 1,4-Naphthoquinones. The action mechanisms underlying these observed effects are primarily due to their ability to react with topoisomerases and to produce semiquinone radicals as well as ROS inside the cell (da Silva et al., 2002). (Kode et al., 2020) synthesized Compound 9a containing 1-methyl, 2- and 3-methoxy substituents within the aromatic ring of phenstatin based indole linked chalcone compounds. This was found to be effective against the SCC-29B human oral cancer cell line, spheroids as well as AW13516, an oral cancer mouse xenograft model. Compound 9a anticancer activity was found to be effected by the disruption of glucose metabolism and cellular integrity wherein the latter was caused by repression of

tubulin polymerization. Compound 9a was found to directly interact with tubulin at the colchicine binding site in addition to interacting with the active sites of key enzymes involved in the pathway of glucose metabolism (Kode et al., 2020). Thus, compound 9a has found great applicability as a favorable tubulin polymerization inhibitor candidate in anti-cancer therapeutics. Compound 9a greatly reduced the tumor volume while not causing any toxicity in murine models. Additionally, it decreased angiogenesis in xenografts of mice, diminished collagen levels and significantly reduced cellular processes including cellular integrity and organization of the cytoskeleton, while disrupting the uptake of glucose in tumor xenografts. The tubulin polymerization was inhibited which led to profilament bending, destabilization and formation of tubulin ring intermediates.

Lupeol (LU) and Oleanolic acid (OA) are members of the class of natural triterpenes and possess wide-ranging biological activities and cytotoxicity against many cancer cell lines. From these two compounds, 6 novel semi-synthetic triterpenes were synthesized and studied for their pharmacological action (Fontana et al., 2022). Compared to its precursor, Lupeol, the lupane-like compounds showed enhanced activity whereas the oleanane-like compounds exhibited more complex properties. Both LU and OA derivatives displayed a pattern of interaction with the NF- κ B p65 subunit that justified the similarity in their capability to hinder the p65 binding to DNA. Also, some of the tested derivatives could augment I κ B- α levels precluding the NF- κ B translocation to the nucleus. This study revealed the pharmacological activity of triterpenes towards leukemia cells, making them valuable anticancer drug candidates.

The different OA and LU derivatives were investigated for their cytotoxic effects against acute myeloid leukemia cancer cell line HL60 as well as its multidrug-resistant (MDR) variant HL60R wherein the latter displayed multidrug resistance, P-gp overexpression, constitutive expression of the NF- κ B transcription factor, inhibition of proteins associated with apoptosis and poor prognosis (Fontana et al., 2022). These derivatives showed more activity than the original compounds and displayed equivalent cytotoxic effects against both HL60 and HL60R cell lines. Also, these compounds remarkably disrupted the NF- κ B pathway both downstream and upstream to NF- κ B activation within the MDR cell line.

All these compounds were able to hinder transcription factor transactivation in the HL60R cell line. Both LU and OA derivatives displayed similar patterns of interaction with the NF- κ B p65 unit, that justified the similarity in their potential to inhibit the interaction of p65 to DNA as well as some of its molecular targets. The capability of many of the derivatives to augment I κ B- α levels precludes the transcription factor from movement to the nucleus, thus accounting for the indirect effect of NF- κ B inhibition. This investigation showed that pre-treatment with OA and LU derivatives could potentiate increased sensitivity of the cancer cells to standard drugs used in chemotherapy, thereby representing novel therapeutic approaches to combat acute myeloid leukemia.

Terpenoids are the largest class of natural compounds and are known for their anticancer activity. (Hussain et al., 2018), explored the anticancer effects of a novel semi-synthetic terpenoid, 16-oxo-cleroda-3,13 (14)E-diene-15-oic acid 1), derived from cleroda diterpene isolated from *Polyalthia longifolia* var. *pendula* against neuroblastoma (Faizi et al., 2008). The γ -amino γ -lactone (PGEA-

AN, 2) of one was chosen for further study as it displayed the highest cytotoxic activity upon initial screening.

PGEA-AN was shown to modulate the p53 system resulting in death of the neuroblastoma cells while not affecting the renal system making it a promising candidate for anticancer activity against neuroblastoma. Further, PGEA-AN augments mitochondrial membrane permeability (MMP). Induction of P53 in neuroblastomas is common observation associated with chemotherapeutic agents (Nikolaev et al., 2003; Lontas and Yeger, 2004). Notwithstanding the mode of cell death, p53 has been implicated in the mitochondrial pathway leading to cell death resulting from apoptosis or necrosis (Cui et al., 2002; Vaseva et al., 2012). The p53 gene directly upregulates BAX, a proapoptotic gene (Toshiyuki and Reed, 1995). BAX overexpression leads to augmentation of apoptosis mediated by multiple factors (Kobayashi et al., 2000). Activation of BAX results in its translocation into mitochondria which in turn increases MMP (Youle and Strasser, 2008), causing reduction or loss of mitochondrial transmembrane potential, pores in the mitochondrial membrane and promotes necrotic or apoptotic cell death (Tsujimoto and Shimizu, 2007).

Peganum harmala L is a medicinal plant of great importance due to its plenitude of alkaloid content rich in β -carbolines (Daoud et al., 2014). report the anticancer activity of a semi-synthetic derivative, B-nine to three formed from two harmane molecules that are bound by a butyl group. This compound showed strong potency and anti-proliferative effects against a human colorectal carcinoma cell line, a human breast cancer cell line and a human lung cancer cell line. A dose-dependent elicitation of apoptosis or necroptosis was observed against all these cell lines in addition to repression of cancer cell migration. Also, B-nine to three exhibited anti-angiogenic effects *in vitro* as observed by the drug-mediated inhibition of tube formation within the human umbilical vascular endothelial cell line (HUVEC).

As per epidemiological findings, chronic inflammation has been implicated in 25% of cancer cases. Hence, blockage of carcinogenesis induced by inflammation could be a viable therapeutic approach for the chemoprevention of cancer. Moreover, anti-inflammatory drugs have been shown to decrease the incidence of cancer. Saponins are natural compounds having tumor inhibitory properties. The triterpenoid derivative of oleanolic acid, 2-cyano-3, 12-dioxooleana-1, 9 (11)-dien-28-oate (CDDO) inhibited NF κ B signaling and displayed antitumoral and anti-inflammatory activities, authenticating its therapeutic potential (Place et al., 2003; Shishodia et al., 2006). This effect was also substantiated in murine models of prostate cancer (Gao et al., 2011).

Semi-synthetic analogs of cycloartane-type saponins (9,19-cyclolanostanes) were prepared (Debeleç-Bütüner et al., 2018) and five of these analogs were investigated for their anticancer activity. Of these, astragenol derivatives 1 and 2, and the cycloastragenol derivatives 3, 4, and 5 showed strong inhibition of NF κ B signaling resulting in the blockage of NF κ B transcriptional activation and suppression of cell proliferation. Therefore, these semi-synthetic compounds displayed strong potential for chemoprevention of prostate cancer driven by the inflammatory NF κ B signaling pathway.

4 Conclusion

Several synthetic drugs have been used to treat cancer but cause long term effects. This review provides an update on advances in the use of secondary metabolites from different African medicinal plants with anticancer potential on different biological models including human cell lines, animals, and human models. Most of the studies that we assessed employed *in vitro* assays with some *in vivo* assays. We report some plants that have contributed to cancer management in Africa, where the anticancer extracts are usually prepared from bark, fruits, leaves, roots, and stems. *In vitro* and *in vivo* studies mentioned in this review have shown that bioactive compounds and metabolites from African medicinal plants use a variety of mechanisms during cancer management. Carrying out *in vitro* studies on anticancer plants is a very important initial step in pharmacological testing. Testing plant phytochemicals on cancer cell lines allow scientists to gauge the anticancer potential of these phytochemicals in a safe and controlled environment of the lab. *In vitro* studies also allow testing of different combinations of phytochemicals on cancer cells to determine any synergistic advantages. Once the effects of the phytochemicals on cancer cells are determined, the phytochemicals are then tested *in vivo* using model organisms such as mice and rats. After the efficacy of the phytochemicals is confirmed *in vivo*, pre-clinical studies are then undertaken to test the phytochemicals on a small population of clinical candidates. If successful, and after approval by appropriate regulatory bodies, the phytochemicals, in drug form, can then be clinically applied in cancer management. Therefore, *in vitro*, and *in vivo* studies of potential anticancer phytochemicals from plants play a crucial role in the ultimate clinical application and commercialization of phytochemicals of these plants, providing alternative cancer management strategies to mankind. However, there is insufficient research on other African medicinal plants for potential use in cancer management. Therefore, there is a need to isolate and evaluate the anticancer potential of the bioactive compounds in the understudied medicinal plants of Africa and elucidate their mechanisms of anticancer activity. Furthermore, more research on animal models is required as it can lead to more clinical studies. Despite the anticancer potential of the reviewed African medicinal plants, there is insufficient data on *in vivo* studies and targets of cancer. *In vivo* studies are crucial for pre-clinical studies and ultimate drug development. Furthermore, toxicological evidence is insufficient in some of the mentioned studies. In some populations, some medicinal plants may be allergenic or harmful, while in other cases, specific plant parts may either be edible or poisonous. Therefore, toxicology investigations are necessary for the determination of adverse effects of some of the plant extracts. They are also important in the establishment of limits of exposure levels.

Many genes, proteins and signaling pathways play important roles in cancer development, progression, and alleviation. Based on the findings of this manuscript, the following genes and pathways should be investigated for preclinical studies as they are significant to cancer biology; the tumour suppressors p21 and p53 as well as the following pathways: NF- κ B, AKT, PI3K, p38-MAPK pathways. In summation, the take home message of this review is that African plants have been shown to have potential anticancer activity. It is important that *in vitro* studies mentioned in this review are advanced to *in vivo* investigations and the *in vivo* studies are elevated to pre-clinical studies. This review has collated

information that may be critical in guiding researchers interested in exploring native African plants for use in cancer management. Figure 2 summarize the different pathways on which different plants their compounds and extracts.

Author contributions

Conceptualization, GG, KM, and AM; methodology, GG, KM, and AM; writing—original draft preparation, GG, SV, PB, KM, TK, and AM; writing—review and editing, GG, SV, PB, KM, TK, DN, GR, and AM. All authors have read and agreed to the published version of the manuscript.

Acknowledgments

We would like to acknowledge the Botswana International University of Science and Technology (BIUST) and the

University of Toronto for providing the resources to complete this manuscript.

Conflict of interest

The authors declare that the research was conducted in the absence of any commercial or financial relationships that could be construed as a potential conflict of interest.

Publisher's note

All claims expressed in this article are solely those of the authors and do not necessarily represent those of their affiliated organizations, or those of the publisher, the editors and the reviewers. Any product that may be evaluated in this article, or claim that may be made by its manufacturer, is not guaranteed or endorsed by the publisher.

References

- Abate, L., Tadesse, M. G., Bachheti, A., and Bachheti, R. K. (2022). Traditional and phytochemical bases of herbs, shrubs, climbers, and trees from Ethiopia for their anticancer response. *BioMed Res. Int.* 2022, 1589877. doi:10.1155/2022/1589877
- Abbas, M. W., Hussain, M., Akhtar, S., Ismail, T., Qamar, M., Shafiq, Z., et al. (2022). Bioactive compounds, antioxidant, anti-inflammatory, anti-cancer, and toxicity assessment of *Tribulus terrestris*—*in vitro* and *in vivo* studies. *Antioxidants* 11, 1160. doi:10.3390/antiox11061160
- Abd-Rabou, A. A., Abdalla, A. M., Ali, N. A., and Zoheir, K. M. (2017). Moringa oleifera root induces cancer apoptosis more effectively than leave nanocomposites and its free counterpart. *Asian Pac. J. cancer Prev. APJCP* 18, 2141–2149. doi:10.22034/APJCP.2017.18.8.2141
- Abebe, W. (2016). An overview of Ethiopian traditional medicinal plants used for cancer treatment. *Eur. J. Med. Plants* 14, 1–16. doi:10.9734/ejmp/2016/25670
- Abutaha, N. (2015). *In vitro* antiproliferative activity of partially purified Withania somnifera fruit extract on different cancer cell lines. *J. Balk. Union Oncol.* 20, 625–630.
- Acero, N., Gradillas, A., Beltran, M., García, A., and Mingarro, D. M. (2019). Comparison of phenolic compounds profile and antioxidant properties of different sweet cherry (*Prunus avium* L.) varieties. *Food Chem.* 279, 260–271. doi:10.1016/j.foodchem.2018.12.008
- Adaramoye, O. A., Sarkar, J., Singh, N., Meena, S., Changkija, B., Yadav, P. P., et al. (2011). Antiproliferative action of *Xylopia aethiopica* fruit extract on human cervical cancer cells. *Phytotherapy Res.* 25, 1558–1563. doi:10.1002/ptr.3551
- Adeloye, D., David, R. A., Aderemi, A. V., Iseolorunkanmi, A., Oyedokun, A., Iweala, E. E., et al. (2016). An estimate of the incidence of prostate cancer in Africa: A systematic review and meta-analysis. *PloS one* 11, e0153496. doi:10.1371/journal.pone.0153496
- Afolayan, A. J., Sharaibi, O. J., and Kazeem, M. I. (2013). Phytochemical analysis and *in vitro* antioxidant activity of *Nymphaea lotus* L. *Int. J. Pharmacol.* 9, 297–304. doi:10.3923/ijp.2013.297.304
- Aggregán, R., Pateiro, M., Bohrer, B. M., Shariati, M. A., Nawaz, A., Gohari, G., et al. (2022). Biological activity and development of functional foods fortified with okra (*Abelmoschus esculentus*). *Crit. Rev. Food Sci. Nutr.* 1–16. doi:10.1080/10408398.2022.2026874
- Agu, K. C., and Okolie, P. N. (2017). Proximate composition, phytochemical analysis, and *in vitro* antioxidant potentials of extracts of *Annona muricata* (Soursop). *Food Sci. Nutr.* 5, 1029–1036. doi:10.1002/fsn3.498
- Ahmad, R., Fatima, A., Srivastava, A., and Khan, M. A. (2017). Evaluation of apoptotic activity of *Withania coagulans* methanolic extract against human breast cancer and Vero cell lines. *J. Ayurveda Integr. Med.* 8, 177–183. doi:10.1016/j.jaim.2017.01.001
- Ahmed, B. T., and Kumar, S. A. (2016). Antioxidant and Antidiabetic properties of *Abelmoschus esculentus* extract—an *in vitro* assay. *Res. J. Biotechnol.* 11, 34–41.
- Ahmed, H. E., Iqbal, Y., Aziz, M. H., Atif, M., Batool, Z., Hanif, A., et al. (2021). Green synthesis of CeO₂ nanoparticles from the *Abelmoschus esculentus* extract: Evaluation of antioxidant, anticancer, antibacterial, and wound-healing activities. *Molecules* 26, 4659. doi:10.3390/molecules26154659
- Al-Asmari, A. K., Albalawi, S. M., Athar, M. T., Khan, A. Q., Al-Shahrani, H., and Islam, M. (2015). Moringa oleifera as an anti-cancer agent against breast and colorectal cancer cell lines. *PloS one* 10, e0135814. doi:10.1371/journal.pone.0135814
- Al-Dabbagh, B., Elhaty, I. A., Al Hrouf, A., Al Sakka, R., El-Awady, R., Ashraf, S. S., et al. (2018). Antioxidant and anticancer activities of *Trigonella foenum-graecum*, *Cassia acutifolia* and *Rhazya stricta*. *BMC complementary Altern. Med.* 18, 240–312. doi:10.1186/s12906-018-2285-7
- Alsdorf, W., Seidel, C., Bokemeyer, C., and Oing, C. (2019). Current pharmacotherapy for testicular germ cell cancer. *Expert Opin. Pharmacother.* 20, 837–850. doi:10.1080/14656566.2019.1583745
- Alves-Silva, J. M., Romane, A., Efferth, T., and Salgueiro, L. (2017). North African medicinal plants traditionally used in cancer therapy. *Front. Pharmacol.* 8, 383. doi:10.3389/fphar.2017.00383
- Amin, A., Gali-Muhtasib, H., Ocker, M., and Schneider-Stock, R. (2009). Overview of major classes of plant-derived anticancer drugs. *Int. J. Biomed. Sci. IJBS* 5, 1–11.
- Amiri, F., Zarnani, A.-H., Zand, H., Koohdani, F., Jeddi-Tehrani, M., and Vafa, M. (2013). Synergistic anti-proliferative effect of resveratrol and etoposide on human hepatocellular and colon cancer cell lines. *Eur. J. Pharmacol.* 718, 34–40. doi:10.1016/j.ejphar.2013.09.020
- Anantharaju, P. G., Reddy, B. D., Padukudru, M. A., Kumari Chitturi, C. M., Vimalambike, M. G., and Madhunapantula, S. V. (2017). Naturally occurring benzoic acid derivatives retard cancer cell growth by inhibiting histone deacetylases (HDAC). *Cancer Biol. Ther.* 18, 492–504. doi:10.1080/15384047.2017.1324374
- Angelova, S., Gospodinova, Z., Krasteva, M., Antov, G., Lozanov, V., Markov, T., et al. (2013). Antitumor activity of Bulgarian herb *Tribulus terrestris* L. on human breast cancer cells. *J. Biosci. Biotechnol.* 2.
- Antognoni, F., Potente, G., Mandrioli, R., Angeloni, C., Freschi, M., Malaguti, M., et al. (2020). Fruit quality characterization of new sweet cherry cultivars as a good source of bioactive phenolic compounds with antioxidant and neuroprotective potential. *Antioxidants* 9, 677. doi:10.3390/antiox9080677
- Arapitsas, P. (2008). Identification and quantification of polyphenolic compounds from okra seeds and skins. *Food Chem.* 110, 1041–1045. doi:10.1016/j.foodchem.2008.03.014
- Ashidi, J., Houghton, P., Hylands, P., and Efferth, T. (2010). Ethnobotanical survey and cytotoxicity testing of plants of South-western Nigeria used to treat cancer, with isolation of cytotoxic constituents from *Cajanus cajan* Millsp. leaves. *J. Ethnopharmacol.* 128, 501–512. doi:10.1016/j.jep.2010.01.009
- Asita, A. O., Heisi, D. H., and Tjale, T. (2015). Modulation of mutagen-induced genotoxicity by two Lesotho medicinal plants in *Allium cepa* L. *Environ. Nat. Resour. Res.* 5, 37. doi:10.5539/enrr.v5n3p37
- Atienza, D. M., Vogel, C. L., Trock, B., and Swain, S. M. (1995). Phase II study of oral etoposide for patients with advanced breast cancer. *Cancer* 76, 2485–2490. doi:10.1002/1097-0142(19951215)76:12<2485::aid-cnrc2820761212>3.0.co;2-j
- Awad, A. B., Gan, Y., and Fink, C. S. (2000). Effect of β -sitosterol, a plant sterol, on growth, protein phosphatase 2A, and phospholipase D in LNCaP cells. *Nutr. cancer* 36, 74–78. doi:10.1207/S15327914NC3601_11
- Ayele, T. (2018). A review on traditionally used medicinal plants/herbs for cancer therapy in Ethiopia: Current status, challenge and future perspectives. *Org. Chem. Curr. Res.* 7, 8. doi:10.4172/2161-0401.1000192

- Bai, L.-P., Zhao, Z.-Z., Cai, Z., and Jiang, Z.-H. (2006). DNA-binding affinities and sequence selectivity of quaternary benzophenanthridine alkaloids sanguinarine, chelerythrine, and nitidine. *Bioorg. Med. Chem.* 14, 5439–5445. doi:10.1016/j.bmc.2006.05.012
- Bakamga-Via, I., Hounda, J. B., Fokou, P. V. T., Tchokouaha, L. R. Y., Gary-Bobo, M., Gallud, A., et al. (2014). Composition and cytotoxic activity of essential oils from *Xylopia aethiopica* (Dunal) A. Rich, *Xylopia parviflora* (A. Rich) Benth. and *Monodora myristica* (Gaertn) growing in Chad and Cameroon. *BMC complementary Altern. Med.* 14, 125–128. doi:10.1186/1472-6882-14-125
- Bala, A., Kar, B., Haldar, P. K., Mazumder, U. K., and Bera, S. (2010). Evaluation of anticancer activity of *Cleome gynandra* on Ehrlich's Ascites Carcinoma treated mice. *J. Ethnopharmacol.* 129, 131–134. doi:10.1016/j.jep.2010.03.010
- Balakrishnan, A. S., Nathan, A. A., Kumar, M., Ramamoorthy, S., and Mothilal, S. K. R. (2017). Withania somnifera targets interleukin-8 and cyclooxygenase-2 in human prostate cancer progression. *Prostate Int.* 5, 75–83. doi:10.1016/j.pnrl.2017.03.002
- Balama, C., Makatta, A., Maduka, S., and Tewe, C. (2015). Nutrient content of dried leaves of *Zanthoxylum chalybeum* Engl. growing in semi-arid areas of Iringa region, Tanzania. *Tanzan. J. For. Nat. Conservation* 84.
- Balogun, F., and Ashafa, A. (2017). Aqueous root extracts of *Dicoma anomala* (Sond.) extenuates postprandial hyperglycaemia *in vitro* and its modulation on the activities of carbohydrate-metabolizing enzymes in streptozotocin-induced diabetic Wistar rats. *South Afr. J. Bot.* 112, 102–111. doi:10.1016/j.sajb.2017.05.014
- Barhoi, D., Upadhyaya, P., Barbhuiya, S. N., Giri, A., and Giri, S. (2021). Aqueous extract of *moringa oleifera* exhibit potential anticancer activity and can be used as a possible cancer therapeutic agent: A study involving *in vitro* and *in vivo* approach. *J. Am. Coll. Nutr.* 40, 70–85. doi:10.1080/07315724.2020.1735572
- Benarba, B., and Pandiella, A. (2018). Colorectal cancer and medicinal plants: Principle findings from recent studies. *Biomed. Pharmacother.* 107, 408–423. doi:10.1016/j.biopha.2018.08.006
- Bioliti, Y. E., Edward, N. B., and Tyeng, T. D. (2020). A chemical overview of *Azanza garckeana*. *Biol. Med. Nat. Prod. Chem.* 9, 91–95. doi:10.14421/biomedich.2020.92.91-95
- Bleckmann, A., Conradi, L.-C., Menck, K., Schmick, N. A., Schubert, A., Rietkötter, E., et al. (2016). β -catenin-independent WNT signaling and Ki67 in contrast to the estrogen receptor status are prognostic and associated with poor prognosis in breast cancer liver metastases. *Clin. Exp. Metastasis* 33, 309–323. doi:10.1007/s10585-016-9780-3
- Bray, F., Laversanne, M., Weiderpass, E., and Soerjomataram, I. (2021). The ever-increasing importance of cancer as a leading cause of premature death worldwide. *Cancer* 127, 3029–3030. doi:10.1002/cncr.33587
- Bray, F., Parkin, D. M., Gnanon, F., Tshisimogo, G., Peko, J.-F., Adoubi, I., et al. (2022). Cancer in sub-saharan Africa in 2020: A review of current estimates of the national burden, data gaps, and future needs. *Lancet Oncol.* 23, 719–728. doi:10.1016/S1470-2045(22)00270-4
- Brown, A. C., Reitzenstein, J. E., Liu, J., and Jadus, M. R. (2005). The anti-cancer effects of poi (*Colocasia esculenta*) on colonic adenocarcinoma cells *in vitro*. *Phytotherapy Res. An Int. J. Devoted Pharmacol. Toxicol. Eval. Nat. Prod. Deriv.* 19, 767–771. doi:10.1002/ptr.1712
- Chen, W.-Y., Chang, F.-R., Huang, Z.-Y., Chen, J.-H., Wu, Y.-C., and Wu, C.-C. (2008). Tubocapsenolide A, a novel withanolide, inhibits proliferation and induces apoptosis in MDA-MB-231 cells by thiol oxidation of heat shock proteins. *J. Biol. Chem.* 283, 17184–17193. doi:10.1074/jbc.M709447200
- Choumessi, A. T., Loureiro, R., Silva, A. M., Moreira, A. C., Pieme, A. C., Tazoacha, A., et al. (2012). Toxicity evaluation of some traditional African spices on breast cancer cells and isolated rat hepatic mitochondria. *Food Chem. Toxicol.* 50, 4199–4208. doi:10.1016/j.fct.2012.08.008
- Christensen, D. K., Armaiz-Pena, G. N., Ramirez, E., Matsuo, K., Zimmerman, B., Zand, B., et al. (2016). SSRI use and clinical outcomes in epithelial ovarian cancer. *Oncotarget* 7, 33179–33191. doi:10.18632/oncotarget.8891
- Cui, H., Schroering, A., and Ding, H.-F. (2002). p53 mediates DNA damaging drug-induced apoptosis through a caspase-9-dependent pathway in SH-SY5Y neuroblastoma cells. *Mol. cancer Ther.* 1, 679–686.
- Cunningham, A., Anoncho, V., and Sunderland, T. (2016). Power, policy and the *Prunus africana* bark trade, 1972–2015. *J. Ethnopharmacol.* 178, 323–333. doi:10.1016/j.jep.2015.11.042
- Custódio, L., Escapa, A. L., Patarra, J., Aligué, R., Alberício, F., Neng, N. R., et al. (2013). Sapwood of carob tree (*Ceratonia siliqua* L.) as a potential source of bioactive compounds. *Rec. Nat. Prod.* 7, 225–229.
- Da Silva, A. J., Buarque, C. D., Brito, F. V., Aurelian, L., Macedo, L. F., Malkas, L. H., et al. (2002). Synthesis and preliminary pharmacological evaluation of new (+/-) 1,4-naphthoquinones structurally related to lapachol. *Bioorg. Med. Chem.* 10, 2731–2738. doi:10.1016/s0968-0896(02)00100-1
- Daoud, A., Song, J., Xiao, F., and Shang, J. (2014). B-9-3, a novel β -carboline derivative exhibits anti-cancer activity via induction of apoptosis and inhibition of cell migration *in vitro*. *Eur. J. Pharmacol.* 724, 219–230. doi:10.1016/j.ejphar.2013.12.038
- De Sousa Ferreira Soares, G., Assreuy, A. M. S., De Almeida Gadelha, C. A., De Moraes Gomes, V., Delatorre, P., Da Conceição Simões, R., et al. (2012). Purification and biological activities of *Abelmoschus esculentus* seed lectin. *protein J.* 31, 674–680. doi:10.1007/s10930-012-9447-0
- Debelec-Bütüner, B., Öztürk, M. B., Tağ, Ö., Akgün, İ. H., Yetik-Anacak, G., Bedir, E., et al. (2018). Cycloartane-type saponin derivatives inhibit NF κ B activation as chemopreventive strategy for inflammation-induced prostate carcinogenesis. *Steroids* 135, 9–20. doi:10.1016/j.steroids.2018.04.005
- Devanesan, S., and Alsali, M. S. (2021). Green synthesis of silver nanoparticles using the flower extract of *Abelmoschus esculentus* for cytotoxicity and antimicrobial studies. *Int. J. Nanomedicine* 16, 3343–3356. doi:10.2147/IJN.S307676
- Dibwe, D. F., Awale, S., Kadota, S., Morita, H., and Tezuka, Y. (2014). Muchimangins G–J, fully substituted xanthones with a diphenylmethyl substituent, from *Securidaca longepedunculata*. *J. Nat. Prod.* 77, 1241–1244. doi:10.1021/np5000445
- Donhouedé, J. C., Salako, K. V., Gandji, K., Idohou, R., Tohou, R., Hounkpèvi, A., et al. (2022). Food and medicinal uses of *Annona senegalensis* pers.: A country-wide assessment of traditional theoretical knowledge and actual uses in Benin, west Africa. *J. Ethnobiol. ethnomedicine* 18, 10–15. doi:10.1186/s13002-022-00510-2
- Dziadek, K., Kopeć, A., Piątkowska, E., and Leszczyńska, T. (2019). High-fructose diet-induced metabolic disorders were counteracted by the intake of fruit and leaves of sweet cherry in wistar rats. *Nutrients* 11, 2638. doi:10.3390/nu11122638
- Economides, M. P., Mccue, D., Borthakur, G., and Pemmaraju, N. (2019). Topoisomerase II inhibitors in AML: Past, present, and future. *Expert Opin. Pharmacother.* 20, 1637–1644. doi:10.1080/14656566.2019.1621292
- El-Seedi, A. R., Burman, R., Mansour, A., Turki, Z., Boulos, L., Gullbo, J., et al. (2013). The traditional medical uses and cytotoxic activities of sixty-one Egyptian plants: Discovery of an active cardiac glycoside from *urinea maritima*. *J. Ethnopharmacol.* 145, 746–757. doi:10.1016/j.jep.2012.12.007
- Elegami, A. A., Bates, C., Gray, A. I., Mackay, S. P., Skellern, G. G., and Waigh, R. D. (2003). Two very unusual macrocyclic flavonoids from the water lily *Nymphaea lotus*. *Phytochemistry* 63, 727–731. doi:10.1016/s0031-9422(03)00238-3
- Eritja, N., Chen, B.-J., Rodríguez-Barrueco, R., Santacana, M., Gatiús, S., Vidal, A., et al. (2017). Autophagy orchestrates adaptive responses to targeted therapy in endometrial cancer. *Autophagy* 13, 608–624. doi:10.1080/15548627.2016.1271512
- Ermakova, S. P., Kang, B. S., Choi, B. Y., Choi, H. S., Schuster, T. F., and Ma, W. Y. (2006). (-)-Epigallocatechin gallate overcomes resistance to etoposide-induced cell death by targeting the molecular chaperone glucose-regulated protein 78. *Cancer Res.* 66, 9260–9269.
- Faizal, A., and Geelen, D. (2013). Saponins and their role in biological processes in plants. *Phytochem. Rev.* 12, 877–893. doi:10.1007/s11101-013-9322-4
- Faizi, S., Khan, R. A., Mughal, N. R., Malik, M. S., Sajjadi, K. E. S., and Ahmad, A. (2008). Antimicrobial activity of various parts of *Polyalthia longifolia* var. pendula: Isolation of active principles from the leaves and the berries. *Phytotherapy Res.* 22, 907–912. doi:10.1002/ptr.2414
- Fang, X. P., Rieser, M. J., Gu, Z. M., Zhao, G. X., and McLaughlin, J. L. (1993). Annonaceous acetogenins: An updated review. *Phytochem. Anal.* 4, 27–48. doi:10.1002/pca.280040108
- Ferreira De Oliveira, J. M. P., Pacheco, A. R., Coutinho, L., Oliveira, H., Pinho, S., Almeida, L., et al. (2018). Combination of etoposide and fisetin results in anti-cancer efficiency against osteosarcoma cell models. *Archives Toxicol.* 92, 1205–1214. doi:10.1007/s00204-017-2146-z
- Fiorito, S., Epifano, F., Bruyère, C., Mathieu, V., Kiss, R., and Genovese, S. (2014). Growth inhibitory activity for cancer cell lines of lapachol and its natural and semi-synthetic derivatives. *Bioorg. Med. Chem. Lett.* 24, 454–457. doi:10.1016/j.bmcl.2013.12.049
- Fontana, G., Badalamenti, N., Bruno, M., Castiglione, D., Notarbartolo, M., Poma, P., et al. (2022). Synthesis, *in vitro* and *in silico* analysis of new oleanolic acid and lupeol derivatives against leukemia cell lines: Involvement of the NF- κ B pathway. *Int. J. Mol. Sci.* 23, 6594. doi:10.3390/ijms23126594
- Foster, K., Oyenih, O., Rademan, S., Erhabor, J., Matsabisa, M., Barker, J., et al. (2020). Selective cytotoxic and anti-metastatic activity in DU-145 prostate cancer cells induced by *Annona muricata* L. bark extract and phytochemical, annonacin. *BMC Complementary Med. Ther.* 20, 375–415. doi:10.1186/s12906-020-03130-z
- Foster, P. A., Newman, S. P., Leese, M. P., Bernietiere, S., Diolet, C., Camara, J., et al. (2008). A new micronized formulation of 2-methoxystriadiol-bis-sulfamate (STX140) is therapeutically potent against breast cancer. *Anticancer Res.* 28, 577–581.
- Fu, Y., Kadioglu, O., Wiench, B., Wei, Z., Wang, W., Luo, M., et al. (2015). Activity of the antiestrogenic cajanin stilbene acid towards breast cancer. *J. Nutr. Biochem.* 26, 1273–1282. doi:10.1016/j.jnutbio.2015.06.004
- Fulda, S., and Debatin, K.-M. (2006). Extrinsic versus intrinsic apoptosis pathways in anticancer chemotherapy. *Oncogene* 25, 4798–4811. doi:10.1038/sj.onc.1209608
- Galluzzi, L., Pedro, B.-S., Manuel, J., Demaria, S., Formenti, S. C., and Kroemer, G. (2017). Activating autophagy to potentiate immunogenic chemotherapy and radiation therapy. *Nat. Rev. Clin. Oncol.* 14, 247–258. doi:10.1038/nrclinonc.2016.183
- Gao, X., Deeb, D., Liu, Y., Arbab, A. S., Divine, G. W., Dulchavsky, S. A., et al. (2011). Prevention of prostate cancer with oleanane synthetic triterpenoid CDDO-Me in the TRAMP mouse model of prostate cancer. *Cancers* 3, 3353–3369. doi:10.3390/cancers3033353

- Gaobotse, G., Trémouillaux-Guiller, J., Venkataraman, S., Sherif, M. K., Makhzoum, A., and Hefferon, K. (2022a). "Plant molecular pharming of biologics to combat HIV," in *Applications in plant biotechnology* (CRC Press), 296–348.
- Gaobotse, G., Venkataraman, S., Mmereke, K. M., Moustafa, K., Hefferon, K., and Makhzoum, A. (2022b). Recent progress on vaccines produced in transgenic plants. *Vaccines* 10, 1861. doi:10.3390/vaccines10111861
- Garrido, M., Paredes, S. D., Cubero, J., Lozano, M., Toribio-Delgado, A. F., Muñoz, J. L., et al. (2010). Jerte Valley cherry-enriched diets improve nocturnal rest and increase 6-sulfatoxymelatonin and total antioxidant capacity in the urine of middle-aged and elderly humans. *Journals Gerontology Ser. A Biomed. Sci. Med. Sci.* 65, 909–914. doi:10.1093/gerona/gdq099
- Gaurav, N., Kumar, A., Tyagi, M., Kumar, D., Chauhan, U., and Singh, A. (2015). Morphology of *Withania somnifera* (distribution, morphology, phytosociology of *Withania somnifera* L. Dunal). *Int. J. Curr. Sci. Res.* 1, 164–173.
- Gavamukulya, Y., Abou-Elella, F., Wamunyokoli, F., and Ael-Shemy, H. (2014). Phytochemical screening, anti-oxidant activity and *in vitro* anticancer potential of ethanolic and water leaves extracts of *Annona muricata* (Graviola). *Asian Pac. J. Trop. Med.* 7, S355–S363. doi:10.1016/S1995-7645(14)60258-3
- Gemed, H. F., Ratta, N., Haki, G. D., Woldegiorgis, A. Z., and Beyene, F. (2015). Nutritional quality and health benefits of okra (*Abelmoschus esculentus*): A review. *J. Food Process Technol.* 6, 2. doi:10.4172/2157-7110.1000458
- Ghanemi, F. Z., Belarbi, M., Fluckiger, A., Nani, A., Dumont, A., De Rosny, C., et al. (2017). Carob leaf polyphenols trigger intrinsic apoptotic pathway and induce cell cycle arrest in colon cancer cells. *J. Funct. Foods* 33, 112–121. doi:10.1016/j.jff.2017.03.032
- Gleye, C., Duret, P., Laurens, A., Hocquemiller, R., and Cavé, A. (1998). cis-Monotetrahydrofuran acetogenins from the roots of *Annona muricata*. *J. Nat. Prod.* 61, 576–579. doi:10.1021/np970494m
- Grace, O., Prendergast, H., Jäger, A., Van Staden, J., and Van Wyk, A. (2003). Bark medicines used in traditional healthcare in KwaZulu-Natal, South Africa: An inventory. *South Afr. J. Bot.* 69, 301–363. doi:10.1016/S0254-6299(15)30318-5
- Greenwell, M., and Rahman, P. (2015). Medicinal plants: Their use in anticancer treatment. *Int. J. Pharm. Sci. Res.* 6, 4103–4112. doi:10.13040/IJPSR.0975-8232.6(10)4103-12
- Gunaratne, R., Nadeeshani, H., Lu, A., Li, J., Zhang, B., Ying, T., et al. (2022). Potential nutraceutical use of *Tribulus terrestris* L. in human health. *Food Rev. Int.*, 1–30. doi:10.1080/87559129.2022.2067172
- Hadisaputri, Y. E., Habibah, U., Abdullah, F. F., Halimah, E., Mutakin, M., Megantara, S., et al. (2021). Antiproliferation activity and apoptotic mechanism of soursop (*Annona muricata* L.) leaves extract and fractions on mcf7 breast cancer cells. *Breast Cancer Targets Ther.* 13, 447–457. doi:10.2147/BCTT.S317682
- Hahn, E. R., Lee, J., and Singh, S. V. (2014). Role of mitogen-activated protein kinases and Mcl-1 in apoptosis induction by withaferin A in human breast cancer cells. *Mol. Carcinog.* 53, 907–916. doi:10.1002/mc.22050
- Hashim, S., Bakht, T., Marwat, K. B., and Jan, A. (2014). Medicinal properties, phytochemistry and pharmacology of *Tribulus terrestris* L. (Zygophyllaceae). *Pak J. Bot.* 46, 399–404.
- Heiduschka, G., Bigenzahn, J., Brunner, M., and Thurnher, D. (2014). Resveratrol synergistically enhances the effect of etoposide in HNSCC cell lines. *Acta otolaryngologica* 134, 1071–1078. doi:10.3109/00016489.2014.888592
- Henley, A. B., Yang, L., Chuang, K.-L., Sahuri-Arisoylu, M., Wu, L.-H., Bligh, S. A., et al. (2017). *Withania somnifera* root extract enhances chemotherapy through 'Priming'. *PLoS One* 12, e0170917. doi:10.1371/journal.pone.0170917
- Huang, W., Yan, Z., Li, D., Ma, Y., Zhou, J., and Sui, Z. (2018). Antioxidant and anti-inflammatory effects of blueberry anthocyanins on high glucose-induced human retinal capillary endothelial cells. *Oxidative Med. Cell. Longev.* 2018, 1862462. doi:10.1155/2018/1862462
- Hussain, S. S., Rafi, K., Faizi, S., Razzak, Z. A., and Simjee, S. U. (2018). A novel, semi-synthetic diterpenoid 16 (R and S)-phenylamino-cleroda-3, 13 (14), Z-dien-15, 16 olide (PGEA-AN) inhibits the growth and cell survival of human neuroblastoma cell line SH-SY5Y by modulating P53 pathway. *Mol. Cell. Biochem.* 449, 105–115. doi:10.1007/s11010-018-3347-3
- Hwang, J. T., Kwak, D. W., Lin, S. K., Kim, H. M., Kim, Y. M., and Park, O. J. (2007). Resveratrol induces apoptosis in chemoresistant cancer cells via modulation of AMPK signaling pathway. *Ann. N. Y. Acad. Sci.* 1095, 441–448. doi:10.1196/annals.1397.047
- Iyer, S., Chaplin, D. J., Rosenthal, D. S., Boulares, A. H., Li, L.-Y., and Smulson, M. E. (1998). Induction of apoptosis in proliferating human endothelial cells by the tumor-specific antiangiogenesis agent combretastatin A-4. *Cancer Res.* 58, 4510–4514.
- Izuegbuna, O. (2022). Leukemia chemoprevention and therapeutic potentials: Selected medicinal plants with anti-leukemic activities. *Nutr. Cancer* 74, 437–449. doi:10.1080/01635581.2021.1924209
- Jabir, M. S., Saleh, Y. M., Sulaiman, G. M., Yaseen, N. Y., Sahib, U. I., Dewir, Y. H., et al. (2021). Green synthesis of silver nanoparticles using *Annona muricata* extract as an inducer of apoptosis in cancer cells and inhibitor for NLRP3 inflammasome via enhanced autophagy. *Nanomaterials* 11, 384. doi:10.3390/nano11020384
- Jaroach, K., Karolak, M., Górski, P., Jaroach, A., Krajewski, A., Ilnicka, A., et al. (2016). Combretastatins: *In vitro* structure-activity relationship, mode of action and current clinical status. *Pharmacol. Rep.* 68, 1266–1275. doi:10.1016/j.pharep.2016.08.007
- Jia, G., Shao, X., Zhao, R., Zhang, T., Zhou, X., Yang, Y., et al. (2021). Portulaca oleracea L. polysaccharides enhance the immune efficacy of dendritic cell vaccine for breast cancer. *Food & Funct.* 12, 4046–4059. doi:10.1039/d0fo02522d
- Jia, H., Yang, Q., Wang, T., Cao, Y., Jiang, Q.-Y., Sun, H.-W., et al. (2016). Rhamnetin induces sensitization of hepatocellular carcinoma cells to a small molecular kinase inhibitor or chemotherapeutic agents. *Biochimica Biophysica Acta (BBA)-General Subj.* 1860, 1417–1430. doi:10.1016/j.bbagen.2016.04.007
- Johnson, T. O., Olatunde, A., and Nwachukwu, L. (2017). Phytochemical composition of *Annona senegalensis* leaf and its antioxidant activity during *Trypanosoma brucei* brucei induced oxidative stress in mice. *J. Pharm. Bioresour.* 14, 219–227.
- Kabbaj, F., Meddah, B., Cherrah, Y., and Faouzi, E. (2012). Ethnopharmacological profile of traditional plants used in Morocco by cancer patients as herbal therapeutics. *Phytopharmacology* 2, 243–256.
- Kaderi, M., Ben Hamouda, G., Zaeir, H., Hanana, M., and Hamrouni, L. (2015). Notes ethnobotanique et phytopharmacologie sur *Cerantonia siliqua* (L.). *Phytothérapie* 13, 144–147. doi:10.1007/s10298-014-0904-4
- Karatoprak, G. Ş., Küpeli Akkol, E., Genç, Y., Bardakçı, H., Yücel, Ç., and Sobarzo-Sánchez, E. (2020). Combretastatins: An overview of structure, probable mechanisms of action and potential applications. *Molecules* 25, 2560. doi:10.3390/molecules25112560
- Kataria, H., Shah, N., Kaul, S. C., Wadhwa, R., and Kaur, G. (2011). Water extract of ashwagandha leaves limits proliferation and migration, and induces differentiation in glioma cells. *Evidence-Based Complementary Altern. Med.* 2011, 267614. doi:10.1093/ecam/nep188
- Kaur, H. (2015). Shantanu, "Anticancer activity of a constituent from *Moringa oleifera* leaves. *J. Chem. Pharm. Res.* 7, 701–705.
- Kelley, D. S., Adkins, Y., Reddy, A., Woodhouse, L. R., Mackey, B. E., and Erickson, K. L. (2013). Sweet bing cherries lower circulating concentrations of markers for chronic inflammatory diseases in healthy humans. *J. Nutr.* 143, 340–344. doi:10.3945/jn.112.171371
- Kelley, D. S., Rasooly, R., Jacob, R. A., Kader, A. A., and Mackey, B. E. (2006). Consumption of Bing sweet cherries lowers circulating concentrations of inflammation markers in healthy men and women. *J. Nutr.* 136, 981–986. doi:10.1093/jn/136.4.981
- Khan, F., Pandey, P., Ahmad, V., and Upadhyay, T. K. (2020). *Moringa oleifera* methanolic leaves extract induces apoptosis and G0/G1 cell cycle arrest via downregulation of Hedgehog Signaling Pathway in human prostate PC-3 cancer cells. *J. Food Biochem.* 44, e13338. doi:10.1111/jfbc.13338
- Kim, H. J., Kim, J. C., Min, J. S., Kim, M.-J., Kim, J. A., Kor, M. H., et al. (2011). Aqueous extract of *Tribulus terrestris* Linn induces cell growth arrest and apoptosis by down-regulating NF-κB signaling in liver cancer cells. *J. Ethnopharmacol.* 136, 197–203. doi:10.1016/j.jep.2011.04.060
- Klein-Júnior, L. C., Campos, A., Niero, R., Corrêa, R., Vander Heyden, Y., and Filho, V. C. (2020). Xanthones and cancer: From natural sources to mechanisms of action. *Chem. Biodivers.* 17, e1900499. doi:10.1002/cbdv.201900499
- Kluska, M., and Woźniak, K. (2021). Natural polyphenols as modulators of etoposide anti-cancer activity. *Int. J. Mol. Sci.* 22, 6602. doi:10.3390/ijms22126602
- Kobayashi, T., Sawa, H., Morikawa, J., Zhang, W., and Shiku, H. (2000). Bax induction activates apoptotic cascade via mitochondrial cytochrome c release and Bax overexpression enhances apoptosis induced by chemotherapeutic agents in DLD-1 colon cancer cells. *Jpn. J. Cancer Res.* 91, 1264–1268. doi:10.1111/j.1349-7006.2000.tb00913.x
- Kode, J., Kovvuri, J., Nagaraju, B., Jadhav, S., Barkume, M., Sen, S., et al. (2020). Synthesis, biological evaluation, and molecular docking analysis of phenstatin based indole linked chalcones as anticancer agents and tubulin polymerization inhibitors. *Bioorg. Chem.* 105, 104447. doi:10.1016/j.bioorg.2020.104447
- Komakech, R., and Kang, Y. (2019). Ethnopharmacological potential of African cherry [*Prunus africana*]. *J. Herb. Med.* 17, 100283. doi:10.1016/j.hermed.2019.100283
- Komakech, R., Yim, N.-H., Shim, K.-S., Jung, H., Byun, J.-E., Lee, J., et al. (2022). Root extract of a micropropagated *Prunus africana* medicinal plant induced apoptosis in human prostate cancer cells (PC-3) via caspase-3 activation. *Evidence-Based Complementary Altern. Med.* 2022, 8232851. doi:10.1155/2022/8232851
- Kuete, V., Sandjo, L. P., Mbaveng, A. T., Zeino, M., and Efferth, T. (2015). Cytotoxicity of compounds from *Xylopia aethiopica* towards multi-factorial drug-resistant cancer cells. *Phytomedicine* 22, 1247–1254. doi:10.1016/j.phymed.2015.10.008
- Kumar, N., Kale, R. K., and Tikku, A. B. (2013). Chemopreventive effect of *Lagenaria siceraria* in two stages DMBA plus croton oil induced skin papillomagenesis. *Nutr. cancer* 65, 991–1001. doi:10.1080/01635581.2013.814800
- Kundu, N., Campbell, P., Hampton, B., Lin, C.-Y., Ma, X., Ambulos, N., et al. (2012). Antimetastatic activity isolated from *Colocasia esculenta* (taro). *Anti-cancer drugs* 23, 200–211. doi:10.1097/CAD.0b013e32834b85e8
- Kuo, C.-Y., Zupkó, I., Chang, F.-R., Hunyadi, A., Wu, C.-C., Weng, T.-S., et al. (2016). Dietary flavonoid derivatives enhance chemotherapeutic effect by inhibiting the DNA damage response pathway. *Toxicol. Appl. Pharmacol.* 311, 99–105. doi:10.1016/j.taap.2016.09.019
- Laszczyk, M. N. (2009). Pentacyclic triterpenes of the lupane, oleanane and ursane group as tools in cancer therapy. *Planta medica* 75, 1549–1560. doi:10.1055/s-0029-1186102

- Lawal, R., Ozaslan, M., Odesanmi, O., Karagoz, I., Kilic, I., and Ebuehi, O. (2012). Cytotoxic and antiproliferative activity of *Securidaca longepedunculata* aqueous extract on Ehrlich ascites carcinoma cells in Swiss albino mice.
- Layos, M. A., Lage, N. N., Chew, B. P., Atienza, L., Mertens-Talcott, S., Talcott, S., et al. (2021). Dark sweet cherry (*Prunus avium*) phenolics enriched in anthocyanins induced apoptosis in MDA-MB-453 breast cancer cells through MAPK-dependent signaling and reduced invasion via akt and p1cy-1 downregulation. *Nutr. Cancer* 73, 1985–1997. doi:10.1080/01635581.2020.1817514
- Leyon, P., and Kuttan, G. (2004). Effect of *Withania somnifera* on B16F-10 melanoma induced metastasis in mice. *Phytotherapy Res. An Int. J. Devoted Pharmacol. Toxicol. Eval. Nat. Prod. Deriv.* 18, 118–122. doi:10.1002/ptr.1378
- Li, A.-N., Li, S., Zhang, Y.-J., Xu, X.-R., Chen, Y.-M., and Li, H.-B. (2014). Resources and biological activities of natural polyphenols. *Nutrients* 6, 6020–6047. doi:10.3390/nu6126020
- Li, Z.-M., Jiang, W.-Q., Zhu, Z.-Y., Zhu, X.-F., Zhou, J.-M., Liu, Z.-C., et al. (2008). Synergistic cytotoxicity of Bcl-xL inhibitor, gossypol and chemotherapeutic agents in non-Hodgkin's lymphoma cells. *Cancer Biol. Ther.* 7, 51–60. doi:10.4161/cbt.7.1.5128
- Lim, T. (2014). "Nymphaea lotus," in *Edible medicinal and non medicinal plants* (Springer), 514–518.
- Liontas, A., and Yeger, H. (2004). Curcumin and resveratrol induce apoptosis and nuclear translocation and activation of p53 in human neuroblastoma. *Anticancer Res.* 24, 987–998.
- Liu, X., Wu, H., Tao, X., Ying, X., and Stien, D. (2021). Two amide glycosides from *Portulaca oleracea* L. and its bioactivities. *Nat. Prod. Res.* 35, 2655–2659. doi:10.1080/14786419.2019.1660333
- Luetragoon, T., Pankla Sranujit, R., Noysang, C., Thongsri, Y., Potup, P., Suphrom, N., et al. (2020). Anti-Cancer effect of 3-Hydroxy- β -Ionone identified from moringa oleifera Lam. Leaf on human squamous cell carcinoma 15 cell line. *Molecules* 25, 3563. doi:10.3390/molecules25163563
- Luo, M., Liu, X., Zu, Y., Fu, Y., Zhang, S., Yao, L., et al. (2010). Cajanol, a novel anticancer agent from *Pigeonpea* [*Cajanus cajan* (L.) Millsp.] roots, induces apoptosis in human breast cancer cells through a ROS-mediated mitochondrial pathway. *Chemico-Biological Interact.* 188, 151–160. doi:10.1016/j.cbi.2010.07.009
- Mahbub, A., Le Maitre, C., Haywood-Small, S., Cross, N., and Jordan-Mahy, N. (2015). Polyphenols act synergistically with doxorubicin and etoposide in leukaemia cell lines. *Cell Death Discov.* 1, 15043–15112. doi:10.1038/cddiscovery.2015.43
- Makhzoum, A., and Hefferon, K. (2022). *Applications in plant biotechnology: Focus on plant secondary metabolism and plant molecular pharming*. CRC Press.
- Maroyi, A. (2018). *Dicoma anomala* sond.: A review of its botany, ethnomedicine, phytochemistry and pharmacology. *Asian J. Pharm. Clin. Res.* 11, 70–77. doi:10.22159/ajpcr.2018.v11i6.25538
- Matias, A. A., Rosado-Ramos, R., Nunes, S. L., Figueira, I., Serra, A. T., Bronze, M. R., et al. (2016). Protective effect of a (poly) phenol-rich extract derived from sweet cherries culls against oxidative cell damage. *Molecules* 21, 406. doi:10.3390/molecules21040406
- McGown, A. T., and Fox, B. W. (1990). Differential cytotoxicity of combretastatins A1 and A4 in two daunorubicin-resistant P388 cell lines. *Cancer Chemother. Pharmacol.* 26, 79–81. doi:10.1007/BF02940301
- Michael, K., Onyia, L., and Jidauna, S. (2015). Evaluation of phytochemicals in *Azanza garckeana* (Gorontula) seed. *J. Agric. Veterinary Sci.* 8, 71–74.
- Misonge, O. J., Kamindu, G. N., Sabina, W., and Muita, G. (2019). An ethnobotanical survey of plants used for the treatment and management of cancer in Embu County, Kenya. *J. Med. Plants* 7, 39–46.
- Mitaine-Offer, A.-C., Pérez, N., Miyamoto, T., Delaude, C., Mirjolet, J.-F., Duchamp, O., et al. (2010). Acylated triterpene saponins from the roots of *Securidaca longepedunculata*. *Phytochemistry* 71, 90–94. doi:10.1016/j.phytochem.2009.09.022
- Mondal, S., and Swamy, M. J. (2020). Purification, biochemical/biophysical characterization and chitoooligosaccharide binding to BGL24, a new PP2-type phloem exudate lectin from bottle gourd (*Lagenaria siceraria*). *Int. J. Biol. Macromol.* 164, 3656–3666. doi:10.1016/j.ijbiomac.2020.08.246
- Monte, L. G., Santi-Gadelha, T., Reis, L. B., Braganhol, E., Prietsch, R. F., Dellagostin, O. A., et al. (2014). Lectin of *Abelmoschus esculentus* (okra) promotes selective antitumor effects in human breast cancer cells. *Biotechnol. Lett.* 36, 461–469. doi:10.1007/s10529-013-1382-4
- Musa, D., Anakaa, T., and Bashir, K. (2017). Phytochemical analysis of crude extracts from *Annona senegalensis* and its antsnake venom potential on albino rats. *FUDMA J. Sci. (FJS) Maiden Ed.* 1, 139–142.
- Musthafa, S. A., Muthu, K., Vijayakumar, S., George, S. J., Murali, S., Govindaraj, J., et al. (2021). Lectin isolated from *Abelmoschus esculentus* induces caspase mediated apoptosis in human U87 glioblastoma cell lines and modulates the expression of circadian clock genes. *Toxicon* 202, 98–109. doi:10.1016/j.toxicon.2021.08.025
- Nabha, S. M., Mohammad, R. M., Wall, N. R., Dutcher, J. A., Salkini, B. M., Pettit, G. R., et al. (2001). Evaluation of combretastatin A-4 prodrug in a non-hodgkin's lymphoma xenograft model: Preclinical efficacy. *Anti-cancer drugs* 12, 57–63. doi:10.1097/00001813-200101000-00008
- Naik, A. V., and Sellappan, K. (2020). *In vitro* evaluation of *Annona muricata* L.(Soursop) leaf methanol extracts on inhibition of tumorigenicity and metastasis of breast cancer cells. *Biomarkers* 25, 701–710. doi:10.1080/1354750X.2020.1836025
- Nam, N.-H. (2003). Combretastatin A-4 analogues as antimitotic antitumor agents. *Curr. Med. Chem.* 10, 1697–1722. doi:10.2174/0929867033457151
- N'guessan, B. B., Asiamah, A. D., Arthur, N. K., Frimpong-Manso, S., Amoateng, P., Amponsah, S. K., et al. (2021). Ethanolic extract of *Nymphaea lotus* L.(Nymphaeaceae) leaves exhibits *in vitro* antioxidant, *in vivo* anti-inflammatory and cytotoxic activities on Jurkat and MCF-7 cancer cell lines. *BMC Complementary Med. Ther.* 21, 22–13. doi:10.1186/s12906-020-03195-w
- Ngulde, S. I., Sandabe, U. K., Abounader, R., Dawson, T. K., Zhang, Y., Iliya, I., et al. (2019). Ethanol extract of *Securidaca longepedunculata* induces apoptosis in brain tumor (U87) cells. *BioMed Res. Int.* 2019, 9826590. doi:10.1155/2019/9826590
- Nihei, Y., Suga, Y., Morinaga, Y., Ohishi, K., Okano, A., Ohsumi, K., et al. (1999). A novel combretastatin A-4 derivative, AC-7700, shows marked antitumor activity against advanced solid tumors and orthotopically transplanted tumors. *Jpn. J. cancer Res.* 90, 1016–1025. doi:10.1111/j.1349-7006.1999.tb00850.x
- Nikolaev, A. Y., Li, M., Puskas, N., Qin, J., and Gu, W. (2003). Parc: A cytoplasmic anchor for p53. *Cell* 112, 29–40. doi:10.1016/s0092-8674(02)01255-2
- Nkwe, D. O., Lotshwao, B., Rantong, G., Matshwele, J., Kwap, T. E., Masisi, K., et al. (2021). Anticancer mechanisms of bioactive compounds from Solanaceae: An update. *Cancers (Basel)* 13, 4989. doi:10.3390/cancers13194989
- Noda, C., He, J., Takano, T., Tanaka, C., Kondo, T., Tohyama, K., et al. (2007). Induction of apoptosis by epigallocatechin-3-gallate in human lymphoblastoid B cells. *Biochem. biophysical Res. Commun.* 362, 951–957. doi:10.1016/j.bbrc.2007.08.079
- Noratto, G., Layosa, M. A., Lage, N. N., Atienza, L., Ivanov, I., Mertens-Talcott, S. U., et al. (2020). Antitumor potential of dark sweet cherry sweet (*Prunus avium*) phenolics in suppressing xenograft tumor growth of MDA-MB-453 breast cancer cells. *J. Nutr. Biochem.* 84, 108437. doi:10.1016/j.jnutbio.2020.108437
- Noronha, V., Sekhar, A., Patil, V. M., Menon, N., Joshi, A., Kapoor, A., et al. (2020). Systemic therapy for limited stage small cell lung carcinoma. *J. Thorac. Dis.* 12, 6275–6290. doi:10.21037/jtd-2019-sclc-11
- Ntie-Kang, F., Zofou, D., Babiaka, S. B., Meudom, R., Scharfe, M., Lifongo, L. L., et al. (2013). AfroDb: A select highly potent and diverse natural product library from african medicinal plants. *PLoS one* 8, e78085. doi:10.1371/journal.pone.0078085
- Obasi, T. C., Braicu, C., Iacob, B. C., Bodoki, E., Jurj, A., Raduly, L., et al. (2018). *Securidaca*-saponins are natural inhibitors of AKT, MCL-1, and BCL2L1 in cervical cancer cells. *Cancer Manag. Res.* 10, 5709–5724. doi:10.2147/CMAR.S163328
- Ochokwu, I., Dasuki, A., and Oshoke, J. (2015). *Azanza garckeana* (goron tula) as an edible indigenous fruit in North eastern part of Nigeria. *J. Biol. Agriculture Healthc.* 5, 26–31.
- Ochwang'i, D. O., Kimwele, C. N., Oduma, J. A., Gathumbi, P. K., Mbaria, J. M., and Kiama, S. G. (2014). Medicinal plants used in treatment and management of cancer in Kakamega County, Kenya. *J. Ethnopharmacol.* 151, 1040–1055. doi:10.1016/j.jep.2013.11.051
- Okwu, D. (2005). Phytochemicals, vitamins and mineral contents of two Nigerian medicinal plants. *Int. J. Mol. Med. Adv. Sci.* 1, 375–381.
- Omara, T., Kiprop, A. K., Ramkat, R. C., Cherutoi, J., Kagoya, S., Moraa Nyangena, D., et al. (2020). Medicinal plants used in traditional management of cancer in Uganda: A review of ethnobotanical surveys, phytochemistry, and anticancer studies. *Evidence-Based Complementary Altern. Med.* 2020, 3529081. doi:10.1155/2020/3529081
- Onyancha, J. M., Gikonyo, N. K., Wachira, S. W., Mwitari, P. G., and Gicheru, M. M. (2018). Anticancer activities and safety evaluation of selected Kenyan plant extracts against breast cancer cell lines. *J. Pharmacogn. Phytotherapy* 10, 21–26. doi:10.5897/jpp2017.0465
- Osafo, N., Boakye, Y. D., Agyare, C., Obeng, S., Foli, J. E., and Minkah, P. A. B. (2017). African plants with antiproliferative properties. *Nat. Prod. Cancer Drug Discov.* doi:10.5772/intechopen.68568
- Osbourne, A. E. (2003). Saponins in cereals. *Phytochemistry* 62, 1–4. doi:10.1016/s0031-9422(02)00393-x
- Ouelbani, R., Bensari, S., Mouas, T. N., and Khelifi, D. (2016). Ethnobotanical investigations on plants used in folk medicine in the regions of Constantine and Mila (North-East of Algeria). *J. Ethnopharmacol.* 194, 196–218. doi:10.1016/j.jep.2016.08.016
- Oyeyemi, I. T., Yekeen, O. M., Odusina, P. O., Ologun, T. M., Ogbade, O. M., Olaleye, O. I., et al. (2015). Genotoxicity and antigenotoxicity study of aqueous and hydro-methanol extracts of *Spondias mombin* L., *Nymphaea lotus* L. and *Luffa cylindrica* L. using animal bioassays. *Interdiscip. Toxicol.* 8, 184–192. doi:10.1515/intox-2015-0028
- Oza, V. P., Parmar, P. P., Kumar, S., and Subramanian, R. (2010). Anticancer properties of highly purified L-asparaginase from *Withania somnifera* L. against acute lymphoblastic leukemia. *Appl. Biochem. Biotechnol.* 160, 1833–1840. doi:10.1007/s12010-009-8667-z
- Pacifico, S., Di Maro, A., Petriccione, M., Galasso, S., Piccolella, S., Di Giuseppe, A. M., et al. (2014). Chemical composition, nutritional value and antioxidant properties of autochthonous *Prunus avium* cultivars from Campania Region. *Food Res. Int.* 64, 188–199. doi:10.1016/j.foodres.2014.06.020

- Pandey, P., and Khan, F. (2021). Jab1 inhibition by methanolic extract of moringa oleifera leaves in cervical cancer cells: A potent targeted therapeutic approach. *Nutr. cancer* 73, 2411–2419. doi:10.1080/01635581.2020.1826989
- Papież, M. A., Krzyściak, W., Szade, K., Bukowska-Straková, K., Kozakowska, M., Hajduk, K., et al. (2016). Curcumin enhances the cytogenotoxic effect of etoposide in leukemia cells through induction of reactive oxygen species. *Drug Des. Dev. Ther.* 10, 557–570. doi:10.2147/DDDT.S92687
- Paragliola, R. M., Corsello, A., Locantore, P., Papi, G., Pontecorvi, A., and Corsello, S. M. (2020). Medical approaches in adrenocortical carcinoma. *Biomedicines* 8, 551. doi:10.3390/biomedicines8120551
- Passos, I. D., and Mironidou-Tzouveleki, M. (2016). "Hallucinogenic plants in the Mediterranean countries," in *Neuropathology of drug addictions and substance misuse* (Elsevier), 761–772.
- Patel, A., Bhatt, M., Soni, A., and Sharma, P. (2021). Identification of steroidal saponins from Tribulus terrestris and their *in silico* docking studies. *J. Cell. Biochem.* 122, 1665–1685. doi:10.1002/jcb.30113
- Pettit, G. R., Singh, S. B., Niven, M. L., Hamel, E., and Schmidt, J. M. (1987). Isolation, structure, and synthesis of combretastatins A-1 and B-1, potent new inhibitors of microtubule assembly, derived from Combretum caffrum. *J. Nat. Prod.* 50, 119–131. doi:10.1021/np50049a016
- Pieme, C. A., Kumar, S. G., Dongmo, M. S., Moukette, B. M., Boyoum, F. F., Ngogang, J. Y., et al. (2014). Antiproliferative activity and induction of apoptosis by Annona muricata (Annonaceae) extract on human cancer cells. *BMC complementary Altern. Med.* 14, 516–610. doi:10.1186/1472-6882-14-516
- Place, A. E., Suh, N., Williams, C. R., Risingsong, R., Honda, T., Honda, Y., et al. (2003). The novel synthetic triterpenoid, CDDO-imidazolide, inhibits inflammatory response and tumor growth *in vivo*. *Clin. Cancer Res.* 9, 2798–2806.
- Potchoo, Y., Richard, D., Sakie, E., Guissou, I., Kini, F., and Yaro, B. (2008). Comparative phytochemical content of leaves extracts of two Annona senegalensis Pers: The one from Togo and the other originates from Burkina Faso. *J. Biol. Sci.* 8, 577–583. doi:10.3923/jbs.2008.577.583
- Prior, R. L., Gu, L., Wu, X., Jacob, R. A., Sotoudeh, G., Kader, A. A., et al. (2007). Plasma antioxidant capacity changes following a meal as a measure of the ability of a food to alter *in vivo* antioxidant status. *J. Am. Coll. Nutr.* 26, 170–181. doi:10.1080/07315724.2007.10719599
- Rady, I., Bloch, M. B., Chamcheu, R.-C. N., Banang Mbeumi, S., Anwar, M. R., Mohamed, H., et al. (2018). Anticancer properties of graviola (Annona muricata): A comprehensive mechanistic review. *Oxidative Med. Cell. Longev.* 2018, 1826170. doi:10.1155/2018/1826170
- Ramachandran, C., Nair, S. M., Escalon, E., and Melnick, S. J. (2012). Potentiation of etoposide and temozolomide cytotoxicity by curcumin and turmeric force in brain tumor cell lines. *J. Complementary Integr. Med.* 9, Article 20. doi:10.1515/1553-3840.1614
- Raobakady, B., Reed, M. J., Leese, M. P., Potter, B. V., and Purohit, A. (2005). Inhibition of MDA-MB-231 cell cycle progression and cell proliferation by C-2-substituted oestradiol mono- and bis-3-O-sulphamates. *Int. J. cancer* 117, 150–159. doi:10.1002/ijc.21066
- Ribeiro, V., Ferreres, F., Macedo, T., Gil-Izquierdo, Á., Oliveira, A. P., Gomes, N. G., et al. (2021). Activation of caspase-3 in gastric adenocarcinoma AGS cells by Xylopia aethiopica (Dunal) A. Rich. fruit and characterization of its phenolic fingerprint by HPLC-DAD-ESI (Ion Trap)-MSn and UPLC-ESI-QTOF-MS2. *Food Res. Int.* 141, 110121. doi:10.1016/j.foodres.2021.110121
- Roduan, M. R., Abd Hamid, R., and Mohtarrudin, N. (2019). Modulation of cancer signalling pathway (s) in two-stage mouse skin tumorigenesis by annonacin. *BMC complementary Altern. Med.* 19, 1–16.
- Rtibi, K., Selmi, S., Grami, D., Saidani, K., Sebai, H., Amri, M., et al. (2017). Ceratonia siliqua L. (immature carob bean) inhibits intestinal glucose absorption, improves glucose tolerance and protects against alloxan-induced diabetes in rat. *J. Sci. Food Agric.* 97, 2664–2670. doi:10.1002/jsfa.8091
- Ruggiero, A., Ariano, A., Triarico, S., Capozza, M. A., Romano, A., Maurizi, P., et al. (2020). Temozolomide and oral etoposide in children with recurrent malignant brain tumors. *Drugs Context* 9, 1–9. doi:10.7573/dic.2020-3-1
- Ruiz, G., Valencia-González, H. A., León-Galicia, I., García-Villa, E., García-Carrancá, A., and Gariglio, P. (2018). Inhibition of RAD51 by siRNA and resveratrol sensitizes cancer stem cells derived from HeLa cell cultures to apoptosis. *Stem cells Int.* 2018, 2493869. doi:10.1155/2018/2493869
- Saidu, I. N., Umar, K. S., and Isa, M. H. (2015). Ethnobotanical survey of anticancer plants in Askira/Uba local government area of Borno State, Nigeria. *Afr. J. Pharm. Pharmacol.* 9, 123–130. doi:10.5897/ajpp2014.4083
- Saleem, A., Ahotupa, M., and Pihlaja, K. (2001). Total phenolics concentration and antioxidant potential of extracts of medicinal plants of Pakistan. *Z. für Naturforsch. C* 56, 973–978. doi:10.1515/znc-2001-11-1211
- Sari, A. N., Bhargava, P., Dhanjal, J. K., Putri, J. F., Radhakrishnan, N., Shefrin, S., et al. (2020). Combination of withaferin-A and CAPE provides superior anticancer potency: Bioinformatics and experimental evidence to their molecular targets and mechanism of action. *Cancers* 12, 1160. doi:10.3390/cancers12051160
- Sawadogo, W. R., Schumacher, M., Teiten, M.-H., Dicato, M., and Diederich, M. (2012). Traditional West African pharmacopeia, plants and derived compounds for cancer therapy. *Biochem. Pharmacol.* 84, 1225–1240. doi:10.1016/j.bcp.2012.07.021
- Senthilnathan, P., Padmavathi, R., Banu, S. M., and Sakthisekaran, D. (2006a). Enhancement of antitumor effect of paclitaxel in combination with immunomodulatory Withania somnifera on benzo (a) pyrene induced experimental lung cancer. *Chemico-biological Interact.* 159, 180–185. doi:10.1016/j.cbi.2005.11.003
- Senthilnathan, P., Padmavathi, R., Magesh, V., and Sakthisekaran, D. (2006b). Chemotherapeutic efficacy of paclitaxel in combination with Withania somnifera on benzo (a) pyrene-induced experimental lung cancer. *Cancer Sci.* 97, 658–664. doi:10.1111/j.1349-7006.2006.00224.x
- Serra, A. T., Duarte, R. O., Bronze, M. R., and Duarte, C. M. (2011). Identification of bioactive response in traditional cherries from Portugal. *Food Chem.* 125, 318–325. doi:10.1016/j.foodchem.2010.07.088
- Shafiq, A., Moore, J., Suleman, A., Faiz, S., Farooq, O., Arshad, A., et al. (2020). Elevated soluble galectin-3 as a marker of chemotherapy efficacy in breast cancer patients: A prospective study. *Int. J. breast cancer* 2020, 4824813. doi:10.1155/2020/4824813
- Shenouda, N. S., Sakla, M. S., Newton, L. G., Besch-Williford, C., Greenberg, N. M., Macdonald, R. S., et al. (2007). Phytosterol Pygeum africanum regulates prostate cancer *in vitro* and *in vivo*. *Endocrine* 31, 72–81. doi:10.1007/s12020-007-0014-y
- Shikder, M. A., Al Hasib, T., and Kabir, M. L. (2020). *Anticancer mechanism of Withania somnifera and its bioactive compounds: A short review along with computational molecular docking study.*
- Shishodia, S., Sethi, G., Konopleva, M., Andreeff, M., and Aggarwal, B. B. (2006). A synthetic triterpenoid, CDDO-Me, inhibits IkappaBalpha kinase and enhances apoptosis induced by TNF and chemotherapeutic agents through down-regulation of expression of nuclear factor kappaB-regulated gene products in human leukemic cells. *Clin. cancer Res.* 12, 1828–1838. doi:10.1158/1078-0432.CCR-05-2044
- Shu, C. W., Weng, J. R., Chang, H. W., Liu, P. F., Chen, J. J., Peng, C. C., et al. (2021). Tribulus terrestris fruit extract inhibits autophagic flux to diminish cell proliferation and metastatic characteristics of oral cancer cells. *Environ. Toxicol.* 36, 1173–1180. doi:10.1002/tox.23116
- Silva, G. R., Vaz, C. V., Catalão, B., Ferreira, S., Cardoso, H. J., Duarte, A. P., et al. (2020). Sweet cherry extract targets the hallmarks of cancer in prostate cells: Diminished viability, increased apoptosis and suppressed glycolytic metabolism. *Nutr. cancer* 72, 917–931. doi:10.1080/01635581.2019.1661502
- Simoni, D., Romagnoli, R., Baruchello, R., Rondanin, R., Rizzi, M., Pavani, M. G., et al. (2006). Novel combretastatin analogues endowed with antitumor activity. *J. Med. Chem.* 49, 3143–3152. doi:10.1021/jm0510732
- Slocum, P. D. (2005). *Waterlilies and lotuses. Species, cultivars, and new hybrids.* Timber Press.
- Solomon, S., Muruganatham, N., and Senthilselvi, M. (2016). Anticancer activity of Abelmoschus esculentus (flower) against human liver cancer. *Int. J. Pharmacol. Biol. Sci.* 6, 154–157. doi:10.21276/ijpbs.2016.6.3.18
- Sparg, S., Light, M., and Van Staden, J. (2004). Biological activities and distribution of plant saponins. *J. Ethnopharmacol.* 94, 219–243. doi:10.1016/j.jep.2004.05.016
- Sreenivasan, S., and Krishnakumar, S. (2015). Synergistic effect of curcumin in combination with anticancer agents in human retinoblastoma cancer cell lines. *Curr. eye Res.* 40, 1153–1165. doi:10.3109/02713683.2014.987870
- Stan, S. D., Hahm, E.-R., Warin, R., and Singh, S. V. (2008). Withaferin A causes FOXO3a- and Bim-dependent apoptosis and inhibits growth of human breast cancer cells *in vivo*. *Cancer Res.* 68, 7661–7669. doi:10.1158/0008-5472.CAN-08-1510
- Sui, M., Yang, H., Guo, M., Li, W., Gong, Z., Jiang, J., et al. (2021). Cajanol sensitizes a2780/taxol cells to paclitaxel by inhibiting the PI3K/akt/NF-κB signaling pathway. *Front. Pharmacol.* 12, 783317. doi:10.3389/fphar.2021.783317
- Sun, B., Qu, W., and Bai, Z. (2003). The inhibitory effect of saponins from Tribulus terrestris on Bcap-37 breast cancer cell line *in vitro*. *Zhong yao cai= Zhongyaochai= J. Chin. Med. Mater.* 26, 104–106.
- Sun, K., Liu, Q.-Y., Wang, A., Gao, Y.-W., Zhao, L.-C., and Guan, W.-B. (2021). Comparative analysis and phylogenetic implications of plastomes of five genera in subfamily Amyridoideae (Rutaceae). *Forests* 12, 277. doi:10.3390/f12030277
- Sung, H., Ferlay, J., Siegel, R. L., Laversanne, M., Soerjomataram, I., Jemal, A., et al. (2021). Global cancer statistics 2020: GLOBOCAN estimates of incidence and mortality worldwide for 36 cancers in 185 countries. *CA a cancer J. Clin.* 71, 209–249. doi:10.3322/caac.21660
- Suphachai, C. (2014). Antioxidant and anticancer activities of Moringa oleifera leaves. *J. Med. Plants Res.* 8, 318–325. doi:10.5897/jmpr2013.5353
- Taiwo, B. J., Popoola, T. D., Van Heerden, F. R., and Fatokun, A. A. (2021). Isolation and characterisation of two quercetin glucosides with potent anti-reactive oxygen species (ROS) activity and an olean-12-en triterpene glucoside from the fruit of Abelmoschus esculentus (L.) moench. *Chem. Biodivers.* 18, e2000670. doi:10.1002/cbdv.202000670
- Talari, A., and Shakappa, D. (2018). Role of pigeon pea (Cajanus cajan L.) in human nutrition and health: A review. *Asian J. Dairy Food Res.* 37, 212–220. doi:10.18805/ajdr.1379
- Teklehaymanot, T. (2009). Ethnobotanical study of knowledge and medicinal plants use by the people in Dek Island in Ethiopia. *J. Ethnopharmacol.* 124, 69–78. doi:10.1016/j.jep.2009.04.005
- Thaiparambil, J. T., Bender, L., Ganesh, T., Kline, E., Patel, P., Liu, Y., et al. (2011). Withaferin A inhibits breast cancer invasion and metastasis at sub-cytotoxic doses by

- inducing vimentin disassembly and serine 56 phosphorylation. *Int. J. cancer* 129, 2744–2755. doi:10.1002/ijc.25938
- Tian, Y., Zhang, C., and Guo, M. (2017). Comparative study on alkaloids and their anti-proliferative activities from three *Zanthoxylum* species. *BMC complementary Altern. Med.* 17, 460–516. doi:10.1186/s12906-017-1966-y
- Toshiyuki, M., and Reed, J. C. (1995). Tumor suppressor p53 is a direct transcriptional activator of the human bax gene. *Cell* 80, 293–299. doi:10.1016/0092-8674(95)90412-3
- Tozer, G. M., Kanthou, C., Parkins, C. S., and Hill, S. A. (2002). The biology of the combretastatins as tumour vascular targeting agents. *Int. J. Exp. pathology* 83, 21–38. doi:10.1046/j.1365-2613.2002.00211.x
- Tremouillaux-Guiller, J., Moustafa, K., Gaobotse, G., and Makhzoum, A. (2020). Plant-made HIV vaccines and potential candidates. *Curr. Opin. Biotechnol.* 61, 209–216. doi:10.1016/j.copbio.2020.01.004
- Tsuda, T., Horio, F., and Osawa, T. (2000). The role of anthocyanins as an antioxidant under oxidative stress in rats. *Biofactors* 13, 133–139. doi:10.1002/biof.5520130122
- Tsujimoto, Y., and Shimizu, S. (2007). Role of the mitochondrial membrane permeability transition in cell death. *Apoptosis* 12, 835–840. doi:10.1007/s10495-006-0525-7
- Tugume, P., Kakudidi, E. K., Buyinza, M., Namaalwa, J., Kamatenesi, M., Mucunguzi, P., et al. (2016). Ethnobotanical survey of medicinal plant species used by communities around Mabira Central Forest Reserve, Uganda. *J. Ethnobiol. ethnomedicine* 12, 5–28. doi:10.1186/s13002-015-0077-4
- Uddin, M., Juraimi, A. S., Hossain, M. S., Nahar, M., Un, A., Ali, M., et al. (2014). Purslane weed (*Portulaca oleracea*): A prospective plant source of nutrition, omega-3 fatty acid, and antioxidant attributes. *Sci. World J.* 2014, 951019. doi:10.1155/2014/951019
- Usenik, V., Stampar, F., Petkovsek, M. M., and Kastelec, D. (2015). The effect of fruit size and fruit colour on chemical composition in 'Kordia' sweet cherry (*Prunus avium* L.). *J. Food Compos. Analysis* 38, 121–130. doi:10.1016/j.jfca.2014.10.007
- Usman, M., Khan, W. R., Yousaf, N., Akram, S., Murtaza, G., Kudus, K. A., et al. (2022). Exploring the phytochemicals and anti-cancer potential of the members of fabaceae family: A comprehensive review. *Molecules* 27, 3863. doi:10.3390/molecules27123863
- Vamsi, K. B., Glory, T. J., Florida, T., Aneesh, N., Rekha, L., and Thangaraj, P. (2020). Gene expression analysis of EGFR and PI3K genes in A549 lung cancer cell line treated with *Withania somnifera* root extract. *Res. J. Biotechnol.* 15, 2.
- Vaseva, A. V., Marchenko, N. D., Ji, K., Tsirka, S. E., Holzmänn, S., and Moll, U. M. (2012). p53 opens the mitochondrial permeability transition pore to trigger necrosis. *Cell* 149, 1536–1548. doi:10.1016/j.cell.2012.05.014
- Vigneshwaran, V., Thirusangu, P., Madhusudana, S., Krishna, V., Pramod, S. N., and Prabhakar, B. (2016). The latex sap of the 'Old World Plant' *Lagenaria siceraria* with potent lectin activity mitigates neoplastic malignancy targeting neovasculature and cell death. *Int. Immunopharmacol.* 39, 158–171. doi:10.1016/j.intimp.2016.07.024
- Visagie, M. H., Birkholtz, L.-M., and Joubert, A. M. (2015). A 2-methoxyestradiol bis-sulphamoylated derivative induces apoptosis in breast cell lines. *Cell & Biosci.* 5, 19–15. doi:10.1186/s13578-015-0010-5
- Von Holtz, R. L., Fink, C. S., and Awad, A. B. (1998). β -sitosterol activates the sphingomyelin cycle and induces apoptosis in LNCaP human prostate cancer cells.
- Wang, H. (1998). Plant-derived anticancer agents currently in clinical use or in clinical trials. *IDrugs investigational drugs J.* 1, 92–102.
- WHO (2020). *Global Health Estimates: Life expectancy and leading causes of death and disability*. World Health Organization.
- Widodo, N., Priyandoko, D., Shah, N., Wadhwa, R., and Kaul, S. C. (2010). Selective killing of cancer cells by *Ashwagandha* leaf extract and its component Withanone involves ROS signaling. *PLoS one* 5, e13536. doi:10.1371/journal.pone.0013536
- Wu, Q., Cho, J.-G., Yoo, K.-H., Jeong, T.-S., Park, J.-H., Kim, S.-Y., et al. (2013). A new phenanthrene derivative and two diarylheptanoids from the roots of *Brassica rapa* ssp. *campestris* inhibit the growth of cancer cell lines and LDL-oxidation. *Archives pharmacol Res.* 36, 423–429. doi:10.1007/s12272-013-0068-8
- Wu, T., Yin, J., Zhang, G., Long, H., and Zheng, X. (2016). Mulberry and cherry anthocyanin consumption prevents oxidative stress and inflammation in diet-induced obese mice. *Mol. Nutr. Food Res.* 60, 687–694. doi:10.1002/mnfr.201500734
- Xie, J., Qian, Y.-Y., Yang, Y., Peng, L.-J., Mao, J.-Y., Yang, M.-R., et al. (2022). Isothiocyanate from *moringa oleifera* seeds inhibits the growth and migration of renal cancer cells by regulating the PTP1B-dependent src/ras/raf/ERK signaling pathway. *Front. Cell Dev. Biol.* 9, 790618. doi:10.3389/fcell.2021.790618
- Yakubu, O. F., Metibemu, D. S., Adelani, I. B., Adesina, G. O., Edokwe, C. B., Oseha, O. E., et al. (2020). *Annona senegalensis* extract demonstrates anticancer properties in N-diethylnitrosamine-induced hepatocellular carcinoma in male Wistar rats. *Biomed. Pharmacother.* 131, 110786. doi:10.1016/j.biopha.2020.110786
- Yang, C., Gundala, S. R., Mukkavilli, R., Vangala, S., Reid, M. D., and Aneja, R. (2015). Synergistic interactions among flavonoids and acetogenins in *Graviola* (*Annona muricata*) leaves confer protection against prostate cancer. *Carcinogenesis* 36, 656–665. doi:10.1093/carcin/bgv046
- Yang, H., Shi, G., and Dou, Q. P. (2007). The tumor proteasome is a primary target for the natural anticancer compound Withaferin A isolated from "Indian winter cherry". *Mol. Pharmacol.* 71, 426–437. doi:10.1124/mol.106.030015
- Yang, Z., Garcia, A., Xu, S., Powell, D. R., Vertino, P. M., Singh, S., et al. (2013). *Withania somnifera* root extract inhibits mammary cancer metastasis and epithelial to mesenchymal transition. *PLoS One* 8, e75069. doi:10.1371/journal.pone.0075069
- Yap, C. V., Subramaniam, K. S., Khor, S. W., and Chung, I. (2017). *Annonacin* exerts antitumor activity through induction of apoptosis and extracellular signal-regulated kinase inhibition. *Pharmacogn. Res.* 9, 378–383. doi:10.4103/pr-pr-19_17
- Yiaile, A. L. (2017). "vitro antiploriferative activity," in *Phytochemical composition and toxicity studies of Fagaropsis angolensis and Prunus africana crude extracts* (University of Nairobi).
- Yiallouris, A., Patrikios, I., Johnson, E. O., Sereti, E., Dimas, K., De Ford, C., et al. (2018). *Annonacin* promotes selective cancer cell death via NKA-dependent and SERCA-dependent pathways. *Cell Death Dis.* 9, 764–813. doi:10.1038/s41419-018-0772-x
- Youle, R. J., and Strasser, A. (2008). The BCL-2 protein family: Opposing activities that mediate cell death. *Nat. Rev. Mol. Cell Biol.* 9, 47–59. doi:10.1038/nrm2308
- Yu, L.-L., Wu, J.-G., Dai, N., Yu, H.-G., and Si, J.-M. (2011). Curcumin reverses chemoresistance of human gastric cancer cells by downregulating the NF- κ B transcription factor. *Oncol. Rep.* 26, 1197–1203. doi:10.3892/or.2011.1410
- Yung, B. C., Li, J., Zhang, M., Cheng, X., Li, H., Yung, E. M., et al. (2016). Lipid nanoparticles composed of quaternary amine-tertiary amine cationic lipid combination (QTsome) for therapeutic delivery of AntimiR-21 for lung cancer. *Mol. Pharm.* 13, 653–662. doi:10.1021/acs.molpharmaceut.5b00878
- Zahoor, M., Ikram, M., Nazir, N., Naz, S., Batiha, G. E.-S., Kamran, A. W., et al. (2021). A comprehensive review on the medicinal importance; biological and therapeutic efficacy of *Lagenaria siceraria* (mol.) (bottle gourd) standley fruit. *Curr. Top. Med. Chem.* 21, 1788–1803. doi:10.2174/1568026621666210701124628
- Zhang, X., Mukerji, R., Samadi, A. K., and Cohen, M. S. (2011). Down-regulation of estrogen receptor- α and rearranged during transfection tyrosine kinase is associated with withaferin a-induced apoptosis in MCF-7 breast cancer cells. *BMC complementary Altern. Med.* 11, 84–10. doi:10.1186/1472-6882-11-84
- Zhang, X., Samadi, A. K., Roby, K. F., Timmermann, B., and Cohen, M. S. (2012). Inhibition of cell growth and induction of apoptosis in ovarian carcinoma cell lines CaOV3 and SKOV3 by natural withanolide Withaferin A. *Gynecol. Oncol.* 124, 606–612. doi:10.1016/j.ygyno.2011.11.044
- Zhao, B.-X., Wang, Y., Zhang, D.-M., Jiang, R.-W., Wang, G.-C., Shi, J.-M., et al. (2011). Flueggines A and B, two new dimeric indolizidine alkaloids from *Flueggea virosa*. *Org. Lett.* 13, 3888–3891. doi:10.1021/ol201410z
- Zhao, R., Gao, X., Cai, Y., Shao, X., Jia, G., Huang, Y., et al. (2013). Antitumor activity of *Portulaca oleracea* L. polysaccharides against cervical carcinoma *in vitro* and *in vivo*. *Carbohydr. Polym.* 96, 376–383. doi:10.1016/j.carbpol.2013.04.023
- Zúñiga, R., Concha, G., Cayo, A., Cikutović-Molina, R., Arevalo, B., González, W., et al. (2020). Withaferin A suppresses breast cancer cell proliferation by inhibition of the two-pore domain potassium (K2P9) channel TASK-3. *Biomed. Pharmacother.* 129, 110383. doi:10.1016/j.biopha.2020.110383
- Zuo, J., Jiang, H., Zhu, Y.-H., Wang, Y.-Q., Zhang, W., and Luan, J.-J. (2016). Regulation of MAPKs signaling contributes to the growth inhibition of 1, 7-dihydroxy-3, 4-dimethoxyxanthone on multidrug resistance A549/taxol cells. *Evidence-Based Complementary Altern. Med.* 2016, 2018704. doi:10.1155/2016/2018704

Glossary

ACAT1 Acetyl-CoA acetyltransferase

Akt Ak strain transforming serine/threonine protein kinase

ASC adaptor protein Apoptosis-associated Speck-like protein containing a CARD BGL24 bottle gourd *Lagenaria siceraria*

Bcl-2 B-Cell Leukemia/lymphoma-2

Bim BH3-containing protein

Con A Concanavalin A

COX-2 CycloOXygenase-2

CRP C-Reactive Protein

DC Dendritic Cell

EGF Epidermal Growth Factor

ENRAGE Extracellular Newly identified ligand for the Receptor for Advanced Glycation End products

ER Estrogen Receptor

ERK Extracellular signal-Regulated Kinase

FOXO3a Forkhead box O3a

GLUT glucose transporter

GPx glutathione peroxidase

GSH reduced glutathione

GSSG Glutathione Disulfide GR Glutathione Reductase

H2O2 Hydrogen peroxide

HSF1 Heat Shock Factor

IC50 Inhibitory Concentration50

IFN-γ Interferon-γ

ING1 Inhibitor of Growth family, member1

IL-12 Interleukin-12

JNK c-Jun N-terminal kinase

LDH Lactate dehydrogenase

LHX3 LIM Homeobox 3

LPS Lipopolysaccharide

MAPK Mitogen-Activated Protein Kinase

MCT4 MonoCarboxylate Transporter 4

MyD88 Myeloid Differentiation primary response 88

NCAM Neural Cell Adhesion Molecule

NF-κB Nuclear Factor-κB

NLRP3 NLR family Pyrin domain containing three

NO synthase Nitric Oxide synthase

NQO1 NADPH quinone oxidoreductase

PI3K Phosphoinositide three Kinase

PAI-1 Plasminogen Activator Inhibitor-1

PFK-1 Phosphofructokinase-1

PLCγ-1 Phosphoinositide-specific Phospholipase γ1

PP2 Phloem Protein 2

RET REarranged during Transfection tyrosine kinase

ROS Reactive Oxygen Species

SCID Severe Combined Immunodeficiency

SOD SuperOxide Dismutase

Sp1/Sp4 Specificity protein transcription factors

STAT3 Signal Transducer and Activator of Transcription three

TFAP2A Transcription Factor AP-2 alpha

Th1 T helper cell

TLR4 Toll-Like Receptor4

TNF-α Tumor Necrosis Factor-α

TPX2 Microtubule-associated Protein

TUNEL Terminal deoxynucleotidyl transferase TdT-catalyzed dUTP-Nick End Labeling

VCAM-1 Vascular Cell Adhesion Molecule-1

VEGF Vascular Endothelial Growth Factor

Frontiers in Pharmacology

Explores the interactions between chemicals and living beings

The most cited journal in its field, which advances access to pharmacological discoveries to prevent and treat human disease.

Discover the latest Research Topics

[See more →](#)

Frontiers

Avenue du Tribunal-Fédéral 34
1005 Lausanne, Switzerland
frontiersin.org

Contact us

+41 (0)21 510 17 00
frontiersin.org/about/contact



Frontiers in Pharmacology

